# BIOSTRATIGRAPHY AND SEDIMENTOLOGY OF TRIASSIC HYDROCARBON-BEARING ROCKS IN NORTHEASTERN BRITISH COLUMBIA

**by**

**MARTYN LEE GOLDING**

**M.Sci., The University of Birmingham, 2008**

**A THESIS SUBMITTED IN PARTIAL FULFILLMENT OF**

**THE REQUIREMENTS FOR THE DEGREE OF**

**DOCTOR OF PHILOSOPHY**

**in**

**THE FACULTY OF GRADUATE AND POSTDOCTORAL STUDIES**

**(Geological Sciences)**

**THE UNIVERSITY OF BRITISH COLUMBIA**

**(Vancouver)**

**April 2014**

**© Martyn Lee Golding, 2014**

## ABSTRACT

The Triassic Montney and Doig formations in the subsurface of northeastern British Columbia are important hydrocarbon reserves for the province. However the age and tectonic setting of these formations, and their outcrop equivalents (Grayling, Toad and Liard formations), are poorly constrained. The collection of conodont and detrital zircon samples from outcrop sections, and from core taken from subsurface hydrocarbon wells, has allowed the biostratigraphy of these formations to be improved, and the tectonic setting to be inferred. The study of new conodont samples, together with re-examination of existing collections, has led to the recognition of more than thirty new species and morphotypes within the Anisian (Middle Triassic) of British Columbia. These new taxa have in turn allowed the recognition of 11 new faunal assemblages that further refine the conodont biostratigraphic scale for the Anisian of British Columbia. Conodont biostratigraphy of the Montney and Doig formations in the subsurface has allowed correlation of these formations with those of surface sections, and also for the first time provided an age for the boundary between them. The boundary is recognised to be diachronous, and it is oldest in the centre of the study area. The basal Doig Formation is condensed, and shows most condensation at the edges of the study area. Both observations imply the presence of palaeo-highs to the west as well as to the east during the Triassic. This conclusion is supported by detrital zircon geochronology, which demonstrates the presence of sediment derived from the Arctic and from the pericratonic Yukon-Tanana terrane in the Triassic rocks of northeastern British Columbia. Previous hypotheses of Permo-Triassic accretion of this terrane onto the North American margin (the Klondike Orogeny) are supported by this study, and the Triassic sediments of northeastern British Columbia are interpreted to have been deposited in the foreland basin of this orogeny.

## PREFACE

This thesis contains material that will be submitted for publication and has involved collaboration with other researchers. The research project was designed by myself with the assistance of J.K. Mortensen, M.J. Orchard and J.P. Zonneveld. I performed fieldwork with the assistance of M.J. Orchard, J.P. Zonneveld, F. Ferri and M. Balini. Some conodont samples were prepared by P. Krauss. The remaining conodont samples and all of the detrital zircon samples were prepared and analysed by myself. I am the lead author on all of the research chapters, each of which has received comments from all of the authors who are listed as contributors.

**Chapter 2 - Taxonomic Revision of Anisian Gondolellidae from Northeastern British Columbia and their Importance for Biostratigraphic Correlation.**

M.L. Golding and M.J. Orchard

A version of this chapter will be submitted for publication. M.J. Orchard provided SEM images that have been incorporated into the chapter as well as providing guidance and comments.

**Chapter 3 - Dating the Doig: Conodonts constrain the age of the Montney-Doig boundary in northeastern British Columbia**

M.L. Golding, M.J. Orchard, J.P. Zonneveld and N. Wilson

A version of this chapter will be submitted for publication. M.J. Orchard provided guidance with the identification of conodont specimens. J.P. Zonneveld assisted with sample selection and collection and provided core photographs and well logs. N. Wilson provided samples and well logs.

**Chapter 4 - Stratigraphy of the Talisman Altares 16-17-083-25W6 well in northeastern British Columbia**

M.L. Golding, M.J. Orchard, J.P. Zonneveld, C.M. Henderson and L. Dunn

A version of this chapter will be submitted for publication. M.J. Orchard provided guidance with the identification of conodont specimens. J.P. Zonneveld assisted with sample selection and collection and provided core photographs and well logs. C.M. Henderson provided samples and assisted with the identification of conodont specimens. L. Dunn provided comments.

**Chapter 5 - Determining the provenance of Triassic sediments in northeastern British Columbia using detrital zircon geochronology – implications for regional tectonics**

M.L. Golding, J.K. Mortensen, F. Ferri, J.P. Zonneveld and M.J. Orchard

A version of this chapter will be submitted for publication. J.K. Mortensen assisted with preparing and analysing detrital zircon samples and provided guidance in interpreting the results. F. Ferri assisted with sample collection in the field, and provided further samples and unpublished data. J.P. Zonneveld and M.J. Orchard assisted with sample collection in the field.

## TABLE OF CONTENTS

**ABSTRACT..... ii**

**PREFACE..... iii**

**TABLE OF CONTENTS..... v**

**LIST OF TABLES.....viii**

**LIST OF FIGURES.....ix**

**ACKNOWLEDGEMENTS..... xiv**

**CHAPTER 1: Introduction.....1**

**1.1 THE TRIASSIC PERIOD.....2**

**1.1.1 The Global Triassic..... 2**

**1.1.2 The End-Permian Mass Extinction.....4**

**1.1.3 The End-Triassic Mass Extinction.....8**

**1.1.4 Triassic Palaeogeography and Climate..... 10**

**1.1.5 The Triassic of British Columbia.....12**

**1.1.6 Triassic Biostratigraphy..... 21**

**1.2 THE WESTERN CANADA SEDIMENTARY BASIN.....27**

**1.2.1 Economic Potential of the Triassic in British Columbia.....30**

**1.3 CORDILLERAN TECTONICS..... 31**

**1.4 THIS STUDY.....35**

**1.4.1 Localities.....38**

**1.4.2 Methods..... 44**

**1.5 STRUCTURE OF THIS THESIS..... 45**

**CHAPTER 2: Taxonomic revision of Anisian Gondolellidae from northeastern British Columbia and their importance for biostratigraphic correlation..... 47**

**2.1 INTRODUCTION.....48**

**2.2 GEOLOGICAL SETTING..... 50**

**2.3 MATERIAL AND METHODS.....53**

**2.4 BIOSTRATIGRAPHY..... 64**

**2.5 CONODONT FAUNAS..... 67**

**2.6 COMPARISON WITH AMMONOID ZONATION IN BC..... 82**

**2.7 CORRELATION.....83**

**2.8 SUMMARY.....86**

**2.9 CONCLUSIONS.....89**

**2.10 SYSTEMATIC PALAEONTOLOGY..... 90**

**CHAPTER 3: Dating the Doig: conodonts constrain the age of the Montney-Doig boundary in northeastern British Columbia.....167**

**3.1 INTRODUCTION.....168**

**3.2 GEOLOGICAL SETTING..... 171**

**3.3 MATERIAL AND METHODS.....176**

**3.4 BIOSTRATIGRAPHY..... 182**

**3.5 CORRELATION OF THE MONTNEY-DOIG BOUNDARY.....198**

**3.6 CONDENSATION OF THE DOIG PHOSPHATE ZONE.....202**

**3.7 IMPLICATIONS.....203**

**3.8 CONCLUSIONS.....205**

**3.9 TAXONOMIC NOTES.....206**

**CHAPTER 4: Stratigraphy of the Talisman Altares 16-17-083-25W6 well in northeastern British Columbia.....211**

**4.1 INTRODUCTION.....212**

**4.2 GEOLOGICAL SETTING..... 213**

**4.3 LITHOLOGY AND SEQUENCE STRATIGRAPHY..... 217**

**4.4 BIOSTRATIGRAPHY..... 226**

**4.5 SYNTHESIS..... 234**

**4.6 CONCLUSIONS.....236**

**4.7 TAXONOMIC NOTES.....237**

**CHAPTER 5: Determining the provenance of Triassic sediments in northeastern British Columbia using detrital zircon geochronology – implications for regional tectonics.....254**

**5.1 INTRODUCTION.....255**

**5.2 GEOLOGICAL SETTING..... 259**

**5.3 MATERIAL AND METHODS.....262**

**5.4 RESULTS.....276**

**5.5 DISCUSSION..... 278**

**5.6 CONCLUSIONS.....292**

**CHAPTER 6: Summary and Further Work.....294**

**6.1 SUMMARY.....295**

**6.2 FURTHER WORK..... 296**

**REFERENCES.....299**

**APPENDIX 1.....338**

**APPENDIX 2.....350**

## LIST OF TABLES

**TABLE 2.1 Location Table for Conodont Samples in Chapter 2..... 59**

**TABLE 2.2 Conodonts Recovered from Samples in Chapter 2..... 63**

**TABLE 2.3 Conodont Morphology Comparison Chart.....94**

**TABLE 3.1 Location Table and Conodonts Recovered from Samples in Chapter 3.....178**

**TABLE 4.1 Conodonts Recovered from Samples in Chapter 4..... 228**

**TABLE 5.1 Location Table for Detrital Zircon Samples in Chapter 5..... 263**

## LIST OF FIGURES

**FIGURE 1.1 Triassic Timescale for North America..... 3**

**FIGURE 1.2 Late Triassic Palaeogeography..... 11**

**FIGURE 1.3 Triassic Outcrop and Locality Map, Northeastern BC..... 14**

**FIGURE 1.4 Correlation Chart of Triassic Formations in Western Canada..... 17**

**FIGURE 1.5 Triassic Ammonoid Biostratigraphy of BC..... 23**

**FIGURE 1.6 Triassic Conodont Biostratigraphy of North America and Tethys..... 26**

**FIGURE 1.7 Map of the Western Canada Sedimentary Basin..... 28**

**FIGURE 1.8 Terrane Map of the Canadian Cordillera.....32**

**FIGURE 1.9 Locality Map of the Williston Lake Area.....39**

**FIGURE 1.10 Locality Map of the Alaska Highway Area.....41**

**FIGURE 1.11 Locality Map of the Liard and Toad River Areas.....42**

**FIGURE 1.12 Locality Map of Subsurface Wells and the Montney Play Trend.....44**

**FIGURE 2.1 Anisian Ammonoid Biostratigraphy of BC.....52**

**FIGURE 2.2 Anisian Ammonoid Biostratigraphy of Nevada..... 54**

**FIGURE 2.3 Anisian Ammonoid Biostratigraphy of Tethys.....55**

**FIGURE 2.4 Locality Map of the Alaska Highway Area.....56**

**FIGURE 2.5 Locality Map of the Liard and Toad River Areas.....56**

**FIGURE 2.6 Locality Map of Subsurface Wells and the Montney Play Trend.....57**

**FIGURE 2.7 Correlation of Conodont Assemblages and Ammonoid Zones in BC..... 65**

**FIGURE 2.8 Anisian Ammonoid Zonation in BC, Nevada and Sverdrup Basin..... 66**

**FIGURE 2.9 Stratigraphic Log of Mile Post 375 East Section.....68**

**FIGURE 2.10 Stratigraphic Log of Petro-Canada Kobes d-048-A/094-B-09 well..... 70**

**FIGURE 2.11 Stratigraphic Log of Talisman Altares 16-17-083-25W6 well.....71**

**FIGURE 2.12 Stratigraphic Log of Murphy Swan d-054-B/093-P9 well..... 73**

**FIGURE 2.13 Stratigraphic Log of Shell Groundbirch 16-02-078-22W6 well..... 74**

**FIGURE 2.14 Stratigraphic Log of East Toad River I Section..... 76**

**FIGURE 2.15 Stratigraphic Log of Mile Post 375 West Section.....77**

**FIGURE 2.16 Stratigraphic Log of North Tetsa Phosphate Section..... 78**

**FIGURE 2.17 Stratigraphic Log of East Toad River II Section.....79**

**FIGURE 2.18 Stratigraphic Log of Yellow Bluffs Section.....81**

**FIGURE 2.19 Standard Multielement Apparatus of *Neogondolella*.....91**

**FIGURE 2.20 Morphological Terminology of Standard *Neogondolella* P1 Element.....95**

**FIGURE 2.21 *Neogondolella bifurcata*.....99**

**FIGURE 2.22 *Neogondolella* ex gr. *constricta* morphotype α..... 104**

**FIGURE 2.23 *Neogondolella* ex gr. *constricta* morphotype β..... 106**

**FIGURE 2.24 *Neogondolella* ex gr. *constricta* morphotype γ..... 107**

**FIGURE 2.25 *Neogondolella* ex gr. *constricta* morphotype δ..... 109**

**FIGURE 2.26 *Neogondolella* ex gr. *constricta* morphotype ε.....111**

**FIGURE 2.27 *Neogondolella* ex gr. *constricta* morphotype ζ.....113**

**FIGURE 2.28 *Neogondolella* ex gr. *transita* morphotype α.....117**

**FIGURE 2.29 *Neogondolella* ex gr. *transita* morphotype β.....118**

**FIGURE 2.30 *Neogondolella* ex gr. *regalis* morphotype α..... 122**

**FIGURE 2.31 *Neogondolella* ex gr. *regalis* morphotype β..... 124**

**FIGURE 2.32 *Neogondolella* ex gr. *regalis* morphotype γ.....125**

**FIGURE 2.33 *Neogondolella* ex gr. *regalis* morphotype δ..... 127**

**FIGURE 2.34 *Neogondolella* ex gr. *regalis* morphotype ε.....128**

**FIGURE 2.35 *Neogondolella* ex gr. *regalis* morphotype ζ.....129**

**FIGURE 2.36 *Neogondolella* ex gr. *regalis* morphotype η..... 131**

**FIGURE 2.37 *Neogondolella* ex gr. *regalis* morphotype θ..... 133**

**FIGURE 2.38 *Neogondolella* ex gr. *regalis* morphotype ι..... 135**

**FIGURE 2.39 *Neogondolella* ex gr. *shoshonensis* morphotypes A and B..... 139**

**FIGURE 2.40 *Neogondolella* ex gr. *shoshonensis* morphotype γ..... 141**

**FIGURE 2.41 *Neogondolella* ex gr. *shoshonensis* morphotype δ..... 142**

**FIGURE 2.42 *Neogondolella* n. sp. A..... 144**

**FIGURE 2.43 *Neogondolella* n. sp. B..... 146**

**FIGURE 2.44 *Neogondolella* n. sp. C..... 148**

**FIGURE 2.45 *Neogondolella* n. sp. D..... 150**

**FIGURE 2.46 *Neogondolella* n. sp. E..... 152**

**FIGURE 2.47 *Neogondolella* n. sp. F..... 154**

**FIGURE 2.48 *Neogondolella* n. sp. G..... 156**

**FIGURE 2.49 *Neogondolella* n. sp. H..... 158**

**FIGURE 2.50 *Paragondolella* ex gr. *excelsa* juveniles..... 161**

**FIGURE 2.51 *Paragondolella* ex gr. *liebermani* morphotype α..... 165**

**FIGURE 2.52 *Paragondolella* ex gr. *liebermani* morphotype β..... 166**

**FIGURE 3.1 Locality Map of Subsurface Wells and the Montney Play Trend..... 170**

**FIGURE 3.2 Correlation Chart of Triassic Formations in Western Canada..... 172**

**FIGURE 3.3 Stratigraphic Log of Petro-Canada Kobes c-074-G/094-B-9 well..... 183**

**FIGURE 3.4 Montney-Doig Boundary, Petro-Canada Kobes c-074-G/094-B-9 well..... 184**

**FIGURE 3.5 Stratigraphic Log of Petro-Canada Kobes d-048-A/094-B-09 well..... 186**

**FIGURE 3.6 Stratigraphic Log of Talisman Altares c-085-I/094-B-01 well..... 188**

**FIGURE 3.7 Stratigraphic Log of Talisman Altares 16-17-083-25W6 well..... 189**

**FIGURE 3.8 Stratigraphic Log of Arc Dawson 07-13-79-15W6 well..... 191**

**FIGURE 3.9 Stratigraphic Log of Murphy Swan d-054-B/093-P9 well..... 192**

**FIGURE 3.10 Stratigraphic Log of Talisman Groundbirch 03-06-078-22W6 well..... 194**

**FIGURE 3.11 Stratigraphic Log of Shell Groundbirch 16-02-078-22W6 well..... 195**

**FIGURE 3.12 Stratigraphic Log of Shell Groundbirch 16-35-078-21W6 well..... 197**

**FIGURE 3.13 NW-SE Cross-Section of Correlated Well Logs..... 199**

**FIGURE 3.14 NE-SW Cross-Section of Correlated Well Logs..... 200**

**FIGURE 3.15 Conodonts Identified in Subsurface BC..... 210**

**FIGURE 4.1 Locality Map of Subsurface Wells and the Montney Play Trend.....213**

**FIGURE 4.2 Isopach Map of the Montney Formation in Northeastern BC.....215**

**FIGURE 4.3 Stratigraphic Log of Talisman Altares 16-17-83-25-W6 well, part 1.....219**

**FIGURE 4.4 Stratigraphic Log of Talisman Altares 16-17-83-25-W6 well, part 2.....220**

**FIGURE 4.5 Belloy-Montney Boundary, Talisman Altares 16-17-83-25-W6 well.....221**

**FIGURE 4.6 Bioclastic Horizon in the Montney Formation..... 222**

**FIGURE 4.7 Montney-Doig Boundary, Talisman Altares 16-17-83-25-W6 well.....224**

**FIGURE 4.8 Timescale Chart for the Lower and Middle Triassic.....230**

**FIGURE 4.9 Conodonts from Talisman Altares 16-17-83-25-W6 well, part 1.....252**

**FIGURE 4.10 Conodonts from Talisman Altares 16-17-83-25-W6 well, part 2.....253**

**FIGURE 5.1 Triassic Outcrop and Locality Map, Northeastern BC..... 258**

**FIGURE 5.2 Map of the Western Canada Sedimentary Basin..... 260**

**FIGURE 5.3 Correlation Chart of Triassic Formations in Western Canada.....261**

**FIGURE 5.4 Locality Map of the Williston Lake Area.....266**

**FIGURE 5.5 Locality Map of the Alaska Highway Area.....268**

**FIGURE 5.6 Anisian Ammonoid Biostratigraphy of BC.....269**

**FIGURE 5.7 Locality Map of Subsurface Wells and the Montney Play Trend.....271**

**FIGURE 5.8 Relative Probability Density Plots, Grouped by Stage and Substage.....274**

**FIGURE 5.9 Relative Probability Density Plots for the Anisian Substages.....275**

**FIGURE 5.10 Relative Probability Density Plots for the Anisian, Grouped by Area.....281**

**FIGURE 5.11 Reference Frame Relative Probability Density Plots.....283**

## ACKNOWLEDGMENTS

Thanks must first go to my supervising committee of Jim Mortensen (UBC), Mike Orchard (Geological Survey of Canada) and J.-P. Zonneveld (University of Alberta), all of whom have provided invaluable guidance, training and encouragement, as well as financial support. My examination committee of Stuart Sutherland, Paul Smith, Dan Moore (all UBC) and Arnaud Brayard (Université de Bourgogne) are also thanked for their comments, which improved the final thesis.

Charles Henderson (Universtiy of Calgary) allowed access to his collections and provided further guidance and comments on chapter 4. Fil Ferri (BC Ministry of Natural Gas Development) accompanied me in the field in 2009, provided unpublished data, and commented on chapter 5. Nick Wilson (Murphy Oil Corp) allowed the use of samples that he had collected, provided subsurface well logs, and commented on chapter 3. Lindsay Dunn (Athabasca Oil Corp) provided comments on chapter 4. Marco Balini (University of Milan) assisted in the field in 2011 and provided comments on incomplete parts of the thesis, as did Luke Beranek (Memorial University Newfoundland). Discussions on various aspects of Triassic stratigraphy, conodonts and tectonics with Rich Friedman (UBC), Chris McRoberts (SUNY Cortland), Leo Krystyn (University of Vienna), Michele Mazza and Marco Levera (both University of Milan), Andrew Caruthers and Pengfei Hou (both UBC) were informative and appreciated. Abbie Wright helped to improve my spelling and grammar.

Jay Scott (Murphy Oil Corp) helped with the provision of well logs. Peter Krauss (Geological Survey of Canada) processed some of the conodont samples and taught me how to process the others. Hillary Taylor (Geological Survey of Canada) picked a number of the conodont samples and helped with cataloguing of the samples. Ryan Olson (BC Oil and Gas Commission) provided access to core held at the storage facility in Charlie Lake, and allowed samples to be taken. Bob Batchelor provided helicopter support during the 2009 field season. Accommodation and logistical support was provided by the Wicked River Outfitters in 2010, and the Tetsa River Lodge in 2011.

Primary funding for this thesis was provided by Geoscience BC.

# CHAPTER 1

# Introduction

## 1.1 THE TRIASSIC PERIOD

### 1.1.1 The Global Triassic

The Triassic was named by Alberti (1834) to encompass three of the facies found in the Germanic Basin; Bunter, Muschelkalk and Keuper. The name was subsequently applied to formations in the Alps by Hauer (1850) and therefore shown to have widespread utility. Mojsisovics *et al*. (1895) divided the Triassic into four series (Scythian, Dinarian, Tirolian, Bajuvarian), whilst Arthaber (1905) utilised three series: Lower, Middle and Upper, thought to be equivalent to the Bunter, Muschelkalk and Keuper, respectively. These divisions are still in use, although some authors (*e.g.* Lucas, 2013) advocate for a return to four series (Scythian, Dinarian, Carnian and Norian) due to the recently realised variability in the length of the existing series. It has now also been realised that the Lower, Middle and Upper Triassic do not correlate exactly with the facies of the Germanic Basin. The Triassic was first recognised in North America due to the discovery of fossils by Gabb (1864) in California; Triassic fossils were later discovered in Canada by Selwyn (1877; see below).

The three series of the Triassic are further subdivided into seven stages: Induan and Olenekian (Kiparisova and Popov, 1956) in the Lower Triassic; Anisian (Waagen and Diener, 1895) and Ladinian (Bittner, 1892) in the Middle Triassic; Carnian, Norian, (Mojsisovics, 1869) and Rhaetian (Gümbel, 1861) in the Upper Triassic (fig. 1.1). In North America, Induan and Olenekian are often replaced by the local terminology Griesbachian, Dienerian, Smithian and Spathian, defined in the Arctic by Tozer (1965). These are considered

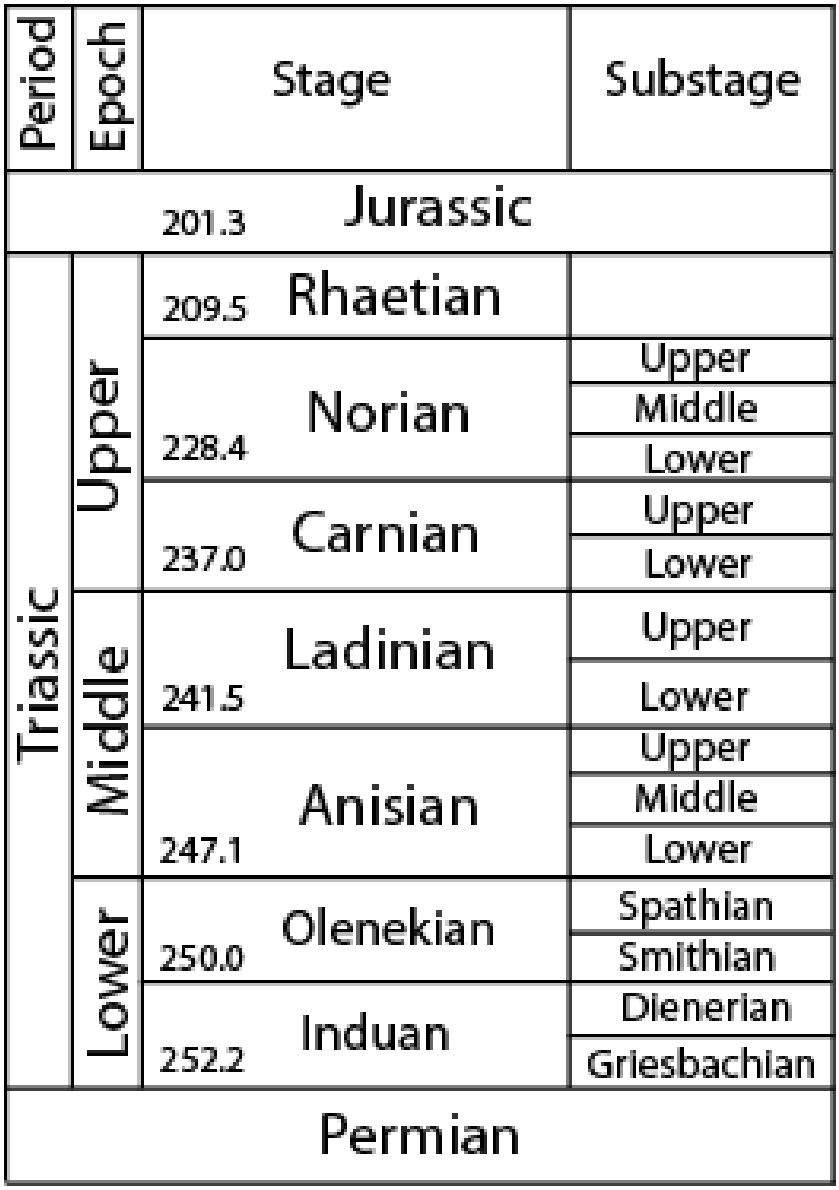



**Figure 1.1.** The Triassic timescale for North America. Based on data from Lucas (2010) and Ogg (2012). Stage boundary ages are in Ma, and taken from Ogg (2012). There is uncertainty over the age of the Induan-Olenekian boundary (Galfetti *et al*., 2007 suggest a date of 251.2 Ma), the Carnian-Norian boundary (Lucas *et al.*, 2012 suggest 221.0 Ma) and the Norian-Rhaetian boundary (Lucas *et al.*, 2012 suggest 201.3 Ma). None of these three boundaries has yet been defined using the GSSP principle, and this leads to part of the uncertainty. See Ogg (2012) and Lucas (2010) for further discussion.

substages of the Induan and Olenekian elsewhere in the world (Lucas, 2010). A number of other names have been applied to divisions of the Triassic and these are summarised in Tozer (1984).

The Triassic is now considered to be the first period of the Mesozoic era, with the latest radiometric dates suggesting that it lasted from approximately 252.2 Ma to 201.3 Ma (Mundil *et al.*, 2010; Shen *et al.*, 2011; Schoene *et al.*, 2010; Ogg, 2012). The base of the Triassic has been defined in Meishan, China, at the first occurrence of the conodont *Hindeodus parvus* (Yin *et al.*, 2001). This boundary with the Permian represents the Palaeozoic-Mesozoic boundary, and is preceeded by the largest mass extinction in Phanerozoic history, the end-Permian mass extinction (Erwin, 2006). The upper boundary with the Jurassic also approximately coincides with another major mass extinction. This situation of having major mass extinctions at both the lower and upper boundaries of the period is unique in the Phanerozoic and therefore the Triassic period represents a particularly interesting chapter in Earth history.

### 1.1.2. The End-Permian Mass Extinction

The end-Permian mass extinction involved the removal of more than 90% of marine species (Raup, 1979), although this number may be an overestimation due to bias in the fossil record (Smith, 2001), and pseudoextinction (McGowan and Smith, 2007). Corals, cephalopods, brachiopods, bryozoans, and crinoids were severely affected (Erwin, 2006); the conodonts, however, had already been reduced in number and did not experience much of an effect during the end-Permian extinction, with only endemics disappearing (Orchard 2007 d). The end-Permian extinction was preceded by a decline in biodiversity that began in the Guadalupian (Clapham *et al.*, 2009), and it contributed to the replacement of the dominant brachiopod fauna by bivalves (Sepkoski, 1981), which had also begun in the Lopingian (Clapham and Bottjer, 2007). The end-Permian extinction did not just reduce diversity, but also caused re-structuring of palaeocommunities, which commonly show a reduction in epifaunal species (Schubert and

Bottjer, 1995). It also led to the reduction in size of some benthic taxa in the Early Triassic aftermath of the extinction (the Lilliput effect; Fraiser and Bottjer, 2004; Payne, 2005; Twitchett *et al.*, 2005; Twitchett, 2007), although this conclusion has been contested in the case of gastropods (Brayard *et al.*, 2010). Global diversity was low in the aftermath of the extinction; however, trace fossil evidence suggests that refugia existed that allowed higher diversity populations to persist (Beatty *et al.*, 2008; Zonneveld *et al.*, 2010 b). There was a relatively long recovery period before overall biodiversity began to increase (Ovtcharova *et al.*, 2006; Lehrmann *et al.*, 2006), although both the conodonts (Orchard, 2007 d) and the ammonoids (Brayard *et al.*, 2009) underwent comparatively rapid recoveries. The aftermath of the extinction led to a global absence of reefs ("reef gap"; Flügel, 2002; although see also Brayard *et al.*, 2011 for an alternative, "reef low" interpretation), chert deposition ("chert gap"; Racki, 1999; Beauchamp and Baud, 2002) and coal beds ("coal gap"; Veevers *et al.*, 1994; Faure *et al.*, 1995; Retallack *et al.*, 1996), as well as an increase in microbial structures, indicating harsh marine conditions in the Lower Triassic such as low oxygen levels and elevated temperature and salinity (Sano and Nakashima, 1997; Jeffrey *et al.*, 2013; Richoz *et al.*, 2013). The extinctions also affected the terrestrial biosphere, with tetrapods (Smith and Ward, 2001; Benton *et al.*, 2004), plants (Retallack, 1995) and insects (Labandeira, 2005) undergoing rapid extinction near to the Permian-Triassic boundary. It has been suggested by some authors that the terrestrial extinctions do not correlate with those of the oceans (*e.g.* Lucas, 2009), whilst other authors maintain that the extinctions are synchronous (*e.g.* Metcalfe and Isozaki, 2009).

A number of mechanisms have been postulated for the end-Permian mass extinction, including volcanism, bolide impact, removal of habitats due to marine regression and anoxia related to marine transgression.

The eruption of the Siberian traps was coincident with the extinctions (Mundil *et al*., 2004) or slightly younger (Burgess and Bowring, 2010). These eruptions are thought to have produced basalt covering up to 7 million square kilometers in as little as 1 million years (Courtillot and Renne, 2003; Nikishin *et al.*, 2002). It is likely that the eruptions played a role in the extinctions by releasing large amounts of $CO_2$, contributing to global warming (Wignall, 2001; Berner, 2002). This warming may in turn may have led to the release of methane from methane hydrate, which then contributed to even greater warming (Erwin, 1993). The Siberian traps erupted in a basin containing large coal deposits known as the Tugusskaya Series, and burning of the coal would also have increased the volume of $CO_2$ and methane in the atmosphere (Retallack and Jahren, 2008). Ash formed by the ignition of these coal beds may also have led to microbial blooms and oceanic anoxia (Grasby *et al.*, 2011). $SO_2$ produced by the eruption would have caused short term cooling of the climate (Renne *et al.*, 1995; Wignall, 2001) and led to the formation of acid rain (Renne *et al.*, 1995) which would have had a detrimental effect on the terrestrial biosphere (Visscher *et al*., 1996).

Evidence for a bolide impact at the Permian-Triassic boundary is limited, with no conclusive evidence yet presented for increased iridium levels that would be indicative of an impact (Koeberl *et al.*, 2004). However there have been reports of shocked quartz (Retallack *et al.*, 1998), fullerenes (Becker *et al.*, 2001) and possible meteorite fragments (Basu *et al.*, 2003), all from Antarctica. No impact crater of the appropriate age has been identified, although the Bedout structure near Australia has been proposed as such (Becker *et al.*, 2004).

Marine regression at the boundary was postulated as an important mechanism for extinction due to gaps in the rock record near to the boundary (Newell, 1963; Maxwell, 1989). Regression

would lead to extinction by reducing the space available for marine organisms to inhabit (Schopf, 1974; Simberloff, 1974). Subsequently however, widespread marine tansgression has been recognised in a number of sections (Wignall and Hallam, 1992, 1993). This is thought to have led to the spread of anoxic water onto continental shelves, leading to extinction through asphyxiation (lack of oxygen; Wignall and Hallam, 1992, 1993). Anoxia may also have led to selective extinction due to hypercapnia (excess of $CO_2$), and $H_2S$ poisoning (Grice *et al.*, 2005; Knoll *et al*., 2007). It has been suggested that marine anoxia persisted into the Griesbachian, inhibiting the recovery of the marine benthic biota that had been most seriously affected by the extinction (Twitchett and Wignall, 1996; Twitchett, 1999; Twitchett *et al*., 2004). In Canada, anoxia may have continued even longer, throughout the Lower Triassic (Woods *et al.*, 2013; Grasby and Beauchamp, 2013). Although some locations show evidence for regression and some for transgression, in others it appears as though the sea-level was fluctuating at around the time of the Permian-Triassic boundary (*e.g.* South China; Yin *et al.*, 2012).

The boundary interval records large variations in the ratios of isotopes of carbon (Payne *et al*., 2004), which suggest that the global carbon cycle was disrupted, either by the addition of large amounts of carbon dioxide, the removal of large amounts of biomass, or both. Two spikes in the carbon isotope record have been identified near the boundary (Korte and Kozur, 2010), and these may coincide with two pulses of extinction (Yin *et al.*, 2012; Song *et al.*, 2013). The ratio of oxygen isotopes reflects sea water temperature, and suggests an interval of global warming coincident with the latest Permian extinctions (Joachimski *et al.*, 2012, 2013). The ratio of strontium isotopes is indicative of the amount of terrestrial weathering, and this seems to increase at the Permian-Triassic boundary (Korte *et al*., 2003). All three of these isotopic

systems may suggest that the climate was becoming warmer at this time, perhaps in relation to an increase in atmospheric $CO_2$.

### 1.1.3 The End-Triassic Mass Extinction

The end-Triassic mass extinction was less severe than the end-Permian, however, up to 76% of species still went extinct (Raup, 1992). Extinction rates were high throughout the Upper Triassic (Tanner *et al.*, 2004), however, some groups appear to have suffered greater extinction in the Rhaetian than during the rest of the Upper Triassic (Hallam, 2002). Bivalves, corals and brachiopods were particuarly affected (McRoberts and Newton, 1995; Stanley, 1988; Harper *et al.*, 1993). This extinction led to the final demise of the conodonts (Clark, 1983). A few specimens of conodonts from Hungary have been recovered above the first appearance of typical Jurassic ammonoids (Kozur, 1993; Pálfy *et al.*, 2007), however, it is uncertain whether these represent re-working or the persistence of conodonts into the Jurassic, as they have only been recovered from one section. The ammonoids were reduced to just one family by the extinction (Tozer, 1981), although both they and the conodonts had suffered extinction throughout the Rhaetian (Hallam, 2002). Terrestrial plants experienced a 95% turnover of their species (McElwain *et al.*, 1999), whilst the evidence for an extinction amongst the tetrapods is ambiguous (Benton, 1994; Cuny, 1995; Tanner and Lucas, 2013).

The extinction not only reduced biodiversity, it also led to changes in the composition of benthic communities, for example in the brachiopod community (Tomašových and Siblík, 2007). There was also a reduction in size of organisms in the aftermath of the extinction, for example in radiolaria (Longridge *et al.*, 2007) and in bivalves (Barras and Twitchett, 2007; Mander *et al.*, 2008).

A number of mechanisms for the extinction have been proposed, including sea-level change (Hallam, 1990), bolide impact (Olsen *et al.*, 1987, 2002 a, b), volcanism (Marzoli *et al.*, 1999; McElwain *et al.*, 1999; Wignall, 2001), release of methane due to melting of methane hydrates (Pálfy *et al.*, 2001; Retallack, 2001) and ocean acidification (Hautmann, 2004).

This extinction has been related to volcanism associated with the Central Atlantic Magmatic Province (CAMP) that was occurring at the same time (Schoene *et al.*, 2010; Blackburn *et al.*, 2013). This volcanism would have released $SO_2$, causing a short, initial period of global cooling (Guex *et al.*, 2004), as well as large amounts of $CO_2$, which would have led to global warming (Pálfy, 2003). This warming would also have disrupted the hydrological cycle, leading to increased freshwater runoff and a salinity decrease in the oceans that may have contributed to the extinction (Brandner, 1984; Ruhl *et al.*, 2011).

Negative carbon isotope anomalies have been recorded from marine sections in Austria (McRoberts *et al.*, 1997), Canada (Ward *et al.*, 2001), Hungary (Pálfy *et al.*, 2001) and England (Hesselbo *et al.*, 2002), as well as from terrestrial sections in Greenland (Hesselbo *et al.*, 2002). Pálfy *et al.*, (2001) attributed these shifts to release of methane from methane hydrate, which may have been related to contemporaneous volcanism (Hesselbo *et al.*, 2002; Pálfy, 2003).

The addition of large amounts of $CO_2$ to the atmosphere due to volcanism and release of methane may in turn have led to oceanic acidification, preventing the precipitation of calcium carbonate and leading to the demise of organisms with an aragonitic or high-Mg calcitic skeleton (Hautmann *et al.*, 2008). This biocalcification crisis has been observed both in shallow water (*e.g.* Northern Calcareous Alps; Galli *et al.*, 2005, and St Audrie's Bay, England; van de Schootbrugge *et al.*, 2007) and in deeper water (*e.g.* Montenegro; Črne *et al.*, 2011). In contrast

to the end-Permian mass extinction, siliceous organisms such as radiolaria suffered relatively little extinction in the latest Triassic (Kiessling and Danelian, 2011).

Evidence for bolide impact at the Triassic-Jurassic boundary is scarce, and is restricted to an iridium anomaly and fern spike in the Newark Basin (Olsen *et al.*, 2002 a, b). These have not been identified elsewhere, nor has a crater of the correct age been identified. The Manicouagan Crater in Québec has been dated to the Norian (Hodych and Gunning, 1992), and appears to be just one of a series of impacts during the Late Triassic (Onoue *et al.*, 2012).

Regression followed by transgression is observed in Triassic-Jurassic boundary sections around the world, including in Germany (Hallam and Wignall, 1999), Austria (McRoberts *et al.*, 1997), England (Hallam, 1990, 1995) and the Sverdrup Basin of Canada (Embry, 1993), although there appears to be no sea-level change in the Queen Charlotte Islands in Western Canada (Tipper *et al.*, 1994), or Asia (Hallam and Wignall, 1999). Regression could have reduced biodiversity at the end of the Triassic due to habitat loss (Newell, 1967). The pattern of regression followed by transgression is observed most commonly in Europe (Hallam, 1990) and may be related to the onset of CAMP magmatism (Hallam and Wignall, 1999).

### 1.1.4 Triassic Palaeogeography and Climate

During the Triassic, most of the landmass of the Earth was concentrated together in a supercontinent known as Pangaea. This continent started to assemble in the Carboniferous and it remained more or less cohesive until the Jurassic, when the North Atlantic Ocean began to open and Pangaea began to split apart (Veevers, 1994). Pangaea was centred on the equator, and extended almost from one pole to the other (Ziegler *et al.*, 1983). The Panthalassa Ocean encircled Pangaea and covered much of the globe, with the Tethys Ocean cutting into the

continent (fig. 1.2). The existence of Pangaea had an important effect on the climate by controlling the distribution of ocean currents. During the Triassic, British Columbia was located at mid-latitudes in the northern hemisphere (Smith *et al.*, 1995; fig. 1.2) and so it experienced a relatively arid climate and was affected by the trade winds (Davies, 1997 a). Its position on the margin of Panthalassa also led to upwelling of nutrient-rich waters along the coast (Davies, 1997 a). Sea-level fluctuated throughout the Triassic, with as many as twelve transgressive-regressive cycles recognised globally (Embry, 1997).

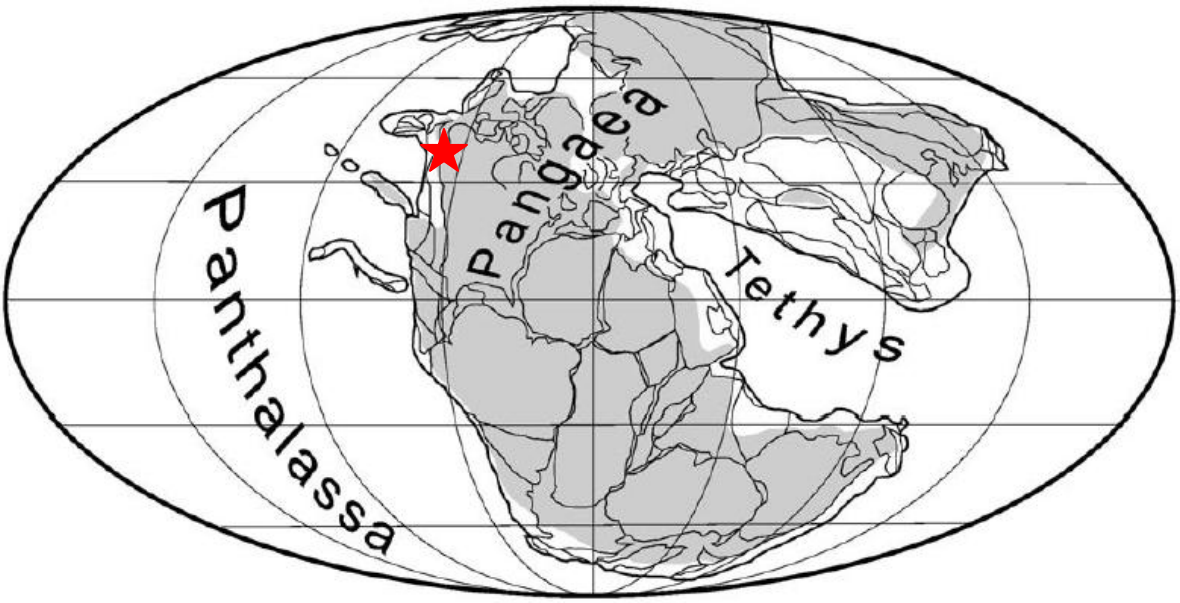



**Figure 1.2.** Late Triassic palaeogeography showing the location of major geographical features. The location of British Columbia at this time is marked by the star. Modified from Preto *et al.* (2010).

Fluctuations in the carbon isotope record during the Lower Triassic (Payne *et al.*, 2004; Horacek *et al.*, 2009) indicate that the environment was repeatedly disturbed, and these fluctuations have been linked to delayed recovery after the end-Permian mass extinction and to subsequent variations in biodiversity (*e.g.* Simms and Ruffel, 1989; Orchard, 2007 d). Strontium isotopes

suggest that globally, the Lower Triassic climate was arid with intermittent humid periods (Korte *et al.*, 2003), whilst oxygen isotopes suggest that the climate was warm until at least the Smithian (Romano *et al.*, 2013). During the Middle Triassic, the eastern part of Tethys appears to have become more humid, whilst western Tethys and North America remained more arid with occasional humid pulses (Preto *et al.*, 2010). Coal formation also resumed at this time (Retallack *et al.*, 1996). The Upper Triassic climate was monsoonal (Preto *et al.*, 2010). Humidity increased markedly during the Middle Carnian, and an increase in rainfall led to what has been termed the Carnian Pluvial Event (Simms and Ruffell, 1989). This widespread event is thought to be related to orogenesis (Hornung and Brandner, 2005), climate change caused by the eruption of the Wrangellia volcanics (Furin *et al.*, 2006) or a peak in monsoon strength (Parrish, 1993). Arid conditions returned during the Upper Carnian and Lower Norian (Simms and Ruffell, 1990) before giving way to a more humid climate again in the Upper Norian and Rhaetian (Korte *et al.*, 2003).

### 1.1.5 The Triassic of British Columbia

The Triassic rocks of British Columbia occur primarily in an outcrop belt which extends through the province in the Rocky Mountain Foothills (fig. 1.3). Triassic rocks are also present in the subsurface of the province east of this outcrop belt, where they are continuous with rocks in the subsurface of Alberta. Other outcrops of Triassic rocks also occur throughout the western half of the province, in the accreted terranes.

The earliest recognition of Triassic rocks in British Columbia came during the expedition of A.R.C. Selwyn in 1875 to the Peace River (Selwyn, 1877). Subsequent work by Dawson (1881) and McConnell (1896) identified further outcrops on the Peace River and surrounding areas. The

Peace River was further investigated by McLearn (1918, 1921, 1930, 1937 a, b, 1940 a, b, 1941 a, b, c, 1947 a, b, 1960), which led to the discovery of a number of sections whose equivalents were sampled on what is now Williston Lake as part of this study: Ne-Parle-Pas Rapids (now Ne-Parle-Pas Point; McLearn, 1937 b); Black Bear Ridge (McLearn, 1960); Brown Hill (McLearn, 1941 a); East Glacier Spur (now Glacier Spur; McLearn, 1947 b); Folded Hill (McLearn, 1941 c) and Beattie Ledge (McLearn, 1940 b). Sections in the Peace River area were further studied by Williams and Bocock (1932), Pelletier (1963) and Gibson (1971). The river was dammed in 1967, leading to the creation of Williston Lake and a number of new outcrops, some of which can be correlated with sections originally investigated before the flooding. These new sections were first visited by E.T. Tozer and M.J. Orchard in 1980-1982, and described by Gibson and Edwards (1990, 1992), Zonneveld *et al.* (1997), and Zonneveld (2010).

The Triassic of the Alaska Highway was first observed by Williams (1944) and Hage (1944), with later collections made by McLearn (1946 a) who collected samples from the locality at Mile Post 375 West. Tozer collected samples from other sections along the highway, including the localities at Mile Post 375 West and East (Tozer, 1967).

Kindle (1944, 1946) first described the Triassic outcrops on the Toad and Liard rivers, naming the Grayling, Toad and Liard formations for rocks exposed on the two rivers. Subsequently, Tozer collected samples from the localities referred to here as Liard-Brimstone (Tozer, 1967) and East Toad River II (Tozer, 1994). The river sections, as well as those on the Alaska Highway, were later recollected by E.T. Tozer and M.J. Orchard in 1983.

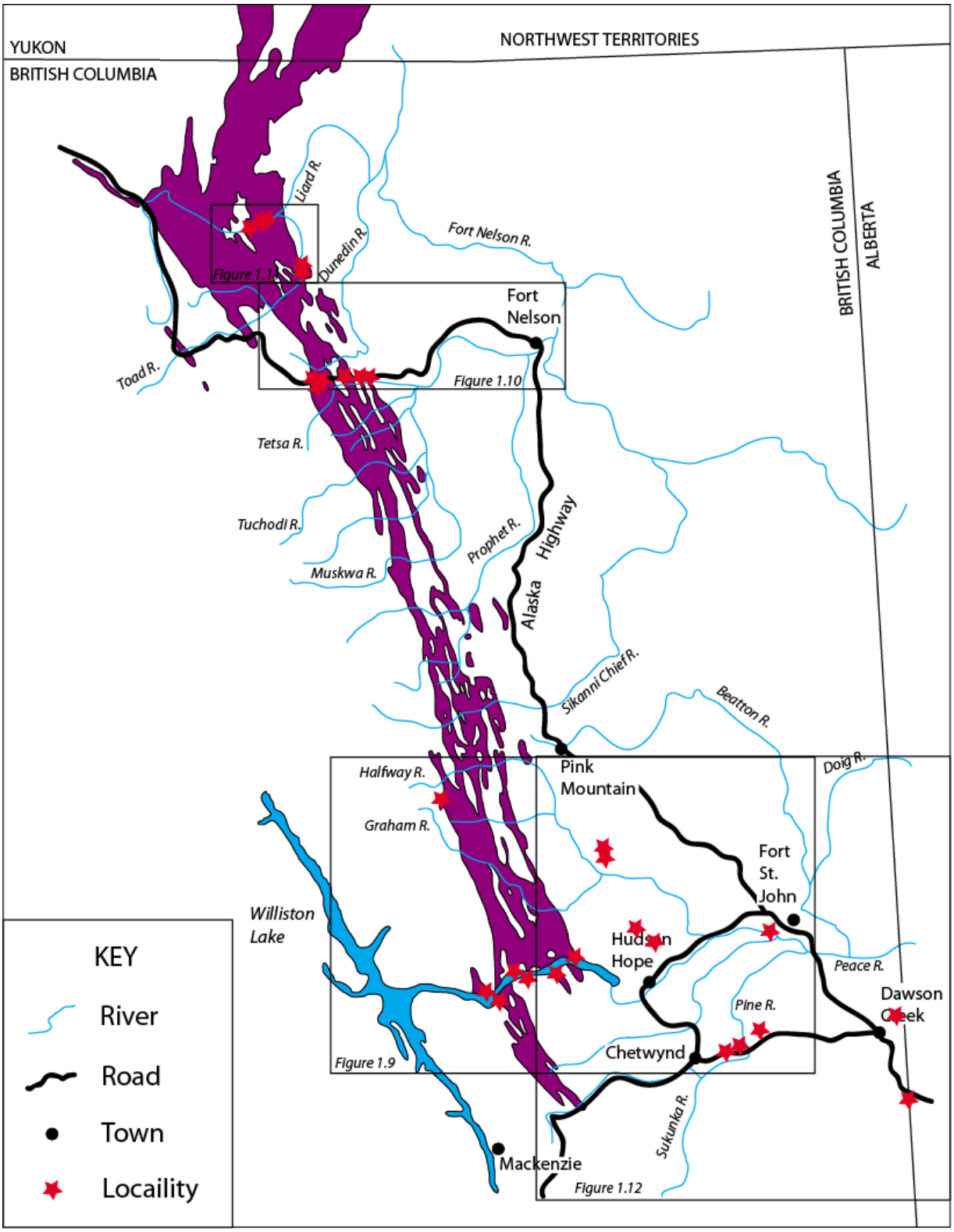



**Figure 1.3.** Map showing Triassic outcrop in northeastern British Columbia. Red stars indicate the location of sections sampled for this study. Boxes indicate the location of figures 1.9-1.12.

Other Triassic localities throughout northeastern B.C. have been studied by Colquhoun (1960, 1962), Muller (1961), Westermann (1962), Pelletier (1960, 1961, 1963, 1964), Pelletier and Stott (1963), Irish (1962, 1970) and Gibson (1969, 1970, 1971, 1972, 1975). The section at South Halfway was first described by Gibson (1971), whilst that at North Tetsa Hill was discovered by Pelletier (1963).

In the subsurface, Triassic rocks were first discerned by Clark (1957) and subsequently named formally by Hunt and Ratcliffe (1959), who utilised the existing Grayling and Toad formation names, as well as proposing the names for the Halfway, Charlie Lake and Baldonnel formations.

McLearn (1921) formally named the first Triassic rocks in B.C., naming the Schooler Creek Formation for rocks found in the Peace River area. Kindle (1946) named the Grayling, Toad and Liard formations for rocks in the Liard River area. Subsequently, McLearn and Kindle (1950) applied the Grayling and Toad formation names to rocks further south in the Peace River area. Above these formations they recognised the "flagstones", the "dark siltstones", the "grey beds" and the "Pardonet beds" (which had previously been named by McLearn, 1940 a); the upper three belonging to the Schooler Creek Formation. In the subsurface, Hunt and Ratcliffe (1959) retained the Toad and Grayling formations, but extended them to a level equivalent to the base of the "grey beds". This name was not retained, however, being broken up into the Halfway, Charlie Lake and Baldonnel formations. In 1960, McLearn raised the "Pardonet beds" to the level of formation. Colquhoun (1962) used these new names for surface outcrop in the Peace River area and introduced the Mount Wright Formation as an equivalent to the "flagstones" and "dark siltstones". In 1962, Armitage defined the Montney and Doig formations in the subsurface

of B.C., considering them together equal to the combined Toad and Grayling formations. Pelletier (1964) chose to restrict the scope of the Liard Formation and correlated it with the Mount Wright Formation, a name which he abandoned. Gibson (1971) removed the Halfway Formation from surface nomenclature and instead extended the Liard Formation up to the base of the Charlie Lake Formation in the Sikanni River-Pine Pass area. He also introduced the Ducette Member as the basal part of the Baldonnel Formation in some areas, the Ludington Formation as a western equivalent to the Charlie Lake Formation and the Bocock Formation as a unit overlying the Pardonet Formation. Zonneveld (2010) maintained this nomenclature but recognised the diachroneity of a number of the boundaries between these formations. He also extended the Ludington Formation to be equivalent in age to the Baldonnel as well as part of the Charlie Lake Formation and considered the Bocock Formation and Ducette Member to be local units.

The current lithostratigraphy used for the Triassic in B.C. is shown in figure 1.4, along with its correlation in the subsurface and with outcrop in Alberta. In Alberta the Triassic rocks are divided into two formations, the Sulphur Mountain Formation and the Whitehorse Formation (Gibson, 1968). The Sulphur Mountain Formation is approximately equal to the Grayling, Toad, Liard and lower part of the Charlie Lake formations in the outcrop of B.C. and to the Montney, Doig, Halfway and lower part of the Charlie Lake formations in the subsurface. The Whitehorse Formation is equivalent to the upper part of the Charlie Lake and Baldonnel formations and the lower part of the Pardonet Formation. The rest of the upper Triassic is missing in Alberta due to erosion beneath a sub-Jurassic unconformity (Gibson, 1971).

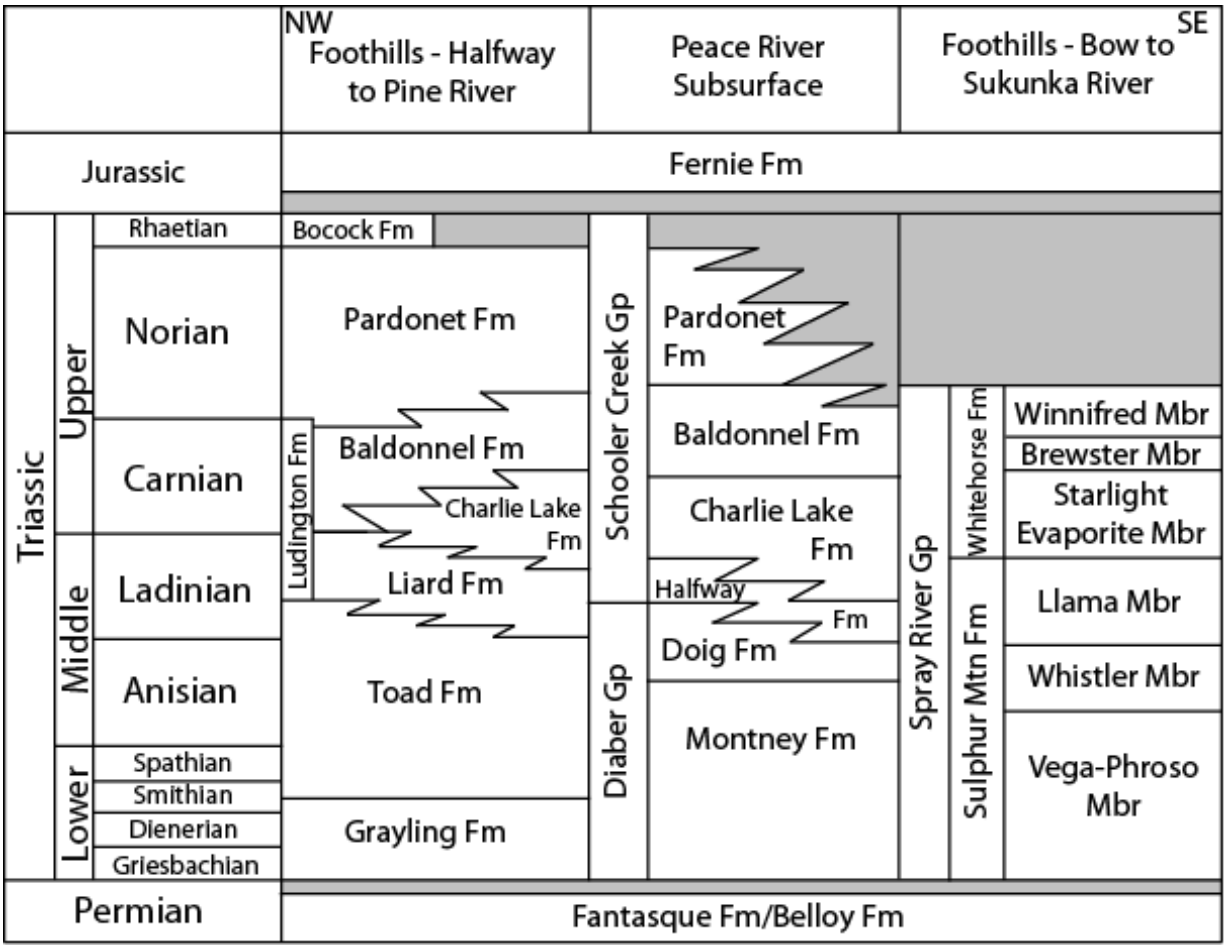



**Figure 1.4.** Correlation chart of Triassic formations in the surface and subsurface of British Columbia and the surface of Alberta. Fm = Formation; Mbr = Member. Stage boundary ages are in Ma, and taken from Ogg (2012).

### *Grayling Formation*

The Grayling Formation unconformably overlies the Permian Fantasque Formation (Gibson, 1971). It consists of a succession of dolomitic siltstone, silty shale and minor amounts of calcareous siltstone, silty limestone, dolomite and fine-grained sandstone that varies in thickness from 35 m at Calnan Creek to 100 m at Clearwater Lake (Gibson, 1975). It is thought to be Griesbachian to Smithian in age (Tozer, 1961).

### *Toad Formation*

The Toad Formation conformably overlies the Grayling Formation. It consists of a thick sequence of argillaceous to calcareous siltstone, silty shale, silty limestone and dolomite, as well as very fine-grained sandstone that varies in thickness from 150 m at Mount Greene to 800 m at South Halfway (Gibson, 1975). It is thought to be Smithian to Ladinian in age (Tozer, 1961; Orchard and Tozer, 1997).

### *Liard Formation*

The Liard Formation overlies and partially interfingers with the Toad Formation. It consists of a sequence of fine to coarse sandstone, calcareous and dolomitic siltstone and sandy to silty dolomite and limestone that varies in thickness from 0 m in the northwest where it is removed by erosion, up to 300 m on the Peace River (Gibson, 1975). It is thought to be Ladinian to lower Carnian in age (Tozer, 1961; Zonneveld, 2010).

### *Charlie Lake Formation*

The Charlie Lake Formation conformably overlies the Liard Formation and the boundary between the two can sometimes be difficult to define (Thompson, 1989). It consists of calcareous and dolomitic siltstone and sandstone, dolostone, limestone and evaporite that varies in thickness from 180 m at Schooler Creek up to 400 m at Mount Withrow (Gibson, 1975). This formation contains few fossils and is thought to be Ladinian to Carnian in age on the basis of stratigraphic position (Zonneveld, 2010).

### *Baldonnel Formation*

The Baldonnel Formation conformably overlies the Charlie Lake Formation and it consists of limestone, dolostone and siltstone that varies in thickness from 80 m on Burnt River to 150 m at Eleven Mile Creek (Gibson, 1975). It is thought to be older in the west, where it is lower to upper Carnian, and younger in the east, where it is upper Carnian to lower Norian in age (Tozer, 1967; Zonneveld and Orchard, 2002).

### *Pardonet Formation*

The Pardonet Formation conformably overlies the Baldonnel Formation and it consists of limestone, dolostone, calcareous silt and shale that varies in thickness from 40 m at Pink Mountain (where it has been eroded) to 130 m at Eleven Mile Creek (Gibson, 1975). It is thought to be Carnian to Rhaetian in age (Tozer, 1967; Orchard, 1991 b; Orchard and Tozer, 1997; Orchard, 2013). It is overlain unconformably by the Jurassic Fernie Formation (Gibson, 1975) or conformably by the Bocock Formation.

### *Ludington Formation*

The Ludington Formation is the western, deep water equivalent of the Liard, Charlie Lake and Baldonnel formations (Gibson, 1993). As such, it is only observed in the most westerly outcrops, where it overlies the Toad Formation. It consists of dolostone, limestone and calcareous siltstone that reaches up to 960 m in thickness at Fiddes Creek (Gibson, 1975; Pelletier, 1964). It is thought to be Ladinian to Carnian in age (Zonneveld, 2010).

### *Bocock Formation*

The Bocock Formation is a local unit that conformably overlies the Pardonet Formation in the foothills region south of Williston Lake. It consists mainly of bioclastic limestone (Zonneveld, 2010) that reaches up to 60 m in thickness at East Carbon Creek (Gibson, 1975). It is thought to be Rhaetian in age (Orchard, 1991 b; Orchard and Tozer, 1997).

### *Montney Formation*

The Montney Formation unconformably overlies the Permian Belloy Formation (Edwards *et al.*, 1994; Henderson *et al.*, 1994). It consists of shale, siltstone and very fine sandstone (Armitage, 1962; Davies *et al.*, 1997). It varies in thickness from 450 m to 0 m at the subcrop edge. It is thought to range from Griesbachian to Anisian in age (Zonneveld, 2010).

### *Doig Formation*

The Doig Formation conformably overlies the Montney Formation and it consists of a basal phosphatic pebble lag, which gives way to shale, siltstone, sandstone and occasional carbonate (Armitage, 1962; Evoy and Moslow, 1995). It varies in thickness from 150 m to 0 m at the subcrop edge. The Montney-Doig boundary is thought to be as old as Smithian in part (Zonneveld, 2010) and estimates for the top of the formation range from Anisian (Qi, 1995) to Ladinian (Hunt and Ratcliffe, 1959).

### *Halfway Formation*

The boundary between the Doig and Halfway formations varies from conformable to abrupt (Zonneveld, 2010). It consists of fine and medium grained sandstone, dolomite and dolomitic

siltstone (Zonneveld, 2010). It is thought to be Ladinian to Carnian in age (Gibson, 1993; Hunt and Ratcliffe, 1959).

### 1.1.6 Triassic Biostratigraphy

Triassic biostratigraphy has primarily centred on the use of ammonoids, both in North America and in Europe. The earliest biostratigraphic timescales constructed for the Triassic were created by Mojsisovics for the Alps (Mojsisovics, 1873, 1879, 1882) and later incorporated data from the Himalayas (Mojsisovics *et al.*, 1895). The Tethyan ammonoid timescale has subsequently been revised by a number of authors, as summarised by Balini *et al.* (2010).

In British Columbia, the first attempts to generate an ammonoid faunal succession for the Triassic were undertaken by McLearn (1941 a, c, 1946 a, b, 1947 a, b, 1953, 1960, 1969). Difficulties in correlation between the ammonoid scales of North America and Tethys eventually led Tozer and Silberling to develop independent timescales based on the ammonoid succession of Arctic Canada (Tozer, 1965), British Columbia (Tozer, 1967) and Nevada (Silberling and Tozer, 1968). Each of these papers included elements of the previous publications, leading to a synthesised ammonoid timescale for the whole of North America.

Further work on the Triassic succession in the western United States has led to the recognition of major differences between the records for Nevada and Canada. Work by Guex *et al.* (2005 a, b) on the Lower Triassic; Silberling and Wallace (1969), Silberling and Nicholls (1982) and Bucher (1988, 1989, 1992 a, b, 1994) on the Middle Triassic; and Balini *et al*. (2007) on the Upper Triassic has led to the addition of a number of new ammonoid zones for the Triassic of Nevada.

In Canada, the ammonoid timescale has been further refined by the work of Tozer (1994) and Bucher (2002); the diagram in figure 1.5 is derived from these works. It shows 38 ammonoid zones for the whole of the Triassic. Correlation between Canada, Nevada and the Tethys is still problematic due to varying completeness of the ammonoid record as demonstrated by Monnet and Bucher (2005, 2007).

Improved correlation between these areas may be achieved utilising conodont biostratigraphy. The conodont timescale has been developed more recently than that of the ammonoids and is still undergoing revision, however, the occurrence of conodont faunas in between ammonoid horizons suggests that a more refined timescale can be developed. If this timescale can in turn be integrated with the ammonoid scale, then it promises to allow much improved correlation between Canada, Nevada and Tethys.

The earliest attempt at creating a conodont timescale for the Triassic was that of Mosher (1968), who recognised a succession of conodont assemblages in both North America and Europe and attempted to correlate the two. This work concentrated mainly on the Middle and Upper Triassic. Sweet (1970) developed the first zonation of the Lower Triassic based on samples from Pakistan. These data sets were integrated by Sweet *et al.* (1971) to create a global stratigraphic scheme for the whole of the Triassic. A number of the zones presented in that paper are still in use. Mosher (1973) studied conodonts collected from the matrix of ammonoid samples used by Tozer (1967) to construct his ammonoid timescale and attempted to tie the two biostratigraphic schemes together for the first time. At approximately the same time, other workers were developing a conodont timescale for the Germanic Muschelkalk (Kozur, 1968) and for the Middle Triassic of Tethys (Budurov and Stefanov, 1972). This work has been updated by Kozur (1989 a, 1999), and

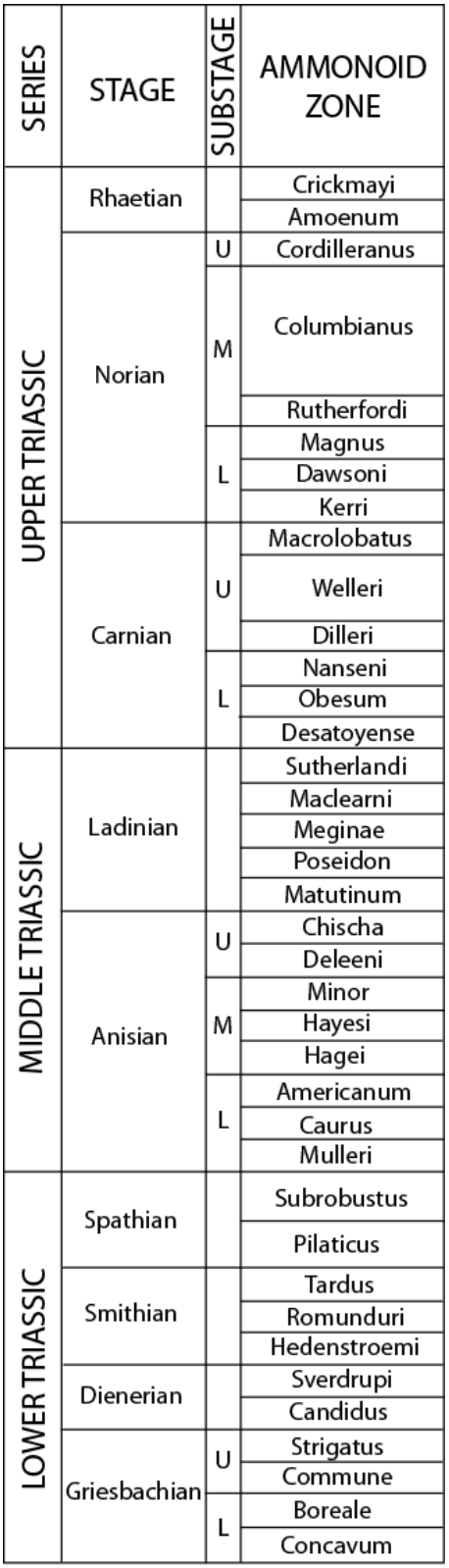



**Figure 1.5.** Ammonoid biostratigraphy for the Triassic of British Columbia. Data from Orchard and Tozer (1997) and Bucher (2002).

integrated conodont and ammonoid scales for Tethys have been presented by Muttoni *et al.* (1998), Krystyn *et al.* (2002) and Kozur (2003).

In North America, the conodont timescale for the Upper Triassic was first revised by Orchard (1983, 1991 a, b). Then, Orchard and Tozer (1997) presented an integrated ammonoid and conodont timescale for the whole of the Triassic of Canada. This introduced a number of new conodont zones based on new species and also pointed out the conodonts that are used for correlation in Tethys but are absent in North America. A number of these North American zones have since been further refined by Orchard and Zonneveld (2009) for the Lower Triassic and by Orchard (2007 a, b, c, 2013) for the Upper Triassic. However, the zones of the Middle Triassic of Canada have not been subjected to such a revision as yet. The current North American conodont timescale is shown in figure 1.6, in comparison with the Tethyan scale.

Other fossil organisms have also been used to generate biostratigraphic schemes for the Triassic. In North America, Carter developed a scheme for the Upper Triassic based on the succession of radiolarian faunas in the Queen Charlotte Islands (Carter *et al.*, 1989; Carter, 1991). This has been intercalibrated with both the ammonoid and conodont schemes of Canada for this time interval (Carter *et al.*, 1989; Carter and Orchard, 2000, 2013). Johns *et al.* (1997) used ichthyoliths to generate a biostratigraphy for the Ladinian to Norian of North America. This was calibrated to both the ammonoid and conodont timescales, but the resolution is very coarse in comparison with these schemes and the use of ichthyoliths as a stratigraphic tool in Triassic has not been widespread. There have also been palynological studies by Jansonius (1962) on the Triassic sediments of subsurface B.C. and Alberta. Utting (1994) developed a palynological zonation for the Sverdrup Basin and there has been some success in recognising these zones in

the Lower Triassic of the subsurface of B.C. and Alberta (Utting *et al.*, 2005). Again, the resolution of the schemes is lower than that of the conodont or ammonoid schemes and they have not been developed for the whole of the Triassic.

Kozur has successfully generated a scheme for the Lower and part of the Middle Triassic in Tethys using conchostracans (*e.g.* Kozur, 1999) and for the Upper Triassic in the Newark Basin in North America (Kozur and Weems, 2007, 2010). Lucas (1998, 1999, 2010) has divided the Triassic into eight faunal assemblages based on terrestrial vertebrates. These schemes allow the division of the terrestrial Triassic but have little bearing on the correlation of the marine rocks; correlation between the marine and terrestrial records is still a work in progress.

The improvement and intercalibration of these multiple biostratigraphic schemes will be important for global correlation. This can only be achieved, however, by a full understanding of the taxonomy of the groups involved.

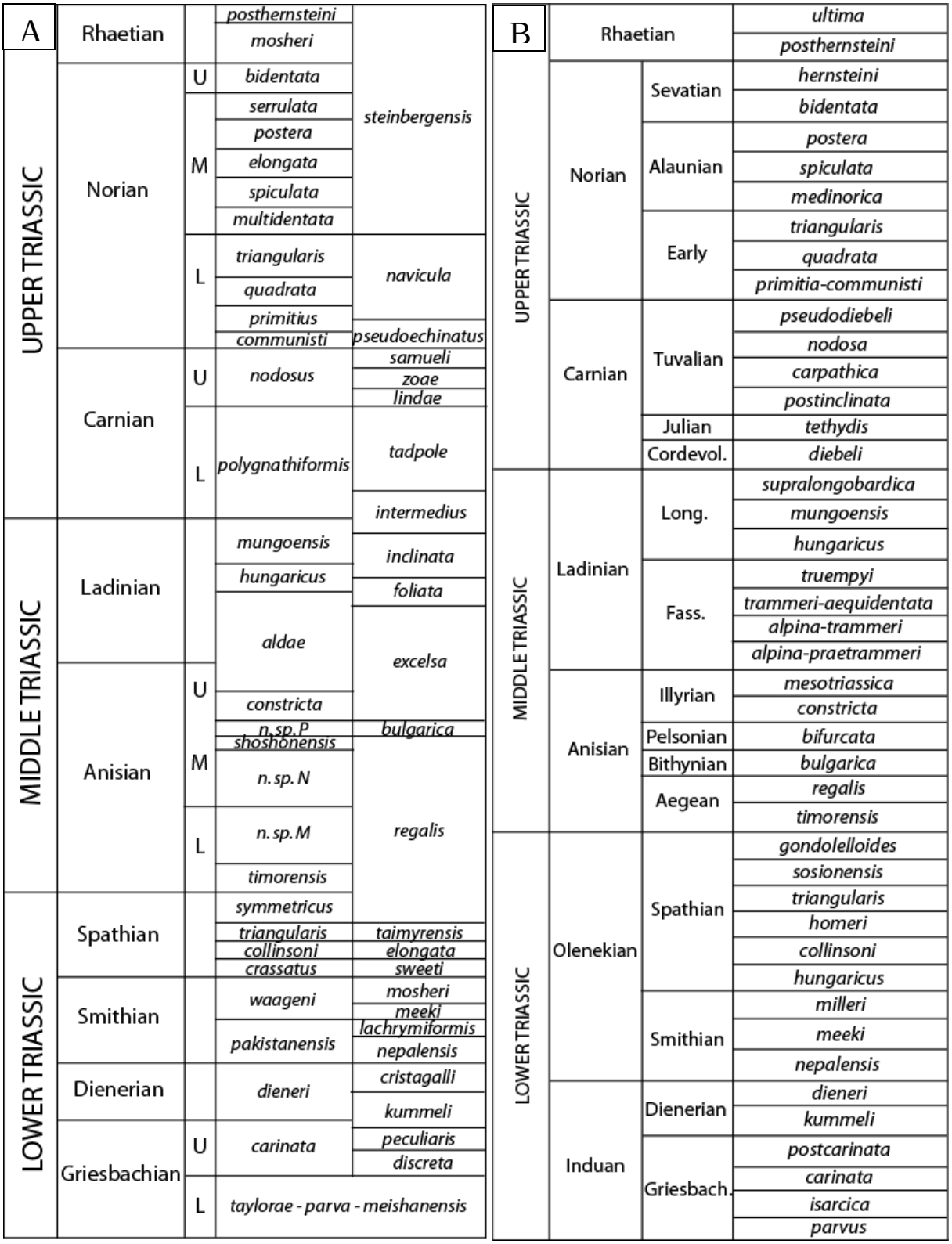



**Figure 1.6.** Conodont biostratigraphy of the Triassic for North America (A) and Tethys (B). Data from Orchard and Tozer (1997) and Kozur (2003).

## 1.2. THE WESTERN CANADA SEDIMENTARY BASIN

The Western Canada Sedimentary Basin is a complex basin that stretches from the Yukon down to the Canada-USA border, beyond which it is thought to be contiguous with other basins in the USA (Ricketts, 1989). It has been subdivided into four sub-basins, recorded by Davies (1997 a) as the Liard Basin, the Peace River Basin, the Continental Margin Basin and the Williston Basin (see fig. 1.7). Each of these has had a slightly different structural history. The Liard Basin formed by transtension, the Peace River Basin formed by a combination of transtension and extension, whilst the Continental Margin Basin is a sag basin (Davies, 1997 a). The oldest rocks found in the basin belong to the Mesoproterozoic Belt-Purcell Supergroup (Ross *et al.*, 1989), which were deposited in an intracratonic basin that formed within the supercontinent Rodinia (Stewart, 1972; Ross and Villeneuve, 2003). This supercontinent rifted apart during the Neoproterozoic, which was recorded by deposition of the Windermere Supergroup (Ross *et al.*, 1989; Colpron *et al.*, 2002). During the Palaeozoic, the basin underwent a period of relative quiescence, as sediment accumulated on the continental margin, before orogenesis in the Mesozoic led to the formation of a foreland baisn (Cant, 1989). The youngest sediments found in the basin are from the Miocene (Leckie, 1989).

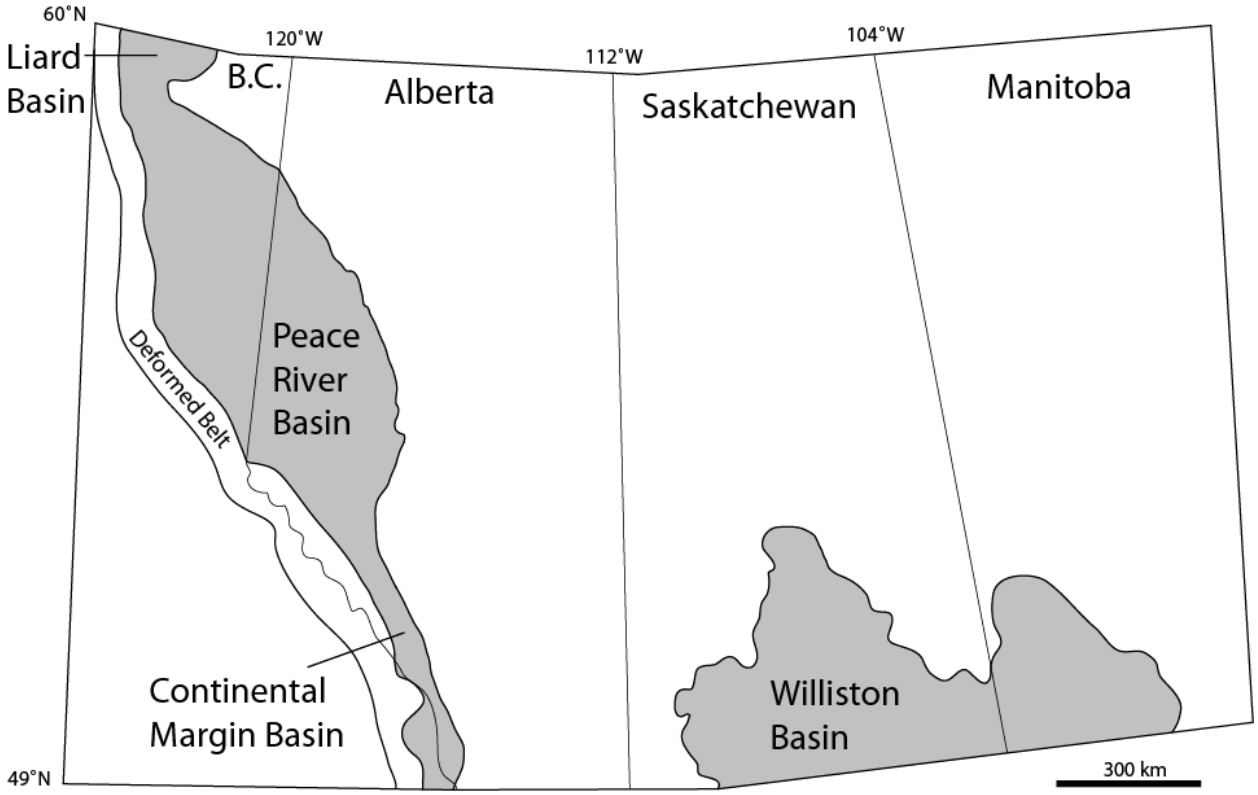



**Figure 1.7.** Map showing the location of the Western Canada Sedimentary Basin in western Canada and the distribution of its sub-basins.

The majority of Triassic sediment was deposited in the Peace River Basin (Gibson and Barclay, 1989) and the present study is focussed on this area. Therefore, the remainder of this section will be dedicated to the Peace River Basin.

The Peace River Basin became a distinct entity during the Mississippian (Richards, 1989; Davies, 1997 a), developing an east-west orientation in response to extension related to the collapse of the Peace River Arch (see below). The basement of the basin consists of Proterozoic to Devonian sedimentary rocks. Faults that formed in the basement during extension continued to exert a strong control on sedimentation throughout the basin's history and were re-activated in some of the younger grabens (Berger *et al.*, 2008). The basin persisted until the Jurassic, at

which time sedimentation was terminated by the Columbian Orogeny (Poulton, 1989). The sediments of the Peace River Basin are now part of the Rocky Mountain Fold and Thrust belt (McMechan and Thompson, 1989; Thompson, 1989) and were affected by the Laramide Orogeny (Poulton, 1989). They underwent further compressional deformation during the Eocene, as well as extensional deformation in the Oligocene (McMechan and Thompson, 1989).

During the Triassic, the Peace River Basin is thought to have been approximately 900 km long and 350 km wide (Davies, 1997 a); the western margin of the basin has typically been considered to have been passive, facing the Panthalassa Ocean (Gibson and Barclay, 1989; Tozer, 1982; Monger, 1989). Triassic sediments within the basin typically thicken from east to west (Gordey, 1991), although there are local, anomalous trends. The Dawson Creek Graben Complex, which includes the Fort St. John Graben and the Hines Creek Graben, exercised a strong control on the distribution of sediment within this basin (Barclay *et al.*, 1990). The graben complex initiated in the Carboniferous in response to extension, which also led to the collapse of the pre-existing Peace River Arch (O'Connell *et al.*, 1990; Barclay *et al.*, 1990). This positive feature had itself exerted a strong influence on the distribution of sediment until the Late Devonian (O'Connell *et al.*, 1990). Its subsequent inversion led to the creation of a local depocentre referred to as the Peace River Embayment (Barclay *et al.*, 1990). The faults of the graben complex continued to be active throughout the Triassic, and thus had significant control on the distribution of Triassic sediment (Berger *et al.*, 2008). The Beatton High was a positive feature during the Permian (Henderson *et al.*, 1994), situated just north of the Fort St. John Graben, whilst the neighbouring Grassy High (Davies and Majid, 1993) became uplifted during the Triassic. Both of these features led to the thinning or erosion of Triassic sediments in their vicinity (Davies, 1997 a). Similarly, the Devonian Leduc Reef trend encircled much of the edge of the Peace River Basin,

leading to thinning of Triassic sediments over the top of these features (Davies, 1997 a). Furthermore, it has been postulated recently that another high area was present to the west of the basin during the Triassic, because of the thinning of sediments near to Williston Lake (Ferri and Zonneveld, 2008). This feature would occupy a similar position to that of the Sukunka Uplift during the Carboniferous and Permian (Richards, 1989). The presence of such a high may be explained by the accretion of the Yukon-Tanana terrane near the end of the Permian (Beranek and Mortensen, 2011). During the Middle Triassic, there is evidence that the salt deposits within the Charlie Lake Formation dissolved, leading to salt collapse and the creation of localised depressions in the basin (Davies, 1997 a).

### 1.2.1 Economic Potential of the Triassic in B.C.

The Triassic rocks of subsurface B.C. and Alberta have been a target for hydrocarbon exploration for a number of years. Exploration targets were initially thick sandstone bodies such as those found in the Doig Formation (Evoy, 1997) and the Halfway Formation (Caplan and Moslow, 1997), and turbidite facies in the Montney Formation (Moslow and Davies, 1997). These were exploited as conventional reservoirs, producing both oil and natural gas.

In recent years, activity has started to focus on unconventional resource plays. This has led to the recognition of large hydrocarbon resources within the Montney and Doig formations. It is estimated that the Montney Formation contains up to 700 trillion cubic feet (Tcf) of natural gas-in-place and the Doig Formation up to 200 Tcf (Walsh *et al.*, 2006). The Montney Formation as a whole is expected to contain 449 Tcf of marketable gas (NEB Report, 2013). This makes these formations two of the most significant natural gas reservoirs in British Columbia, representing around 22% of the natural gas reserves of B.C. (OGC Report, 2013). Production from these

formations reached 1.6 billion cubic feet (Bcf) per day in 2012, with a cumulative total of approximately 1.5 Tcf produced to that point (Adams, 2013).

## 1.3. CORDILLERAN TECTONICS

The Canadian Cordillera comprises a number of terranes that are interpreted to represent the remains of volcanic arcs and the intervening oceanic crust that have been accreted onto the North American continent (fig. 1.8). The term "terrane" is used here to indicate fault bounded blocks that contain assemblages of rocks with a similar geological history (Coney *et al.*, 1980). A large number of terranes have been identified within the Cordillera (Wheeler *et al.*, 1991; Colpron *et al.*, 2006) and these can be grouped into three different "tectonic entities" (Nelson and Colpron, 2007): the North American continent and its parautochthonous terranes (Cassiar and Kootenay terranes); the pericratonic terranes (Slide Mountain, Yukon-Tanana, Quesnellia, and Stikinia terranes); and the exotic terranes (Cache Creek, Wrangellia and Alexander terranes).

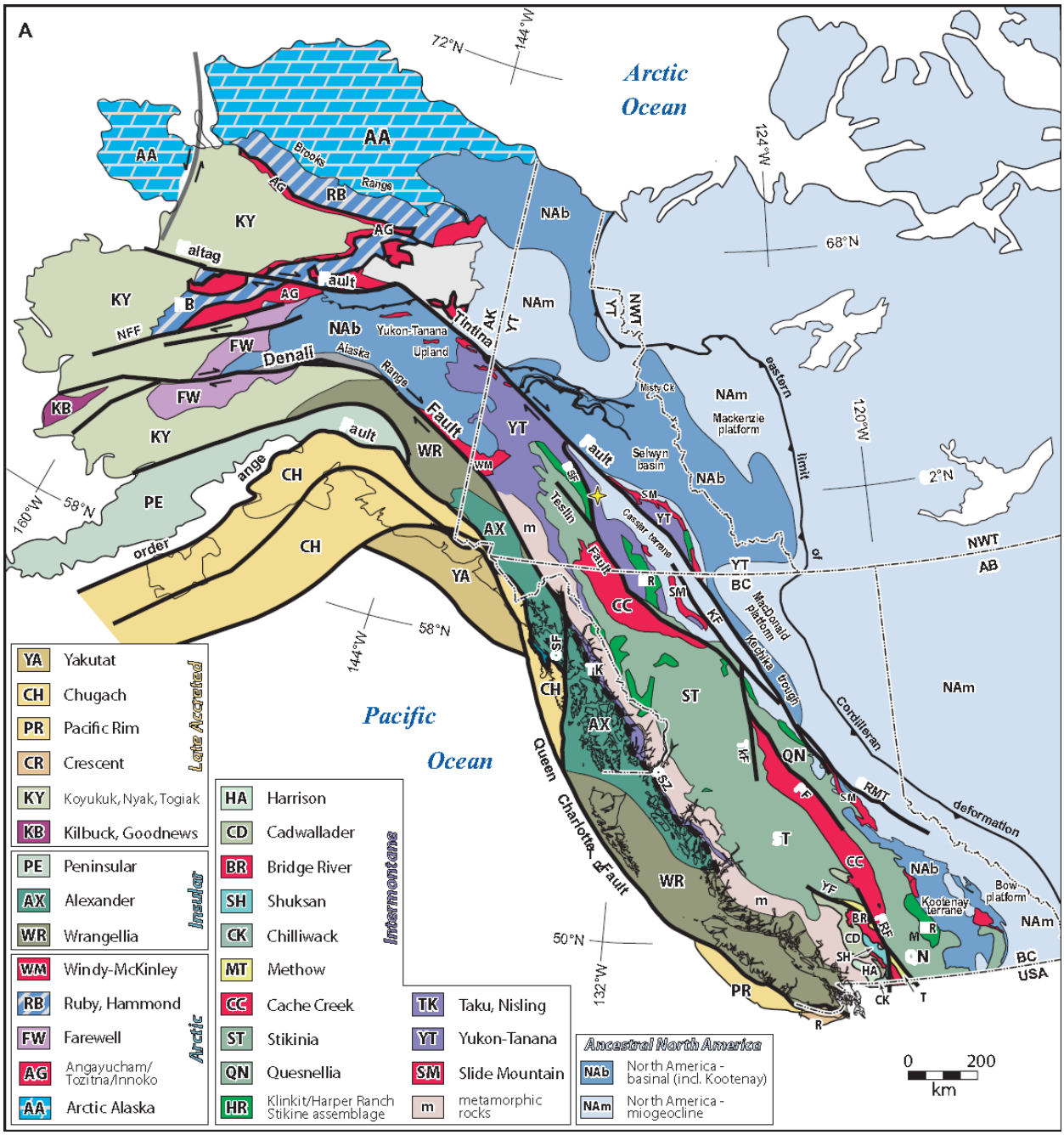



**Figure 1.8.** Terrane map of the Canadian Cordillera. NA = North America (including Cassiar and Kootenay Terranes), YT = Yukon-Tanana, QN = Quesnellia, ST = Stikinia, CC = Cache Creek, SM = Slide Mountain, AX = Alexander, WR = Wrangellia. From Nelson and Colpron (2007).

The western margin of North America initally formed due to rifting during the break-up of the supercontinent Rodinia during the Late Proterozoic and Early Palaeozoic (Colpron *et al.*, 2002). The rocks of the Cassiar and Kootenay terranes began to be deposited during the Cambrian, and are thought to have been formed on the North American continent (Ferri and Melville, 1994; Logan and Colpron, 2006). These terranes have subsequently been displaced laterally along the margin of North America, but they do not appear to have been separated from the continent by oceanic crust at any point. Continued rifting during the Devonian led to the separation of continental crust that would become the basement of the Yukon-Tanana, Quesnellia and Stikinia terranes. The Slide Mountain terrane is thought to represent the remains of oceanic crust formed between the parautochthonous terranes and the pericratonic terranes; the Slide Mountain Ocean is thought to have opened during the Mississippian (Ferri, 1997). Volcanic arcs were built on all three of the pericratonic terranes from the Devonian until the Permian due to west-facing subduction (Ferri, 1997; Logan, 2004; Nelson *et al*., 2006). The Slide Mountain Ocean began to close in the Permian (Ferri, 1997) and the Yukon-Tanana terrane became the first of the pericratonic terranes to collide with and overthrust the North American margin and the Cassiar terrane in the Late Permian (Beranek and Mortensen, 2011). Slivers of the Slide Mountain terrane were also thrust onto the margin, forming isolated bands including the Sylvester allochthon (Nelson, 1993). Following the accretion of Quesnellia in the Permo-Triassic (Klepacki, 1985; Schiarizza, 1989), subduction continued to the east under North America and to the west under Stikinia; at this time Stikinia appears to have been rotating above the subduction zone, enclosing the Cache Creek terrane between it and Quesnellia (Nelson and Mihalynuk, 1993; Mihalynuk *et al.*, 1994; Nokleberg *et al.*, 2000). Stikinia collided with Quesnellia in the Middle Jurassic and arc volcanism ceased in these terranes. The exotic Alexander and

Wrangellia terranes formed as oceanic arcs during the Precambrian and Devonian, repectively (Juras, 1987; Gehrels *et al.,* 1996). These two terranes were amalgamated by the Pennsylvanian (Gardner *et al.,* 1988) and were accreted to North America by the end of the Middle Jurassic (Gehrels, 2001). Successive continental volcanic arcs were built on the new margin of North America during the Jurassic, Cretaceous (including the formation of the Coast Plutonic Complex) and from the Palaeocene until recent times (Nelson and Colpron, 2007, and references therein). This volcanic and intrusive activity has been accompanied by strike-slip faulting that has shuffled the constituents of the Canadian Cordillera, most notably along the Tintina, Fraser, Yalakom and Denali faults during the Eocene (Umhoeffer and Schiarizza, 1996; Lowey, 1998; Gabrielse *et al.*, 2006).

This thesis focuses on the tectonic situation at the North American margin during the Triassic; therefore, it is concerned primarily with the interactions between the North American continent and the Yukon-Tanana and Quesnellia terranes. Permian-Triassic accretion of the Quesnellia Terrane has been suggested (Nelson and Colpron, 2007). The evidence for accretion of the Yukon-Tanana terrane during the Permian comes from observations in the Yukon (Beranek and Mortensen, 2011). Nelson *et al.* (2006) advocated for Permian accretion on the basis of the age of eclogite formation, the age of synorogenic conglomerate deposition and the timing of thrust faulting in the terrane. Detrital zircon provenance studies by Beranek *et al.* (2010 a) and Beranek and Mortensen (2011) found evidence that Early Triassic sediment in the Selwyn Basin was partly derived from the Yukon-Tanana terrane. By dating a pluton that cut across the accretionary boundary as Late Permian, Beranek and Mortensen (2011) found further support for the Late Permian accretion model. They named this accretionary event the Klondike Orogeny.

Late Permian orogenesis also implies the formation of a foreland basin into which the Triassic sediments were shed. This basin would be expected to be continuous along much of the North American margin in northwestern Canada, and therefore detrital zircon provenance studies of the Triassic rocks of British Columbia should find a similar pattern to that uncovered in the Yukon. Previous studies of this type have failed to record this signal. Ross *et al.* (1997) carried out the first detrital zircon study of Triassic sedimentary rocks in the WCSB and determined that all of the sediment was derived either from the North American craton or from the Innuitian orogenic wedge in the Arctic. Boghossian *et al*. (1996) used neodymium isotopes to determine whether the sediments of the WCSB had been derived from a juvenile or evolved crustal source and found that significant juvenile sediment was deposited, with signatures later attributed to derivation from the Arctic (Garzione *et al.*, 1997). Palaeocurrent indicators from the Triassic rocks of B.C. were reported by Pelletier (1965) and Arnold (1994), all of which suggested transport from the east or northeast to the west. The overall thickening of Triassic sediments to the west (Gordey *et al.*, 1991) also suggests derivation of the sediment from the east.

## 1.4 THIS STUDY

As discussed in the previous sections, the Triassic Period was an important time in terms of North American tectonics and the formation of economically important hydrocarbon bearing rocks. This study was conceptualized to help to address questions regarding the timing of terrane accretion in the Canadian Cordillera and also the timing and mechanism of formation of the hydrocarbon-bearing rocks.

The first step in understanding timing and rates of geological processes is the establishment of a robust, accurate and precise chronological scale. In the absence of radiometric dates from time-

equivalent units such as ash beds or lava flows, biostratigraphy is a major tool in the development of such a scheme. The previous sections have discussed the evolution of ammonoid and conodont biostratigraphic scales for the Triassic. Ammonoids are a limited tool when considering correlation between surface outcrop and the subsurface, due to their almost complete absence in subsurface core. Questions about the timing of development of units in the subsurface cannot be answered using ammonoids. The conodont scale, however, is not as well developed as that of the ammonoids, and the first goal of this study is to try to create a more precise conodont timescale. This has been approached by examining new conodont collections from both surface and subsurface sections, as well as existing conodont collections held by the Geological Survey of Canada. The collections from the surface sections can be related to ammonoid collections in the same sections, allowing the calibration of the two schemes. The conodont faunal assemblages recognised in this study occur in both the surface and the subsurface, allowing correlation between the two.

As discussed previously, a signifcant portion of British Columbia's natural gas reserves are produced in the Doig Phosphate Zone. The formation of this unit in unclear, although it has been related to a period of transgression. The age of the Montney-Doig boundary is poorly constrained. If the Doig Phosphate Zone was formed during transgression, a simple test would be that the Montney-Doig boundary should be diachronous in the direction of the transgression, which in this instance would have been west to east. The new conodont collections from the subsurface are concentrated around the Montney-Doig boundary and allow its age to be determined across a wide geographic area.

The third goal of this study is to test the hypothesis that terrane accretion in the Canadian Cordillera began prior to the Triassic. As mentioned previously, detrital zircon studies of Triassic sedimentary rocks in the Yukon identified zircon populations that could only have been derived from the Yukon-Tanana terrane. It has therefore been suggested that this terrane collided with the North American margin prior to the Triassic (Beranek and Mortensen, 2011). If this is the case, then similar detrital zircon signatures should be present in the Triassic rocks of British Columbia. Detrital zircon studies lead to the reconstruction of sedimentary transport pathways. Changes in the detrital zircon population with time allow the recognition of changes in source area and hence in depositional systems. Collecting detrital zircon samples together with conodont samples enables these changes to be placed in a relative timescale. Detrital zircon samples have been collected from both the surface and the subsurface to determine changes in sedimentary patterns over a wide geographical area.

Fieldwork was carried out across three field seasons. In 2009, the South Halfway section was studied, in 2010 sections on Williston Lake were visited and in 2011 fieldwork was carried out on the Alaska Highway. In addition, in 2010 cores from oil wells from throughout the study area were examined and sampled at the Charlie Lake Core Facility. Additional samples for detrital zircon analysis were collected from Williston Lake by J.-P. Zonneveld in 2012. Existing conodont collections of M.J. Orchard were examined at the Geological Survey of Canada in Vancouver and are incorporated into this study.

In total, 122 new conodont samples and 88 new detrital zircon samples were collected from 17 outcrop sections and 7 subsurface wells. A total of 31 of the detrital zircon samples were productive, as were 67 of the conodont samples. In addition, 46 existing samples from 4

subsurface wells were examined, and 30 of them contained conodonts. An additional 19 existing conodont samples from 9 surface sections in northeastern B.C. were also examined. Therefore, a total of 116 conodont samples and 31 detrital zircon samples were utilised for this study. All of the samples are listed in Appendix 1.

The samples range in depositional age from Griesbachian to Rhaetian; however, no samples were collected from rocks of Norian age. The distribution of these samples can be broken up into five geographic areas: Williston Lake and surrounding area; Alaska Highway and surrounding area; Toad River; Liard River and Subsurface B.C. The geology of the sections in each of these areas is summarised below.

### 1.4.1 Localities

***Williston Lake Area (fig. 1.9)***

Ursula Creek – Shale, sandstone and carbonate belonging to the Grayling, Toad and Ludington formations and ranging in age from Griesbachian to Carnian.

Ne-Parle-Pas Point – Siltstone, bioclastic siltstone, carbonate, shale and gravel lag beds belonging to the Pardonet Formation and ranging in age from Norian to Hettangian.

Pardonet Creek – Siltstone, bioclastic siltstone, shale and gravel beds belonging to the Pardonet and Fernie formation and ranging in age from Norian to Hettangian.

Black Bear Ridge – Siltsone, carbonate and gravel beds belonging to the Ludington and Pardonet formations and ranging in age from Carnian to Hettangian.

Brown Hill – Shale, siltstone, carbonate and breccia belonging to the Toad, Liard, Charlie Lake, Baldonnel and Pardonet formations and ranging in age from Anisian to Norian.

Glacier Spur – Shale, siltstone, sandstone and carbonate belonging to the Toad, Liard and Charlie Lake formations and ranging in age from Ladinian to Carnian.

.

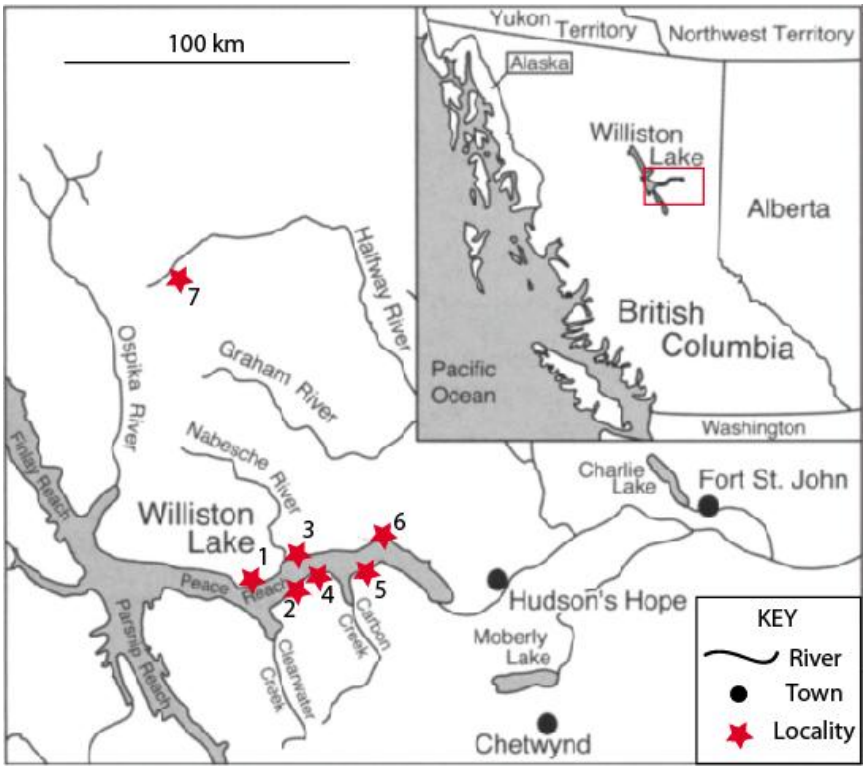



**Figure 1.9.** Map of Williston Lake, showing the location of sections sampled for this study. 1) Pardonet Creek; 2) Ne-Parle-Pas Point; 3) Black Bear Ridge; 4) Glacier Spur; 5) Brown Hill; 6) East Carbon Creek; 7) South Halfway. Modified from Zonneveld *et al.* (2001).

Folded Hill – Shale, fine to medium grained sandstone and carbonate belonging to the Toad, Liard and Charlie Lake formations and ranging in age from Ladinian to Carnian.

East Carbon Creek – Siltstone, sandstone and carbonate belonging to the Charlie Lake and Baldonnel formations and ranging in age from Carnian to Norian.

Beattie Ledge – Shale, siltstone, sandstone, carbonate and breccia belonging to the Toad, Liard and Charlie Lake formations and ranging in age from Ladinian to Carnian.

South Halfway – Siltstone, fine sandstone and carbonate belonging to the Toad and Liard formations and ranging in age from Ladinian to Carnian.

***Alaska Highway Area (fig. 1.10)***

Mile Post 386 – Siltstone with nodular carbonate beds that belong to the Toad Formation and are Ladinian in age.

Sanitary Landfill – Siltstone belonging to the Toad Formation that is Middle Triassic in age.

North Tetsa Phosphate West – Siltstone belonging to the Toad Formation that is Middle Triassic in age.

North Tetsa Phosphate – Siltstone and carbonate belonging to the Toad Formation that is Anisian in age.

Yellow Bluffs – Siltstone and carbonate that belongs to the Toad Formation and is Anisian in age.

Mile Post 375 West – Siltstone and carbonate belonging to the Toad Formation that is Anisian in age.

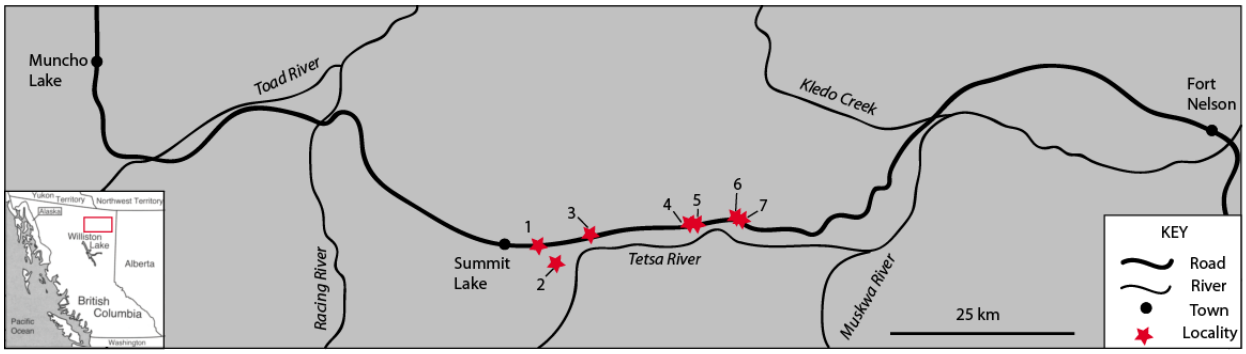



**Figure 1.10.** Map of the Alaska Highway, showing the location of sections sampled for this study. 1) Mile Post 386; 2) North Tetsa Hill; 3) North Tetsa Phosphate; 4) Oyster Springs; 5) Yellow Bluffs; 6) Mile Post 375 West; 7) Mile Post 375 East.

Oyster Springs – Siltstone and carbonate belonging to the Toad Formation that is Anisian in age.

Mile Post 375 East – Siltstone with carbonate nodules that belongs to the Toad Formation and is Anisian in age.

North Tetsa Hill – Siltstone of the Toad Formation that is Anisian in age.

***Liard River Area (fig. 1.11)***

North Liard – Siltstone of the Toad Formation that is Anisian in age.

Liard-Crusty – Siltstone of the Toad Formation that is Anisian in age.

Liard-Brimstone – Siltstone of the Toad Formation that is Anisian in age.

***Toad River Area (fig. 1.11)***

East Toad River I – Siltstone of the Toad Formation that is Anisian in age.

East Toad River II – Siltstone of the Toad Formation that is Anisian in age.

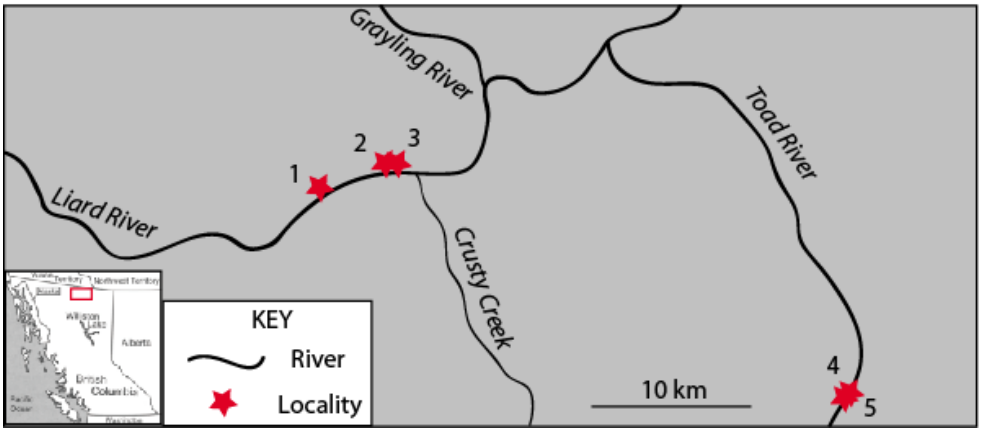



**Figure 1.11.** Map showing the location of sections on the Liard and Toad Rivers in northeastern B.C. 1) Liard-Brimstone; 2) Liard-Crusty; 3) North Liard; 4) East Toad River I; 5) East Toad River II.

***Subsurface B.C. (fig. 1.12)***

Petro-Canada Kobes c-074-G/094-B-9 – Siltstone belonging to the Montney and Doig formations, ranging from Smithian to Anisian in age.

Petro-Canada Kobes d-048-A/094-B-09 – Siltstone belonging to the Montney and Doig formations, ranging from Spathian to Anisian in age.

Talisman Altares c-085-I/094-B-01 – Siltstone belonging to the Doig Formation that is Anisian in age.

Talisman Altares 16-17-083-25W6 – Siltstone belonging to the Montney and Doig formations, ranging from Greisbachian to Anisian in age.

Arc Dawson 07-13-79-15W6 – Siltstone belonging to the Montney and Doig formations, that is Anisian in age.

Rocor Monias 08-22-82-20W6 – Siltstone belonging to the Montney and Doig formations, that is Middle Triassic in age.

Murphy Swan d-054-B/093-P9 – Siltstone belonging to the Doig Formation that is Anisian in age.

Talisman Groundbirch 03-06-078-22W6 – Siltstone belonging to the Montney and Doig formations, ranging from Spathian to Anisian in age.

Shell Groundbirch 16-02-078-22W6 – Siltstone belonging to the Montney and Doig formations, ranging from Anisian to Ladinian in age.

Shell Groundbirch 16-35-078-21W6 – Siltstone belonging to the Montney and Doig formations, ranging from Smithian to Anisian in age.

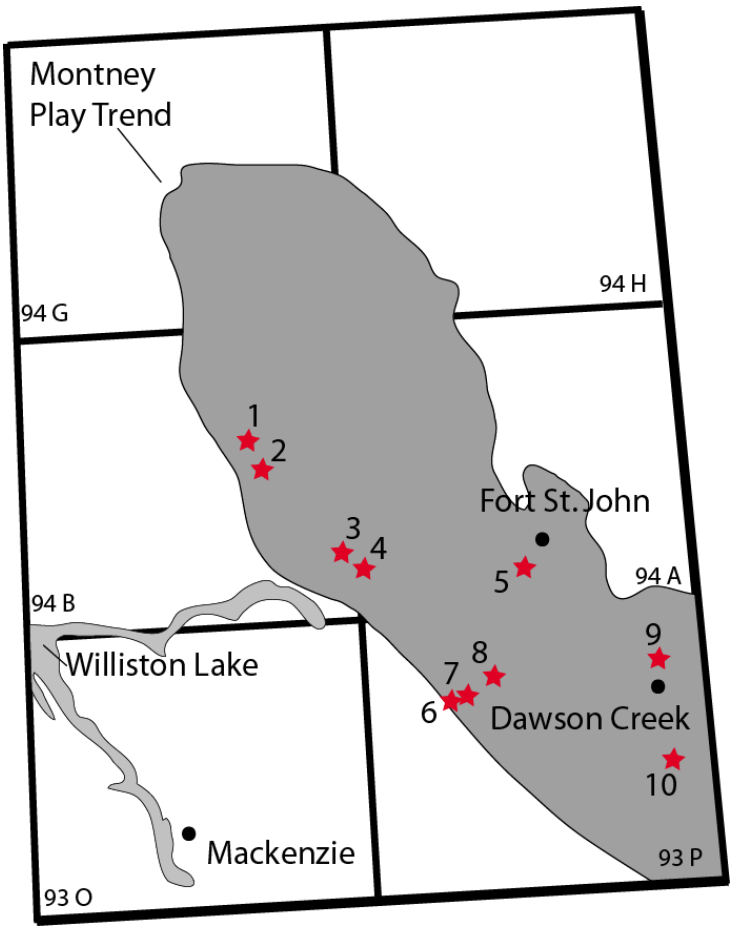



**Figure 1.12.** Map showing location of the sampled wells in British Columbia and their relationship to the Montney Play Trend. 1) Petro-Canada Kobes c-074-G/094-B-9; 2) Petro-Canada Kobes d-048-A/094-B-09; 3) Talisman Altares c-085-I/094-B-01; 4) Talisman Altares 16-17-083-25W6; 5) Rocor Monias 08-22-82-20W6; 6) Talisman Groundbirch 03-06-078-22W6; 7) Shell Groundbirch 16-02-078-22W6; 8) Shell Groundbirch 16-35-078-21W6; 9) Arc Dawson 07-13-79-15W6; 10) Murphy Swan d-054-B/093-P9. Montney Play Trend after Hayes (2012).

### 1.4.2 Methods

The conodont samples were processed at the University of British Columbia and at the Geological Survey of Canada in Vancouver, British Columbia. Samples were approximately 2 kg in weight. They were crushed, weighed and dissolved in buffered 10% dilute acetic acid, for a period of 10 – 14 days. The samples were then sieved to retain the 850 μm – 90 μm fraction.

This was then rinsed, dried and put through sodium polytungstate with a specific gravity of 2.85. The heavy fraction was retained and conodonts were picked under a light microscope. Images of all the conodonts were obtained using the SEM facility at the Geological Survey of Canada in Vancouver. Existing conodont collections were viewed at the Geological Survey of Canada in Vancouver and at the University of Calgary, and had been processed in a similar fashion to the new collections.

The detrital zircon samples were processed at the Pacific Centre for Isotopic and Geochemical Research at the University of British Columbia. Samples were approximately 2 kg in weight. They were cleaned, crushed, ground, passed over a Wilfley table, dry sieved and put through methylene iodide. The heavy fraction was picked in ethanol under a light microscope. Representative zircon populations were selected for analysis and set in epoxy resin. These were analyzed using the Thermo Finnegan Element2 Laser Ablation Inductively-Coupled-Plasma Mass Spectrometer at the Pacific Centre for Isotopic and Geochemical Reseach at the University of British Columbia, using methods as described in Beranek and Mortensen (2011).

## 1.5 STRUCTURE OF THIS THESIS

This thesis is presented as a series of four papers, representing different aspects of work on the biostratigraphy and sedimentology of the Triassic of northeastern British Columbia. The first paper deals with taxonomic revision of the Middle Triassic conodont faunas of British Columbia and the introduction of a new biostratigraphic scheme for this time period based upon the successive appearance of conodont faunal assemblages. It is possible to correlate these new assemblages with the existing ammonoid zonation. The next paper deals with using the revised condont faunas to determine the age of Montney-Doig boundary in the subsurface, with

implications for the formation of the Doig Phosphate Zone. The next paper continues the focus on the subsurface, using conodont collections to develop a biostratigraphy integrated with sequence stratigraphy for the entire Montney Formation as preserved in the Talisman Altares 16-17-83-25W6 well. The fourth paper moves on to using the ammonoid and conodont biostratigraphy to constrain the stratigraphic position of detrital zircon samples, which are used to determine the provenance of the Triassic sediments. This in turn has implications for the tectonic evolution of western North America during this time.

# CHAPTER 2

## Taxonomic Revision of Anisian Gondolellidae from Northeastern British Columbia and their Importance for Biostratigraphic Correlation

## 2.1 INTRODUCTION

The ammonoid fossil record for the Anisian of British Columbia (B.C.) is well established, and allows the recognition of eight ammonoid zones and two subzones (Tozer, 1994; Bucher, 2002). In comparison, the conodont biostratigraphic record is less well resolved, in part because of problems with taxonomy. Improving the resolution of the conodont biozonation scheme and its calibration with the ammonoid scheme is essential for correlation where ammonoid faunas are absent, particularly in the subsurface. Improved correlation will in turn allow greater precision in the timing of events that were occurring in North America during the Anisian. This was a time of significant tectonic activity on the western margin of North America, with collision between the continent and pericratonic terranes beginning in the latest Permian (Beranek and Mortensen, 2011). Also at this time, important hydrocarbon bearing rocks were forming in British Columbia. The occurrence of such events can only be understood with the help of a refined and widely applicable biochronological scale. Biostratigraphy therefore has importance for both the tectonics and the economics of B.C.

The first step towards achieving such a scale is a revision of the major conodont groups found in B.C. during the Anisian. Previously, very few different conodont species have been identified from the Anisian of North America, with most specimens being assigned to broadly defined concepts of *Neogondolella mombergensis* (Tatge), *N. regalis* Mosher, *N. constricta* (Mosher and Clark), *N. shoshonensis* Nicora and *Paragondolella excelsa* Mosher. New species were identified by Orchard and Tozer (1997) but these have yet to be described, which limits their usefulness in correlation. The recognition of so few species obscures variability within the major groups and so prevents the creation of a refined biostratigraphic scheme.

In order to facilitate the revision of the major conodont groups, new collections were made from Anisian outcrops on the Alaska Highway, as well as from cores taken from hydrocarbon wells drilled in the subsurface of B.C. In addition, existing samples were reviewed at the Geological Survey of Canada. The Survey has made abundant collections of Anisian conodonts from northeastern B.C. over the years, but little has so far been published on the faunas recovered. Samples come from localities on the Alaska Highway, Liard River and Toad River; some of these localities are designated as the type sections for the North American ammonoid zones of the Anisian. This study includes a large number of samples collected from numerous localities across northeastern B.C., and is also the first study to incorporate subsurface data from B.C. in the formation of a conodont biostratigraphic scheme.

A number of new morphotypes belonging to *N.* ex gr. *regalis, N.* ex gr. *constricta, N.* ex gr. *shoshonensis, P.* ex gr. *excelsa* have been identified, as well as a number of new species that cannot be placed within the revised diagnoses for these groups. Some of these conodont species and morphotypes are able to be linked to the ammonoid scale, and allow a number of new, informal faunal assemblages to be identified that help to improve local biostratigraphic correlation. Some of the new species can be recognised in Nevada as well. The record of the Anisian in Nevada is even more complete than that of B.C. and recognition of zones that allow correlation between these two areas will allow the development of a conodont biostratigraphic scheme for the whole of western North America. Furthermore, some of the species identified in the course of this revision can be identified in Tethys, such as *N. bifurcata* (Budurov and Stefanov). These species allow sections in B.C. to be correlated globally, although their stratigraphic range is quite large. This means that the global correlation within the Anisian is not

as precise at the moment as the local and regional correlation facilitated by the new species and morphotypes.

## 2.2 GEOLOGICAL SETTING

The Anisian rocks of surface B.C. belong to the Toad Formation. This formation was defined originally on the Toad River by Kindle (1944) and consists primarily of siltstone, shale, fine grained sandstone and carbonate (Zonneveld, 2010). It formed in deep water and shows evidence for deposition from turbidity currents (Ferri *et al.*, 2010). The Toad Formation is not recognised in the subsurface, where Anisian rocks belong to the upper part of the Montney Formation and the lower part of the Doig Formation, which are lateral equivalents of the Toad Formation. Both subsurface formations were defined by Armitage (1962) at the Texaco NFA Buick Creek No. 7 6-26-87-21W6 well in B.C. The Montney Formation consists of shale, siltstone and very fine sandstone (Zonneveld, 2010). The top of the formation is marked by an emergent surface, bioturbated by the *Glossifungites* ichnogenus. The base of the Doig Formation is a condensed section formed during transgression over this surface. The condensed section is rich in phosphate and is termed the Doig Phosphate Zone (Edwards *et al.*, 1994). Equivalent phosphate-rich horizons can be recognised in the Toad Formation in surface outcrop. Above this zone, the Doig Formation is primarily siltstone and sandstone. The Montney and Doig formations represent deposition in a wide range of environments, from offshore turbidites (*e.g.* Moslow, 2000) to the shoreface (*e.g.* Evoy and Moslow, 1995).

All of the Anisian rocks of B.C. were deposited on the margin of the Ancestral North American continent. They were formed in the Peace River sub-basin of the Western Canada Sedimentary Basin (WCSB). The Peace River Basin is a transpressional basin that stretches from the B.C.-

Yukon border down into the United States (Davies, 1997 a). The basin was initiated during the Mississippian and deposition continued until the Jurassic (Gibson and Barclay, 1989; Poulton, 1989). During the Triassic, rock units currently present in northeastern B.C. were situated at mid-latitude north of the equator and the climate was arid. A significant amount of sediment deposited in the basin is thought to have been windblown (Davies, 1997 a) and palaeocurrent indicators suggest that the bulk of the sediment was derived from the continent (Pelletier, 1965; Arnold, 1994). However, anomalous thinning of Triassic sediments to the west in outcrop led Ferri and Zonneveld (2008) to suggest the presence of a palaeo-high to the west of the WCSB during the Triassic. This is supported by detrital zircon work (Beranek *et al.*, 2010 a; Beranek and Mortensen, 2011; see chapter 5) that confirms earlier hypotheses about collision of Yukon-Tanana terrane and the North American margin during the Permian (Nelson *et al.*, 2006; Beranek and Mortensen, 2011).

In North America, the Anisian is divided into the Lower, Middle and Upper Anisian sub-stages, whilst in the Tethys region the Anisian is divided into the Aegean, Bithynian, Pelsonian and Illyrian sub-stages (figs. 2.1-2.3). Tozer recognised seven ammonoid zones in the Anisian of B.C. (Tozer, 1967, 1994; Silberling and Tozer, 1968), and Bucher (2002) added an additional zone first recognised in Nevada (fig. 2.1). The Lower Anisian of B.C. consists of the Mulleri Zone, the Caurus Zone and the Americanum Zone; the Caurus Zone is further divided into two subzones, the Bufonis Subzone (Caurus I) and the Nahwisi Subzone (Caurus II). The Middle Anisian consists of the Hagei, Hayesi and Minor zones. The Upper Anisian contains the Deleeni and Chischa zones. The samples examined as part of this study range from the Lower to the Upper Anisian; however, no samples from the Mulleri or Hagei zones were available.




**Figure 2.1.** Chart showing the ammonoid biozonation of the Anisian in British Columbia, based on the work of Tozer (1994) and Bucher (2002).

In Nevada, the ammonoid record is far more extensive (fig. 2.2). A total of 13 ammonoid zones and 31 subzones have been recognized (Silberling and Wallace, 1969; Silberling and Nichols, 1982; Bucher, 1988, 1989, 1992 a, b, 1994; Bucher and Orchard, 1995). In Tethys, a number of ammonoid scales based upon sequences in Italy and Hungary exist. The scheme shown in fig. 2.3 is a composite based on the work of Mietto and Manfrin (1995) and Monnet and Bucher (2007). It includes six ammonoid zones and 14 subzones. Correlation of the ammonoid timescale between the Canadian Arctic, B.C., Nevada and Tethys has been problematic and no judgement on ammonoid correlation is made here.

## 2.3 MATERIAL AND METHODS

New material was collected from four sections on the Alaska Highway in northeastern B.C. (Tuchodi Lakes map area 094 K), as well as from seven cores taken from the subsurface of B.C. in the vicinity of Fort St. John (Halfway River map area 094 B, Charlie Lake map area 094 A and Dawson Creek map area 093 P). Existing collections made by the Geological Survey of Canada were also examined. These existing collections also came from northeastern B.C.: three sections on the Alaska Highway (Tuchodi Lakes map area 094 K; two of which have been re-sampled in the new collections); a further section in the Tetsa River area (Tuchodi Lakes map area 094 K); three sections on the Liard River (Toad River map area 094 N); and two sections on the Toad River (Toad River map area 094 N).

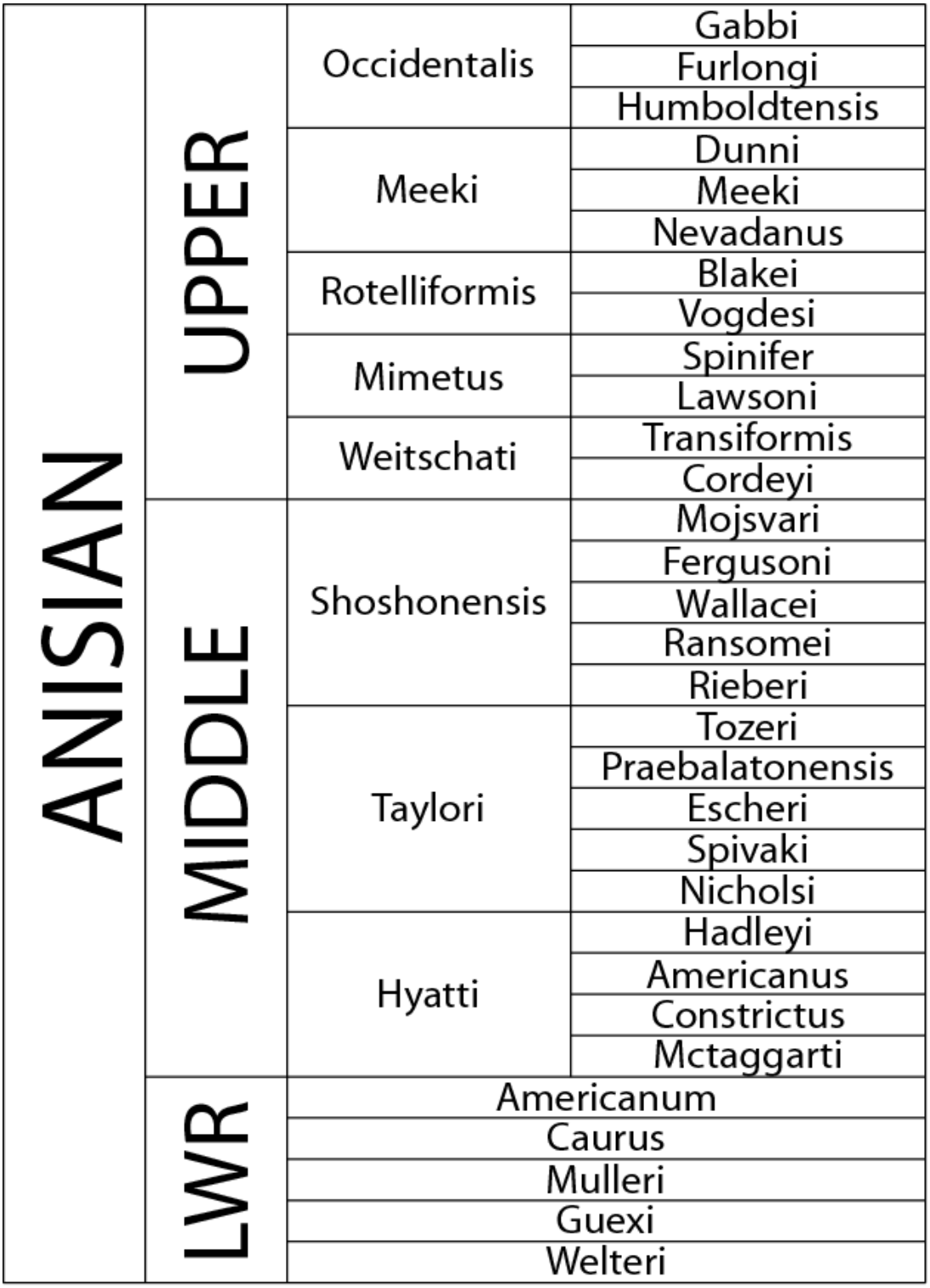



**Figure 2.2.** Chart showing the ammonoid biozonation of the Anisian in Nevada, based primarily on the scheme presented in Monnet and Bucher (2005).

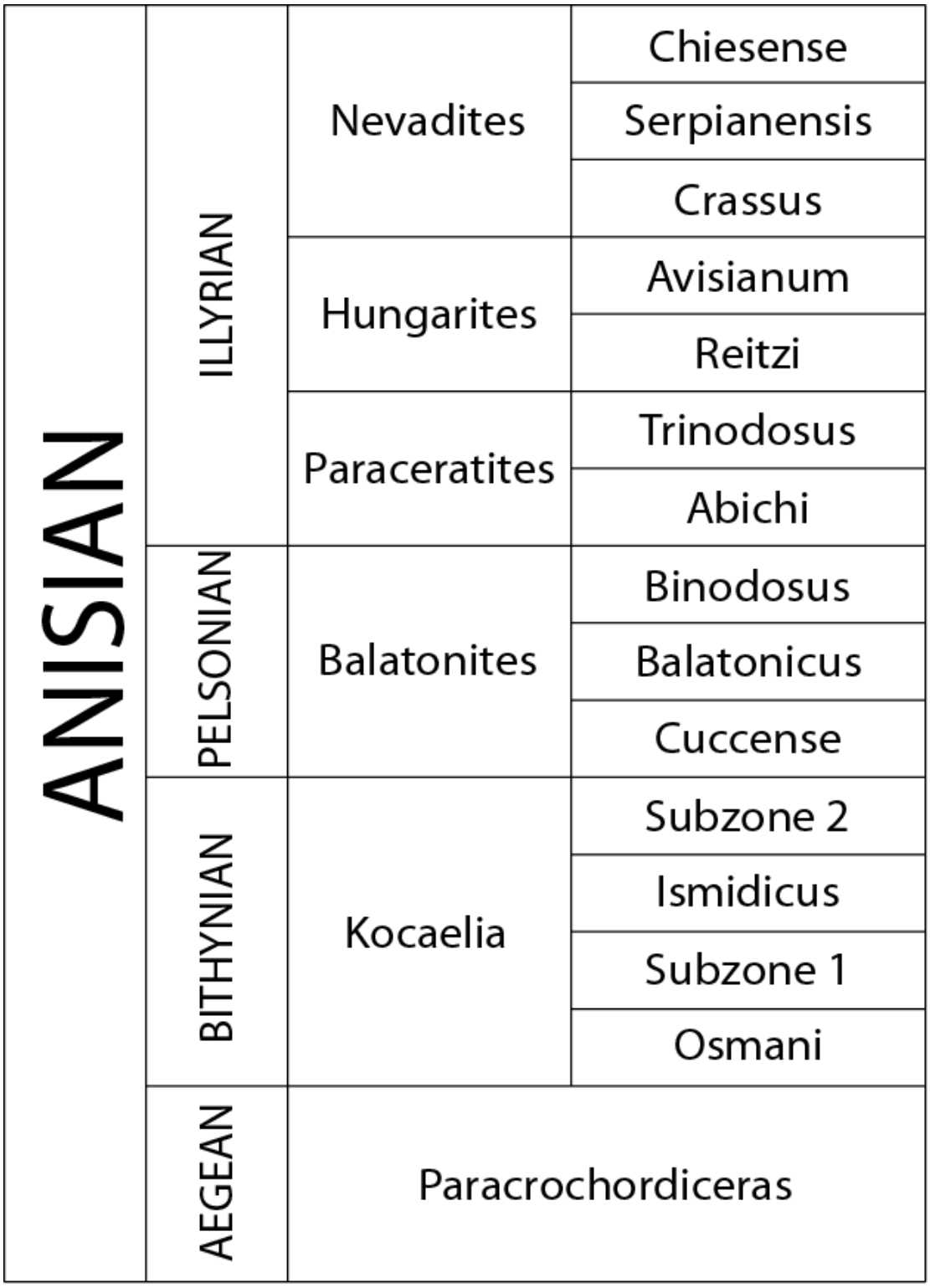



**Figure 2.3.** Chart showing a composite ammonoid biozonation for the Anisian of Tethys, based on the work of Mietto and Manfrin (1995).

On the Alaska Highway, sections were examined at Oyster Springs, Yellow Bluffs, North Tetsa Phosphate and Mile Post 375 West (fig. 2.4). Previous collections were examined from the sections at Yellow Bluffs and Mile Post 375 West, as well as from the section at Mile Post 375 East (fig. 2.4). The section at North Tetsa Hill is in the vicinity of the Alaska Highway (fig. 2.4). The sections on the Liard River are referred to here as North Liard, Liard-Crusty and Liard-Brimstone (fig. 2.5). The sections on the Toad River are referred to here as East Toad River I and II (fig. 2.5).

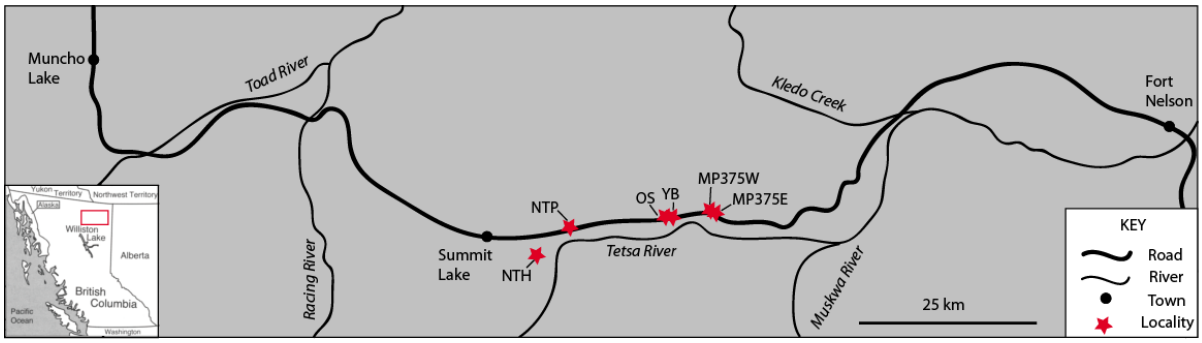



**Figure 2.4.** Map showing the location of sections on the Alaska Highway in northeastern B.C. NTH = North Tetsa Hill, NTP = North Tetsa Phosphate, OS = Oyster Springs, YB = Yellow Bluffs, MP375W = Mile Post 375 West, MP375E = Mile Post 375 East.

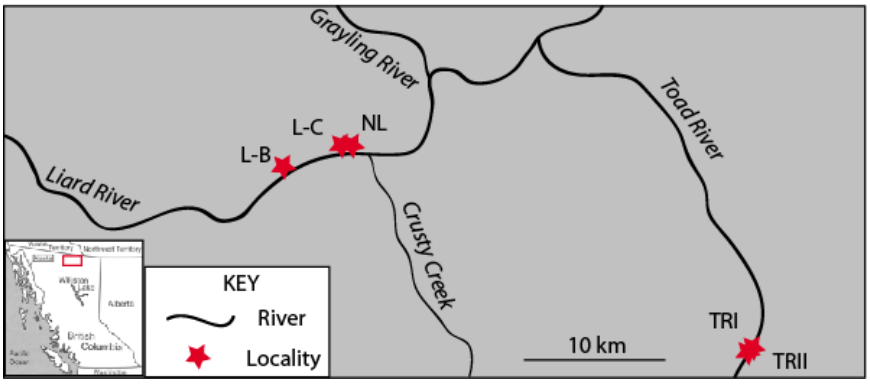



**Figure 2.5.** Map showing the location of sections on the Liard and Toad Rivers in northeastern B.C. L-B = Liard-Brimstone, L-C = Liard-Crusty, NL = North Liard, TRI = East Toad River I, TRII = East Toad River II.

The seven cores sampled from the subsurface are as follows: Petro-Canada Kobes d-048-A/094-B-09; Petro-Canada Kobes c-074-G/094-B-9; Talisman Altares c-085-I/094-B-01; Talisman Altares 16-17-083-25W6; Arc Dawson 07-13-79-15W6; Murphy Swan d-054-B/093-P9 and Shell Groundbirch 16-02-078-22W6 (fig. 2.6).

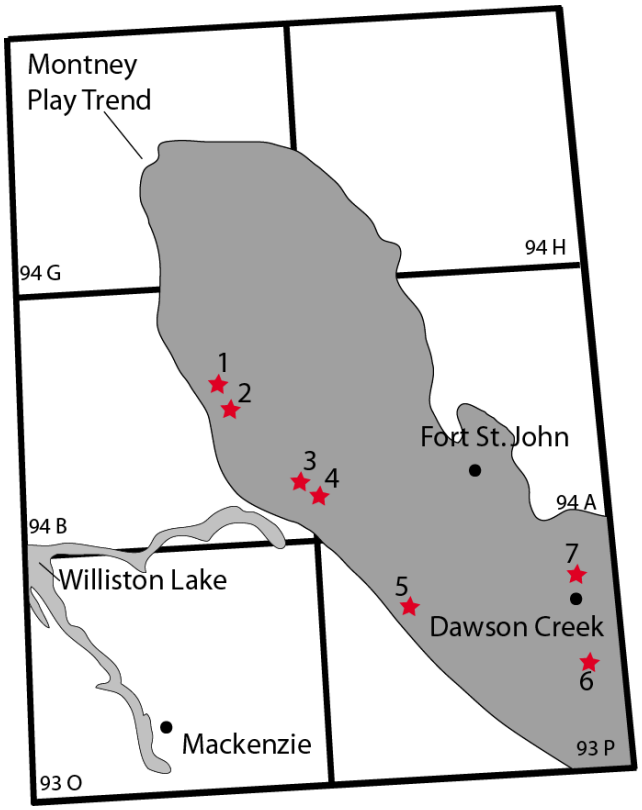



**Figure 2.6.** Map showing the location of subsurface sections and their relation to the Montney hydrocarbon Play Trend. 1 = Petro-Canada Kobes c-074-G/094-B-9, 2 = Petro-Canada Kobes d-048-A/094-B-09, 3 = Talisman Altares c-085-I/094-B-01, 4 = Talisman Altares 16-17-083-25W6, 5 = Shell Groundbirch 16-02-078-22W6, 6 = Murphy Swan d-054-B/093-P9, 7 = Arc Dawson 07-13-79-15W6. Montney Play Trend after Adams (2012).

The new samples were collected from calcareous siltstone beds from the Toad Formation on the Alaska Highway, and from the age equivalent Montney and Doig formations in the subsurface. Samples were approximately 2 kg in weight. Processing was carried out at the Geological Survey

of Canada and the University of British Columbia, using a similar methodology to that outlined in Stone (1987) and Jeppsson *et al.* (1999). Samples were cleaned using sand abrasion before being manually crushed. The fragments were then transferred to containers of 10% dilute acetic acid, buffered with spent solution. After 10 days in the acid, samples were sieved, and the 850 μm – 90 μm fraction was retained and dried. This was then put through sodium polytungstate with a specific gravity of 2.85. The heavy fraction was retained and picked under a light microscope. Images of the conodonts were obtained using the scanning electron microscope facility at the Geological Survey of Canada in Vancouver. Existing collections also came from the Toad Formation, and were processed in a similar way to the new collections.

A total of 70 new samples were collected for this study; 34 from the subsurface and 36 from the Alaska Highway. Of these, 23 contained conodonts that could be identified and were used in this study (table 2.1). 19 samples were examined in the collections of the Geological Survey of Canada; 10 from the Alaska Highway and surrounding area, 5 from the Toad River and 4 from the Liard River (table 2.1). Therefore a total of 42 samples were used for this study. From these samples, 31 taxa were identified (table 2.2). These were assigned to 13 species belonging to two genera. Seven of the species are new, and five of the species have been further divided into 23 morphotypes, 22 of which are new. All taxa identified are described in detail in the systematic palaeontology section.

**Table 2.1.** Samples collected for this study (broken down into those from the Alaska Highway and those from the subsurface) and samples collected previously and held in the collections at the GSC-Pacific in Vancouver. PCK = Petro-Canada Kobes, TA = Talisman Altares, AD = Arc Dawson, MS = Murphy Swan, SG = Shell Groundbirch.

| New Samples – Alaska Highway | | | | | |
|---|---|---|---|---|---|
| **Field No.** | **Locality** | **GSC No.** | **Height above Base (m)** | **Formation** | **Productive** |
| MG-11-OS C1 | Oyster Springs | N/A | 0.00 | Toad | No |
| MG-11-OS C1a | Oyster Springs | N/A | 3.30 | Toad | No |
| MG-11-OS C2 | Oyster Springs | N/A | 6.00 | Toad | Yes |
| MG-11-OS C3 | Oyster Springs | N/A | 9.00 | Toad | No |
| MG-11-OS C4 | Oyster Springs | N/A | 17.90 | Toad | No |
| MG-11-YB-C1 | Yellow Bluffs | N/A | 1.70 | Toad | No |
| MG-11-YB-C2 | Yellow Bluffs | N/A | 1.70 | Toad | No |
| MG-11-YB-C3 | Yellow Bluffs | N/A | 3.00 | Toad | No |
| MG-11-YB-C4 | Yellow Bluffs | N/A | 3.00 | Toad | No |
| MG-11-YB-C5 | Yellow Bluffs | N/A | 3.75 | Toad | No |
| MG-11-YB-C6 | Yellow Bluffs | N/A | 3.75 | Toad | No |
| MG-11-YB-C7 | Yellow Bluffs | N/A | Talus | Toad | Yes |
| MG-11-YB-C8 | Yellow Bluffs | N/A | 10.00 | Toad | No |
| MG-11-YB-C9 | Yellow Bluffs | N/A | 10.00 | Toad | Yes |
| MG-11-YB-C10 | Yellow Bluffs | N/A | 8.00 | Toad | Yes |
| MG-11-YB-C11 | Yellow Bluffs | N/A | 13.00 | Toad | No |
| MG-11-YB-C12 | Yellow Bluffs | N/A | 13.00 | Toad | Yes |
| MG-11-YB-Cfloat | Yellow Bluffs | N/A | Talus | Toad | No |
| MG-11-NTP-C0 | North Tetsa Phosphate | N/A | -0.30 | Toad | Yes |
| MG-11-NTP-C1 | North Tetsa Phosphate | N/A | 0.45 | Toad | No |
| MG-11-NTP-C2 | North Tetsa Phosphate | N/A | 2.60 | Toad | No |
| MG-11-NTP-C3 | North Tetsa Phosphate | N/A | 2.70 | Toad | No |
| MG-11-NTP-C4 | North Tetsa Phosphate | N/A | 2.80 | Toad | No |
| MG-11-NTP-C5 | North Tetsa Phosphate | N/A | 3.18 | Toad | No |
| MG-11-NTP-C6 | North Tetsa Phosphate | N/A | 3.40 | Toad | Yes |
| MG-11-NTP-C7 | North Tetsa Phosphate | N/A | 4.30 | Toad | Yes |
| MG-11-NTP-C8 | North Tetsa Phosphate | N/A | 5.60 | Toad | No |
| MG-11-NTP-C9 | North Tetsa Phosphate | N/A | 7.55 | Toad | No |
| MG-11-NTP-C10 | North Tetsa Phosphate | N/A | 9.55 | Toad | No |

| New Samples – Alaska Highway | | | | | |
|---|---|---|---|---|---|
| **Field No.** | **Locality** | **GSC No.** | **Height above Base (m)** | **Formation** | **Productive** |
| MG-11-NTP-C11 | North Tetsa Phosphate | N/A | 10.60 | Toad | No |
| MG-11-NTP-C12 | North Tetsa Phosphate | N/A | 11.35 | Toad | No |
| MG-11-NTP-C13 | North Tetsa Phosphate | N/A | >11.35 | Toad | Yes |
| MG-11-MP375W-C0 | Mile Post 375 West | N/A | -1.00 | Toad | No |
| MG-11-MP375W-C1 | Mile Post 375 West | N/A | 0.00 | Toad | No |
| MG-11-MP375W-C2 | Mile Post 375 West | N/A | 10.00 | Toad | No |
| MG-11-MP375W-C3 | Mile Post 375 West | N/A | 27.00 | Toad | Yes |
| **New Samples – Subsurface B.C.** | | | | | |
| **Field No.** | **Well Name** | **GSC No.** | **Depth in Well (m)** | **Formation** | **Productive** |
| MG-11-C28 | PCK d-048-A/094-B-09 | N/A | 1968.25 | Montney | No |
| MG-11-C29 | PCK d-048-A/094-B-09 | N/A | 1967.85 | Montney | No |
| MG-11-C30 | PCK d-048-A/094-B-09 | N/A | 1967.30-1967.50 | Doig | Yes |
| MG-11-C31 | PCK d-048-A/094-B-09 | N/A | 1966.00-1967.00 | Doig | No |
| MG-11-C32 | PCK d-048-A/094-B-09 | N/A | 1964.80-1965.00 | Doig | No |
| MG-11-C33 | PCK d-048-A/094-B-09 | N/A | 1965.00-1965.40 | Doig | Yes |
| MG-11-JP17 | PCK c-074-G/094-B-9 | N/A | 1945.60-1945.80 | Montney | No |
| MG-11-JP18 | PCK c-074-G/094-B-9 | N/A | 1946.90-1947.15 | Montney | No |
| MG-11-JP19 | PCK c-074-G/094-B-9 | N/A | 1951.50-1952.00 | Montney | No |
| MG-11-JP20 | PCK c-074-G/094-B-9 | N/A | 1858.60-1858.90 | Doig | Yes |
| MG-11-JP21 | PCK c-074-G/094-B-9 | N/A | 1860.30-1860.60 | Doig | No |
| MG-11-C13 | TA c-085-I/094-B-01 | N/A | 2370.61-2369.96 | Doig | Yes |
| MG-11-C14 | TA c-085-I/094-B-01 | N/A | 2368.88-2368.04 | Doig | No |
| MG-11-C15 | TA c-085-I/094-B-01 | N/A | 2366.75-2366.06 | Doig | No |
| MG-11-C16 | TA c-085-I/094-B-01 | N/A | 2315.22-2314.50 | Doig | No |
| MG-11-C18 | TA c-085-I/094-B-01 | N/A | 2306.82-2306.01 | Doig | No |
| MG-11-C1 | TA 16-17-083-25W6 | N/A | 2258.30-2257.43 | Montney | No |
| MG-11-C3 | TA 16-17-083-25W6 | N/A | 2255.30-2254.44 | Doig | No |
| MG-11-C7 | TA 16-17-083-25W6 | N/A | 2242.35-2241.46 | Doig | No |
| MG-11-C8 | TA 16-17-083-25W6 | N/A | 2239.75-2238.74 | Doig | Yes |

| New Samples – Subsurface B.C. | | | | | |
|---|---|---|---|---|---|
| **Field No.** | **Well Name** | **GSC No.** | **Depth in Well (m)** | **Formation** | **Productive** |
| MG-11-C9 | TA 16-17-083-25W6 | N/A | 2237.05-2236.09 | Doig | Yes |
| MG-11-C10 | TA 16-17-083-25W6 | N/A | 2234.57-2234.10 | Doig | Yes |
| MG-11-C21 | AD 07-13-79-15W6 | N/A | 2054.68-2054.48 | Doig | No |
| MG-11-C22 | AD 07-13-79-15W6 | N/A | 2054.30-2054.05 | Doig | Yes |
| MG-10-JP1 | MS d-054-B/093-P9 | N/A | 2548.45 | Doig | No |
| MG-10-JP2 | MS d-054-B/093-P9 | N/A | 2549.66 | Doig | Yes |
| MG-10-JP3 | MS d-054-B/093-P9 | N/A | 2551.80 | Doig | No |
| MG-10-JP4 | MS d-054-B/093-P9 | N/A | 2553.40 | Doig | No |
| MG-10-JP5 | MS d-054-B/093-P9 | N/A | 2553.80 | Doig | Yes |
| MG-10-JP6 | MS d-054-B/093-P9 | N/A | 2556.25 | Doig | No |
| MG-10-JP7 | MS d-054-B/093-P9 | N/A | 2556.90 | Doig | Yes |
| MG-10-JP8 | MS d-054-B/093-P9 | N/A | 2557.30 | Doig | No |
| SG-3073 | SG 16-02-078-22W6 | N/A | 3073.00 | Montney | Yes |
| SG-30348 | SG 16-02-078-22W6 | N/A | 3034.80 | Doig | Yes |
| **GSC Collections – Alaska Highway, Liard River, Toad River** | | | | | |
| **Field No.** | **Locality** | **GSC No.** | **Height above Base (m)** | **Formation** | **Productive** |
| 83-TE211A | North Liard | 99574 | Unknown | Toad | Yes |
| 83-TE211B | North Liard | 99575 | Unknown | Toad | Yes |
| 82-B9F | Liard-Crusty | C-090852 | Unknown | Toad | Yes |
| 00-TE-X | Liard-Brimstone | 42349 | Unknown | Toad | Yes |
| 83-215B | East Toad River I | 99588 | 2.00 | Toad | Yes |
| 83-215E | East Toad River I | 99591 | 5.25 | Toad | Yes |
| 83-215F | East Toad River I | 99592 | 6.00 | Toad | Yes |
| 83-205A | East Toad River II | 99565 | 5.00 | Toad | Yes |
| 83-205B | East Toad River II | 99564 | 10.00 | Toad | Yes |
| 00-TE-X | North Tetsa Hill | 46499 | Unknown | Toad | Yes |
| 92-AH2 | Yellow Bluffs | C-201902 | 0.00 | Toad | Yes |
| 92-AH21 | Yellow Bluffs | C-201921 | 21.50 | Toad | Yes |
| 94-TE68294 | Mile Post 375 West | 68294 | 0.00 | Toad | Yes |

| GSC Collections – Alaska Highway, Liard River, Toad River | | | | | |
|---|---|---|---|---|---|
| **Field No.** | **Locality** | **GSC No.** | **Height above Base (m)** | **Formation** | **Productive** |
| 92-AH26 | Mile Post 375 West | C-201926 | 10.00 | Toad | Yes |
| 92-AH25 | Mile Post 375 West | C-201925 | 27.00 | Toad | Yes |
| 92-AH22 | Mile Post 375 East | C-201922 | 4.00 | Toad | Yes |
| HB-655 | Mile Post 375 East | C-209952 | 18.00 | Toad | Yes |
| HB-656 | Mile Post 375 East | C-302187 | 22.00 | Toad | Yes |
| 82-AH6 | Mile Post 375 East | C-101077 | 25.00 | Toad | Yes |

| Locality | Sample | Ammonoid Zone | Conodont Assemblage | n. sp. B | Reg alpha | n .sp. E | Reg beta | Reg delta | Reg zeta | Reg eta | n. sp. H | Reg iota | n. sp. A | Reg gamma | Bifurcata | Con alpha | Reg theta | Reg epsilon | Shosh D | n. sp. G | Shosh C | Shosh B | Con epsilon | n. sp. C | n. sp. D | Con zeta | Con delta | Lieb alpha | Lieb beta | Con gamma | Con beta | n. sp. F | Tran alpha | Tran beta |
|---|---|---|---|---|---|---|---|---|---|---|---|---|---|---|---|---|---|---|---|---|---|---|---|---|---|---|---|---|---|---|---|---|---|
| MP375 East | 92-AH22 | Caurus I | n. sp. B | x | | | | | | | | | | | | | | | | | | | | | | | | | | | | | |
| d-48-A/94-B-9 | 5 | N/A | Reg α | | x | x | x | | | | | | | | | | | | | | | | | | | | | | | | | | |
| d-48-A/94-B-9 | 1 | N/A | Reg δ | | x | | | x | | | | | | | | | | | | | | | | | | | | | | | | | |
| N Liard River | 83-TE 211A | Caurus II | Reg δ | x | | | | x | x | | | | | | | | | | | | | | | | | | | | | | | | |
| Liard-Brimstone | 42349 | Caurus II | Reg δ | | | | | x | | | | | | | | | | | | | | | | | | | | | | | | | |
| MP375 East | HB-655 | Americanum | Reg η | | x | | | | x | x | x | | | | | | | | | | | | | | | | | | | | | | |
| 16-17-83-25W6 | 20 | N/A | Reg η | | | | | | | x | | | | | | | | | | | | | | | | | | | | | | | |
| d-54-B/93-P-9 | MG 2556 | N/A | Reg ι | | | | | | | | | x | | | | | | | | | | | | | | | | | | | | | |
| 16-17-83-25W6 | 21 | N/A | Reg ι | | | | | | | | | x | | | | | | | | | | | | | | | | | | | | | |
| SG 16-02-078-22 | 3073 | N/A | Reg ι | | | | | | | | | x | | | | | | | | | | | | | | | | | | | | | |
| d-54-B/93-P-9 | MG 2553 | N/A | n. sp. A | | | | | | | | | x | x | x | | | | | | | | | | | | | | | | | | | |
| MP375 East | HB-656 | Hayesi | n. sp. A | | | | | | | | | | x | | x | x | | | | | | | | | | | | | | | | | |
| c-85-I/94-B-1 | 1 | N/A | n. sp. A | | | | x | | | | | | | x | | | | | | | | | | | | | | | | | | | |
| 16-17-83-25W6 | 22 | N/A | n. sp. A | | x | | | | | | | x | | x | | | | | | | | | | | | | | | | | | | |
| 7-13-79-15W6 | 2 | N/A | n. sp. A | | x | | | | | | | x | x | | | | | | | | | | | | | | | | | | | | |
| MP375 East | 82-AH6 | Hayesi | Reg θ | | | | | | | | | | x | | | | x | | | | | | | | | | | | | | | | |
| MP375 West | 68294 | Hayesi | Reg θ | | x | | | | | | | | x | x | | | x | x | | | | | | | | | | | | | | | |
| Liard-Crusty | 82-B9F | Hayesi | Reg θ | | x | | | | | | | | | | | | | | | | | | | | | | | | | | | | |
| N Liard River | 83-TE 211B | Hayesi | Reg θ | | | | | | | | | | | | | | x | | | | | | | | | | | | | | | | |
| E Toad River I | 83-215B | Hayesi | Reg θ | | x | | | | | | | | | | | | | | | | | | | | | | | | | | | | |
| North Tetsa Phosphate | NTP-C0 | N/A | Reg θ | | x | | | | | | | | | | | | | | | | | | | | | | | | | | | | |
| North Tetsa Phosphate | NTP-C6 | N/A | Shosh | | | | | | | | | | | | | | | | x | | | | | | | | | | | | | | |
| North Tetsa Phosphate | NTP-C7 | N/A | Shosh | | | | | | | | | | | | | x | | | | | | | | | | | | | | | | | |
| North Tetsa Phosphate | NTP-C13 | N/A | Shosh | | | | | | | | | | | | | | | | | x | | | | | | | | | | | | | |
| E Toad River II | 83-205A | Minor | Shosh | | | | | | | | | | | | | | | | x | | x | | | | | | | | | | | | |
| E Toad River I | 83-215E | Minor | Shosh | | | | | | | | | | | | | x | | | x | | x | x | | | | | | | | | | | |
| MP375 West | 92-AH26 | Minor | Shosh | | | | | | | | | | | | | x | | | x | | | | x | x | x | | | | | | | | |
| c-74-G/94-B-9 | 4 | N/A | Shosh | | | | x | | | | | x | | | | | | | | | | x | | | | | | | | | | | |
| SG 16-02-078-22 | 30348 | N/A | Shosh | | | | | | | | x | | | | x | | | | | | | | | x | | | | | | | | | |
| North Tetsa Hill | 46499 | Minor | Shosh | | | | | | | | | | | | | | | | | | | | | | x | | | | | | | | |
| d-54-B/93-P-9 | MG 2549 | N/A | Shosh | | | | | | | | | | | | | | | | | x | | | | | | | | | | | | | |
| E Toad River I | 83-215F | Deleeni | Con ζ | | | | | | | | | | | | | | | | | | | | x | x | | x | | | | | | | |
| Yellow Bluffs | YB-C7 | N/A | Con ζ | | | | | | | | | | | | | | | | | | | | | | | | x | | | | | | |
| Yellow Bluffs | 92-AH2 | Deleeni | Lieb | | | | | | | | | | | | | x | | | | | | | | | x | x | | x | x | | | | |
| Yellow Bluffs | YB-C10 | N/A | Lieb | | | | | | | | | | | | | x | | | | | | | | | | | | | | | | | |
| Yellow Bluffs | YB-C9 | N/A | Lieb | | | | | | | | | | | | | x | | | | | | | | | | | x | | | | | | |
| Yellow Bluffs | YB-C12 | N/A | Lieb | | | | | | | | | | | | | | | | | | | | | | | | x | | | | | | |
| E Toad River II | 83-205B | Deleeni | Lieb | | | | | | | | | | | | | x | | | | | | | | | | | x | | x | x | x | | |
| MP375 West | 92-AH25 | Deleeni | Lieb | | | | | | | | | | | | | | | | | | | | | | | | x | x | | | | | |
| Mile Post 375 West | MP375W-C3 | Deleeni | Lieb | | | | | | | | | | | | | x | | | | | | | | | | | | | | | | | |
| Yellow Bluffs | 92-AH21 | Chischa | Tran | | | | | | | | | | | | | | | | | | | | | | | | | | | x | | x | x |
| Oyster Springs | OS-C2 | N/A | Tran | | | | | | | | | | | | | | | | | | | | | | | | | | | x | | x | |

**Table 2.2.** Conodonts recovered from each of the productive samples, in approximate stratigraphic order. Oldest sample is at the top of the table. Conodont faunal assemblages are shown for each sample, as is the ammonoid zone when known. Reg = *regalis*, Con = *constricta*, Shosh = *shoshonensis*, Lieb = *liebermani*, Tran = *transita*.

## 2.4 BIOSTRATIGRAPHY

The ammonoid scale for B.C. has been generated through the work of McLearn (1941 a, c, 1946 a, b, 1947 a, b, 1953, 1960, 1969), Tozer (1961, 1965, 1967, 1982, 1994), Silberling and Tozer (1969), and Bucher (2002). Orchard and Tozer (1997) presented an integrated ammonoid and conodont scale for the whole of the Triassic, principally based on material from B.C. and the Canadian Arctic. The Anisian portion of their scheme, compared with the B.C. ammonoid zonation, is shown in figure 2.7 along with the new conodont faunal assemblages described in this paper. Orchard and Tozer (1997) recognised ten conodont zones; however, some are age equivalent. There is a maximum of seven sequential zones in their scheme. B.C. includes an important fossil record for the Anisian stage. However, work on the ammonoid faunas of Nevada has led to the recognition of an even more complete ammonoid biostratigraphy for the Anisian (Silberling and Wallace, 1969; Silberling and Nichols, 1982; Bucher, 1988, 1989, 1992 a, b, 1994; Bucher and Orchard, 1994). The most recent correlation of the Anisian ammonoid zones of Nevada with those of B.C. and the Arctic is shown in figure 2.8 (from Monnet and Bucher, 2005).

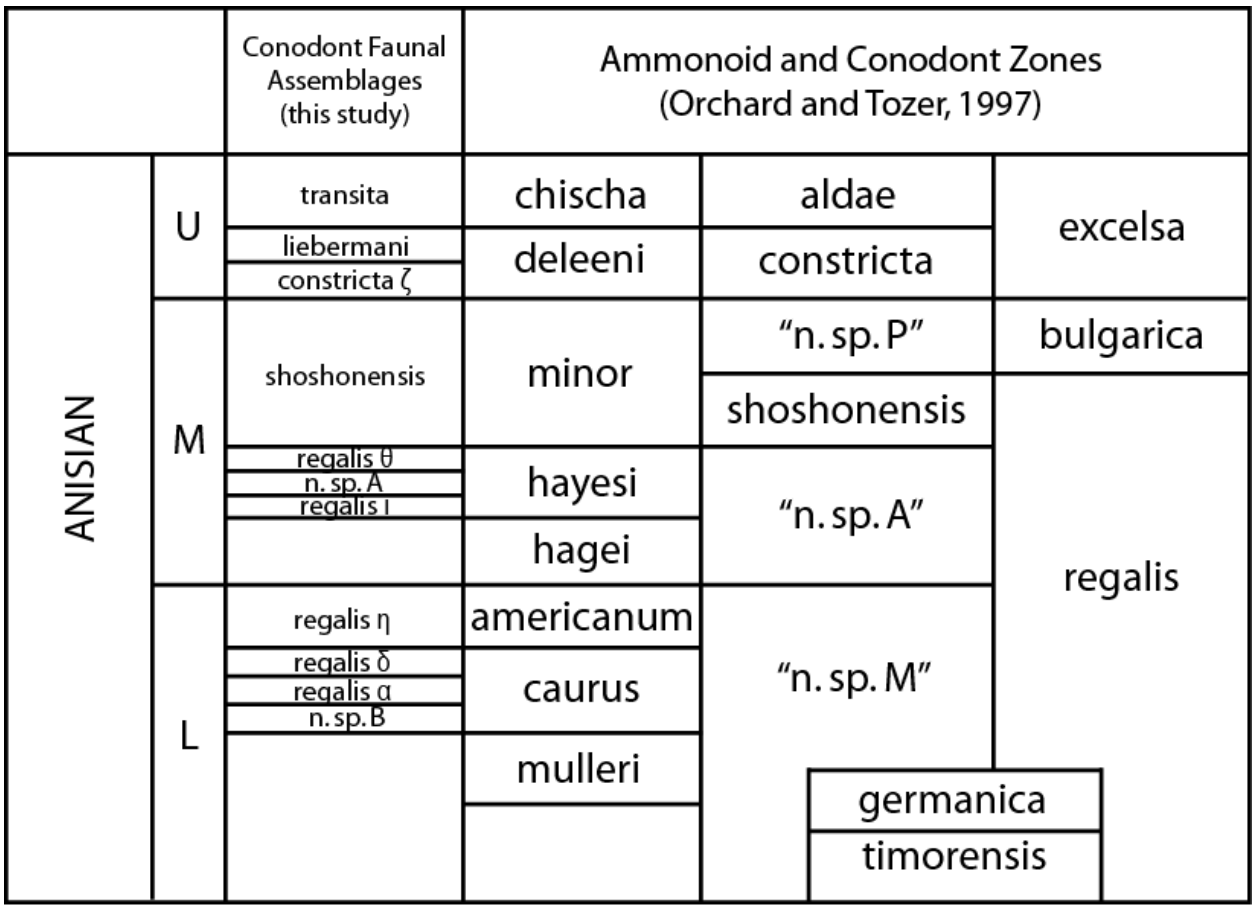



**Figure 2.7.** Chart showing the correlation between the new conodont faunal assemblages proposed in this study and the existing ammonoid and conodont biozonation for the Anisian of B.C.

The revision of the B.C. conodonts from the Anisian has allowed the recognition of eleven informal conodont faunas (fig. 2.7). The existing collections of conodonts from the Alaska Highway had initially been made in conjunction with collections of ammonoids, which allows the correlation of the conodont samples with the North American ammonoid zones of Tozer (1994). These samples are identified in table 2.1. From this table, it can be seen that certain conodont species are associated with particular ammonoid zones. Where these species are found in other samples, it can be suggested that the samples correlate with the corresponding ammonoid zones, even though no ammonoids were found with the samples. This in turn leads to

the recognition of further species that are indicative of particular ammonoid zones and allows samples where these occur to be assigned to an ammonoid zone, and so on.

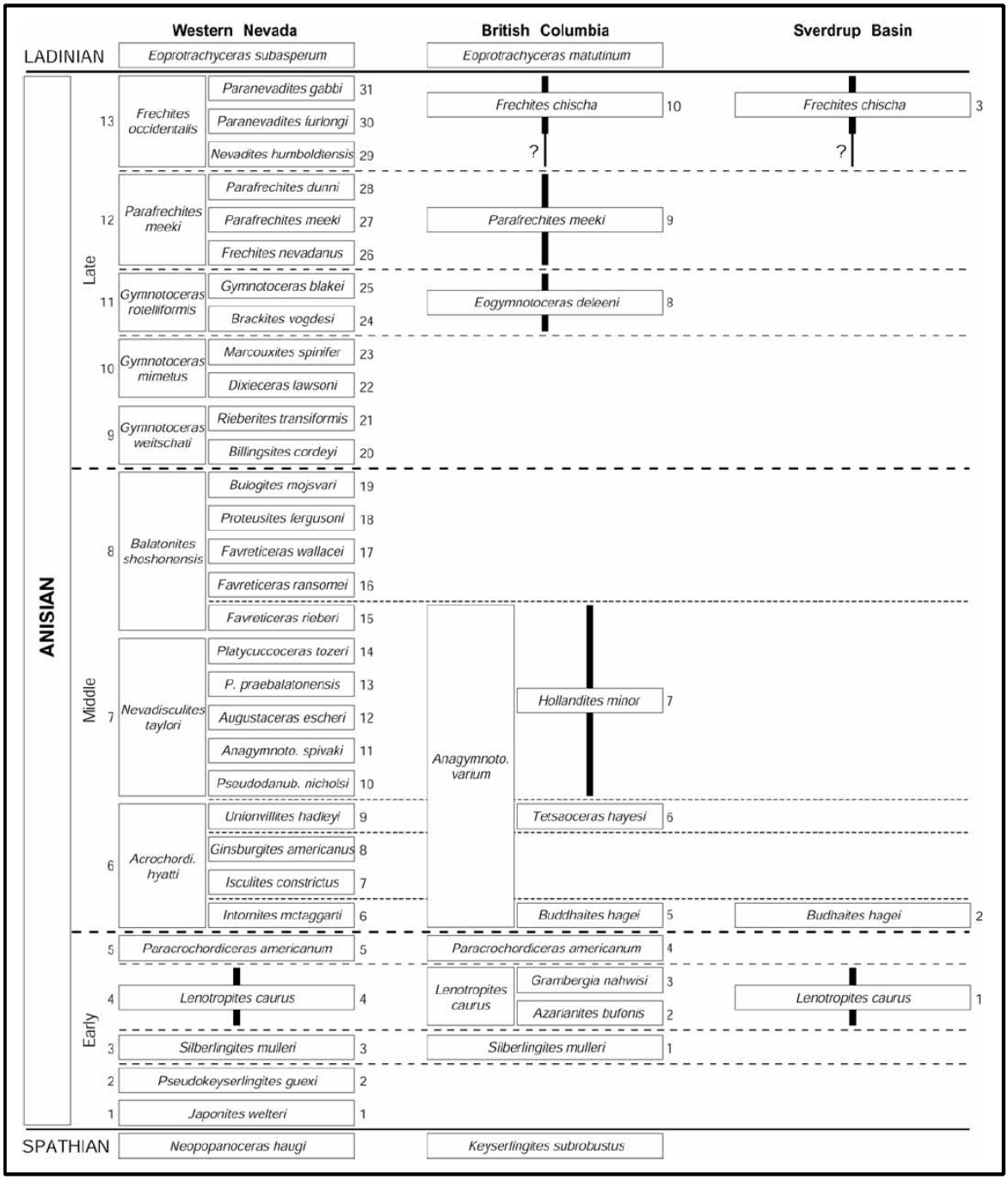



**Figure 2.8.** Chart showing the correlation of Anisian ammonoid zones between Nevada, British Columbia and the Sverdrup Basin in the Arctic. From Monnet and Bucher (2005).

The conodont faunas are defined on the basis of the conodonts that occur within them; there is a general lack of superposition of these faunas in section. Where successions of samples do occur, it has been possible to discriminate further faunas based on their order of appearance. Those sections with conodont faunas in sequence are illustrated in figures 2.9 – 2.17. This biostratigraphic scheme is currently a hybrid, containing faunal assemblages equivalent in concept to both assemblage biozones and interval biozones. Because of the hybrid nature of the scheme and the lack of superposition of assemblages in multiple sections, it is thought best to keep these faunal assemblages informal at this time, pending further work.

## 2.5 CONODONT FAUNAS

### Lower Anisian

#### *N. n. sp. B Faunal Assemblage*

The base of this faunal assemblage is defined by the first appearance of *N.* n. sp. B. This is the only conodont to occur within this assemblage, which correlates approximately to the Caurus I Subzone. It is only observed in the Mile Post 375 East section, where it occurs with ammonoids of this subzone. The top of this assemblage is defined by the first appearance of *N.* ex gr. *regalis* morphotype α.

#### *N. ex gr. regalis α Faunal Assemblage*

The base of this faunal assemblage is defined by the first appearance of *N.* ex gr. *regalis* morphotype α. Also appearing for the first time in this assemblage are *N.* ex gr. *regalis* morphotype β and *N.* n. sp. E, the latter being restricted to this assemblage. The assemblage is only observed in the Petro-Canada Kobes d-048-A/094-B-09 well, where it occurs beneath the

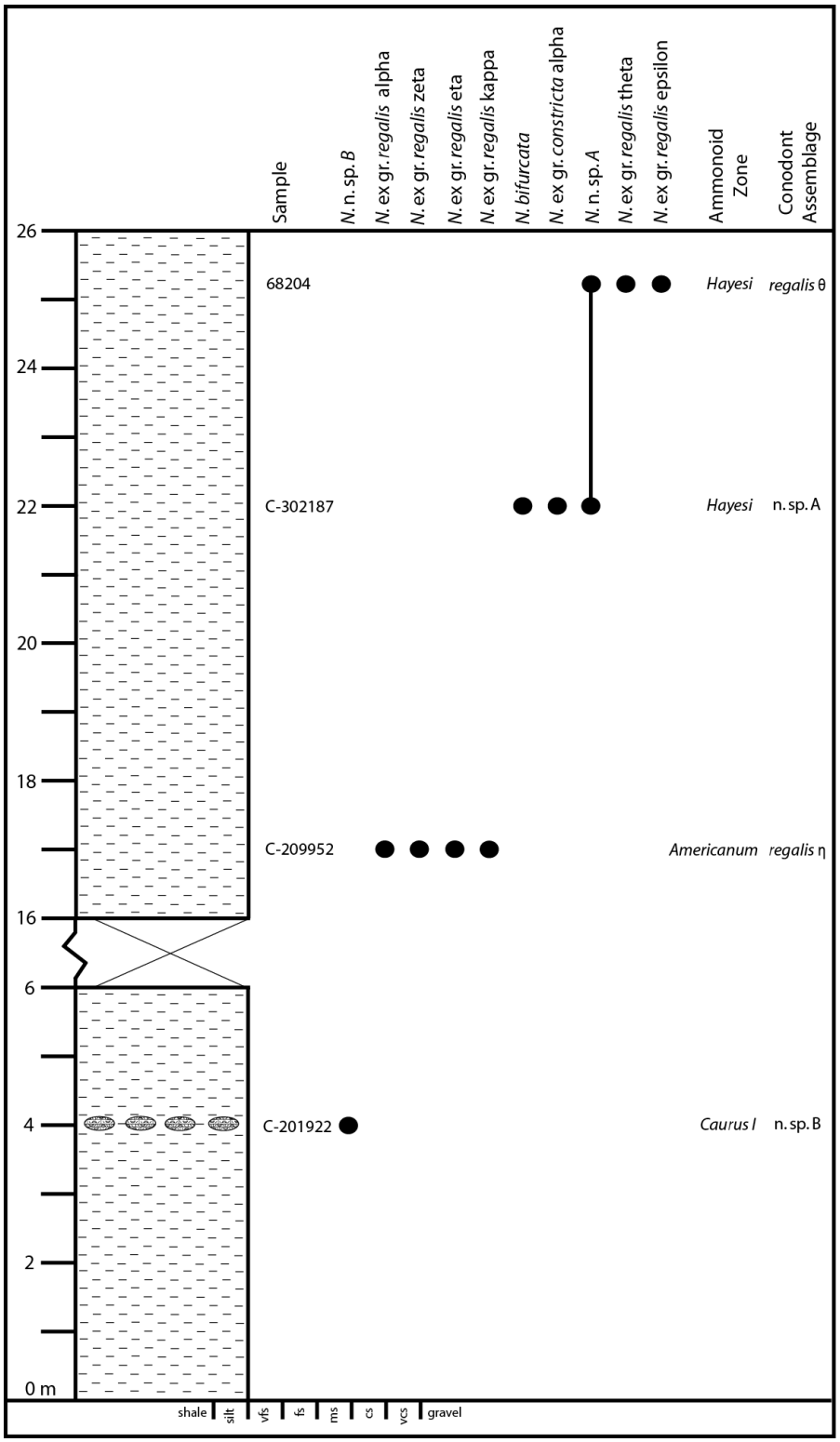



**Figure 2.9.** Stratigraphic log of the section at Mile Post 375 East, showing the location and composition of conodont samples from this section, and the position of ammonoid zones and conodont faunal assemblages present.

first occurrence of *N.* ex gr. *regalis* δ (fig. 2.10). It is uncertain whether this assemblage correlates with the Caurus I or Caurus II subzone, or between the two. The top of the assemblage is defined by the appearance of *N.* ex gr. *regalis* morphotype δ.

***N. ex gr. regalis δ Faunal Assemblage***

The base of this faunal assemblage is defined by the first appearance of *N.* ex gr. *regalis* morphotype δ. Also appearing for the first time in this assemblage is *N.* ex gr. *regalis* morphotype ζ, whist *N.* n. sp. B disappears within it. *N.* ex gr. *regalis* morphotype δ is restricted to this assemblage. The assemblage directly overlies the *N.* ex gr. *regalis* α Faunal Assemblage in the Petro-Canada Kobes d-048-A/094-B-09 well (fig. 2.10). It is also observed in the North Liard River and Liard-Brimstone sections, where it occurs with ammonoids of the Caurus II Subzone. The top of this assemblage is defined by the first appearance of *N.* ex gr. *regalis* η.

***N. ex gr. regalis η Faunal Assemblage***

The base of this faunal assemblage is defined by the first appearance of *N.* ex gr. *regalis* morphotype η. Also appearing for the first time in this assemblage is *N.* n. sp. H, whilst *N.* ex gr. *regalis* morphotype ζ disappears within this assemblage. *N.* ex gr. *regalis* morphotype α is also present. This assemblage occurs above the *N.* n. sp. B Faunal Assemblage in the Mile Post 375 East section (fig. 2.9), where it is associated with ammonoids of the Americanum Zone. It is also present in the Talisman Altares 16-17-083-25W6 well, where it is overlain by the *N.* ex gr. *regalis* ι Faunal Assemblage (fig. 2.11). The top of this assemblage is defined by the first appearance of *N.* ex gr. *regalis* morphotype ι.

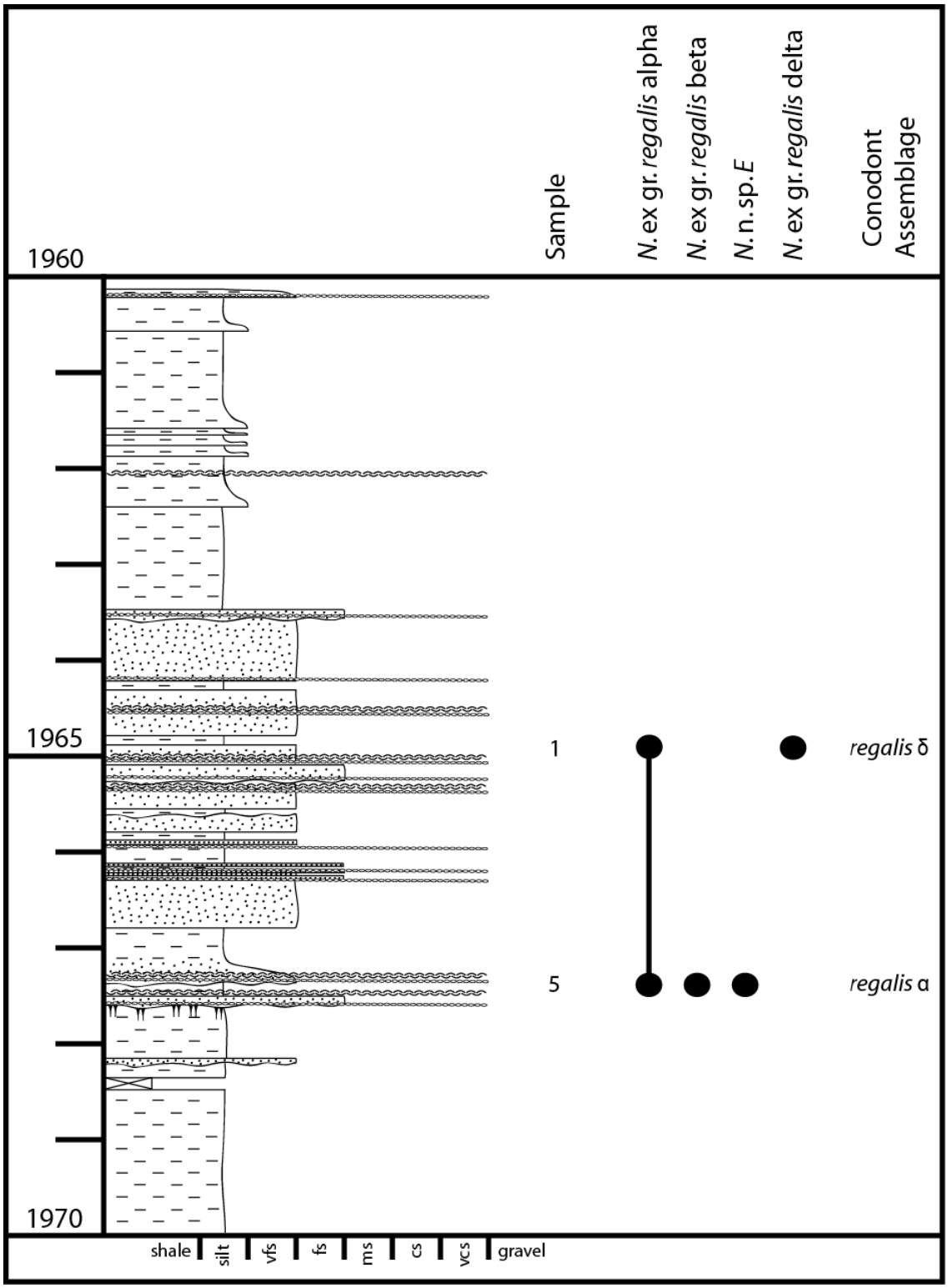



**Figure 2.10.** Stratigraphic log of the core from the Petro-Canada Kobes d-048-A/094-B-09 well, showing the location and composition of conodont samples from this core, and the position of conodont faunal assemblages present.

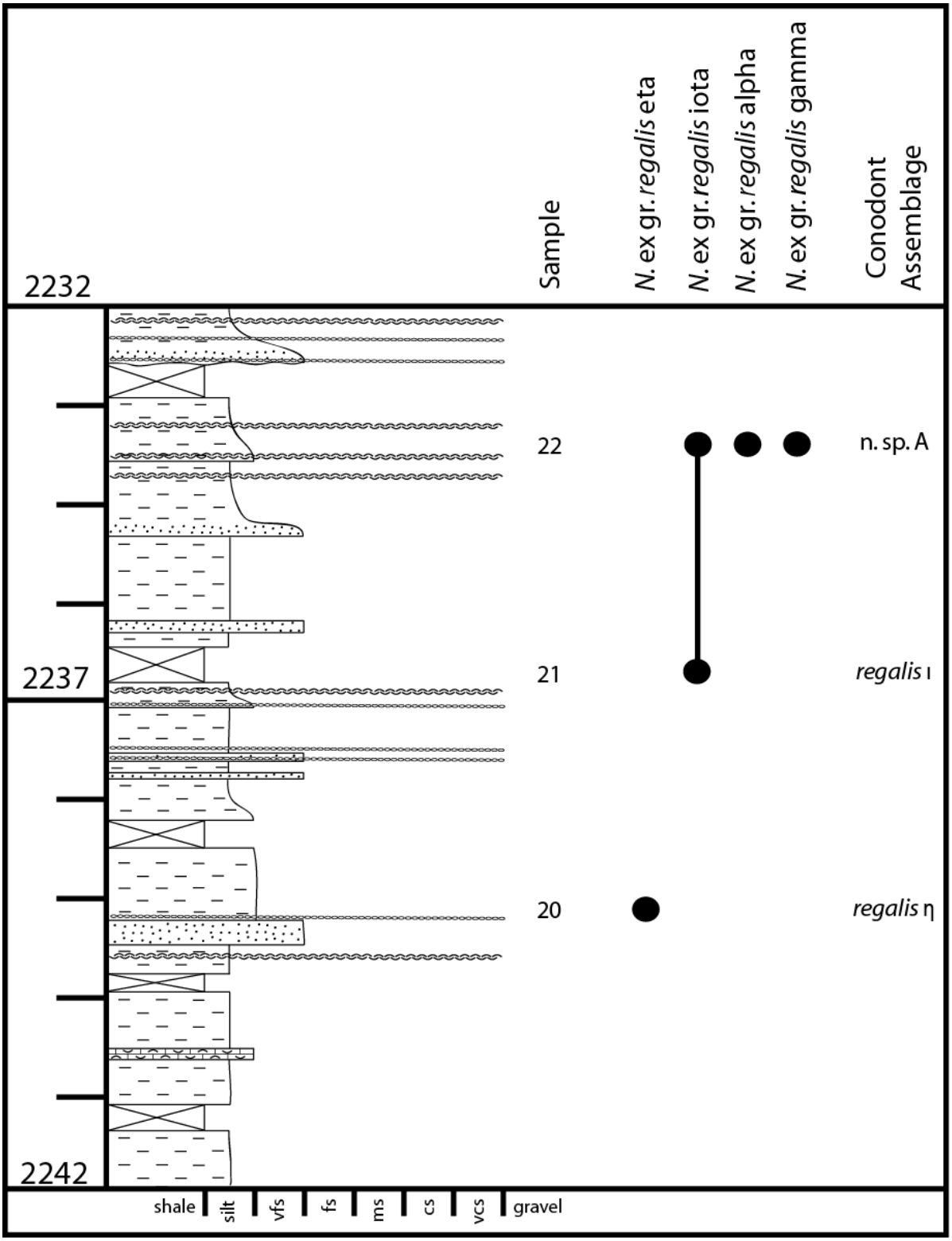



**Figure 2.11.** Stratigraphic log of the core from the Talisman Altares 16-17-083-25W6 well, showing the location and composition of conodont samples from this core, and the position of conodont faunal assemblages present.

**Middle Anisian**

***N. ex gr. regalis ι Faunal Assemblage***

The base of this faunal assemblage is defined by the first appearance of *N.* ex gr. *regalis* morphotype ι. This is the only conodont observed in this assemblage. It is observed in the Talisman Altares 16-17-083-25W6 well, where it directly overlies the *N.* ex gr. *regalis* η Faunal Assemblage (fig. 2.11), in the Murphy Swan d-54-B/093-P-9 well, where it appears below the first occurrence of the *N.* n. sp. A Faunal Assemblage (fig. 2.12) and in the Shell Groundbirch 16-02-078-22W6 well (fig. 2.13). This faunal assemblage does not occur with any ammonoids; however, its conodont fauna is most similar to that of the Hayesi Zone; *N.* ex gr. *regalis* morphotype ι is never found with Lower Anisian conodonts, but does occur higher in the Murphy Swan d-54-B/093-P-9 well with conodonts of the Middle Anisian. The top of this faunal assemblage is defined by the appearance of *N.* n. sp. A.

***N. n. sp. A Faunal Assemblage***

The base of this faunal assemblage is defined by the first appearance of *N.* n. sp. A. The first appearances of *N. bifurcata, N.* ex gr. *constricta* morphotype α and *N.* ex gr. *regalis* γ also occur in this assemblage. *N.* ex gr. *regalis* morphotypes α, β and ι are also present. This assemblage immediately overlies the *N.* ex gr. *regalis* α Faunal Assemblage in the Mile Post 375 East section (fig. 2.9). It is also observed in the Murphy Swan d-54-B/093-P-09 well (fig. 2.12), where it overlies the *N.* ex gr. *regalis* morphotype ι Faunal Assemblage, and also in the Arc Dawson 07-13-079-15W6, Talisman Altares 16-17-083-25W6 and Talisman Altares c-085-I/094-B-09 wells. It occurs with ammonoids of the Hayesi Zone at the Mile Post 375 East section. The top of the assemblage is defined by the first appearance of *N.* ex gr. *regalis* morphotype θ.

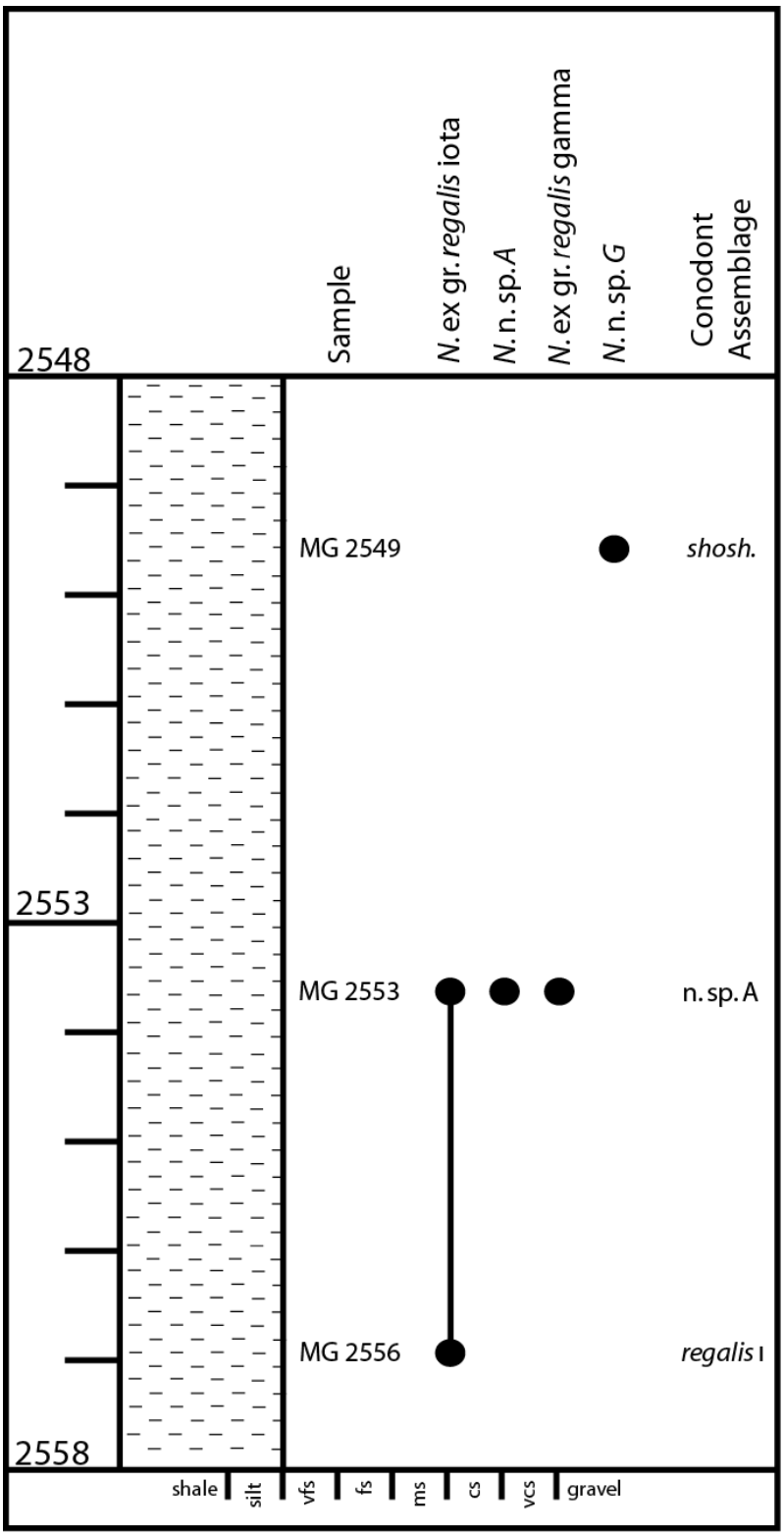



**Figure 2.12.** Stratigraphic log of the core from the Murphy Swan d-054-B/093-P9 well, showing the location and composition of conodont samples from this core, and the position of conodont faunal assemblages present. Shosh. = *shoshonensis* faunal assemblage.

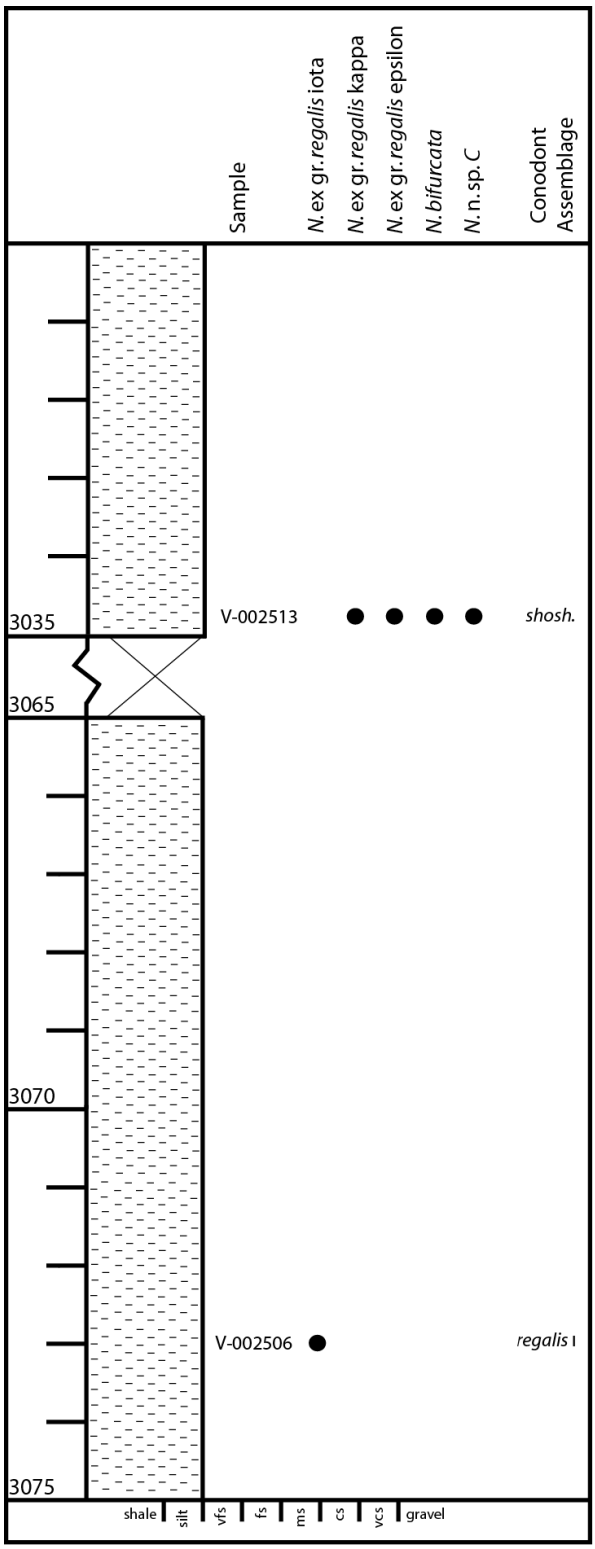



**Figure 2.13.** Stratigraphic log of the core from the Shell Groundbirch 16-02-078-22W6 well, showing the location and composition of conodont samples from this core, and the position of conodont faunal assemblages present. Shosh. = *shoshonensis* faunal assemblage.

***N. ex gr. regalis θ Faunal Assemblage***

The base of this faunal assemblage is defined by the first appearance of *N.* ex gr. *regalis* morphotype θ, which is restricted to this assemblage. *N.* ex gr. *regalis* morphotype ε is also restricted to this assemblage. The last appearances of *N.* ex gr. *regalis* morphotypes α and γ and *N.* n. sp. A occur in this assemblage, and *N.* ex gr. *regalis* morphotype ι is also present. In the Mile Post 375 East section, *N.* ex gr. *regalis* θ appears together with *N.* n. sp. A, above the first appearance of that species (fig. 2.9). This assemblage is also observed in the Mile Post 375 West (fig. 2.14), East Toad River I (fig. 2.15), North Tetsa Phosphate (fig. 2.16), Liard-Crusty and North Liard River sections. It occurs with ammonoids of the Hayesi Zone in both the Mile Post 375 East and West sections. The top of this faunal assemblage is defined by the first appearance of *N.* ex gr. *shoshonensis.*

***N. ex gr. shoshonensis Faunal Assemblage***

The base of this faunal assemblage is defined by the first appearance of morphotypes of *N.* ex gr. *shoshonensis.* This assemblage is equivalent in concept to an assemblage zone. The first appearances of *N.* ex gr. *constricta* morphotype ε, *N.* n. sp. C, *N.* n. sp. D and *N.* n. sp. G also occur in this assemblage, as do the last appearances of *N.* ex gr. *regalis* morphotypes β and ι and *N.* n. sp. H. Also present in this assemblage is *N.* ex gr. *constricta* α. This assemblage is observed at the Mile Post 375 West, East Toad River I and North Tetsa Phosphate sections, where it overlies the *N.* ex gr. *regalis* morphotype θ Faunal Assemblage (figs. 2.14, 2.15, 2.16), as well as the sections at East Toad River II (fig. 2.17), North Tetsa Hill, the Shell Groundbirch 16-02-78-22W6 well (fig. 2.13), the Petro-Canada Kobes c-074-G/094-B-09 well and the Murphy Swan

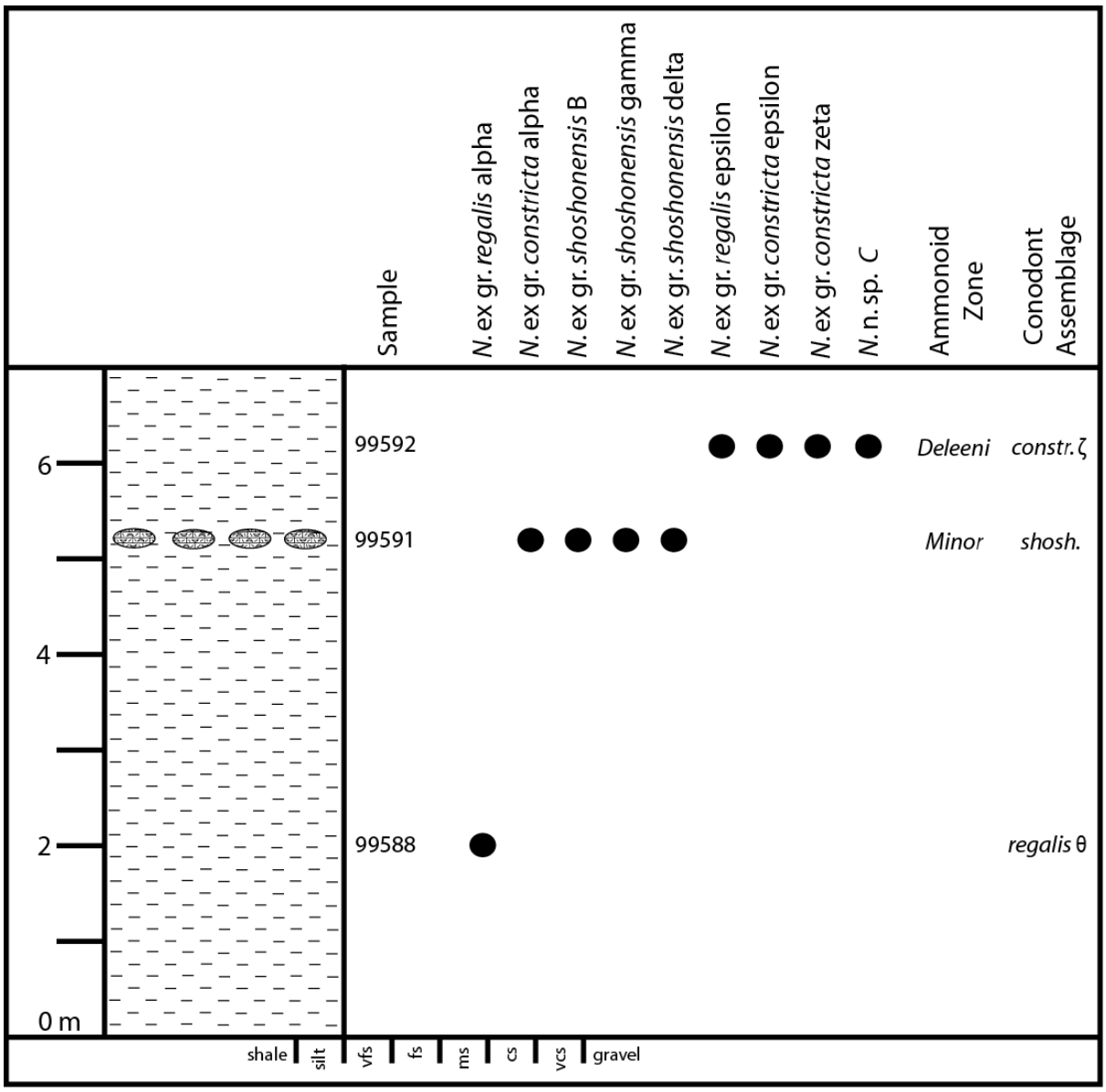



**Figure 2.14.** Stratigraphic log of the section at East Toad River I, showing the location and composition of conodont samples from this section, and the position of ammonoid zones and conodont faunal assemblages present. Shosh. = *shoshonensis* faunal assemblage, constr. ζ = *constricta* ζ faunal assemblage.

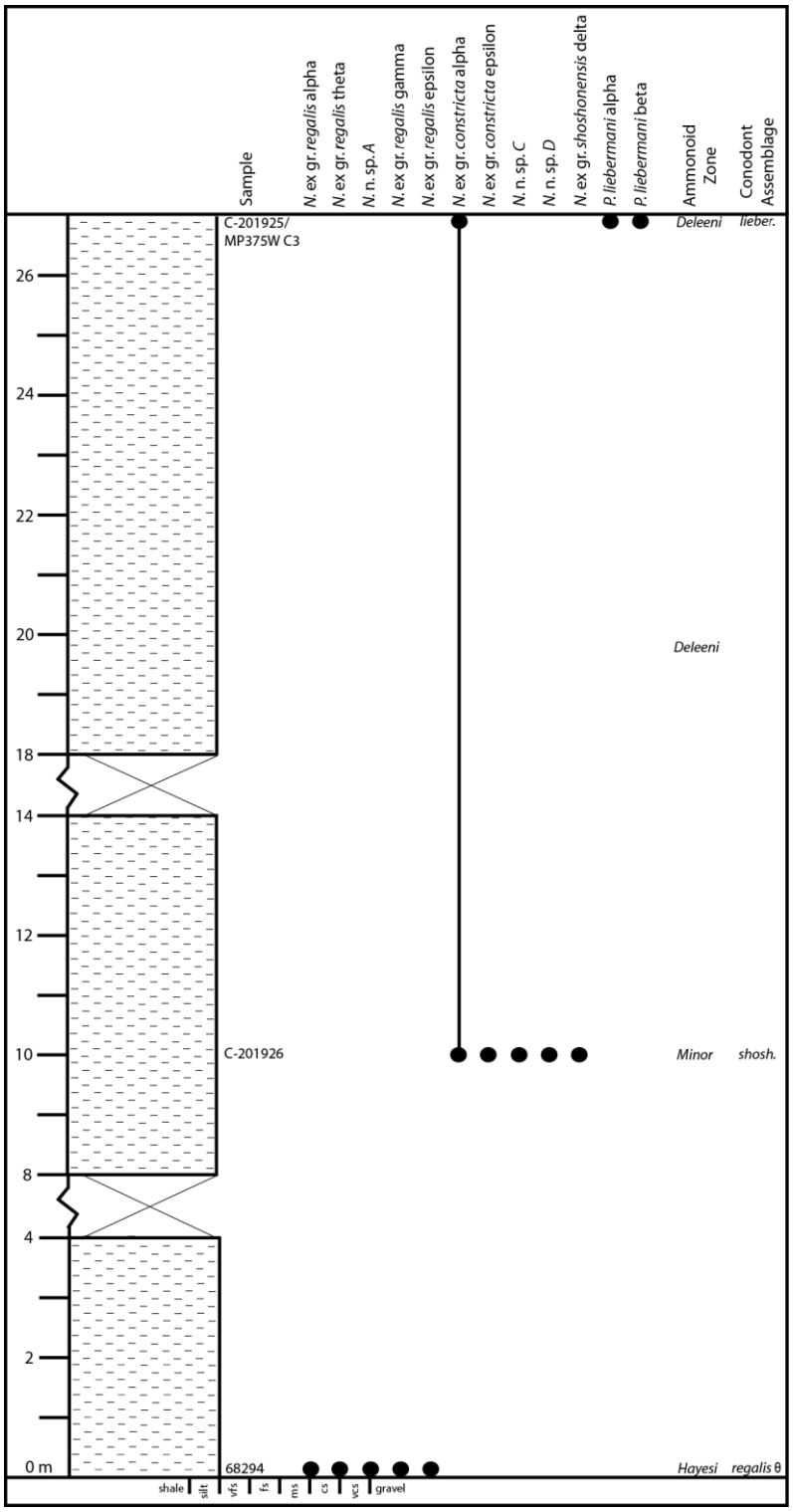



**Figure 2.15.** Stratigraphic log of the section at Mile Post 375 West, showing the location and composition of conodont samples from this section, and the position of ammonoid zones and conodont faunal assemblages present. Shosh. = *shoshonensis* faunal assemblage, lieber. = *liebermani* faunal assemblage.

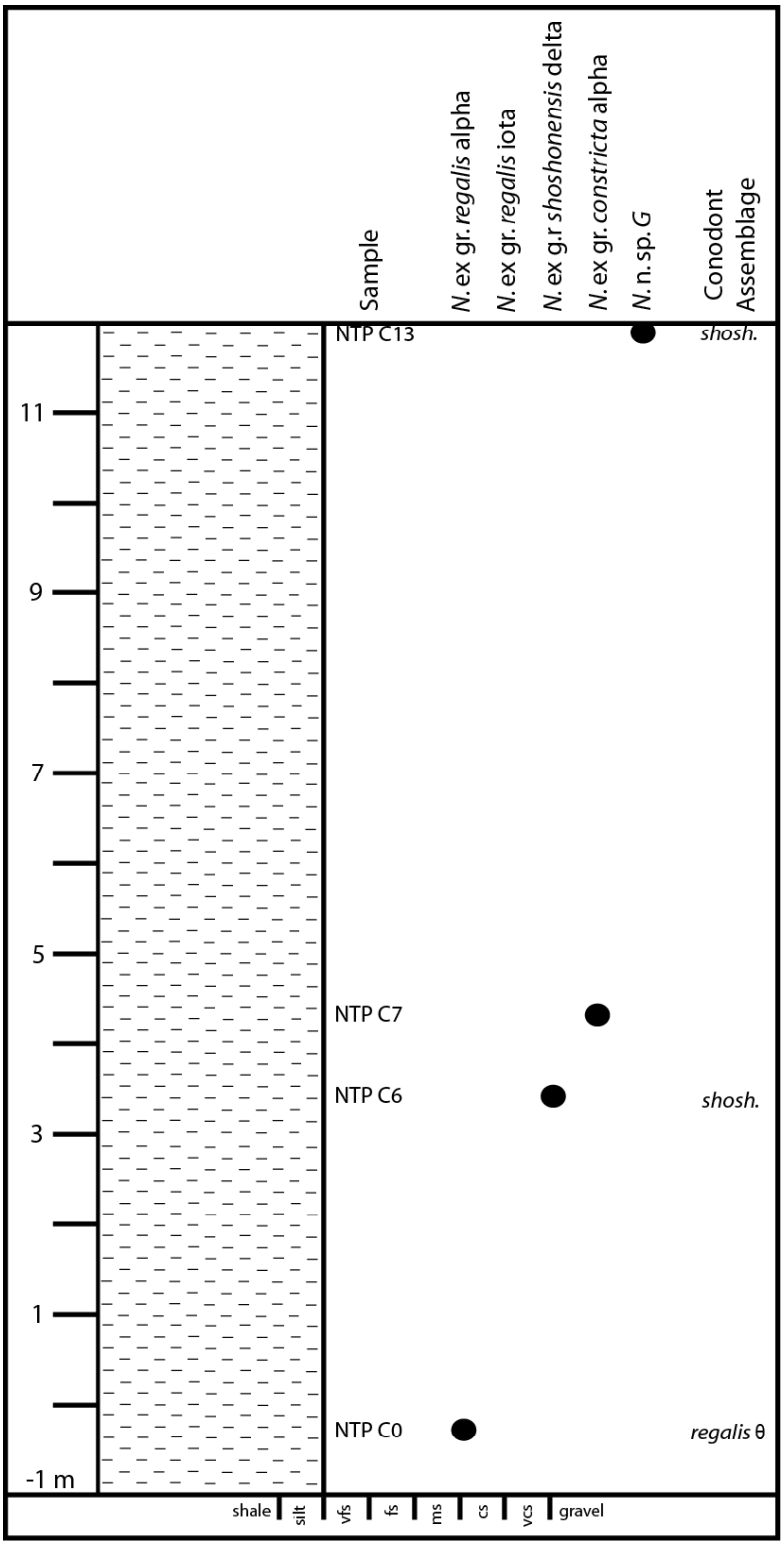



**Figure 2.16.** Stratigraphic log of the section at North Tetsa Phosphate, showing the location and composition of conodont samples from this section, and the position of ammonoid zones and conodont faunal assemblages present. Shosh. = *shoshonensis* faunal assemblage.

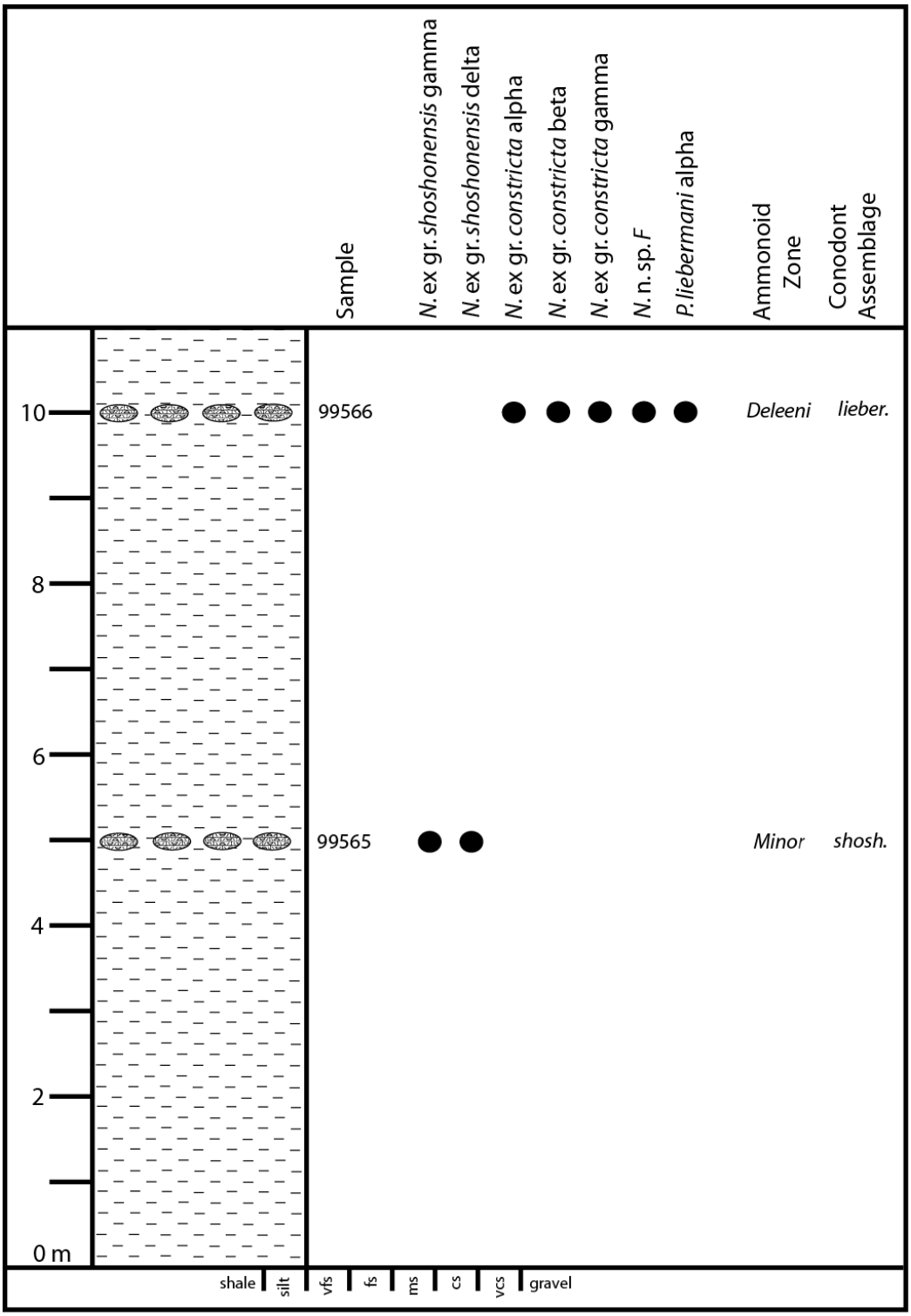



**Figure 2.17.** Stratigraphic log of the section at East Toad River II, showing the location and composition of conodont samples from this section, and the position of ammonoid zones and conodont faunal assemblages present. Shosh. = *shoshonensis* faunal assemblage, lieber. = *liebermani* faunal assemblage.

d-054-B/093-P-09 well (fig. 2.12). Morphotypes of *N.* ex gr. *shoshonensis* occur with ammonoids of the Minor Zone at Mile Post 375 West and East Toad River I. They appear to be restricted to this ammonoid zone, as are *N.* n. sp. D and *N.* n. sp. G. Therefore, this faunal assemblage is considered equivalent to the Minor Zone. The top of the faunal assemblage is defined by the disappearance of *N.* ex gr. *shoshonensis*.

**Upper Anisian**

***N. ex gr. constricta ζ Faunal Assemblage***

The base of this faunal assemblage is defined by the first appearance of *N.* ex gr. *constricta* morphotype ζ. It also contains the first appearance of *N.* ex gr. *constricta* morphotype δ and the last appearances of *N.* ex gr. *constricta* morphotype ε and *N.* n. sp. C. This assemblage is observed at the East Toad River I section (fig. 2.14), where it directly overlies the *N.* ex gr. *shoshonensis* Faunal Assemblage and in talus at the Yellow Bluffs section. It occurs with ammonoids of the Deleeni Zone at East Toad River I. The top of the assemblage is defined by the appearance of *P. liebermani.*

***P. liebermani Faunal Assemblage***

The base of this faunal assemblage is defined by the first appearance of *P. liebermani* morphotypes α and β. It also contains the first appearance of *N.* ex gr. *constricta* morphotypes β and γ and *N.* n. sp. F. Two of these, *N.* ex gr. *constricta* morphotype γ and *N.* n. sp. F, are restricted to this assemblage. It also contains the last appearances of *N.* ex gr. *constricta* morphotypes α, δ and ζ and *N.* n. sp. G. In the Yellow Bluffs section, *P. liebermani* morphotype

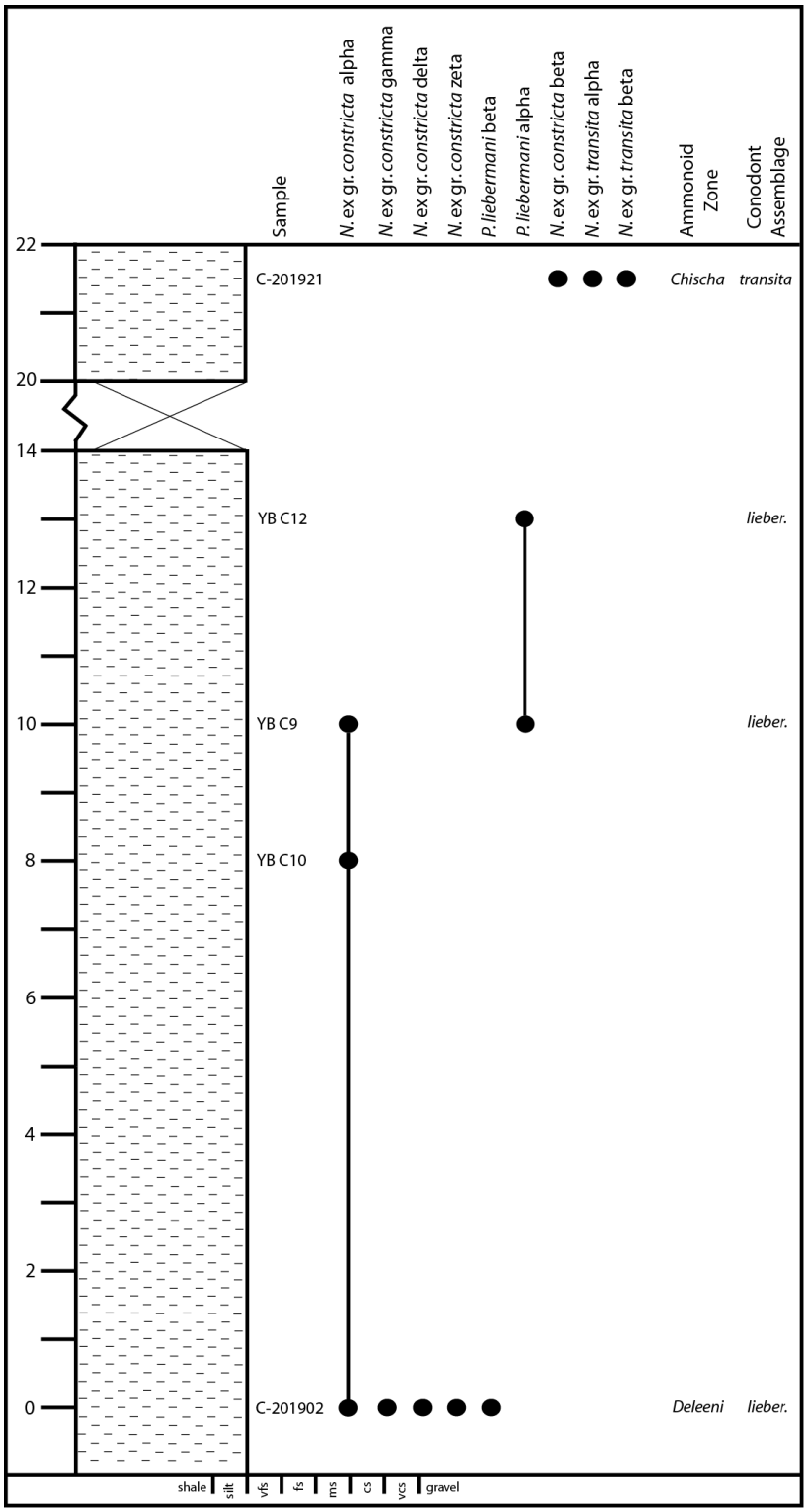



**Figure 2.18.** Stratigraphic log of the section at Yellow Bluffs, showing the location and composition of conodont samples from this section, and the position of ammonoid zones and conodont faunal assemblages present. Lieber. = *liebermani* faunal assemblage.

α occurs first and morphotype β occurs higher in the section (fig. 2.18). In the Mile Post 375 West section the two morphotypes of *P. liebermani* occur together (fig. 2.15). In the East Toad River II section this assemblage occurs above the *N.* ex gr. *shoshonensis* Faunal Assemblage (fig. 2.17). It occurs with ammonoids of the Deleeni Zone at Yellow Bluffs and Mile Post 375 West. The top of this assemblage is defined by the first appearance of *N.* ex gr. *transita. P. liebermani* is not observed in the *N.* ex gr. *transita* Faunal Assemblage, although it is found as high as the Ladinian Meginae Zone in other sections in B.C.

***N. ex gr. transita Faunal Assemblage***

The base of this faunal assemblage is defined by the first appearance of *N.* ex gr. *transita*. It occurs together with *N.* ex gr. *constricta* morphotype β. The assemblage is observed in the Yellow Bluffs section, where it immediately overlies the *P. liebermani* Faunal Assemblage (fig. 2.18) and in the Oyster Springs section. It occurs with ammonoids of the Chischa Zone at Yellow Bluffs. The top of this assemblage is undefined, as the strata immediately overlying the Chischa Zone in B.C. have not been sampled as part of this study. Unpublished data from Nevada suggests that similar morphotypes of *N.* ex gr. *transita* occur in the Ladinian Subasperum Zone (approximately equivalent to the Matutinum Zone in B.C.).

## 2.6 COMPARISON WITH AMMONOID ZONATION IN B.C.

The new conodont scheme allows refinements of some parts of the Anisian timescale in B.C. that were not possible using the existing ammonoid scheme. It allows the recognition of the upper and lower parts of the Caurus ammonoid Zone; it improves the resolution within the Hayesi ammonoid Zone, recognising three assemblages equivalent to this zone; and also within the Deleeni ammonoid Zone, where two assemblages are recognised.

In some parts of the stratigraphic column, however, the new scheme does not represent as much of an improvement. No samples were collected from the Mulleri or Hagei ammonoid Zones and so the conodont scheme has gaps equivalent to these zones at the moment. The new conodont assemblages do not represent an improvement in the resolution of the Minor or Chischa ammonoid Zones.

## 2.7 CORRELATION

Some of the taxa recognised in this study are found in Arctic Canada, Nevada and Europe, allowing correlation between these areas and B.C.

All five of the species groups defined in this study have representatives in the Anisian of Nevada, Europe, or both. *N.* ex gr. *constricta* appears earlier in B.C. than in Nevada (Hayesi Zone opposed to Rotelliformis Zone), and continues for longer into the Ladinian (Meginae Zone opposed to Subasperum Zone; Nicora and Kovács, 1984). In Europe, again it appears later (Balatonicus Zone) and disappears earlier (Poseidon Zone) than in B.C (Kovács and Kozur, 1980).

So far, *N.* ex gr. *transita* has only been described from the Upper Anisian of B.C., whilst in Nevada it ranges from the Lower Anisian to the Ladinian (Nicora, 1976; Kozur *et al.*, 1994). In Europe, it straddles the Anisian-Ladinian boundary, ranging from Illyrian to Fassanian (Budurov and Stefanov, 1972, 1973, 1984).

*N.* ex gr. *regalis* has been identified in Europe, ranging from the Aegean to the Bithynian (Kovács and Kozur, 1980). In Nevada, it once again has a shorter range than in B.C., appearing

only in the Hayesi Zone (compared to the Subrobustus Zone) and disappearing in the Minor Zone (opposed to the Deleeni Zone; Mosher, 1973).

*N.* ex gr. *shoshonensis* has a much longer range in Nevada than in B.C. It appears in the Shoshonensis Zone and ranges up into the Occidentalis Zone in Nevada (Nicora, 1976), whilst in B.C. it is restricted to the Minor Zone. In Europe, however, it is restricted to the Trinodosus Zone, which is slightly younger than the Minor Zone in B.C (Nicora, 1976).

*P.* ex gr. *excelsa* has not been described from Nevada. Its range in Europe is broad, from the Trinodosus Zone in the Illyrian to the Archelaus Zone (=Neumayri Zone; Mietto and Manfrin, 1995) in the Longobardian (Kovács, 1994). It occurs earlier in B.C. (Hayesi Zone) and disappears at approximately the same time (Meginae Zone).

Other taxa recognised in this study can also be found in various sections in Arctic Canada, Nevada and Europe. *N.* n. sp. E is known from the Canadian Arctic (Orchard, 2008), where it occurs in the Svartfjeld Member of the Blind Fiord Formation at Spath Creek. Its occurrence here is just above that of ammonoids belonging to the Subrobustus Zone (Tozer, 1967). This is uppermost Spathian. *N.* n. sp. E does not occur with ammonoids in B.C.; however, it does appear with other conodonts that in turn are found only with conodonts belonging to the Caurus II Subzone (Lower Anisian). This species is likely to be restricted to the uppermost Spathian and lowest Anisian. In Nevada it is known from the Lower Anisian Welteri Zone (Orchard, 2008), which is thought to be slightly older than the Caurus Zone (Bucher, 1989).

*N. bifurcata* is found in the Shoshonensis Zone to the Occidentalis Zone of Nevada. In B.C., this species occurs earlier, during the Hayesi Zone (= Hadleyi Subzone of Nevada) and disappears earlier, in the Minor Zone (= Taylori and lowermost Shoshonensis Zones of Nevada). In Europe,

it ranges from the base of the Bithynian to the lower Illyrian (Kovács and Rálisch-Felgenhauer, 2005).

It is obvious from the above that the ranges of some of these groups are clearly quite distinct in different areas. This is likely because of broad taxonomic concepts used in the past to define species and groups of species, which obscures the true stratigraphic range of the groups. Continued revision of these species or species groups should allow the recognition of better defined species, with amended stratigraphic ranges. This in turn will allow the refinement of correlations between different parts of the world during the Anisian. At present, the best defined cosmopolitan species, *N. bifurcata*, also has the longest stratigraphic range and so is less helpful for precise global correlation.

The conodont faunal assemblages recognised in this study clearly have regional significance and allow correlation across B.C., including from the surface to the subsurface. This is one of the major benefits of utilising conodonts for stratigraphic purposes; they are abundant often when other fossils such as ammonoids are absent. This allows stratigraphic ages to be determined in areas such as subsurface B.C., where ammonoid fossils are virtually absent from the whole of the Triassic, due to the limited amount of rock collected during drilling. At present, these faunal assemblages are not recognised outside of B.C. However, it is hoped that further work on specimens from Nevada will allow recognition of similar assemblages there, and lead to more precise correlation. Further collection of samples from both Nevada and B.C., in between ammonoid horizons, should also allow the sequence of conodont faunas to be confirmed, rejected or improved. It will also lead to the filling in of gaps in the stratigraphic record of the Anisian, which are caused in part by the discontinuous nature of the ammonoid occurrences. At

present, the ammonoid zonation for the Anisian is most complete in Nevada and gaps in the record have been noticed in B.C. Conodont collections from B.C. and Nevada will help to close these gaps and improve calibration between the two ammonoid faunas, and allow correlation of Anisian strata over much of North America.

## 2.8 SUMMARY

The recognition of 22 new morphotypes and seven new species of conodont from the Anisian of B.C. represents an important first step in the revision of the Gondolellidae. The use of species groups and morphotypes illustrates the broad range of morphological diversity within some of the traditionally defined species. Some of these morphotypes also have stratigraphic significance, as evidenced by their inclusion in the new timescale. This may suggest that they represent more than just intraspecific variability, and in fact may be new species in and of themselves that have evolved at a particular time.

*N.* ex gr. *regalis* shows the greatest range of morphological diversity, with as many as ten morphotypes. Some of these are clearly separated by time, for example the Lower Anisian is characterised by morphotypes α, β, δ, and ζ, whilst the Middle Anisian includes morphotypes γ, ε, θ and ι. There may be a case for separating these morphotypes into separate species based on their different stratigraphic range. Morphotypes such as morphotypes γ and ζ may also represent new species due to their unique platform morphologies.

*N.* ex gr. *constricta* is also diverse. Again, a number of these morphotypes may be separated from the species, or the species may be raised to generic level to incorporate the diversity at the species level. *N. constricta* could be retained for the forms that can be clearly linked with the

constricted juveniles, such as morphotypes α and β. The adult morphotypes would be considered independent species, as *N. balkanica* and *N. cornuta* are; these two species can be clearly recognised by reference to the holotypes, and they can be shown to exist in Nevada as well as in Tethys, and so it is probably not advisable to consider such well defined species as merely morphotypes of *N. constricta*, even if the juveniles are similar. It may be more useful to consider the juveniles as being similar in all three species. When they have been considered as separate species, the stratigraphic range of *N. balkanica* and *N. cornuta* appears to be similar but not identical to that of *N. constricta* s.s.

*N.* n. sp. G appears to be transitional between species belonging to the *N. constricta* group and those belonging to the *N. shoshonensis* group. *N.* ex gr. *constricta* appears first in B.C., with morphotype α occurring in the n. sp. A Faunal Assemblage (within the Hayesi Zone). *N.* n. sp. G then occurs in the *shoshonensis* Faunal Assemblage, together with morphotypes of *N.* ex gr. *shoshonensis*. The earlier appearance of *N.* ex gr. *constricta* would suggest that it is the ancestor of *N.* n. sp. G and *N.* ex gr. *shoshonensis*; however, because the latter two species apparently appear together, it is not clear if *N.* n. sp. G is a true transitional form, or another side-branch in this evolutionary lineage. Such a lineage cannot be recognised in Nevada, where the first occurrence of *N.* ex gr. *constricta* is above that of *N.* ex gr. *shoshonensis* (Nicora and Kovács, 1984).

The Middle Anisian and lower part of the Upper Anisian contain the majority of the species belonging to *N.* ex gr. *constricta*. In the uppermost Anisian and Ladinian, the faunas are instead dominated by *N.* ex gr. *transita*. These groups share a number of morphological features and therefore may be closely related. This pattern of replacement of *N.* ex gr. *constricta* with *N.* ex

gr. *transita* in the Upper Anisian is also seen in Nevada, with *N.* ex gr. *transita* appearing alongside *N.* ex gr. *constricta* in the Occidentalis Zone (Upper Anisian) and continuing on its own into the Subasperum Zone (Ladinian).

The new species recognised as part of this study would previously have been categorised as *N. regalis, N. constricta* or even *N. mombergensis*. It is clear from looking at multiple specimens from separate localities that these new species show distinct morphological features. Comparison of the new species with the holotypes of *N. regalis, N. constricta* and *N. mombergensis* also precludes their assignment to these existing species. The new species represent only the most robust species concept; it is likely that as work continues, other morphotypes will come to be considered as new species, or become further split.

This study represents only the first step in a comprehensive revision of the Anisian Gondolellidae. Further work is required, but this revision has already led to the recognition of eleven new conodont faunal assemblages that can be used to divide the Anisian in B.C. Most of these assemblages can be correlated directly with the well established ammonoid zones, and in some cases they represent an improvement in precision over these zones. A number of them can also be recognised in the subsurface, which demonstrates the usefulness of a conodont scheme in correlating between areas which are devoid of ammonoids. Some of the assemblages are equivalent to interval zones and some are akin to assemblage zones. The scheme as it stands is therefore not ideal; a scheme based solely upon interval zones that can be tied to a specific section of rock is desirable (Tozer, 1971). A number of the faunal assemblages have only been observed in one section thus far and should be regarded as less reliable than those that appear in more than one section. Further collecting will allow the extent and reality of these assemblages

to be assessed. This will be an important step towards defining zones in place of the faunal assemblages. Further work on Nevadan faunas will allow us to tell whether these faunal assemblages can be correlated into Nevada and if they have regional as well as local utility.

## 2.9 CONCLUSIONS

- A total of 31 conodont taxa are recognised from the Anisian of B.C. Of these, 22 are new morphotypes belonging to five existing species groups and seven are new species.
- The recognition of these new taxa has allowed the creation of a conodont biostratigraphic scheme for the Anisian, consisting of a succession of 11 conodont faunal assemblages.
- These assemblages are defined as equivalent to either interval biozones or assemblage biozones.
- The majority of the assemblages can be tied directly to the existing ammonoid biozonation for the Anisian of B.C., and in some instances a number of conodont faunal assemblages can be recognised within the range of one ammonoid zone.
- These faunal assemblages allow correlation between the surface outcrop and subsurface of B.C. and are therefore useful at a local scale.
- Some of the new conodont taxa can be recognised in the Anisian of Nevada. Further work should allow the creation of a similar sequence of faunal assemblages in Nevada that can be correlated with the one presented in this study for B.C. This would make the conodont scheme more regional in utility.

## 2.10 SYSTEMATIC PALAEONTOLOGY

The family Gondolellidae (Lindström, 1970) includes a wide variety of genera that are united primarily on the basis of similarity between their multielement apparatuses (Orchard, 2005). A typical *Neogondolella* multielement apparatus is shown in figure 2.19 to illustrate the form of these elements and to define the multielement terminology used in this paper, which follows that of Purnell *et al.* (2000). The family has been divided up further into seven subfamilies by Orchard (2005). Although this suprageneric classification is based mainly upon the structure and morphology of the multielement apparatus, it is clear that the greatest morphological diversity within the Gondolellidae is displayed by the P1 elements. These elements have traditionally been used to define species and genera, and are of more use for biostratigraphy than the relatively conservative ramiform elements. Most of the specimens of Gondolellidae from the Anisian of North America have previously been referred to one of two genera: *Neogondolella* or *Paragondolella*. Anisian samples are dominated by these two genera. Specimens belonging to these genera however show relatively little morphological variation, and therefore only a few species names have been applied. The majority of specimens from the Anisian of North America have been assigned to one of six species: *N. mombergensis, N. bulgarica, N. constricta, N. regalis, N. shoshonensis* and *P. excelsa.* These names have been applied to a wide range of morphologies, which has obscured variation and in turn led to a very coarse resolution for conodont biostratigraphic schemes covering this interval. Ritter (1989) went so far as to consider all of the Anisian conodonts in Nevada as belonging to *N. mombergensis*. *N. mombergensis* and *N. bulgarica* were both defined in Europe and it is not clear that any specimens from B.C. can be assigned to either of these species on the basis of comparison with the holotypes. Both of these species are in need of taxonomic revision; however, this is beyond the scope of this study.

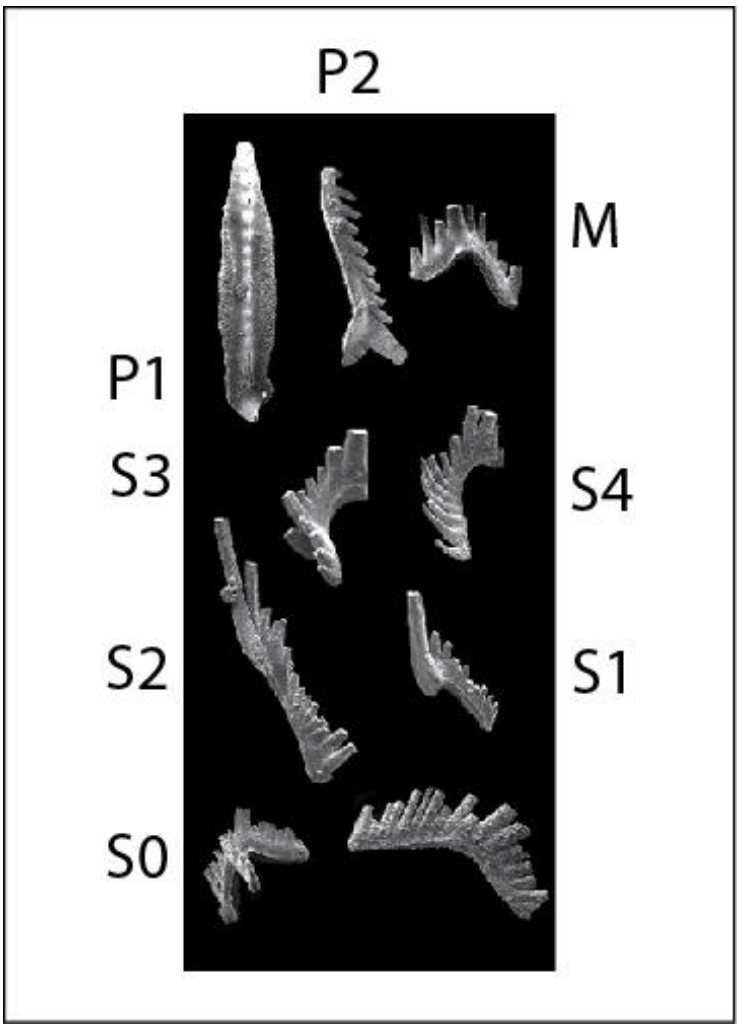



**Figure 2.19.** A standard multielement apparatus of *Neogondolella* (this example is *N.* ex gr. *constricta* from the Ladinian Prida Formation of Fossil Hill, Nevada). From Orchard (2005); apparatus nomenclature after Goudemand *et al.* (2012 b).

.Specimens representing the remaining four species as well as *N. transita* have been recovered during this study. All of these species show great morphological variation and therefore it has been practical to refer instead to species groups (*N.* ex gr. *constricta*, *N.* ex gr. *transita*, *N.* ex gr. *regalis*, *N.* ex gr. *shoshonensis* and *P.* ex gr. *excelsa*) consisting of morphotypes. The group concept recognises the range of morphological variation whilst still implying close relationship between these morphotypes. Further study will determine which, if any, of the morphotypes are

the most robust, and these can then be elevated to species status. Alternatively, if a large number of the morphotypes are considered to represent real taxonomic entities, then it may be advisable to elevate them to the rank of species, with the species group being raised to genus level. For now, it is considered best to leave most of these morphotypes in open nomenclature, pending further study of their geographic and stratigraphic range, their ontogeny and the composition of their multielement apparatuses. Some specimens are viewed as unique enough to be considered as belonging to new species at this stage; however, they are again kept in open nomenclature for the same reasons as outlined above. The species groups can be defined by the combination of a few morphological characteristics such as the height of the carina and the position of the basal pit. These characteristics are summarised in table 2.3, which includes the five main species groups as well as the seven new species identified in this study.

Species and species groups identified in this study are currently assigned to the genera *Neogondolella* and *Paragondolella*. However, the assignment to the genus *Neogondolella* is somewhat uncertain, especially because the genus is currently defined on its distinctive ramiform elements. Although such elements have been recovered during this study, it has not been possible to match ramiform elements with the platform elements of particular species. The type species of *Neogondolella*, *N. mombergensis*, has a distinctive carina that is lowest in the middle and higher at the anterior and posterior and this has been used by previous workers as a defining feature for *Neogondolella*. However *N.* ex gr. *regalis*, for example, does not share this type of carina. For the moment, species are retained within *Neogonodolella* pending further revision, which may result in the definition of new genera, as stated previously.

The morphological terms applied to Triassic Gondolellidae are sometimes poorly defined, and used in different ways by different authors. An example of this is the term *keel*, which has been used by authors working on Triassic faunas to refer to the grooved attachment surface anterior of the basal cavity, although this is not truly a keel as defined for Palaeozoic conodonts (Kozur, 1989 b). Figure 2.20 shows a "standard" Gondolellid P1 element in three views, with labels indicating the descriptive morphological terminology used in this study. The Gondolellidae here are considered to be part of the order Ozarkodinida (Dzik, 1976), following Dzik (1991) and Donoghue *et al.* (2008; equivalent to their Ozarkodinina).

| | Carina | Basal Pit and Keel | Platform Anterior | Platform Posterior |
|---|---|---|---|---|
| ***N.* ex gr. *constricta*** | Low; rises to anterior and posterior | Pit is terminal within keel | Tapers to end of element | Constricted in juveniles and some adults |
| ***N.* ex gr. *transita*** | Low; rises to anterior and posterior | Keel continues posterior of pit as secondary keel | Tapers to end of element | Constricted |
| ***N.* ex gr. *regalis*** | Uniformly high; may become lower to posterior | Pit is terminal within keel | Tapers to end of element | Variable |
| ***N.* ex gr. *shoshonensis*** | High; rises to anterior and posterior | Pit is terminal within keel | Narrows abruptly | Narrows abruptly |
| ***P.* ex gr. *excelsa*** | High; becomes lower to anterior and posterior | Pit is terminal within keel | Tapers to end of element | Variable |
| ***N.* n. sp. A** | Low; unfused | Pit is terminal within keel | Tapers to end of element | Tapers to end of element |
| ***N.* n. sp. B** | Low; fused | Pit is terminal within keel | Narrows close to end of element | Rounded |
| ***N.* n. sp. C** | Moderately high; moderately fused | Pit is terminal within keel | Tapers to end of element | Narrows near end of element |
| ***N.* n. sp. D** | Low; rises to anterior | Pit is terminal within keel | Tapers to end of element | Variable |
| ***N.* n. sp. E** | Low; rises to anterior and posterior | Pit is terminal within keel | Narrows abruptly | Rounded |
| ***N.* n. sp. F** | Low; becomes lower to anterior and posterior | Pit is terminal within keel | Tapers to end of element | Quadrate |
| ***N.* n. sp. G** | High; becomes lower to the posterior | Pit is terminal within keel | Narrows abruptly | Constricted |

**Table 2.3.** Comparison table showing the variation in major morphological features between the main conodont species groups and new species identified in this study.

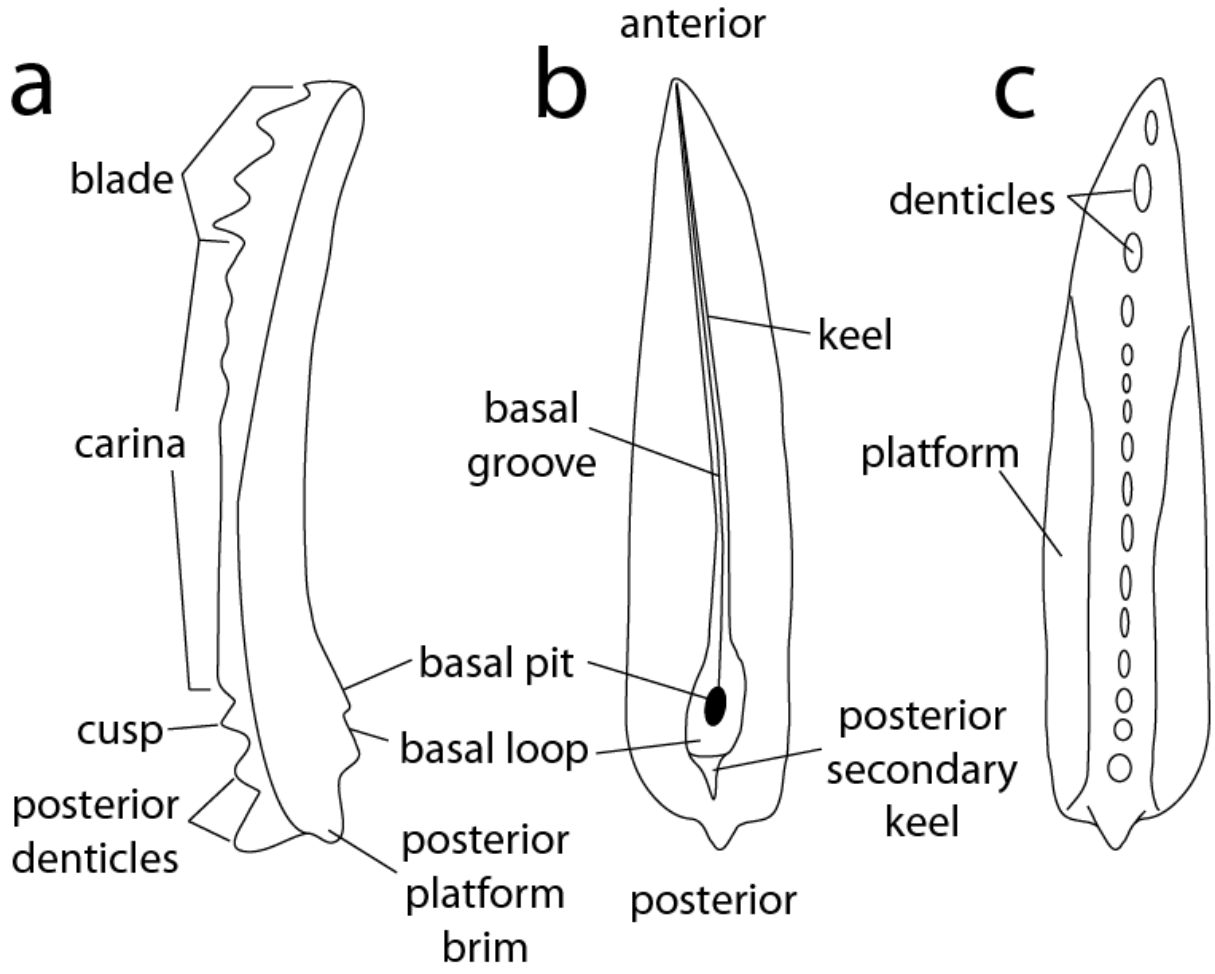



**Figure 2.20.** Three views of a typical P1 element of *Neogondolella* showing the main features referred to in this paper and defining the terminology used; a = lateral view, b = lower view, c = upper view.

## Class CONODONTA Eichenberg, 1930

## Order OZARKODINIDA Dzik, 1976

## Family GONDOLELLIDAE Lindström, 1970

### Genus *Neogondolella* Bender and Stoppel, 1965

*Type Species: Gondolella mombergensis* Tatge, 1956

The genus *Neogondolella* was erected for species of Triassic conodonts similar to *Gondolella,* but without platform ornamentation (Bender and Stoppel, 1965). Since then, a number of different criteria have been used to determine the scope of *Neogonodolella*, including the shape of the carina and the nature of the basal pit. The species that are assigned here to *Neogondolella* are variable in their appearance, but have all been assigned to *Neogondolella* by different authors. It may be appropriate to separate some of these species, in particular the *regalis* group and the *constricta* group, into separate genera in the future.

#### ***Neogondolella bifurcata*** (Budurov and Stefanov, 1972)

Figure 2.21

1972 *Paragondolella bifurcata* n. sp. – Budurov and Stefanov, p. 843, Pl. 1, figs. 1-25, Pl. 2, figs. 1-9.

***Holotype:*** Bu 1039/1; Budurov and Stefanov, 1972, Pl. 1, figs. 1-3.

***Age of Holotype:*** Trinodosus Zone, Illyrian, Anisian, Middle Triassic.

***Type Stratum:*** Unknown.

***Type Locality:*** Golo Bardo Mountains, near Pernik, Bulgaria.

***Diagnosis:*** Species of *Neogondolella* with wedge shaped platform and blunted posterior platform margin. Platform is flat and tapers to the anterior. Carina is high at the anterior end of the element and becomes lower at the posterior end, where it is bifurcated with at least one denticle offset on either side of the carina.

***Description:*** Specimens have a wedge shaped platform that is widest at the posterior of the element and tapers evenly towards the anterior. None of the recovered specimens preserve the anterior of the element. At the posterior of the element, the platform flares to the sides before terminating posterior to the cusp. Some of the elements have lateral platform projections near the posterior due to the degree of this flaring. The posterior of the platform is quadrate to sub-rounded, and a small posterior platform brim is formed. Reticulation is present on the margins of the platform. In side view, the platform is arched, thick and has slightly upturned margins. Denticles are laterally compressed and upright, except for the posteriormost denticles which become inclined. The carina is high and uniformly fused along its length. At the posterior of the element the carina splits into two, with at least one denticle on either side aligned at an acute angle to the rest of the carina. These denticles may be fused to the carina or free, and are inclined posteriorly. Keel is low, flat and broad, terminating in a closed, oval basal loop around the sub-terminal basal pit. Sometimes there are secondary keels present, posterior to the basal loop.

***Comparisons:*** *N. hanbulogi* (Sudar and Budurov) has a similar platform shape but its margins are more strongly upturned. *N. bulgarica* (Budurov and Stefanov) has a terminal cusp with no posterior platform brim. Neither of these species exhibit posterior bifurcation of the carina.

***Remarks:*** Kovács and Papšová (1986) noted that carinal bifurcation is present in a number of species of *Neogondolella* (*Gondolella* of those authors), and therefore claim that it cannot be used as distinguishing feature for *N. bifurcata*. However, those specimens with carinal bifurcation were still included in *N. bifurcata* by Kovács and Papšová, along with other specimens previously assigned to *N. navicula* (Huckriede). In B.C., only examples with a carinal bifurcation have been recovered, and they are restricted to the Hayesi Zone. It is therefore possible that the forms of *N. bifurcata* similar to the holotype, with a bifurcated carina, have a geographical and stratigraphical range that differs from other forms. No juveniles of this species have been observed in our samples; nor is it clear that juveniles of this species have been figured in the literature.

***Occurrence in B.C.:*** *Localities* - GSC Locality C-302187 (93/HB656), Mile Post 375 East; 3034.8 m below Kelly Bushing, Shell Groundbirch 16-02-078-22W6 well.

*Faunal Assemblages* - *N.* n. sp. A Faunal Assemblage to *shoshonensis* Faunal Assemblage.

*Ammonoid Zones* - Hayesi Zone to Minor Zone (Middle Anisian).

***Other Occurrences:*** Shoshonensis Zone (Middle Anisian) to Occidentalis Zone (Upper Anisian) of Nevada (Nicora, 1976); Ismidicus Zone (Bithynian) to Balatonicus Zone (Pelsonian) of Turkey (Nicora, 1976); Osmani Zone (Bithynian) to Trinodosus Zone (Illyrian) of Hungary (Kovács and Rálisch-Felgenhauer, 2005); Balatonicus Zone (Pelsonian) to Trinodosus Zone (Illyrian) of former Yugoslavia (Sudar, 1982); Lower Pelsonian to Lower Illyrian of Slovakia and Bulgaria (Budurov and Stefanov 1972; Kovács and Papšova, 1986; Pevný and Salaj, 1997); Illyrian of Italy (Pisa *et al.*, 1980) and Germany (Rafek, 1977).

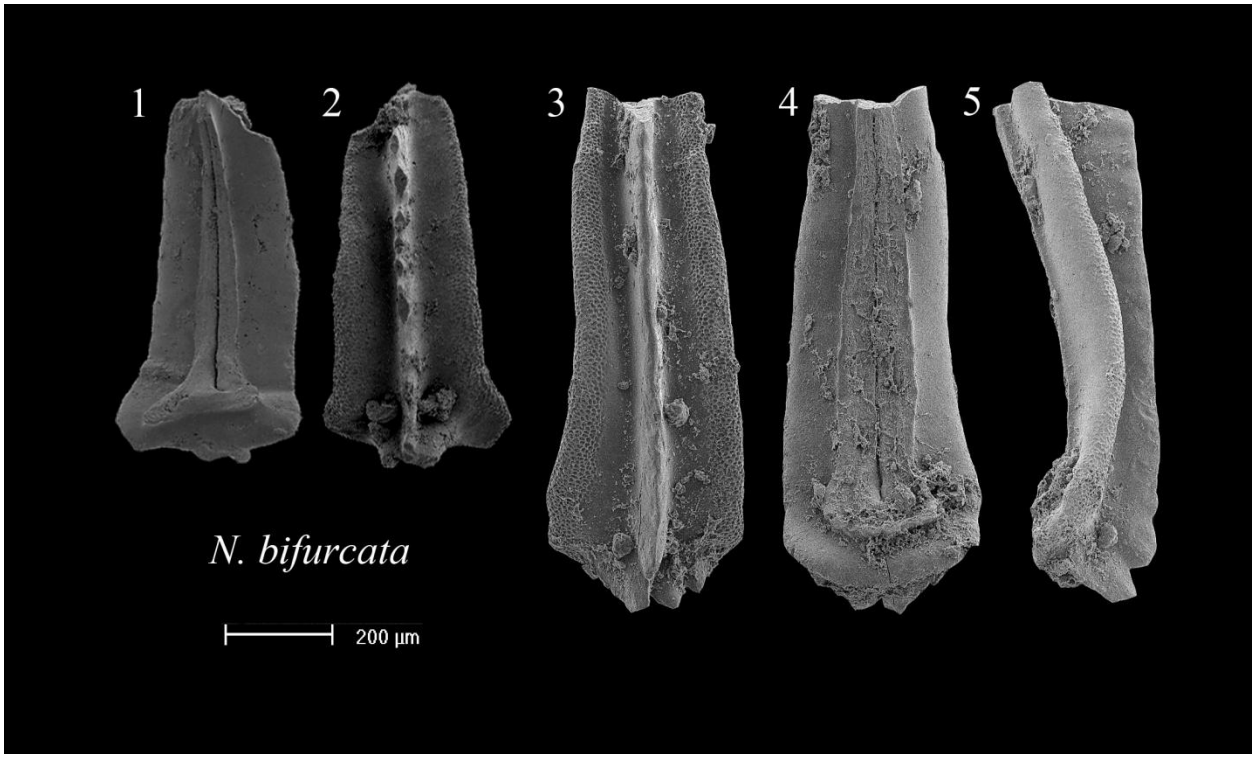



**Figure 2.21.** *Neogondolella bifurcata* (Budurov and Stefanov, 1972). 1-2, GSC Locality C-302187, Mile Post 375 East. 3-5, 3034.8 m below Kelly Bushing, Shell Groundbirch 16-02-078-22W6 well.

***Neogondolella* ex gr. *constricta*** (Mosher and Clark)

Figures 2.22 – 2.27

***Central Species:*** *Gondolella constricta* Mosher and Clark, 1965

1965 *Gondolella constricta* n. sp. – Mosher and Clark, p. 560, Pl. 65, figs. 11, 14, 15, 18, 19, 21, 22, 24, 25.

***Holotype:*** USNM 145189, US National Museum; Mosher and Clark, 1965, Pl. 65, figs. 21, 24, 25.

***Age of Holotype:*** Rotelliformis Zone of the Late Anisian, Middle Triassic.

***Type Stratum:*** Prida Formation.

***Type Locality:*** Sample FH-3, Fossil Hill, Nevada.

***Allied Taxa:*** *N. cornuta* Budurov and Stefanov, 1972

*N. balkanica* Budurov and Stefanov, 1975

*G. constricta* morphotypes α and β Kovács *et al.*, 1990

*G. constricta postcornuta* Kovács, 1994

***Key Features:*** This group is introduced to accommodate common Middle Triassic specimens of *Neogondolella* that share certain morphological characteristics. Species of this group all have narrow platforms. The posterior of the platform may be constricted in front of the cusp; sometimes this is present in small growth stages but disappears with growth. The carina is low in the middle, rising to both the anterior and posterior. This forms a pseudo-blade at the anterior of the element. The pit is terminal with respect to the keel.

***Description:*** Platform margins vary from biconvex to sub-parallel, with the widest part of the platform either at midpoint or in the anterior third of the element. Platform extends all the way to the anterior end of the element, leaving no free blade. In some morphotypes, a platform brim is always present, whilst in others a brim only develops in adult specimens. Platform is always constricted at the posterior in juveniles; sometimes this constriction disappears with growth. Reticulation is present on the margins of the platform. In side view, elements are arched and platform is thin with upturned margins, becoming thicker with growth. Cusp is always large and

varies from upright to posteriorly inclined. Sometimes it is terminal, but often there is a posterior denticle that may become larger than the cusp in adults. Carina is low, becoming higher to the anterior. Denticles are free in juveniles and fused in adults, often more strongly in the middle of the carina, becoming more discrete to the anterior. They are inclined and asymmetrical. Keel is low and narrow in juveniles, becoming wider with growth. It terminates in a rounded to sub-rounded, closed basal loop surrounding a deeply excavated, subterminal basal pit.

***Comparisons:*** *N.* ex gr. *regalis* has a much higher and more fused carina and lacks a posterior platform constriction at any growth stage. *P. szaboi* (Kovács) also has a higher, more fused carina. *N. mombergensis* (Tatge) has a similar carina to *N.* ex gr. *constricta,* but again lacks posterior platform constriction at any growth stage. *N.* ex gr. *transita* has a secondary keel formed posterior to the basal loop.

***Remarks:*** Nicora and Kovács (1984) united *N. constricta* with *N. cornuta* and *N. balkanica.* These authors considered *N. constricta* to represent the juvenile form of the species, whilst *N. cornuta* and *N. balkanica* represented two morphotypes of the mature stage. Kovács *et al.* (1990) referred to these two morphotypes as morphotype α and β. These authors also introduced two further morphotypes of *N. constricta*: morphotype $\alpha_1$ (which is equivalent to *N. longa* Budurov and Stefanov) and morphotype γ. Kozur *et al.* (1994) considered morphotype γ to represent *N. mesotriassica* (Kozur and Mostler) and separated all four morphotypes from *N. constricta* into individual species again. In this study, *N. longa* and *N. mesotriassica* are considered to be part of *N.* ex gr. *transita* (see below). No indisputable representatives of *N. cornuta, N. balkanica* or *N. constricta postcornuta* were identified in our samples. Instead, populations of a number of different morphotypes of *N.* ex gr. *constricta* could be identified, with adult specimens that do

not resemble *N. cornuta*, *N. balkanica* or *N. constricta postcornuta*. In B.C., at least, it appears as though these species may be absent. Budurov and Sudar (1989) erected the genus *Pridaella* for a number of species including *N. cornuta*, *N. balkanica* and *N. constricta*, based on a multielement apparatus that was never figured. This genus name may be available in a more restricted sense for this group. The apparatus of *N.* ex gr. *constricta* has been figured by Orchard and Rieber (1999) and Orchard (2005), and appears to be the similar to those belonging to other species of *Neogondolella.* For now, it is appropriate to consider all the species named above as members of *N.* ex gr. *constricta,* until a more comprehensive revision of these species can be undertaken. In addition, the seven new morphotypes belonging to *N.* ex. gr. *constricta* that are recognised here are kept in open nomenclature pending such a revision.

***Occurrence in B.C.:*** Hayesi Zone (Middle Anisian) to Meginae Zone (Ladinian).

***Other Occurrences:*** Members of the *N. constricta* group have been reported from the Rotelliformis Zone (Upper Anisian) to Subasperum Zone (Ladinian) of Nevada (Nicora and Kovács, 1984); Balatonicus Zone (Pelsonian) to Poseidon Zone (Ladinian) of Hungary (Kovács and Kozur, 1980); Pelsonian to Fassanian of Slovakia (Pevný and Salaj, 1997), Slovenia (Kolar-Jurkovšek, 1983) and Bosnia (Sudar, 1986); Illyrian to Fassanian of Bulgaria (Budurov and Stefanov, 1972) and Poland (Zawidzka, 1975; Trammer, 1975); Illyrian of Germany (Rafek, 1977).

*Morphotype α*

Figure 2.22

***Diagnosis:*** Morphotype of *N.* ex gr. *constricta* with posterior platform constriction in juveniles that becomes diminished in larger specimens. Platform brim is absent in juveniles, but develops in larger specimens. Posterior denticle is always present, with a similar posterior inclination to the cusp. In juveniles, the cusp is larger than the posterior denticle, but with growth the posterior denticle becomes larger than the cusp.

***Comparisons:*** *N.* ex gr. *constricta* morphotype β has both a posterior platform brim and a posterior platform constriction at all stages of growth. *N.* ex gr. *constricta* morphotype γ has parallel rather than biconvex platform margins. Large specimens of *N.* ex gr. *constricta* morphotype δ have a rounded posterior platform margin and a large terminal cusp. *N.* ex gr. *constricta* morphotype ε has a rounded posterior platform margin and a more robust cusp and posterior denticle. Large specimens of *N.* ex gr. *constricta* morphotype ζ have more parallel platform margins, a quadrate posterior margin and no posterior denticle. *N. lindstroemi* Budurov and Stefanov has a similar platform outline and carina to medium growth stages, but does not have the distinctive cusp and posterior denticle.

***Remarks:*** Some specimens show weak crenulation on the anterior third of the platform margins. This feature is similar to that seen in younger species of *Neogondolella* (such as *N. liardensis* Orchard) and *Paragondolella* (such as *P. inclinata* (Kovács)).

***Occurrence in B.C.:*** *Localities* - GSC Locality 99591 (83/215E), East Toad River I; GSC Locality 99566 (83/205B), East Toad River II; GSC Locality C-201902 (92/AH2), Sample YB C9 and Sample YB C10, all Yellow Bluffs; Sample NTP C7, North Tetsa Phosphate; GSC Locality C-201926 (92/AH26) and Sample MP375W C3, both Mile Post 375 West; GSC Locality C-302187 (93/HB656), Mile Post 375 East.

*Faunal Assemblages* - *N.* n. sp. A Faunal Assemblage to *liebermani* Faunal Assemblage.

*Ammonoid Zones* - Hayesi Zone (Middle Anisian) to Deleeni Zone (Upper Anisian).

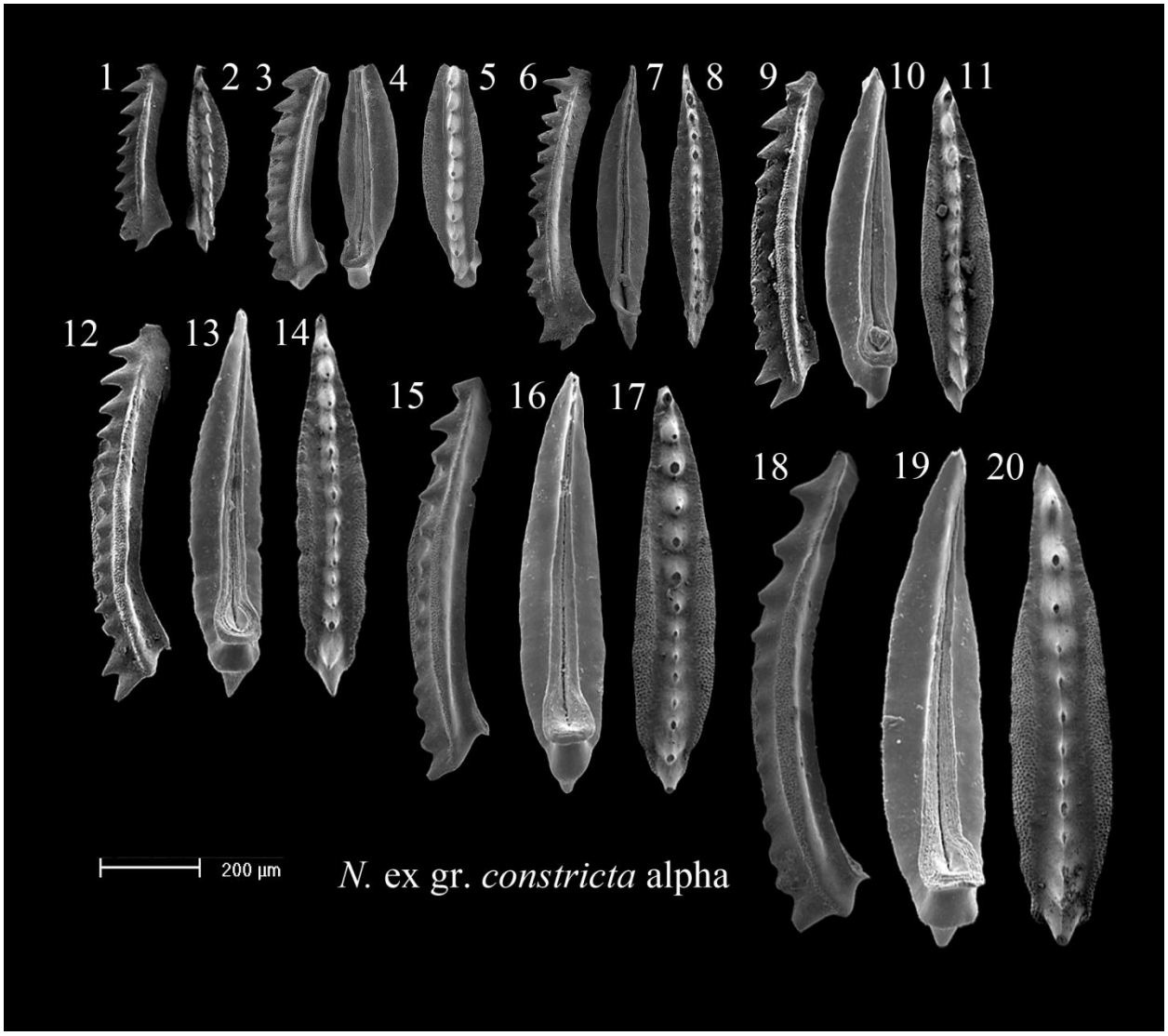



**Figure 2.22.** *Neogondolella* ex gr. *constricta* morphotype α. 1-2, 9-14, GSC Locality 99566, East Toad River II. 3-5, NTP C7, North Tetsa Phosphate. 6-8, GSC Locality C-201926, Mile Post 375 West. 15-20, GSC Locality C-201902, Yellow Bluffs.

*Morphotype β*

Figure 2.23

***Diagnosis:*** Morphotype of *N.* ex gr. *constricta* with a posterior platform constriction that is present at all growth stages. A thin posterior platform brim is present at all growth stages, as is a posterior denticle. In juveniles the cusp is larger than the posterior denticle, but with growth the denticle becomes larger than the cusp.

***Comparisons:*** *N.* ex gr. *constricta* morphotype γ has parallel rather than biconvex platform margins. *N.* ex gr. *constricta* morphotypes δ and ε have rounded posterior margins. Juveniles assigned to *N. lindstroemi* are similar to the juveniles of *N.* ex gr. *constricta* morphotype β, however the adults of *N. lindstroemi* develop a much broader platform with no posterior constriction. Morphotypes of *N.* ex gr. *shoshonensis* have a higher carina than *N.* ex gr. *constricta* morphotype β and a platform that narrows to the posterior rather than becoming constricted. *N.* n. sp. G has a higher carina and lacks a posterior platform brim.

***Occurrence in B.C.:*** *Localities* - GSC Locality 99566 (83/205B), East Toad River II; Sample OS C2, Oyster Springs; GSC Locality C-201921 (92/AH21), Yellow Bluffs.

*Faunal Assemblages* - *liebermani* Faunal Assemblage to *transita* Faunal Assemblage.

*Ammonoid Zones* - Deleeni Zone to Chischa Zone (Upper Anisian).

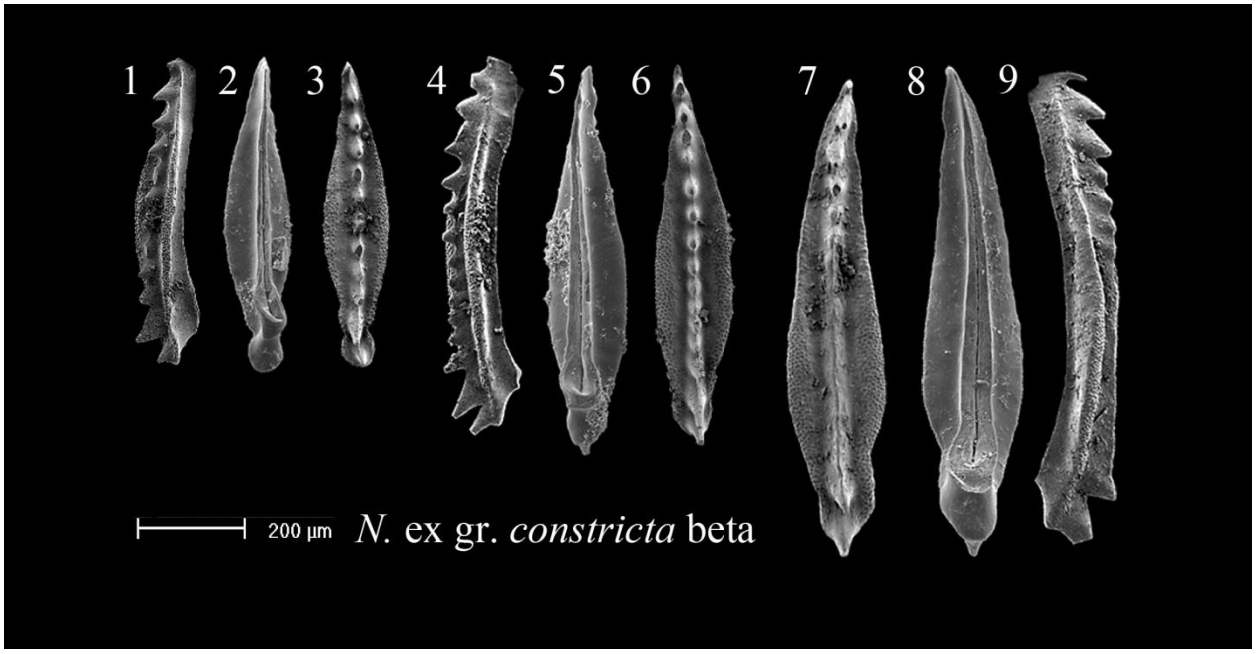



**Figure 2.23.** *Neogondolella* ex gr. *constricta* morphotype β. 1-6, GSC Locality C-201921, Yellow Bluffs. 7-9, GSC Locality 99566, East Toad River II.

*Morphotype γ*

Figure 2.24

***Diagnosis:*** Morphotype of *N.* ex gr. *constricta* with parallel to sub-parallel platform margins. Posterior platform constriction and posterior platform brim both present at all growth stages. Posterior denticle always present; it is much smaller than the cusp in juveniles, but becomes larger than the cusp in larger growth stages.

***Comparisons:*** *N.* ex gr. *constricta* morphotype δ does not possess such a strong posterior platform constriction. *N.* ex gr. *constricta* morphotype ε has a rounded posterior margin and a more robust cusp and posterior denticle. *N.* ex gr. *constricta* morphotype ζ does not have a posterior platform constriction or posterior denticle.

***Occurrence in B.C.:*** *Localities* - GSC Locality 99566 (83/205B), East Toad River II; GSC Locality C-201902 (92/AH2), Yellow Bluffs.

*Faunal Assemblages* - *liebermani* Faunal Assemblage.

*Ammonoid Zones* - Deleeni Zone (Upper Anisian).

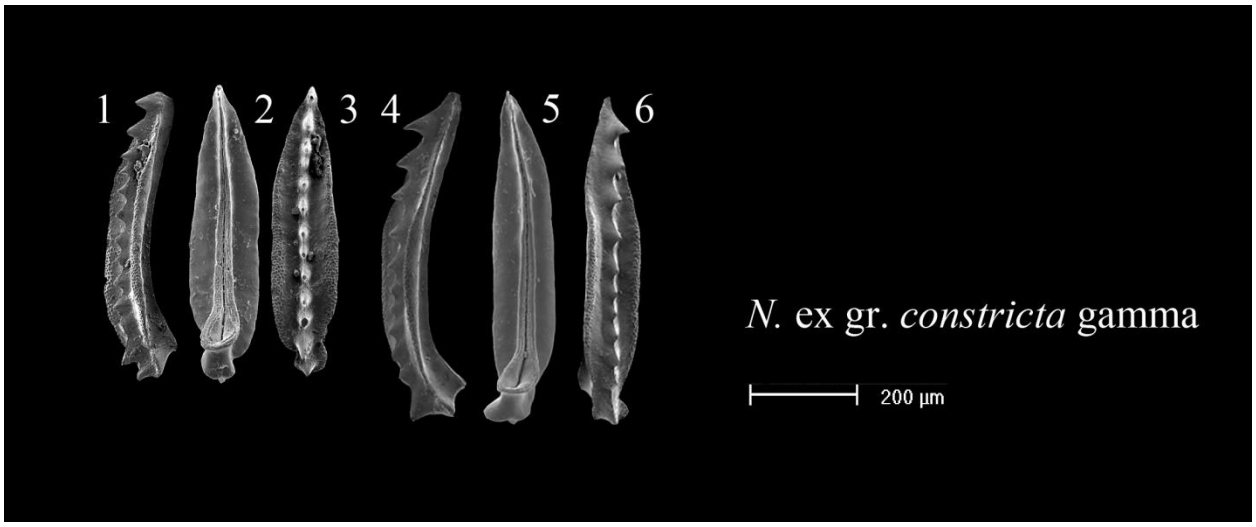



**Figure 2.24.** *Neogondolella* ex gr. *constricta* morphotype γ. 1-3, GSC Locality 99566, East Toad River II. 4-6, GSC Locality C-201902, Yellow Bluffs.

*Morphotype δ*

Figure 2.25

***Diagnosis:*** Large morphotype of *N.* ex gr. *constricta* with parallel to sub-parallel platform margins and a rounded posterior margin. Posterior platform brim is present. Cusp is large, inclined and terminal, with no posterior denticle present.

***Comparisons:*** *N.* ex gr. *constricta* morphotype ε has a rounded posterior margin but also possesses a posterior denticle similar in size to its cusp. *N.* ex gr. *constricta* morphotype ζ has a quadrate posterior margin. *N. balkanica* has an upright rather than inclined cusp, whilst *N. cornuta* has an inclined cusp, but no posterior platform brim.

***Remarks:*** Only large growth stages of this morphotype are known. It is included within *N.*ex gr. *constricta* because of the similarity between its carina and those of other adults included in the same group.

***Occurrence in B.C.:*** *Localities* - GSC Locality C-201902 (92/AH2) and Sample YB C7, both Yellow Bluffs.

*Faunal Assemblages* - *constricta* ζ Faunal Assemblage to *liebermani* Faunal Assemblage.

*Ammonoid Zones* - Deleeni Zone (Upper Anisian).

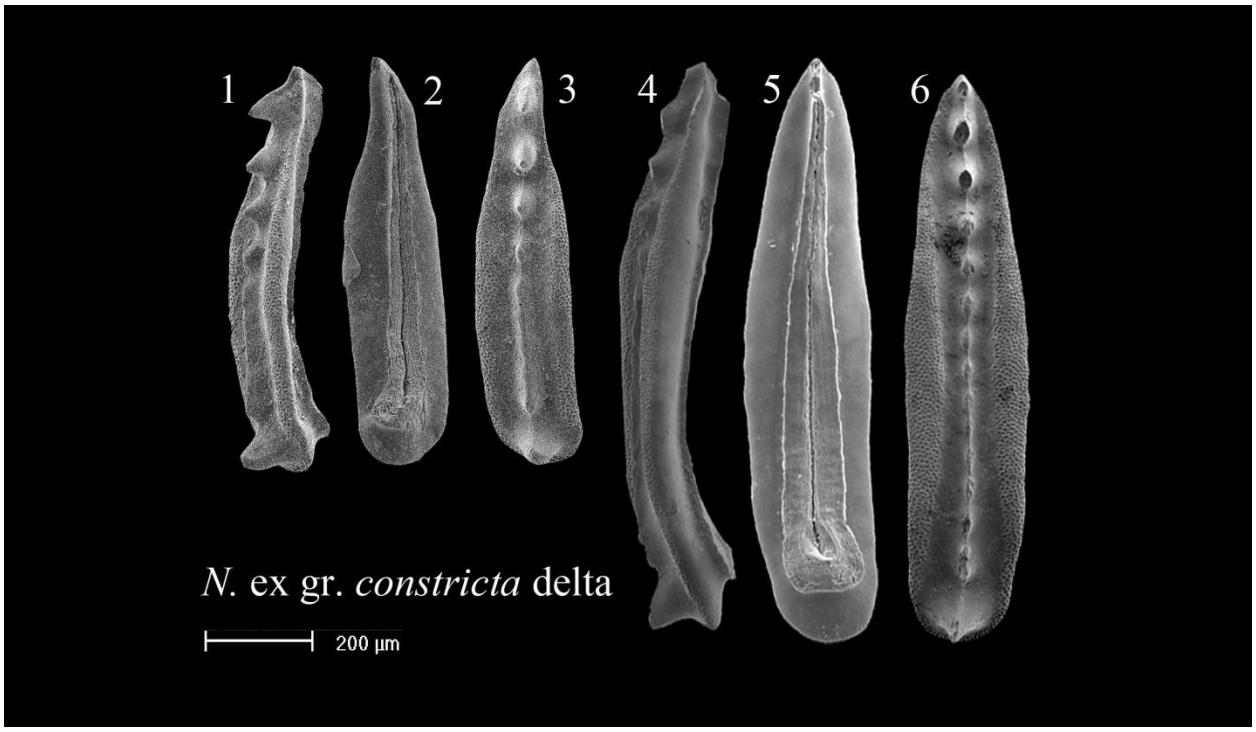



**Figure 2.25.** *Neogondolella* ex gr. *constricta* morphotype δ. 1-3, YB C7, Yellow Bluffs. 4-6, GSC Locality C-201902, Yellow Bluffs.

*Morphotype ε*

Figure 2.26

***Diagnosis:*** Large morphotype of *N.* ex gr. *constricta* with sub-parallel platform margins in the posterior two thirds of the element and a rounded posterior platform margin. Posterior platform brim and posterior denticle are always present. Element sometimes has an asymmetrical posterior.

***Comparisons:*** *N.* ex gr. *constricta* morphotype ζ has a quadrate posterior margin, a more inclined cusp and no posterior denticle. *N. cornuta* and *N. tardocornuta* both lack a posterior platform brim, and the posterior denticle in *N. cornuta* is more inclined. *N. balkanica* has an

upright cusp and platform brim, but its anterior denticles are asymmetrical in profile whilst those in *N.* ex gr. *constricta* morphotype ε are symmetrical throughout.

***Remarks:*** Only large growth stages of this morphotype are known. It is included within *N.*ex gr. *constricta* because of the similarity between its carina and those of other adults included in the same group.

***Occurrence in B.C.:*** *Localities* - GSC Locality 99592 (83/215F), East Toad River I; GSC Locality C-201926 (92/AH26), Mile Post 375 West.

*Faunal Assemblages* - *shoshonensis* Faunal Assemblage to *constricta* ζ Faunal Assemblage.

*Ammonoid Zones* - Minor Zone (Middle Anisian) to Deleeni Zone (Upper Anisian).

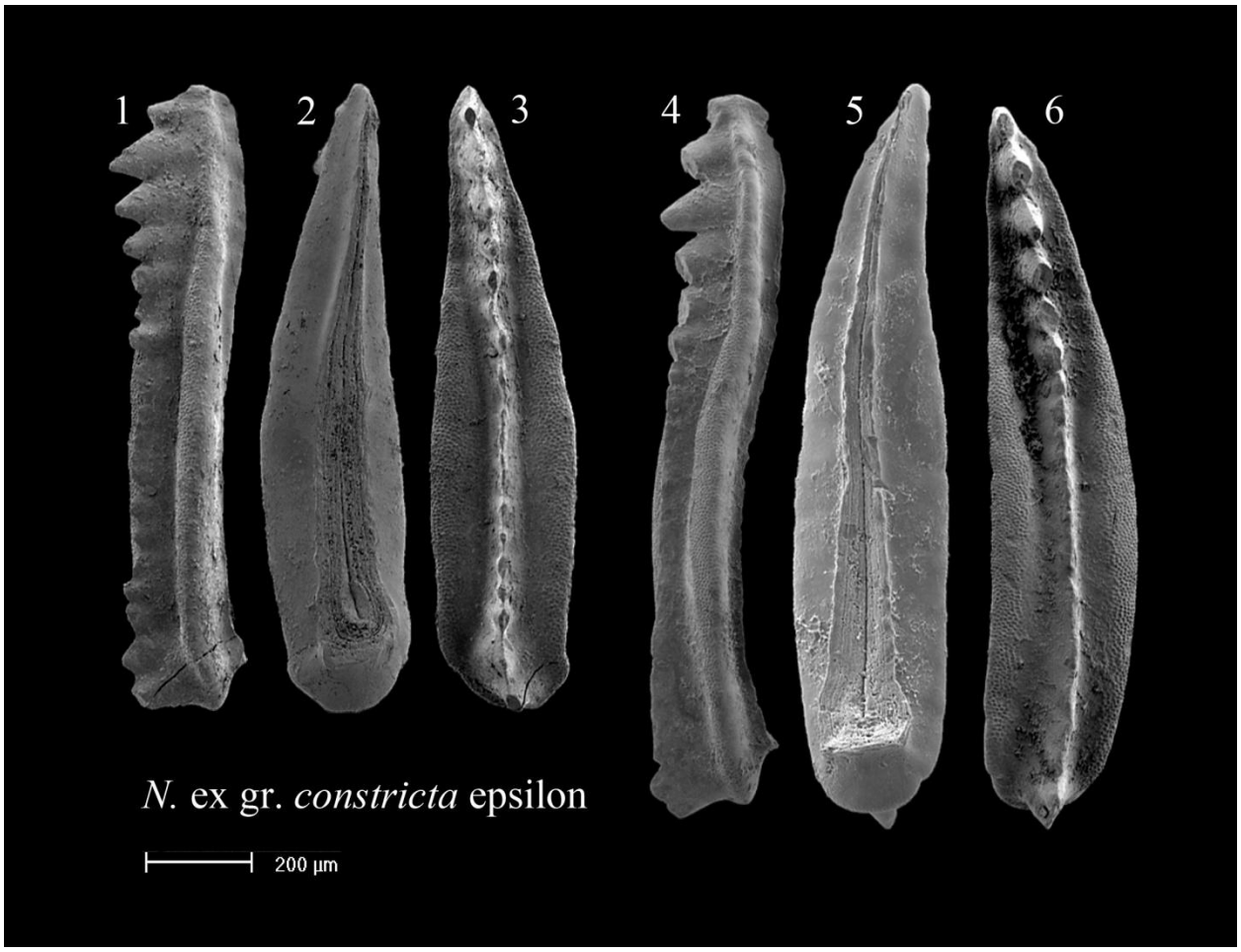



**Figure 2.26.** *Neogondolella* ex gr. *constricta* morphotype ε. 1-3, GSC Locality C-201926, Mile Post 375 West. 4-6, GSC Locality 99592, East Toad River I.

*Morphotype ζ*

Figure 2.27

***Diagnosis:*** Large morphotype of *N.* ex gr. *constricta* with parallel platform margins in the posterior two thirds of the element and a quadrate posterior platform margin. Posterior platform brim is present, but there is no posterior denticle. Element is curved laterally at its posterior end.

***Comparisons:*** See above.

***Remarks:*** Only large growth stages of this morphotype are known. It is included within *N.*ex gr. *constricta* because of the similarity between its carina and those of other adults included in the same group.

***Occurrence in B.C.:*** *Localities* - GSC Locality 99592 (83/215F), East Toad River I; GSC Locality C-201902 (92/AH2), Yellow Bluffs.

*Faunal Assemblages* - *constricta* ζ Faunal Assemblage to *liebermani* Faunal Assemblage.

*Ammonoid Zones* - Deleeni Zone (Upper Anisian).

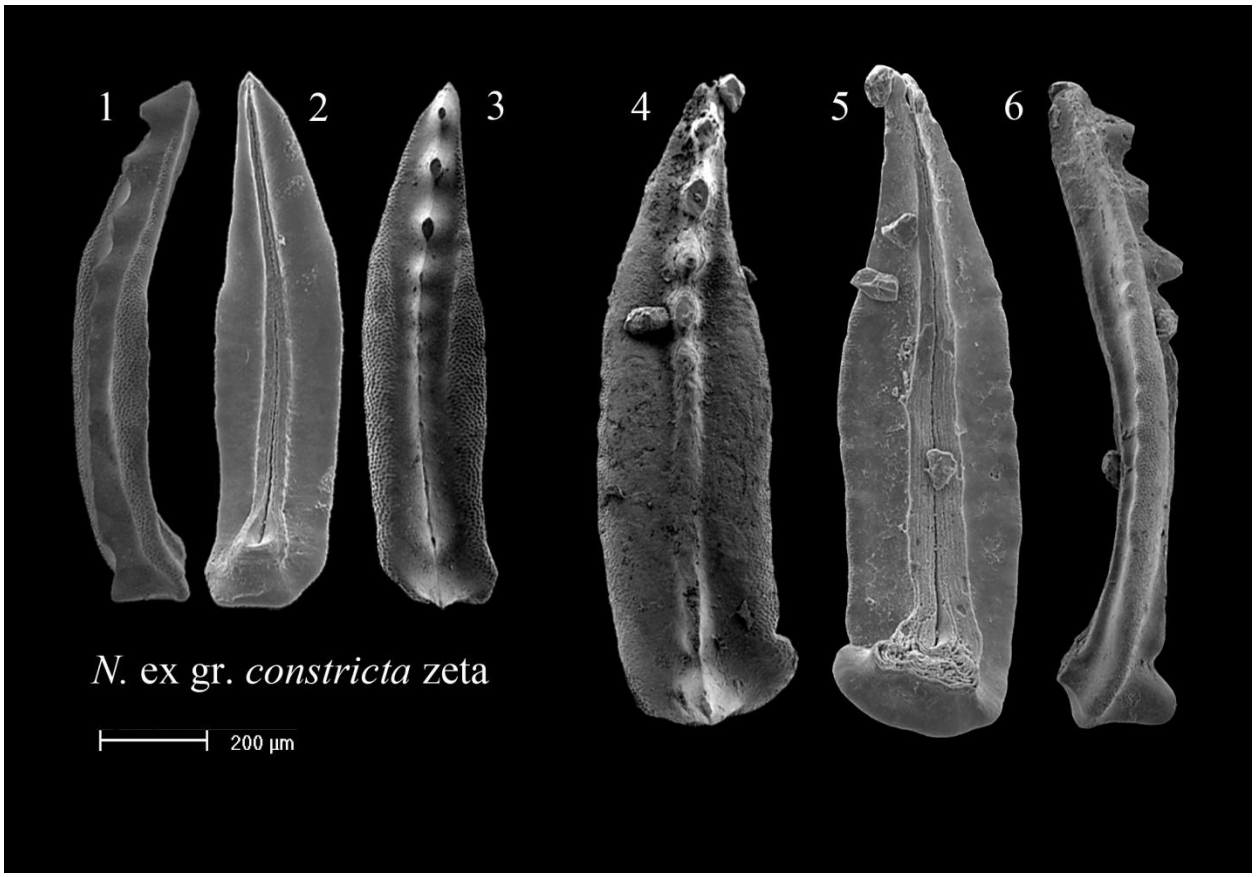



**Figure 2.27.** *Neogondolella* ex gr. *constricta* morphotype ζ. 1-3, GSC Locality C-201902, Yellow Bluffs. 4-6, GSC Locality 99592, East Toad River I.

***Neogondolella* ex gr. *transita*** (Kozur and Mostler)

Figures 2.28 – 2.29

***Central Species:*** *Gondolella transita* Kozur and Mostler, 1971

1971 *Gondolella transita* n. sp. – Kozur and Mostler, p. 12, Pl. 2, fig. 12

***Holotype:*** Kozur and Mostler, Pl. 2, fig. 12

***Age of Holotype:*** Curionii Zone, Fassanian, Ladinian, Middle Triassic.

***Type Stratum:*** Buchenstein Formation.

***Type Locality:*** Felsöörs, Balaton Highlands, Hungary.

***Allied Taxa:*** *N. bakalovi* Budurov and Stefanov, 1972

*N. excentrica* Budurov and Stefanov, 1972

*N. basisymmetrica* Budurov and Stefanov, 1972

*N. longa* Budurov and Stefanov, 1973

*N. lindstroemi* Budurov and Stefanov, 1973

*N. pseudolonga* Kovács, Kozur and Mietto, 1980

*G. mesotriassica* Kozur and Mostler, 1982

*N. tardocornuta* Budurov and Stefanov, 1984

*N. aldae* Kozur, Krainer and Mostler, 1994

*N. ladinica* Kozur, Krainer and Mostler, 1994

***Key Features:*** This group is introduced to include Middle Triassic specimens of *Neogondolella* that share certain morphological characteristics. Species of this group have relatively long, narrow platforms with asymmetrical posteriors. The basal pit is subterminal with respect to the posterior end of the keel and a secondary keel is developed posterior of the basal pit and loop. The carina is generally low, becoming higher to the anterior and posterior.

***Description:*** Platform margins vary from biconvex to parallel. Platform is broadest either at the midpoint or in the anterior third of the element. Margins taper evenly to the anterior end of the element, leaving no free blade. Posterior platform brim can be present or absent. Platform is constricted at the posterior end of the element. Reticulation is present on the platform margins. In side view, element is arched and platform is thin with upturned margins. Cusp is similar in size to denticles of the carina. At least one posterior denticle is always present and the terminal denticle is often larger than the cusp. Carina is low, becoming higher to the anterior and posterior. Denticles are fused, becoming more discrete to the anterior. Denticles are all inclined and asymmetrical. Keel is low and narrow, becoming wider with growth. It terminates in a rounded to sub-rounded, closed basal loop surrounding a subterminal basal pit. The keel extends beyond the basal loop and forms a pointed or bifid secondary posterior keel.

***Comparisons:*** *N.* ex gr. *constricta* also has a narrow platform, but the basal loop is simple and no secondary keel is developed. *P. trammeri* (Kozur) and *P. eotrammeri* (Krystyn) have short secondary keels developed, but have much broader platforms and higher carinae. *P. alpina* (Kozur and Mostler) and *P. szaboi* sometimes have a secondary keel, but they also possess a free blade.

***Remarks:*** Members of this group have previously been included in some authors' understanding of *N. constricta.* Kovács *et al.* (1990) considered both *N. longa* and *N. pseudolonga* to be morphotypes or sub-species of *N. constricta.* They also described a morphotype of *N. constricta* (morphotype γ) that Kozur *et al.* (1994) considered to be *N. mesotriassica.* Here, *N. longa*, *N. pseudolonga* and *N. mesotriassica* are treated as independent species of the *transita* group. None

of the above named species have been recognised in the samples collected for this study, however two new morphotypes belonging to *N.* ex gr. *transita* have been identified.

***Occurrence in B.C.:*** Chischa Zone (Upper Anisian).

***Other Occurrences:*** Members of the *N. transita* group have been reported from the Hyatti Zone (Lower Anisian) to Subasperum Zone (Ladinian) of Nevada (Nicora, 1976; Kozur *et al.*, 1994); Illyrian to Fassanian of Bulgaria (Budurov and Stefanov 1972, 1973, 1984) and Slovakia (Pevný and Salaj, 1997); Fassanian of Hungary (Kozur and Mostler, 1971), Italy (Kovács *et al.*, 1980), and Austria (Kozur *et al.*, 1994).

*Morphotype α*

Figure 2.28

***Diagnosis:*** Morphotype of *N.* ex gr. *transita* with asymmetrically developed posterior secondary keel, the lateral profile of which rises to the posterior. Posterior denticle and platform brim present. Platform margins are asymmetrical, as is the posterior platform margin where one of the postero-lateral corners is more developed. Platform tapers sharply in the anterior third but there is no free blade.

***Comparisons:*** *N. transita* morphotype β has no posterior platform brim, and a longer platform. *N. mesotriassica* also has a longer platform and a secondary keel that does not rise to the posterior in lateral profile. *N. basisymmetrica* has a rounded posterior platform margin and lacks a posterior platform brim. *N. ladinica* also lacks a posterior platform brim.

***Occurrence in B.C.:*** *Localities* - Sample OS C2, Oyster Springs; GSC Locality C-201921 (92/AH21), Yellow Bluffs.

*Faunal Assemblages* - *transita* Faunal Assemblage.

*Ammonoid Zones* - Chischa Zone (Upper Anisian).

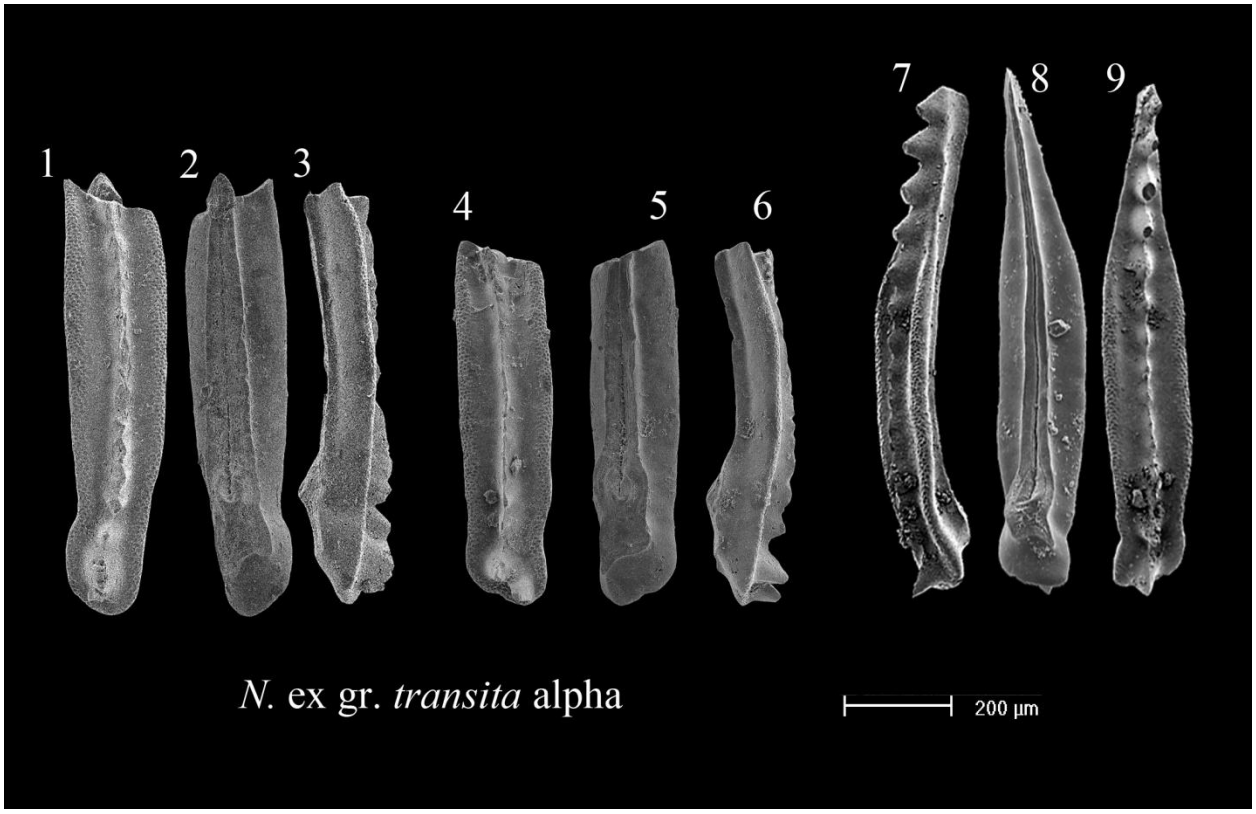



**Figure 2.28.** *Neogondolella* ex gr. *transita* morphotype α. 1-6, OS C2, Oyster Springs. 7-9, GSC Locality C-201921, Yellow Bluffs.

*Morphotype β*

Figure 2.29

***Diagnosis:*** Morphotype of *N.* ex gr. *transita* with long, slender platform. Posterior margin is rounded, and there is no posterior platform brim. In lateral profile, the secondary keel continues on the same trajectory as the main keel.

***Comparisons:*** *N. mesotriassica* and *N. tardocornuta* both have broader platforms. *N. ladinica* has a secondary keel that rises to the posterior in lateral profile. *N. pseudolonga* has a more pronounced posterior platform constriction and a unique narrow basal loop. *N. basisymmetrica* has a similar secondary keel but its platform is relatively broader and tapers to the anterior for more of the element length.

***Occurrence in B.C.:*** *Localities* - GSC Locality C-201921 (92/AH21), Yellow Bluffs.

*Faunal Assemblages* - *transita* Faunal Assemblage.

*Ammonoid Zones* - Chischa Zone (Upper Anisian).




**Figure 2.29.** *Neogondolella* ex gr. *transita* morphotype β. 1-6, GSC Locality C-201921, Yellow Bluffs.

***Neogondolella* ex gr. *regalis*** Mosher

Figures 2.30 – 2.39

***Key Species:*** *Neogondolella regale* Mosher, 1970

1970 *Neogondolella regale* n. sp. – Mosher, p. 741, Pl. 110, figs. 1, 2, 4, 5.

***Holotype:*** GSC 25048, Geological Survey of Canada, Ottawa; Mosher, 1970, Pl. 110, figs. 1, 4.

***Age of Holotype:*** Hayesi Zone of Middle Anisian, Middle Triassic.

***Type Stratum:*** Toad Formation.

***Type Locality:*** GSC Locality 68294, Mile Post 375 West on the Alaska Highway, B.C.

***Key Features:*** Species of this group have a uniformly very high, fused carina at all growth stages. The upper profile of the carina is generally uniform, becoming lower at the posterior end in some morphotypes due to the arch in the element. The carina is made up of a large number of closely spaced denticles that are laterally compressed.

***Description:*** Platform margins are biconvex to sub-parallel. Platform is widest at midpoint or in the anterior third of the element. Platform margins taper evenly to the anterior end of the element, leaving no free blade. There is no posterior brim, and some elements show a posterior platform constriction. Reticulation is present on the platform margins. In side view, the elements are arched and the platform is thin with upturned margins. Cusp is large and posteriorly inclined. Posterior denticle is always present, and may be smaller or larger than the cusp. Carina is uniformly high and fused. Denticles are inclined and symmetrical. Keel is low and narrow, terminating in a sub-rounded basal loop that surrounds the sub-terminal basal pit.

***Comparisons:*** The carina of *N.* ex gr. *regalis* is much higher than that of *N. mombergensis* or *N.* ex gr. *constricta.* Carina of *P.* ex gr. *excelsa* is highest in the middle and becomes lower to the anterior and posterior. *N.* ex gr. *shoshonensis* has a less fused carina that becomes lower in the middle. Comparison with *N. bulgarica* is difficult due to the poorly described and illustrated type material of *N. bulgarica* in Budurov and Stefanov (1975). Nicora (1977) considered elements of *N. bulgarica* to be more curved than those of *N.* ex gr. *regalis*. *N. bulgarica* also appears to have a less well-fused carina than *N.* ex gr. *regalis*. It may be possible to unite the more curved morphotypes of *N.* ex gr. *regalis* described here with morphotypes of *N. bulgarica*, but this will require study of the type material and a revision of *N. bulgarica*, which is beyond the scope of the present study.

***Remarks:*** Ten new morphotypes of *Neogondolella* ex gr. *regalis* are recognised herein. None exactly resemble the holotype of Mosher (1970), however they have been assigned to this species group due to their similarity to the paratypes. The holotype of *N. regalis* may be an aberrant form, because it does not resemble the paratypes or any specimens that have been recovered from the type locality, or any specimens that have been subsequently assigned to this species. If *N. regalis* is to be maintained then it will have to be recognised on the basis of the paratypes. The new morphotypes are assigned to *N.* ex gr. *regalis* due to the uncertainty in the definition of the species.

***Occurrence in B.C.:*** Subrobustus Zone (Spathian; Mosher, 1973) to Deleeni Zone (Upper Anisian).

***Other Occurrences:*** Members of the *N. regalis* group have been reported from the Subrobustus Zone (Spathian) of the Canadian Arctic (Orchard, 2008); Hagei Zone to Minor Zone (Middle

Anisian) of Nevada (Mosher, 1973); Aegean to Bithynian of Poland (Trammer, 1972; Narkiewicz, 1999), Greece and Turkey (Nicora, 1977), Bulgaria (Budurov, 1976) and former Yugoslavia (Sudar, 1986).

*Morphotype α*

Figure 2.30

***Diagnosis:*** Morphotype of *N.* ex gr. *regalis* with a biconvex platform that is widest at the midpoint of the element. Small growth stages exhibit a posterior platform constriction. A small posterior denticle is present at all growth stages. Upper profile of carina is of uniform height for most of the length of the element, becoming lower at the posterior end due to curvature of the element.

***Comparisons:*** *N.* ex gr. *regalis* morphotype β has a platform that is widest in the posterior third of the element. *N.* ex gr. *regalis* morphotype γ and *N.* n. sp. G both have a posterior platform constriction. *N.* ex gr. *regalis* morphotypes δ and ε both have platforms that are widest at the posterior end of the element. *N.* ex gr. *regalis* morphotype ζ has an asymmetrical posterior platform margin. The carina of *N.* ex gr. *regalis* morphotype η has a uniform upper profile along its whole length. The platform of *N.* ex gr. *regalis* morphotype θ is sometimes broadest in the posterior half of the element and the cusp and posterior denticle are both much larger than those in equal sized specimens of *N.* ex gr. *regalis* morphotype α. *N.* ex gr. *regalis* morphotype ι has a relatively wider platform and a posterior denticle that is larger than the cusp. *N.* n. sp. H has an indented platform margin.

***Occurrence in B.C.:*** *Localities* - GSC Locality 99588 (83/215B), East Toad River I; GSC Locality C-90852 (82/B9F), Liard-Crusty; Sample NTP C0, North Tetsa Phosphate; GSC Locality C-201922 (92/AH22) and GSC Locality C-302187 (HB655), both Mile Post 375 East; GSC Locality 68294, Mile Post 375 West; 1967.30-1967.50 m and 1965.00-1965.40 m below Kelly Bushing, Petro-Canada Kobes d-048-A/094-B-09 well; 2054.30-2054.05 m below Kelly Bushing, Arc Dawson 07-13-079-15W6 well.

*Faunal Assemblages* - *regalis* α Faunal Assemblage to *regalis* θ Faunal Assemblage.

*Ammonoid Zones* - Caurus Zone (Lower Anisian) to Minor Zone (Middle Anisian).

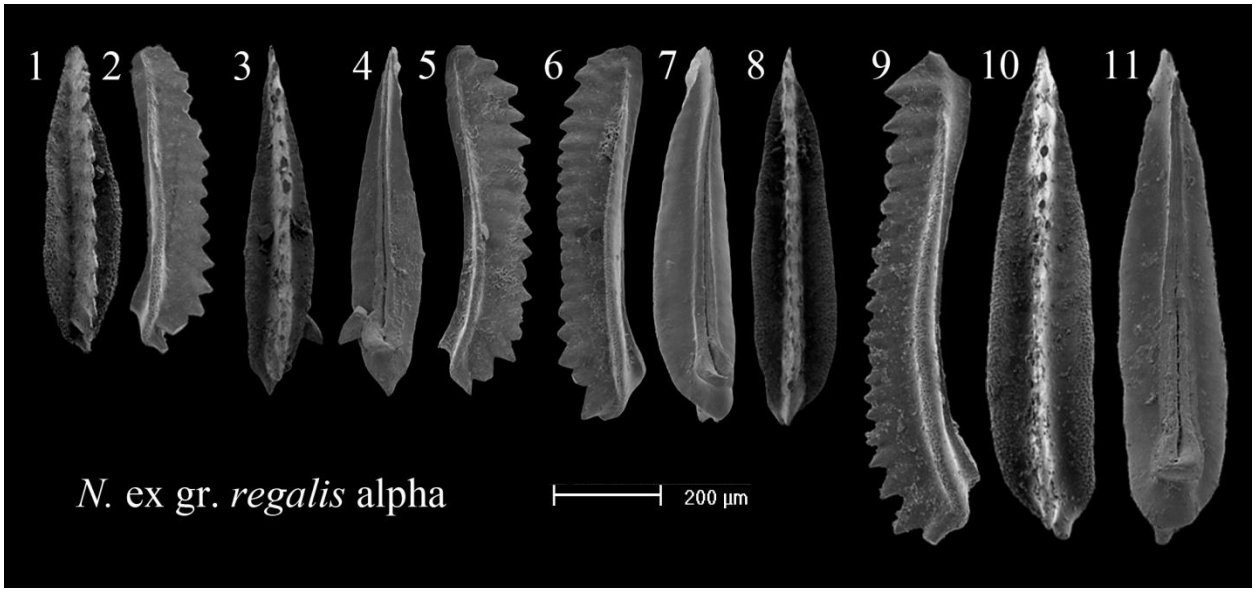



**Figure 2.30.** *Neogondolella* ex gr. *regalis* morphotype α. 1-2, GSC Locality C-201922, Mile Post 375 East. 3-5, GSC Locality C-90852, Liard-Crusty. 6-8, GSC Locality 99588, East Toad River I. 9-11, GSC Locality C-302187, Mile Post 375 East.

*Morphotype β*

Figure 2.31

***Diagnosis:*** Morphotype of *N.* ex gr. *regalis* with a platform that is biconvex and widest in the posterior third of the element. There is no posterior platform brim and at least one posterior denticle is present at all growth stages. Upper profile of carina is of uniform height for most of the length of the element, becoming lower at the posterior end due to curvature of the element.

***Comparisons:*** *N.* ex gr. *regalis* morphotypes γ and ι have a platform that is widest close to the midpoint of the element and morphotype γ also has a posterior platform constriction. *N.* ex gr. *regalis* morphotypes δ and ε both have a platform that is widest at the posterior margin of the element. *N.* ex gr. *regalis* morphotype η has a uniformly high carina. *N.* ex gr. *regalis* morphotype θ has a larger cusp and posterior denticle than *N.* ex gr. *regalis* morphotype β.

***Occurrence in B.C.:*** *Localities* - 1858.60-1858.90 m below Kelly Bushing, Petro-Canada Kobes c-074-G/094-b-09 well; 1967.30-1967.50 m below Kelly Bushing, Petro-Canada Kobes d-048-A/094-b-09 well.

*Faunal Assemblages* - *regalis* α Faunal Assemblage to *shoshonensis* Faunal Assemblage.

*Ammonoid Zones* - Caurus Zone (Lower Anisian) to Minor Zone (Middle Anisian).

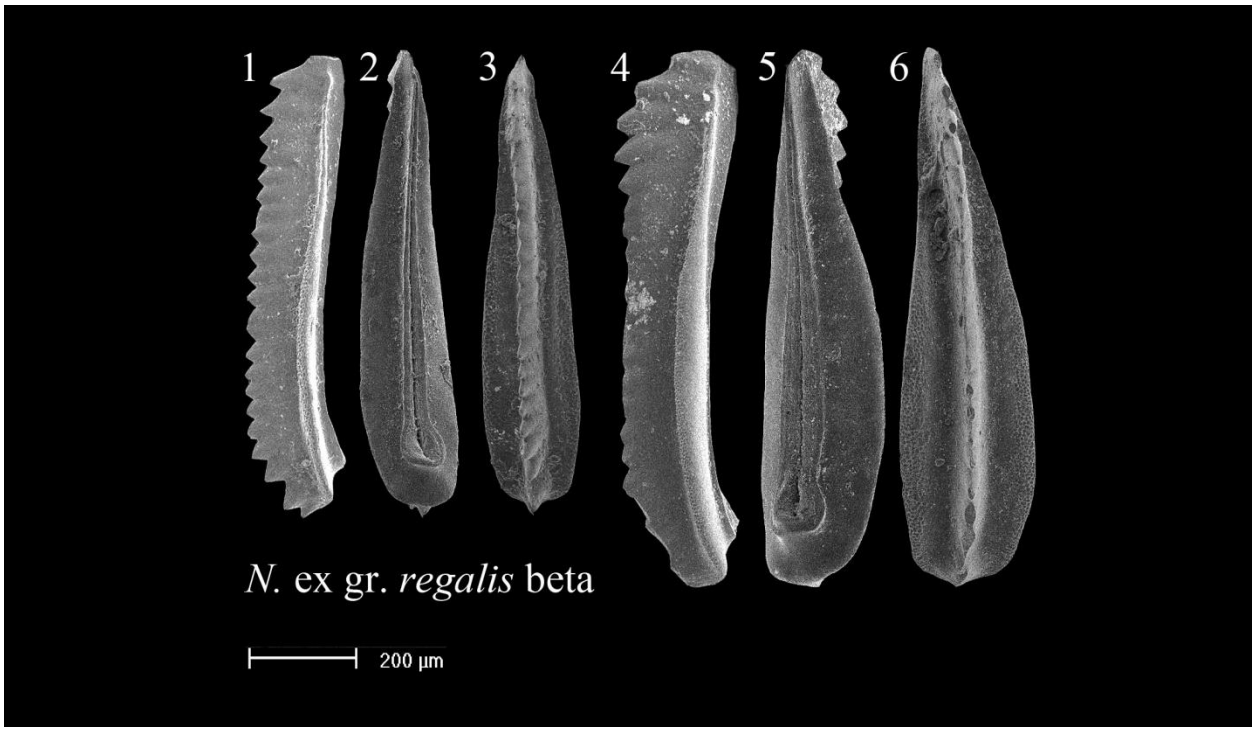



**Figure 2.31.** *Neogondolella* ex gr. *regalis* morphotype β. 1-3, 1858.60-1858.90 m below Kelly Bushing, Petro-Canada Kobes c-074-G/094-b-09 well. 4-6, 1967.30-1967.50 m below Kelly Bushing, Petro-Canada Kobes d-048-A/094-b-09 well.

*Morphotype γ*

Figure 2.32

***Diagnosis:*** Morphotype of *N.* ex gr. *regalis* with narrow, biconvex platform with a constriction in the posterior sixth of the element. Posterior denticle is present at all growth stages and is similar in size, shape and orientation to the cusp.

***Comparisons:*** *N.* ex gr. *constricta* morphotype α has a much lower and less fused carina. *N.* ex gr. *constricta* morphotype β also has a lower carina, as well as a more pronounced posterior platform constriction. *N.* ex gr. *constricta* morphotypes δ and ε both have lower carinae and a

more rounded posterior platform margin. *N.* ex gr. *regalis* morphotype ζ does not have a posterior platform constriction, instead having an asymmetrical posterior platform margin. *N.* n. sp. G has a lower and less fused carina and a posterior platform constriction that begins in the posterior third of the element, as does *N.* ex gr. *shoshonensis*.

***Occurrence in B.C.:*** *Localities* - GSC Locality 68294, Mile Post 375 West; 2370.61-2369.96 m below Kelly Bushing, Talisman Altares c-085-I/094-B-01 well; 2234.57-2234.10 m below Kelly Bushing, Talisman Altares 16-17-083-25W6 well; 2553.80 m below Kelly Bushing, Murphy Swan d-054-B/094-P-09 well.

*Faunal Assemblages* - n. sp. A Faunal Assemblage to *regalis* θ Faunal Assemblage.

*Ammonoid Zones* - Hayesi Zone (Middle Anisian).

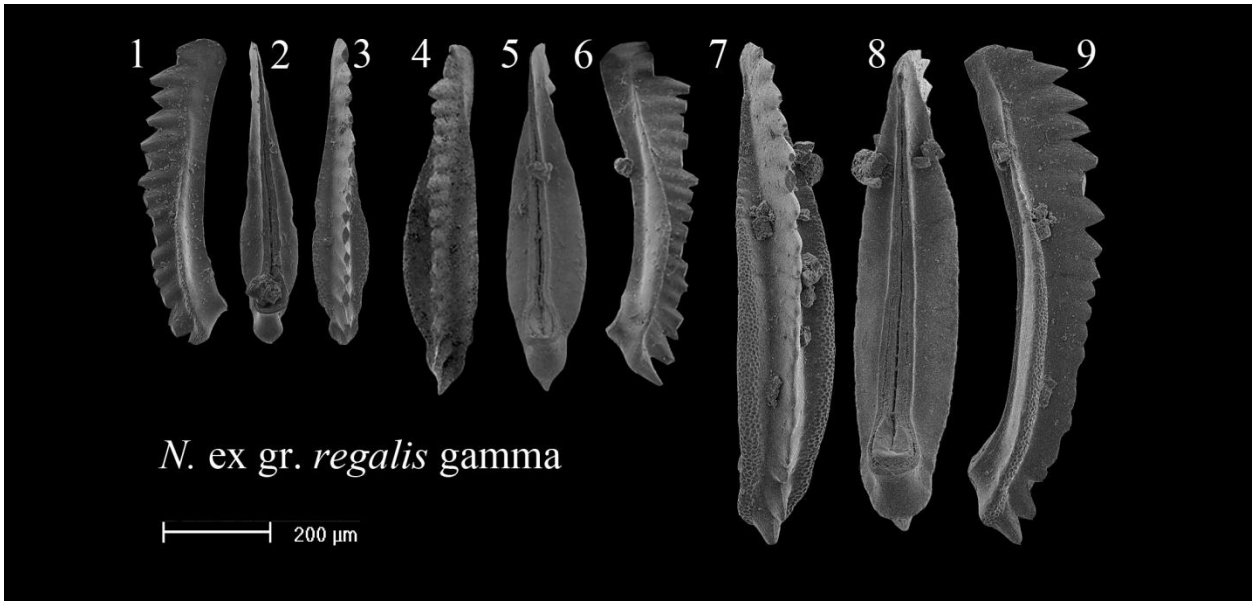



**Figure 2.32.** *Neogondolella* ex gr. *regalis* morphotype γ. 1-3, 7-9, 2553.80 m below Kelly Bushing, Murphy Swan d-054-B/094-P-09 well. 4-6, GSC Locality 68294, Mile Post 375 West.

*Morphotype δ*

Figure 2.33

***Diagnosis:*** Large morphotype of *N.* ex gr. *regalis* with triangular platform that is widest at the quadrate posterior margin. There is no posterior platform brim, and posterior denticle is larger than the cusp. Upper profile of carina is of uniform height throughout. Basal loop is quadrate at the posterior.

***Comparisons:*** *N.* ex gr. *constricta* morphotype ζ has a quadrate posterior margin, but has a lower carina and no posterior denticle. *N.* ex gr. *regalis* morphotype ε has a posterior platform brim and a cusp and posterior denticle that are both much larger than the rest of the denticles. The carina of *N.* ex gr. *regalis* morphotype η is similar to that of *N.* ex gr. *regalis* morphotype δ but its platform is a different shape. Some specimens of *N.* ex gr. *regalis* morphotype δ have accessory nodes adjacent to the posterior of the carina, similar to those in *N. bifurcata.* However, the carina of *N. bifurcata* rises to the anterior rather than maintaining a uniform height.

***Remarks:*** No juvenile specimens of this morphotype were observed.

***Occurrence in B.C.:*** *Localities* - GSC Locality 99574 (83/211A), North Liard River; GSC Locality 42349, Liard-Brimstone; 1965.00-1965.40 m below Kelly Bushing, Petro-Canada Kobes d-048-A/094-B-09 well.

*Faunal Assemblages* - *regalis* δ Faunal Assemblage.

*Ammonoid Zones* - Caurus II Subzone (Lower Anisian).

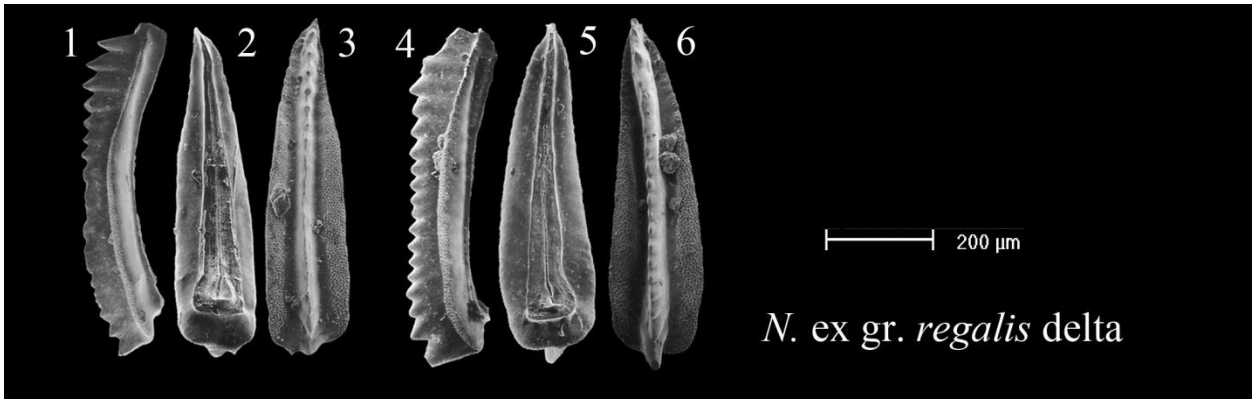



**Figure 2.33.** *Neogondolella* ex gr. *regalis* morphotype δ. 1-3, GSC Locality 99574, North Liard River. 4-6, GSC Locality 42349, Liard-Brimstone.

*Morphotype ε*

Figure 2.34

***Diagnosis:*** Morphotype of *N.* ex gr. *regalis* with triangular platform that is widest at the quadrate posterior margin. Posterior platform brim present. Posterior denticle is much larger than cusp, and both are much larger than the rest of the denticles and are strongly inclined to the posterior. Fixed anterior blade present.

***Comparisons:*** *N.* ex gr. *constricta* morphotype ζ has a lower carina and platform margins that begin to taper to the anterior closer to the end of the element. The carina of *N.* ex gr. *regalis* morphotype θ is similar to that of *N.* ex gr. *regalis* morphotype ε but it lacks an anterior blade.

***Occurrence in B.C.:*** *Localities* - GSC Locality 68294, Mile Post 375 West.

*Faunal Assemblages* - *regalis* θ Faunal Assemblage.

*Ammonoid Zones* - Hayesi Zone (Middle Anisian).

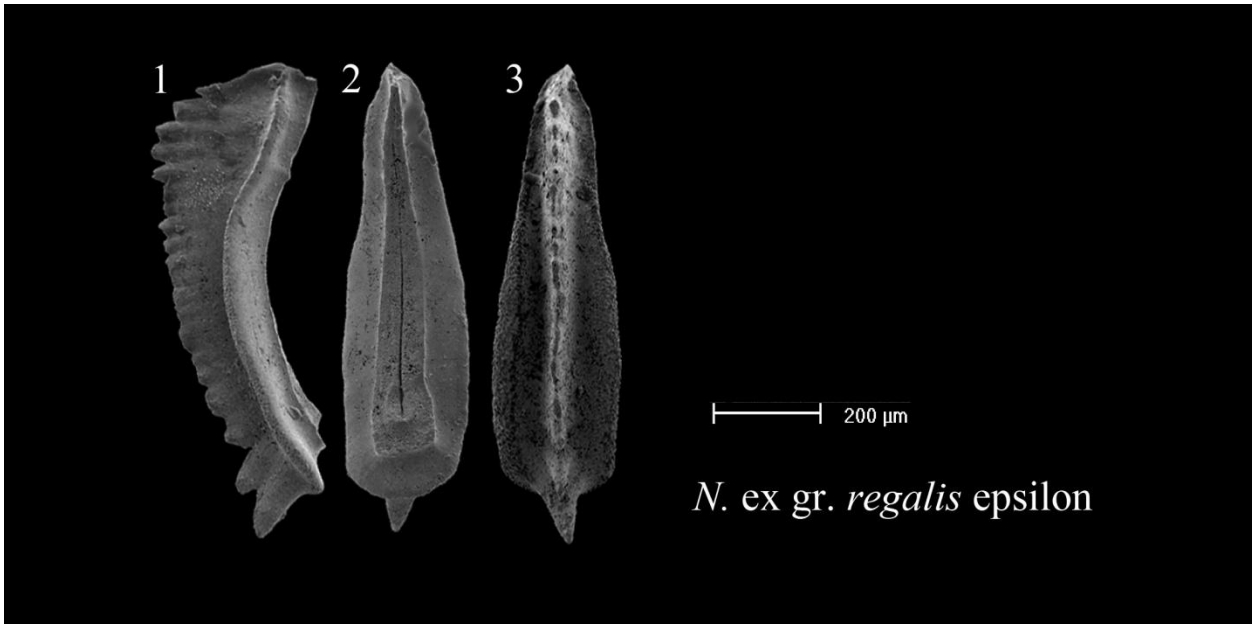



**Figure 2.34.** *Neogondolella* ex gr. *regalis* morphotype ε. 1-3, GSC Locality 68294, Mile Post 375 West.

*Morphotype ζ*

Figure 2.35

***Diagnosis:*** Morphotype of *N.* ex gr. *regalis* with biconvex platform margins, the outer one of which is shorter than the inner. This gives the posterior platform margin an asymmetrical appearance. There is no posterior platform brim. Cusp and posterior denticle are the same size, are much larger than the other denticles, and are strongly inclined to the posterior. Carina is high and rises to the anterior and the posterior.

***Comparisons:*** *N. mombergensis* is downturned in the posterior of the element and has a lower carina in the middle of the element. *N. prava* (Kozur) also has a lower carina. Neither species has one platform margin that is shorter than the other, which is the case in *N.* ex gr. *regalis*

morphotype ζ. Some morphotypes of *N.* ex gr. *transita* have asymmetrical platforms, but they also possess a posterior secondary keel which is absent in *N.* ex gr. *regalis* morphotype ζ.

***Occurrence in B.C.:*** *Localities* - GSC Locality 99574 (83/211A), North Liard River; GSC Locality C-302187 (93/HB656), Mile Post 375 East.

*Faunal Assemblages* - *regalis* δ Faunal Assemblage to *regalis* η Faunal Assemblage.

*Ammonoid Zones* - Caurus II Subzone to Americanum Zone (Lower Anisian).

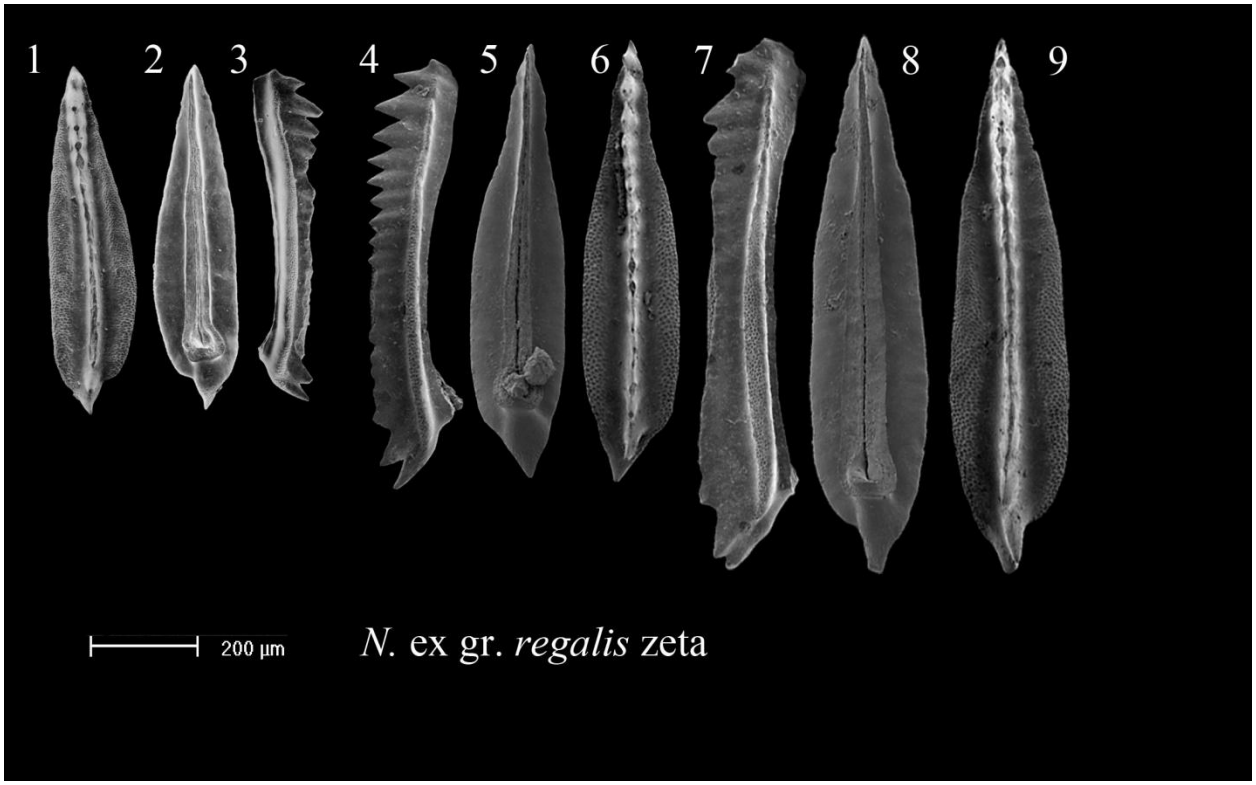



**Figure 2.35.** *Neogondolella* ex gr. *regalis* morphotype ζ. 1-3, GSC Locality 99574, North Liard River. 4-9, GSC Locality C-209952, Mile Post 375 East.

*Morphotype η*

Figure 2.36

***Diagnosis:*** Morphotype of *N.* ex gr. *regalis* with platform margins that are straighter on one side of the element than the other. Carina is high and fused, with upper margin straight in lateral profile. Posterior platform brim is absent. Cusp and posterior denticle are similar in size to each other and to the rest of the denticles. Element may be slightly arched.

***Comparisons:*** *N.* ex gr. *regalis* morphotype θ has a distinctive cusp and posterior denticle that are not present in *N.* ex gr. *regalis* morphotype η. *N.* ex gr. *regalis* morphotype ι has a biconvex platform and a prominent posterior denticle.

***Occurrence in B.C.:*** *Localities* - GSC Locality C-302187 (HB655), Mile Post 375 East; 2239.75-2238.74 m below Kelly Bushing, Talisman Altares 16-17-083-25W6 well.

*Faunal Assemblages* - *regalis* η Faunal Assemblage.

*Ammonoid Zones* - Americanum Zone (Lower Anisian).

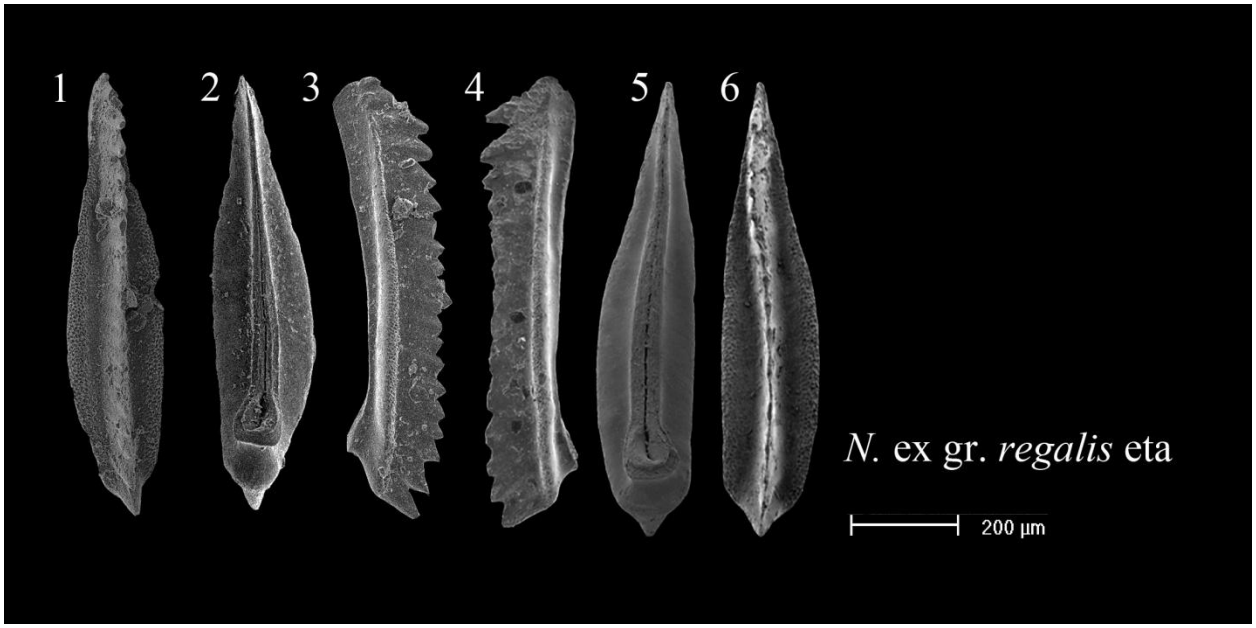



**Figure 2.36.** *Neogondolella* ex gr. *regalis* morphotype η. 1-3, 2239.75-2238.74 m below Kelly Bushing, Talisman Altares 16-17-083-25W6 well. 4-6, GSC Locality C-302187, Mile Post 375 East.

*Morphotype θ*

Figure 2.37

***Diagnosis:*** Morphotype of *N.* ex gr. *regalis* with a platform that is broadest at midpoint or in the posterior half of the element. Posterior platform margin is rounded or quadrate and posterior platform brim is present. Posterior denticle is larger than cusp, and both are inclined to the posterior.

***Comparisons:***. *N.* ex gr. *regalis* morphotype ι has a more pointed posterior platform margin and no posterior platform brim. *N.* n. sp. A has a pointed posterior platform margin and a much larger, terminal cusp with no posterior denticle or platform brim.

***Occurrence in B.C.:*** *Localities* - GSC Locality 99575 (83/211B), North Liard River; GSC Locality 68294, Mile Post 375 West; GSC Locality 68204 (82/AH6), Mile Post 375 East.

*Faunal Assemblages* - *regalis* θ Faunal Assemblage.

*Ammonoid Zones* - Hayesi Zone (Middle Anisian).

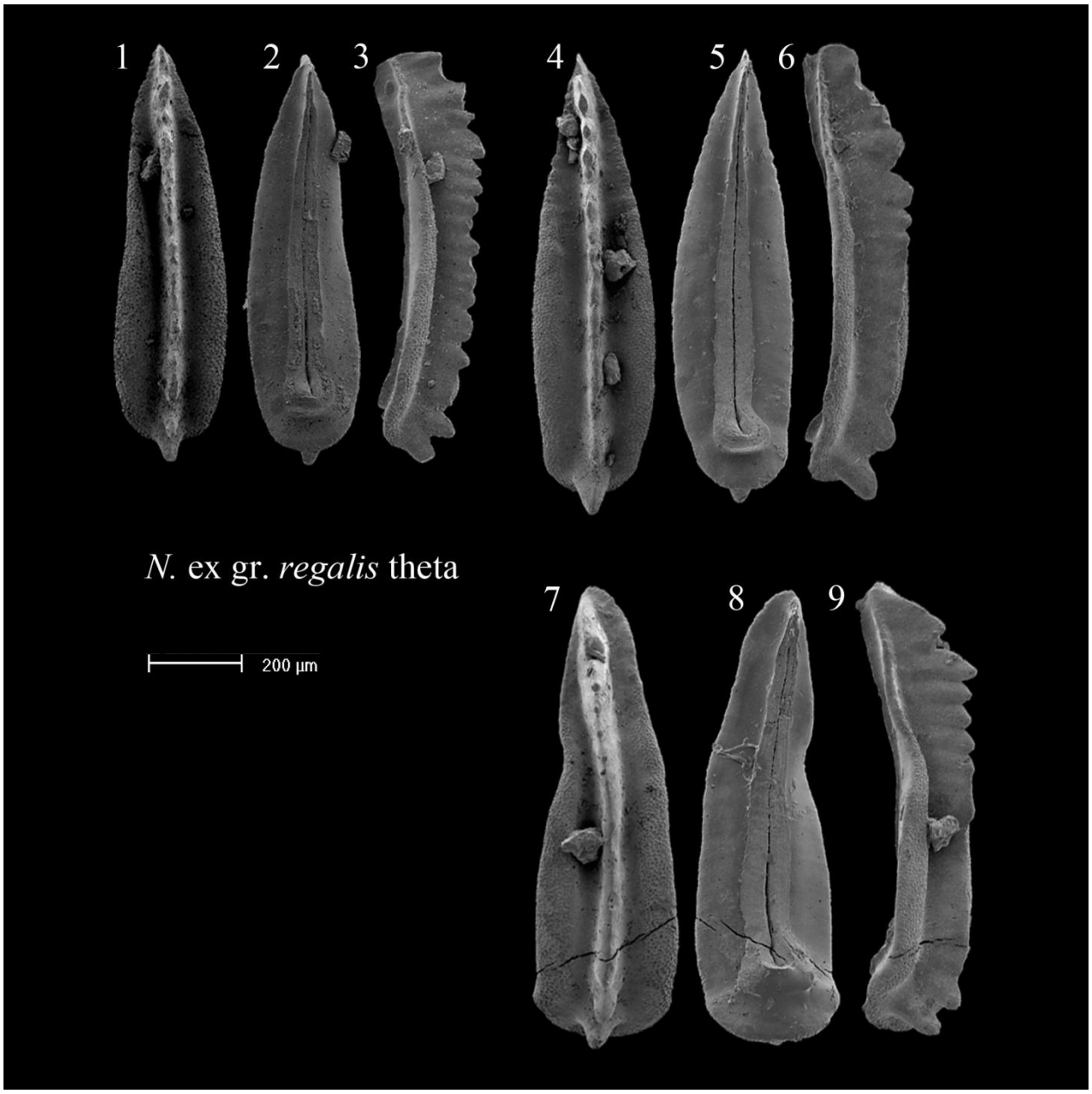



**Figure 2.37.** *Neogondolella* ex gr. *regalis* morphotype θ. 1-3, 7-9, GSC Locality 68294, Mile Post 375 West. 4-6, GSC Locality 68204, Mile Post 375 East.

*Morphotype ι*

Figure 2.38

***Diagnosis:*** Morphotype of *N.* ex gr. *regalis* with biconvex platform that is widest at its midpoint. Slight platform constriction is present in smaller growth stages. Posterior platform brim is absent. Posterior denticle is larger than cusp and is inclined. Carina is high and fused. Keel extends beyond basal pit in largest specimens.

***Comparisons:*** *N.* ex gr. *constricta* morphotype α possesses a similar platform but has a posterior constriction, a lower carina and a posterior denticle that is always similar in size to the cusp. *N.* n. sp. A has a terminal cusp and a less fused carina.

***Occurrence in B.C.:*** *Localities* - 2054.30-2054.05 m below Kelly Bushing, Arc Dawson 07-13-79-15W6 well; 2553.80 m and 2556.90 m below Kelly Bushing, Murphy Swan d-054-B/094-P-09 well; 3073.00 m below Kelly Bushing, Shell Groundbirch 16-02-078-22W6 well.

*Faunal Assemblages* - *regalis* ι Faunal Assemblage to *shoshonensis* Faunal Assemblage.

*Ammonoid Zones* - Hayesi Zone to Minor Zone (Middle Anisian).

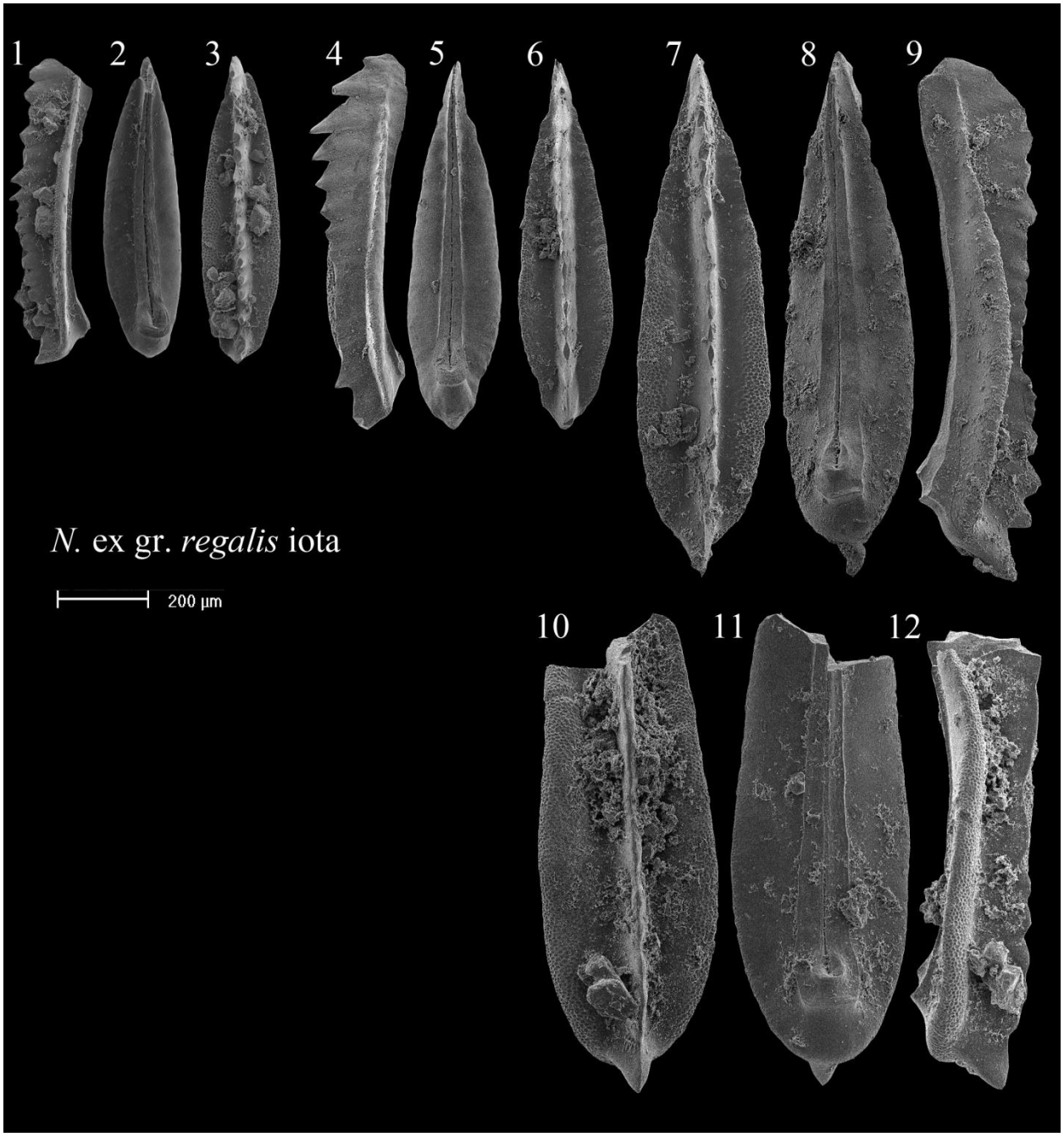



**Figure 2.38.** *Neogondolella* ex gr. *regalis* morphotype ι. 1-3, 2553.80 m below Kelly Bushing, Murphy Swan d-054-B/094-P-09 well. 4-6, 2556.90 m below Kelly Bushing, Murphy Swan d-054-B/094-P-09 well. 7-9, 3073.00 m below Kelly Bushing, Shell Groundbirch 16-02-078-22W6 well. 10-12, 2054.30-2054.05 m below Kelly Bushing, Arc Dawson 07-13-79-15W6 well.

***Neogondolella* ex gr. *shoshonensis*** Nicora

Figures 2.39 – 2.42

***Key Species:*** *Neogondolella shoshonensis* Nicora, 1976

1976 *Neogondolella shoshonensis* n. sp. – Nicora, p. 640-642, Pl. 83, figs. 1-15; Pl. 84, fig. 17.

***Holotype:*** CO 133, Institute of Paleontology, Milan; Nicora, 1976, Pl. 83, figs. 6a-b.

***Age of Holotype:*** Shoshonensis Zone, Middle Anisian, Middle Triassic.

***Type Stratum:*** Prida Formation.

***Type Locality:*** Sample N 112, Tobin Range, Nevada.

***Key Features:*** Species of this group have platforms that typically taper progressively from the midpoint of the element to both the anterior and posterior, sometimes with denticles on a free posterior process. Other specimens have wider and rounded posterior margins. Carina is highest at the ends of the element, and lowest in the middle. The posterior end of the element is downturned, and the denticles change from upright to inclined, giving the carina a fan-shaped upper margin at the posterior of the element.

***Description:*** Platform is biconvex to sub-parallel, with its greatest width at the midpoint of the element. Platform margins taper evenly to the anterior but there is no free blade. The posterior end of the platform is very variable, sometimes surrounding the cusp and forming a brim, sometimes tapering to the posterior end of the element, and sometimes becoming constricted in front of the cusp. Reticulation is present on the platform margins. In side view, the element is arched and the platform margins upturned. Cusp is similar in size to the adjacent denticles or

slightly larger; one or more posterior denticles may be present. All of the denticles are inclined, but the cusp and adjacent denticles are inclined more strongly. Carina is lowest in the middle and becomes higher to both the anterior and posterior. Denticles are fused, some more so than others. Keel is narrow and extends into a narrow, oval basal loop surrounding a subterminal basal pit.

***Comparisons:*** *Neogondolella mombergensis* is similar but has a cusp that is much larger than the denticles and there is no change in the inclination of its denticles. *N. haslachensis* (Tatge) has a biconvex platform but the carina is of a uniform height and the denticles are more discrete; it is also found at a higher stratigraphic level than *N.* ex gr. *shoshonensis*. Some morphotypes of *N.* ex gr. *constricta* show similar posterior and anterior constriction, but their carina is lower and fewer denticles become inclined to the posterior. *N.* ex gr. *regalis* has a high carina but it is uniform in lateral profile when compared with *N.* ex gr. *shoshonensis*.

***Remarks:*** Nicora (1976) recognised two morphotypes of *N. shoshonensis*, morphotypes A and B. The holotype for the species belongs to morphotype A, which has a rounded posterior as opposed to the more common tapered posterior. No examples of this morphotype have been found in British Columbia or elsewhere, and it may represent a form that is endemic to Nevada. However, specimens belonging to morphotype B as well as two new morphotypes, here designated morphotypes γ and δ, are recognised and assigned to *N.* ex gr. *shoshonensis*. The largest forms of this group lose the strongly reduced posterior platform of the smaller growth stages (fig. 2.42) and it is not always clear which morphotype these largest specimens belong to.

***Occurrence in B.C.:*** Minor Zone (Middle Anisian).

***Other Occurrences:*** Members of the *N. shoshonensis* group have been reported from the Shoshonensis Zone (Middle Anisian) to Occidentalis Zone (Upper Anisian) of Nevada (Nicora, 1976); Trinodosus Zone (Illyrian) of Turkey (Nicora, 1976; Assereto, 1974).

*Morphotype A* (sensu Nicora, 1976)

Figure 39

***Diagnosis:*** An atypical morphotype of *N.* ex gr. *shoshonensis* whose platform tapers to the anterior but remains wide until the posterior end of the element. It surrounds the sub-terminal cusp and a posterior platform brim is present. The platform has a constriction in the posterior third of large growth stages.

***Comparisons:*** The platform of *N.* ex gr. *shoshonensis* morphotype B tapers to the posterior and is narrower at the end of the element; there is no posterior brim present. *N.* ex gr. *shoshonensis* morphotype γ and small growth stages of *N.* ex gr. *shoshonensis* morphotype δ have platforms that narrow in the posterior third of the element, leaving the carina to continue on a posterior process. The larger specimens of *N.* ex gr. *shoshonensis* morphotype D have a similar platform to morphotype A, but without a constriction.

***Remarks:*** The holotype of *N. shoshonensis* belongs to this morphotype, which differs in platform shape from the other morphotypes assigned to *N.* ex gr. *shoshonensis* by Nicora (1976) and this study. It may be that this morphotype represents the only true *N. shoshonensis* and the other morphotypes belong to a different, closely related species.

***Occurrence in B.C.:*** None.

***Other Occurrences:*** Shoshonensis Zone (Middle Anisian) to Rotelliformis Zone (Upper Anisian) of Nevada (Nicora, 1976).

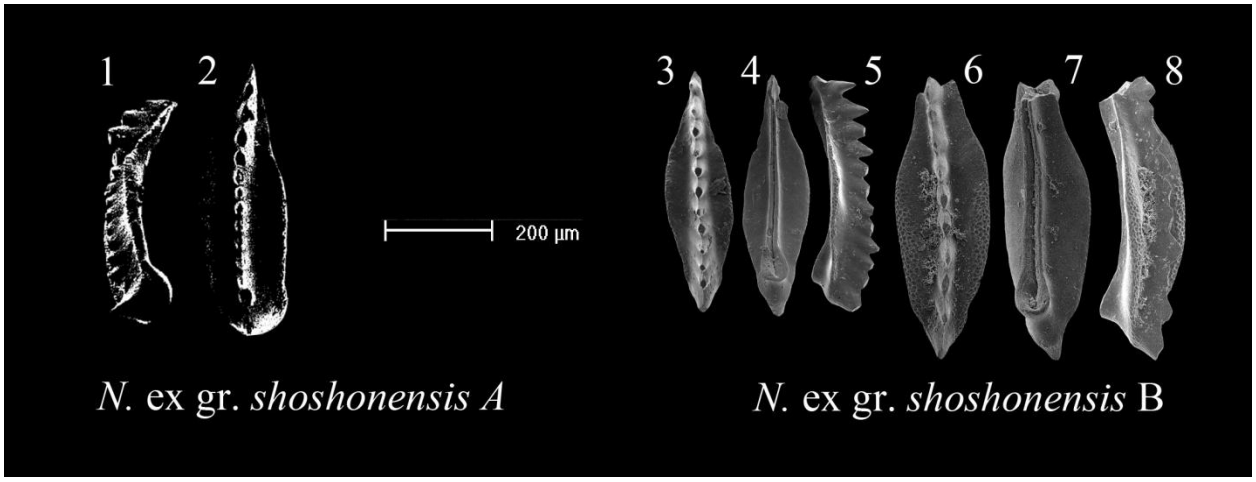



**Figure 2.39.** *Neogondolella* ex gr. *shoshonensis* morphotype A (from Nicora, 1976). 1-2, N 112, Tobin Range, Nevada. *Neogondolella* ex gr. *shoshonensis* morphotype B. 3-5, GSC Locality 99591, East Toad River I. 6-8, 1858.60-1858.90 m below Kelly Bushing, Petro-Canada Kobes c-074-G/094-B-09 well.

*Morphotype B* (sensu Nicora, 1976)

Figure 2.39

***Diagnosis:*** Morphotype of *N.* ex gr. *shoshonensis* whose platform is strongly biconvex and narrowed in the anterior one third of the element length. Platform tapers from the midpoint to the posterior and continues to the end of the element. Cusp is terminal and there is no posterior process.

***Comparisons:*** In both *N.* ex gr. *shoshonensis* morphotype γ and δ, the platform terminates in the posterior third of the element, leaving the carina to continue on a posterior process. *N.* ex gr.

*shoshonensis* morphotype B has a more distinct anterior platform narrowing than any of the other morphotypes.

***Occurrence in B.C.:*** *Localities* - GSC Locality 99591 (83/215E), East Toad River I; 1858.60-1858.90 m below Kelly Bushing, Petro-Canada Kobes c-074-G/094-B-09 well.

*Faunal Assemblages* - *shoshonensis* Faunal Assemblage.

*Ammonoid Zones* - Minor Zone (Middle Anisian).

***Other Occurrences:*** Shoshonensis Zone (Middle Anisian) to Occidentalis Zone (Upper Anisian) of Nevada; Trinodosus Zone (Illyrian) of Turkey (Nicora, 1976; Assereto, 1974).

*Morphotype γ*

Figure 2.40

***Diagnosis:*** Morphotype of *N.* ex gr. *shoshonensis* whose biconvex platform narrows abruptly in the posterior third of the element. The platform may terminate completely, or continue to the posterior end as a narrow ridge.

***Comparisons:*** *N.* ex gr. *shoshonensis* morphotype δ has a longer, narrower platform, a shorter posterior process and a carina that is very low in the middle of the element.

***Occurrence in B.C.:*** *Localities* - GSC Locality 99591 (83/215E), East Toad River I; GSC Locality 99565 (83/205A), East Toad River II. *Faunal Assemblages* - *shoshonensis* Faunal Assemblage. *Ammonoid Zones* - Minor Zone (Middle Anisian).

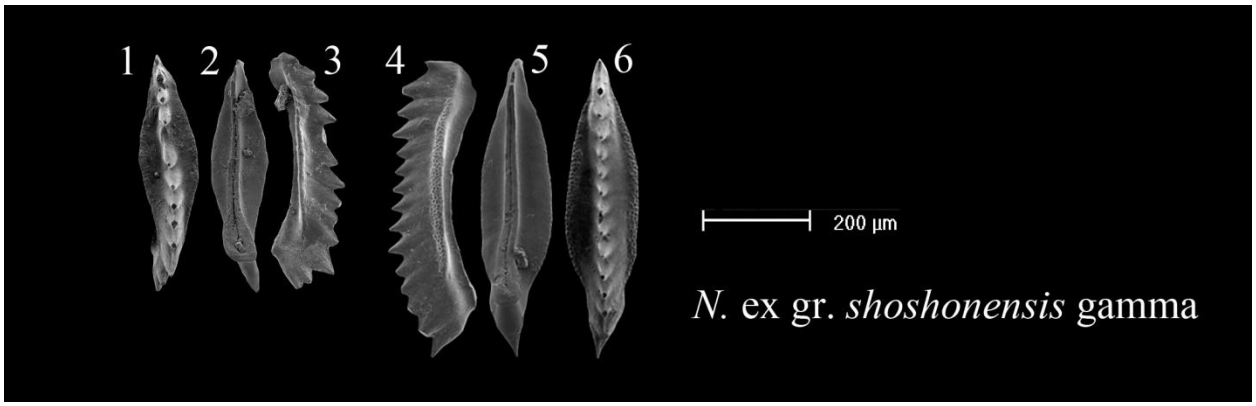



**Figure 2.40.** *Neogondolella* ex gr. *shoshonensis* morphotype γ. 1-3, GSC Locality 99591, East Toad River I. 4-6, GSC Locality 99565, East Toad River II.

*Morphotype δ*

Figure 2.41

***Diagnosis:*** Morphotype of *N.* ex gr. *shoshonensis* whose platform margins vary from weakly to strongly biconvex. Platform narrows in the posterior sixth of the element in small growth stages, leaving the carina to continue on a posterior process. This process becomes smaller with growth and is overgrown in adult specimens. Carina is very low in the middle third of the element.

***Comparisons:*** See above.

***Occurrence in B.C.:*** *Localities* - GSC Locality 99591 (83/215E), East Toad River I; GSC Locality 99565 (83/205A), East Toad River II; Sample NTP C6, North Tetsa Phosphate; GSC Locality C-201926 (92/AH26), Mile Post 375 West.

*Faunal Assemblages* - *shoshonensis* Faunal Assemblage.

*Ammonoid Zones* - Minor Zone (Middle Anisian).

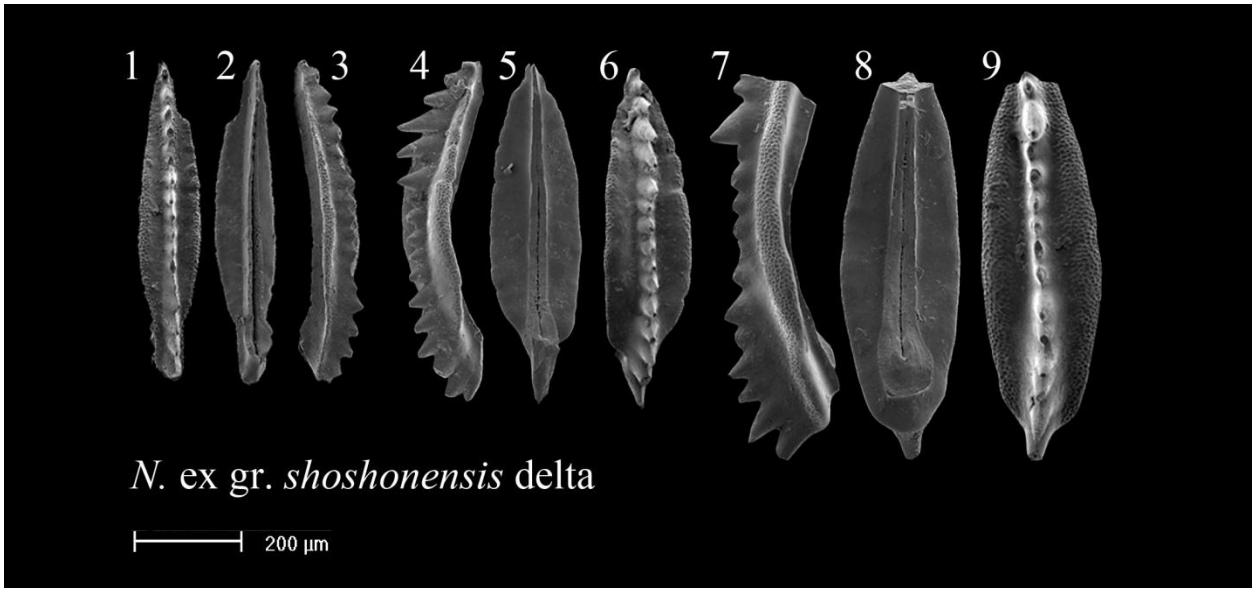



**Figure 2.41.** *Neogondolella* ex gr. *shoshonensis* morphotype δ. 1-3, GSC Locality C-201926, Mile Post 375 West. 4-6, GSC Locality 99565, East Toad River II. 7-9, GSC Locality 99591, East Toad River I.

### ***Neogondolella* n. sp. A**

Figure 2.42

1997 *Neogondolella* n. sp. N – Orchard and Tozer, p. 682

***Holotype:*** 97-2-5 (fig. 2.42, 9-11).

***Age of Holotype:*** Hayesi Zone, Middle Anisian, Middle Triassic.

***Type Stratum:*** Toad Formation.

***Type Locality:*** GSC Locality 68204, Mile Post 375 East on the Alaska Highway, B.C.

***Diagnosis:*** Species of *Neogondolella* with biconvex platform that narrows to a point at both the anterior and posterior ends of the element. Cusp is prominent, inclined and terminal. There is no

posterior denticle and no posterior brim. Carina is low, of an even height for most of its length and denticles are discrete. In the largest specimens, a higher, fixed blade develops at the anterior of the carina.

***Description:*** Platform is biconvex and widest at, or just posterior of, the midpoint of the element. Platform margins taper evenly to both the anterior and posterior, leaving no free blade and no posterior platform brim. Posterior margin of the platform is pointed. Reticulation is present on the platform margins. In side view, element is arched and platform is thin with upturned margins. Cusp is very large and inclined. There is never a posterior denticle present. Carina is uniformly high in juveniles but in adults it is lower. Denticles are unfused and inclined. Keel is high and narrow, terminating in an open, subcircular basal loop surrounding the subterminal basal pit.

***Comparisons:*** *N.* ex gr. *constricta* morphotype α has a lower carina and a posterior platform constriction. Morphotype of *N.* ex gr. *regalis* have much higher carinae with a more even upper profile.

***Occurrence in B.C.:*** *Localities* - GSC Locality 68294, Mile Post 375 West; GSC Locality C-302187 (93/HB656), Mile Post 375 East; GSC Locality 68204 (82/AH6), Mile Post 375 East; 2054.30-2054.05 m below Kelly Bushing, Arc Dawson 07-13-79-15W6 well; 2553.80 m below Kelly Bushing, Murphy Swan d-054-B/094-P-09 well.

*Faunal Assemblages* - n. sp. A Faunal Assemblage to *regalis* θ Faunal Assemblage.

*Ammonoid Zones* - Hayesi Zone (Middle Anisian).




**Figure 2.42.** *Neogondolella* n. sp. A. 1-2, 6-8, 2553.80 m below Kelly Bushing, Murphy Swan d-054-B/094-P-09 well. 3-5, 9-11, GSC Locality 68204, Mile Post 375 East. 12-13, GSC Locality 68294, Mile Post 375 West.

### ***Neogondolella* n. sp. B**

Figure 2.43

***Holotype:*** 97-1-2 (fig. 2.43, 4-6).

***Age of Holotype:*** Subzone II, Caurus Zone, Lower Anisian, Middle Triassic.

***Type Stratum:*** Toad Formation.

***Type Locality:*** GSC Locality 99574, North Liard River, B.C.

***Diagnosis:*** Species of *Neogondolella* with a platform that is widest in the posterior third of the element. Platform is asymmetrical with a more convex outer margin and a straight to undulating inner margin. Platform narrows very close to the anterior of the element leaving a very short free blade. Carina is uniformly low and laterally deflected at the posterior.

***Description:*** Platform is asymmetrical with its widest point in the posterior third of the element. Platform margins taper to the anterior before narrowing sharply close to the end of the element. Posterior platform margin is rounded and a posterior platform brim is present. Reticulation covers much of the platform margins. In side view, element is arched and platform is thick with upturned margins. Cusp is small and similar in size to adjacent denticles. Posterior denticle is present. Carina is low, rising to the anterior. Posterior end of the carina is laterally deflected. Denticles are uniformly fused along its length. They are inclined and asymmetrical. Keel is low and wide, terminating in a closed, oval basal loop surrounding the subterminal basal pit.

***Comparisons:*** *N.* ex gr. *constricta* morphotype δ does not have an anterior platform constriction and has a less fused carina. The platform of *N.* n. sp. C tapers to the anterior but is not constricted; it also has a posterior platform constriction and more discrete denticles. *N.* n. sp. D also has a posterior platform constriction. *N.* n. sp. E has an anterior constriction that occurs much closer to the midpoint of the element. *N. hanbulogi* does not have an anterior platform constriction.

***Occurrence in B.C.:*** *Localities* - GSC Locality 99574 (83/211A), North Liard River; GSC Locality C-201922 (92/AH22), Mile Post 375 East.

*Faunal Assemblages* - n. sp. B Faunal Assemblage to *regalis* δ Faunal Assemblage.

*Ammonoid Zones* - Caurus Zone (Lower Anisian).




**Figure 2.43.** *Neogondolella* n. sp. B. 1-3, GSC Locality C-201922, Mile Post 375 East. 4-6, GSC Locality 99574, North Liard River.

### ***Neogondolella* n. sp. C**

Figure 2.44

***Holotype:*** 97-5-16 (fig. 2.44, 7-9).

***Age of Holotype:*** Deleeni Zone, Upper Anisian, Middle Triassic.

***Type Stratum:*** Toad Formation.

***Type Locality:*** GSC Locality 99592, East Toad River I, B.C.

***Diagnosis:*** Relatively short and broad species of *Neogondolella* with margins that are sub-parallel to biconvex and taper strongly to the anterior. Platform narrows slightly in the posterior third of the element. Posterior platform margin is rounded, and a narrow posterior platform brim is present in adult specimens. Carina is moderately high and fused.

***Description:*** Platform biconvex to sub-parallel, with widest point at or slightly anterior of midpoint. Platform margins taper strongly to the anterior end of the element but leave no free blade. To the posterior, the platform margins either taper evenly or show a weak narrowing before continuing to the end of the element, where they form a rounded posterior margin. Posterior platform brim is always present. Reticulation is present on platform margins. In side view, element is arched and platform is thin with weakly upturned margins. Cusp is small and similar in size to the adjacent denticles. Posterior denticle is always present and is similar in size to or smaller than the cusp. Carina is low, becoming higher to the anterior. Denticles are weakly fused, rounded and inclined. Keel is low and narrow, terminating in a large, closed, oval basal loop that surrounds the subterminal basal pit.

***Comparisons:*** This species is relatively short and broad compared with other species of *Neogondolella* from the Middle Triassic. Elements of *N.* n. sp. D are similar but have a more differentiated anterior blade. The narrow posterior platform differentiates this species from *N. hanbulogi.*

***Occurrence in B.C.:*** *Localities* - GSC Locality 99592 (83/215F), East Toad River I; GSC Locality C-201926 (92/AH26), Mile Post 375 West; 3034.8 m below Kelly Bushing, Shell Groundbirch 16-02-078-22W6 well.

*Faunal Assemblages* - *shoshonensis* Faunal Assemblage to *constricta* ζ Faunal Assemblage.

*Ammonoid Zones* - Minor Zone (Middle Anisian) to Deleeni Zone (Upper Anisian).

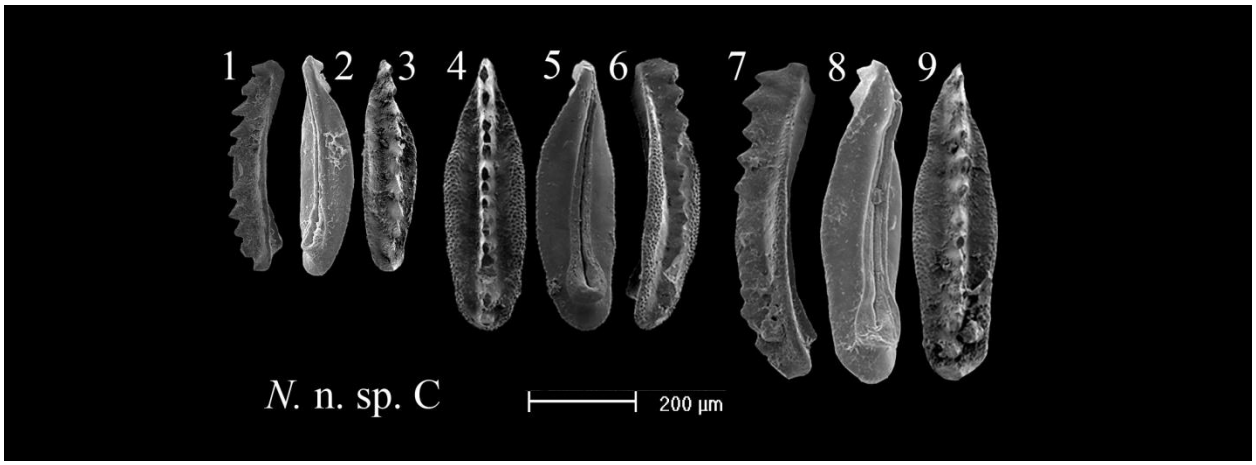



**Figure 2.44.** *Neogondolella* n. sp. C. 1-3, 7-9, GSC Locality 99592, East Toad River I. 4-6, GSC Locality C-201926, Mile Post 375 West.

### *Neogondolella* n. sp. D

Figure 2.45

***Holotype:*** fig. 2.45, 3-4.

***Age of Holotype:*** Minor Zone, Middle Anisian, Middle Triassic.

***Type Stratum:*** Toad Formation.

***Type Locality:*** GSC Locality 46499, North Tetsa Hill, B.C.

***Diagnosis:*** Species of *Neogondolella* with broad, biconvex platform that tapers asymmetrically in the posterior sixth of the element. Posterior denticle is always present and commonly offset from the carina. Carina is low and partially fused. To the anterior, an upstanding fixed blade is differentiated from the carina.

***Description:*** Platform is biconvex, with widest point at midpoint of the element. Platform margins taper evenly to the anterior, leaving a short free blade in some specimens. Platform is constricted to the posterior. Posterior platform margin varies from rounded to quadrate, platform brim is sometimes present in the quadrate forms. Reticulation is present on the platform margins. In side view, element is strongly arched and platform is thin with strongly upturned margins. These upturned margins form adcarinal troughs. Cusp is small, rarely larger than adjacent denticles. Posterior denticle is always present, often larger than the cusp and commonly offset from the rest of the carina. Carina is low and rises to the anterior. Denticles are inclined and weakly fused. Keel is low but varies in width. It terminates in a closed, subcircular to oval basal loop that surrounds the subterminal basal pit.

***Comparisons:*** *N.* ex gr. *constricta* morphotypes α and β both have a cusp and posterior denticle that are distinctly larger than the other denticles, and the elements are narrower than those of *N.* n. sp. D. *N.* n. sp. G and *N.* ex gr. *regalis* γ both have a higher carina. Posterior platform constriction differentiates this species from *N. hanbulogi.*

***Occurrence in B.C.:*** *Localities* - GSC Locality C-201926 (92/AH26), Mile Post 375 West; GSC Locality 46499, North Tetsa Hill.

*Faunal Assemblages* - *shoshonensis* Faunal Assemblage.

*Ammonoid Zones* - Minor Zone (Middle Anisian).

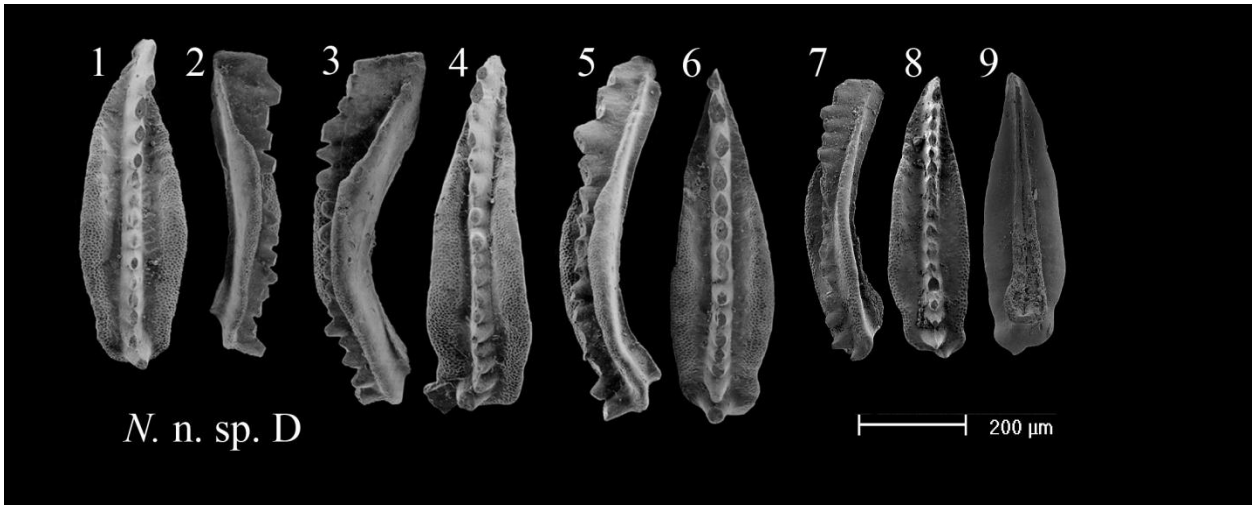



**Figure 2.45.** *Neogondolella* n. sp. D. 1-6, GSC Locality 46499, North Tetsa Hill. 7-9, GSC Locality C-201926, Mile Post 375 West.

### ***Neogondolella* n. sp. E**

Figure 2.46

2008 *Neogondolella* sp. C – Orchard, p. 405-407, figs. 5.17-5.19

***Holotype:*** fig. 2.46, 1-3.

***Age of Holotype:*** Unknown.

***Type Stratum:*** Doig Formation.

***Type Locality:*** 1967.30-1967.50 m below Kelly Bushing, Petro-Canada Kobes d-048-A/094-B-09 well, B.C.

***Diagnosis:*** Species of *Neogondolella* with a platform that abruptly narrows in the anterior third of the element at weak geniculation points. There is no free blade, but the high carina in the

anterior forms a pseudo-blade. The carina is low in the middle third of the element but rises to both the anterior and posterior. The posterior of the platform is sub-rounded and there is a posterior brim. Cusp is large and posteriorly inclined. Basal pit and loop are both very narrow.

***Description:*** Platform widest at midpoint of the element. Platform is constricted in the anterior third, but continues to the end of the element, leaving no free blade. Platform margins taper to the posterior, forming a rounded posterior margin with a posterior platform brim. Reticulation is present on the platform margins. In side view, the element is gently arched and the platform is thick with slightly upturned margins. Cusp is large and posteriorly inclined; there is no posterior denticle present. Carina is low in the middle, becoming higher to the anterior. Denticles are fused, becoming more discrete to the anterior. They are inclined and asymmetrical. Keel is low and narrow, terminating in a closed, circular to sub-quadrate basal loop that surrounds the subterminal basal pit.

***Comparisons:*** The anterior constriction of this species serves to separate it from most of its contemporaries. *Neogondolella joanae* Orchard from the Smithian of B.C. is similar but has a more fused carina and a pointed posterior margin. *Columbitella elongata* (Sweet), from the Spathian, has more upturned margins. Some species of *Metapolygnathus* are similar, in particular *M. acuminatus* Orchard from the Carnian of B.C.; other than by stratigraphic position, this species can be separated by its possession of a free blade, which is not present in *N.* n. sp. E.

***Occurrence in B.C.:*** *Localities* - 1967.30-1967.50 m below Kelly Bushing, Petro-Canada Kobes d-048-A/094-B-09 well.

*Faunal Assemblages* - *regalis* α Faunal Assemblage.

***Other Occurrences:*** Subrobustus Zone (Spathian) of Canadian Arctic (Orchard, 2008); Welteri Zone (Lower Anisian) of Nevada (Orchard, 2008).

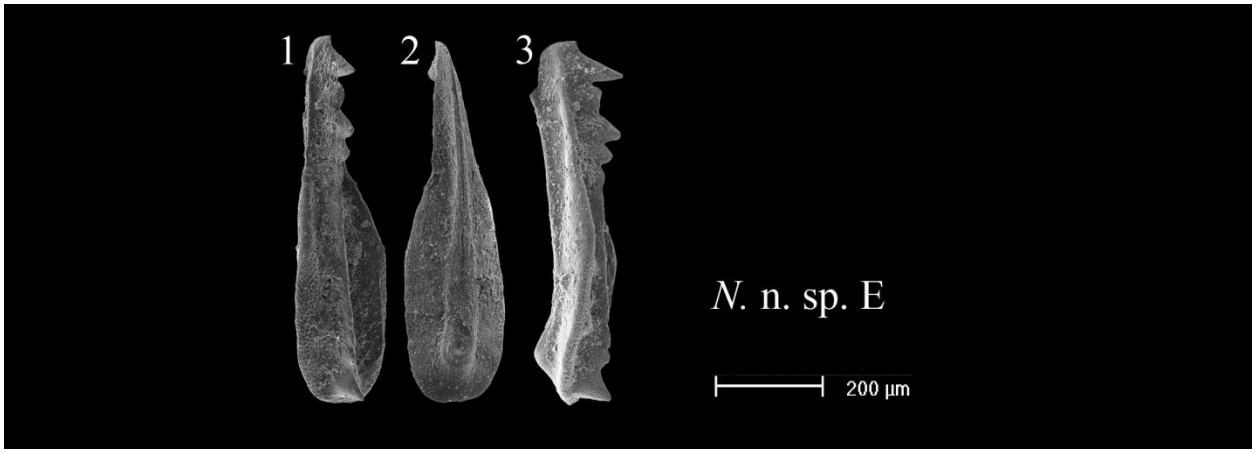



**Figure 2.46.** *Neogondolella* n. sp. E. 1-3, 1967.30-1967.50 m below Kelly Bushing, Petro-Canada Kobes d-048-A/094-B-09 well.

### *Neogondolella* n. sp. F

Figure 2.47

***Holotype:*** 97-6-2 (fig. 2.47, 1-3)

***Age of Holotype:*** Deleeni Zone, Upper Anisian, Middle Triassic.

***Type Stratum:*** Toad Formation.

***Type Locality:*** GSC Locality 99566, East Toad River II, B.C.

***Diagnosis:*** Species of *Neogondolella* with straight platform margins and a blunted posterior margin. Carina is low at the posterior and in the middle of the element, but rises to the anterior

where it forms a high fixed blade. Denticles are fused. Narrow platform brim is present and the keel is wide.

***Description:*** Platform margins sub-parallel, with widest part of the platform at the posterior of the element. Platform margins taper evenly in the anterior third to the end of the element, leaving no free blade. Posterior platform margin is quadrate and a posterior platform brim is present. Reticulation present on platform margins. In side view, element is arched and platform is thick with upturned margins. Cusp is small and a posterior denticle of similar size is present. Carina is low, rising to the anterior, and is uniformly fused. Denticles are inclined. Keel is low and wide, terminating in an open, sub-circular basal loop that surrounds the subterminal basal pit.

***Comparisons:*** The marked differentiation of the blade and carina in this species separates it from most others described herein. *N.* ex gr. *constricta* morphotype ζ has a similar platform shape to *N.* n. sp. F, but its carina is much less fused and does not rise as steeply to the anterior. *N.* ex gr. *regalis* morphotypes δ and ε also both have similar platforms to *N.* n. sp. F, but their carinae are much higher for the whole of their length; morphotype ε also lacks a posterior platform brim. *P.* ex gr. *excelsa* have a carina that is highest in the middle of the element. The carina of *P. inclinata* (Kovács) has a similar profile to that of *N.* n. sp. F but is higher. The carina of *P. sulcata* Orchard is even lower in the posterior half of the element than that of *N.* n. sp. F, and the posterior platform margin of *P. sulcata* is typically rounded.

***Occurrence in B.C.:*** *Localities* - GSC Locality 99566 (83/205B), East Toad River II.

*Faunal Assemblages* - *liebermani* Faunal Assemblage.

*Ammonoid Zones* - Deleeni Zone (Upper Anisian).

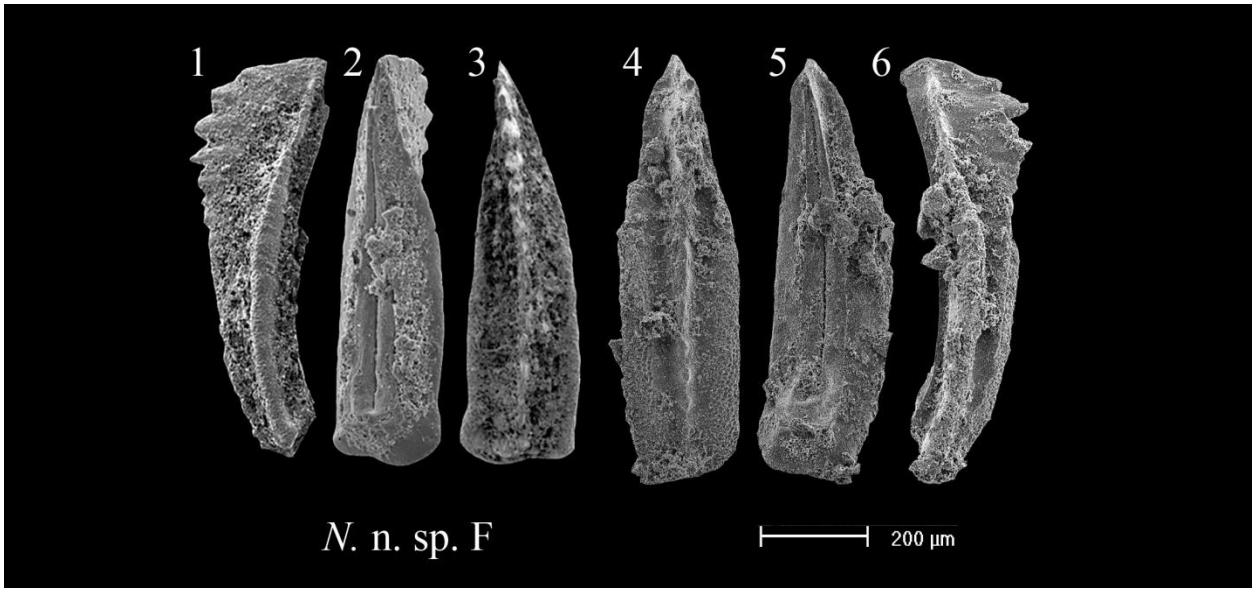



**Figure 2.47.** *Neogondolella* n. sp. F. 1-3, GSC Locality 99566, East Toad River II. 4-6, MP386 C3, Mile Post 386.

### *Neogondolella* n. sp. G

Figure 2.48

***Holotype:*** fig. 2.48, 4-6.

***Age of Holotype:*** Minor Zone, Middle Anisian, Middle Triassic.

***Type Stratum:*** Toad Formation.

***Type Locality:*** Sample NTP C13, North Tetsa Phosphate, B.C.

***Diagnosis:*** Species of *Neogondolella* with moderately high and fused carina. The platform is constricted at the posterior. The platform margins taper in the anterior third to the end of the

element. There is no posterior platform brim at any growth stage, and a posterior denticle that is smaller than the cusp is always present.

***Description:*** Platform biconvex and widest at the midpoint. Platform margins taper from this point to the anterior, narrowing close to the end of the element. Margins also taper to the posterior, becoming constricted just anterior of the cusp. There is no posterior platform brim. Reticulation is present on the platform margins. In side view, element is arched and platform is thin with upturned margins. Cusp is slightly larger than the other denticles, including the posterior denticle that is always present. Carina is high, with an arched upper profile. It is fused most strongly in the middle third of its length. The denticles are inclined and asymmetrical; those near the posterior of the element are more strongly inclined than the others. Keel is high and narrow, terminating in a subcircular basal loop that surrounds the subterminal basal pit.

***Comparisons:*** *N.* ex gr. *constricta* has a carina that is lower than that of *N.* n. sp. G and which becomes higher to the anterior and posterior. *N.* ex gr. *shoshonensis* has a carina that is high like that of *N.* n. sp. G but it is low in the middle and rises to the anterior and posterior. The carina of *N.* ex gr. *regalis* morphotype γ contains more denticles than that of *N.* n. sp. G and they are more tightly spaced.

***Remarks:*** This species appears to be transitional between *N.* ex gr. *constricta* with which it shares a posterior platform constriction and *N.* ex gr. *shoshonensis* with which it shares a comparatively high carina. The stratigraphic range of *N.* n. sp. G overlaps with that of both *N.* ex gr. *constricta* and *N.* ex gr. *shoshonensis*.

***Occurrence in B.C.:*** *Localities* - Sample NTP C13, North Tetsa Phosphate; 2549.66 m below Kelly Bushing, Murphy Swan d-054-B/093-P9 well.

*Faunal Assemblages* - *shoshonensis* Faunal Assemblage.

*Ammonoid Zones* - Minor Zone (Middle Anisian).

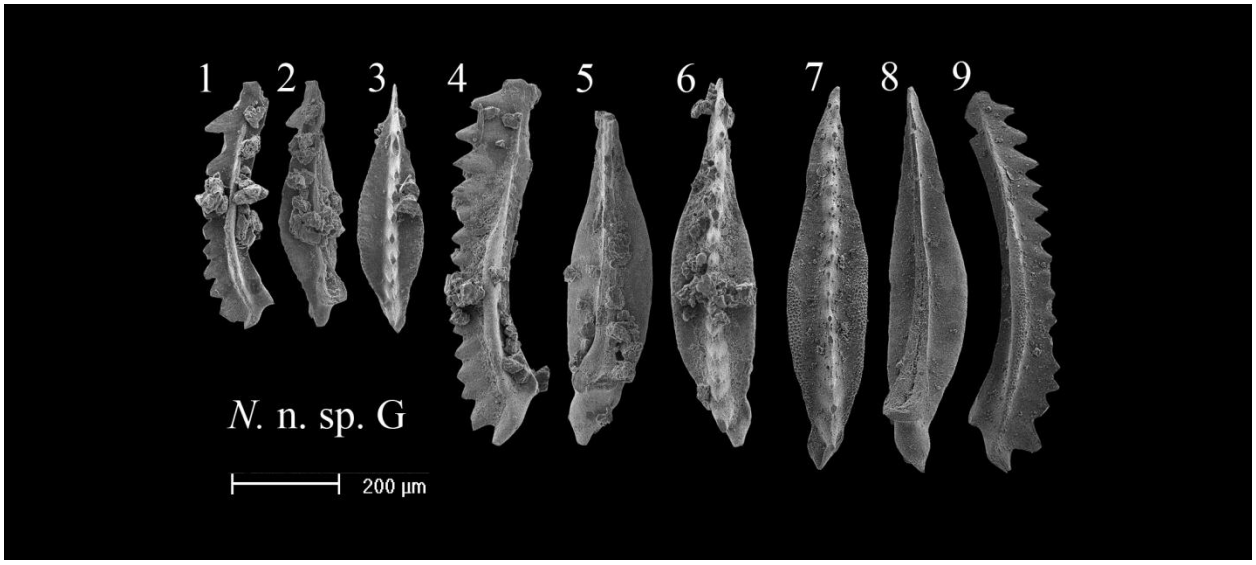



**Figure 2.48.** *Neogondolella* n. sp. G. 1-6, C13, North Tetsa Phosphate. 7-9, 2549.66 m below Kelly Bushing, Murphy Swan d-054-B/093-P9 well.

### ***Neogondolella* n. sp. H**

Figure 2.49

***Holotype:*** fig. 2.49, 4-6

***Age of Holotype:*** Americanum Zone, Lower Anisian, Middle Triassic.

***Type Stratum:*** Toad Formation.

***Type Locality:*** GSC Sample Number C-209952, Mile Post 375 East, B.C.

***Diagnosis:*** Species of *Neogondolella* with biconvex platform margins. Inner platform margin is indented at all growth stages. The widest point of the platform varies from the anterior to the posterior of the element. Posterior margin is narrowly to broadly rounded. Cusp is similar in size to the rest of the carina, which is high and fused, becoming increasingly fused with growth.

***Description:*** Platform biconvex. Position of the widest part is variable, and can be in the anterior, posterior or midpoint of the the element. Platform margins taper from the widest point to the anterior of the element; there is no free blade. The outer platform margin also tapers evenly to the posterior of the element, however the inner margin is indented in the posterior third of the element. Some specimens show a posterior constriction of the platform. In juveniles, posterior margin is pointed, whilst in adults it is rounded. Posterior platform brim also develops with growth. Reticulation is present on the platform margins. In side view, element is arched and platform is thin with upturned margins, becoming thicker with growth. Cusp is similar in size to other denticles and is inclined. Posterior denticle is always present; it is smaller than the cusp in juveniles, but becomes larger than the cusp with growth. Carina is high with an arched upper profile. Denticles are inclined and fused, becoming increasingly fused with growth. Keel is low and narrow in juveniles, becoming wider with growth. It terminates in an open, circular basal loop that surrounds the subterminal basal pit.

***Comparisons:*** *N. hanbulogi* and *N. bulgarica* have similar upturned margins; only *N. hanbulogi* has a platform brim like *N.* n. sp. H, but it does not have such indented platform margins.

***Occurrence in B.C.:*** *Localities* - GSC Locality C-209952 (HB/655), Mile Post 375 East; 3034.8 m below Kelly Bushing, Shell Groundbirch 16-02-078-22W6 well.

*Faunal Assemblages* - *regalis* η Faunal Assemblage to *shoshonensis* Faunal Assemblage.

*Ammonoid Zones* - Americanum Zone (Lower Anisian) to Minor Zone (Middle Anisian).

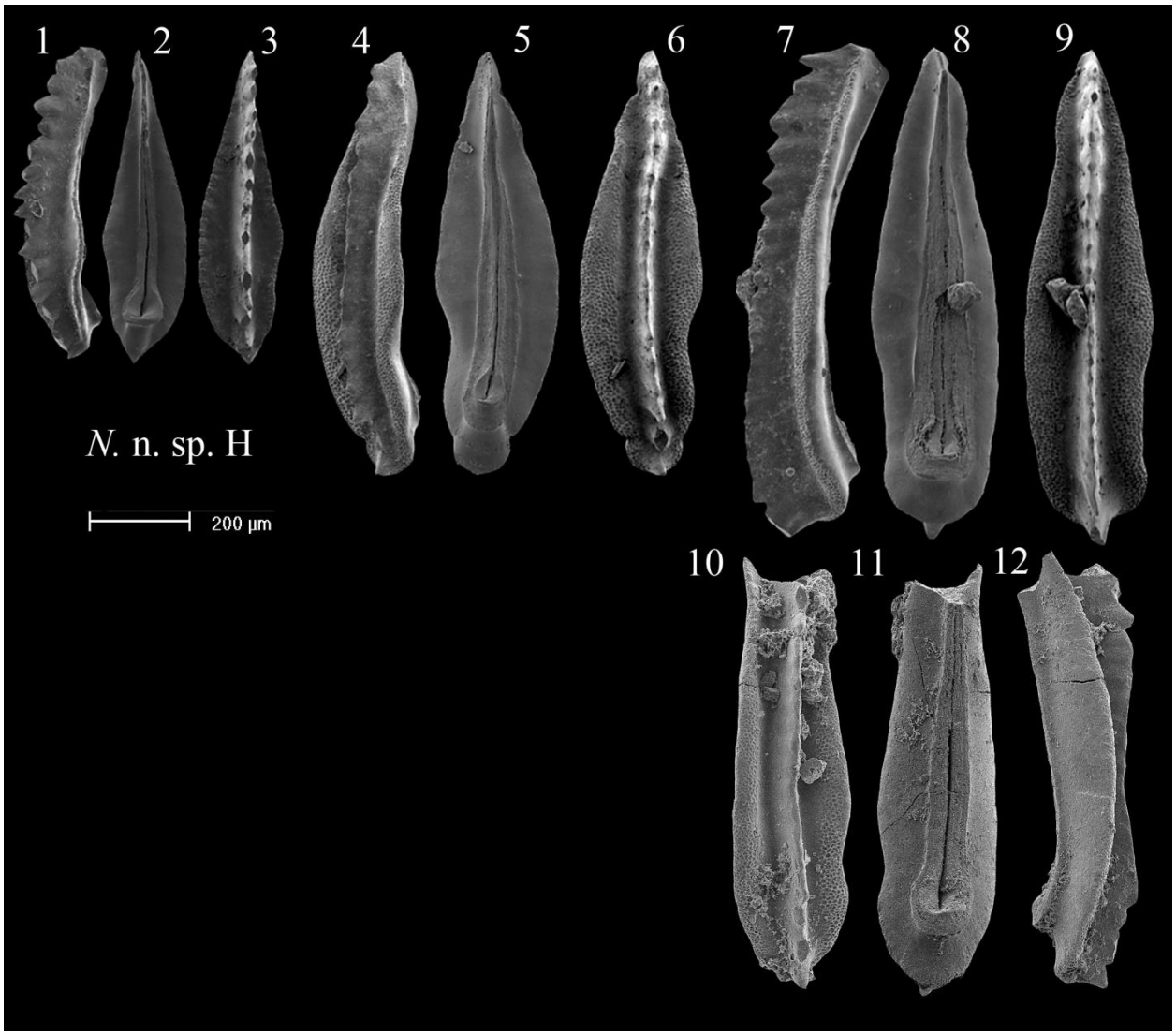



**Figure 2.49.** *Neogondolella* n. sp. H. 1-3, 1858.60-1858.90 m below Kelly Bushing, Petro-Canada Kobes c-074-G/094-B-09 well. 4-6, 3034.8 m below Kelly Bushing, Shell Groundbirch 16-02-078-22W6 well.

## Genus *Paragondolella* Mosher, 1968

*Type Species: Paragondolella excelsa* Mosher, 1968

The genus *Paragondolella* was originally introduced for species whose juvenile growth stages lacked a platform, which appeared with growth (Mosher, 1968). This was shown to be common to other genera by Kozur and Mostler (1971). Vrielynck (1987) and Kozur (1989 b) re-defined *Paragondolella* based on its very high carina, as seen in the holotype of the type species, *P. excelsa.* This latter definition of *Paragondolella* is followed here. It is possible that forms of *Neogondolella* with high carinae, such as *N.* ex gr. *regalis*, belong in *Paragondolella* or their own genus, as they do not possess the same carina as the type species of *Neogondolella, N. mombergensis.*

### *Paragondolella* ex gr. *excelsa* Mosher

Figures 2.50 – 2.52

***Key Species:*** *Paragondolella excelsa* Mosher, 1968

1968 *Paragondolella excelsa* n. sp. – Mosher, p. 938-939, Pl. 118, figs. 1-8.

***Holotype:*** USNM 159211, US National Museum, Washington; Mosher, 1968, Pl. 118, figs. 7-8.

***Age of Holotype:*** Anisian, Middle Triassic.

***Type Stratum:*** Schreyeralmkalk.

***Type Locality:*** Sample Fr-7, Feuerkogel, Austria.

***Allied Taxa:*** *P. postexcelsa* Budurov, Sudar and Mirauta, 1989

*G. liebermani* Kovács and Krystyn, 1994

*G. fueloepi* Kovács, 1994

***Key Features:*** This group is introduced to accommodate common Middle Triassic specimens of *Paragondolella* that share the following morphological characteristics. Species of this group have a broad, flat platform, often with biconvex margins. A posterior platform brim is present in adults and there is no anterior free blade. Carina is high and typically has an arched profile that is highest in the middle of the element. Pit is relatively large and open, and is situated terminally with respect to the keel.

***Description:*** Platform biconvex, widest at midpoint in juveniles. In some adults, the widest point moves to the anterior or posterior third of the element. Platform tapers evenly to the anterior, leaving no free blade. A posterior platform brim develops in adults. Reticulation is absent from most juveniles, but is present on the platform margins of larger specimens. In side view the element is arched, and the platform margins upturned. Cusp is large and inclined, there is often a posterior denticle that remains small at all growth stages. Carina is high and fused, but varies in height. Denticles are inclined and asymmetrical. Keel is narrow and high, expanding into a rounded to sub-rounded basal loop that surrounds the subterminal basal pit.

***Comparisons:*** *P. szaboi* does not have a posterior platform brim and has more upturned margins. *P. alpina* has a free blade. *P. trammeri* has a much narrower platform and a more expanded basal cavity. Morphotypes of *N.* ex gr. *regalis* have a high carina but it is not arched and the platform is much longer and narrower than that of *P.* ex gr. *regalis*.

***Remarks:*** The carina of *P. excelsa* was described by Mosher (1968) as being highest at the anterior; however in the illustration of the holotype it can be seen that the carina is highest in the middle of the element. Of the species belonging to this group, so far only *P. excelsa* and *P. liebermani* have been identified from North America. Mosher (1968) illustrated examples of the juveniles of *P. excelsa* s.s., but juveniles of *P. fueloepi, P. liebermani* and *P. postexcelsa* have not been figured and so it is unclear whether, and how, the juveniles of these species differ from those of *P. excelsa.* In this study, adult specimens belonging to *P. liebermani* were identified, along with juvenile specimens that could not be assigned to one of the four species and so are referred to here as belonging to *P.* ex gr. *excelsa* (fig. 2.50).

***Occurrence in B.C.:*** Hayesi Zone (Middle Anisian) to Deleeni Zone (Upper Anisian).

***Other Occurrences:*** Illyrian (Anisian) to Fassanian (Ladinian) of Austria (Mosher, 1968); Trinodosus Zone (Illyrian) to Archelaus Zone (Longobardian) of Hungary and Greece (Kovács, 1994); Fassanian to Longobardian (Ladinian) of Bulgaria, Romania and former Yugoslavia (Budurov and Sudar, 1989).

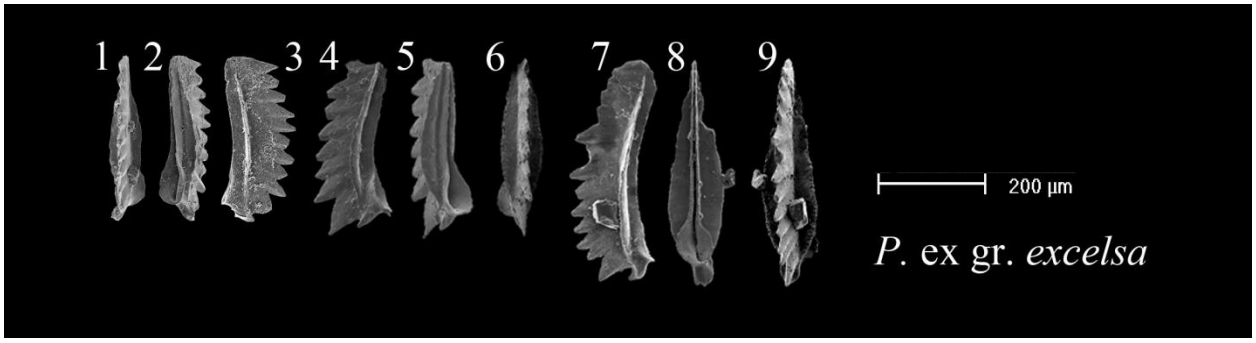



**Figure 2.50.** *Paragondolella* ex gr. *excelsa* juveniles. 1-3, MP375W C3, Mile Post 375 West. 4-6, GSC Locality 68204, Mile Post 375 East. 7-9, GSC Locality C-201926, Mile Post 375 West.

***Paragondolella liebermani*** (Kovács and Krystyn, 1994)

Figures 2.51 – 2.52

1994 *Gondolella liebermani* n. sp. – Kovács and Krystyn, *in* Kovács, p. 492-493, Pl. 6, figs. 1-3.

***Holotype:*** T 6469, Museum of the Hungarian Geological Survey, Budapest; Kovács, 1994, Pl. 6, figs. 1a-d.

***Age of Holotype:*** Trinodosus Zone, Illyrian, Anisian, Middle Triassic.

***Type Stratum:*** Buchenstein Formation.

***Type Locality:*** Bed No. 5, Vászoly, Öreghegy Hill, Balaton Highlands, Hungary.

***Diagnosis:*** A member of *Paragondolella* ex gr. *excelsa* in which the platform is relatively long and narrow.

***Description:*** Platform is biconvex and widest at the midpoint, or slightly to the anterior or posterior of this point. Platform tapers to the anterior and there is no free blade. Posterior platform brim is present. Reticulation is present on the margins of the posterior two thirds of the platform. In side view, element is arched, platform is thin with upturned margins. Cusp is upright and there is no posterior denticle. Carina is high and uniformly fused, rising to the anterior of the element. Denticles vary from upright to inclined and are symmetrical. Keel is narrow and high, developing into an open, rounded basal loop that surrounds the subterminal, deeply excavated basal pit.

***Comparisons:*** *P. excelsa* sensu stricto has a biconvex platform, that is relatively shorter and broader than in *P. liebermani*. *P. postexcelsa* has a carina that decreases in height more rapidly to the posterior than to the anterior and so has a different profile to that of *P. liebermani*. It also has more of an arch to the element. *P. fuelopi* has a platform that shows downstepping to the anterior in side view.

***Remarks:*** Two morphotypes of *P. liebermani* are recognised in this study based on differences in platform shape. Juveniles here assigned to *P.* ex gr. *excelsa* may be examples of juvenile *P. liebermani*.

***Occurrence in B.C.:*** Deleeni Zone (Upper Anisian).

***Other Occurrences:*** Trinodosus Zone to Reitzi Zone (Illyrian) of Hungary and Greece (Kovács, 1994).

*Morphotype α*

Figure 2.51

***Diagnosis:*** Morphotype of *P. liebermani* with platform that is relatively long and narrow with subparallel margins. Platform margins narrow slightly near the posterior end of the element. Platform is initially widest near midpoint of the element. The narrowing seen in smaller specimens becomes diminished with growth.

***Comparisons:*** Platform in *P. liebermani* morphotype β is broader and shorter, with more biconvex margins.

***Remarks:*** The carina becomes lower in larger specimens (fig. 2.51, 10-12). The holotype of *P. liebermani* as figured by Kovács (1994) appears to belong to this morphotype.

***Occurrence in B.C.:*** *Localities* - GSC Locality 99566 (83/205B), East Toad River II; Sample YB C9 and Sample YB C12, both Yellow Bluffs; GSC Locality C-201925 (92/AH25), Mile Post 375 West.

*Faunal Assemblages* - *liebermani* Faunal Assemblage.

*Ammonoid Zones* - Deleeni Zone (Upper Anisian).

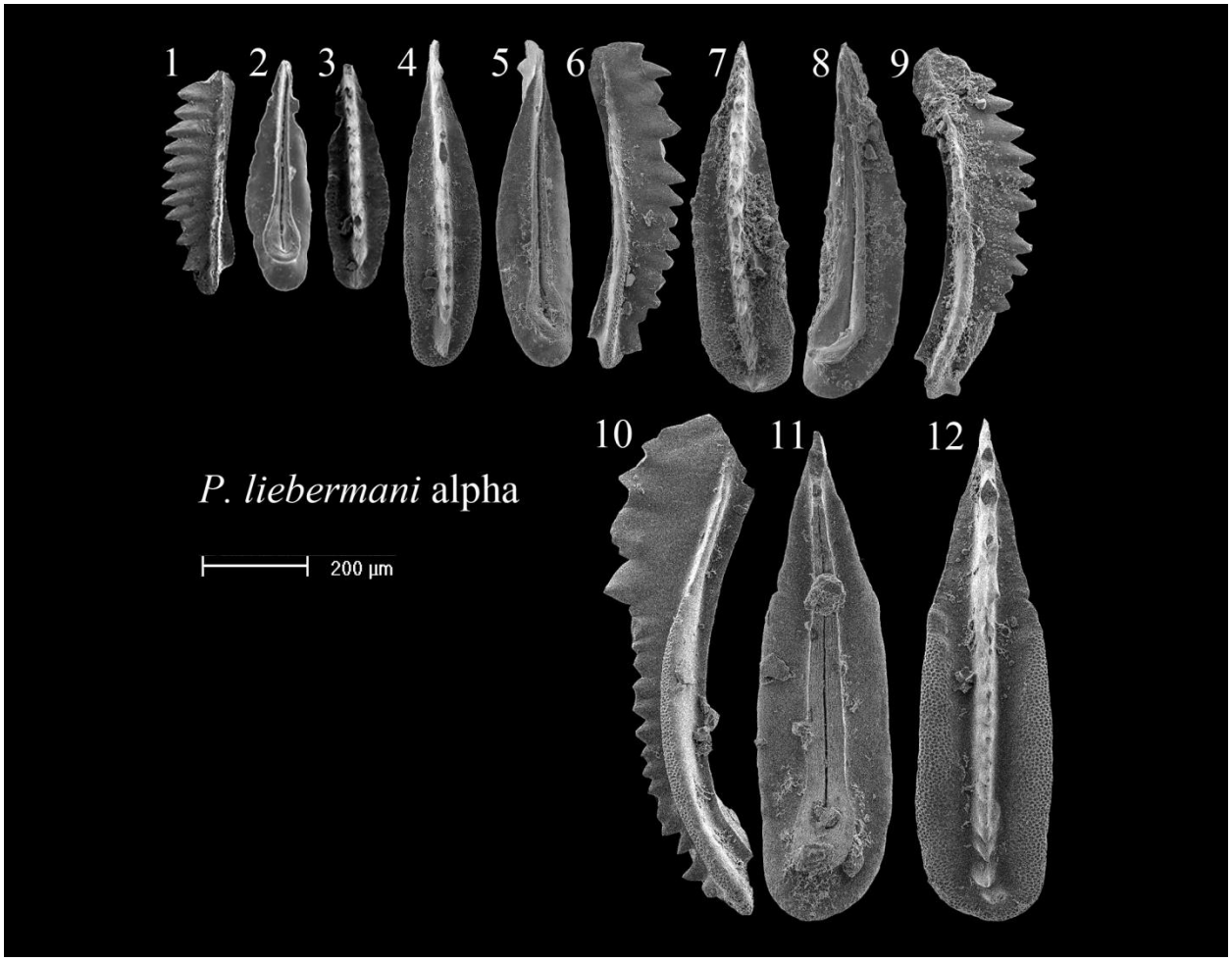



**Figure 2.51.** *Paragondolella liebermani* morphotype α. 1-3, GSC Locality 99566, East Toad River II. 4-6, YB C9, Yellow Bluffs. 7-9, MP386 C4, Mile Post 386. 10-12, YB C12, Yellow Bluffs.

*Morphotype β*

Figure 2.52

***Diagnosis:*** Morphotype of *P. liebermani* with a biconvex platform that is relatively short and broad and widest at the midpoint of the element.

***Comparisons:*** See above.

***Remarks:*** This morphotype is close to *P. excelsa* and may be transitional between this species and *P. liebermani*.

***Occurrence in B.C.:*** *Localities* - GSC Locality C-201902 (92/AH2), Yellow Bluffs; GSC Locality C-201925 (92/AH25), Mile Post 375 West.

*Faunal Assemblages* - *liebermani* Faunal Assemblage.

*Ammonoid Zones* - Deleeni Zone (Upper Anisian).

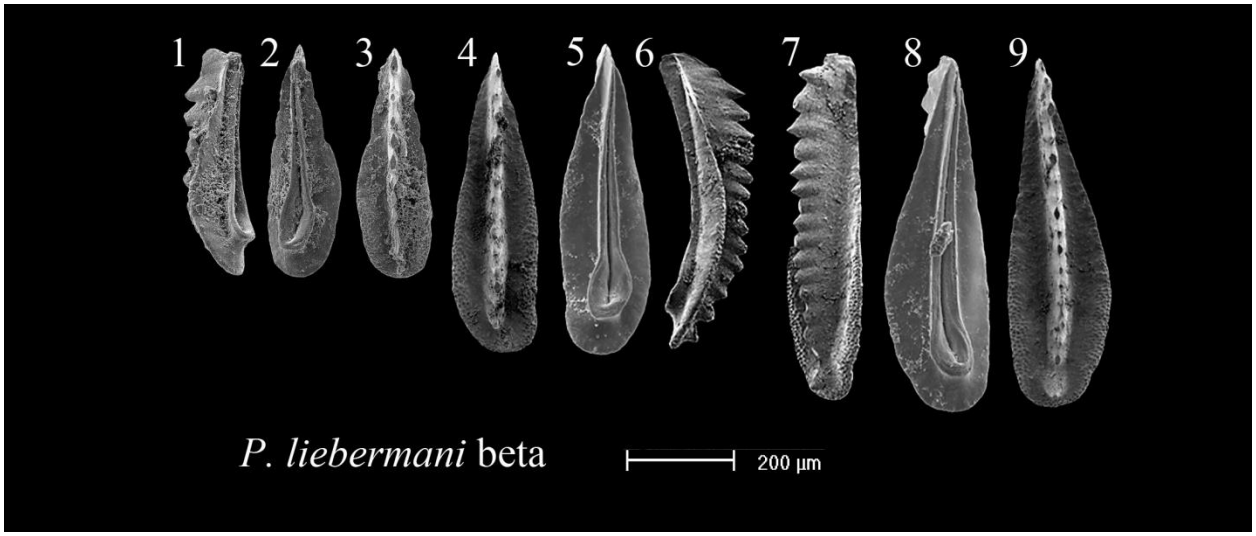



**Figure 2.52.** *Paragondolella liebermani* morphotype β. 1-3, MP386 C4, Mile Post 386. 4-9, GSC Locality C-201925, Mile Post 375 West.

# CHAPTER 3

## Dating the Doig: Conodonts constrain the age of the Montney-Doig boundary in northeastern British Columbia

## 3.1 INTRODUCTION

The Montney and Doig formations are important natural gas sources and reservoirs in northeastern British Columbia. It is thought that together they contain as much as 900 Tcf of natural gas (Walsh *et al.*, 2006), and they contain up to 22% of British Columbia's natural gas reserves (OGC Report, 2013). Thus far, much of the research on these units has focused on the Montney Formation, due in part to the longer history of drilling in this formation, and the larger size of its reserves. As of 2013, the majority of production comes from the Montney Formation (Adams, 2013). The Doig Formation is comparatively quite poorly understood. The boundary between the two formations is marked in most areas by a heavily bioturbated interval, containing burrows belonging to the *Glossifungites* ichnofacies (Zonneveld, 2010). This is overlain by an intraclast lag and a zone of high phosphate content (Gibson and Barclay, 1989), known informally as the Doig Phosphate Zone (Edwards *et al.*, 1994). This is an important part of the formation, as much of the hydrocarbon in the Doig Formation may have been generated in this zone (Riediger *et al.*, 1990). As much as 200 Tcf of natural gas is estimated to be contained within the Doig Formation, with up to 70 Tcf of this within the Doig Phosphate Zone (Walsh *et al.*, 2006). The mechanisms behind the formation of the phosphate zone are poorly understood, although it is widely recognized that the surface marks the onset of a marine transgression (*e.g.* Barss *et al.*, 1964; Gibson and Barclay, 1989; Gibson, 1993; Edwards *et al.*, 1994). The age of the zone, and therefore also the age of the Montney-Doig boundary, is not well constrained. Estimates have placed the age of the boundary in the Spathian (Zonneveld, 2010), Anisian (Qi, 1995) and Ladinian (Armitage, 1962). The boundary is commonly drawn in figures at approximately the Spathian-Anisian boundary, although there has been little biostratigraphic work done to support this. Additionally, it is not clear whether this boundary is diachronous or

not. If it is diachronous, then it is important to understand the extent of the diachroneity, and to know where the boundary is oldest or youngest. This will also have implications for the age and duration of the Doig Phosphate Zone. The top of the Doig Phosphate Zone, however, is not always easy to distinguish from the overlying part of the Doig Formation, making the duration of the zone difficult to determine.

In order to constrain the age of the Montney-Doig boundary (and the base of the Doig Phosphate Zone), samples were collected for conodont analysis from nine wells in the Kobes-Altares-Groundbirch region of northeastern British Columbia (fig. 3.1). All of these nine wells intercept the Montney-Doig boundary. Six of the wells are aligned in a roughly northwest-southeast orientation, approximately parallel to the strike of the Triassic beds in this region. The remaining three wells are perpendicular to this trend, aligned approximately northeast-southwest. This allows a three-dimensional model of the boundary to be created in this area.

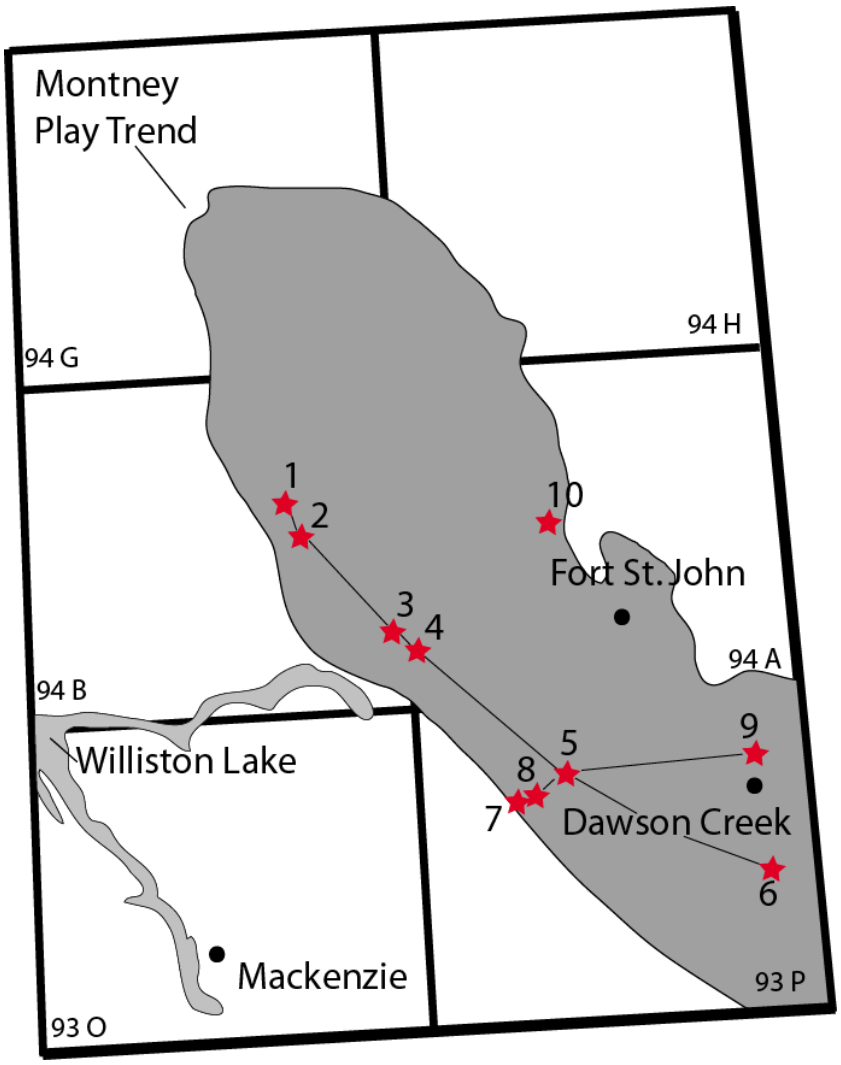



**Figure 3.1.** Map showing location of the sampled wells in British Columbia and their relationship to the Montney Play Trend. Also shown is the location of the Texaco NFA Buick Creek No. 7 6-26-87-21W6 well, which is the type well for both the Montney and Doig formations. Lines between wells indicate the location of the cross-section lines in figures 12 and 13. 1) Petro-Canada Kobes c-074-G/094-B-9; 2) Petro-Canada Kobes d-048-A/094-B-09; 3) Talisman Altares c-085-I/094-B-01; 4) Talisman Altares 16-17-083-25W6; 5) Shell Groundbirch 16-35-078-21W6; 6) Murphy Swan d-054-B/093-P9; 7) Talisman Groundbirch 03-06-078-22W6; 8) Shell Groundbirch 16-02-078-22W6; 9) Arc Dawson 07-13-79-15W6; 10) Texaco NFA Buick Creek No. 7 6-26-87-21W6. Montney Play Trend after Hayes (2012).

## 3.2 GEOLOGICAL SETTING

Both the Montney Formation and the Doig Formation were first defined by Armitage (1962) in the Texaco N.F.A. Buick Creek No. 7 well (6-26-87-21W6) in British Columbia (fig. 3.1). Together they make up the Daiber Group (Armitage, 1962).

The Montney Formation consists of up to 450 m of dark grey siltstone and sandstone with very minor amounts of shale. It was formed in a variety of depositional environments, from offshore turbidites and submarine fans in the west, to more proximal shoreface, deltaic and intertidal environments in the east (Markhasin, 1997; Moslow and Davies, 1997; Davies *et al.*, 1997; Kendall, 1999; Moslow, 2000; Panek, 2000; Zonneveld *et al.*, 2010 a). The Montney Formation in Alberta was divided into three units by Davies *et al.* (1997), with a lower sandstone unit, a middle coquina unit and an upper siltstone unit. This was expanded on by Dixon (2000), who defined two new units within the Montney Formation in B.C.: a lower siltstone-sandstone unit equivalent to the whole of the Montney Formation in Alberta (the middle coquina member is missing in B.C.) and an upper shale unit that is absent in Alberta. Dixon's stratigraphic subdivision has not been subsequently adopted by any other Montney workers. More commonly, the 'Shale Member' has been termed the Upper Montney Formation and the 'Siltstone-Sandstone Member' has been divided into the Lower and Middle Montney Formation. The Montney Formation is further subdivided by different companies in a number of different ways, commonly using letter designations.

The oldest part of the Montney Formation in British Columbia is earliest Triassic (Griesbachian; Lower Induan) in age (see chapter 4). The Montney Formation is equivalent to the Grayling and lower part of the Toad formations in the surface outcrop of British Columbia north of the Pine

River (Gibson, 1971). It is also equivalent to the Vega-Phroso Siltstone member of the Sulphur Mountain Formation in British Columbia south of the Pine River and in Alberta (Gibson, 1968; see fig. 3.2).

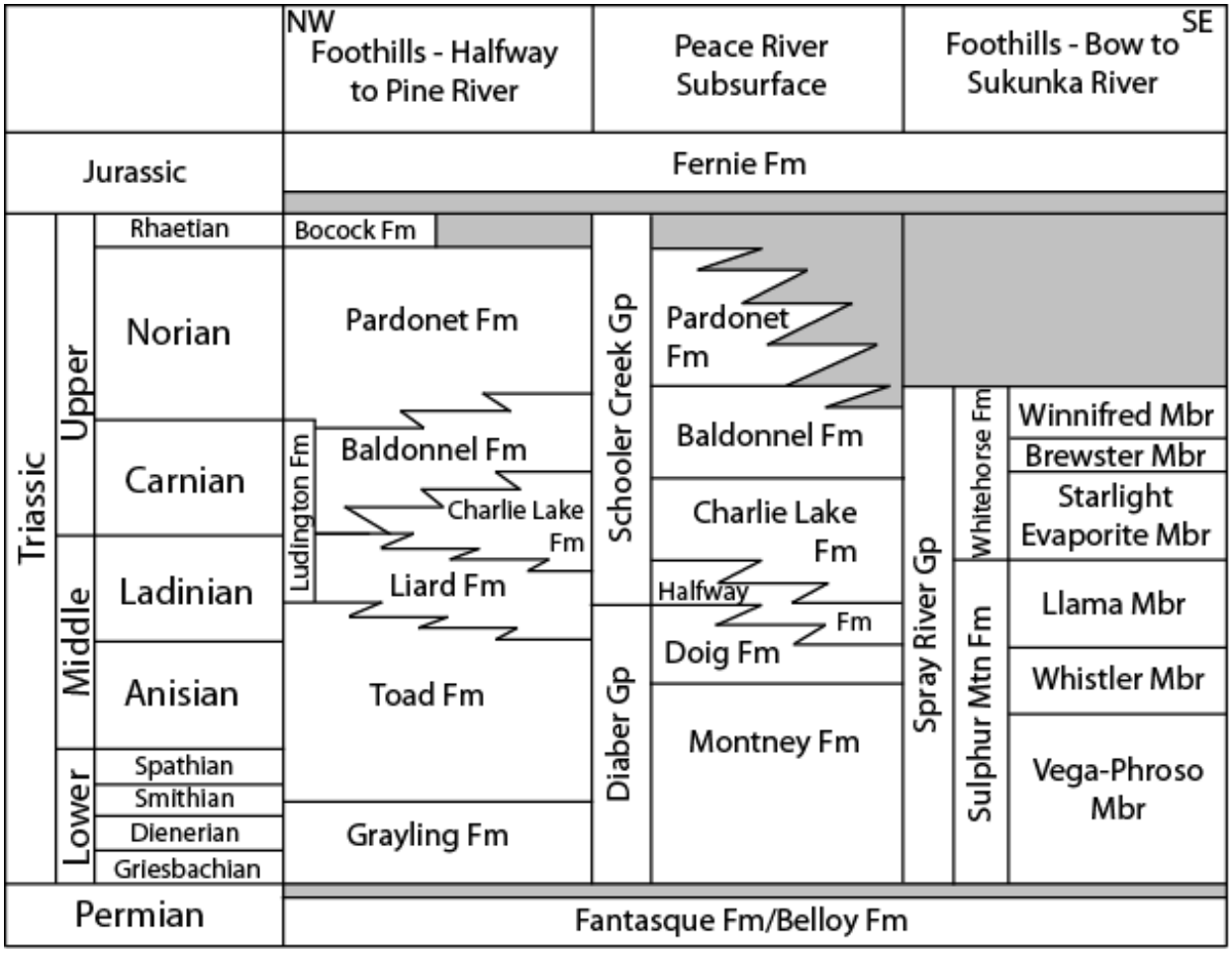



**Figure 3.2.** Correlation chart of Triassic formations in the surface and subsurface of British Columbia and the surface of Alberta. Fm = Formation; Mbr = Member. Stage boundary ages are in Ma, and taken from Ogg (2012).

The Doig Formation immediately overlies the Montney Formation, and consists of up to 150 m of siltstone, shale, sandstone, and generally minor amounts of bioclastic packstone and

grainstone. It was formed in a range of environments, including offshore, offshore transition and shoreface (Evoy and Moslow, 1995).

Davies (1997 a) informally subdivided the Doig Formation into three units. The lowest part of the formation consists of a phosphate-rich gravel lag that is informally termed the Doig Phosphate Zone (Edwards *et al.*, 1994). This can vary from 10 m thick to over 80 m locally and can be identified in core samples, as well as in gamma ray logs by its very high signal, due to uranium's affinity for phosphate. The Doig Phosphate Zone commonly overlies a *Glossifungites*-demarcated discontinuity surface. The *Glossifungites* ichnofacies includes trace fossils emplaced within a firm substrate (Seilacher, 1967; Frey and Pemberton, 1985; MacEachern *et al.*, 1992), and their presence implies an hiatus in deposition at the Montney-Doig boundary. This supports the interpretation that the Doig Phosphate Zone represents a marine transgression over a coplanar lowstand surface of erosion and transgressive surface of erosion.

The phosphate is preserved in a variety of forms. Towards the basal contact the phosphate occurs as phosphatized clasts, phosphatic sand and layered grains. Many of the larger clasts consist of phosphatic pebbles comprised of smaller phosphatic grains. The nature of the layered clasts indicates that they underwent multiple cycles of burial, phosphatization, uplift and erosion (Pufahl and Grimm, 2003). Thus, the Doig Phosphate Zone is interpreted to represent a condensed section. The presence of ichnogenera indicative of both the *Glossifungites* and *Trypanites* ichnofacies allows for the recognition of a number of disconformities within the Doig Phosphate Zone, which suggest periods of erosional and/or non-deposition during the formation of the zone (see chapter 4). The upper part of the Doig Formation (a few metres to several 10s of metres above the phosphate zone) contains sand bodies (commonly referred to as ATSBs;

anomalously thick sand bodies) that have been variably interpreted as depression fill of grabens (Wittenburg, 1992) or slumps (Qi, 1995), as shoreface deposits (Evoy, 1997), delta channels (Harris, 2000), barrier islands (Rahman, 2005), or incised-valley fill (Rahman and Henderson, 2005). Dixon (2011) considered the graben interpretation to be the most likely, based on regional correlations. However, as these features occur throughout the Western Canada Sedimentary Basin (WCSB), and as they are highly variable in the nature of their lithological fill, it is herein considered likely that no single interpretation explains the formation of all of these bodies.

The highest part of the Doig Formation consists of muddy sandstone thought to have been formed in a lower shoreface environment that underlies the cleaner sands of the Halfway Formation (Evoy, 1998).

As with all hydrocarbon-bearing stratigraphic units, the Doig Formation is both a lithostratigraphic entity as well as an economic and political entity. The lithostratigraphic base of the Doig Formation occurs at the base of the Doig Phosphate Zone. In defining this formation, the British Columbia government follows this practice; however, the Alberta government does not. Thus, although the actual Montney-Doig contact should be placed at the base of the phosphate zone, in Alberta the economic hydrocarbon boundary is placed lower, at the base of a regionally extensive siltstone body (Davies and Hume, 2011). This unit was referred to informally as the Gordondale Member of the Montney Formation by Davies (1997 a) but was never formalized and no type-well or section was designated. Subsequently, the lower part of the Jurassic Fernie Formation was formally redesignated the Gordondale Member, and a type-well designated (Asgar-Deen *et al*., 2004). Thus, this name is no longer available to be used for a member of either the Doig or the Montney Formation. Commonly, this unit is now referred to

as the ‘Lower Doig Siltstone Member’; however, this unit has not been formalized, nor formally removed from the Montney Formation and added to the Doig Formation. This issue requires formal treatment that falls outside the purview of the present paper and it is not further discussed herein.

The Doig Formation is equivalent to the upper part of the Toad Formation and the lower part of the Liard Formation in British Columbia north of Pine River (Gibson, 1971), and the Whistler member of the Sulphur Mountain Formation in British Columbia south of Pine River and in Alberta (Edwards *et al.*, 1994; Davies *et al.*, 1997; see fig. 3.2).

The Montney and Doig formations have been interpreted to record two large-scale cycles of sea-level transgression and regression (Gibson and Barclay, 1989). The Montney Formation was deposited during the first of these and consists of several smaller scale transgressive-regressive cycles. Two transgressive-regressive cycles were recognized in the Induan (Griesbachian-Dienerian) part of the succession in the Pedigree-Ring-Border-Kahntah area near the subcrop erosional limit of the Montney (Utting *et al.*, 2005). The lower part of the Doig Formation was deposited during a marine transgression, whilst the upper part formed during a regional marine regression that continued during the formation of the overlying Halfway and Charlie Lake Formations (Gibson and Barclay, 1989; Gibson, 1993). The absolute depth of the Montney Formation is not well constrained, although the shape of the clinoforms in seismic sections and the presence of shallow water trace fossils and conodonts suggest that the formation was deposited in a nearshore to shelf environment (Edwards *et al.*, 1994). At several stages during its development the Doig Phosphate Zone was emergent (see chapter 4). Some of the overlying sandstone bodies have been interpreted to represent shallow water or deltaic deposits

(Wittenberg, 1992; Evoy, 1997; Harris, 2000; Rahman, 2005). The overlying Halfway Formation represents continued regression over the Doig Formation, being deposited in a beach-barrier island environment (Barclay and Leckie, 1986; Cant, 1986; Willis, 1992; Caplan, 1992; Willis and Moslow, 1994; Caplan and Moslow, 1997, 1999).

The sediments of the Montney and Doig formations were deposited within the Peace River Basin, a sub-basin of the WCSB that forms an arcuate trend throughout British Columbia and Alberta (Davies, 1997 a). This basin is thought to have initiated during the Mississippian due to collapse of the Peace River Arch, possibly during an interval of transtension (Davies, 1997 a). Within this basin, a series of graben structures (Fort St. John Graben, Dawson Creek Graben) formed in response to initial subsidence of the previously emergent Peace River Arch in the Mississippian (Cant, 1988; Davies, 1997 a). The further subsidence and collapse of this arch to form the Peace River Embayment (Barclay *et al.*, 1990) and continued movement on the graben structures (Davies, 1997 a) were important controls on the distribution of sediment deposited during the Triassic, as well as the current distribution of producing oil and gas fields within the Montney and Doig plays (Berger *et al.*, 2009).

## 3.3 MATERIAL AND METHODS

Cores from nine wells were logged for this study and a total of 102 samples were collected from the Montney and Doig formations for conodont analysis. Cores were examined at the Charlie Lake Core Facility in British Columbia. The cores come from the following nine wells: Petro-Canada Kobes c-074-G/094-B-9; Petro-Canada Kobes d-048-A/094-B-09; Talisman Altares c-085-I/094-B-01; Talisman Altares 16-17-083-25W6; Arc Dawson 07-13-79-15W6; Murphy Swan d-054-B/093-P9; Talisman Groundbirch 03-06-078-22W6; Shell Groundbirch 16-02-078-

22W6 and Shell Groundbirch 16-35-078-21W6. All intervals are recorded in standard drilling depths which record the interval below the Kelly Bushing (KB) on the drill rig floor. The location of these wells is shown in figure 3.1, and the location of each of the samples is listed in table 3.1. Other wells were observed to assess the nature of the contact throughout the basin but were not sampled for biostratigraphic analyses.

The samples were processed at the Geological Survey of Canada in Vancouver and at the University of British Columbia. They were crushed, weighed and dissolved in buffered 10% dilute acetic acid, for a period of 10 – 14 days. The samples were then sieved to retain the 850μm - 90μm fraction. This was then rinsed, dried and put through sodium polytungstate with a specific gravity of 2.85. The heavy fraction was retained and conodonts were picked under a light microscope. Images of all the conodonts were obtained using the SEM facility at the Geological Survey of Canada in Vancouver.

After processing, 49 of the 102 samples were found to contain conodonts that could be identified (see table 3.1).

| Well | Formation | Depth (m) | Conodonts Identified |
|---|---|---|---|
| PCK c-074-G/094-B-9 | Montney | 1951.50-1952.00 | None |
| PCK c-074-G/094-B-9 | Montney | 1946.90-1947.15 | *Bo. buurensis, Ns. crassatus, Nv. waageni* |
| PCK c-074-G/094-B-9 | Montney | 1945.60-1945.80 | None |
| PCK c-074-G/094-B-9 | Doig | 1860.30-1860.60 | *Ng. regalis β, Ng. regalis ε, Ng.* n. sp. D, *Ng.* n. sp. H, *Ng. shoshonensis* |
| PCK c-074-G/094-B-9 | Doig | 1858.60-1858.90 | *Ng.* ex gr. *regalis* |
| PCK d-048-A/094-B-09 | Montney | 1968.25 | None |
| PCK d-048-A/094-B-09 | Montney | 1967.85 | *Ch. timorensis, Ns. triangularis* |
| PCK d-048-A/094-B-09 | Doig | 1967.30-1967.50 | *Tr. homeri, Ng. n.sp. I, Ng. regalis α, Ng. regalis β* |
| PCK d-048-A/094-B-09 | Doig | 1966.00-1967.00 | None |
| PCK d-048-A/094-B-09 | Doig | 1964.80-1965.00 | None |
| PCK d-048-A/094-B-09 | Doig | 1965.00-1965.40 | *Ng. regalis α, Ng. regalis δ* |
| TA c-085-I/094-B-01 | Doig | 2370.61-2369.96 | *Ng. regalis β, Ng. regalis γ, Ng.* n. sp. B |
| TA c-085-I/094-B-01 | Doig | 2368.88-2368.04 | None |
| TA c-085-I/094-B-01 | Doig | 2366.75-2366.06 | None |
| TA c-085-I/094-B-01 | Doig | 2315.22-2314.50 | None |
| TA c-085-I/094-B-01 | Doig | 2306.82-2306.01 | None |
| TA 16-17-083-25W6 | Montney | 2530.10-2530.40 | *Cl. meishanensis* |
| TA 16-17-083-25W6 | Montney | 2527.50-2528.50 | *Cl.* sp. |
| TA 16-17-083-25W6 | Montney | 2523.20-2524.10 | None |
| TA 16-17-083-25W6 | Montney | 2515.30-2516.30 | None |
| TA 16-17-083-25W6 | Montney | 2514.30-2515.30 | None |
| TA 16-17-083-25W6 | Montney | 2499.80-2501.70 | None |
| TA 16-17-083-25W6 | Montney | 2495.00-2496.00 | None |
| TA 16-17-083-25W6 | Montney | 2490.50-2491.50 | *Cl. carinata* |
| TA 16-17-083-25W6 | Montney | 2484.00-2484.80 | None |
| TA 16-17-083-25W6 | Montney | 2470.00-2470.75 | *Ns. cristagalli* |
| TA 16-17-083-25W6 | Montney | 2453.00-2453.75 | None |
| TA 16-17-083-25W6 | Montney | 2447.80-2448.80 | None |
| TA 16-17-083-25W6 | Montney | 2431.80-2432.40 | None |
| TA 16-17-083-25W6 | Montney | 2424.50-2425.50 | *Nv. waageni* |

| Well | Formation | Depth (m) | Conodonts Identified |
|---|---|---|---|
| TA 16-17-083-25W6 | Montney | 2420.50-2421.20 | None |
| TA 16-17-083-25W6 | Montney | 2402.40-2403.30 | *Nv. waageni, Ns. posterolongatus, Ns. pakistanensis, G. bransoni, P. meeki* |
| TA 16-17-083-25W6 | Montney | 2394.00-2395.00 | *Sc. mosheri, Sc. phryna, Co. conservativa* |
| TA 16-17-083-25W6 | Montney | 2393.20-2394.10 | *Sc. mosheri, G. bransoni* |
| TA 16-17-083-25W6 | Montney | 2388.70-2389.60 | *Sc. mosheri, Co. conservativa* |
| TA 16-17-083-25W6 | Montney | 2384.00-2385.00 | *Ng.* sp. D |
| TA 16-17-083-25W6 | Montney | 2380.10-2381.00 | None |
| TA 16-17-083-25W6 | Montney | 2370.70-2371.50 | *Ng.* sp., *Nv.* sp. |
| TA 16-17-083-25W6 | Montney | 2368.00-2369.00 | None |
| TA 16-17-083-25W6 | Montney | 2356.00-2357.00 | None |
| TA 16-17-083-25W6 | Montney | 2330.80-2332.20 | None |
| TA 16-17-083-25W6 | Montney | 2322.00-2323.00 | None |
| TA 16-17-083-25W6 | Montney | 2304.40-2305.30 | None |
| TA 16-17-083-25W6 | Montney | 2276.50-2277.50 | None |
| TA 16-17-083-25W6 | Montney | 2263.75-2264.70 | None |
| TA 16-17-083-25W6 | Montney | 2281.25-2282.00 | None |
| TA 16-17-083-25W6 | Montney | 2258.00-2259.00 | *Ng.* sp. |
| TA 16-17-083-25W6 | Montney | 2257.43-2258.30 | *Ng.* sp. A |
| TA 16-17-083-25W6 | Doig | 2256.00-2257.00 | None |
| TA 16-17-083-25W6 | Doig | 2254.44-2255.30 | *Ng.* sp. |
| TA 16-17-083-25W6 | Doig | 2252.00-2253.00 | *Ng.* ex gr. *regalis* |
| TA 16-17-083-25W6 | Doig | 2243.00-2244.00 | *Ng.* ex gr. *regalis* |
| TA 16-17-083-25W6 | Doig | 2241.46-2242.35 | *Ng.* sp. |
| TA 16-17-083-25W6 | Doig | 2240.00-2241.00 | *Ng.* sp. |
| TA 16-17-083-25W6 | Doig | 2238.74-2239.75 | *Ng. regalis α* |
| TA 16-17-083-25W6 | Doig | 2236.09-2237.05 | *Ng.* ex gr. *regalis* |
| TA 16-17-083-25W6 | Doig | 2234.10-2234.57 | *Ng. regalis α, Pa. excelsa* |
| AD 07-13-79-15W6 | Doig | 2054.68-2054.48 | None |
| AD 07-13-79-15W6 | Doig | 2054.30-2054.05 | *Ng. regalis α, Ng.* n. sp. C, *Ng.* n. sp. D |
| MS d-054-B/093-P9 | Doig | 2557.30 | None |

| Well | Formation | Depth (m) | Conodonts Identified |
|---|---|---|---|
| MS d-054-B/093-P9 | Doig | 2556.90 | *Ng.* n. sp. B |
| MS d-054-B/093-P9 | Doig | 2556.25 | None |
| MS d-054-B/093-P9 | Doig | 2553.80 | *Ng. regalis γ, Ng.* n. sp. B, *Ng.* n. sp. C |
| MS d-054-B/093-P9 | Doig | 2553.40 | None |
| MS d-054-B/093-P9 | Doig | 2551.80 | None |
| MS d-054-B/093-P9 | Doig | 2549.66 | *Ng. constricta γ* |
| MS d-054-B/093-P9 | Doig | 2548.45 | None |
| TG 03-06-078-22W6 | Montney | 3884.25 | None |
| TG 03-06-078-22W6 | Montney | 3486.00 | *Ng. discreta* |
| TG 03-06-078-22W6 | Montney | 3350.10 | *Ns. brevissimus, Tr. homeri, Nv.* sp. |
| TG 03-06-078-22W6 | Montney | 3348.40 | None |
| TG 03-06-078-22W6 | Doig | 3202.80 | None |
| TG 03-06-078-22W6 | Doig | 3192.50 | *Ng.* sp. |
| TG 03-06-078-22W6 | Doig | 3185.00 | *Ng.* sp. |
| SG 16-02-078-22W6 | Montney | 3150.40 | None |
| SG 16-02-078-22W6 | Montney | 3127.54 | None |
| SG 16-02-078-22W6 | Montney | 3113.00 | None |
| SG 16-02-078-22W6 | Montney | 3094.80 | None |
| SG 16-02-078-22W6 | Montney | 3094.40 | None |
| SG 16-02-078-22W6 | Montney | 3089.00 | None |
| SG 16-02-078-22W6 | Montney | 3084.90 | None |
| SG 16-02-078-22W6 | Montney | 3073.00 | *Ch. timorensis, Ng.* ex gr. *regalis, Ng.* n. sp. B |
| SG 16-02-078-22W6 | Montney | 3067.60 | *Ch.* sp., *Ng.* sp. |
| SG 16-02-078-22W6 | Montney | 3057.60 | None |
| SG 16-02-078-22W6 | Montney | 3052.50 | *Ng.* ex gr. *regalis, Ng.* sp. "A" |
| SG 16-02-078-22W6 | Montney | 3045.50 | *Ng.* sp. "A" |
| SG 16-02-078-22W6 | Montney | 3039.30 | *Ng.* sp. "A", *Ng.* sp. "O" |
| SG 16-02-078-22W6 | Doig | 3034.80 | *Ng. bifurcata, Ng. regalis ε, Ng.* n. sp. F, *Ng.* n. sp. H, *Ch.* sp. |
| SG 16-02-078-22W6 | Doig | 3034.60 | *Ng.* sp. "O" |
| SG 16-02-078-22W6 | Doig | 3029.20 | None |

| Well | Formation | Depth (m) | Conodonts Identified |
|---|---|---|---|
| SG 16-02-078-22W6 | Doig | 3020.30 | *Ng.* sp. "A", *Ng.* sp. "O" |
| SG 16-02-078-22W6 | Doig | 2999.20 | *Ng.* ex gr. *constricta*, *Ng.* ex gr. *shoshonensis*, *Ng.* sp. "F" |
| SG 16-35-078-21W6 | Montney | 2971.80 | *Sc. mosheri*, *Ng.* sp. |
| SG 16-35-078-21W6 | Montney | 2970.37 | *Sc. mosheri*, *Ns. pakistanensis* |
| SG 16-35-078-21W6 | Montney | 2969.00 | *Sc. mosheri*, *Ng.* sp. |
| SG 16-35-078-21W6 | Montney | 2781.00 | None |
| SG 16-35-078-21W6 | Montney | 2773.20 | *Ch. timorensis*, *Ng.* ex gr. *regalis*, *Ng.* n. sp. B |
| SG 16-35-078-21W6 | Montney | 2765.50 | None |
| SG 16-35-078-21W6 | Montney | 2763.20 | None |
| SG 16-35-078-21W6 | Doig | 2758.40 | *Ng.* ex gr. *regalis*, *Ng.* sp. |
| SG 16-35-078-21W6 | Doig | 2753.75 | None |
| SG 16-35-078-21W6 | Doig | 2749.00 | None |

**Table 3.1.** Conodont samples from wells in northeastern B.C., showing their depth below KB, the formation from which they were collected, and the conodonts that were recovered. PCK = Petro-Canada Kobes, TA = Talisman Altares, AD = Arc Dawson, MS = Murphy Swan, TG = Talisman Groundbirch, SG = Shell Groundbirch, *Bo = Borinella*, *Ns. = Neospathodus*, *Nv. = Novispathodus*, *Ng. = Neogondolella*, *Ch. = Chiosella*, *Tr. = Triassospathodus*, *Cl. = Clarkina*, *G. = Guanxidella*, *P. = Paulella*, *Sc. = Scythogondolella*, *Co. = Conservatella*, *Pa. = Paragondolella.*

## 3.4 BIOSTRATIGRAPHY

### *Petro-Canada Kobes c-074-G/094-B-9*

Core from this well covers the interval from 1955 m to 1855 m below KB. Five samples were collected from this core, and three contained identifiable conodonts (see table 3.1; fig. 3.3).

The Montney-Doig boundary is at 1861 m (fig. 3.4). The lowest productive sample comes from 1946.90-1947.15 m, in the Montney Formation. This sample contains *Borinella buurensis*, *Neospathodus crassatus* and *Novispathodus waageni*. *B. buurensis* and *Nv. waageni* are indicative of the uppermost part of the *waageni* Zone (Orchard, 2008), equivalent to the Tardus ammonoid Zone, which is uppermost Smithian. *Ns. crassatus* is indicative of lowermost Spathian (Orchard, 1995) and so this sample must closely approximate the Smithian-Spathian boundary.

The sample from 1860.30-1860.60 m comes from the Doig Formation and contains *Neogondolella regalis* morphotypes β and ε, *N.* n. sp. D, *N.* n. sp. H and *N. shoshonensis.* These conodonts are typical of the Minor ammonoid Zone (see chapter 2), which is Middle Anisian (Tozer, 1994). The Lower-Middle Triassic boundary must therefore occur between 1947.15 m and 1860.60 m. The sample at 1858.60-1858.90 m also contains conodonts from the Minor ammonoid Zone. The Montney-Doig boundary is Spathian or Anisian in this well. The top of the Doig Phosphate Zone is at 1828 m.

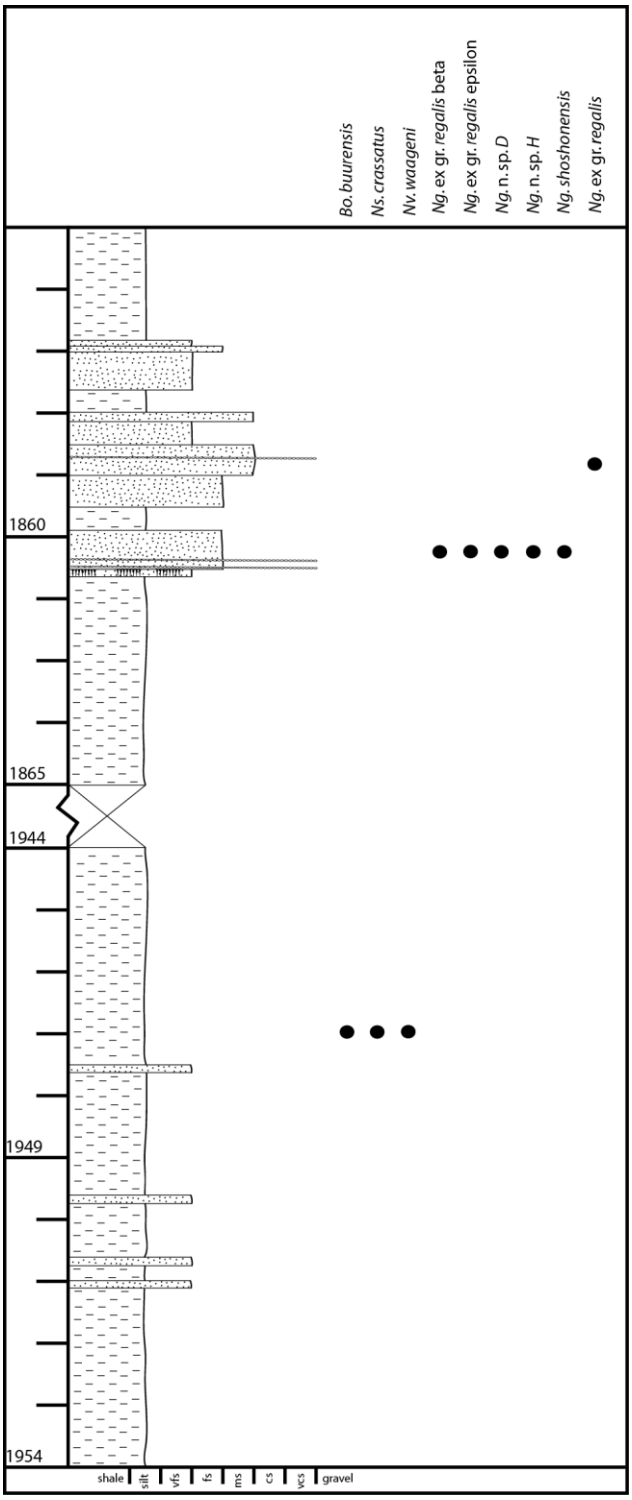



**Figure 3.3.** Lithological log and position of conodont samples in the Petro-Canada Kobes c-074-G/094-B-9 well.

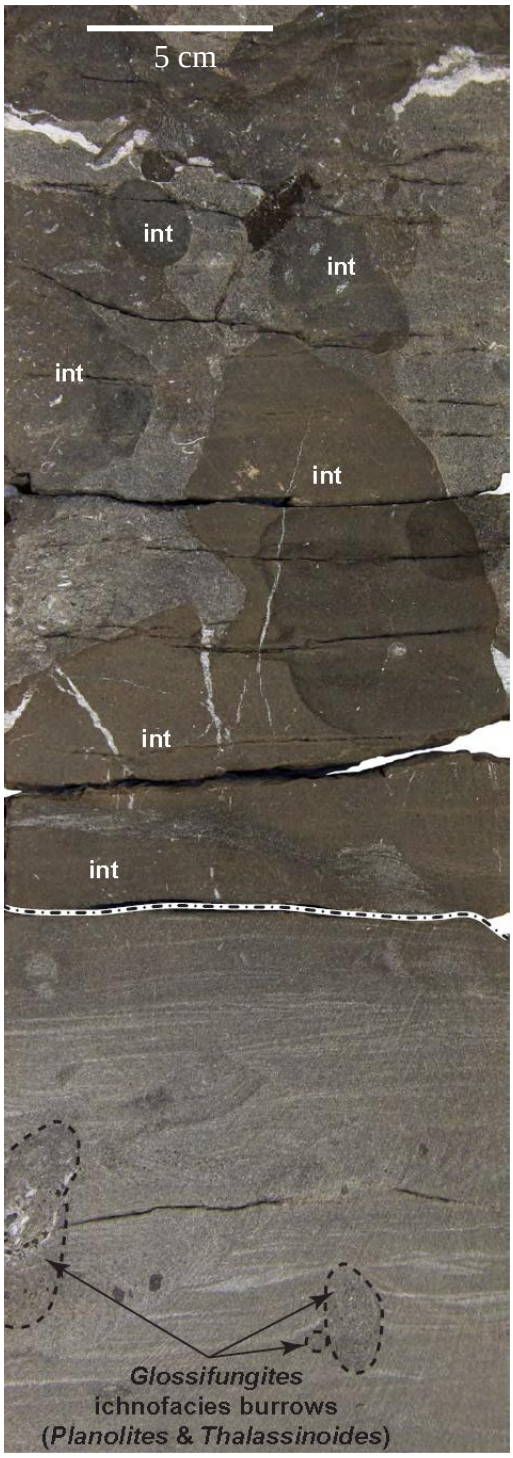



**Figure 3.4.** The Montney-Doig boundary in the Petro-Canada Kobes c-074-G/94-B-09 well. The contact in this well occurs where intraclast-rich bioclastic grainstone of the lower Doig Formation erosionally overlies dolomitic siltstone of the upper Montney Formation. A low-diversity Glossifungites assemblage occurs at the contact, which is demarcated by a dashed line. int = intraclast.

***Petro-Canada Kobes d-048-A/094-B-09***

Core from this well covers the interval from 2066 m to 1957 m below KB. Six samples were collected from this core, and three contained identifiable conodonts (see table 3.1; fig. 3.5).

The Montney-Doig boundary occurs at 1967.50 m. Immediately below the boundary in the Montney Formation, the sample from 1967.85 m contains *Chiosella timorensis* and *Novispathodus triangularis*, indicating that the sample is either uppermost Spathian or lowermost Anisian (Orchard *et al.*, 2007 a, b; Goudemand *et al*., 2012 a). The sample from 1967.30 – 1967.50 m comes from above the boundary in the Doig Formation and contains *Triassospathodus homeri*, which is also indicative of the uppermost Spathian or lowermost Anisian (Orchard, 1995; Orchard *et al.*, 2007 a, b; Goudemand *et al.*, 2012 a). These samples suggest that the Montney-Doig boundary in this well could be upper Spathian or lower Anisian, and probably closely approximates the Spathian-Anisian boundary. The sample from 1965.00 – 1965.40 m comes from the Doig Formation and contains *Neogondolella regalis* morphotypes α and δ which correspond to the Caurus ammonoid zone (see chapter 2), which is Lower Anisian (Tozer, 1994). The top of the Doig Formation occurs at 1849 m in this well.

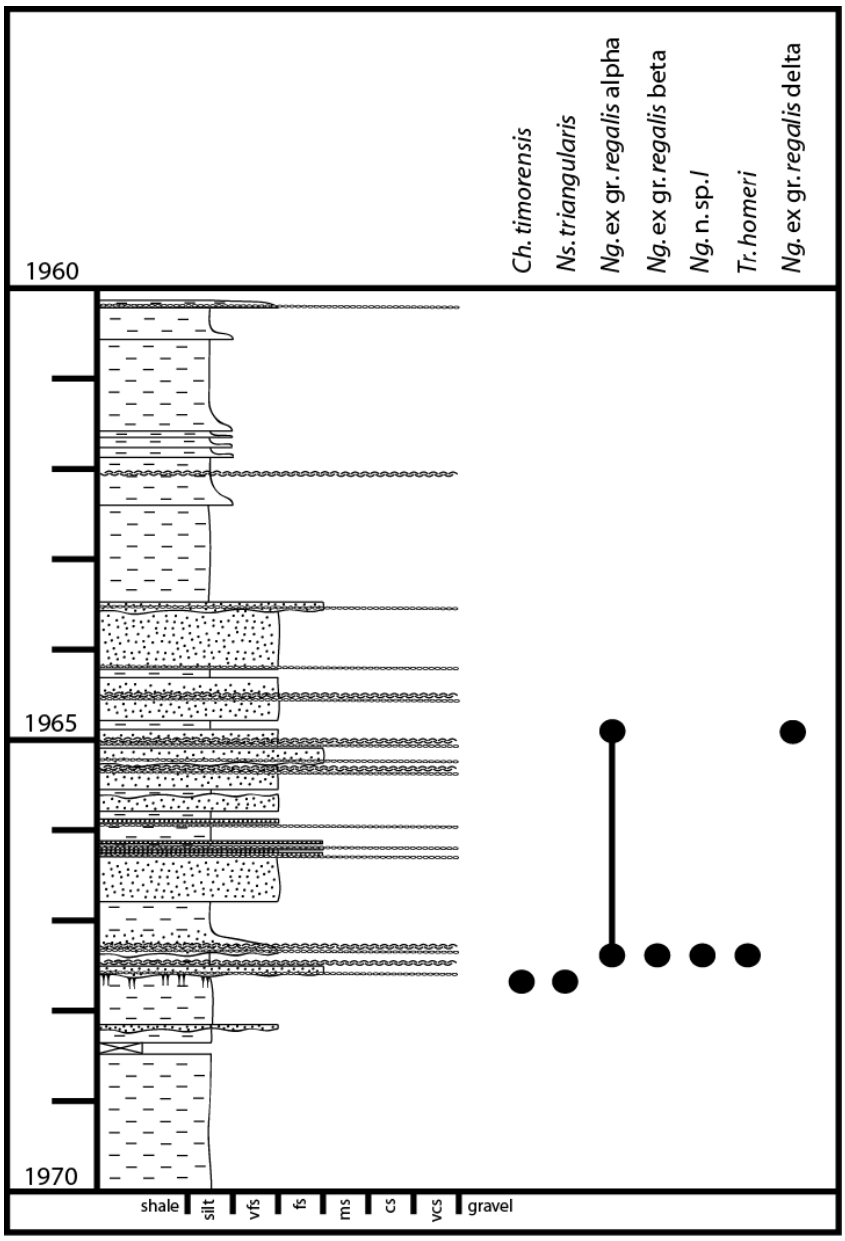



**Figure 3.5.** Lithological log and position of conodont samples in the Petro-Canada Kobes d-048-A/094-B-09 well.

***Talisman Altares c-085-I/094-B-01***

Core from this well covers the interval from 2465 m to 2444 m and 2372 m to 2359 m below KB. Five samples were collected from this core; however, only one of them contained identifiable conodonts (see table 3.1; fig. 3.6).

The Montney-Doig boundary occurs at 2387 m. The single productive sample comes from 2370.61 – 2369.96 m below KB, in the Doig Formation. It contains *Neogondolella regalis* morphotypes β and γ and *Neogondolella* n. sp. B. These species suggest that the sample belongs to the Hayesi ammonoid zone (see chapter 2), making it Middle Anisian in age (Tozer, 1994). This sample occurs approximately 17 m above the Montney-Doig boundary, and indicates that the boundary may be Anisian in this well. The top of the Doig Formation is at 2345 m.

***Talisman Altares 16-17-083-25W6***

Core from this well covers the interval from 2530 m to 2230 m below KB. Forty one samples were collected from this core, and twenty-one contained identifiable conodonts (see table 3.1; fig. 3.7). The biostratigraphy of this well is described in detail in chapter 4.

The Montney-Doig boundary occurs at 2257.35 m. The sample at 2384.00 – 2385.00 m from the Montney Formation contains *Neogondolella* sp. D (sensu Orchard and Zonneveld, 2009) which is indicative of the Spathian. The lowest sample from the Doig Formation comes from 2256.00 – 2257.00 m and contains *Neogondolella* sp. A (sensu Orchard, 2008), also indicative of the Spathian. The Montney-Doig boundary is therefore Spathian in this well. Above the boundary, at 2252.00 – 2253.00 m, the first Anisian conodonts (*N.* ex gr. *regalis*) appear, suggesting that the

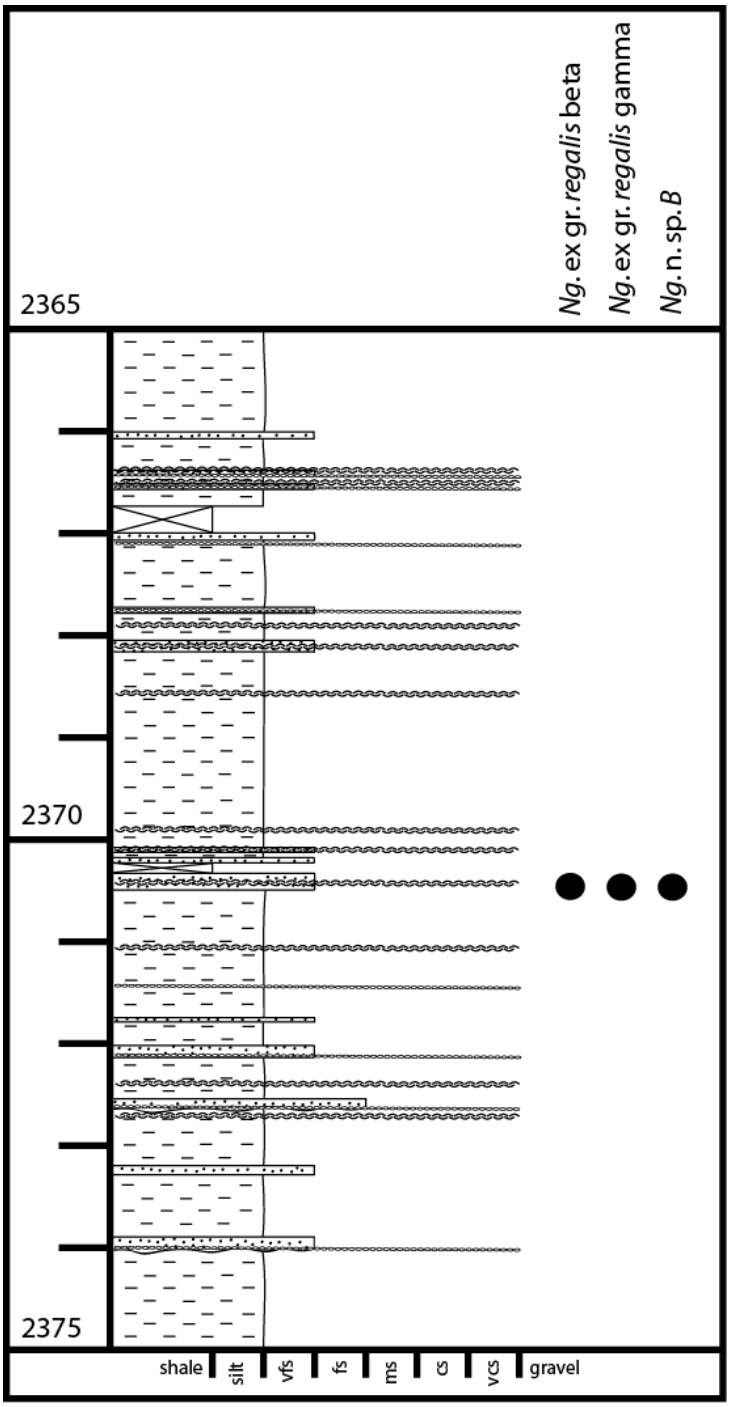



**Figure 3.6.** Lithological log and position of conodont samples in the Talisman Altares c-085-I/094-B-01 well.

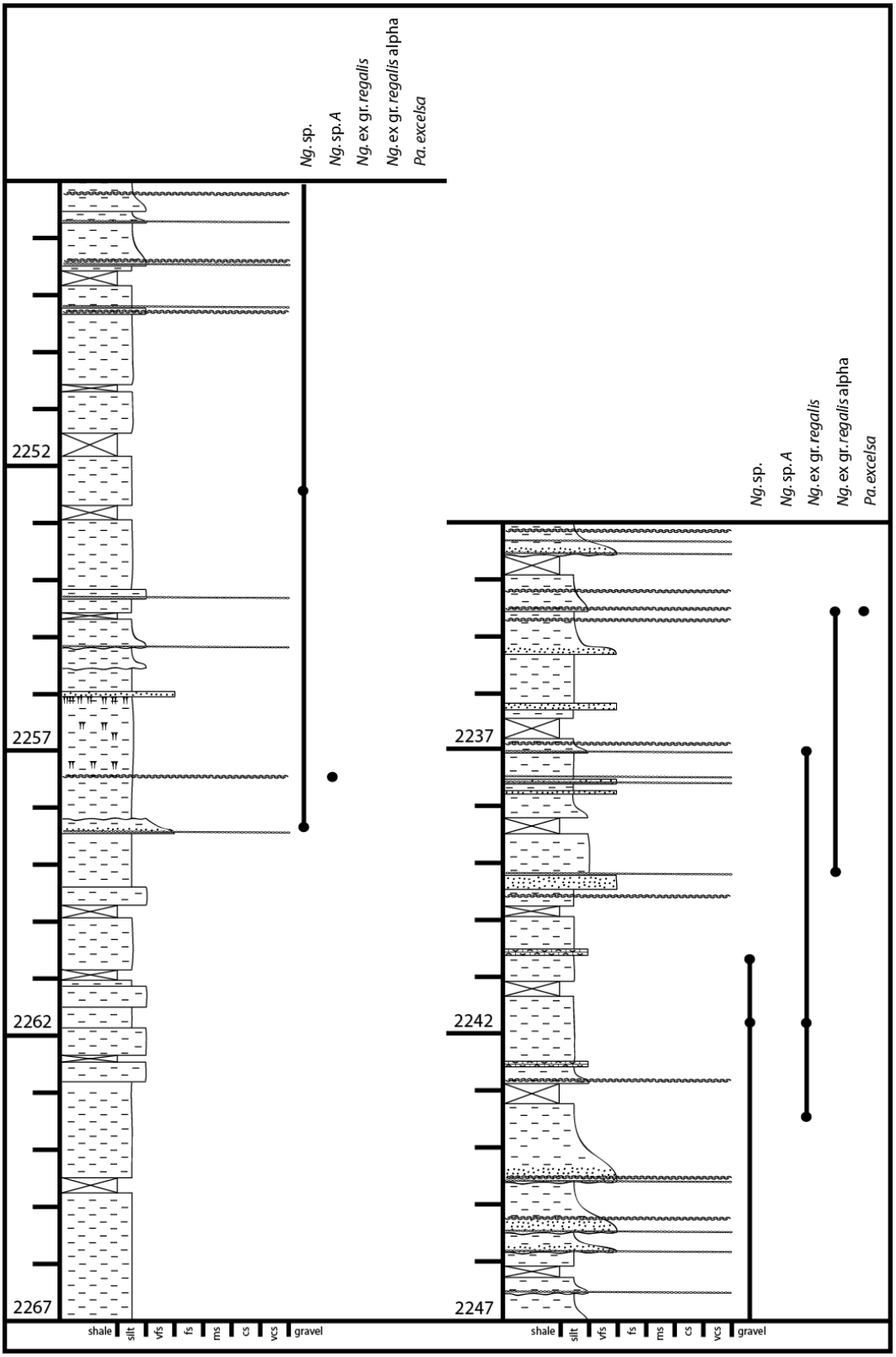



**Figure 3.7.** Lithological log and position of conodont samples in the Talisman Altares 16-17-083-25W6 well.

Spathian-Anisian boundary occurs between 2256.00 m and 2253.00 m. The highest conodont collection comes from 2234.10 – 2234.57 m and contains *Paragondolella* ex gr. *excelsa,* which is typical of the Upper Anisian *excesla* Zone (Orchard and Tozer, 1997). This species group also extends into the Ladinian. This means that the Doig Phosphate Zone encompasses most, if not all, of the Anisian in this well. The top of the Doig Formation is not observed.

***Arc Dawson 07-13-79-15W6***

Core from this well covers the interval from 2109 m to 2054 m below KB. Two samples were collected from this core, and only one of them contained identifiable conodonts (see table 3.1; fig. 3.8).

The Montney-Doig boundary occurs at 2058 m. The single productive sample comes from 2054.30 – 2054.05 m, in the Doig Formation. It contains *Neogondolella regalis* morphotype α, *N.* n. sp. C and *N.* n. sp. D. These suggest that the sample is equivalent to the Hayesi ammonoid Zone (see chapter 2), which belongs to the Middle Anisian. The Montney-Doig boundary occurs approximately 4 m below this sample and is therefore likely to be Anisian in this well. The top of the Doig Formation is at 1977 m.

***Murphy Swan d-054-B/093-P9***

Core from this well covers the interval from 2584 m to 2548 m below KB. Eight samples were collected from this core, and three of them contained identifiable conodonts (see table 3.1; fig. 3.9).

The Montney-Doig boundary occurs at 2563 m. The lowest productive sample comes from 2556.90 m, in the Doig Formation. It contains *Neogondolella* n. sp. B, which is indicative of the

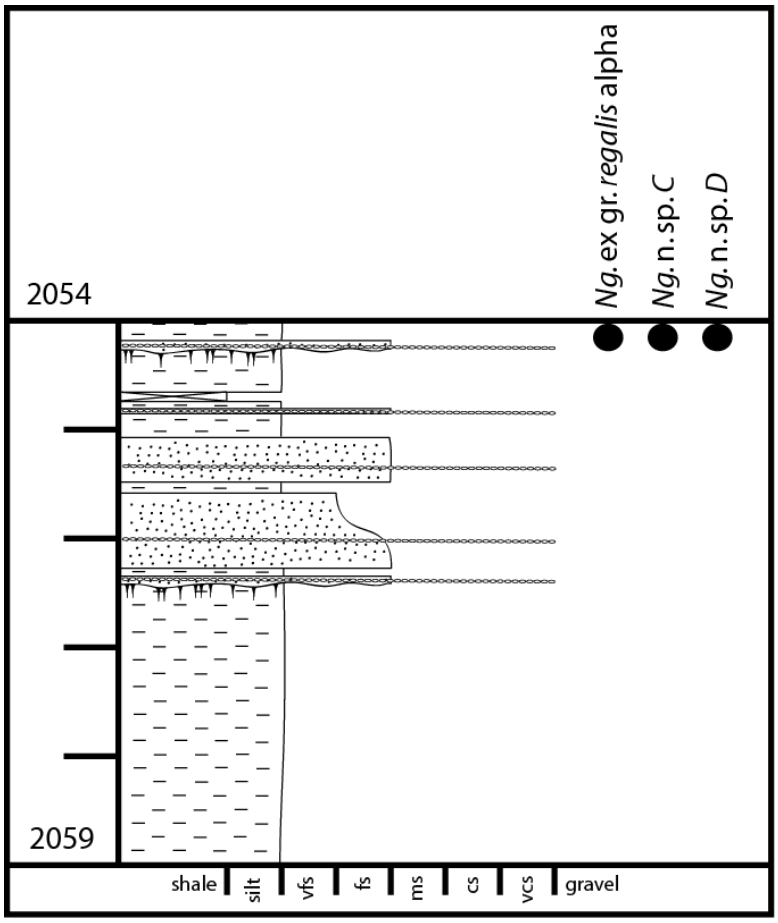



**Figure 3.8.** Lithological log and position of conodont samples in the Arc Dawson 07-13-79-15W6 well.

Hayesi ammonoid Zone (see chapter 2) from the Middle Anisian. The Montney-Doig boundary is approximately 6 m below this sample and is likely Anisian in this well. The sample from 2553.80 also contains *N.* n. sp. B as well as *N.* n. sp. C and *N. regalis* morphotype γ and is also from the Hayesi ammonoid Zone (see chapter 2). The highest sample from 2549.66 m contains *N. constricta* morphotype γ which is indicative of the Deleeni ammonoid Zone (see chapter 2)

from the Upper Anisian (Tozer, 1994). The Middle-Upper Anisian boundary therefore occurs between 2553.80 m and 2549.66 m. The top of the Doig Formation is at 2465 m.

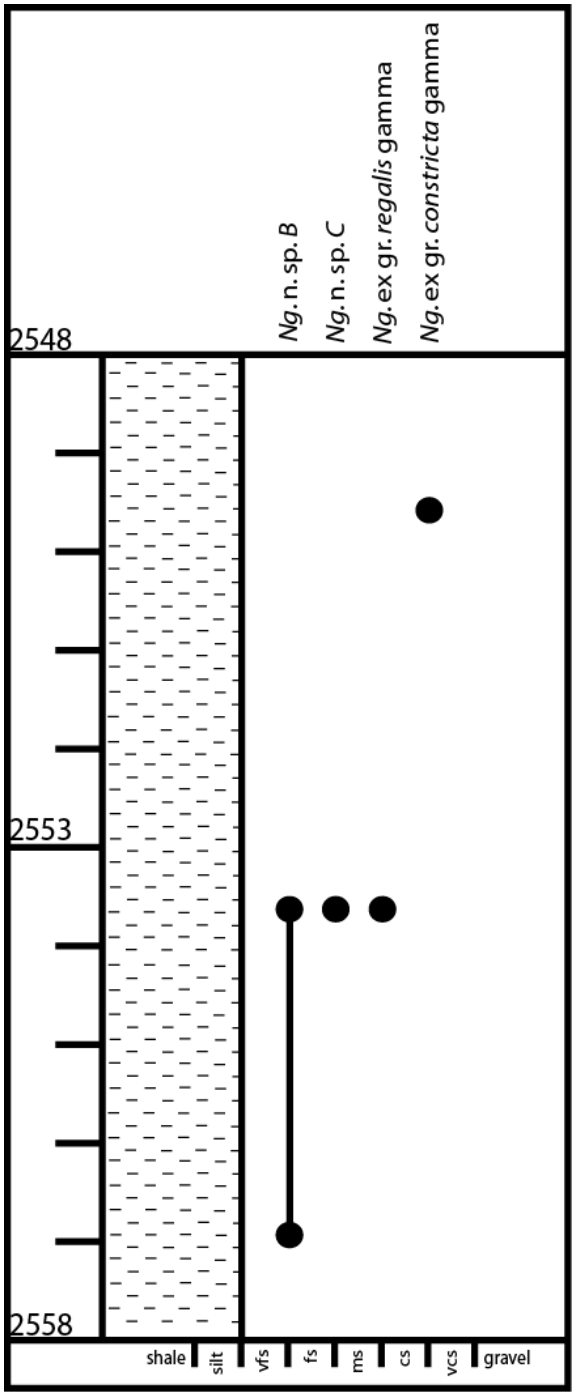



**Figure 3.9.** Lithological log and position of conodont samples in the Murphy Swan d-054-B/093-P9 well.

***Talisman Groundbirch 03-06-078-22W6***

Core from this well covers the interval from 3362 m to 3344 m and 3200 m to 3184 m below KB. Seven samples were collected from this core, and four of them contained identifiable conodonts (see table 3.1; fig. 3.10).

The Montney-Doig boundary occurs at 3287 m. The highest sample from the Montney Formation comes from 3350.10 m and contains *Neospathodus brevissimus, Triassospathodus homeri* and *Novispathodus* sp. The presence of *N. brevissimus* and *T. homeri* suggests that this sample comes from the Spathian (Orchard, 1995). The sample at 3185.00 m comes from the Doig Formation and contains species of *Neogondolella* belonging to the Anisian. The Montney-Doig boundary in this well occurs between the Spathian and the Anisian. The top of the Doig Phosphate Zone occurs at 3200 m, and is therefore confined to the Anisian in this well.

***Shell Groundbirch 16-02-078-22W6***

Core from this well covers the interval from 3176 m to 2995 m below KB. Eighteen samples were collected from this core, and nine of them contained identifiable conodonts (see table 3.1; fig. 3.11).

The Montney-Doig boundary occurs at 3060 m. The sample from 3073.00 m comes from the Montney Formation and it contains *Chiosella timorensis, Neogondolella* ex. gr. *regalis* and *Neogondolella* n. sp. B. The presence of *C. timorensis* with *N.* n. sp. B indicates that this sample is from the Hayesi ammonoid Zone (see chapter 2), in the Middle Anisian.

The lowest sample from the Doig Formation is at 3034.86 m and contains *Neogondolella bifurcata, Neogondolella regalis* morphotype ε, *Neogondolella* n. sp. F, *Neogondolella* n. sp. H

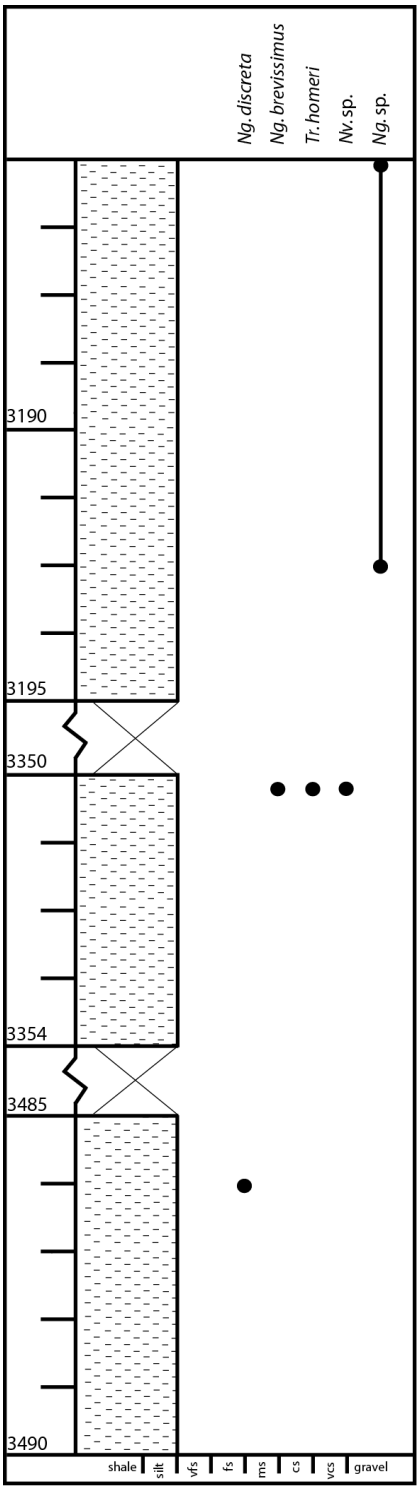



**Figure 3.10.** Lithological log and position of conodont samples in the Talisman Groundbirch 03-06-078-22W6 well.

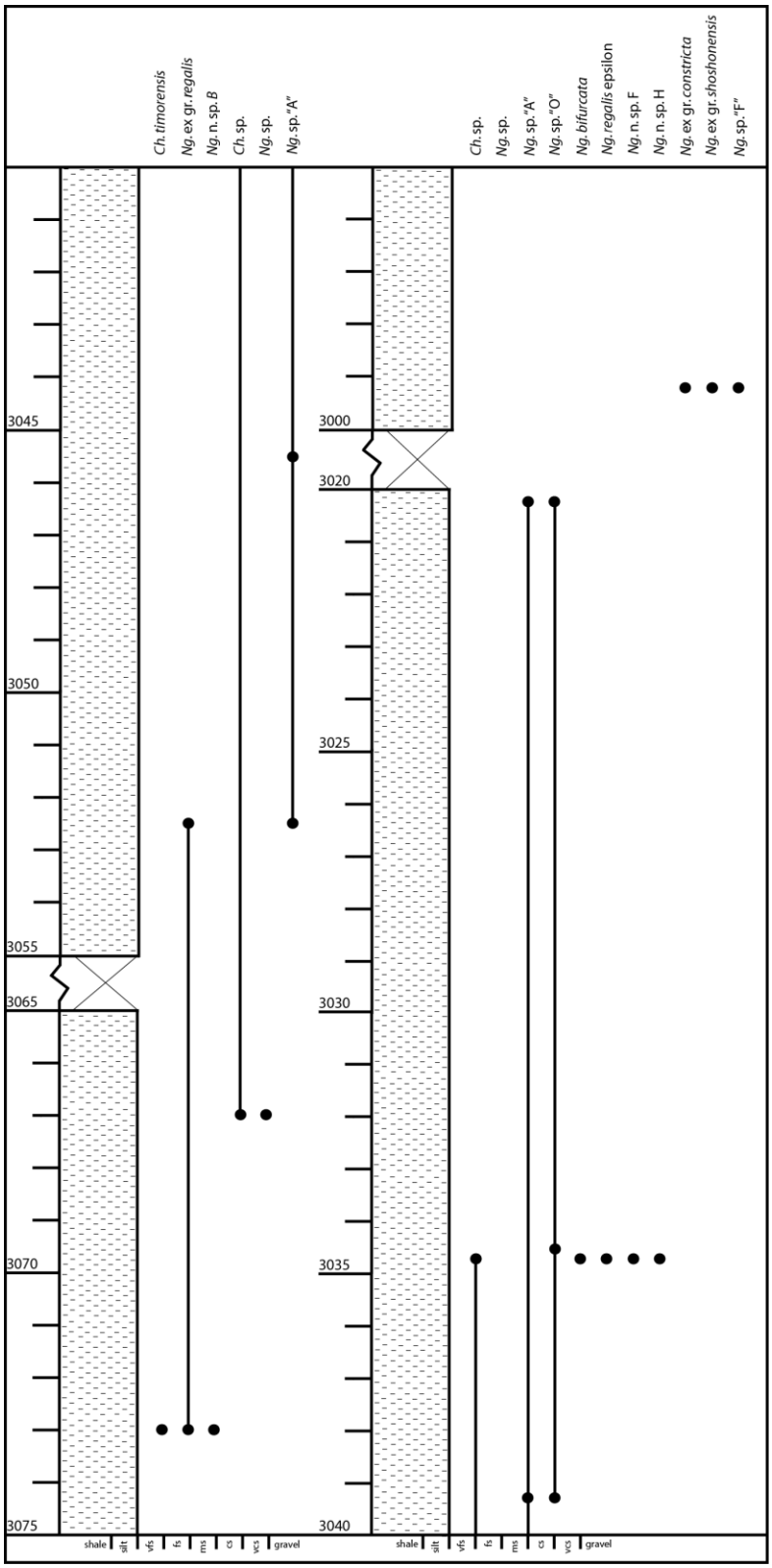



**Figure 3.11.** Lithological log and position of conodont samples in the Shell Groundbirch 16-02-078-22W6 well.

and *Chiosella* sp. *N. bifurcata* indicates Lower – Middle Anisian (Budurov and Stefanov, 1972), *N.* n. sp. H suggests Minor Zone, whilst *N.* n. sp. F suggests Minor Zone or Deleeni Zone (see chapter 2). Together, therefore, these conodonts suggest that the sample is from the Minor Zone, in the uppermost Middle Anisian. Therefore, the Montney-Doig boundary occurs in the Middle Anisian in this well.

The sample from 2999.20 m is from the Doig Formation and contains *Neogondolella* ex gr. *constricta*, *Neogondolella shoshonensis*, and *Neogondolella* n. sp. "F". *N. constricta* first appears in the Deleeni Zone in North America and can be found up into the Ladinian (Nicora and Kovács, 1984), *N. shoshonensis* appears in the Minor Zone and persists at least to the Anisian-Ladinian boundary (Nicora, 1977), while *N.* n. sp. "F" is typical of the Subasperum Zone in the lowest Ladinian of Nevada. Together, these conodonts suggest that this sample very closely approximates the Anisian-Ladinian boundary. The top of the Doig Phosphate Zone occurs at 2958 m, therefore in this well the Doig Phosphate Zone extends into the Ladinian.

***Shell Groundbirch 16-35-078-21W6***

Core from this well covers the interval from 2760 m to 2724 m below KB. Ten samples were collected from this core, and five of them contained identifiable conodonts (see table 3.1; fig. 3.12).

The Montney-Doig boundary is at 2769 m. The lowest productive sample comes from 2971.80 m, in the Montney Formation. It contains *Scythogondolella mosheri* and *Neospathodus* sp. *Scythogondolella mosheri* indicates the *mosheri* Zone (Orchard and Zonneveld, 2009), which is upper Smithian. *Sc. mosheri* appears up to 2969.00 m. The highest sample from the Montney

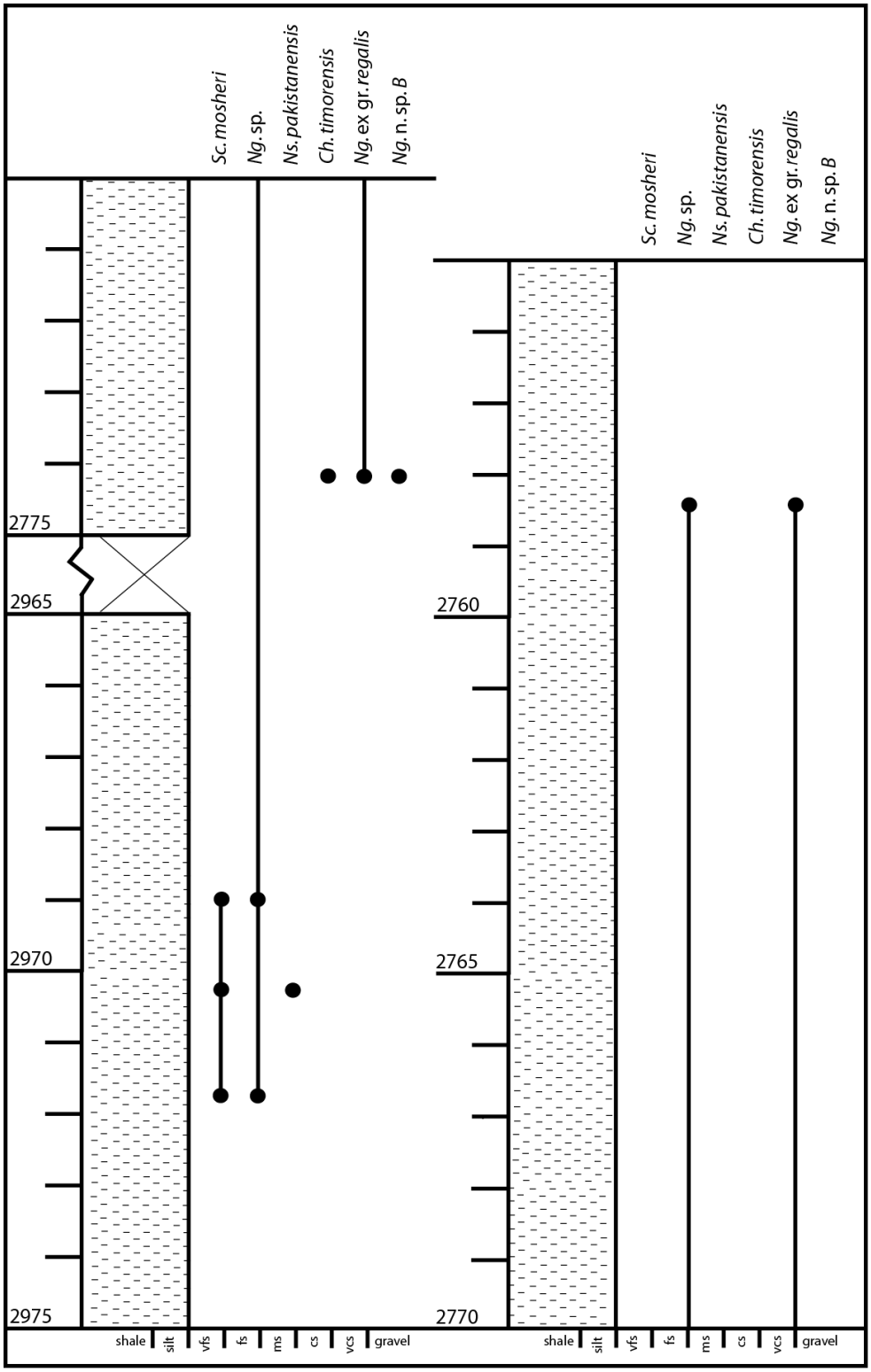



**Figure 3.12.** Lithological log and position of conodont samples in the Shell Groundbirch 16-35-078-21W6 well.

Formation is from 2773.20 m and it contains *Chiosella timorensis*, *Neogondolella* ex. gr. *regalis* and *Neogondolella* n. sp. B. This fauna indicates the uppermost Spathian or the Anisian. The lowest sample from the Doig Formation comes from 2758.40 m and contains *Neogondolella* ex. gr. *regalis* and *Neogondolella* sp. This sample is also Spathian or Anisian. The Montney-Doig boundary must therefore be close to the Spathian-Anisian boundary in this well. The top of the Doig Phosphate Zone is 2694 m.

### 3.5 CORRELATION OF THE MONTNEY-DOIG BOUNDARY

Conodont biostratigraphy has allowed the age of the Montney-Doig boundary to be determined in different wells in the study area. It has been well established that conodonts are susceptible to re-working after deposition (Purnell and Donoghue, 2005, and references therein). This has led some authors to suggest that they are unsuitable for biostratigraphical study (*e.g.* Macke and Nichols, 2007). However, in this instance, evidence of re-working of the conodonts is lacking. Conodonts from multiple levels in the cores occur with each other in predictable groups, and the groups appear in a predictable order that has been established in other sections in North America. For example, conodonts indicative of the Anisian never occur below those indicative of the Spathian, in any of the cores. The range of element sizes recovered at a particular level also argues against re-working, as this process should lead to size-sorting of the elements (McGoff, 1991). In this study, therefore, the sequence of conodont faunas is taken to represent a true and accurate biostratigraphy, that is suitable for dating the Montney-Doig boundary.

It is clear from the conodont biostratigraphy of these wells that the Montney-Doig contact is diachronous in the study area. It ranges in age from upper Spathian in the Talisman Altares

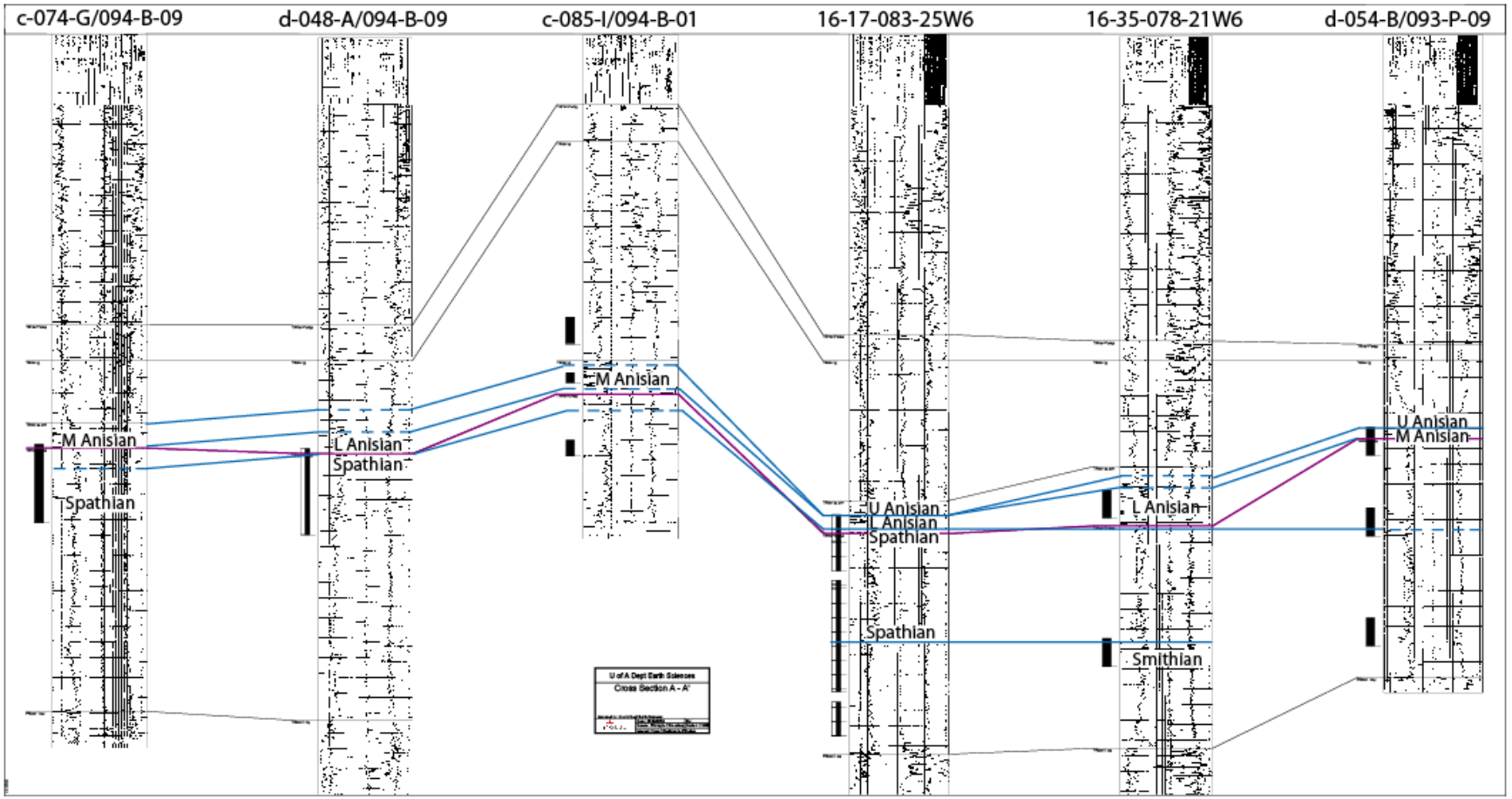



**Figure 3.13.** Cross-section of gamma ray logs running NW-SE, showing the position of Montney-Doig boundary (in purple) as well as stage and substage boundaries (in blue). Dashed lines indicate uncertainty in the placement of the stage boundaries in a particular well. Stage and substage boundary names are placed at the depth at which conodonts indicative of that age were recovered.

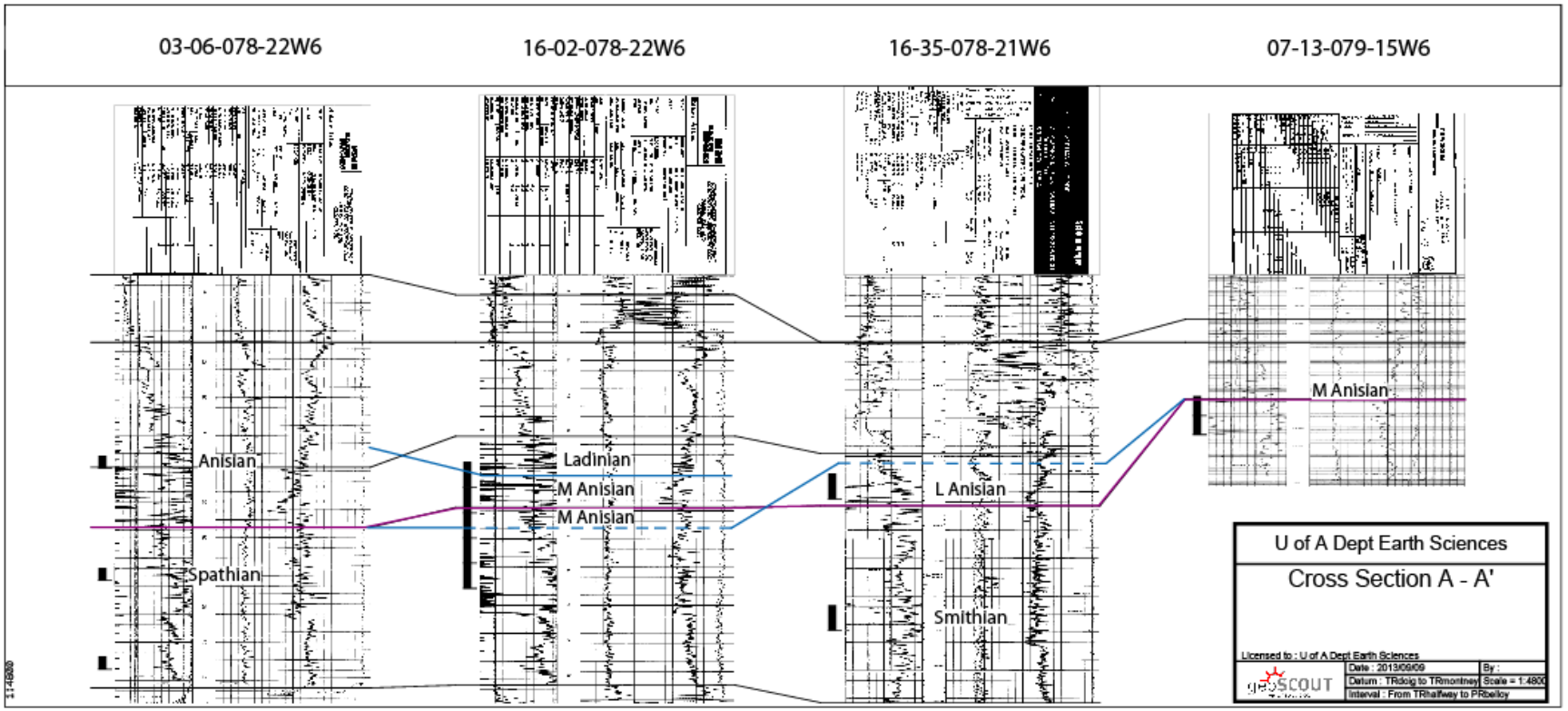



**Figure 3.14.** Cross-section of gamma ray logs running NE-SW, showing the position of Montney-Doig boundary (in purple) as well as stage and substage boundaries (in blue). Dashed lines indicate uncertainty in the placement of the stage boundaries in a particular well. Stage and substage boundary names are placed at the depth at which conodonts indicative of that age were recovered.

16-17-83-25W6 well up to the Middle Anisian in the Shell Groundbirch 16-02-78-22W6 well. The correlation of the boundary in these wells is shown in figures 3.13 and 3.14. The cross-section in figure 3.13 runs approximately northwest-southeast, parallel to regional strike. It demonstrates that the boundary is oldest in the Altares area, and is younger to both the northwest and southeast.

The cross-section in figure 3.14 runs approximately northeast-southwest, parallel to regional stratigraphical dip, and perpendicular to the cross-section in figure 3.13. The two cross-sections intersect at the Shell Groundbirch 16-35-78-21W6 well. This figure demonstrates that the Montney-Doig boundary is also diachronous in this direction. The boundary is oldest in the southwestern part of the section, where it roughly approximates the Spathian-Anisian boundary. To the northeast, the boundary is up to Middle Anisian in age.

The variation in age of the Montney-Doig boundary is thus quite substantial, from Spathian in the Altares region (at approximately 56.201389 N; 121.906667 W) up to Middle Anisian in the Dawson region (at approximately 55.846389 N; 120.203333 W), over a distance of approximately 120 km. Ogg (2012) gives the age of the Spathian-Anisian boundary as 247.06 Ma. He does not provide a date for the Lower-Middle Anisian boundary, but does give an age of 244.94 Ma for the base of the Balatonicus ammonoid zone, which is the lowest zone of the Pelsonian sub-stage in Europe and is equivalent to the base of the Middle Anisian in North America. This gives a minimum age range of 2.12 million years for the Montney-Doig boundary in northeastern British Columbia.

## 3.6 CONDENSATION OF THE DOIG PHOSPHATE ZONE

By its very nature as an interval enriched in phosphate, the Doig Phosphate Zone is similar to condensed sections elsewhere (Glen *et al.*, 1994; Föllmi, 1996). Condensation is necessary to allow the accumulation and concentration of layered phosphate grains (Pufahl and Grimm, 2003). The average rate of deposition for the Doig Formation in the Talisman Altares 16-17-083-25W6 well is approximately 4 metres per million years, compared with approximately 54 metres per million years for the Montney Formation in the same well (see chapter 4). However, it is clear from figures 3.13 and 3.14 that the Doig Phosphate Zone does not demonstrate equal condensation throughout the study area.

In the Talisman Groundbirch 03-06-078-22W6 well, the Doig Phosphate Zone is confined to the Anisian. In the Shell Groundbirch 16-02-078-22W6 well, it begins in the lowest Anisian and encompasses all of the Anisian as well as the lower part of the Ladinian. In the Murphy Swan d-54-B/93-P-9 well, the top of the Middle Anisian occurs approximately 10 m above the Montney-Doig boundary, whilst in the Talisman Altares c-085-I/094-B-01 well it occurs 17 m above the boundary.

The Doig Phosphate Zone appears to be more condensed in the Swan and eastern Groundbirch regions, and relatively expanded in the Altares and western Groundbirch regions. Again using ages from Ogg (2012), 60 metres included in the Doig Phosphate Zone in the Shell Groundbirch 16-02-078-22W6 well accumulated in approximately 7 million years, whilst in the Talisman Groundbirch 03-06-078-22W6 well, the 87 metres of the Doig Phosphate Zone took a maximum of 3 million years to be deposited. Although these numbers are approximate, they give an indication of the degree of variability in condensation.

## 3.7 IMPLICATIONS

Previous publications have depicted the boundary between the Montney and Doig formations as approximating the Spathian-Anisian boundary (*e.g.* Gibson and Barclay, 1989; Davies *et al.*, 1997; Zonneveld, 2010). The evidence from this study shows that although this may be true in some areas (*e.g.* the Kobes and eastern Groundbirch areas), the boundary in northeastern British Columbia is in fact diachronous, and shows great variability in age and duration over relatively short distances. The boundary is oldest in the centre of the studied region, and is younger to both the northwest and southeast. It is also younger to the west and east. This pattern has implications for the models of formation of the Doig Phosphate Zone. If the zone formed during a simple west-east marine transgression, the boundary between the Montney and Doig formations should be oldest in the west and youngest in the east. This is clearly not the case. The pattern of diachroneity of the base of the Doig Formation may imply that the Doig Phosphate Zone sediments occurred due to transgression within a partially enclosed basin rather than on an open shelf. Alternatively, it may imply that transgression did not have a role in the formation of this zone, with local tectonic effects playing a greater part.

Variability in the degree of condensation of the Doig Phosphate Zone implies that there are previously unidentified palaeo-highs that affected sedimentation patterns during the Triassic in northeastern British Columbia. The zone is most highly condensed in the south of the region, with sediment deposition rates slowest in the eastern Groundbirch and Swan areas. This implies that a palaeo-high was present during the Triassic in the south of the region, causing less sediment to be deposited here in comparison with more northerly areas.

These two inferences lead to the further implication that sediment was not necessarily shed directly to the west off of the North American continent during the Early and Middle Triassic. It is possible that some sediment was derived from the south or the west. The pattern of sedimentation in the study area suggests a basin with highs to the west and south as well as to the east. The presence of a palaeo-high to the west during the Triassic has previously been suggested by Ferri and Zonneveld (2008) on the basis of sediment thickness patterns. The location of this regional high is coincident with that of the Paleozoic West Alberta Ridge and the Sukunka Uplift (Moore, 1989; Richards, 1989) and thus may imply that this geomorphological entity was rejuvenated during the early Mesozoic, likely as a result of regional tectonic events. The suggested occurrence of a regional high generated by tectonic events has been supported by the detrital zircon work of Beranek *et al.* (2010 a), Beranek and Mortensen (2011) and of this study (see chapter 5), that documents the Permo-Triassic collision between North America and the pericratonic Yukon-Tanana terrane. This orogeny, termed the Klondike Orogeny, led to regional uplift west of the WCSB and provided a westerly source for sediment being shed into the basin at this time (Beranek and Mortensen, 2011). This underscores the fact that basin-scale stratal architecture in the WCSB is a function of Western Canadian influences and tectonics, and that correlation of Triassic stratigraphic events in the WCSB with global fluctuations in sea-level is not necessarily correct.

Triassic sediment of the WCSB was likely deposited in a backarc or embryonic foreland basin setting (sensu Ferri and Zonneveld, 2008). This study suggests that collision and formation of a western high must have occurred prior to the deposition of the Doig Formation and therefore during the Spathian or earlier.

## 3.8 CONCLUSIONS

- The Montney-Doig boundary in northeastern British Columbia is diachronous, varying in age from Spathian to Middle Anisian. It is oldest in the Altares area and youngest in the Dawson area.
- The base of the Doig Phosphate Zone is diachronous. Formation of this zone commenced earliest in the Altares region.
- The Doig Phosphate Zone is condensed relative to the Montney Formation. However, it is not condensed equally throughout northeastern B.C. It is most highly condensed in the Swan and eastern Groundbirch areas, whilst being relatively expanded in the Altares and western Groundbirch areas.
- The thickness of the Doig Phosphate Zone is reasonably constant across the study area, but the depositional rates vary.
- The Doig Formation was not formed by simple east-west transgression as previously thought.
- Palaeo-highs were likely present to the south and west of the study area during the Triassic, as well as to the east. It is suggested that these formed in response to the Klondike Orogeny that took place during Permian and Early Triassic time. Sediment of the Doig Formation was therefore deposited in a foreland basin and sourced from locations in the west as well as from the North American continent to the east.
- Additional work is required to constrain the age of the Montney-Doig boundary in Alberta, as well as the ages of the Lower-Middle and Middle-Upper Montney Formation boundaries. This will improve our understanding of sedimentation patterns during the Triassic in the Western Canada Sedimentary Basin.

## 3.9 TAXONOMIC NOTES

The majority of the conodonts recovered for this study are described in chapters 2 and 4, and are not discussed further here. Brief descriptions of the remaining, stratigraphically important conodont species are given below. The synonymy lists emphasise North American occurrences of these species. Illustrated specimens are housed at the GSC-Pacific Vancouver.

*Borinella buurensis* Dagys, 1984

Fig. 3.15, parts 1-3

1984 *Borinella buurensis* n. sp., Dagys, p. 12-13, pl. 2, figs. 6-10; pl. 3, fig. 1; pl. 11, figs. 1-4; pl. 12, figs. 1-2; pl. 16, figs. 1-4.

2008 *Borinella buurensis* Dagys, Orchard, p. 400-402, figs. 5.9-5.13.

*Description:* Elements with a biconvex platform that tapers more strongly to the anterior than to the posterior. Platform is very flat in side view. Posterior is rounded and posterior platform brim is present. Denticles are discrete and become more widely spaced to the anterior of the element. Cusp is large and separated from the rest of the carina.

*Comparisons: Borinella megacuspa* has a more robust cusp and thicker platform. *B. nepalensis* has a narrower platform.

*Remarks:* The examples of *B. buurensis* figured by Orchard (2008) all have a denticle posterior to the cusp that is offset from the carina, which is not present in these specimens.

*Occurrence:* Montney Formation, Petro-Canada Kobes c-074-G/094-B-9 well.

*Chiosella timorensis* (Nogami, 1968)

Fig. 3.15, parts 4-5

1968 *Gondolella timorensis* n. sp., Nogami, p. 127-128, pl. 10, figs. 17-21

1992 *Chiosella timorensis* (Nogami), Orchard and Bucher, pl. 1, figs. 1-8

1994 *Chiosella timorensis* (Nogami), Orchard, pl. 1, figs. 1-10, 12-14

*Description:* Large elements with platform reduced to a ridge running the length of the element. Carina is uniformly high and fused, with denticles inclined. They become more inclined at the posterior end of the element. Keel is deeply excavated and terminates in a large, sub-triangular basal loop.

*Comparisons:* The ridge or platform of *Chiosella gondolelloides* does not reach the posterior end of the element.

*Occurrence:* Montney Formation, Petro-Canada Kobes d-048-A/094-B-09 well, Shell Groundbirch 16-02-078-22W6 well.

*Neospathodus brevissimus* Orchard, 1995

Fig. 3.15, parts 9-10

1995 *Neospathodus brevissimus* n. sp., Orchard, p. 119, figs. 3.14, 3.15, 3.20-3.22

*Description:* Elements lacking a platform. Blade is very short and high, with upright to slightly inclined denticles. Basal cavity is large and subcircular.

*Comparisons: Neospathodus crassatus* has a relatively longer and lower blade. *Novispathodus triangularis* has a triangular rather than circular basal cavity.

*Occurrence:* Montney Formation, Talisman Groundbirch 03-06-078-22W6 well.

*Neospathodus crassatus* Orchard, 1995

Fig. 3.15, parts 11-12

1995 *Neospathodus crassatus* n. sp., Orchard, p. 120, figs. 2.19, 2.25-2.27

*Description:* Elements lacking a platform. Blade is relatively long and low, with inclined denticles. Basal cavity is large and expanded with thick margins. It is sub-triangular in shape and downturned at the posterior margin.

*Comparisons: Novispathodus triangularis* has a much shorter and higher blade and a smaller basal cavity with less robust margins.

*Occurrence:* Montney Formation, Petro-Canada Kobes c-074-G/094-B-9 well.

*Novispathodus triangularis* (Bender, 1970)

Fig. 3.15, parts 7-8

1970 *Spathognathodus triangularis* n. sp., Bender, p. 530, pl. 5, figs. 22a. b

1992 *Neospathodus triangularis* Bender, Orchard and Bucher, pl. 1, fig. 15

*Description:* Elements lacking a platform. Blade is relatively short and high, with inclined denticles. Basal cavity is large and triangular in shape. Basal cup is folded, forming a ridge on the upper surface of the cup that runs towards the blade.

*Comparisons:* See above.

*Occurrence:* Montney Formation, Petro-Canada Kobes d-048-A/094-B-09 well.

*Triassospathodus homeri* (Bender, 1970)

Fig. 3.15, parts 13-14

1970 *Spathognathodus homeri* n. sp., Bender, p. 528-529, pl. 5, figs. 16a, b, c

1992 *Neospathodus homeri* (Bender), Orchard and Bucher, pl. 1, figs. 11-12

1994 *Neospathodus* ex gr. *homeri* (Bender), Orchard, pl. 1, figs. 11, 15-18

2007 *Triassospathodus* ex gr. *homeri* (Bender), Lucas and Orchard, fig 7, parts 8-9

2009 *Triassospathodus* ex gr. *homeri* (Bender), Orchard and Zonneveld, p. 788, fig. 15, parts 38-40

*Description:* Elements lacking a platform. Blade is very narrow, relatively long and high. Denticles are inclined. Downturned process bearing three denticles is present posterior of the cusp. Basal cavity is small, narrow and sub-circular.

*Comparisons: Neospathodus anhuiensis* has more numerous denticles and a longer posterior process.

*Occurrence:* Montney Formation, Talisman Groundbirch 03-06-078-22W6 well; Doig Formation, Petro-Canada Kobes d-048-A/094-B-09 well.

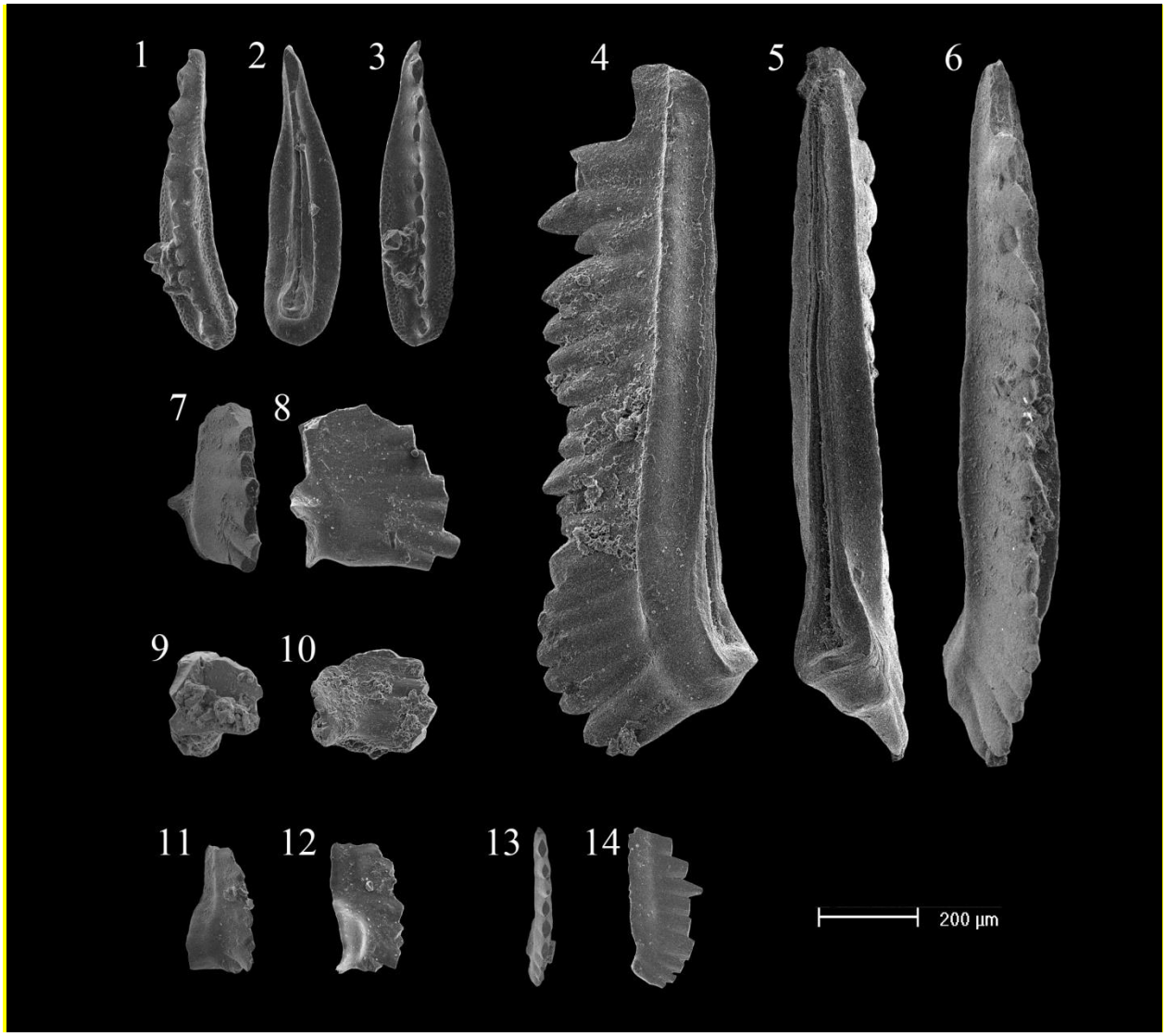



**Figure 3.15.** Conodont elements from the Montney and Doig formations, northeastern B.C. 1-3, *Borinella buurensis*, Montney Formation, at 1946.90-1947.15 m in the Petro-Canada Kobes c-074-G/094-B-9 well. 4-6, *Chiosella timorensis*, Montney Formation, at 1967.85 m in the Petro-Canada Kobes d-048-A/094-B-09 well. 7-8, *Neospathodus triangularis*, Montney Formation, at 1967.85 m in the Petro-Canada Kobes d-048-A/094-B-09 well. 9-10, *Neospathodus brevissimus*, Montney Formation, at 3350.10 m in the Talisman Groundbirch 03-06-078-22W6 well. 11-12, *Neospathodus crassatus*, Montney Formation, at 1946.90-1947.15 m in the Petro-Canada Kobes c-074-G/094-B-9 well. 13-14, *Triassospathodus homeri*, Doig Formation, at 1967.30-1967.50 m in the Petro-Canada Kobes d-048-A/094-B-09 well.

# CHAPTER 4

# Stratigraphy of the Talisman Altares 16-17-083-25W6 well in northeastern British Columbia

## 4.1 INTRODUCTION

The 16-17-083-25W6 well (surface location 56.201495° N; 121.906891° W) was drilled in the Altares area of British Columbia (fig. 4.1) by Talisman Energy Inc. in 2009 and was cored from 2230 m to 2530 m below Kelly Bushing (KB). Approximately 270 metres of core was recovered. This core encompasses the entire thickness of the Montney Formation in the Altares field, as well as the lower part of the Doig Formation and the upper part of the Belloy Formation. This is the only core drilled thus far that samples the entirety of the Montney Formation, and as such is a unique source of information on the lithology and age of this economically important formation.

Both the Montney and Doig formations are large unconventional reservoirs for natural gas and, in some areas, associated liquid hydrocarbons. It is estimated that the Montney Formation in British Columbia contains up to 700 Tcf of natural gas-in-place and the Doig Formation up to 200 Tcf (Walsh *et al.*, 2006). The Montney Formation as a whole is expected to contain 449 Tcf of marketable natural gas (NEB Report, 2013). This makes these formations two of the most significant natural gas reservoirs in British Columbia, representing around 22% of the natural gas reserves of British Columbia (OGC Report, 2013). Production from these formations in British Columbia reached 1.6 Bcf per day in 2012, with a cumulative total of approximately 1.5 Tcf produced to that point (Adams, 2013).

The core from the Talisman Altares 16-17-083-25W6 well has been lithologically logged and sampled for conodont biostratigraphy. These samples encompass the whole of the Montney Formation and the lower part of the Doig Formation and represent the most complete record of conodont biostratigraphy for the Lower and Middle Triassic in the subsurface of British Columbia.

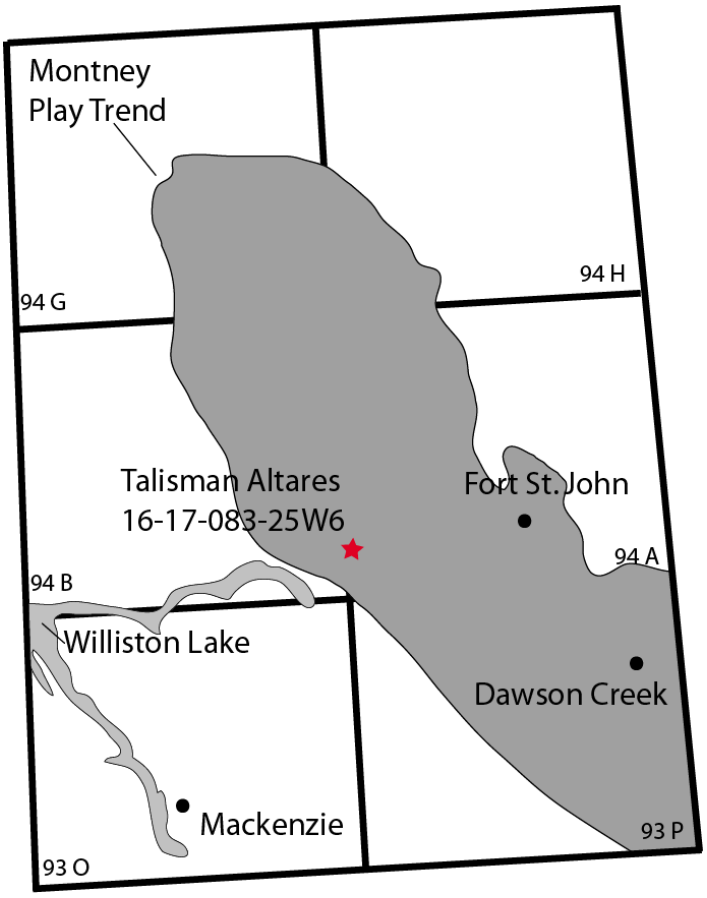



**Figure 4.1.** Location of the Talisman Altares 16-17-083-25W6 well in British Columbia and its position with respect to the Montney Play Trend. Montney Play Trend after Hayes (2012).

## 4.2 GEOLOGICAL SETTING

The Montney and Doig formations were deposited in the Western Canada Sedimentary Basin (WCSB) during the Triassic. At this time, this portion of British Columbia was situated at mid-latitude in the northern hemisphere, where the climate was likely arid and affected by seasonal trade winds and periodic upwelling (Davies, 1997 a). Traditionally, the Montney and Doig formations are both thought to have been deposited in a passive margin setting (Edwards *et al.*,

1994), although anomalous thicknesses in outcrop equivalents suggest that a topographic high may have existed towards the west (Ferri and Zonneveld, 2008; see chapter 3). Paleocurrent indicators and sedimentary provenance analysis suggests that during the Triassic, the majority of sediment was transported from the east (Pelletier, 1965; Arnold, 1994; Davies, 1997 b; Ross *et al.*, 1997). Recent studies have shown, however, that a small component may also have been derived from the north and west (see chapter 5).

The Montney Formation was first defined at the Texaco Buick Creek No. 7 well (100/06-26-87-21W6; 56.5702°N; 121.236°W) in British Columbia by Armitage (1962). In the type well, the Montney Formation consists of 267 metres (875 feet) of siltstone with minor sandstone, carbonate and shale (Armitage, 1962). It reaches a thickness of 450 m in the west and thins to 0 m at the eastern subcrop edge. It extends through much of northeastern B.C. and western Alberta (fig 4.2). The Montney Formation varies in depositional environment throughout the WCSB, including successions deposited in offshore settings by turbidity currents (Moslow and Davies, 1997; Kendall, 1999; Moslow, 2000) and others deposited in more proximal environments (Markhasin, 1997; Panek, 2000). Fossil data from this formation and equivalents are sparse and so age assignments are uncertain, but it is commonly represented as being latest Permian to Spathian in age (*e.g.* Gibson and Barclay, 1989; Davies *et al.*, 1997; Zonneveld, 2010; Zonneveld *et al*., 2010 b, c; Schoepfer *et al.*, 2012). The Grayling and the lower part of the Toad Formation in the outcrop belt of northeastern British Columbia north of the Pine River are equivalents of the Montney Formation (Gibson, 1971). The Vega, Phroso, Meosin Mountain and lower part of the Whistler members of the Sulphur Mountain Formation are equivalents in Alberta and in British Columbia south of Pine River (Gibson, 1968; Orchard and Zonneveld, 2009). The Montney Formation in Alberta was divided into three units by Davies *et al.* (1997),

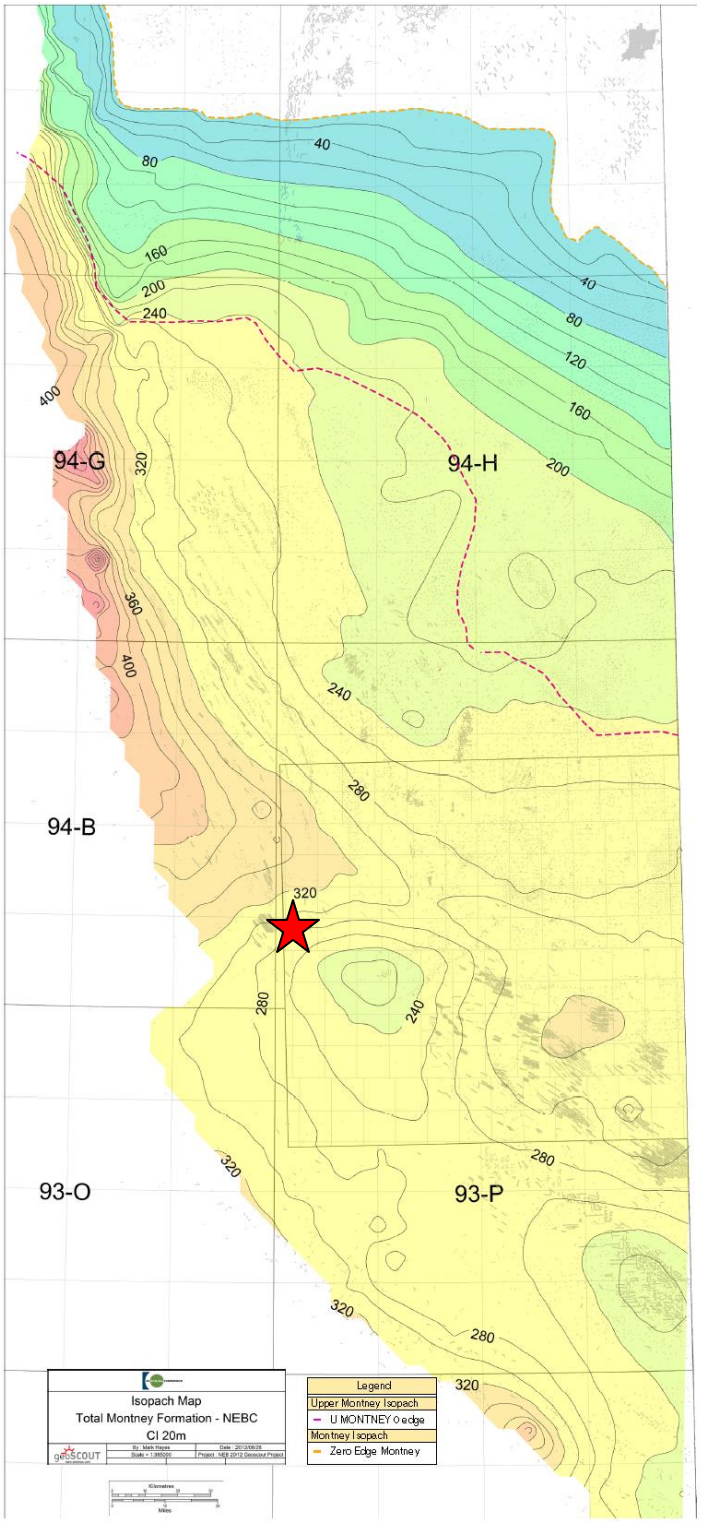



**Fig. 4.2.** Isopach map of the Montney Formation in northeastern BC. Contour intervals are in metres. Location of the Talisman Altares 16-17-083-25W6 well is indicated with a star. Modified from Hayes (2012).

whilst in B.C. it was divided into two units by Dixon (2000). No lithostratigraphic subdivision has achieved wide acceptance and thus, for the purposes of this paper, the Montney is divided into the Lower Montney, the Middle Montney and the Upper Montney Formation.

The Doig Formation was also first defined at the Texaco Buick Creek No. 7 well (Armitage, 1962), where it consists of 81 metres (265 feet) of siltstone, sandstone and minor amounts of shale and phosphate. The formation reaches a maximum thickness of 150 m and thins to 0 m at the eastern subcrop edge. The lowest part of the formation is dominated by phosphate-rich siltstone and is referred to as the Doig Phosphate Zone (Edwards *et al.*, 1994). Above this, the formation becomes sand-rich and includes thick sandstone bodies that have been a previous target for conventional oil exploration (Evoy and Moslow, 1995). The Doig Formation is interpreted to have been deposited at shallow depths, with the Doig Phosphate Zone representing a condensed section formed during transgression (Gibson and Barclay, 1989). The sandstone-rich upper part of the formation is thought to have formed in shallower water, locally as graben fill (Wittenburg, 1992; Dixon, 2011), slumps (Qi, 1995), shoreface deposits (Evoy, 1997), delta channels (Harris, 2000), barrier islands (Rahman, 2005), or incised-valley fill (Rahman and Henderson, 2005). The Doig Formation is thought to be Anisian to Ladinian in age (Gibson and Barclay, 1989; Davies *et al.*, 1997; Zonneveld, 2010). The upper part of the Toad Formation and the lower part of the Liard Formation in the outcrop belt of northeastern British Columbia north of the Pine River are the equivalents of the Doig Formation (Gibson, 1971), as are the upper part of the Whistler and lower part of the Llama members of the Sulphur Mountain Formation in outcrop in Alberta and northeastern British Columbia south of the Pine River (Gibson, 1968).

## 4.3 LITHOLOGY AND SEQUENCE STRATIGRAPHY

### *Observations*

The core from the Talisman Altares 16-17-083-25W6 well consists of 270 m of siltstone, sandstone and carbonate (figs. 4.3, 4.4). The lowest part of the core intersects partially silicified, glauconitic, sandy carbonate (bioclastic packstone) belonging to the Permian Belloy Formation. This carbonate is heavily bioturbated and contains abundant sponge spicules. It is herein interpreted to have been deposited on a proximal carbonate ramp.

The boundary between the Belloy and Montney formations is marked by an abrupt change in lithology, from sandy bioclastic packstone to grey-brown siltstone (fig. 4.5). It is considered to be an unconformity based on biostratigraphic data and thus is interpreted to be a coplanar lowstand surface of erosion and transgressive surface of erosion. Although no diagnostic fossils were recovered from the Belloy Formation in this well, the youngest fossils recorded from the formation or equivalents elsewhere are conodonts that are mid-Changhsingian (Schoepfer *et al.*, 2012, 2013; figure 2 in Zubin-Stathopoulos *et al.*, 2012). This is much younger than previous reports of a Roadian-Wordian (Guadalupian) age (Henderson, 1988; Henderson *et al.*, 1994). The oldest fossils from the Montney Formation are conodonts that are latest Permian or Griesbachian in age (see below), suggesting that a fraction of the Lopingian is missing between the two formations.

Above the transgressive surface, the offshore basal Montney Formation consists primarily of siltstone (fig. 4.3). There are rare thin beds (2 to 10 cm) of very fine and fine sandstone. Minor amounts of pyrite are present throughout this part of the core, and become more common from approximately 2450 m to 2420 m where it occurs in association with nodules of phosphate.

Within this interval, the depositional environment changes from distal offshore to proximal offshore. The sediment is still dominated by siltstone with lesser amounts of very fine sandstone. At 2430 m the depositional environment changes again to offshore transition, and at 2423 m it changes to offshore. This change to offshore deposition coincides with the boundary between the Lower and Middle Montney Formation.

The first significant deposits of carbonate in the Montney Formation occur at 2404 m (fig. 4.3). The base of the first carbonate bed is interpreted to represent a change from offshore deposition to offshore transition. The carbonate beds are heterolithic bioclastic units, and occur as lenses and laminae within a background of siltstone sedimentation (fig. 4.6). The highest bioclastic carbonate bed occurs at 2390 m, but bioclastic material remains abundant until 2387 m, above which the depositional environment is interpreted to change back to offshore and sedimentation is again dominated by siltstone. This change to offshore deposition coincides with the boundary between the Middle and Upper Montney Formations (fig. 4.3).

The lowest part of the Upper Montney Formation is referred to here as the Upper Montney Phosphate. The sediment is predominantly siltstone, but it is also relatively rich in phosphatic nodules, blebs, and biogenic phosphate such as fish bones. At 2380 m the depositional environment is interpreted to change to proximal offshore, and then back to offshore at 2360 m (fig. 4.4). The main lithology is still siltstone; however, two thick beds of hummocky cross-stratified very fine sandstone at approximately 2345 m indicate an offshore transition environment. These beds are overlain by a flooding surface that marks the return of offshore deposition and siltstone.

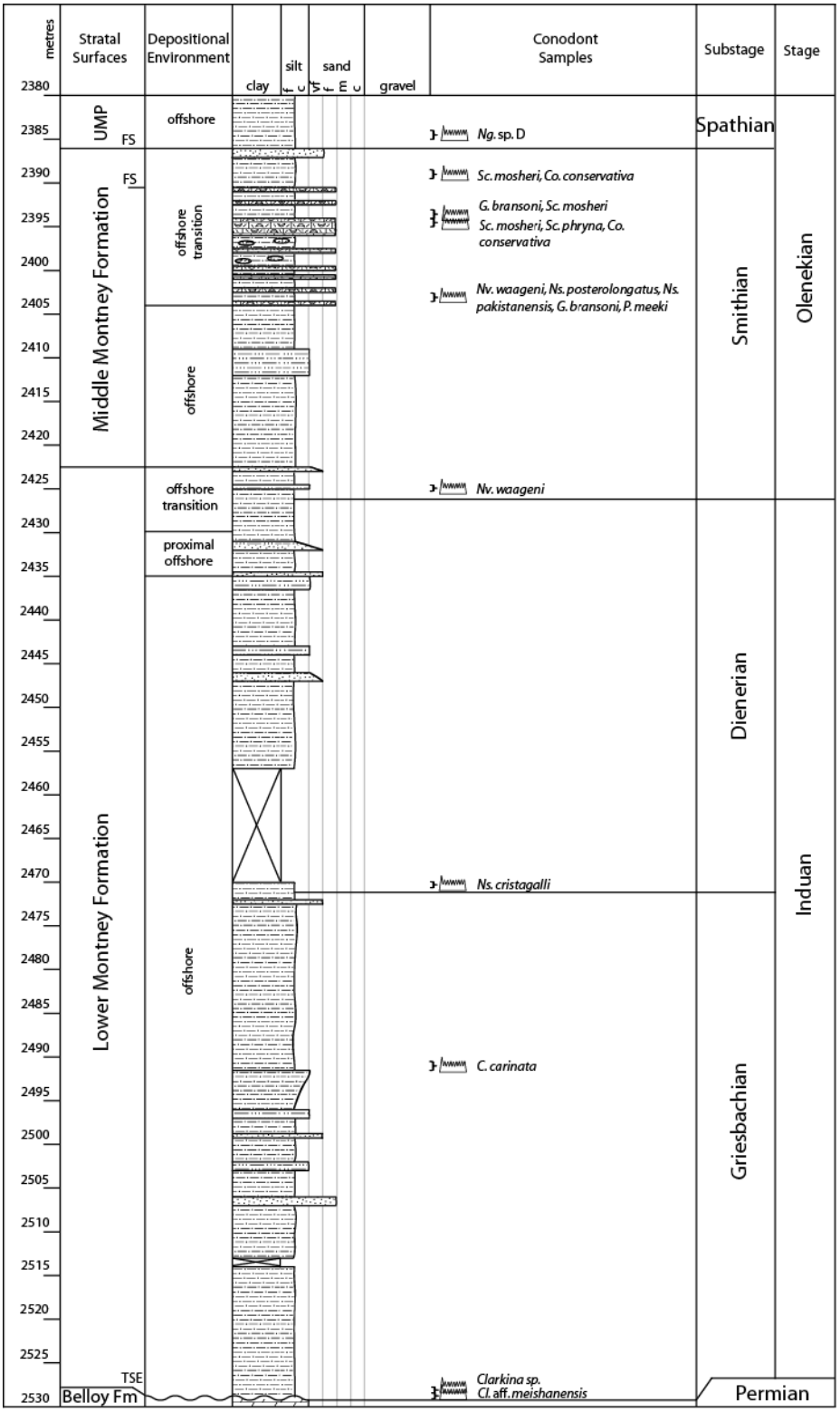



**Figure 4.3.** Lithological log of the Talisman Altares 16-17-83-25-W6 well, showing formation boundaries, depositional environment, the position of conodont samples and stage boundaries. Part 1 of 2.

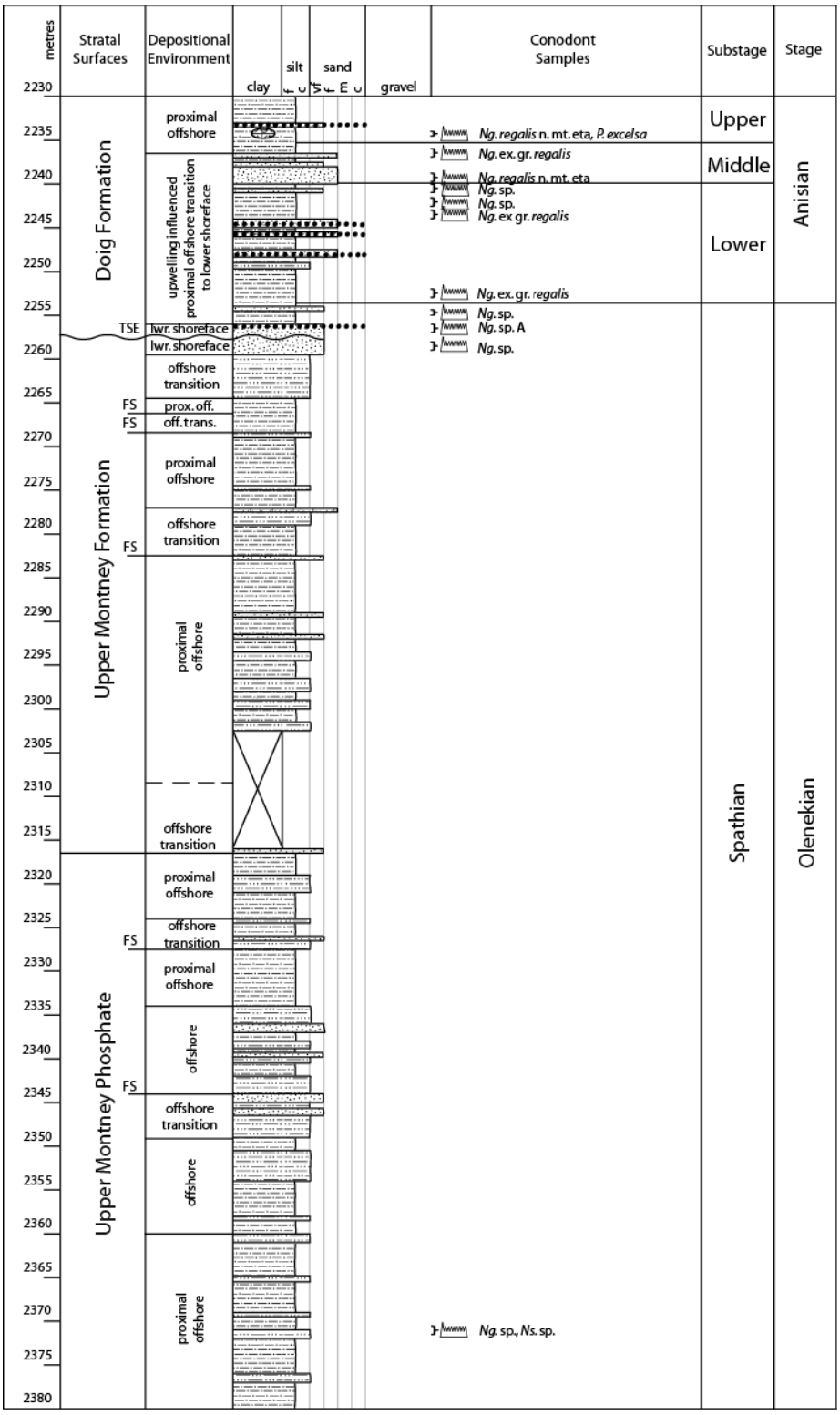



**Figure 4.4.** Lithological log of the Talisman Altares 16-17-83-25-W6 well, showing formation boundaries, depositional environment, the position of conodont samples and stage boundaries. Part 2 of 2.

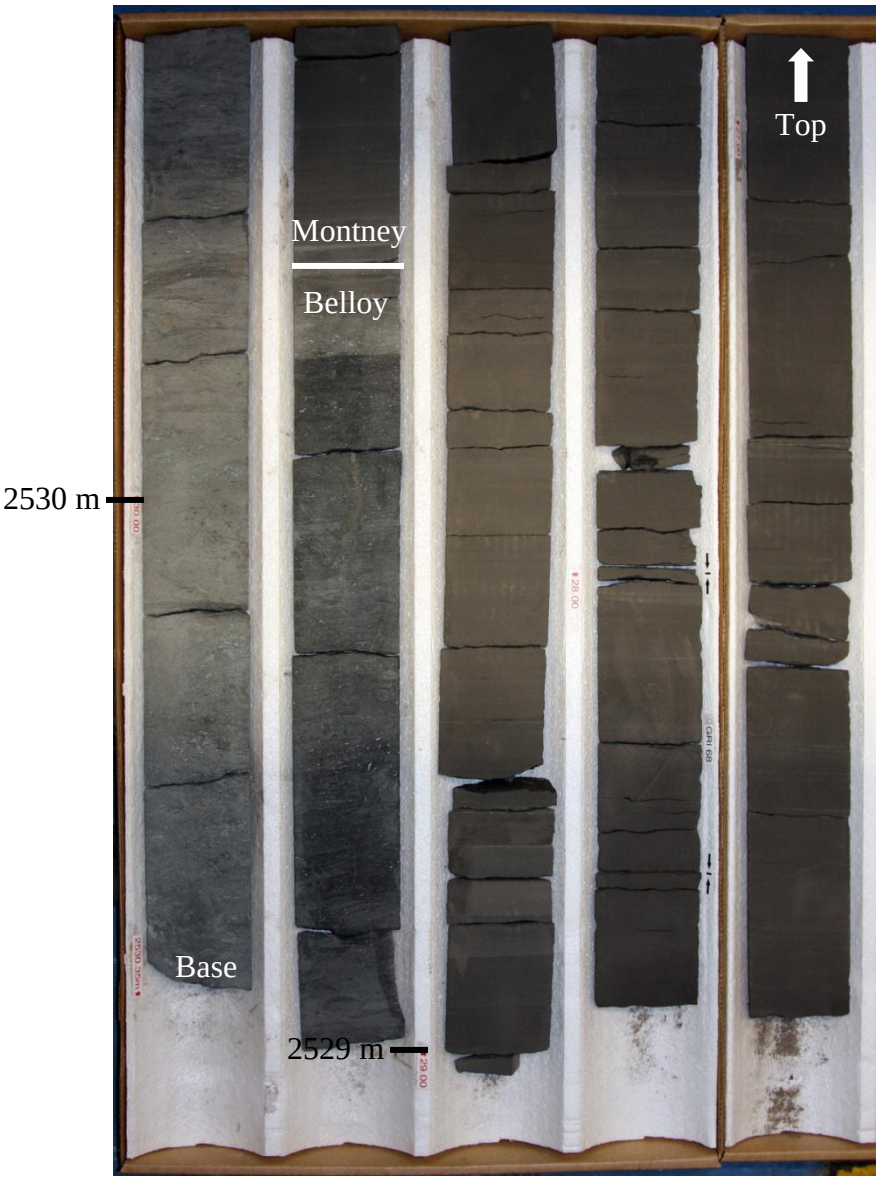



**Figure 4.5.** Boundary between the light grey, bioclastic Permian Belloy Formation and the dark brown, laminated siltstone of the Griesbachian Montney Formation in the Talisman Altares 16-17-083-25W6 well. Base of core is to the left and top of core is to the right.

The depositional environment is interpreted to alternate between distal offshore, proximal offshore and offshore transition over the next 85 m, with sedimentation dominated by siltstone, very fine sandstone and rare fine sandstone. The top of the Upper Montney Phosphate occurs at 2316 m, above which phosphate is rare in the Montney Formation (fig. 4.4.).

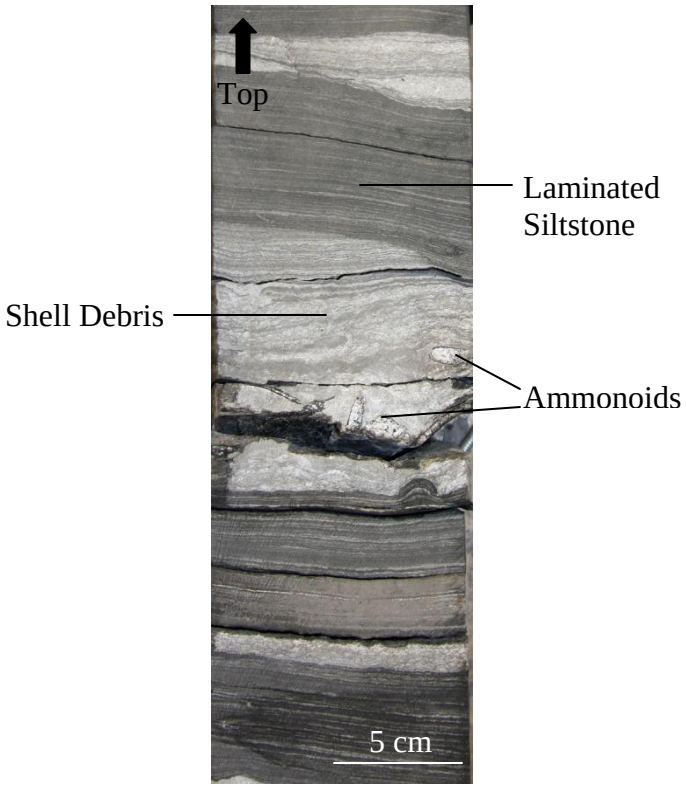



**Figure 4.6.** Bioclastic interval within the Middle Montney Formation. Note the ammonoid fossils and shell debris supported in the siltstone. From 2399 m below KB in the Talisman Altares 16-17-083-25W6 well.

At 2260 m a significant change in depositional environment is interpreted to have occurred, as thick beds of fine sandstone were deposited. The presence of cross-lamination and the trace fossil assemblage of this unit suggest that it was deposited in the lower shoreface. Above this thick package of sand is an erosional unconformity at 2257 m. This surface marks the boundary between the Upper Montney and Doig formations. A low-diversity *Glossifungites* assemblage, consisting of *Skolithos* and *Thalassinoides,* demarcates the Montney-Doig unconformity in this well as well as within many other wells throughout British Columbia and Alberta (fig. 4.7). Overlying the unconformity is fine-grained sandstone with bioclasts, climbing ripples and trace

fossils that suggest deposition in the upper shoreface. There is also a high proportion of phosphate grains. Above the sandstone, siltstone once again predominates; however, this time it is rich in phosphate and bioclasts and has layers that are heavily bioturbated with several *Glossifungites* and *Trypanites* assemblages indicating disconformity surfaces. This succession is interpreted to represent deposition in the proximal offshore transition to lower shoreface environment. The abundant phosphate in the lowest part of the Doig Formation occurs regionally and thus the lower part of the Doig Formation is commonly referred to as the Doig Phosphate Zone (Edwards *et al.*, 1994).

The return of carbonate concretions at 2236 m marks the base of sediments interpreted to have been deposited in the proximal offshore environment (fig. 4.4). Phosphatic siltstone continues to the top of the core, and the top of the Doig Phosphate Zone is not observed in this well.

***Discussion***

The Montney Formation in the Talisman Altares 16-17-083-25W6 well consists predominantly of siltstone with lesser amounts of very fine and fine sandstone. In this sense it closely resembles the core from the type well for the Montney Formation at Buick Creek (Armitage, 1962; see above). The boundaries between the Lower, Middle and Upper Montney Formation have been distinguished in this core and these units may be correlated between wells. The zone of bioclastic carbonate, which occurs from 2404 m to 2390 m, is a distinctive lithological unit, as are the two phosphate-rich intervals (2450 m to 2420 m and 2387 m to 2316 m). This second unit is referred to herein as the Upper Montney Phosphate. It may be possible to recognise these marker units in other wells and to use them for correlation.

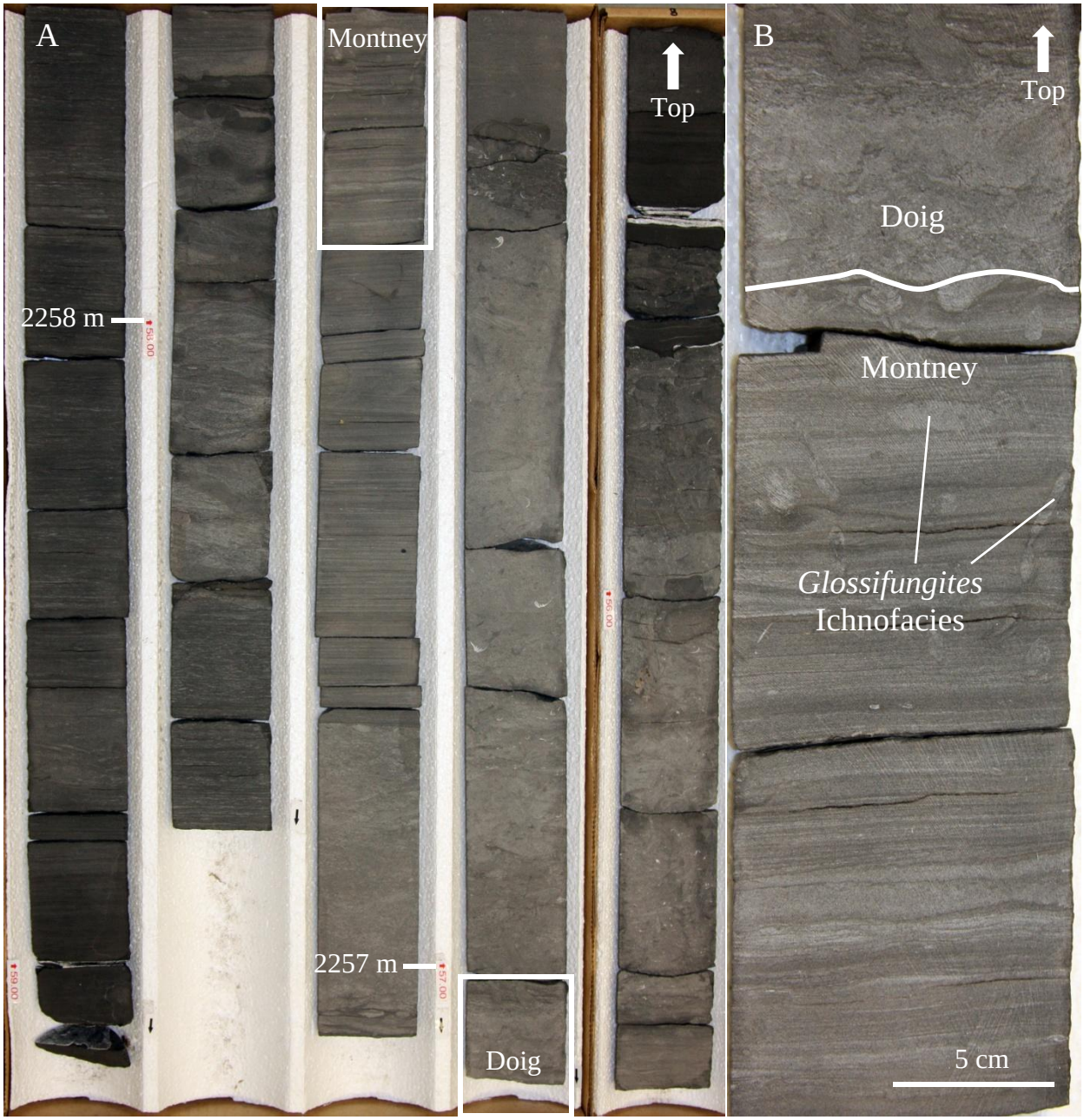



**Fig. 4.7.** The Montney-Doig boundary in the Talisman Altares 16-17-083-25W6 well. A) Overview of the boundary interval. Montney Formation is predominantly laminated siltstone, whilst the Doig Formation contains more abundant bioclastic material. Boundary is at the top of the middle sleeve. Location of figure 7B is shown by the white box. B) Close-up of the boundary. Note the irregular nature of the contact, bioturbation in the Doig Formation and the presence of burrows belonging to the *Glossifungites* ichnofacies, bringing sediment down into the laminated Montney Formation.

The Doig Formation differs from the Montney Formation mainly in the proportion of sandstone to siltstone, which is higher in the Doig Formation. The *Glossifungites*-demarcated discontinuity surface that is commonly used to identify the boundary between the two formations is well developed in this core, as are a number of similar surfaces above the boundary.

This core records a number of changes in depositional environment, which are interpreted to reflect changes in relative sea level (*i.e.* either regional or global fluctuations in sea-level, or more local fluctuations in the balance between sediment input and the creation of accommodation space). Depositional environments vary from offshore to lower shoreface within the Montney Formation. A total of seven apparent flooding surfaces are recognised in this core, although the utilization of these surfaces as parasequence boundaries would necessitate correlation on a regional basis. A sequence boundary is identified at the boundary between the Belloy Formation and the Montney Formation. This is a coplanar lowstand surface of erosion and transgressive surface of erosion (Posamentier and Vail, 1988) and as such is equivalent to both the maximum regressive surface and the maximum flooding surface (Catuneanu *et al.*, 2011). This surface comprises a sequence boundary in the "genetic sequence" scheme of Galloway (1989) and the "T-R sequence" scheme of Embry and Johannessen (1992). It corresponds to the regional Permian-Triassic sequence boundary of Embry (1997). The boundary between the Montney Formation and the Doig Formation is also a coplanar lowstand surface of erosion and transgressive surface (Posamentier and Vail, 1988). It fits the definition of a sequence boundary in the "T-R sequence" schemes of Johnson and Murphy (1984) and Embry and Johannessen (1992). It is possible to correlate both of these surfaces between wells in B.C. These surfaces are also recognised in Alberta (Markhasin, 1997; Kendall, 1999; Panek, 2000). However, in Alberta the provincial government places the Montney-Doig boundary at a lower

horizon than that chosen in B.C. (Davies and Hume, 2011) and so although sequence boundaries are recognised at the formation boundary in both provinces, they are not correlative. Furthermore, sequence boundaries have also been identified at the Lower-Middle and Middle-Upper Montney boundaries in Alberta (Markhasin, 1997; Kendall, 1999; Panek, 2000). These sequence boundaries cannot be identified in the Talisman Altares 16-17-083-25W6 core. Additional work is necessary to establish stratigraphic equivalency between Montney successions in the two provinces.

## 4.4 BIOSTRATIGRAPHY

### *Methods*

In total, 41 samples were collected from the Talisman Altares 16-17-083-25W6 core for conodont analysis. Due to the relatively large size of sample required for conodont analysis, most of the samples were collected from a significant length of the core; very few are spot samples. The samples cover a range of up to one metre. The lowest sample comes from a depth of 2530.10 – 2530.40 m below KB, and the highest comes from 2234.10 – 2234.57 m.

Nineteen of these samples were processed at the University of Calgary. They were crushed, weighed and dissolved in buffered 10% dilute acetic acid for one week. Many of the samples were subjected to a combination of acetic acid dissolution followed by boiling in quaternary O in order to disaggregate the minor clay fraction. The samples were sieved to retain the >75 μm fraction. The dried insoluble residue was then separated in tetrabromoethane with a specific gravity of 2.85. Conodonts were picked from the heavy fraction under a binocular microscope using a fine wet brush. Images were obtained using the SEM at the University of Calgary Faculty of Medicine Imaging Facility.

The remaining twenty-two samples were processed in the micropalaeontology laboratories at the University of British Columbia. These samples were crushed, weighed and dissolved in buffered 10% dilute acetic acid, for a period of 10 days. The samples were then sieved to retain the 850 μm – 90 μm fraction. This was then rinsed, dried and put through sodium polytungstate with a specific gravity of 2.85. The heavy fraction was retained and conodonts were picked under a light microscope. Images of the conodonts were obtained using the SEM facility at the GSC-Pacific.

***Results***

Out of the 41 samples processed, 30 produced conodonts. Nine of these contained only indeterminate fragments or ramiform elements, leaving 21 samples with identifiable conodonts. The conodonts found in each of the samples are shown in table 4.1 and in figures 4.3 and 4.4. They range in age from Griesbachian to Anisian. The Greisbachian, Dienerian, Smithian and Spathian stages were introduced for the Lower Triassic by Tozer (1965). In North America they are usually considered to be stages (e.g. Orchard and Tozer, 1997), whilst in other parts of the world they are considered to be substages of the Induan (Griesbachian and Dienerian) and Olenekian (Smithian and Spathian) stages (fig. 4.8).

The stratigraphically lowest conodonts recovered come from 2528.50 – 2529.00 m in the Lower Montney Formation. This collection contains *Clarkina* aff. *meishanensis*, which is indicative of the *meishanensis* Zone of the Canadian Arctic (Henderson and Baud, 1997; Algeo *et al.*, 2012), which is latest Changhsingian. *C. meishanensis* has however been identified above the Permian-Triassic boundary in China (Zhang *et al.*, 1995) and India (Orchard and Krystyn, 1998), and so may indicate lowest Griesbachian. This implies that the lowest part of the Montney Formation is

| Sample | Formation | Depth (m) | Conodonts Identified |
|---|---|---|---|
| JPZ - 1 | Lower Montney | 2528.50-2529.00 | *Cl.* aff. *meishanensis* |
| CMH - 19 | Lower Montney | 2527.50-2528.50 | *Cl.* sp. |
| JPZ - 2 | Lower Montney | 2523.20-2524.10 | None |
| CMH - 18 | Lower Montney | 2515.30-2516.30 | None |
| JPZ - 3 | Lower Montney | 2514.30-2515.30 | None |
| JPZ - 4 | Lower Montney | 2499.80-2501.70 | None |
| CMH - 17 | Lower Montney | 2495.00-2496.00 | None |
| CMH - 16 | Lower Montney | 2490.50-2491.50 | *Cl. carinata* |
| JPZ - 5 | Lower Montney | 2484.00-2484.80 | None |
| CMH - 15 | Lower Montney | 2470.00-2470.75 | *Ns. cristagalli* |
| CMH - 14 | Lower Montney | 2453.00-2453.75 | None |
| JPZ - 6 | Lower Montney | 2447.80-2448.80 | None |
| JPZ - 7 | Lower Montney | 2431.80-2432.40 | None |
| CMH - 13 | Lower Montney | 2424.50-2425.50 | *Nv. waageni* |
| JPZ - 8 | Middle Montney | 2420.50-2421.20 | None |
| JPZ - 9 | Middle Montney | 2402.40-2403.30 | *Nv. waageni, Ns. pakistanensis, Ns. posterolongatus, G. bransoni, P. meeki* |
| CMH - 12 | Middle Montney | 2394.00-2395.00 | *Sc. mosheri, Sc. phryna, Co. conservativa* |
| JPZ - 10 | Middle Montney | 2393.20-2394.10 | *Sc. mosheri, G. bransoni* |
| JPZ - 11 | Middle Montney | 2388.70-2389.60 | *Sc. mosheri, Co. conservativa* |
| CMH - 11 | Upper Montney | 2384.00-2385.00 | *Ng.* cf. n. sp. D (sensu Orchard, 2007 d) |
| CMH - 10 | Upper Montney | 2380.10-2381.00 | None |
| CMH - 9 | Upper Montney | 2370.70-2371.50 | *Ng.* sp., *Ns.* sp. |
| JPZ - 12 | Upper Montney | 2368.00-2369.00 | None |
| CMH - 8 | Upper Montney | 2356.00-2357.00 | None |
| JPZ - 13 | Upper Montney | 2330.80-2332.20 | None |
| CMH - 7 | Upper Montney | 2322.00-2323.00 | None |
| JPZ - 14 | Upper Montney | 2304.40-2305.30 | None |
| CMH - 6 | Upper Montney | 2281.25-2282.00 | None |
| JPZ - 15 | Upper Montney | 2276.50-2277.50 | None |
| JPZ - 16 | Upper Montney | 2263.75-2264.70 | None |

| Sample | Formation | Depth (m) | Conodonts Identified |
|---|---|---|---|
| CMH - 5 | Upper Montney | 2258.00-2259.00 | *Ng.* sp. |
| MLG - 1 | Upper Montney | 2257.43-2258.30 | None |
| CMH - 3 | Doig | 2256.00-2257.00 | *Ng.* cf. sp. A (Orchard, 2008) |
| MLG - 3 | Doig | 2254.44-2255.30 | *Ng.* sp. |
| CMH - 4 | Doig | 2252.00-2253.00 | *Ng.* ex gr. *regalis* |
| CMH - 2 | Doig | 2243.00-2244.00 | *Ng.* ex gr. *regalis* |
| MLG - 7 | Doig | 2241.46-2242.35 | *Ng.* sp. |
| CMH - 1 | Doig | 2240.00-2241.00 | *Ng.* sp. |
| MLG - 8 | Doig | 2238.74-2239.75 | *Ng.* ex gr. *regalis* |
| MLG - 9 | Doig | 2236.09-2237.05 | *Ng.* ex gr. *regalis* |
| MLG - 10 | Doig | 2234.10-2234.57 | *Ng. regalis* morphotype η, *Pa. excelsa* |

**Table 4.1.** Conodont samples from the Talisman Altares 16-17-083-25W6 well, showing their depth below KB, the formation from which they were collected, and the conodonts that were recovered. *Ng. = Neogondolella, Cl. = Clarkina, Ns. = Neospathodus, Nv. = Novispathodus, G. = Guanxidella, P. = Paulella, Sc. = Scythogondolella, Co. = Conservatella, Pa. = Paragondolella.*

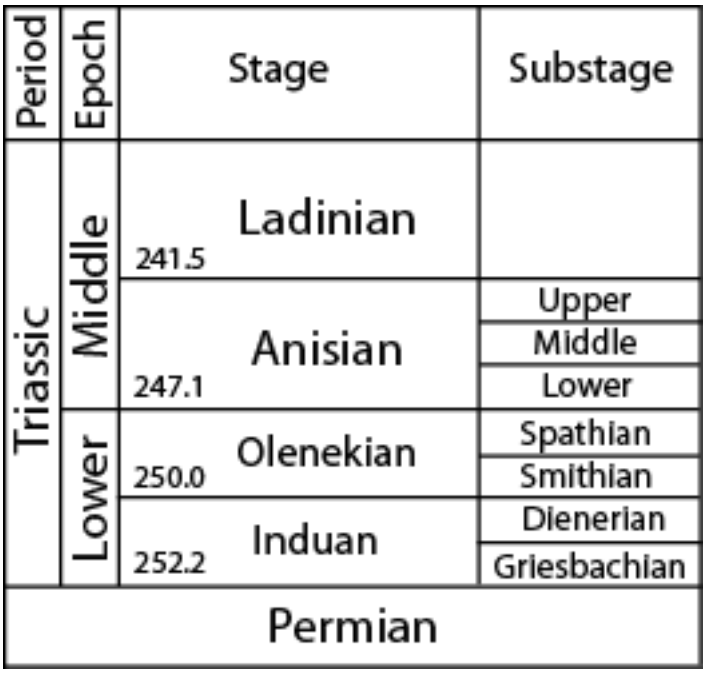



**Figure 4.8.** Timescale chart for the Lower and Middle Triassic, showing stages and substages as defined globally following Visscher (1992). Previously in North America, Griesbachian, Dienerian, Smithian and Spathian were considered to be stages rather than substages, but they are now regarded as informal substages of the Induan and Olenekian. Given the definition of the PTB, the original Griesbachian (Tozer, 1965, 1967) is now assigned to the uppermost Permian (Ogg, 2012). Ages are given in Ma and come from Ogg (2012). The age of the Induan-Olenekian boundary is uncertain; Ogg (2012) favoured a 250 Ma age based on cyclostratigraphic correlation, but Galfetti et al (2007) show that the boundary is 251.2 Ma (+/- 0.2 Myrs) based on U-Pb ages in China.

close to the Permian-Triassic boundary. Above this, additional species of *Clarkina* were found, consistent with assignment to the Griesbachian. At 2490.50 – 2491.50 m, *Clarkina carinata* appears. This indicates the *carinata* Zone (Henderson and, Baud 1997; Algeo *et al.*, 2012), which is Griesbachian in age.

The oldest Dienerian conodont, *Neospathodus cristagalli*, appears at 2470.00 – 2470.50 m (fig. 4.3). This indicates the *cristagalli* Zone (Sweet *et al.*, 1971), which is upper Dienerian in age. This means that the Griesbachian-Dienerian boundary must occur within the Lower Montney

Formation, between 2490.50 m and 2470.50 m (fig. 4.3). This means that the Griesbachian in this well has a minimum thickness of 39.6 m and a maximum thickness of 59.6 metres.

*Novispathodus waageni* occurs at 2424.50 – 2425.50 m and is indicative of the *waageni* Zone (Orchard and Tozer, 1997), which is Smithian. This means that the Dienerian-Smithian boundary also occurs within the Lower Montney Formation in this well, between 2470.00 m and 2425.50 m (fig. 4.3), and that the Dienerian has a maximum thickness of 66.0 m.

*Neospathodus posterolongatus, Neospathodus pakistanensis, Guangxidella bransoni* and *Paulella meeki* all appear for the first time at 2402.40 – 2403.30 m, within the Middle Montney Formation. This fauna is indicative of the *meeki* Zone (Orchard and Zonneveld, 2009), which is equivalent to the lower part of the *waageni* Zone. This implies that the Lower-Middle Montney Formation boundary is Smithian in age in this well.

The first occurrence of Spathian conodonts is at 2384.00 – 2385.00 m, at the base of the Upper Montney Phosphate. This collection contains the first occurrence of *Neogondolella* sp. D (sensu Orchard and Zonneveld, 2009). This conodont is indicative of the lower Spathian. The underlying sample, at 2388.70 – 2389.60 m, contains *Scythogondolella mosheri* and *Conservatella conservativa*, both indicative of the Smithian *mosheri* Zone. This means that the Smithian-Spathian boundary occurs close to the Middle-Upper Montney Formation boundary, between 2388.70 m and 2385.00 m (fig. 4.3), and that the Smithian has a maximum thickness of 85 m.

The lowest conodont collection from the Doig Formation comes from 2256.00 – 2257.00 m and contains the first appearance of *Neogondolella* sp. A (sensu Orchard, 2008), which indicates latest Spathian. This means that the Montney-Doig boundary is Spathian in age in this well.

The first occurrence of *Neogondolella.* ex gr. *regalis* is at 2252.00 – 2253.00 m within the Doig Formation. This conodont group is indicative of the uppermost Spathian and the Anisian (Orchard and Tozer, 1997; Orchard, 2008; Orchard and Zonneveld, 2009). The conodonts from the collection at 2254.44 – 2255.30 m are not age-diagnostic, and therefore there is uncertainty about the position of the Spathian-Anisian boundary. It must occur within the Doig Formation, between 2256.00 m and 2253.00 m (fig. 4.4). This means that the maximum thickness for the Spathian is 135.7 m.

The occurrence of two new morphotypes of *Neogondolella* ex gr. *regalis* at 2238.74 – 2239.75 m indicates the Middle Anisian, whilst the first occurrence of *Paragondolella* ex gr. *excelsa* at 2234.10 – 2234.57 m indicates the Upper Anisian or Ladinian (Orchard and Tozer, 1997). The minimum thickness for the Anisian is 23 m, however this thickness incorporates the Lower, Middle and at least part of the Upper Anisian.

***Discussion***

The Triassic component of the Talisman Altares 16-17-083-25W6 core begins close to Changhsinghian-Griesbachian boundary. The core encompasses the Griesbachian, Dienerian, Smithian, Spathian and Anisan, with the top of the core in the Upper Anisian.

The Lower-Middle Montney boundary occurs above a sample containing conodonts belonging to the *waageni* Zone, and below conodonts belonging to the *meeki* Zone, which is equivalent to the lower part of the *waageni* Zone. This constrains the age of the boundary very tightly in this well, placing it within the Smithian, equivalent to the *meeki* Zone. This correlates with the upper part of the Romunduri ammonoid Zone (Orchard and Tozer, 1997), which is younger than previous

estimates for the age of this boundary based on studies in Alberta. Markhasin (1997) and Kendall (1999) equated the Lower-Middle Montney boundary to the Dienerian-Smithian boundary.

The Middle-Upper Montney boundary occurs above a sample containing conodonts belonging to the *mosheri* Zone, which is uppermost Smithian, and immediately below a sample containing Spathian conodonts. It therefore closely approximates the Smithian-Spathian boundary. Again, this is younger than the ages suggested for this boundary in Alberta; Markhasin (1997), Kendall (1999) and Panek (2000) all placed it within the Smithian.

The Montney-Doig boundary occurs within the Spathian, close to the Spathian-Anisian boundary. It is not possible at this time to constrain this to the level of biozone, and therefore its age is less precisely constrained than that of the Lower-Middle Montney boundary. The Anisian conodonts from the Doig Formation do appear to record the lowest Anisian, and this is also found in other wells in northeastern B.C. (see chapter 3). Although the Montney-Doig boundary occurs within the Spathian in the Talisman Altares 16-17-083-25W6 well, in other wells in northeastern B.C. it is found to be Lower and even Middle Anisian in age (see chapter 3). The Talisman Altares 16-17-083-25W6 well is significant for recording the oldest age for the Montney-Doig boundary in northeastern B.C. that has been determined thus far. No biostratigraphic data for the Doig Formation in Alberta has so far been presented, making the age of the boundary there unknown, and correlation between the two provinces impossible.

Although the exact positions of the stage and substage boundaries are uncertain, it can be discerned that the substages of the Lower Triassic incorporate approximately equal thicknesses of sediment in this well. The Griesbachian is slightly thinner than the Dienerian and Smithian, whilst the Spathian appears to be thicker than the other stages. The Anisian is much thinner than

all of the Lower Triassic stages, and this supports the suggestion that the Doig Formation represents temporally condensed deposition (Edwards *et al.*, 1994). Using estimates for the ages of Triassic stage boundaries given in Ogg (2012) and the thicknesses reported above, the average rate of deposition for the Doig Formation encountered in this well is approximately 4 metres per million years, compared with approximately 54 metres per million years for the Montney Formation. In surrounding outcrop sections Henderson (2011) indicated deposition rates for Montney equivalents from 10 to 80 metres per million years. The rate of sedimentation for the Doig Formation is very low. However, the figure for the Doig Formation is likely an underestimation, due to the presence of a large number of disconformities. This suggests that the sedimentation that formed the lower part of the Doig Formation was episodic. It is possible that rather than accumulating more slowly than the Montney Formation, the Doig Formation simply records more gaps in sedimentation.

## 4.5 SYNTHESIS

The core from the Talisman Altares 16-17-83-25W6 well contains 270 m of sediment spanning the Lower Permian to the Middle Triassic. It records the boundaries between the Belloy and Montney formations, the Lower-Middle Montney, Middle-Upper Montney and the Montney-Doig. The Belloy-Montney boundary is interpreted to be a coplanar lowstand surface of erosion and transgressive surface of erosion that is unconformable and may represent as much as 1.0 million years of missing time. The lowest part of the Montney Formation is close to the Permian-Triassic boundary in age. The Lower Montney Formation is predominantly siltstone deposited in an offshore and proximal offshore environment during the Griesbachian, Dienerian and Smithian. A distinctive phosphate- and pyrite-rich interval occurs in the Lower Montney

Formation, and was deposited during the Dienerian. The Middle Montney Formation is also predominantly siltstone deposited in an offshore and offshore transition environment, but it is much thinner than the Lower Montney Formation. Also, it contains the first and only substantial interval of carbonate within the core. The carbonate formed during the Smithian in an offshore transition environment. Carbonate deposition and preservation is similarly restricted to the Smithian elsewhere in Canada (Zonneveld, 2011). The top of the Middle Montney Formation is a flooding surface that marks the return to offshore deposition and is also equivalent to the Smithian-Spathian boundary; this is the only stage boundary to occur coincident with an interpreted sequence stratigraphic surface in this core. Above the flooding surface, the sediment is rich in phosphate and is referred to as the Upper Montney Phosphate. This unit is entirely Spathian, and contains a higher proportion of sandstone to siltstone than the lower parts of the Montney Formation. The depositional environment fluctuates relatively rapidly between offshore, offshore transition and proximal offshore. Above the zone of phosphate enrichment is the remainder of the Upper Montney Formation. This is also entirely Spathian and contains sediment deposited in shallower water than any of the rest of the Montney Formation. Thick beds of sandstone deposited in a lower shoreface environment occur at the top of the formation. They are overlain by the Montney-Doig boundary, which is herein interpreted as a coplanar lowstand surface of erosion and transgressive surface of erosion. The boundary occurs within the Spathian, and although it is an unconformity, it appears as though little of the upper Spathian is missing in this core. The basal part of the overlying Doig Phosphate Zone is Spathian and was deposited in a lower shoreface-offshore transition environment. The Spathian-Anisian boundary occurs within sediment deposited in these environments, as does the Lower-Middle Anisian boundary. Sediment deposited in a proximal offshore environment is still rich in phosphate and records the

Middle-Upper Anisian boundary. Neither the top of the Doig Phosphate Zone nor the top of the Anisian are observed in this core. A number of disconformities are present in the Doig Phosphate Zone, and the formation of phosphate indicates slow deposition rates. Together these factors make the Doig Phosphate Zone far more condensed than the Montney Formation. The Doig Phosphate Zone is at least 27 m thick in this core, whilst the Upper Montney Phosphate is approximately 71 m thick. Both may be useful units for correlation between wells.

## 4.6 CONCLUSIONS

- The core from the Talisman Altares 16-17-83-25W6 well records deposition of the Montney and Doig formations in offshore, proximal offshore, offshore transition and lower shoreface environments.
- Unconformities mark the boundaries between the Belloy and Montney formations, and between the Montney and Doig formations. The Belloy-Montney unconformity represents up to 1.0 million years of missing time, whilst the Montney-Doig unconformity appears to represent very little missing time in this well.
- The Montney Formation spans the Griesbachian to the Spathian, whilst the Doig Formation spans the Spathian to the Anisian; its upper boundary is not observed.
- The stage boundaries as observed in this core rarely occur at inferred changes in depositional environment – meaning that they are not controlled by the environmental sensitivities of the fossils used to define them.
- The stage boundaries as observed in this core rarely occur at sequence stratigraphic surfaces – meaning that they record continuous sedimentation across the boundaries.

- The Montney-Doig boundary is older than has been previously assumed and does not equate to a stage boundary in this well, underscoring that one should not assume that lithological boundaries equate to time boundaries.
- The Doig Phosphate Zone is highly condensed compared to the Montney Formation and represents most of the Anisian in this well. This is partly due to the high number of disconformities demarcated by *Glossifungites* and *Trypanites* assemblages. These disconformity surfaces are not present in the Upper Montney Phosphate, which is thicker than the Doig Phosphate Zone, but accumulated much more quickly in the Spathian.
- The two main sequence stratigraphic boundaries can be correlated throughout B.C. and into Alberta. However, a number of sequences present in Alberta were not identified in this well.

## 4.7 TAXONOMIC NOTES

This section provides brief taxonomic descriptions of the 18 conodont species that were identified in the Talisman Altares 16-17-83-25W6 well. A detailed taxonomy is not attempted here, as it has already been covered for these species in other publications (*e.g.* Orchard, 2008; Orchard and Zonneveld, 2009; see chapter 2). In the following section, some species are referred to the genus *Clarkina* and others to the genus *Neogondolella.* The distinction of these two genera, and the relationship between them is unclear because the mutlielement appartatuses of these genera are not unambiguously defined (see discussion in Orchard 2008, p. 402, 405). It is beyond the scope of this paper to try to resolve this nomenclatural issue, therefore both names are used, with *Clarkina* used for Upper Permian and lowermost Triassic species, and *Neogondolella* used for younger species. The synonymy lists emphasise North American

occurrences of these species. Illustrated specimens are housed at the GSC-Pacific Vancouver, or at the University of Calgary.

*Clarkina carinata* (Clark, 1959)

Figure 4.9, parts 22-24

1959 *Gondolella carinata* n. sp., Clark, pp. 308-309, pl. 44, figs. 15-19

1994 *Neogondolella carinata* (Clark), Orchard *et al.*, p. 833, pl. 3, figs. 1-4, 10-14

1997 *Neogondolella carinata* (Clark), Markhasin, pl. 1, fig. 3

1999 *Neogondolella carinata* (Clark), Kendall, pp. 232-233, pl. 2, figs. 4-7

2000 *Neogondolella carinata* (Clark), Panek, pp. 91-92, pl. 1, figs. 1-6

*Description:* Elements with flat, broad platform that is widest in the middle of the element and is constricted anterior of the terminal cusp. Carina is low and denticles are discrete. Cusp is distinct, upright and surrounded by a platform brim.

*Comparisons: Neogondolella planata* lacks a posterior platform constriction and a higher carina. *N. taylorae* and *N. nevadensis* both have a platform that is widest in the posterior third of the element. *N. meishanensis* has an inclined cusp.

*Occurrence:* Lower Montney Formation.

*Clarkina* aff. *meishanensis* (Zhang *et al.*, 1995)

Figure 4.9, parts 19-21

1995 *Clarkina meishanensis* n. sp., Zhang *et al.*, p. 674, pl. 2, figs. 4, 5, 6

*Description:* Elements with a wedge shaped platform that is widest at the posterior and tapers to the anterior. At the posterior, the platform is blunted and terminates at the cusp, with no posterior brim. In side view the platform is flat. Carina is low, denticles are distinct and upright. Cusp is terminal and large relative to the other denticles. It is inclined to the posterior. Keel is low and quite wide, terminating in a circular basal loop.

*Comparisons: Clarkina carinata* also has a low carina, but has a platform that is broadest at mid-length and its cusp is upright. *Neogondolella nevadensis* has a more bulbous posterior and the platform margins taper more steeply to the anterior.

*Remarks:* Only one specimen was preserved, and it does not closely resemble the holotype of *Clarkina meishanensis.* It does however resemble those examples from the Canadian Arctic illustrated by Algeo *et al.* (2012).

*Occurrence:* Lower Montney Formation

*Conservatella conservativa* (Müller, 1956)

Figure 4.9, part 9

1956 *Ctenognathodus conservativa* n. sp., Müller, p. 821, pl. 95, figs. 25-27

1997 *Neospathodus conservativus* (Müller), Markhasin, pl. 2, figs. 9-10

2008 *Conservatella conservativa* (Müller), Orchard, p. 402, fig. 8, parts 20, 21

2009 *Conservatella conservativa* (Müller), Orchard and Zonneveld, p. 778, fig. 13, parts 31-34

*Description:* These elements have a discrete, upright cusp and denticles, that are laterally compressed. Element is narrow and there is no platform. Basal cavity is elongate and inverted. Basal margin rises towards the posterior of the element.

*Comparisons:* The denticles of *Discretella discreta* are more discrete than those of *Conservatella conservativa,* and it often has a longer posterior process. *Neospathodus spitiensis* has more inclined denticles.

*Occurrence:* Middle Montney Formation

*Guangxidella bransoni* (Müller, 1956)

Figure 4.9, parts 1-3

1956 *Neoprioniodus bransoni* n. sp., Müller, p. 829, pl. 95, figs. 19-21

2009 *Guangxidella bransoni* (Müller), Orchard and Zonneveld, p. 780, fig. 15, parts 26-28

*Description:* Elements with straight basal margin, but bowed in upper view. Denticles are rounded, inclined and closely spaced but unfused. Basal cavity is wide and sub-rounded to diamond-shaped. There is no platform.

*Comparisons: Guanxidella bicuspidatus* (Müller) is unbowed, with a heart-shaped basal cavity and even more closely spaced denticles.

*Occurrence:* Middle Montney Formation

*Neogondolella* ex. gr. *regalis* Mosher, 1970

Figure 4.10, parts 13-15

1970 *Neogondolella regale* n. sp., Mosher, pp. 741-742, pl. 110, figs. 1, 2, 4, 5

1973 *Neogondolella regale* Mosher, Mosher, p. 169, pl. 19, figs. 21, 28, 29, 32

2008 *Neogondolella* ex. gr. *regalis* Mosher, Orchard, p. 405, fig. 5, parts 22-25

2009 *Neogondolella* ex. gr. *regalis* Mosher, Orchard and Zonneveld, p.782, fig. 15, parts 32, 33

*Description: Neogondolella regalis* is a species that requires revision due to the wide range of morphological variation of elements assigned to this species. The designation "*Neogondolella* ex. gr. *regalis"* is here used to refer to a group of elements with a high, fused carina and biconvex platform margins. These could not be placed in one of the two morphotypes of *Neogondolella regalis* described below.

*Comparisons:* The high carina of this group distinguishes it from *N. mombergensis* and *N. constricta*. *P. excelsa* has a high carina, but it is highest in the middle and becomes lower to the anterior and posterior.

*Occurrence:* Doig Formation

*Neogondolella* ex gr. *regalis* morphotype η (see chapter 2)

Figure 4.10, parts 4-6

*Description:* Elements with high, fused carina typical of *Neogondolella* ex gr. *regalis.* This morphotype has a platform with biconvex margins, that only taper towards the anterior in the anterior third, and towards the posterior in the posterior sixth of the element. Platform terminates at the cusp and there is no posterior platform brim. In side view, the platform is flat and straight. Cusp is prominent and inclined posteriorly. Posterior denticle is present. Keel is narrow and forms a sub-quadrate to sub-circular basal loop.

*Comparisons:* The biconvex margins and lack of posterior platform constriction in this morphotype distinguish it from other morphotypes of *Neogondolella* ex gr. *regalis.*

*Occurrence:* Doig Formation

*Neogondolella* cf. sp. A Orchard, 2008

Figure 4.10, parts 10-12

2008 *Neogondolella* sp. A, Orchard, p. 405, figs. 5.14-5.16, 5.21, 5.26-5.28, 5.32-5.33

*Description:* Narrow elements with platforms that taper to a point at both the anterior and posterior ends. There is no posterior platform brim. Cusp is terminal, inclined and in larger specimens a conspicuous gap appears between it and the carina.

*Comparisons: N. regalis* has a cusp that is fused with its carina. *N.* n. sp. D (sensu Orchard, 2007d) possesses a posterior platform brim.

*Occurrence:* Upper Montney Formation

*Neogondolella* cf. n. sp. D Orchard, 2007 d

Figure 4.10, parts 16-17

2007 *Neogondolella* n. sp. D, Orchard, p. 99, fig. 1

2009 *Neogondolella* n. sp. D, Orchard and Zonneveld, p. 782, fig. 15, parts 29-31

*Description:* Elements that are widest at midpoint and taper to the anterior. Posterior platform margin is rounded and a posterior platform brim is present. Cusp is inclined and terminal. Carina is low and unfused.

*Comparisons: N. regalis* has a higher and more strongly fused carina.

*Occurrence:* Upper Montney Formation

*Neospathodus cristagalli* (Huckriede, 1958)

Figure 4.9, parts 25-27

1958 *Spathognathodus cristagalli* n. sp. Huckriede, pp. 161-162, pl. 10, figs. 14-15

1997 *Neospathodus cristagalli* (Huckriede), Markhasin, pl. 2, fig. 11

1999 *Neospathodus cristagalli* (Huckriede), Kendall, pp. 236-237, pl. 3, figs. 9-12

2009 *Neospathodus cristagalli* (Huckriede), Orchard and Zonneveld, p. 782, fig. 14, parts 14, 15, 20

*Description:* Elements with no platform and a basal margin that rises to the posterior. Cusp is short, broad, triangular and separated from the denticle of the carina. Basal cavity is oval in outline. Posterior denticle fused with cusp may be present.

*Comparisons:* The basal margin of *Neospathodus pakistanensis* is downturned at the posterior tip, rather than upturned as in *Neospathodus cristagalli.* The margin of *Sweetospathodus kummeli* is upturned, however the posterior tip of this species is inturned and the cusp is fused with the rest of the carina.

*Occurrence:* Lower Montney Formation

*Neospathodus pakistanensis* Sweet, 1970

Figure 4.9, parts 10-12

1970 *Neospathodus pakistanensis* n. sp., Sweet, pp. 254-255, pl. 1, figs 16, 17

1999 *Neospathodus pakistanensis* Sweet, Kendall, pp. 238-239, pl. 3, fig. 17

2008 *Neospathodus pakistanensis* Sweet, Orchard, p. 407, fig. 8, parts 10-12

2009 *Neospathodus pakistanensis* Sweet, Orchard and Zonneveld, p. 784, fig. 13, parts 18-21, 25, 26

*Description:* Elements with no platform and straight basal margin. Denticles are highest near the midpoint of the element, becoming lower to the anterior and posterior. Denticles are inclined to the posterior and laterally compressed. Basal cavity is large and subrounded, and posterior tip is downturned.

*Comparisons: Novispathodus waageni* has a basal cavity that is wholly upturned to the posterior, and has shorter elements with denticles of the same height as *Neospathodus pakistanensis.* The basal cavity of *Neospathodus posterolongatus* is extended to the posterior, giving it a diamond shape. *Neospathodus novaehollandae* has been included within *Neospathodus pakistanensis* by

Orchard (2010), whilst Metcalfe *et al.* (2013) separate it by the presence of a mid-lateral ridge on the element.

*Occurrence:* Middle Montney Formation

*Neospathodus posterolongatus* Zhao and Orchard, 2007

Figure 4.9, parts 16-18

2004 *Neospathodus waageni* subsp. B, Zhao *et al.*, pp. 42-43, fig. 2

2007 *Neospathodus posterolongatus* n. sp., Zhao and Orchard in Zhao *et al.*, p. 36, pl. 1, figs. 2A-2C

2008 *Neospathodus posterolongatus* Zhao and Orchard, Orchard, p. 407, fig. 8, parts 3, 4

2009 *Neospathodus posterolongatus* Zhao and Orchard, Orchard and Zonneveld, p. 784, fig. 14, parts 7, 8, 16, 17, 21, 22

*Description:* Elements with no platform and basal margin that is straight or downturned anteriorly. Denticles are highest just posterior of the midpoint of the element, and they become lower to the anterior and posterior. Denticles are rounded, inclined and weakly fused. There are denticles posterior to the cusp located on a posterior process. Basal cavity is either flat or upturned towards the posterior. It is widest under the cusp, but extends underneath the posterior process, giving the basal cavity a diamond shape in basal view. The widest parts of the basal cavity extend beyond the margins of the element.

*Comparisons:* The diamond shaped basal cavity separates this species from *Novispathodus waageni* and *Neospathodus pakistanensis*. *Neospathodus cristagalli* also has a basal cavity that extends and is upturned to the posterior, but has a more well defined cusp. *Neospathodus spitiensis* has an even more extended posterior process. The extended process of *Triassospathodus homeri* is downturned rather than upturned.

*Occurrence:* Middle Montney Formation

*Novispathodus waageni* (Sweet, 1970)

Figure 4.9, parts 13-15

1970 *Neospathodus waageni* n. sp., Sweet, pp. 260-261, pl. 1, figs. 11, 12

1997 *Neospathodus waageni* Sweet, Markhasin, pl. 2, figs. 13-18

1999 *Neospathodus waageni* Sweet, Kendall, p. 239, pl. 4, figs. 1-9 only

2000 *Neospathodus waageni* Sweet, Panek, pp. 94-95, pl. 2, fig. 6

2008 *Neospathodus waageni* Sweet, Orchard, p. 407, fig. 8, parts 1, 2, 8, 9

2009 *Novispathodus waageni* (Sweet), Orchard and Zonneveld, p. 785, fig. 13, parts 1-10, 14, 15

*Description:* Short elements with high denticles and no platform. Denticles are laterally compressed and highest at, or just posterior to, the midpoint of the element. They decrease rapidly in height towards the anterior and posterior. Denticles are upright and weakly fused.

Cusp is distinct and a small, posterior denticle is always present. Basal cavity is wide, circular, and may be upturned to the posterior.

*Comparisons:* A number of subspecies and morphotypes of *Novispathodus waageni* have been recognised; however it is not possible to assign these specimens to any of the subspecies with confidence. The specimens illustrated are most similar to examples illustrated by Goel (1977) from the Himalayas. *Novispathodus waageni eowaageni* has upright denticles and a circular basal cavity, but this is not upturned to the posterior. *Nv. waageni waageni* has more inclined denticles at the posterior of the carina. *Ns. posterolongatus* has a more elongate rather than rounded basal cavity. *Nv. latiformis* has platform flanges developed even in small specimens.

*Occurrence:* Lower and Middle Montney Formation

*Paragondolella excelsa* Mosher, 1968

Figure 4.10, parts 7-9

1968 *Paragondolella excelsa* n. sp., Mosher, pp. 938-939, pl. 118, figs. 1-8

1973 *Metapolygnathus excelsa* (Mosher), Mosher, pp. 163-164, pl. 20, fig. 8

*Description:* Elements with a very high, fused carina that is highest in the posterior third of the elements. Carina becomes lower rapidly to the posterior and the denticles become inclined. Carina becomes lower more gradually towards the anterior, and the denticles remain upright. Denticle is sometimes present posterior to the cusp. Platform is biconvex and narrow, tapering to the anterior and posterior, but terminating before it reaches the cusp. Platform is flat and straight in side view. Keel is high, narrow, and forms a narrow, flared basal loop that is wider than the platform.

*Comparisons: Paragondolella liebermani* is closely related but has a uniformly high carina; the upper margin of the carina of *Paragondolella excelsa* is semi-circular in comparison. *Neogondolella regalis* also has a high carina, but a much longer and wider platform.

*Occurrence:* Doig Formation

*Paulella meeki* (Paull, 1983)

Figure 4.10, parts 1-3

1983 *Gladigondolella meeki* n. sp., Paull, pp. 189-191, figs. 1A-1O

1997 *Gladigondolella meeki* Paull, Markhasin, pl. 1, fig. 18

1999 *Gladigondolella* cf. *meeki* Paull, Kendall, pp. 231-232, pl. 2, fig. 16

2000 *Gladigondolella* cf. *meeki* Paull, Panek, p. 95, pl. 2 fig. 7

2005 *Meekella meeki* (Paull), Orchard, p. 84, fig. 9

2008 *Paulella meeki* (Paull), Orchard, p. 408, fig. 6, parts 1-3

2009 *Paulella meeki* (Paull), Orchard and Zonneveld, p. 785, fig. 12, parts 4-9, 17-21

*Description:* Large platform elements with biconvex platform margins. Platform is widest at the midpoint of the element and it tapers evenly to the anterior and posterior. Level with the cusp, the platform tapers sharply, and is deflected as it follows the offset posterior process. Platform is crenulated at the anterior end. Carina is high and fused, of even height along the whole length. Denticles are laterally compressed and inclined at the posterior, but upright towards the anterior.

Cusp is large and distinct, and the offset posterior process carries 1-3 posterior denticles. Keel is wide and basal cavity is inverted. Keel continues on the posterior process.

*Comparisons: Scythogondolella crenulata* and *Scythogondolella milleri* have platform crenulation, but no posterior process. Species of *Gladigondolella* have a posterior process but generally have a much narrower platform and a basal pit situated closer to the mid length of the element.

*Occurrence:* Middle Montney Formation

*Scythogondolella mosheri* (Kozur and Mostler, 1976)

Figure 4.9, parts 6-8

1976 *Gondolella mosheri* n. sp., Kozur and Mostler, p. 8, pl. 1, figs. 9-12

2008 *Scythogondolella mosheri* (Kozur and Mostler), Orchard, p. 410, fig. 5, parts 1-4

2009 *Scythogondolella mosheri* (Kozur and Mostler), Orchard and Zonneveld, p. 786, fig. 15, parts 10-19

*Description:* Short elements with comparatively wide platform. Platform is widest near to the posterior of the element, and it tapers evenly to the anterior. Platform tapers sharply to the posterior, and terminates in front of the cusp. This gives the platform an overall teardrop or heart shape in upper view. Cusp is large and separate from the rest of the carina. It is laterally compressed and inclined. Carina is uniformly low and partially fused, with upright and laterally compressed denticles. Keel is narrow, basal cavity is large, flared and sub-circular in outline.

*Comparisons: Scythogondolella phryna* has a much higher, fused and semi-circular carina. The platform of *Scythogondolella milleri* is more highly crenulated. *Scythogondolella lachrymiformis* has a more elongate platform. *Scythogondolella rhomboidea* has a diamond-shaped basal cavity.

*Occurrence:* Middle Montney Formation

*Scythogondolella phryna* Orchard and Zonneveld, 2009

Figure 4.9, parts 4-5

2009 *Scythogondolella phryna* n. sp., Orchard and Zonneveld, p. 786, fig. 16, parts 10-16, 20-24

*Description:* Elements with narrow, biconvex platform. Platform is widest at the midpoint of the element, and it tapers evenly to both the anterior and posterior. It does not reach the posterior end of the element, terminating before the cusp. Platform is flat in side view, whilst the element is arched. Carina is very high, and it is highest at the midpoint of the element. It becomes lower to the anterior and posterior, forming a semi-circular upper margin to the carina. The denticles are fused for only part of their length, and they are rounded. Those at the posterior are inclined, whilst those to the anterior are upright. Cusp is distinct but similar in size to the neighbouring denticles. Keel is narrow at the anterior and widens to the posterior before forming a wide, sub-circular basal loop.

*Comparisons:* The high carina of *Scythogondolella phryna* distinguishes it *Scythogondolella lachrymiformis*, whilst it has a much narrower platform than *Scythogondolella ellesmerensis*.

*Occurrence:* Middle Montney Formation

**Fig. 4.9**

**Parts 1-3.** *Guangxidella bransoni*, from the Middle Montney, at 2402.40-2403.30 m.

**Parts 4-5.** *Scythogondolella phryna*, from the Middle Montney, at 2394.00-2395.00 m.

**Parts 6-8.** *Scythogondolella mosheri*, from the Middle Montney, at 2393.20-2394.10 m.

**Part 9.** *Conservatella conservativa*, from the Middle Montney, at 2388.70-2389.60 m.

**Parts 10-12.** *Neospathodus pakistanensis*, from the Middle Montney, at 2402.40-2403.30 m.

**Parts 13-15.** *Neospathodus waageni*, from the Middle Montney, at 2402.40-2403.30 m.

**Parts 16-18.** *Neospathodus posterolongatus*, from the Middle Montney, at 2402.40-2403.30 m.

**Parts 19-21.** *Clarkina* aff. *meishanensis*, from the Lower Montney, at 2528.50-2529.00 m.

**Parts 22-24.** *Clarkina carinata*, from the Lower Montney, at 2490.50-2491.50 m.

**Parts 25-27.** *Neospathodus cristagalli*, from the Lower Montney, at 2470.00-2470.75 m.

**Fig. 4.10**

**Parts 1-3.** *Paulella meeki*, from the Middle Montney, at 2402.40-2403.30 m.

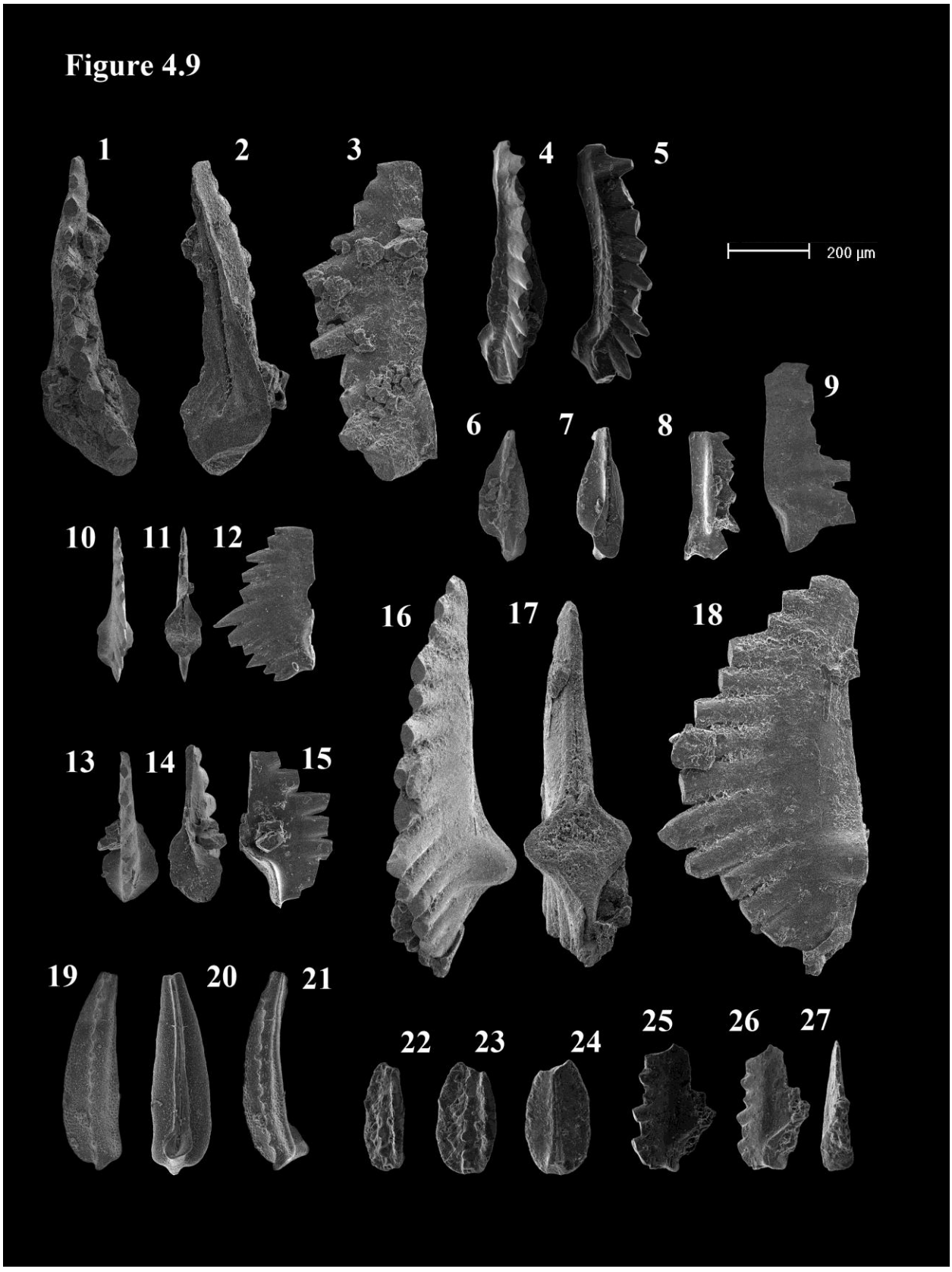
**Parts 4-6.** *Neogondolella* ex gr. *regalis* morphotype η, from the Doig, at 2238.74-2239.75 m.

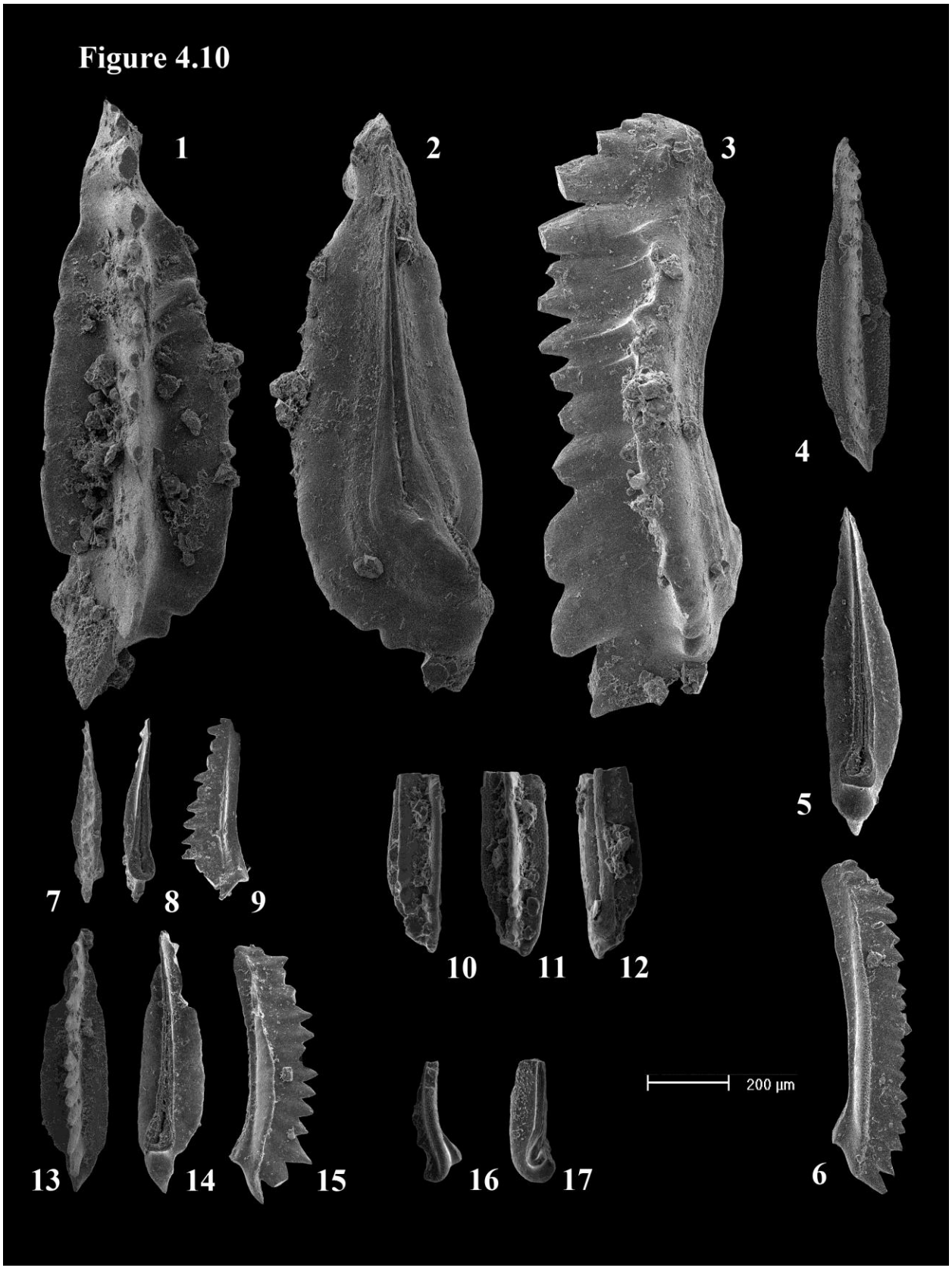
**Parts 7-9.** *Paragondolella excelsa*, from the Doig, at 2234.10-2234.57 m.

**Parts 10-12.** *Neogondolella* cf. sp. A (sensu Orchard, 2008), from the Doig, at 2256.00-2257.00 m.

**Parts 13-15.** *Neogondolella* ex gr. *regalis*, from the Doig, at 2238.74-2239.75 m.

**Parts 16-17.** *Neogondolella* cf. n. sp. D (sensu Orchard, 2007 d), from the Upper Montney, at 2384.00-2385.00 m.


Figure 4.9
1
2
3
4
5
200 µm
6
7
8
9
10
11
12
16
17
18
13
14
15
19
20
21
22
23
24
25
26
27


Figure 4.10
1
2
3
4
5
6
7
8
9
10
11
12
13
14
15
16
17
200 µm

# CHAPTER 5

## Determining the provenance of Triassic sediments in northeastern British Columbia using detrital zircon geochronology – implications for regional tectonics

## 5.1 INTRODUCTION

A number of recent studies have utilised the isotopic dating of detrital zircons to determine provenance of sediments in northern and western Canada (e.g., Garzione *et al.*, 1997; Ross *et al.*, 1997; Gehrels and Ross, 1998; Mortensen *et al.*, 2007; Leslie, 2009; Beranek *et al.*, 2010 a, b; Beranek and Mortensen, 2011; Anfinson *et al.*, 2012; Lemiuex *et al.*, 2011; Hadlari *et al.*, 2012). The ages obtained from detrital zircon grains provide an indication of the age of any igneous rock units from which the clastic detritus was derived, either directly through erosion or indirectly, having been reworked from previously deposited sedimentary units that initially contained the zircons. Especially when combined with whole rock geochemistry and Nd isotopic studies such as those of Boghossian *et al.* (1996), Unterschutz *et al.* (2002) and Beranek (2009), the resulting data set can constrain sedimentary provenance as well as the regional tectonic setting during deposition.

The study of Ross *et al.* (1997) was the first to examine the provenance of Triassic sediments in the Western Canada Sedimentary Basin (WCSB). On the basis of U-Pb ages for 57 single zircon grains from two localities, they determined that all of the Triassic sediment was derived from Laurentia and the Innuitian foreland wedge. These samples came from the Liard Formation in northern British Columbia and the Whitehorse Formation in southern British Columbia and were analysed using thermal ionization mass spectrometry (TIMS) methods. Beranek *et al.* (2010 a) and Beranek and Mortensen (2011) analysed a larger suite of samples from the Triassic of the Yukon that were deposited in the WCSB and the Selwyn Basin. They analysed a total 2,068 grains from 29 samples using laser ablation inductively-coupled-plasma mass spectrometry (LA-ICP-MS) methods. The advance of technology led to the generation of this considerably larger

data set, which allowed the authors to reach conclusions regarding the provenance of Triassic sediments that were different to those of Ross *et al.* (1997). Although the majority of the sediment was interpreted to have been derived from Laurentia and the Arctic, in agreement with Ross *et al.* (1997), a number of zircon grains gave anomalously young, mainly Permian, ages (Beranek and Mortensen, 2011). Zircons of this age have no known source in Laurentia or the Arctic, and the overlap of these ages with those of dated intrusions and volcanic rocks in the Yukon-Tanana terrane led Beranek (2009; see also Beranek *et al.*, 2010 a; Beranek and Mortensen, 2011) to conclude that the Yukon-Tanana terrane had impinged upon the ancestral North American margin prior to the Triassic, during the latest Permian. The timing of this event fits with the conclusions of Nelson *et al.* (2006), who advocated for Permian collision of the Yukon-Tanana terrane on the basis of the age of eclogite formation, the age of synorogenic conglomerate deposition and the timing of thrust faulting in the terrane. The recognition of collision in the Permian pushes back the date for the initiation of orogenesis related to terrane accretion in the northern part of the Canadian Cordillera from its previously accepted age in the Jurassic (e.g., Monger and Price, 2002). Further south in the Cordillera, the Antler Orogeny had already occurred during the Devonian and Mississippian. Beranek and Mortensen (2011) named this latest Permian orogenic event the Klondike Orogeny and concluded that the Triassic strata in the Yukon were deposited in the foreland basin associated with this orogeny. This period of orogenesis in the northern Cordillera occurred at approximately the same time as the Sonoman Orogeny in the southern Cordillera (Mortensen *et al.*, 2007).

The work of Nelson *et al.* (2006) and Beranek and Mortensen (2011) in the northern Cordillera makes it necessary to re-evaluate the conclusions of Ross *et al.* (1997) concerning the provenance of Triassic sediment in the WCSB. The model of deposition in a foreland basin of

the Klondike Orogeny implies that the Triassic rocks of the WCSB should contain a component of detrital zircon grains sourced from the Yukon-Tanana terrane, similar to the Triassic rocks of the WCSB, Selwyn and Earn basins in the Yukon. Beranek *et al.* (2010 a) suggest that the similarity of detrital zircon signatures from the Toad Formation in the southern Yukon and in the WCSB (Ross *et al.*, 1997) indicates that there was uninterrupted sedimentation along the margin of western North America during the Triassic.

In order to test the hypotheses of pre-Triassic orogenesis and the lateral correlation of Triassic rocks in the Yukon and British Columbia, a detrital zircon study of Triassic sedimentary rocks in the WCSB was undertaken. A total of 69 samples were collected from 15 sections, of which 31 yielded datable zircon. Of the 1,257 zircon grains that were analyzed from these samples, 979 produced concordant ages. The samples were collected from outcrop sections on Williston Lake (Halfway River map area) and the Alaska Highway (Tuchodi Lakes map area), as well as from subsurface cores taken from natural gas wells (Dawson Creek, Charlie Lake and Halfway River map areas). The location of these sections are shown in figure 1. The depositional ages of all of the samples analyzed were well constrained on the basis of ammonoid and conodont biochronology, and ranged from the Spathian (Lower Triassic) to the Rhaetian (Upper Triassic). The result of this undertaking, presented here, is the most extensive detrital zircon geochronological study in terms of geographic range, stratigraphic coverage and volume of samples analysed thus far undertaken in the Triassic of British Columbia.

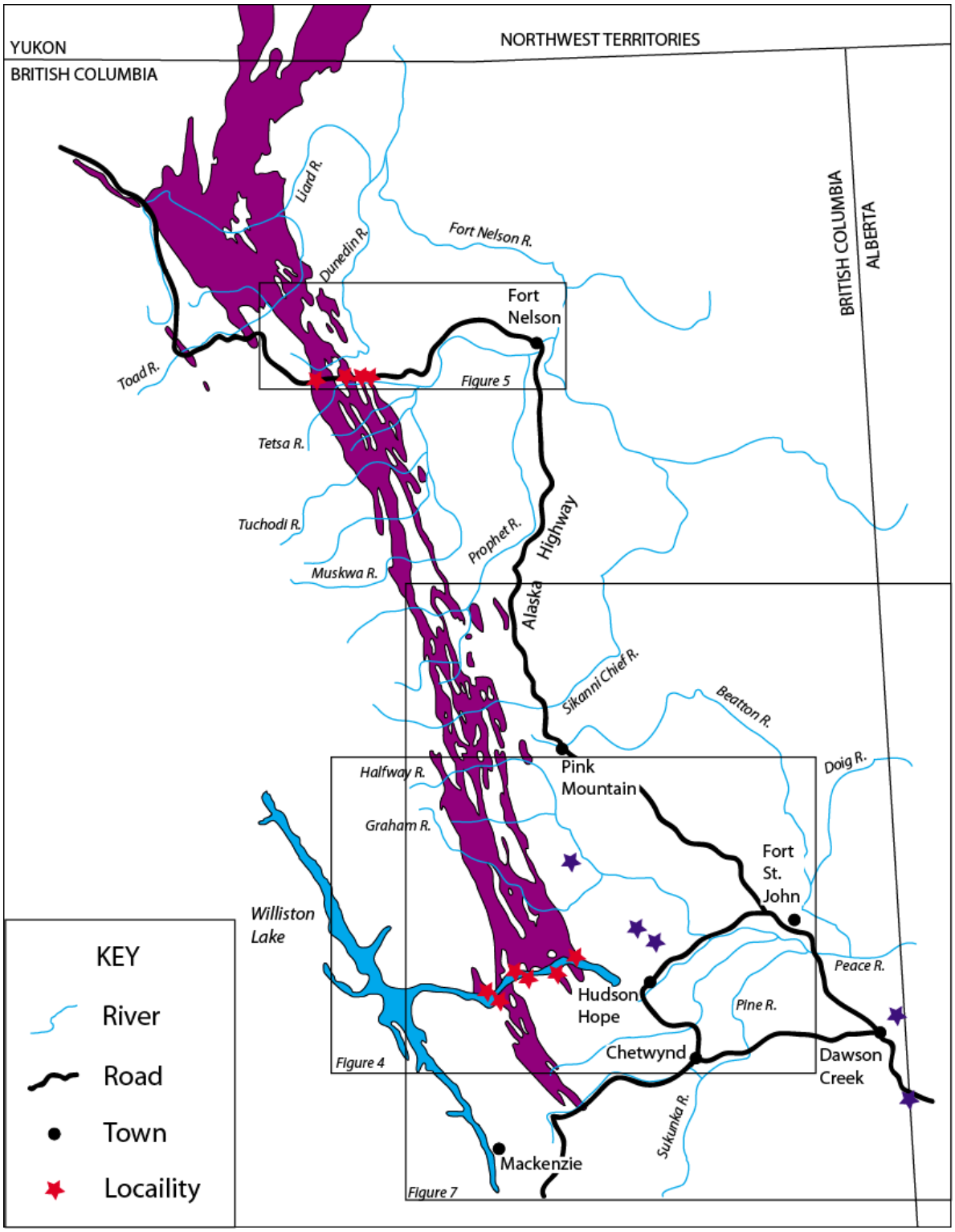



**Figure 5.1.** Map of British Columbia, western Alberta, southeastern Yukon and southwestern NWT, showing the location of Triassic outcrop in purple. Red stars indicate the location of outcrop sections sampled for this study, blue stars indicate the location of subsurface wells. The areas of figures 4, 5 and 7 are shown in outline.

## 5.2 GEOLOGICAL SETTING

The Western Canada Sedimentary Basin (WCSB; Fig. 5.2) was a long-lived and structurally complex basin that initially developed in the Mesoproterozoic and continued to exist until the Jurassic (Davies, 1997 a; Ross *et al*., 1989; Poulton, 1989). The basin extended from southeastern Yukon to the USA-Canada border and is divided into a number of sub-basins; this study is restricted to sediments deposited in the Peace River Basin (fig. 5.1; Davies, 1997 a). During the Triassic, the WCSB was situated at mid-latitudes in the northern hemisphere, in an arid environment (Davies, 1997 a). Because of this setting, it is thought that much of the sediment was deposited by wind and sourced from the Laurentian craton to the east.

Triassic strata that crop out in northeastern British Columbia are divided into six regional formations (Zonneveld, 2010). Not all of these formations can be confidently correlated with rock units in the subsurface, where six formations have also been identified (fig. 5.3). In outcrop, the oldest part of the Triassic consists of siltstone and shale of the Grayling Formation, which was not sampled for this study. Overlying this is the Toad Formation, which consists of argillaceous to calcareous siltstone, silty shale, silty limestone and dolomite, as well as very fine-grained sandstone. The Toad Formation interfingers with the Liard Formation, which consists of fine to coarse sandstone, calcareous and dolomitic siltstone and sandy to silty dolomite and limestone. The upper boundary of this formation is difficult to place due to its transitional nature. The overlying Charlie Lake Formation, comprising of mainly dolostone, limestone and evaporite, was not sampled for this study.

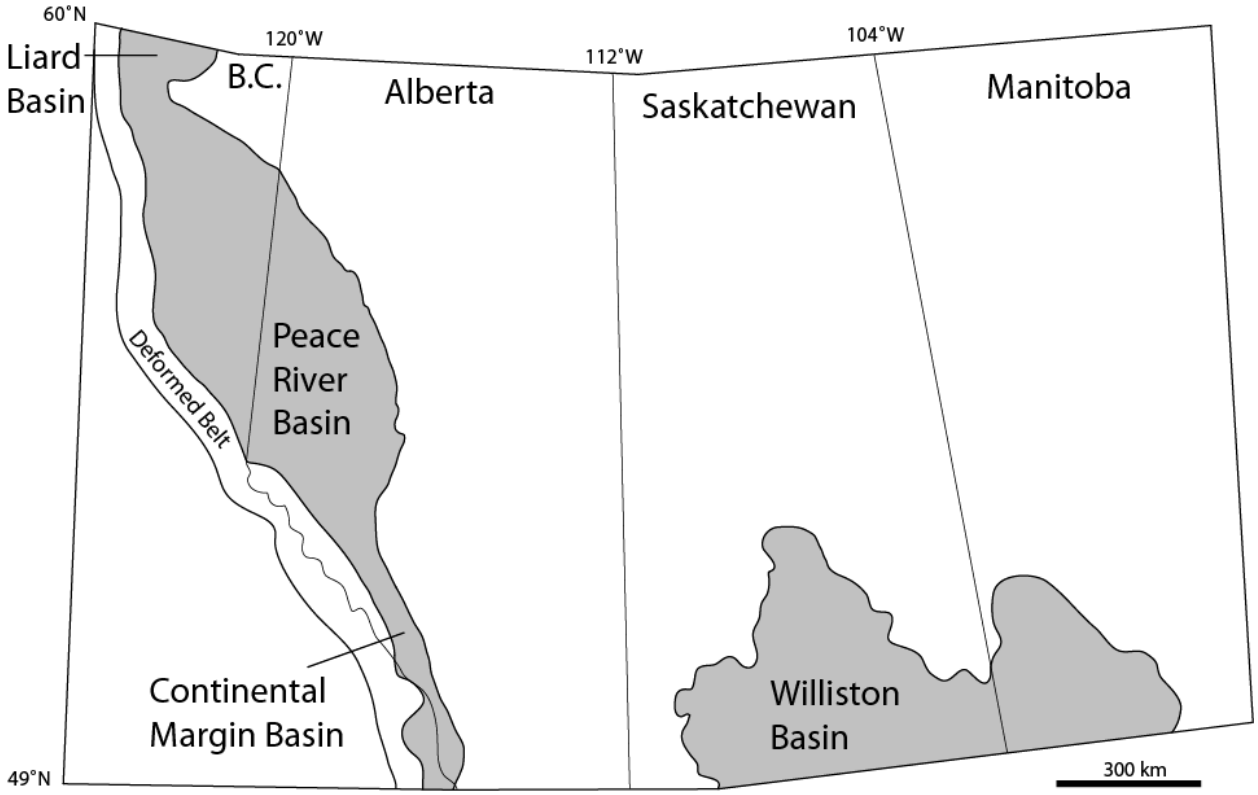



**Figure 5.2.** Map showing the location of the Western Canada Sedimentary Basin in western Canada and the distribution of its sub-basins.

Stratigraphically above the Charlie Lake Formation is the Baldonnel Formation, which is characterised by a sequence of limestone, dolostone and siltstone. The Pardonet Formation consists of halobiid-rich limestone, dolostone, calcareous siltstone and shale. The youngest formation of the Triassic is the Bocock Formation, consisting of carbonate and locally overlying the Pardonet Formation. This unit was not sampled for this study; neither were the carbonates and calcareous siltstones of the Ludington Formation, which is a deep water equivalent of the Liard, Charlie Lake and Baldonnel formations, and that is restricted to the western Rocky Mountain Foothills.

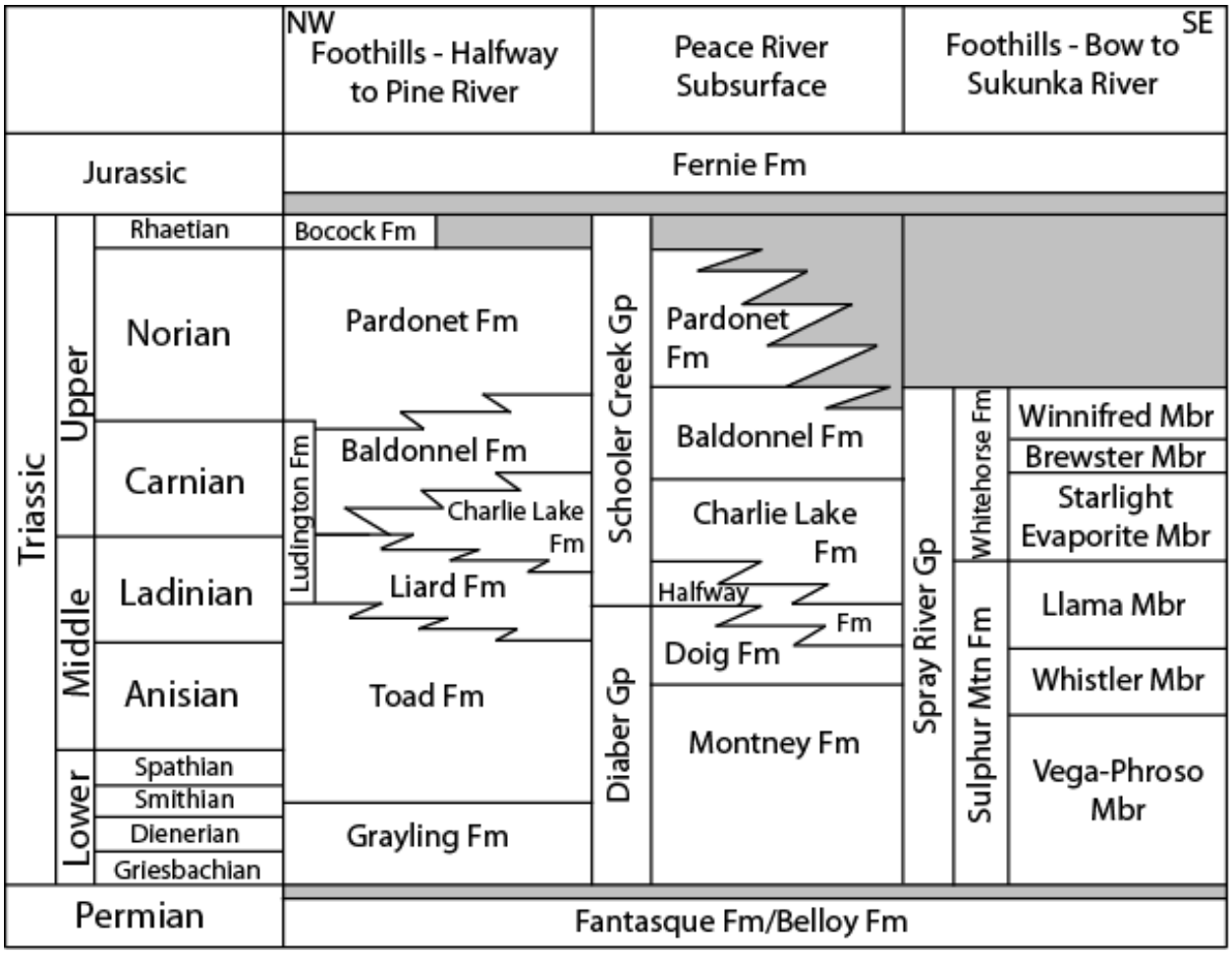



**Figure 5.3.** Correlation chart of Triassic formations in the surface and subsurface of British Columbia and the surface of Alberta. Fm = Formation; Mbr = Member. Stage boundary ages are in Ma, and taken from Ogg (2012).

In the subsurface, the oldest part of the Triassic is represented by the Montney Formation, which consists of siltstone, shale and very fine sandstone. It is correlated with the Grayling Formation and lower part of the Toad Formation in outcrop (fig. 5.3; Gibson, 1971). The top of the Montney Formation is marked by a firmground that is overlain by phosphate-rich sediments of the Doig Formation, which comprises shale, siltstone, sandstone and carbonate. It is the equivalent of the upper part of the Toad Formation and the lower part of the Liard Formation, as

recognized in surface outcrop (Gibson, 1971). The Halfway Formation is equivalent to the upper part of the Liard Formation, but was not sampled for this study. The remaining subsurface formations correlate with their surface equivalents (fig. 5.3), but were not sampled.

## 5.3 MATERIAL AND METHODS

Sixty-nine samples were collected for detrital zircon analysis using LA-ICP-MS methods from fifteen sections in northeastern British Columbia (fig. 5.1; table 5.1). Additional samples were collected for conodont analysis in order to determine the depositional age of the samples, and ammonoids were also collected from some of the sections for similar purposes. Some of the sections had previously been visited and sampled for fossils, whilst others were new sections. None of the sections have formerly been sampled for detrital zircon analysis. Many of the sampled rock units were relatively fine grained, and detrital zircons that were sufficiently coarse to permit isotopic dating were scarce to absent in many of the samples.

The sampled sections can be divided into three main areas: Williston Lake area, Alaska Highway, and subsurface British Columbia (figs. 5.4, 5.5 and 5.6).

### *Williston Lake Area*

Samples from Williston Lake come from the eastern extension of this reservoir in north-central British Columbia, known as the Peace Reach (fig. 5.4). Six sections were sampled on Peace Reach; from west to east these are: Ne-Parle-Pas Point; Pardonet Creek; Black Bear Ridge; Brown Hill; Glacier Spur and East Carbon Creek. All sections have been described by Zonneveld (2010).

| Williston Lake | | | | |
|---|---|---|---|---|
| **Locality** | **Height (m)** | **Age** | **Zircon?** | **Formation** |
| Ne-Parle-Pas Point | 37.20 | Rhaetian | Y | Pardonet |
| Ne-Parle-Pas Point | 41.20 | Rhaetian | N | Pardonet |
| Ne-Parle-Pas Point | 41.20 | Rhaetian | Y | Pardonet |
| Ne-Parle-Pas Point | 41.75 | Rhaetian | N | Pardonet |
| Ne-Parle-Pas Point | 42.50 | Rhaetian | N | Pardonet |
| Ne-Parle-Pas Point | 42.80 | Rhaetian | N | Pardonet |
| Ne-Parle-Pas Point | 43.00 | Rhaetian | N | Pardonet |
| Ne-Parle-Pas Point | 43.20 | Rhaetian | Y | Pardonet |
| Ne-Parle-Pas Point | 47.25 | Rhaetian | Y | Pardonet |
| Ne-Parle-Pas Point | 48.40 | Rhaetian | Y | Pardonet |
| Ne-Parle-Pas Point | 51.00 | Rhaetian | N | Pardonet |
| Ne-Parle-Pas Point | 51.20 | Rhaetian | N | Pardonet |
| Pardonet Creek | 3.60 | Rhaetian | Y | Pardonet |
| Pardonet Creek | 14.35 | Rhaetian | Y | Pardonet |
| Pardonet Creek | 15.45 | Rhaetian | N | Pardonet |
| Pardonet Creek | 15.70 | Rhaetian | N | Pardonet |
| Black Bear Ridge | 242.00 | Rhaetian | Y | Pardonet |
| Black Bear Ridge | 242.00 | Rhaetian | Y | Pardonet |
| Brown Hill | 191.00 | Anisian | Y | Toad |
| Brown Hill | 239.00 | Anisian | Y | Toad |
| Glacier Spur | 122.60 | Ladinian | Y | Liard |
| Glacier Spur | 149.00 | Ladinian | Y | Liard |
| Glacier Spur | 255.00 | Ladinian | Y | Liard |
| Glacier Spur | 293.80 | Ladinian | Y | Liard |
| Glacier Spur | 304.00 | Ladinian | Y | Liard |
| East Carbon Creek | 76.00 | Carnian | Y | Baldonnel |
| **Alaska Highway** | | | | |
| **Locality** | **Height (m)** | **Age** | **Zircon?** | **Formation** |
| Mile Post 386 | 10.25 | Ladinian | N | Toad |
| Mile Post 386 | 17.50 | Ladinian | Y | Toad |
| North Tetsa Phosphate | 2.60 | Middle Anisian | N | Toad |
| North Tetsa Phosphate | 2.70 | Middle Anisian | Y | Toad |
| North Tetsa Phosphate | 2.80 | Middle Anisian | Y | Toad |
| North Tetsa Phosphate | 10.60 | Middle Anisian | N | Toad |
| North Tetsa Phosphate | 11.85 | Middle Anisian | N | Toad |
| Oyster Springs | ? | Upper Anisian | Y | Toad |
| Oyster Springs | 3.30 | Upper Anisian | Y | Toad |
| Oyster Springs | ? | Upper Anisian | N | Toad |
| Mile Post 375 West | N/A | Middle Anisian | Y | Toad |
| **Subsurface British Columbia** | | | | |
| **Locality** | **Depth (m)** | **Age** | **Zircon?** | **Formation** |
| PCK d-048-A/094-B-09 | 1968.25 | Spathian/Anisian | N | Montney |

| Subsurface British Columbia | | | | |
|---|---|---|---|---|
| **Locality** | **Depth (m)** | **Age** | **Zircon?** | **Formation** |
| PCK d-048-A/094-B-09 | 1967.85 | Spathian/Anisian | N | Montney |
| PCK d-048-A/094-B-09 | 1967.30-1967.50 | Spathian/Anisian | N | Doig |
| PCK d-048-A/094-B-09 | 1966.00-1967.00 | Spathian/Anisian | N | Doig |
| PCK d-048-A/094-B-09 | 1964.80-1965.90 | Lower Anisian | N | Doig |
| PCK d-048-A/094-B-09 | 1965.00-1965.40 | Lower Anisian | Y | Doig |
| TA c-085-I/094-B-01 | 2374.17-2373.25 | Middle Anisian | Y | Doig |
| TA c-085-I/094-B-01 | 2315.22-2314.50 | Anisian? | Y | Doig |
| TA c-085-I/094-B-01 | 2310.89-2310.00 | Anisian? | Y | Doig |
| TA c-085-I/094-B-01 | 2306.82-2306.01 | Anisian? | N | Doig |
| TA c-085-I/094-B-01 | 2295.92-2295.36 | Anisian? | N | Doig |
| TA 16-17-083-25W6 | 2258.30-2257.43 | Spathian | N | Montney |
| TA 16-17-083-25W6 | 2256.22-2255.98 | Spathian | Y | Doig |
| TA 16-17-083-25W6 | 2255.30-2254.44 | Spathian | N | Doig |
| TA 16-17-083-25W6 | 2248.52-2248.05 | Lower Anisian | N | Doig |
| TA 16-17-083-25W6 | 2247.75-2247.21 | Lower Anisian | N | Doig |
| TA 16-17-083-25W6 | 2245.79-2244.62 | Lower Anisian | N | Doig |
| TA 16-17-083-25W6 | 2242.35-2241.46 | Lower Anisian | N | Doig |
| TA 16-17-083-25W6 | 2239.75-2238.74 | Middle Anisian | N | Doig |
| TA 16-17-083-25W6 | 2237.05-2236.09 | Middle Anisian | N | Doig |
| TA 16-17-083-25W6 | 2234.57-2234.10 | Upper Anisian | N | Doig |
| TA 16-17-083-25W6 | 2233.61-2233.08 | Upper Anisian | N | Doig |
| AD 07-13-79-15W6 | 2056.35-2055.68 | Middle Anisian | Y | Montney |
| AD 07-13-79-15W6 | 2054.30-2054.05 | Middle Anisian | Y | Doig |
| MS d-54-B/093-P-9 | 2557.30 | Middle Anisian | N | Doig |
| MS d-54-B/093-P-9 | 2556.90 | Middle Anisian | N | Doig |
| MS d-54-B/093-P-9 | 2556.25 | Middle Anisian | N | Doig |
| MS d-54-B/093-P-9 | 2553.80 | Middle Anisian | N | Doig |
| MS d-54-B/093-P-9 | 2553.40 | Middle Anisian | N | Doig |
| MS d-54-B/093-P-9 | 2551.80 | Middle Anisian | Y | Doig |
| MS d-54-B/093-P-9 | 2549.66 | Upper Anisian | N | Doig |
| MS d-54-B/093-P-9 | 2548.45 | Upper Anisian | N | Doig |

**Table 5.1.** Table showing locality, depth/height in section, stratigraphic age and formation of detrital zircon samples, as well as whether datable zircon was recovered or not.

*Ne-Parle-Pas Point.* This section consists of approximately 50 metres of fossiliferous siltstone, carbonate, and phosphatic gravel lag beds, all belonging to the Pardonet Formation. This section encompasses both the Norian-Rhaetian boundary, and the Triassic-Jurassic boundary. Twelve

samples were collected from lag beds in the Rhaetian part of the section, and five of these produced datable zircons.

*Pardonet Creek.* This section is approximately 25 metres thick and also consists of fossiliferous siltstone, carbonate, and gravel lag beds belonging to the Pardonet Formation. It also spans both the Norian-Rhaetian and Triassic-Jurassic boundary. Four samples were collected from lag beds in the Rhaetian part of the sections, and two produced datable zircons.

*Black Bear Ridge.* This section consists of 270 metres of siltstone, shale and bioclastic limestone belonging to the Ludington and Pardonet formations. This section includes the Carnian-Norian, Norian-Rhaetian and Triassic-Jurassic boundaries. Two samples were collected from one lag bed in the Rhaetian part of the Pardonet Formation and both produced datable zircons. The Rhaetian is much more condensed here than at either the Ne-Parle-Pas Point or Pardonet Creek localities.

*Brown Hill.* This section consists of approximately 920 metres of shale, siltstone, sandstone and carbonate belonging to the Toad, Liard, Charlie Lake, Baldonnel and Pardonet formations. This section encompasses much of the Triassic, and ranges from Anisian to Norian in age. Two samples were collected from the Toad Formation, and are Anisian in depositional age. Both produced datable zircons.

*Glacier Spur.* This section is situated along strike from Brown Hill. It is 370 metres thick, and it too consists of shale, siltstone, sandstone and carbonate belonging to the Toad, Liard and Charlie Lake formations. This section encompasses the Ladinian-Carnian boundary. Five samples were collected from the Ladinian part of the Liard Formation, and all of them contained datable zircons.

*East Carbon Creek.* This is a 110 metre section of siltstone, sandstone and bioclastic limestone with gravel lag beds throughout. These rocks belong to the Charlie Lake and Baldonnel formations. One sample was collected from the Carnian aged Baldonnel Formation, and it contained datable zircons.

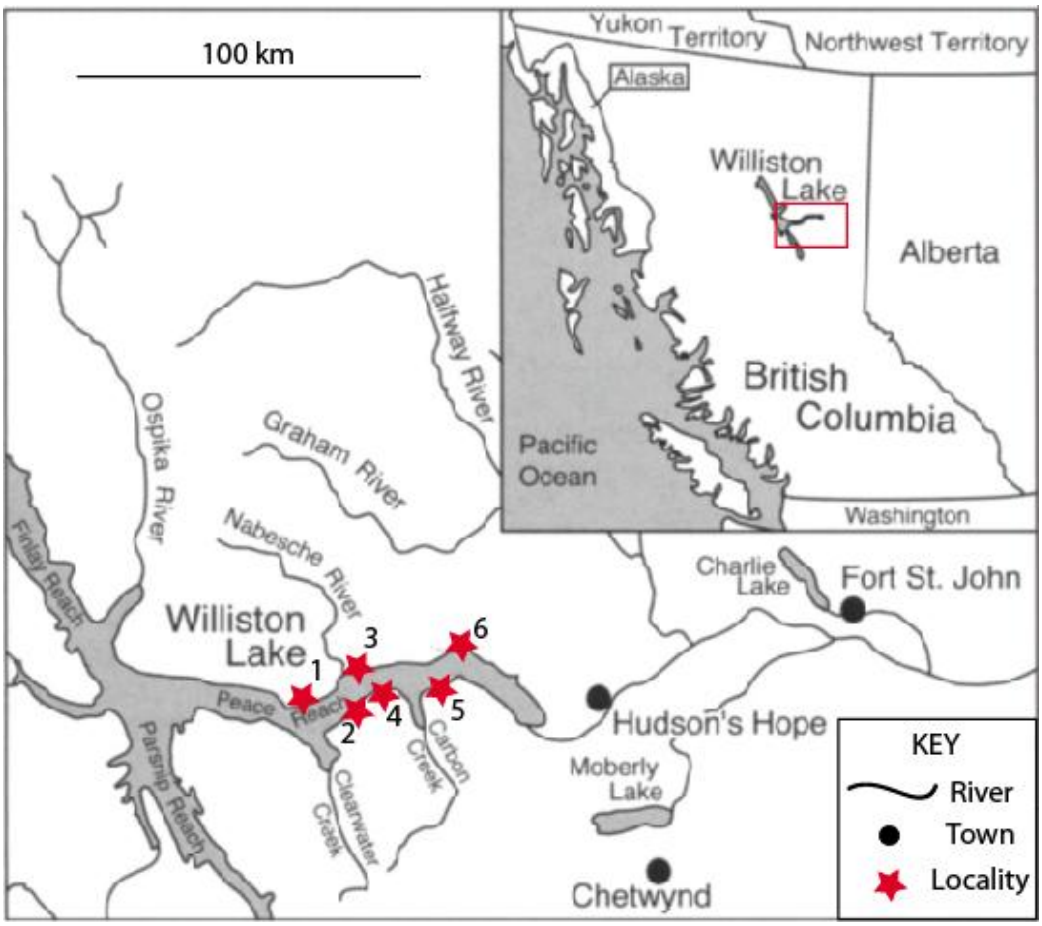



**Figure 5.4.** Map of Williston Lake, showing the location of sections sampled for this study. 1) Pardonet Creek; 2) Ne-Parle-Pas Point; 3) Black Bear Ridge; 4) Glacier Spur; 5) Brown Hill; 6) East Carbon Creek. Modified from Zonneveld *et al.* (2001). Black Bear Ridge (3) contains zircons with a Rhaetian age.

### *Alaska Highway*

The Alaska Highway cuts through exposures of Triassic rock as it runs east-west west of Fort Nelson. Four sections were sampled in the Tuchodi Lakes map area (NTS 094 K; fig. 5.5). From west to east, these sections are: Mile Post 386; North Tetsa Phosphate; Oyster Springs and Mile Post 375 West. The section at Mile Post 375 West is described in Tozer (1967); the other sections have not yet been formally described.

*Mile Post 386.* This section has its base at UTM 410890E 6503721N (NAD83). It consists of 17.75 metres of siltstone and sandstone belonging to the Toad Formation. This section contains ammonoids belonging to the Ladinian Meginae Zone (Tozer, 1994; fig 5.6). Two samples were collected, and one contained datable zircons.

*North Tetsa Phosphate.* This section has its base at UTM 416937E 6503965N (NAD 83). It consists of 17.85 metres of siltstone and sandstone, also belonging to the Toad Formation. Ammonoids from this section indicate the presence of the Middle Anisian Hayesi Zone (Tozer, 1994; fig. 5.6). Five samples were collected from this section, and two contained datable zircons.

*Oyster Springs.* This section has its base at UTM 425012E 6502735N (NAD83). It consists of 18.53 metres of siltstone, sandstone and carbonate belonging to the Toad Formation. This section contains conodonts equivalent in age to the Chischa Zone, which is Upper Anisian in age (Tozer, 1994; fig. 5.6). Three samples were collected, and two contained datable zircons.

*Mile Post 375 West.* This section was described by Tozer (1967). The section belongs to the Toad Formation and contains ammonoids belonging to the Hayesi, Minor and Deleeni zones of the Middle and Upper Anisian (fig. 5.6). One sample was collected from between Bed 1 and Bed

2 of Tozer (1967), placing it in either the Hayesi or Minor zone from the Middle Anisian (Tozer, 1994; fig. 5.6). This sample contained datable zircons.

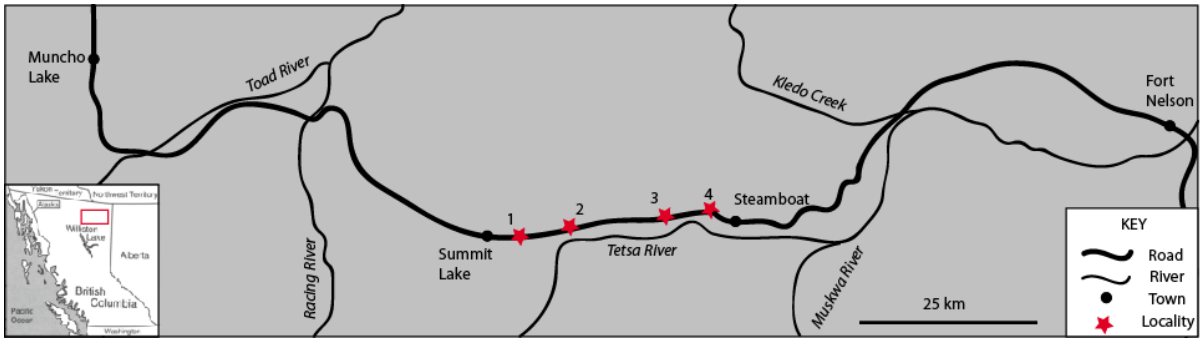



**Figure 5.5.** Map of the Alaska Highway, showing the location of sections sampled for this study. 1) Mile Post 386; 2) North Tetsa Phosphate; 3) Oyster Springs; 4) Mile Post 375 West.

***Subsurface British Columbia***

As described previously, subsurface equivalents of the rock units examined on Williston Lake and the Alaska Highway exist in British Columbia and Alberta (fig. 5.2). A number of natural gas wells have intercepted these Triassic rocks, and cores taken from five of these wells were sampled. All of the wells come from the area around Fort St John: in the Kobes, Altares, Swan and Dawson areas (fig. 5.7). From northwest to southeast, the wells are: Petro-Canada Kobes d-048-A/094-B-09; Talisman Altares c-085-I/094-B-01; Talisman Altares 16-17-083-25W6; Arc Dawson 07-13-79-15W6 and Murphy Swan d-54-B/093-P-9 (fig. 5.7). The core from the Talisman Altares 16-17-083-25W6 well is described in more detail in chapter 4.

*Petro-Canada Kobes d-048-A/094-B-09.* The core from this well consists of 9.00 metres of siltstone and very fine sandstone belonging to the Montney and Doig formations. Conodont biochronology indicates that both formations in this well are Anisian in age. Two samples were

taken from the Montney Formation, and four from the Doig Formation. Only one sample, from the Doig Formation, produced datable zircons.

*Talisman Altares c-085-I/094-B-01*. The core from this well consists of 84.17 metres of siltstone and fine sandstone belonging to the Doig Formation. Conodont biochronology indicates an Anisian age. Five samples were collected, three of which contained datable zircons.




**Figure 5.6.** Chart showing the Anisian ammonoid zones of British Columbia. Data compiled from Tozer (1994) and Bucher (2002).

*Talisman Altares 16-17-083-25W6.* The logged core from this well consists of 34.00 metres of siltstone and fine sandstone belonging to the Montney and Doig formations. Conodont biochronology indicates that the Montney Formation and lower part of the Doig Formation are Spathian in age, whilst the upper part of the Doig Formation in this well is Anisian. One sample was collected from the Montney Formation, and ten samples from the Doig Formation. The one sample from the Montney was the only one that contained datable zircons.

*Arc Dawson 07-13-79-15W6.* The core from this well consists of 4.50 metres of siltstone and fine sandstone belonging to the Montney and Doig formations. Conodont biochronology indicates that this core is Anisian in age. Two samples were collected, one from the Montney Formation and one from the Doig Formation. Both samples produced datable zircons.

*Murphy Swan d-54-B/093-P-09.* The core from this well consists of 36.00 m of siltstone and fine sandstone belonging to the Montney and Doig formations. Conodont biochronology indicates that the core is Anisian in age. Eight samples were collected from the Doig Formation but only one contained datable zircons.

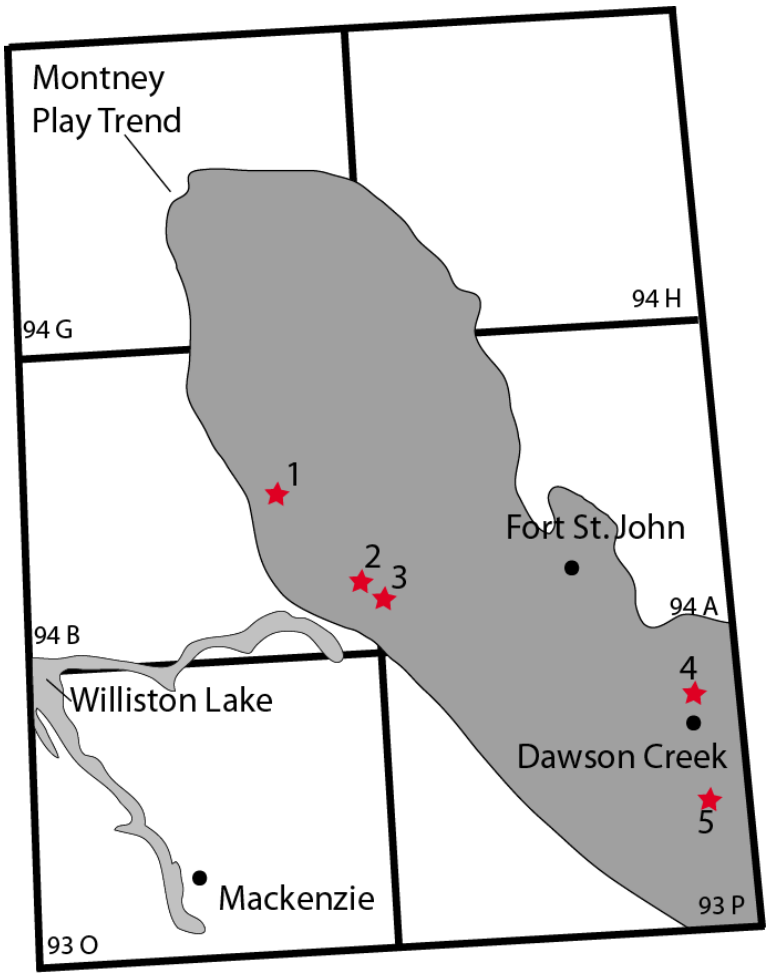



**Figure 5.7.** Map of northeastern British Columbia showing the location of sampled wells and their relationship to the Montney natural gas play trend. 1) Petro-Canada Kobes d-048-A/094-B-09; 2) Talisman Altares c-085-I/094-B-01; 3) Talisman Altares 16-17-083-25W6; 4) Arc Dawson 07-13-79-15W6; 5) Murphy Swan d-054-B/093-P9. Montney Play Trend after Hayes (2012). Arc Dawson 07-13-79-15W6 (4) contains zircon with a Permian age.

### *Detrital Zircon Processing and Analysis*

Samples collected were approximately 2 kg in weight. They were cleaned, crushed, ground, passed over a Wilfley table, dry sieved and put through methylene iodide. The heavy fraction was picked in ethanol under a stereoscopic microscope. Zircons were selected for analysis and set in epoxy resin. Zircons were selected as randomly as possible; however, there was a

necessary bias towards larger grains in many of the samples, with the larger zircons preferentially selected for the following three reasons:

- The majority of samples came from siltstones, and therefore the grain size was much smaller than typically employed for detrital zircon studies. This prevented many of the smaller grains from being isolated using tweezers.
- Since the smallest spot-size on the laser is 15 μm, grains have to be significantly larger than this to be ablated by the laser.
- Smaller grains that were large enough to be ablated produced lower count rates of uranium and lead, commonly leading to highly imprecise and/or discordant results.

The abundance of zircon and size of the grains determined how many grains were selected for analysis from each sample. The smallest sample produced 8 grains, whereas the largest produced 60 grains, which was used as the upper limit. However, not all of the zircon grains analysed in all samples produced concordant results, and the total number of concordant analyses varied from 7 to 53 per sample. Dodson *et al.* (1988) suggested that 60 grains needed to be analysed to have a 95% probability that an age component that makes up 5% of the total population will be recovered. Vermeesch (2004) raised this number to 117 grains. Košler (2011), however, found that only 40 grains needed to be analysed to detect the 5% population. In this study, only eleven of the thirty-one samples produced more than 40 concordant analyses; therefore, this represents another possible source of uncertainty in our results.

A total of 1,257 grains were analyzed using the Thermo Finnegan Element2 Laser Ablation Inductively-Coupled-Plasma Mass Spectrometer at the University of British Columbia. The analytical methodology is as described by Beranek and Mortensen (2011). Laser power was

typically 40 % and the spot size was 15 μm. Line analyses rather than spot analyses were conducted to reduce the effects of laser-induced elemental fractionation (Košler, 2008, 2012). Unknowns were analysed along with samples of the 337 Ma PL standard (external standard; Sláma *et al.*, 2008) to correct for mass and elemental fractionation, and samples of the 197 Ma KL standard (internal standard) to measure data quality. Data were reduced using the Glitter macro for Excel, version 4.4 (van Achterbergh *et al.*, 2001; Jackson *et al.*, 2004) and then processed using the Isoplot macro (Ludwig, 2003). Ages with a ($^{207}Pb/^{236}U$)/($^{206}Pb/^{238}U$) discordance of greater than +10% or -5% were rejected from the analysis. This resulted in 278 analyses being rejected. The high number is thought to be due to the small size of the majority of the zircons, leading to a higher susceptibility to post-crystallization Pb-loss, and hence more discordant analyses. A total of 979 zircons gave concordant dates. The final data set for each sample was analysed with the Age Pick macro (Gehrels, 2009) to identify age populations within each sample. The data for all of the concordant analyses is shown in Appendix 2. Results are also presented as probability density plots (Dodson *et al.*, 1988; Ludwig, 2003) in figures 5.8 and 5.9.

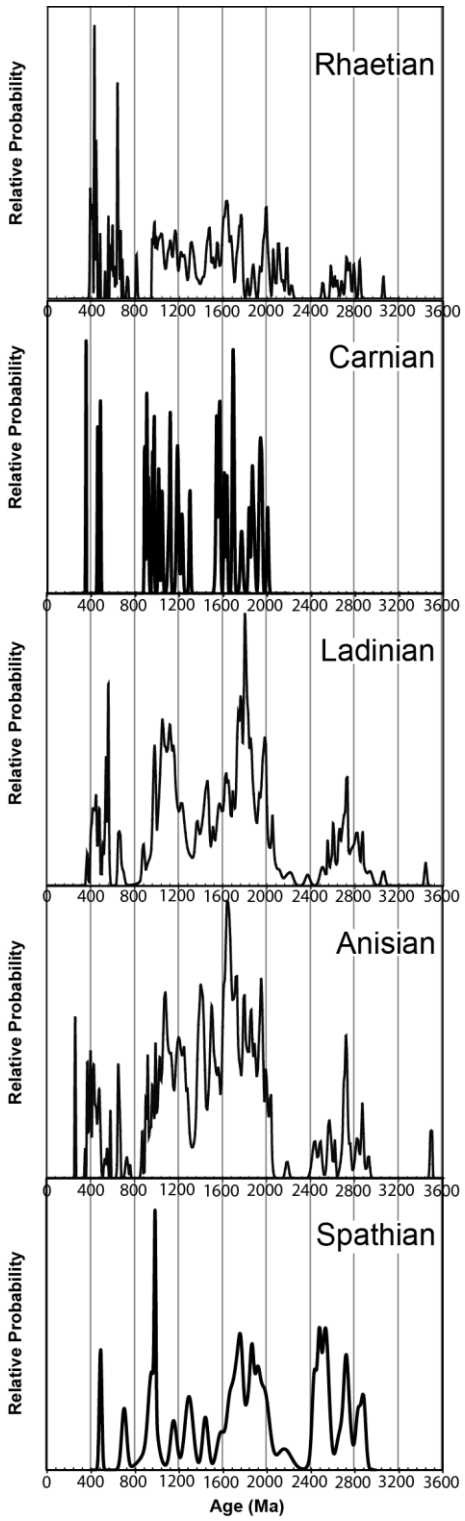



**Figure 5.8.** Relative probability density plots of all detrital zircon samples grouped by stage and substage. Note that the Rhaetian plot excludes the data from Black Bear Ridge; see text for details. No samples were collected from rocks of Norian age.

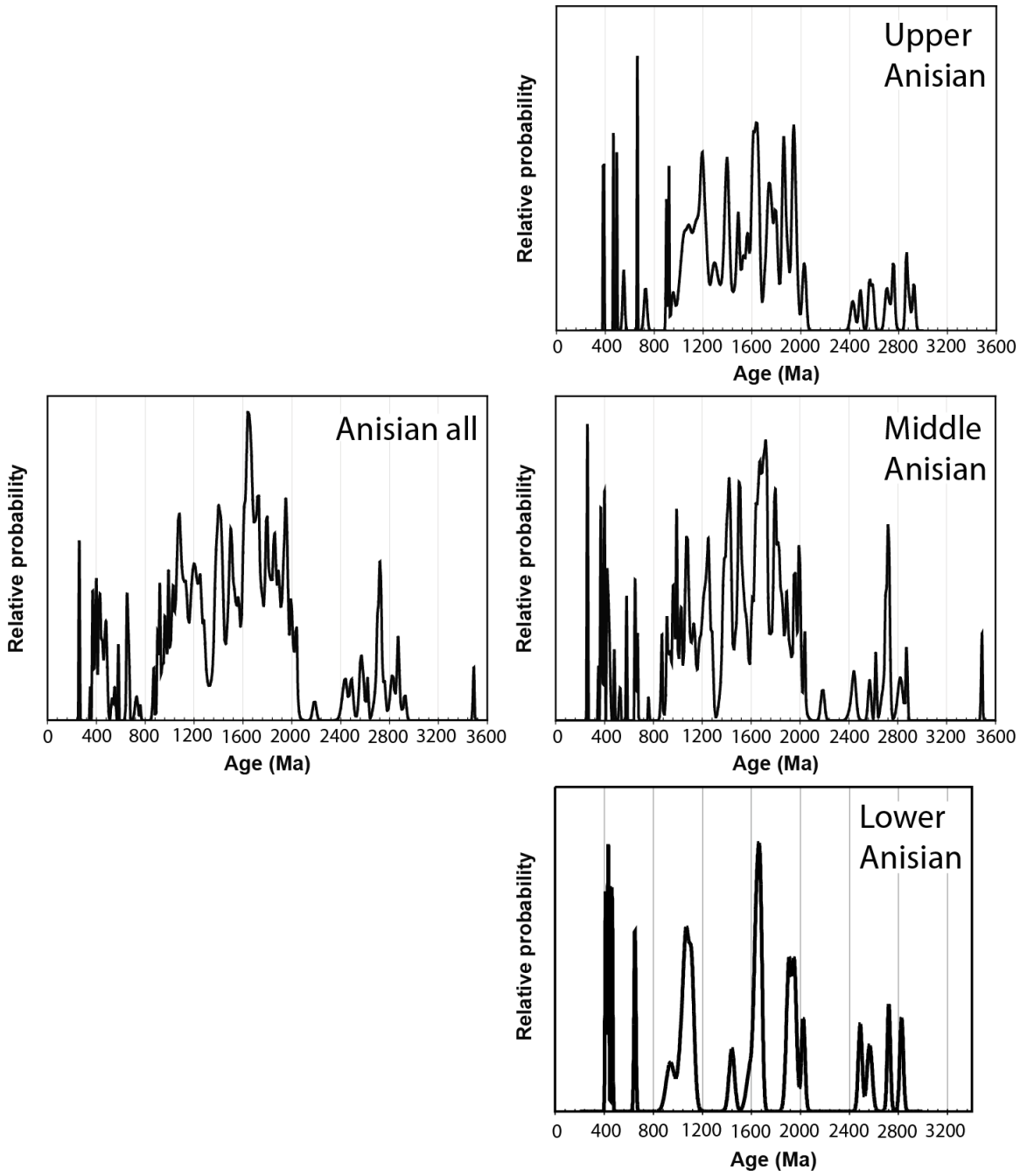



**Figure 5.9.** Relative probability density plots of all detrital zircon samples from the Anisian, grouped by substage.

## 5.4 RESULTS

### *Spathian*

The only Spathian sample comes from the Talisman Altares 16-17-83-25W6 well. This sample consists of 33 analyses and shows age peaks at 348 Ma and 450-480 Ma, and a range of ages from 840-1350 Ma, and 1550-2000 Ma with peaks at 1556 Ma, 1687 Ma, 1859 Ma and 1937 Ma (fig. 5.8).

### *Anisian*

A total of 14 samples are Anisian in age and they include a total of 285 zircon analyses. Identified populations include 375-401 Ma, 415-485 Ma, 648-670 Ma, 834-2081 Ma and 2385-2930 Ma. There are peaks at 386 Ma, 395 Ma, 424 Ma, 432 Ma, 476 Ma, 661 Ma, 854 Ma, 869 Ma, 919 Ma, 965 Ma, 991 Ma, 1079 Ma, 1247 Ma, 1415 Ma, 1504 Ma, 1654 Ma, 1797 Ma, 1855 Ma, 1952 Ma, 2471 Ma, 2571 Ma, 2616 Ma, 2718 Ma and 2870 Ma (fig. 5.8).

#### *Lower Anisian*

The only sample from the Lower Anisian is from the Petro-Canada Kobes d-48-A/94-B-9 well. This sample consists of 32 zircon analyses and shows peaks in age at 1092 Ma, 1656 Ma and 1928 Ma (fig. 5.9).

#### *Middle Anisian*

Six samples of Middle Anisian age were analyzed and they generated a total of 154 zircon ages. Identified populations range from 391-397 Ma, 420-434 Ma, 837-2053 Ma, 2610-2618 Ma, 2673-2777 Ma and 2849-2896 Ma. There are peaks at 396 Ma, 424 Ma, 854 Ma, 869 Ma, 914

Ma, 964 Ma, 991 Ma, 1030 Ma, 1078 Ma, 1251 Ma, 1421 Ma, 1506 Ma, 1683 Ma, 1798 Ma, 1957 Ma, 1990 Ma, 2031 Ma, 2718 Ma and 2872 Ma (fig. 5.9).

*Upper Anisian*

Three samples can be assigned to the Upper Anisian and they produced a total of 99 ages. Identified populations range from 901-2027 Ma, 2721-2761 Ma, 2829-2832 Ma and 2882-2897 Ma. There are peaks at 901 Ma, 920 Ma, 1098 Ma, 1191 Ma, 1396 Ma, 1494 Ma, 1625 Ma, 1747 Ma, 1865 Ma, 1941 Ma, 2020 Ma and 2755 Ma (fig. 5.9).

***Ladinian***

There are six samples that come from the Ladinian, and these samples produced a total of 256 ages. Identified populations range from 387-393 Ma, 399-584 Ma, 637-681 Ma, 793-2231 Ma and 2414-3043 Ma. There are peaks at 415 Ma, 435 Ma, 473 Ma, 540 Ma, 559 Ma, 659 Ma, 885 Ma, 984 Ma, 1063 Ma, 1112 Ma, 1378 Ma, 1459 Ma, 1637 Ma, 1695 Ma, 1804 Ma, 1980 Ma, 2045 Ma, 2554 Ma, 2605 Ma, 2660 Ma, 2725 Ma, 2809 Ma, 2864 Ma (fig. 5.8).

***Carnian***

The only sample taken from the Carnian comes from East Carbon Creek on Williston Lake. This sample consists of 34 analyses, with age peaks at 984 Ma, 1378 Ma, 1433 Ma, 1768 Ma, 1871 Ma, 2486 Ma, 2726 Ma and 2857 Ma (fig. 5.8).

***Rhaetian***

A total of nine samples were collected from the Rhaetian, all of them from Williston Lake. The two samples from Black Bear Ridge contained zircons that were predominantly Triassic in age;

these were removed from the dataset used to produce the relative probability density diagrams because they are thought to reflect a coeval felsic ash component in the sample, and their ages therefore do not bear on the provenance of the sample. The significance of these zircons will be discussed in a separate publication. The remaining seven samples consist of 199 analyses. Identified populations range from 380-451 Ma, 468-482 Ma, 570-596 Ma, 604-610 Ma, 628-654 Ma, 657-660 Ma, 936-1811 Ma, 1819-2209 Ma, 2585-2635 Ma, 2690-2786 Ma and 2809-2830 Ma. There are peaks at 386 Ma, 393 Ma, 412 Ma, 426 Ma, 442 Ma, 475 Ma, 578 Ma, 588 Ma, 636 Ma, 954 Ma, 970 Ma, 1020 Ma, 1062 Ma, 1155 Ma, 1192 Ma, 1310 Ma, 1466 Ma, 1631 Ma, 1757 Ma, 1823 Ma, 1871 Ma, 1989 Ma, 2055 Ma, 2102 Ma, 2175 Ma, 2615 Ma, 2737 Ma and 2783 Ma (fig. 5.8).

## 5.5 DISCUSSION

### *Temporal Trends in Detrital Zircon Signatures*

The relative probability density diagrams in figures 5.8 and 5.9 show that the detrital zircon signature for sediments deposited in the Western Canada Sedimentary Basin remained fairly consistent during the Triassic. Samples from the Lower, Middle and Upper Triassic all have three main populations of zircon: an "Archean – Palaeoproterozoic" population (approximately 2400 Ma – 2900 Ma); a "Proterozoic" population (800 Ma – 2100 Ma); and a "Neoproterozoic - Lower Palaeozoic" population (800 Ma – 400 Ma). The only exception to this is the sample from the single Carnian sample that was analyzed, which lacks an Archean population; this may be due to the low number of analyses available from this time period. There is a notable scarcity of zircon grains in the range of approximately 2100-2400 Ma. The absence of zircon of this age has been noted in other studies, and has been ascribed to the paucity of rocks of this age in Western

Canada, with only the 2324-1990 Ma Buffalo Head Terrane in Alberta as a possible source (Villeneuve *et al.*, 1993). There are also only very rare zircons older than 2900 Ma, although a very minor component of zircon present in the Anisian and Ladinian yields ages of approximately 3400-3500 Ma. The Proterozoic population also falls into two groups, at approximately 800-1250 Ma and 1250-2100 Ma. The Proterozoic population dominates the samples from the Anisian, Ladinian and Carnian. Although there are very few zircon ages in the range from 500-800 Ma in the Spathian, Anisian, Ladinian and Carnian samples, there is a much larger input of zircons of this age range in Rhaetian samples. Although all of the stages contain zircons in the 320-500 Ma range, there are generally fewer zircons of this age. The exception is again in the Rhaetian, where the proportion of zircons from this age range increases. The youngest age obtained from zircon in these samples (with the exception of the possibly tuffaceous Triassic zircons in the Rhaetian sample from Williston Lake) was 320 Ma, except for one Anisian sample which yielded a single zircon with an age of 260 Ma (Late Permian). This sample came from the Arc Dawson 07-13-79-15W6 well. The Anisian is the only stage that contains zircon of this age.

***Geographical Trends in Detrital Zircon Signatures***

The set of detrital zircon samples used for this study come from three widely separated geographical areas: the Alaska Highway, Williston Lake and subsurface British Columbia. The only sample from the Spathian is from the subsurface, and the only sample from the Carnian is from Williston Lake, as are all of the samples from the Rhaetian. The samples from the Ladinian are mainly from Williston Lake, together with one from the Alaska Highway. Direct comparisons between the three areas can therefore only be made for the Anisian. Fourteen

samples in total are from the Anisian: five from the Alaska Highway, two from Williston Lake and seven from the subsurface. Figure 5.10 shows relative probability density plots for these samples grouped by geographic location. In the southern part of the study area, the samples from Williston Lake and from the subsurface have roughly similar detrital zircon signatures. The main difference between the two areas is in the relative proportion of younger (<800 Ma) zircons. The samples from the subsurface have a relatively high proportion of zircon younger than 800 Ma compared to those from Williston Lake. Also, all of the younger peaks that are present in the Williston Lake samples are present in the subsurface; however, peaks are present in the subsurface samples that are not present in Williston Lake samples. The youngest zircons in the Williston Lake samples are approximately 430 Ma, whilst the subsurface samples also contain zircon that ranges from 260 Ma to 420 Ma. The Anisian samples from the subsurface contain the youngest pre-Triassic detrital zircon of any age and geographic location. The Williston Lake samples also contain much older zircon than the subsurface samples, including a grain approximately 3598 Ma, which is much older than the oldest grain (2825 Ma) from the subsurface.

In comparison with the more southerly samples, the samples from the Alaska Highway are most similar to those from Williston Lake (fig. 5.10). The Alaska Highway samples do not contain any grains as young as those found in the subsurface samples. They also have older grains similar in age to the oldest grains found in the Williston Lake samples. The main difference between north and south in the study area is the presence in the northern samples of zircon that falls into the range of 650 Ma to 850 Ma. Grains of this age are absent in all of the southern samples.

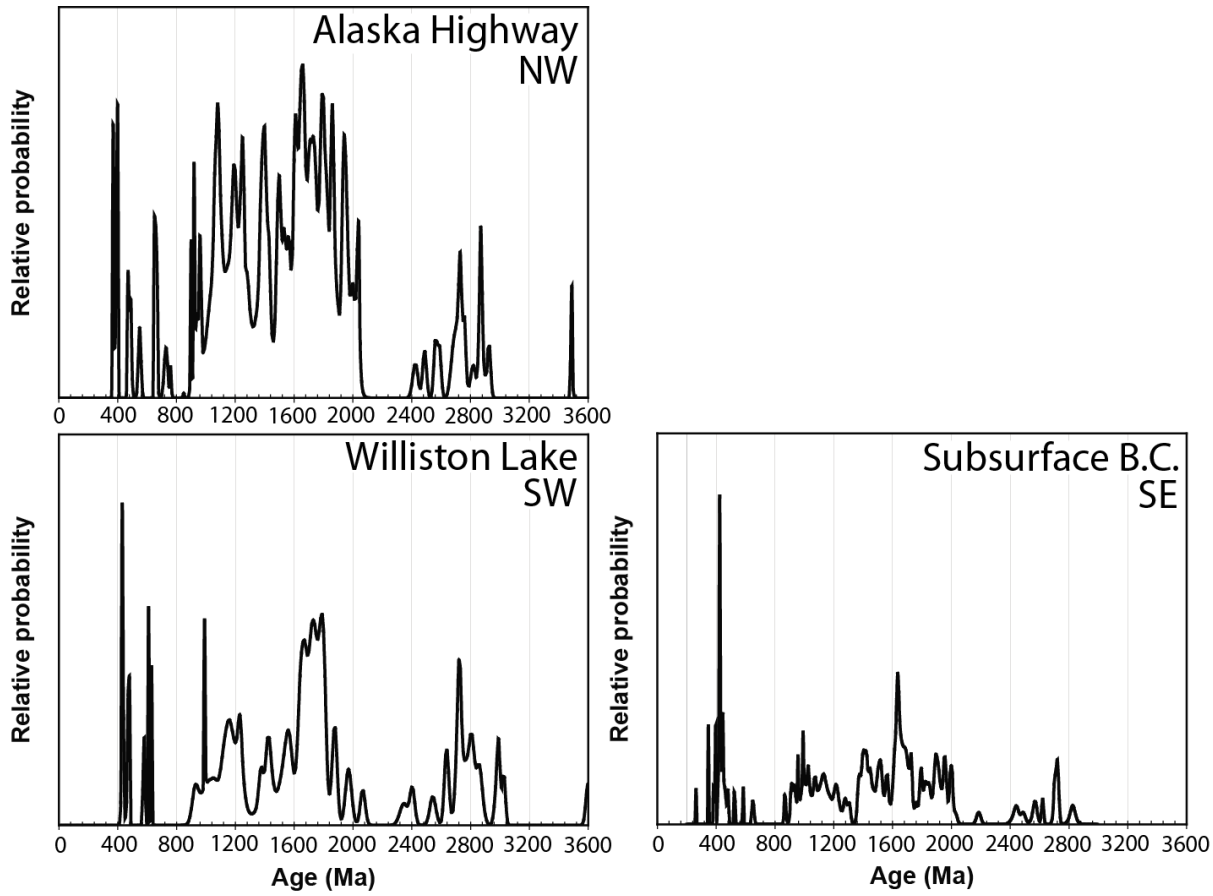



**Figure 5.10.** Relative probability density plots of all detrital zircon samples from the Anisian, grouped by geographic location.

### *Provenance of the Zircon Populations*

Beranek *et al.* (2010 b) presented an Arctic reference frame and a Northwest Laurentian reference frame compiled from detrital zircon studies of the Neoproterozoic to Triassic continental margin strata of these areas. The use of these reference frames makes it possible to determine whether the detrital zircon signatures that were observed in this study are compatible with derivation from sediment from North America.

The Arctic reference frame refers to Palaeozoic rocks in Alaska and Arctic Canada that contain zircons with ages ranging from 400 to 680 Ma. These ages are not found in the crystalline rocks of Laurentia, and therefore represent a unique fingerprint for the Arctic area. Beranek *et al.* (2010 b) suggest that zircons of this age were likely formed during early Palaeozoic Caledonian magmatism in eastern Laurentia and western Baltica and during Ediacaran magmatism in northern Baltica and the Arctic Alaska-Chukotka terrane (Stephens and Gee, 1985; Gehrels *et al.*, 1999; Amato *et al.*, 2009). They were then deposited in the foreland basin associated with the Innuitian Orogen during the mid-Palaeozoic, as allochthonous terranes collided with the northern margin of North America (Trettin *et al.*, 1991). This reference frame is based on the studies of McNicoll *et al.* (1995), Gehrels *et al.* (1999), Miller *et al.* (2006) and Amato *et al.* (2009).

The Northwest Laurentian reference frame refers to Neoproterozoic to Triassic rocks from the Canadian Cordilleran miogeocline (Boghossian *et al.*, 1996; Garzione *et al.*, 1997; Ross *et al.*, 1997; Gehrels and Ross, 1998). These have three distinctive signatures, with detrital zircon age ranges of 1800 – 2000 Ma, 1400 – 1600 Ma and 1000 – 1300 Ma. These zircons are interpreted to have been derived initially from the Precambrian basement of central and western Laurentia (Hoffman, 1989; Villeneuve *et al.*, 1993). The fact that detrital zircons in Cambrian sediments deposited on the passive margins of Laurentia (that could only be sourced from the craton) reflect the Laurentian Precambrian basement supports this interpretation (Hadlari *et al.*, 2012).

The relative probability density diagrams for the two reference frames are reproduced from Beranek *et al.* (2010 b) in figure 5.11.

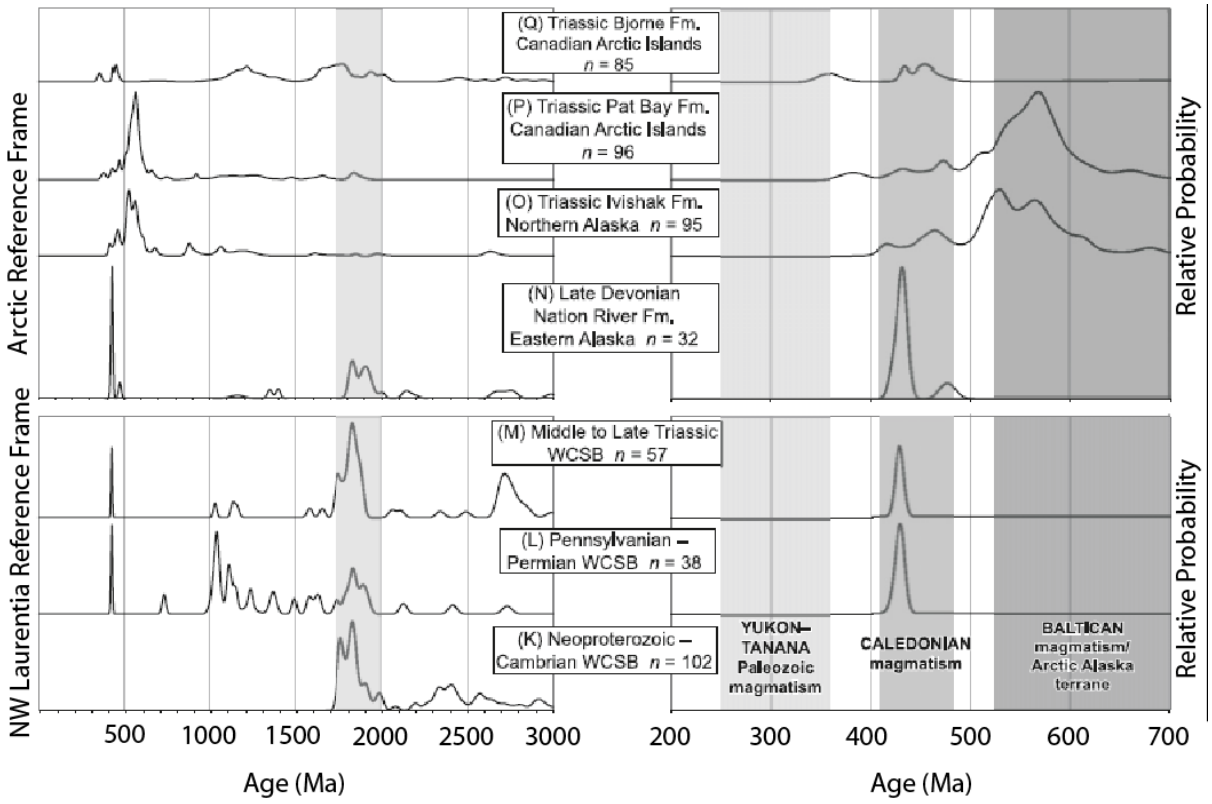



**Figure 5.11.** Relative probability density plots of the Arctic and NW Laurentia reference frames. Modified from Beranek *et al.* (2010 b).

By comparison with these diagrams, it is clear that the majority of the sediment deposited throughout the Triassic in the WCSB was sourced from northwestern Laurentia. Although these zircons yield the expected age ranges to have been initially derived from Precambrian provinces, it is likely that at least some of them have been re-worked from older formations in the Cordillera.

Zircons with ages compatible with the Arctic reference frame are also present. This supports the suggestion of Ross *et al.* (1997) that some of the sediment deposited in the WCSB during the Triassic was sourced from the Innuitian orogenic wedge.

There are, however, zircon ages that do not match with either of the two North American reference frames as recognised by Beranek *et al.* (2010 b). These are the Archean zircons, Proterozoic zircons with ages from 1800 – 1600 Ma and 1000 – 800 Ma, and zircons younger than 400 Ma.

Archean zircon is present in some of the samples described by Gehrels and Ross (1998), but not in the abundance that it is observed in the Triassic, either in samples from this study or in the samples described by Ross *et al.* (1997). It is possible that this represents direct sourcing from the Precambrian rocks that make up the North American craton. Archean rocks of suitable ages to provide sources for the Archean detrital zircons are present in abundance in the Slave, Rae and Hearn provinces of western Canada (Hoffman, 1989; Villeneuve *et al.*, 1993).

Zircons with ages of 1800 – 1600 Ma are present in samples described by Gehrels and Ross (1998) from Pennsylvanian-Permian rocks of the WCSB, but not from older rocks. This signature is also present in the Triassic samples of Beranek *et al.* (2010 b) from the continental margin in the Yukon. These zircons may have been re-worked from immediately underlying local sources during the Triassic, and some may represent deposition by longshore drift from the Yukon.

Zircon from 1000 – 800 Ma is present in Neoproterozoic to Carboniferous rocks of the Mackenzie Mountains (Leslie, 2009), and in Triassic rocks from the Arctic (Miller *et al.*, 2006). Leslie (2009) recovered zircon of this age from the Neoproterozoic Katherine and Little Dal groups, the Neoproterozoic Keele Formation, the Cambrian Sekwi Formation, the Ordovician Franklin Mountain Formation, and the Carboniferous Tsichu Group. In the Arctic, zircon of this age is present in the Lower Triassic Ivishak Formation of Alaska, the Middle Triassic Tolbon

Formation of Chukotka and the Upper Triassic Otuk Formation of Alaska (Miller *et al.*, 2006). Miller *et al.* (2006) suggest that these zircons were derived from the granitoids on the Taimyr peninsula in Siberia, which have been dated from 840 – 1004 Ma (Pease *et al.*, 2001; Pease and Vernikovsky, 2000; Vernikovsky *et al.*, 1988). Zircons in our samples may have been derived directly from these sources, or re-worked from older parts of the Triassic sequence in the Arctic.

There are only 16 grains of zircon younger than 400 Ma. Thirteen are Devonian, two are Mississippian and one is Permian. Magmatic rocks of these ages are rare in the Canadian Cordillera; however, some are present. The Lower and Middle Devonian grains have a possible source in the Middle Ordovician-Middle Devonian Marmot Formation of the Misty Creek Embayment near the Yukon-NWT border, which contains tuffs (Cecile *et al.*, 1982). The majority of Marmot Formation volcanism has been dated to the Ordovician (460-444 Ma; Leslie, 2009); however, it is thought to persist until the Middle Devonian (Cecile *et al.*, 1982; Leslie, 2009). The Upper Devonian grains may have been derived from the Earn Group in south central Yukon, which locally includes trachyte and rhyolite (Hunt, 2002). The Devonian grain dated at 368 Ma is relatively imprecise, but overlaps with the ages of the Exshaw Tuff (363 Ma; Richards *et al.*, 2002) in the Laurentian miogeocline in British Columbia, the Fyre Lake Succession (360-365 Ma) and Kudz Ze Kayah metavolcanic rocks (360 Ma; Piercey *et al.*, 2002), in the Yukon-Tanana terrane in the Yukon, and the Eagle Bay volcanics (360 Ma; Bailey *et al.*, 2001) in the Kootenay terrane in British Columbia. The single grain dated to 367 Ma has a much smaller error and could have been derived from either the Fyre Lake Succession or the Exshaw Tuff. Detrital zircons from the Late Devonian Imperial Formation and the Mississippian Tuttle Formation in the northern Yukon and the Northwest Territories have been dated at approximately 360 – 395 Ma (Beranek *et al.*, 2010 b; Lemieux *et al.*, 2011) and therefore these

formations may also represent a possible source for these grains, although they are much more distant from the location of our samples. These Devonian grains could also have been derived originally from intrusive rocks in the Arctic Alaska-Chukotka terrane (McClelland *et al.*, 2006; Lane, 2007; Amato *et al.*, 2009) and the Pearya terrane (Trettin *et al.*, 1987).

The Mississippian grain dated at 348 Ma is very close in age to tonalite of the Dorsey assemblage in northern British Columbia (349 Ma; Nelson *et al.*, 1998), whilst the grain at 346 Ma is possibly derived from metavolcanics and intrusives of the Wolverine Lake succession in the Yukon (345 Ma; Piercey *et al.*, 2002).

A single zircon is dated at 260 Ma. Permian felsic volcanics have been reported from the McGregor Subassemblage near McLeod Lake in central British Columbia (Struik, 1994), but these have not been dated. Ferri and Friedman (2002) reported an age of 281 Ma from Permian intrusions in the Snowshoe Group of the Kootenay Terrane, but this is not close in age to the 260 Ma zircon and the intrusions are gabbro, and thus unlikely to be a source of zircon. The only likely sources for this zircon are igneous and metamorphic rocks of the Yukon-Tanana terrane, to the west of the miogeocline. The Sulphur Creek orthogneiss in the Dawson area was initially dated at 262 Ma by Mortensen (1990) and subsequently revised by Beranek and Mortensen (2011) to approximately 260 Ma. The comagmatic Klondike Schist has yielded age estimates from 263 – 253 Ma (Mortensen, 1990, 1992; Villeneuve *et al.*, 2003; Nelson *et al.*, 2006). Metaporphyry and metatuff bodies in the Nasina Assemblage in Yukon and eastern Alaska are dated at 267 Ma – 253 Ma (Mortensen, 1992; Dusel-Bacon *et al.*, 2006), whilst a sill that intrudes this assemblage in the Yukon has been dated at 259 Ma (Beranek and Mortensen, 2011). In the Campbell Range belt, felsic rocks have been dated at 260 – 259 Ma (Murphy *et al.*, 2006).

All of these sources are likely to be related to the same period of magmatism and all could represent possible sources for the Permian zircon in our samples.

### *Explaining the Trends in the Triassic Detrital Zircon Signatures*

The vast majority of the detrital zircon recovered in this study are consistent with derivation from the North American margin. This source area remains a significant contributor to the detrital zircon signature throughout the Triassic. Detrital zircon derived from the Arctic is also consistently deposited throughout the Triassic, meaning that for the entire period, sediment was being shed into the Western Canada Sedimentary Basin from two directions. This was previously suggested by Ross *et al.* (1997), but this has not been widely acknowledged in regional discussions of Triassic deposition in the basin.

The main change in sedimentation patterns appears to occur during the Rhaetian stage, when there is a proportional increase in the amount of zircon derived from the Arctic reference frame relative to the zircon derived from the Northwest Laurentian reference frame. This change may reflect a shift in sediment transport pathways, with the pathway from the north becoming relatively more open and the pathway from the east becoming relatively closed. Alternatively it may reflect the exposure of new sources of younger sediment after erosion of overlying units during the earlier parts of the Triassic. However, the sediments deposited during the Rhaetian are relatively condensed compared to sediments deposited during the rest of the Upper Triassic. For example, on Williston Lake, the Rhaetian is 20 m thick at Ne-Parle-Pas Point, 15 m thick at Pardonet Creek and less than 5 m thick at Black Bear Ridge. This may have allowed the preservation of more of the Arctic signal compared with the rest of the relatively expanded

Triassic, where the signal may have been swamped by the sediment being shed from western Laurentia.

Beranek and Mortensen (2011) presented evidence for the accretion of the Yukon-Tanana terrane against the margin of North America during latest Permian time. They termed this event the Klondike Orogeny, and constrained the age of this orogeny in the Yukon by the age of a post-tectonic intrusion. Detrital zircon studies by the same authors show the earliest occurrence of zircons derived from the Yukon-Tanana terrane in the Olenekian (late Early Triassic) strata of the North American margin. This implies that a foreland basin to the Klondike Orogeny had initiated by the Olenekian and persisted until the Carnian (Beranek and Mortensen, 2011). Post-Carnian Triassic strata in the eastern Yukon reflected a renewed input of detrital zircon from the Laurentian margin to the east.

The single Permian zircon grain found in the present study is likely to have been derived from the Yukon-Tanana terrane or from uplifted pericratonic and western-most miogeoclinal rocks of North America, and this supports the model of terrane accretion and orogeny along the western margin of North America during the Permian-Triassic as advocated by Beranek and Mortensen (2011). The Permian grain comes from the Middle Anisian, consistent with, but not in direct support of, the hypothesis of foreland basin deposition beginning during the Olenekian. It is plausible that zircons from the Yukon-Tanana terrane would appear later in the marginal sediments of British Columbia than those of the Yukon, as it would take time for these grains to be transported south from the site of collision. Beranek (2009) and Beranek and Mortensen (2011) suggested that the widespread similarity of Late Triassic detrital zircon signatures across the North American margin, the Slide Mountain Terrane and the Yukon-Tanana Terrane was due

to the presence of a Late Triassic overlap assemblage. No evidence for such an assemblage has yet been identified in British Columbia.

No other Permian zircon has been recovered from the Triassic of the Western Canada Sedimentary Basin, in this study or in any previous work (see below). There are a number of possible explanations for this relative lack of Yukon-Tanana derived zircon in sediments of the foreland basin. Ferri and Zonneveld (2008) suggested that erosion during the Jurassic-Cretaceous Laramide Orogeny preferentially removed the more westerly Triassic rocks that would have been most likely to contain such zircons. If the area of uplift in the west related to the Klondike Orogeny was separated from the miogeoclinal wedge of the WCSB by sufficient distance, sediment from the west would form a separate, eastward tapering wedge that would only interfinger with the most distal parts of the westward tapering wedge of the WCSB, if at all. The overlap between the two wedges, if it existed, likely occurred in the region of the western Rocky Mountains where all Triassic sediment has been eroded.

Beranek and Mortensen (2011) suggested that these strata have been structurally buried by Jurassic and Cretaceous thrust faulting. It may also be that the topographic relief of the hinterland block during and following the Klondike Orogeny was not that high, and it may therefore have represented a relatively local source of sediment for the basin that did not contribute significant amounts of sediment to the basin farther to the south (Beranek and Mortensen, 2011). A final explanation may be that the rate of deposition of sediment sourced from the North American continent during the Triassic was so high that it has swamped the signal from the Yukon-Tanana terrane. The single Permian grain recovered was collected from the Doig Phosphate Zone (Edwards *et al.,* 1994), which is a condensed section. The Late Triassic

zircons from Black Bear Ridge were collected from a lag bed, again representing condensation. This condensation of the sections may be the reason that a rare, but still significant, number of young zircons were recovered from these sections, whilst they appear to be absent in other, more expanded sections. If detrital zircon studies are to continue in the Triassic of the Western Canada Sedimentary Basin in the future, it may be best to focus on similar condensed sections.

The similarity between detrital zircon signatures from the Alaska Highway, Williston Lake and subsurface B.C. during the Anisian suggests that there was little geographic variation in provenance of sediment during this stage. The northernmost samples contain zircon in the 650 – 850 Ma range that is absent in southern samples. Zircons of this age are found in the Pennsylvanian-Permian rocks of the WCSB (Gehrels and Ross, 1998) so this may indicate more re-working of underlying formations in the north of the study area than in the south. However, the similarity between samples from the north and south suggest that structural features such as the Peace River Embayment (Barclay *et al.*, 1990) had little effect on the distribution of sediment along the North American margin. The youngest zircon is found in the southeast of the study area, in samples from the subsurface. This supports the idea of widespread continuous sedimentation on the margin; the samples closest to the craton would be the least likely to contain zircon sourced from Yukon-Tanana, but its presence in these samples suggests that by the Anisian sedimentation from the west was widespread enough to leave a signature in even the most easterly of samples.

### *Comparison with Other Studies from British Columbia*

This study represents the first major detrital zircon study of Triassic rocks in British Columbia. However, data from isolated samples have been published previously.

Ross *et al*. (1997) presented data from two samples collected in British Columbia, one from the Liard Formation on the Alaska Highway (Middle Triassic) and one from the Whitehorse Formation west of Kananaskis, southwest of Calgary (Late Triassic). Both of these samples show similar signals to those from this study, with the majority of sediment interpreted to be derived from the North American craton and marginal sediments, with a smaller input from the Innuitian orogenic wedge (Ross *et al.*, 1997). In comparison to the samples from this study, the Archean age population is missing, as are grains younger than 400 Ma.

Ferri (2009) reported data from a single sample collected from the base of the Liard Formation (Ladinian) at Clearwater Creek, north of Williston Lake. This sample has a more similar detrital zircon signature to those from the Middle Triassic of this study, showing a small number of Archean and Paleoproterozoic grains, a large proportion of Neoproterozoic grains and a number of late Neoproterozoic to early Palaeozoic grains. This sample also contained Devonian grains and a single Mississippian grain. The Devonian grains are dated as 395 Ma and 358 Ma. The 395 Ma grain is similar in age to plutons in the Brooks Range of the Yukon (390 Ma; Dillon *et al.*, 1987), or it may have been re-worked from the Imperial or Tuttle formations. The 358 Ma grain is very similar in age to the Quesnel Lake gneiss (357.2 Ma; Ferri *et al.*, 1999) and the Gilliland Tuff (357 Ma; Erdmer *et al.*, 2005). The Mississippian grain is dated as 347 Ma and may be derived from the either the Dorsey assemblage or the Wolverine Lake succession.

Ferri *et al.* (2010) presented data from a second sample collected from the base of the Liard Formation, in the South Halfway section located near to the Halfway River. This sample also shows three main populations of Archean, Proterozoic and early Paleozoic grains, similar to the samples of this study. One Devonian grain dated at 371 Ma and one Mississippian grain dated at 341 Ma were recovered. The Devonian grain is close in age to the Mount Sedgwick Pluton in the Yukon (370 Ma; Mortensen and Bell, 1991) and other plutons in its vicinity (367 – 375 Ma; Lane, 2007). It may also have been reworked from the Imperial or Tuttle formations. The Mississippian grain is very close in age to that of a metavolcanic schist from the Turnagain River area (339.7 Ma; Erdmer *et al.*, 2005).

## 5.6 CONCLUSIONS

- Detrital zircon studies of Triassic formations in northeastern B.C. support previous conclusions that the majority of sediment deposited at this time was derived from re-worked sediment on the North American continental margin and in the Arctic.
- Although patterns of deposition remained fairly constant throughout the Triassic, a relative increase in the proportion of sediment derived from the Arctic occurred during the Rhaetian.
- Devonian and Mississippian grains occur throughout the Triassic and signify direct derivation from local igneous bodies as well as from re-working of older sedimentary rocks.
- A single Permian grain was found in the Middle Anisian, indicating either derivation from igneous bodies on the Yukon-Tanana terrane or from distal parts of the North

American margin. This implies close proximity between the Yukon-Tanana terrane and the North American margin during the Triassic.

- Geographically widespread samples show similar detrital zircon signatures during the Anisian, suggesting that sedimentation was widespread and uniform along the margin of North America at this time.
- The detrital zircon evidence suggests that the Triassic sediments of the Western Canada Sedimentary Basin were deposited in a foreland basin, formed in response to the latest Permian Klondike Orogeny.

# CHAPTER 6

## Summary and Further Work

## 6.1 SUMMARY

This study has led to the recognition of more than thirty new conodont taxa from the Triassic of northeastern British Columbia. The recognition of these new morphotypes and species is the first step towards revision of the broadly defined species groups that have been identified in the Triassic thus far in North America. Their recognition also allows the construction of a preliminary biostratigraphic scheme for the Anisian of British Columbia based on the succession of conodont faunal assemblages. This informal scheme helps to improve the resolution of the exisiting conodont and ammonoid biostratigraphic schemes and also allows correlation between surface outcrop, where both ammonoids and conodonts are abundant, and the subsurface, where ammonoids are extremely rare. The biostratigraphic scheme has the potential to act as the basis for conodont scheme that allows correlation between British Columbia, the Canadian Arctic and Nevada, and therefore have regional utility.

The new informal conodont scheme, in combination with the existing one, has allowed the first dating of the Montney-Doig boundary in northeastern British Columbia. This has led to the realisation that the boundary between the two formations does not equate to the Spathian – Anisian boundary as previously thought, but is in fact diachronous. The conodont biostratigraphy has also allowed the degree of condensation in the basal Doig Formation to be calculated. The regional pattern of diachroneity and condensation around the Montney-Doig boundary is also different to what was expected. Rather than recording the west – east younging that would be expected from deposition during transgression, it appears instead that the oldest parts of the Doig Formation occur in the centre of the study area and become younger to the east, west and north. The degree of condensation in the lowest Doig Formation also increases in these directions. This

pattern is consistent with the Doig Formation being deposited in a basin, with palaeo-highs located to the north and west as well as to the east. Previously both the Montney and Doig formations were thought to have been deposited in a passive margin setting, facing the Panthalassa Ocean to the west.

The existence of high ground to the west of the Peace River Basin during the Triassic is consistent with the model of latest Permian orogenesis due to the accretion of the pericratonic Yukon-Tanana Terrane (the Klondike Orogeny). This model is also supported by sedimentary provenance studies using detrital zircon. This is the most extensive study carried out thus far on the provenance of Triassic rocks in British Columbia, and it supports previous hypotheses that suggest most of the sediment deposited in the Western Canada Sedimentary Basin during the Triassic was sourced from either the North American craton or from the Innuitian orogenic wedge in the Arctic. Zircons derived from rocks of the Yukon-Tanana Terrane have also been identified for the first time in the Triassic of British Columbia. This is consistent with the model of latest Permian accretion. The overall similarity of detrital zircon signatures across northeastern British Columbia (including the subsurface) and throughout the Triassic indicate that the sedimentation patterns were very conservative at this time. This is consistent with the hypothesis of a foreland basin associated with the Klondike Orogeny exisiting in British Columbia throughout the Triassic.

## 6.2 RECOMMENDATIONS FOR ADDITIONAL WORK

This project represents the initial stages of research in a number of areas and additional work in each of these areas is desirable.

In terms of conodont taxonomy and biostratigraphy, it will be necessary to continue the revision of Anisian Gondolellidae. Further taxonomic revision will lead to a better understanding of the species present and allow a more precise and accurate biostratigraphic zonation to be constructed. The faunal assemblages recognised at the moment may persist and be raised to the level of zones, or they may be further subdivided. The collection of additional material in British Columbia, Arctic Canada and Nevada will also help in the revision of Anisian Gondolellidae, as well as helping to refine correlation between these areas.

In order to more completely understand the formation and distribution of the Montney and Doig formations, the next step should be to extend the biostratigraphic part of this study into Alberta. The correlation of the Montney-Doig boundary between these two provinces is not well established, and conodont biostratigraphy will help to solve this problem. It will enable assessment of how the age of the boundary varies in the east, and whether this fits with the pattern of diachroneity observed in British Columbia. It is likely that deposition of the Montney and Doig formations is even more complex than suggested by this study.

At present, the number of detrital zircons sourced from the Yukon-Tanana Terrane is very small and they are restricted to sediment deposited during the Anisian. This study has, however, identified areas where other detrital zircons from this source may be recovered. The zircons are present in very low numbers and so the greatest likelihood of recovery is in conditions where the zircons have been concentrated. This includes lag beds and condensed sections. In expanded sections, there appears to have been too much sediment being shed from North America for the small number of zircons sourced from the west to be recovered.

This kind of detrital zircon study should be continued and expanded because of the low resolution of the present study. It is not clear at this time if accretion occurred at the same time in British Columbia as it did in the Yukon, or if orogenesis was more complex. It is clear that a foreland basin was established by the Middle Triassic in British Columbia, and therefore future studies should focus on earlier time periods to see if the timing of accretion and foreland basin initiation can be better constrained. The Klondike Orogeny has been dated as latest Permian in the Yukon; hence, a provenance study investigating Permian sediments in British Columbia would be useful. In the Yukon, an overlap asssemblage was identified in the Upper Triassic but this event has not been recognised in British Columbia. Additional studies focused on the Upper Triassic of British Columbia would therefore also be useful. This study concentrated on evidence from detrital zircons to determine sedimentary provenance. However there are other geochemical techniques, such as the study of Nd isotopes and whole rock geochemistry of sedimentary rocks, that can be used to corroborate the evidence from detrital zircons, to fill gaps in the record, and to further develop our understanding of what the source areas for Triassic sediment were. Studies of this nature would complement the existing detrital zircon record.

This study is interdisciplinary in nature, and this style of research shows promise for answering a number of geological questions. Biostratigraphy, sedimentology and sedimentary provenance are all interrelated and therefore they cannot be fully understood in isolation. The combination of techniques used in this study has allowed different lines of evidence to be reviewed and understood in terms of the Triassic tectonics of British Columbia, and this multi-themed approach helps to strengthen the support for its conclusions.

# REFERENCES

Adams, C., 2013. Summary of shale gas activity in northeast British Columbia 2012. B.C. Ministry of Energy and Mines, 1-27

Alberti, F. von, 1834. Beitrag zu einer Monographie des Bunten Sandsteins, Muschelkalks und Keupers, und die Verbindung dieser Gebilde zu einer Formation, Stuttgart und Tübingen, Verlag der J. G. Cotta'sschen Buchhandlung

Algeo, T., Henderson, C.M., Ellwood, B., Rowe, H., Elswick, E., Bates, S., Lyons, T., Hower, J.C., Smith, C., Maynard, B., Hays, L.E., Summons, R.E., Fulton, J. and Freeman, K.H., 2012. Evidence for a diachronous Late Permian marine crisis from the Canadian Arctic region. Geological Society of America Bulletin, **124**, 1424-1448

Amato, J.M., Toro, J., Miller, E.L., Gehrels, G.E., Farmer, G.L., Gottlieb, E.S. and Till, A.B., 2009. Late Proterozoic – Paleozoic evolution of the Arctic Alaska-Chukotka terrane based on U-Pb igneous and detrital zircon ages: implications for Neoproterozoic paleogeographic reconstructions. Geological Society of America Bulletin, **121**, 1219-1235

Anfinson, O.A., Leier, A.L., Embry, A.F. and Dewing, K., 2012. Detrital zircon geochronology and provenance of the Neoproterozoic to Late Devonian Franklinian Basin, Canadian Arctic Islands. Geological Society of America Bulletin, **124**, 415-430

Armitage, J.H., 1962. Triassic oil and gas occurrences in northeastern British Columbia, Canada. Journal of the Alberta Society of Petroleum Geologists, **10**, 35-56

Arnold, K.J., 1994. Origin and distribution of aeolian sandstones in the Triassic Charlie Lake Formation, northeastern British Columbia. Unpublished MSc. Thesis. University of Alberta. 320 p.

Arthaber, G. von, 1905. Die alpine Trias des Mediterran-Gebietes. *In,* Frech, F. (ed.), Lethaea Geognostica, pt. II, Das Mesozoicum. Trias. Schweizerbart'schen, Stuttgart, 223–391, 417–472

Asgar-Deen, M., Riediger, C. and Hall, R., 2004. The Gordondale Member: designation of a new member in the Fernie Formation to replace the informal "Nordegg Member" nomenclature of the subsurface of west-central Alberta. Bulletin of Canadian Petroleum Geology, **52**, 201-214

Assereto, R., 1974. Aegean and Bithynian: Proposal for two new Anisian substages. *In,* The Stratigraphy of the Alpine-Mediterranean Triassic, Zapfe, H. (ed.), Schriftenreihe der erdwissenschaftlichen Komission, Österreichische Akadamie der Wissenschaften, **2**, 23-39

Bailey, S.L., Paradis, S. and Johnston, S.T., 2001. New insights into metavolcanic successions and geochemistry of the Eagle Bay assemblage, south-central British Columbia. *In,* Current Research 2001-A8. Geological Survey of Canada Paper 2001-A8, 16 p.

Balini, M., Jenks, J.F., McRoberts, C.A. and Orchard, M.J., 2007. The Ladinian-Carnian boundary succession at South Canyon (New Pass Range, central Nevada). *In*, Triassic of the American West, Lucas, S.G. and Spielmann, J.A. (eds.), New Mexico Museum of Natural History and Science Bulletin, **40**, 127-138

Balini, M., Lucas, S.G., Jenks, J.F. and Spielmann, J.A., 2010. Triassic ammonoid biostratigraphy: an overview. Geological Society of London Special Publication, **334**, 221-262

Barclay, J.E. and Leckie, D.A., 1986. Tidal-inlet reservoirs in the Triassic Halfway Formation. *In,* Meijer Drees, N.C. *et al.* (eds.), Canadian Society of Petroleum Geologists Core Conference, 4.1-4.6

Barclay, J.E., Krause, F.F., Campbell, R.I. and Utting, J., 1990. Dynamic casting of the Dawson Creek Graben Complex: Carboniferous-Permian Peace River Embayment, Western Canada. *In,* Geology of the Peace River Arch, O'Connell, S.C. and Bell, J.S. (eds.), Bulletin of Canadian Petroleum Geology, **38A**, 115-145

Barss, D.L., Best, E.W. and Meyers, N., 1964. Chapter 9: Triassic. *In,* Geological History of Western Canada, McCrossan, R.G. and Glaister, R.P. (eds.), Alberta Society of Petroleum Geologists, Calgary, 113-136

Barras, C.G. and Twitchett, R.J., 2007. Response of the marine infauna to Triassic-Jurassic environmental change: ichnological data from southern England. Palaeogeography, Palaeoclimatology, Palaeoecology, **244**, 223-241

Basu, A.R.M., Petaev, M.I., Poreda, R.J., Jacobsen, S.B. and Becker, L., 2003. Chondritic meteorite fragments associated with the Permian-Triassic boundary in Antarctica. Science, **302**, 1388-1392

Beauchamp, B. and Baud, A., 2002. Growth and demise of Permian biogenic chert along northwest Pangaea: evidence for end-Permian collapse of thermohaline circulation. Palaeogeography, Palaeoclimatology, Palaeoecology, **184**, 37-63

Beatty, T.W., Zonneveld, J.P. and Henderson, C.M., 2008. Anomalously diverse Early Triassic ichnofossil assemblages in northwestern Pangaea: a case for a shallow-marine habitable zone. Geology, **36**, 771-774

Becker, L., Poreda, R.J., Hunt, A.G., Bunch, T.E. and Rampino, M., 2001. Impact event at the Permian-Triassic boundary: evidence from extraterrestrial Noble Gases in fullerenes. Science, **291**, 1530-1533

Becker, L., Poreda, R.J., Basu, A.R., Pope, K.O., Harrison, T.M., Nicholson, C. and Iasky, R., 2004. Bedout: a possible end-Permian impact crater offshore of northwestern Australia. Science, **304**, 1469-1474

Bender, H., 1970. Zur Gliederung der Mediterranen Trias II. Die Conodontenchronologie der Mediterranen Trias. Annales Geologiques des Pays Helleniques, **19**, 465-540

Bender, H. and Stoppel, D., 1965. Perm-Conodonten. Geologisches Jahrbuch, **82**, 331-364

Benton, M.J., 1994. Late Triassic to Middle Jurassic extinctions among continental tetrapods: testing the pattern. *In,* In the Shadow of the Dinosaurs, Fraser, N.C., Sues, H.-D. (eds.), Cambridge University Press, 366– 397

Benton, M.J., Tverdokhlebov, V.P. and Surkov, M.V., 2004. Ecosystem remodelling amongst vertebrates at the Permian-Triassic boundary in Russia. Nature, **432**, 97-100

Beranek, L.P., 2009. Provenance and paleotectonic setting of North American Triassic strata in Yukon: the sedimentary record of pericratonic terrane accretion in the northern Canadian Cordillera. Unpublished PhD Thesis. University of British Columbia. 338 p.

Beranek, L.P. and Mortensen, J.K., 2011. The timing and provenance record of the Late Permian Klondike orogeny in northwestern Canada and arc-continent collision along western North America. Tectonics, **30**, 1-23

Beranek, L.P., Mortensen, J.K., Orchard, M.J. and Ullrich, T., 2010 a. Provenance of North American Triassic strata from west-central and southeastern Yukon: Correlations with coeval strata in the Western Canada Sedimentary Basin and Canadian Arctic Islands. Canadian Journal of Earth Sciences, **47**, 53-73

Beranek, L.P., Mortensen, J.K., Lane, L.S., Allen, T., Fraser, T., Hadlari, T. and Zantvoort, W., 2010 b. Detrital zircon geochronology of the western Ellesmerian clastic wedge, northwestern Canada: Insights on Arctic tectonics and the mid-Paleozoic evolution of the northern Cordilleran miogeocline. Geological Society of America Bulletin, **122**, 1899-1911

Berger, Z., Boast, M. and Mushayandebvu, M., 2008. The contribution of integrated HRAM studies to exploration and exploitation of unconventional plays in North America, part 1. Canadian Society of Petroleum Geologists Reservoir, **35**, 10, 42-47

Berger, Z., Boast, M. and Mushayandebvu, M., 2009. The contribution of integrated HRAM studies to exploration and exploitation of unconventional plays in North America, part 2. Canadian Society of Petroleum Geologists Reservoir, **36**, 2, 40-45

Berner, R.A., 2002. Examination of hypotheses for the Permian-Triassic boundary extinction by carbon cycle modelling. Proceedings of the National Academy of Sciences of the United States of America, **99**, 4172-4177

Bittner, A., 1892. Was ist norisch? Jahrbuch Geologischen Reichsanstalt, **42**, 387-396

Blackburn, T.J., Olsen, P.E., Bowring, S.A., McLean, N.M., Kent, D.V., Puffer, J., McHone, G., Rasbury, E.T. and Et-Touhami, M., 2013. Zircon U-Pb geochronology links the end-Triassic mass extinction with the Central Atlantic Magmatic Province. Science, **340**, 941-945

Boghossian, N.D., Patchett, P.J., Ross, G.M. and Gehrels, G.E., 1996. Nd isotopes and the source of sediments in the miogeocline of the Canadian Cordillera. The Journal of Geology, **104**, 259-277

Brandner, R., 1984. Meeresspiegelschwankungen und Tektonik in der Trias der NW-Tethys. Jahrbuch der Geologischen Bundesanstalt, **126**, 435-475

Brayard, A., Escarguel, G., Bucher, H., Monnet, C., Brühwiler, T., Goudemand, N., Galfetti, T. and Guex, J., 2009. Good genes and good luck: ammonoid diversity and the end-Permian mass extinction. Science, **325**, 1118-1121

Brayard, A., Nützel, A., Stephen, D.A., Bylund, K.G., Jenks, J. and Bucher, H., 2010. Gastropod evidence against the Early Triassic Lilliput effect. Geology, **38**, 147-150

Brayard, A., Vennin, E., Olivier, N., Bylund, K.G., Jenks, J., Stephen, D.A., Bucher, H., Hofmann, R., Goudemand, N. and Escarguel, G., 2011. Transient metazoan reefs in the aftermath of the end-Permian mass extinction. Nature Geoscience, **4**, 693-697

Bucher, H., 1988. A new Middle Anisian (Middle Triassic) ammonoid zone from northwestern Nevada (USA). Eclogae Geologicae Helvetiae, **81**, 723-762

Bucher, H., 1989. Lower Anisian ammonoids from the northern Humboldt Range (northwestern Nevada, USA) and their bearing upon the Lower-Middle Triassic boundary. Eclogae Geologicae Helvetiae, **82**, 945-1002

Bucher, H., 1992 a. Ammonoids of the Hyatti Zone and the Anisian transgression in the Star Peak Group, northwestern Nevada, USA. Palaeontographica Abteilung A, **223**, 137-166

Bucher, H., 1992 b. Ammonoids of the Shoshonensis Zone (Middle Anisian, Middle Triassic) from northwestern Nevada (USA). Jahrbuch der Geologischen Bundesanstalt Wien, **135**, 425-465

Bucher, H., 1994. New ammonoids from the Taylori Zone (Middle Anisian, Middle Triassic) from northwestern Nevada (USA). Mémoires de Géologie (Lausanne), **22**, 1-8

Bucher, H., 2002. Early Anisian (Middle Triassic) ammonoid biostratigraphy of northeastern British Columbia. Eclogae Geologicae Helvetiae, **95**, 277-287

Bucher, H. and Orchard, M.J., 1995. Intercalibrated ammonoid and conodont succession, Upper Anisian-Lower Ladinian of Nevada. Albertiana, **15**, 66-71

Budurov, K. and Stefanov, S.A., 1972. Plattform-Conodonten und ihre Zonen in der Mittleren Trias Bulgariens. Mitteilungen der Gesellschaft der Geologie- und Bergbaustudenten, Österreich, **21**, 829-852

Budurov, K. and Stefanov, S.A., 1973. Etliche neue Plattform-Conodonten aus der Mitteltrias Bulgariens. Comptes rendus de l'Academie bulgare des Sciences, **26**, 803-806

Budurov, K. and Stefanov, S.A., 1975. Neue Daten über die Conodontenchronologie der Balkaniden Mittleren Trias. Comptes rendus de l'Academie bulgare des Sciences, **28**, 791-794

Budurov, K. and Stefanov, S.A., 1984. *Neogondolella tardocornuta* sp. n. (Conodonta) from the Ladinian in Bulgaria. Comptes rendus de l'Academie bulgare des Sciences, **37**, 605-607

Budurov, K. and Sudar, M.N., 1989. New Conodont Taxa from the Middle Triassic. Geology of Himalayas – Palaeontology, Stratigraphy and Structure Contributions to Himalayan Geology, **4**, 250-254

Burgess, S.D. and Bowring, S.A., 2010. Evaluating a link between eruption of the Siberian Traps and the End-Permian Mass Extinction with high-precsion geochronology. EGU General Assembly 2010, 11490

Cant, D.J., 1986. Hydrocarbon trapping in the Halfway Formation (Triassic), Wembley Field, Alberta. Bulletin of Canadian Petroleum Geology, **34**, 329-338

Cant, D.J., 1988. Regional structure and development of the Peace River Arch, Alberta: a Paleozoic failed-rift system. Bulletin of Canadian Petroleum Geology, **36**, 284-295

Cant, D.J., 1989. Lower Zuni Sequence: Middle Jurassic to Middle Cretaceous. *In*, Western Canada Sedimentary Basin – a Case History, Ricketts, B.D. (ed.), Canadian Society of Petroleum Geologists, Special Publication, **30**, 251-268

Caplan, M.L., 1992. Sedimentology, stratigraphy and petrography of the Middle Triassic Halfway Formation, Peejay Field, northeastern British Columbia. Unpublished M.Sc. Thesis. University of Alberta. 312p.

Caplan, M.L. and Moslow, T.F., 1997. Tectonic controls on preservation of Middle Triassic Halfway reservoir facies, Peejay Field, northeastern British Columbia: a new petroleum exploration model. *In*, Triassic of the Western Canada Sedimentary Basin, Moslow, T.F. and Wittenberg, J. (eds.), Bulletin of Canadian Petroleum Geology, **45**, 595-613

Caplan, M.L. and Moslow, T.F., 1999. Depositional origin and facies variability of a Middle Triassic barrier island complex, Peejay Field, northeastern British Columbia. American Association of Petroleum Geologists Bulletin, **83**, 128-153

Carter, E.S., 1991. Late Triassic radiolarian biostratigraphy of the Kunga Group, Queen Charlotte Islands, British Columbia. *In,* Evolution and hydrocarbon potential of the Queen Charlotte Basin, Woodsworth, G.J. (ed.), Geological Survey of Canada Paper 90-10, 195-201

Carter, E.S. and Orchard, M.J., 2000. Intercalibrated conodont-radiolarian biostratigraphy and potential datums for the Carnian-Norian boundary within the Upper Triassic Peril Formation, Queen Charlotte Islands, British Columbia. Geological Survey of Canada Current Research 2000-A7

Carter, E.S. and Orchard, M.J., 2013. Intercalibration of conodont and radiolarian faunas from the Carnian-Norian boundary interval in Haida Gwaii, British Columbia, Canada. *In,* The Triassic System, Tanner, L.H., Spielmann, J.A. and Lucas, S.G. (eds.), New Mexico Museum of Natural History and Science Bulletin, **61**, 67-92

Carter, E.S., Orchard, M.J. and Tozer, E.T., 1989. Integrated ammonoid-conodont-radiolarian biostratigraphy, Late Triassic Kunga Group, Queen Charlotte Islands, British Columbia. Geological Survey of Canada Paper 89-1H, 23-30

Catuneanu, O., Galloway, W.E., Kendall, C.G.St.C, Miall, A.D., Posamentier, H.W., Strasser, A. and Tucker, M.E., 2011. Sequence stratigraphy: methodology and nomenclature. Newsletters on Stratigraphy, **44**, 173-245

Cecile, M., Fritz, W.H., Norford, B.S. and Tipnis, R.S., 1982. The lower Paleozoic Misty Creek Embayment, Selwyn Basin, Yukon and Northwest Territories. Geological Survey of Canada Bulletin 335

Clapham, M.E. and Bottjer, D.J., 2007. Permian marine paleoecology and its implications for large-scale decoupling of brachiopod and bivalve abundance and diversity during the Lopingian (Late Permian). Palaeogeography, Palaeoclimatology, Palaeoecology, **249**, 283-301

Clapham, M.E., Shen, S. and Bottjer, D.J., 2009. The double mass extinction revisited: reassessing the severity, selectivity, and causes of the end-Guadalupian biotic crisis (Late Permian). Paleobiology, **35**, 32-50

Clark, L.M., 1957. Fort St. John sets pace for Peace River gas fields. Oil and Gas Journal, **55**, 132-134

Clark, D.L., 1959. Conodonts from the Triassic of Nevada and Utah. Journal of Paleontology, **33**, 305-312

Clark, D.L., 1983. Extinction of conodonts. Journal of Paleontology, **57**, 652-661

Colpron, M., Logan, J. and Mortensen, J.K., 2002. U-Pb age constraint for late Neoproterozoic rifting and initiation of the lower Paleozoic passive margin of western Laurentia. Canadian Journal of Earth Science, **39**, 133-143

Colpron, M., Nelson, J.L. and Murphy, D.C., 2006. A tectonostratigraphic framework for the pericratonic terranes of the northern Canadian Cordillera. *In,* Paleozoic Evolution and Metallogeny of Pericratonic Terranes at the Ancient Pacific Margin of North America, Canadian and Alaskan Cordillera, Colpron, M. and Nelson, J.L. (eds.), Geological Association of Canada Special Paper, **45**, 323-360

Colquhoun, D.J., 1960. Triassic stratigraphy of western central Canada. Unpublished PhD Thesis. University of Illinois.

Colquhoun, D.J., 1962. Triassic stratigraphy in the vicinity of Peace River Foothills, British Columbia. Edmonton Geological Society 4th Field Trip Guidebook, 57-88

Coney, P.J., Jones, D.L. and Monger, J.W.H., 1980. Cordilleran suspect terranes. Nature, **288**, 329-333

Courtillot, V.E. and Renne, P.R., 2003. On the ages of flood basalt events. Comptes Rendus Geoscience, **335**, 113-140

Črne, A.E., Weissert, H., Goričan, S. and Bernasconi, S., 2011. A biocalcification crisis at the Triassic-Jurassic boundary recorded in the Budva Basin (Dinarides, Montenegro). Geological Society of America Bulletin, **123**, 40-50

Cuny, G., 1995. French vertebrate faunas and the Triassic-Jurassic boundary. Palaeogeography, Palaeoclimatology, Palaeoecology, **119**, 343-358

Dagys, A.A., 1984. Early Triassic conodonts of northern Middle Siberia (in Russian). Transactions of the Institute of Geology and Geophysics, Academy of Sciences USSR, Siberian Branch, **554**, 1-69

Davies, G.R., 1997 a. The Triassic of the Western Canada Sedimentary Basin: tectonic and stratigraphic framework, paleogeography, paleoclimate and biota. *In*, Triassic of the Western Canada Sedimentary Basin, Moslow, T.F. and Wittenberg, J. (eds.), Bulletin of Canadian Petroleum Geology, **45**, 434-460

Davies, G.R., 1997 b. Aeolian sedimentation and bypass, Triassic of western Canada. *In*, Triassic of the Western Canada Sedimentary Basin, Moslow, T.F. and Wittenberg, J. (eds.), Bulletin of Canadian Petroleum Geology, **45**, 624-642

Davies, G.R. and Hume, D., 2011. "Upper" Montney – "Lower" Doig: quo vadis? Recovery – Candian Society of Petroleum Geologists Joint Annual Convention, Calgary

Davies, G.R. and Majid, H., 1993. "Grassy High", northeastern British Columbia: a structural high with eroded Upper Triassic section coincident with optimum Mississippian hydrothermal dolomite reservoir development. Canadian Society of Petroleum Geologists, Pangaea Conference, Program and Abstracts, 70

Davies, G.R., Moslow, T.F. and Sherwin, M.D., 1997. The Lower Triassic Montney Formation, west-central Alberta. *In*, Triassic of the Western Canada Sedimentary Basin, Moslow, T.F. and Wittenberg, J. (eds.), Bulletin of Canadian Petroleum Geology, **45**, 474-505

Dawson, G.M., 1881. Report on an exploration from Port Simpson on the Pacific coast to Edmonton on the Saskatchewan, embracing a portion of the northern part of British Columbia and the Peace River country. Geological and Natural History Survey of Canada, Report of Progress 1879-80, part B, 1-177

Dillon, J.T., Tilton, G.R., Decker, J. and Kelly, M.J., 1987. Resource implications of magmatic and metamorphic ages for Devonian igneous rocks in the Brooks Range. *In*, Alaskan North Slope Geology, Tailleur, I. And Weimer, P. (eds.), Society of Economic Paleontologists and Mineralogists (Pacific Section), **2**, 713-722

Dixon, J., 2000. Regional lithostratigraphic units in the Triassic Montney Formation of western Canada. Bulletin of Canadian Petroleum Geology, **48**, 80-83

Dixon, J., 2011. A review of the character and interpreted origins of thick, mudstone-encased sandstone bodies in the Middle Triassic Doig Formation of western Canada. Bulletin of Canadian Petroleum Geology, **59**, 261-276

Dodson, M.H., Compston, W., Ireland, I.S. and Wilson, J.F., 1988. A search for ancient detrital zircons in Zimbabwean sediments. Journal of the Geological Society of London, **145**, 977-983

Donoghue, P.C.J., Purnell, M.A., Aldridge, R.J. and Zhang, S., 2008. The interrelationships of "complex" conodonts (Vertebrata). Journal of Systematic Palaeontology, **6**, 119-153

Dusel-Bacon, C., Hopkins, M.J., Mortensen, J.K., Dashevsky, S.S., Bressler, J.R. and Day, W.C., 2006. Paleozoic tectonic and metallogenic evolution of the pericratonic rocks of east-central Alaska and adjacent Yukon. *In,* Paleozoic Evolution and Metallogeny of Pericratonic Terranes at the Ancient Pacific Margin of North America, Canadian and Alaskan Cordillera, Colpron, M. and Nelson, J.L. (eds.), Geological Association of Canada Special Paper, **45**, 25-74

Dzik, J., 1976. Remarks on the evolution of Ordovician conodonts. Acta Palaeontologica Polonica, **21**, 395-455

Dzik, J., 1991. Evolution of the oral apparatuses in the conodont chordates. Acta Palaeontologica Polonica, **36**, 265-323

Edwards, D.E., Barclay, J.E., Gibson, D.W., Kvill, G.E. and Halton, E., 1994. Triassic strata of the Western Canada Sedimentary Basin. *In,* Geological Atlas of the Western Canada Sedimentary Basin, Mossop, G.D and Shetsen, I. (eds.), Canadian Society of Petroleum Geologists and Alberta Research Council, Calgary, 259-275

Embry, A.F., 1993. Transgressive-regressive (T-R) sequence analysis of the Jurassic succession of the Sverdrup Basin, Canadian Arcitc Archipelago. Canadian Journal of Earth Science, **30**, 301-320

Embry, A.F., 1997. Global sequence boundaries of the Triassic and their identification in the Western Canada Sedimentary Basin. *In,* Triassic of the Western Canada Sedimentary Basin, Moslow, T.F. and Wittenberg, J. (eds.), Bulletin of Canadian Petroleum Geology, **45**, 415-433

Embry, A.F. and Johannessen, E.P., 1992. T-R sequence stratigraphy, facies analysis and reservoir distribution in the uppermost Triassic-Lower Jurassic succession, western Sverdrup Basin, Arctic Canada. *In,* Arctic Geology and Petroleum Potential, Vorren, T.O., Bergsager, E., Dahl-Stamnes, O.A., Holter, E., Johansen, B., Lie, E. and Lund, T.B. (eds.), Norwegian Petroleum Society Special Publication, **2**, 121-146

Erdmer, P., Mihalynuk, M.G., Gabrielse, H., Heaman, L. and Creaser, R.A., 2005. Mississippian volcanic assemblage conformably overlying Cordilleran miogeoclinal strata, Turnagain River area, northern British Columbia, is not part of an accreted terrane. Canadian Journal of Earth Sciences, **42**, 1449-1465

Erwin, D.H., 1993. The Great Paleozoic Crisis: Life and Death in the Permian. Columbia University Press.

Erwin, D.H., 2006. Extinction: How Life on Earth Nearly Ended 250 Million Years Ago. Princeton University Press.

Evoy, R.W., 1997. Lowstand shorefaces in the Middle Triassic Doig Formation, Buick Creek Field, northeastern British Columbia. Bulletin of Canadian Petroleum Geology, **45**, 537-552

Evoy, R.W., 1998. Reservoir sedimentology of the Doig Formation, Buick Creek Field, northeastern British Columbia. Canadian Society of Petroleum Geologists Annual Conference on Oil and Gas Pools of the Western Canada Sedimentary Basin, Calgary, 1996, S-51, 127-135

Evoy, R.W. and Moslow, T.F., 1995. Lithofacies associations and depositional environments in the Middle Triassic Doig Formation, Buick Creek Field, northeastern British Columbia. Bulletin of Canadian Petroleum Geology, **43**, 461-475

Faure, K., de Witt, M.J. and Willis, J.P., 1995. Late Permian global coal hiatus linked to $^{13}C$-depleted $CO_2$ flux into the atmosphere during the final consolidation of Pangaea. Geology, **23**, 507-510

Ferri, F., 1997. Nina Creek Group and Lay Range Assemblage, north-central British Columbia: remnants of late Paleozoic oceanic and arc terranes. Canadian Journal of Earth Science, **34**, 854-874

Ferri, F., 2009. Geology of the Jones Peak Area (NTS94B/02 and 07), Halfway River map sheet (94B). *In,* Geoscience Reports 2009, B.C. Ministry of Energy, Mines and Petroleum Resources, 5-23

Ferri, F. and Melville, D.M., 1994. Bedrock geology of the Germansen Landing – Manson Creek area, British Columbia (93 N/9, 10, 15; 94 C/2). British Columbia Ministry of Energy, Mines and Petroleum Resources, Bulletin 91

Ferri, F. and Zonneveld, J.-P., 2008. Were Triassic rocks of the Western Canada Sedimentary Basin deposited in a Foreland? Canadian Society of Petroleum Geologists Reservoir, **35**, 10, 12-14

Ferri, F., Rees, C., Nelson, J.L. and Legun, A., 1999. Geology and mineral deposits of the northern Kechika Trough between Gataga River and the 60$^{th}$ parallel. British Columbia Ministry of Energy and Mines, Geological Survey Branch, Bulletin **107**

Ferri, F., Golding, M.L., Mortensen, J.K., Zonneveld, J.P. and Orchard, M.J., 2010. Toad Formation (Montney and Doig equivalent) in northwestern Halfway River map area, British Columbia (NTS 094B/14). *In,* Geoscience Reports 2010, B.C. Ministry of Energy, 21-34

Flügel, E., 2002. Triassic reef patterns. *In,* Phanerozoic Reef Patterns, Kiessling, W., Flügel, E. and Golonka, J. (eds.), SEPM Special Publication, **72**, 391-462

Föllmi, K.B., 1996. The phosphorous cycle, phosphogenesis and marine phosphate-rich deposits. Earth Science Reviews, **40**, 55-124

Fraiser, M.L. and Bottjer, D.J., 2004. The non-actualistic Early Triassic gastropod fauna: a case study of the Lower Triassic Sinbad Limestone Member. Palaios, **19**, 259-275

Frey, R.W. and Pemberton, S.G., 1985. Biogenic Structures in Outcrops and Cores. I. Approaches to Ichnology. Bulletin of Canadian Petroleum Geology, **33**, 72-115

Furin, S., Preto, N., Rigo, M., Roghi, G., Gianolla, P., Crowley, J. and Bowring, S.A., 2006. A high-precision U/Pb zircon age from the Triassic of Italy — implications for the Carnian rise of calcareous nannoplankton and dinosaurs. Geology, **34**, 1009–1012

Gabb, W.M., 1864. Descriptions of the Triassic fossils of California and the adjacent territories. Geological Survey of California, Paleontology, 1, 19-35

Gabrielse, H., Murphy, D.C. and Mortensen, J.K., 2006. Cretaceous and Cenozoic dextral orogen-parallel displacements, magmatism and paleogeography, north-central Canadian Cordillera. *In,* Paleogeography of the North American Cordillera: evidence for and against large-scale displacements, Haggart, J.W., Monger, J.W.H. and Enkin, R.J. (eds.), Geological Association of Canada Special Paper 46, 255-276

Galfetti, T., Bucher, H., Ovtcharova, M., Schaltegger, U., Brayard, A., Brühwiler, T., Goudemand, N., Weissert, H., Hochuli, P.A., Cordey, F. and Guodun, K.A., 2007. Timing of the Early Triassic carbon cycle perturbations inferred from new U-Pb ages and ammonoid biochronozones. Earth and Planetary Science Letters, **258**, 593-604

Galli, M.T., Jadoul, F., Bernasconi, S.M. and Weissert, H., 2005. Anomalies in global carbon cycling and extinction at the Triassic/Jurassic boundary: evidence from a marine C-isotope record. Palaeogeography, Palaeoclimatology, Palaeoecology, **216**, 203-214

Galloway, W.E., 1989. Genetic stratigraphic sequences in basin analysis, I. Architecture and genesis of flooding-surface bounded depositional units. American Association of Petroleum Geologists Bulletin, **73**, 125-142

Gardner, M.C., Bergman, S.C., Cushing, G.W., MacKevett Jr., E.M., Plafker, G., Campbell, R.B., Dodds, C.J., McClelland, W.C. and Mueller, P.A., 1988. Pennsylvanian pluton stitching of Wrangellia and the Alexander terrane, Wrangell Mountains, Alaska. Geology, **16**, 967-971

Garzione, C.N., Patchett, P.J., Ross, G.M. and Nelson, J.L., 1997. Provenance of Paleozoic sedimentary rocks in the Canadian Cordilleran miogeocline: a Nd isotopic study. Canadian Journal of Earth Sciences, **34**, 1603-1618

Gehrels, G.E., 2001. Geology of the Chatham Sound region, southeast Alaska and coastal British Columbia. Canadian Journal of Earth Sciences, **38**, 1579-1599

Gehrels, G.E., 2009. Age Pick program, University of Arizona Laserchron Center

Gehrels, G.E. and Ross, G.M., 1998. Detrital zircon geochronology of Neoproterozoic to Permian miogeoclinal strata in British Columbia and Alberta. Canadian Journal of Earth Sciences, **35**, 1380-1401

Gehrels, G.E., Butler, R.F. and Bazard, D.R., 1996. Detrital zircon geochronology of the Alexander terrane, southeastern Alaska. Geological Society of America Bulletin, **108**, 722-734

Gehrels, G.E., Johnsson, M.J. and Howell, D.G., 1999. Detrital zircon geochronology of the Adams Argillite and Nation River Formation, East-Central Alaska, U.S.A. Journal of Sedimentary Research, **69**, 135-144

Gibson, D.W., 1968. Triassic stratigraphy between the Athabasca and Smoky Rivers of Alberta. Geological Survey of Canada Paper 67-65

Gibson, D.W., 1969. Triassic stratigraphy of the Bow River – Crowsnest Pass region, Rocky Mountains of Alberta and British Columbia. Geological Survey of Canada Paper 68-29

Gibson, D.W., 1970. Triassic stratigraphy, Pine Pass area, northeastern British Columbia. Edmonton Geological Society Field Conference Guidebook, 23-38

Gibson, D.W., 1971. Triassic stratigraphy of the Sikanni Chief River – Pine Pass region, Rocky Mountain Foothills, northeastern British Columbia. Geological Survey of Canada Paper 70-31

Gibson, D.W., 1972. Triassic stratigraphy of the Pine Pass – Smoky River area, Rocky Mountain Foothills and Front Ranges of British Columbia and Alberta. Geological Survey of Canada Paper 71-30

Gibson, D.W., 1975. Triassic rocks of the Rocky Mountain Foothills and Front Ranges of northeastern British Columbia and west-central Alberta. Geological Survey of Canada Bulletin 247

Gibson, D.W., 1993. Triassic. *In,* Sedimentary cover of the craton in Canada, Stott, D.F. and Aitken, J.D. (eds.), Geology of Canada, No. 5, 294-320

Gibson, D.W and Barclay, J.E., 1989. Middle Absaroka Sequence – the Triassic stable craton. *In,* Western Canada Sedimentary Basin – a Case History, Ricketts, B.D. (ed.), Canadian Society of Petroleum Geologists, Special Publication, **30**, 219-232

Gibson, D.W. and Edwards, D.E., 1990. Triassic stratigraphy of the Williston Lake area, northeastern British Columbia. Field Trip Guidebook, Basin Perspectives, Canadian Society of Petroleum Geologists Convention

Gibson, D.W. and Edwards, D.E., 1992. Triassic stratigraphy and sedimentary environments of the Williston Lake area and adjacent subsurface plains, northeastern British Columbia. American Association of Petroleum Geologists Field Trip Guidebook

Glen, C.R., Föllmi, K.B, Riggs, S.R., Baturin, G.B., Grimm, K.A., Trappe, J., Abed, A.M., Galli-Olivier, C., Garrison, R.E., Ilyin, A.V., Jehl, C., Rohrlich, V., Sadaoah, R.M.Y., Schidlowski, M., Sheldon, R.E. and Siegmund, H., 1994. Phosphorous and phosphorites: sedimentology and environments of formation. Eclogae Geologicae Helvetiae, **87**, 747-788

Goel, R.K., 1977. Conodonts from Spiti (Himachal Pradesh), India. Journal of Paleontology, **51**, 1085-1101

Gordey, S.P., Geldsetzer, H.H.J., Bamber, E.W., Henderson, C.M., Richards, B.C., McGugan, A., Gibson, D.W. and Poulton, T.P., 1991. Upper Devonian to Middle Jurassic Assemblages, Part A: Ancestral North America. *In*, Geology of the Cordilleran Orogen in Canada, Gabrielse, H. and Yorath, C.J. (eds.). Geological Survey of Canada, Geology of Canada, **4**, 219-327

Goudemand, N., Orchard, M.J., Bucher, H. and Jenks, J., 2012 a. The elusive origin of *Chiosella timorensis* (Conodont Triassic). Geobios, **45**, 199-207

Goudemand, N., Orchard, M.J., Tafforeau, P., Urdy, S., Brühwiler, T., Brayard, A., Galfetti, T. and Bucher, H., 2012 b. Early Triassic conodont clusters from South China: Revision of the architecture of the 15 element apparatuses of the superfamily Gondolelloidea. Palaeontology, **55**, 1021-1034

Grasby, S.E. and Beauchamp, B. 2013. Recurrent Early Triassic anoxia in NW Pangaea. Geological Society of America Abstracts with Programs, **45**, 883

Grasby, S.E., Hamei, H. and Beauchamp, B., 2011. Catastrophic dispersion of coal fly ash into oceans during the latest Permian extinction. Nature Geoscience, **4**, 104-107

Grice, K., Cao, C., Love, G.D. Böttcher, M.E., Twitchett, R.J., Grosjean, E., Summons, R.E., Turgeon, S.C., Dunning, W. and Jin, Y., 2005. Photic zone euxinia during the Permian-Triassic superanoxic event. Science, **307**, 706-709

Gümbel, C.W. von, 1861. Geognostiche Beschreibungdes bayerischen Alpengebirges und seines Vorlands. Perthes, Gotha.

Guex, J., Bartolini, A., Atudorei, V. and Taylor, D., 2004. High-resolution ammonite and carbon isotope stratigraphy across the Triassic–Jurassic boundary at New York Canyon (Nevada). Earth and Planetary Science Letters, **225**, 29–41

Guex, J., Hungerbrühler, A., Jenks, J., Taylor, D. and Bucher, H., 2005 a. Dix-huit nouveaux genres d'ammonites du Spathien (Trias inférieur) de l'Ouest américain (Idaho, Nevada, Utah et Californie): Note préliminaire. Bulletin de Géologie Lausanne, **362**, 1–31

Guex, J., Hungerbrühler, A., Jenks, J., Taylor, D. and Bucher, H., 2005 b. Dix-neuf espèces d'ammonites du Spathien (Trias inférieur) de l'Ouest américain (Idaho, Nevada, Utah et Californie): Note préliminaire. Bulletin de Géologie Lausanne, **363**, 1–25

Hadlari, T., Davis, W.J., Dewing, K., Heaman, L.M., Lemiuex, Y., Ootes, L., Pratt, B.R. and Pyle, L.J., 2012. Two detrital zircon signatures for the Cambrian passive margin of northern Laurentia highlighted by new U-Pb results from northern Canada. Geological Society of America Bulletin, **124**, 1155-1168

Hage, 1944. Geology adjacent to the Alaska Highway between Fort St. John and Fort Nelson, British Columbia. Geological Survey of Canada Paper 44-30

Hallam, A., 1990. The end-Triassic mass extinction event. *In,* Global Catastrophes in Earth History: An Interdisciplinary Conference on Impacts, Volcanism, and Mass Mortality, Sharpton, V.L. and Ward, P.D. (eds.), Geological Society of America Special Paper, **247**, 577–583

Hallam, A., 1995. Major bio-events in the Triassic and Jurassic. *In,* Global Events and Event Stratigraphy, Walliser, O.H. (ed.), Springer-Verlag, 265–283

Hallam, A. 2002. How catastrophic was the end-Triassic mass extinction? Lethaia, **35**, 147-157

Hallam, A. and Wignall, P.B., 1999. Mass extinctions and sea-level changes. Earth Science Reviews, **48**, 217-250

Harper, D.A.T., Brunton, C.H.C., Cocks, L.R.M., Copper, P., Doyle, E.N., Jeffrey, A.L., Owen, E.F., Parkes, M.A., Popov, L.E. and Prosser, C.D., 1993. Brachiopoda. *In,* The Fossil Record, vol. 2, Benton, M.J. (ed.), Chapman and Hall, 427– 462

Harris, R.G., 2000. Triassic Doig Formation sand bodies in the Peace River area of western Canada: Depositional and structural models and the impact of diagenesis on reservoir properties. Unpublished MSc. Thesis. University of British Columbia. 205 p.

Hauer, F.R. von, 1850. Uber die Gliederung des Alpen-Kalks in den Ost-Alpen. Neues Jahrbuch, **1850**, 584

Hautmann, M., 2004. Effect of end-Triassic $CO_2$ maximum on carbonate sedimentation and marine mass extinction. Facies, **50**, 257-261

Hautmann, M., Benton, M.J. and Tomašových, A., 2008. Catastrophic ocean acidification at the Triassic-Jurassic boundary. Neues Jahrbuch für Geologie und Paläontologie-Abhandlungen, 249, 119-127

Hayes, M., 2012. Montney Formation Play Atlas NEBC. BC Oil and Gas Commission Technical Report.

Henderson, C.M., 1988. Conodont paleontology and biostratigraphy of the Upper Carboniferous to Lower Permian Canyon Fiord, Belcher Channel, Nansen, an unnamed, and Van Hauen formations, Canadian Arctic Archipelago. Unpublished PhD Thesis. University of Calgary. 287 p.

Henderson, C.M., 2011. Biostratigraphic correlation and shale fabric of Lower Triassic strata, east-central British Columbia (NTS 093I, O, P); in Geoscience BC Summary of Activities 2010, Geoscience BC, Report 2011-1, 223-228

Henderson, C.M. and Baud, A., 1997. Correlation of the Permian-Triassic boundary in Arctic Canada and comparison with Meishan, China. *In,* Stratigraphy, Proceedings of the 30th International Geological Congress, Wang, N. and Remane, J. (eds.), **11**, 143-152

Henderson, C.M., Richards, B.C. and Barclay, J.E., 1994. Permian strata of the Western Canada Sedimentary Basin. *In,* Geological Atlas of the Western Canada Sedimentary Basin, Mossop, G.D and Shetsen, I. (eds.), Canadian Society of Petroleum Geologists and Alberta Research Council, Calgary, 251-258

Hesselbo, S.P., Robinson, S.A., Surlyk, F. and Piasecki, S., 2002. Terrestrial and marine extinction at the Triassic-Jurassic boundary synchronized with major carbon-cycle perturbation: a link to initiation of massive volcanism? Geology, **30**, 251-254

Hodych, J.P. and Gunning, G.R., 1992. Did the Manicouagan impact trigger end-of-Triassic extinction? Geology, **20**, 51-54

Hoffman, P.F., 1988. United Plates of America, the birth of a craton: Early Proterozoic assembly and growth of Laurentia. Annual Review of Earth and Planetary Sciences, **16**, 543-603

Horacek, M., Koike, T. and Richoz, S., 2009. Lower Triassic $\delta^{13}C$ isotope curve from shallow marine carbonates in Japan, Panthalassa realm: confirmation of the Tethys $\delta^{13}C$ curve. Journal of Asian Earth Sciences, **36**, 481-490

Hornung, T. and Brandner, R., 2005. Biostratigraphy of the Reingraben Turnover (Hallstatt Facies Belt): local black shale events controlled by the regional tectonics, climatic change and plate tectonics. Facies, **51**, 460–479

Huckriede, R., 1958. Die Conodonten der mediterranen Trias und ihr stratigraphischer Wert. Paläontologische Zeitschrift, **32**, 10-14

Hunt, J.A., 2002. Volcanic-associated massive sulphide (VMS) mineralization in the Yukon-Tanana terrane and coeval strata of the North American miogeocline in the Yukon and adjacent areas. Indian and Northern Affairs Canada, Exploration and Geological Services Division, Yukon Region, Bulletin 12

Hunt, A.D. and Ratcliffe, J.D., 1959. Triassic stratigraphy, Peace River area, Alberta and British Columbia, Canada. Bulletin of the American Association of Petroleum Geologists, **43**, 563-589

Irish, E.J.W., 1962. Geology of Halfway River, British Columbia. Geological Survey of Canada Map 37-1961

Irish, E.J.W., 1970. Halfway River map-area, British Columbia. Geological Survey of Canada Paper 69-11

Jackson, S.E., Pearson, N.J., William, L., Griffin, W.L. and Belousova, E.A., 2004. The application of laser ablation microprobe-inductively coupled plasma-mass spectrometry (LAM-ICP-MS) to in situ U-Pb zircon geochronology. Chemical Geology, **211**, 47-69

Jansonius, J., 1962. Palynology of Permian and Triassic sediments, Peace River area, Western Canada. Paleontographica Abteilung B, **110**, 35-98

Jeffrey, B.M., Elrick, M. and Atudorei, V., 2013. Widespread Lower Triassic (Smithian) microbial mound complex across southern Utah: facies architecture and implication for post P-T paleoceanographic conditions. Geological Society of America Abstracts with Programs, **45**, 232

Jeppsson, L., Anehus, R. and Fredholm, D., 1999. The optimal acetate buffered acetic acid technique for extracting phosphatic fossils. Journal of Paleontology, **73**, 964-972

Joachimski, M.M., Lai, X., Shen, S., Jiang, H., Luo, G., Chen, B., Chen, J. and Sun, Y., 2012. Climate warming in the latest Permian and the Permian-Triassic mass extinction. Geology, **40**, 195-198

Joachimski, M.M., Alekseev, A.S., Lai, X., Shen, S., Grigoryan, A., Jiang, H. and Luo, G., 2013. Catastrophic climate warming in the latest Permian to Early Triassic: evidence from oxygen isotopes. Geological Society of America Abstracts with Programs, **45**, 89

Johns, M.J., Barnes, C.R. and Orchard, M.J., 1997. Taxonomy and biostratigraphy of Middle and Late Triassic elasmobranch ichthyoliths from northeastern British Columbia. Geological Survey of Canada Bulletin 502

Johnson, J.G. and Murphy, M.A., 1984. Time-rock model for Siluro-Devonian continental shelf, western United States. Geological Society of America Bulletin, **96**, 1349-1359

Juras, S.S., 1987. Geology of the polymetallic volcanogenic Buttle Lake camp, with emphasis on the Price Hillside, Central Vancouver Island, British Columbia, Canada. Unpublished PhD Thesis. University of British Columbia. 279 p.

Kendall, D.R., 1999. Sedimentology and stratigraphy of the Lower Triassic Montney Formation, Peace River Basin, subsurface of northwestern Alberta. Unpublished MSc. Thesis. University of Calgary. 368 p.

Kiessling, W. and Danelian, T., 2011. Trajectories of Late Permian – Jurassic radiolarian extinction rates: no evidence for an end-Triassic mass extinction. Fossil Record, **14**, 95-101

Kindle, E.D., 1944. Geological reconnaissance along Fort Nelson, Liard and Beaver Rivers, northeastern British Columbia and southeastern Yukon. Geological Survey of Canada Paper 44-16

Kindle, E.D., 1946. The Middle Triassic of Liard River, British Columbia, Appendix I. *In*, A Middle Triassic (Anisian) fauna in Halfway, Sikanni Chief and Tetsa valleys, northeastern British Columbia. Geological Survey of Canada Paper 46-1

Kiparisova, L.D. and Popov, Y.N., 1956. Subdivision of the Lower series of the Triassic system into stages. Doklady Akademii Nauk SSSR, **109**, 842-845 (in Russian)

Klepacki, D.W., 1985. Stratigraphy and structural geology of the Goat Range area, southeastern British Columbia. Unpublished PhD Thesis. Massachusetts Institute of Technology. 286 p.

Knoll, A.H., Bambach, R.K., Payne, J.L., Pruss, S. and Fischer, W., 2007. Paleophysiology and end-Permian mass extinction. Earth and Planetary Science Letters, **256**, 295-313

Koeberl, C., Farley, K.A., Peucker-Ehrenbrink, B. and Sephton, M.A., 2004. Geochemistry of the end-Permian extinction event in Austria and Italy: no evidence for an extraterrestrial component. Geology, **30**, 1053-1056

Kolar-Jurkovšek, T., 1983. Srednjetriasni konodonti Slovenije. Rudarsko-Metalurški Zbornik, **30**, 323-364

Korte, C. and Kozur, H.W., 2010. Carbon-isotope stratigraphy across the Permian-Triassic boundary: a review. Journal of Asian Earth Sciences, **39**, 215-235

Korte, C., Kozur, H.W., Bruckschen, P. and Veizer, J., 2003. Strontium isotope evolution of Late Permian and Triassic seawater. Geochimica et Cosmochimica Acta, **67**, 47-62

Košler, J., 2008. Laser ablation sampling strategies for concentration and isotope ratio analyses by ICP-MS. *In*, Laser-Ablation-ICPMS in the Earth Sciences, Sylvester, P. (ed.), Mineralogical Association of Canada Short Course Series, **40**, 79-92

Košler, J., 2011. U-Pb detrital zircon analysis – results of inter-laboratory comparison. Detrital Zircon Workshop, Goldschmidt Conference, Prague 2011

Košler, J., 2012. U-Pb geochronology and Hf isotope geochemistry of detrital zircon in sedimentary systems, Sylvester, P. (ed.), Mineralogical Association of Canada Short Course Series, **42**, 185-202

Kovács, S., 1994. Conodonts of stratigraphical importance from the Anisian/Ladinian boundary interval of the Balaton Highland, Hungary. Rivista Italiana di Paleontologia e Stratigrafia, **99**, 473-514

Kovács, S. and Kozur, H.W., 1980. Some remarks on Middle and Upper Triassic platform conodonts. Recent Researches in Geology, **6**, 541-581

Kovács, S. and Papšová, J., 1986. Conodonts from the *Paraceratites binodosus* Zone (Middle Triassic) from the Mecsek Mts., southern Hungary and from the Choč nappe of the Low Tatra Mts., Czechoslovakia. Geologický Zborník – Geologica Carpathica, **37**, 59-74

Kovács, S. and Rálisch-Felgenhauer, E., 2005. Middle Anisian (Pelsonian) platform conodonts from the Triassic of the Mecsek Mts. (South Hungary) – Their taxonomy and stratigraphic significance. Acta Geologica Hungarica, **48**, 69-105

Kovács, S., Kozur, H.W. and Mietto, P., 1980. *Gondolella pseudolonga* n. sp. (Conodontophorida), an important Lower Ladinian guide form. Geologisch-Paläontologische Mitteilungen Innsbruck, **10**, 217-221

Kovács, S., Nicora, A., Szabó, I. and Balini, M., 1990. Conodont biostratigraphy of Anisian-Ladinian boundary sections in the Balaton Upland (Hungary) and in the Southern Alps (Italy). Courier Forschungsinstitut Senckenberg, **118**, 171-195

Kozur, H.W., 1968. Conodonten aus dem Muschelkalk des germanischen Binnen-beckens und ihr stratigraphischer Wert. Teil I: Conodonten vom Plattformtyp und stratigraphische Bedeutung der Conodonten aus dem Oberen Muschelkalk. Geologie, **17**, 930-946

Kozur, H.W., 1989 a. Significance of events in conodont evolution for the Permian and Triassic stratigraphy. Courier Forschungsinstitut Senckenberg, **117**, 385-408

Kozur, H.W, 1989 b. The taxonomy of the Gondolellid conodonts in the Permian and Triassic. Courier Forschungsinstitut Senckenberg, **117**, 409-469

Kozur, H.W., 1993. First evidence of Liassic in the vicinity of Csővár (Hungary), and its palaeogeographic and palaeotectonic significance. Jahrbuch Geolgische Bundesanstalt, **136**, 89–98

Kozur, H.W., 1999 The correlation of the Germanic Buntsandstein and Muschelkalk with the Tethyan scale. Zentralblatt für Geologie und Paläontologie, Teil I, **7-8**, 701-725

Kozur, H.W., 2003. Integrated ammonoid, conodont and radiolarian zonation of the Triassic and some remarks to Stage/Substage subdivision and the numeric age of the Triassic stages. Albertiana, **28**, 57-74

Kozur, H.W. and Mostler, H., 1971. Probleme der Conodontenforschung in der Trias. Geologisch-Paläontologische Mitteilungen Innsbruck, **1**, 1-19

Kozur, H.W. and Mostler H., 1976. Neue conodonten aus dem Jungpaläozoikum und der Trias. Geologisch-Paläontologische Mitteilungen Innsbruck, **636**, 1-40

Kozur, H.W. and Mostler, H., 1982. Neue Conodonten aus dem Illyr und Fassan der Profile Fellbach und Karalm (Gailtaler Alpen, Kärnten, Österreich). Geologisch-Paläontologische Mitteilungen Innsbruck, **11**, 291-298

Kozur, H.W. and Weems, R.E., 2007. Upper Triassic conchostrachan biostratigraphy of the continental rift basins of eastern North America: its importance for correlating Newark Supergroup events with the Germanic Basin and the international geologic timescale. *In,* The Global Triassic, Lucas, S.G. and Spielmann, J.A. (eds.), New Mexico Museum of Natural History and Science Bulletin, **41**, 137-188

Kozur, H.W. and Weems, R.E., 2010. The biostratigraphic importance of conchostracansin the continental Triassic of the northern hemisphere. Geological Society of London Special Publication, **334**, 315-417

Kozur, H.W., Krainer, K. and Mostler, H., 1994. Middle Triassic conodonts from the southern Karawanken Mountains (Southern Alps) and their stratigraphic importance. Geologisch-Paläontologische Mitteilungen Innsbruck, **19**, 165-200

Krystyn, L., Gallet, Y., Besse, J. and Marcoux, J., 2002. Integrated Upper Carnian to Lower Norian biochronology and implications for the Upper Triassic magnetic polarity time scale. Earth and Planetary Science Letters, **203**, 343-351

Labandeira, C.C., 2005. The fossil record of insect extinction: new approaches and future directions. American Entomologist, **51**, 14-29

Lane, L.S., 2007. Devonian-Carboniferous paleogeography and orogenesis, northern Yukon and adjacent Arctic Alaska. Canadian Journal of Earth Sciences, **44**, 679-694

Leckie, D.A., 1989. Upper Zuni Sequence: Middle Cretaceous to Lower Tertiary. *In*, Western Canada Sedimentary Basin – a Case History, Ricketts, B.D. (ed.), Canadian Society of Petroleum Geologists, Special Publication, **30**, 269-284

Lehrmann, D.J., Ramezani, J., Bowring, S.A., Martin, M.W., Montgomery, P., Enos, P., Payne, J.L., Orchard, M.J., Hongmei, W. and Jiayong, W., 2006. Timing of recovery from the end-

Permian extinction: geochronologic and biostratigraphic constraints from south China. Geology, **34**, 1053-1056

Lemieux, Y., Hadlari, T. and Simonetti, A., 2011. Detrital zircon geochronology and provenance of Devono-Mississippian strata in the northern Canadian Cordilleran miogeocline. Canadian Journal of Earth Sciences, **48**, 515-541

Leslie, C.D., 2009. Detrital zircon geochronology and rift-related magmatism: Central Mackenzie Mountains, Northwest Territories. Unpublished M.Sc. Thesis, University of British Columbia. 224p.

Lindström, M., 1970. A suprageneric taxonomy of the conodonts. Lethaia, **3**, 427-445

Logan, J.M., 2004. Preliminary lithogeochemistry and polymetallic VHMS mineralization in Early Devonian and (?) Early Carboniferous volcanic rocks, Foremore property. Geological Fieldwork 2003, BC Ministry of Energy and Mines Paper 2004-1, 105-124

Logan, J.M. and Colpron, M., 2006. Stratigraphy, geochemistry, syngenetic sulphide occurrences and tectonic setting of the lower Paleozoic Lardeau Group, northern Selkirk Mountains, British Columbia. *In*, Paleozoic Evolution and Metallogeny of Pericratonic Terranes at the Ancient Pacific Margin of North America, Canadian and Alaskan Cordillera, Colpron, M. and Nelson, J.L. (eds.), Geological Association of Canada Special Paper, **45**, 323-360

Longridge, L.M., Carter, E.S., Smith, P.L. and Tipper, H.W., 2007. Early Hettangian ammonites and radiolarians from the Queen Charlotte Islands, British Columbia and their bearing on the definition of the Triassic–Jurassic boundary. Palaeogeography, Palaeoclimatology, Palaeoecology, **244**, 142-169

Lowey, G.W., 1998. A new estimate of the amount of displacement on the Denali fault system based on the occurrence of carbonate megaboulders in the Dezadesh Formation (Jura-Cretaceous), Yukon, and the Nutzotin Mountains sequence (Jura-Cretaceous), Alaska. Bulletin of Canadian Petroleum Geology, **46**, 379-386

Lucas, S.G., 1998. Global Triassic tetrapod biostratigraphy and biochronology. Palaeogeography, Palaeoclimatology, Palaeoecology, **143**, 347-384

Lucas, S.G., 1999. The epicontinental Triassic, an overview. Zentralblatt für Geologie und Paläontologie Teil 1, 475‑496

Lucas, S.G., 2009. Timing and magnitude of tetrapod extinctions across the Permo-Triassic boundary. Journal of Asian Earth Sciences, **36**, 491–502

Lucas, S.G., 2010. The Triassic chronostratigraphic scale: history and status. Geological Society of London Special Publication, **334**, 17-39

Lucas, S.G., 2013. A new Triassic timescale. *In,* The Triassic System, Tanner, L.H., Spielmann, J.A. and Lucas, S.G. (eds.), New Mexico Museum of Natural History and Science Bulletin, **61**, 366-374

Lucas, S.G. and Orchard, M.J., 2007. Triassic lithostratigraphy and biostratigraphy north of Currie, Elko County, Nevada. *In,* The Global Triassic, Lucas, S.G. and Spielmann, J.A. (eds.), New Mexico Museum of Natural History and Science Bulletin, **41**, 119-126

Lucas, S.G., Tanner, L.H., Kozur, H.W., Weems, R.E. and Heckert, A.B., 2012. The Late Triassic timescale: age and correlation of the Carnian-Norian boundary. Earth Science Reviews, **114**, 1-18

Ludwig, K.R., 2003. User's manual for Isoplot/Ex. 3.00: A Geochronological Toolkit for Microsoft Excel. Berkley Geochronology Center Special Publication 1a, 55p.

MacEachern, J.A., Raychaudhuri, I. and Pemberton, S.G., 1992. Stratigraphic Applications Of The Glossifungites Ichnofacies: Delineating Discontinuities In The Rock Record. Applications of Ichnology to Petroleum Exploration. SEPM Core Workshop 17, 169-198

Macke, D.L. and Nichols, K.M., 2007. Conodonts viewed as evolving heavy-mineral grains. *In,* The Global Triassic, Lucas, S.G. and Spielmann, J.A. (eds.), New Mexico Museum of Natural History and Science Bulletin, **41**, 262-267

Mander, L., Twitchett, R.J. and Benton, M.J., 2008. Palaeoecology of the Late Triassic extinction in southwest UK. Journal of the Geological Society of London, 165, 319–332

Markhasin, B., 1997. Sedimentology and stratigraphy of the Lower Triassic Montney Formation, subsurface of northwestern Alberta. Unpublished MSc. Thesis. University of Calgary. 212 p.

Marzoli, A., Renne, P.R., Piccirillo, E.M., Ernesto, M., Bellieni, G. and de Min, A., 1999. Extensive 200-million-year-old continental flood basalts of the Central Atlantic Magmatic Province. Science, **284**, 616-618

Maxwell, W.D., 1989. The end-Permian mass extinction. *In,* Mass extinctions: processes and evidence, Donovan, S.K. (ed.), Bellhaven Press, London, 152-173

McClelland, W.C., Schmidt, J.M. and Till, A.B., 2006. New U-Pb SHRIMP ages from Devonian felsic volcanic and Proterozoic plutonic rocks of the southern Brooks Range, Alaska. Geological Society of America Abstracts with Programs, **38**, 12

McConnell, R.G., 1896. Report on an exploration of the Finlay and Omineca River. Geological Survey of Canada, Annual Report, **7**, 6-40

McElwain, J.C., Beerling, D.J. and Woodward, F.I., 1999. Fossil plants and global warming at the Triassic-Jurassic boundary. Science, **285**, 1386-1390

McGoff, H.J., 1991. The hydrodynamics of conodont elements. Lethaia, **24**, 235-247

McGowan, A.J. and Smith, A.B., 2007. Ammonoids across the Permian/Triassic boundary: a cladistic perspective. Palaeontology, **50**, 573-590

McLearn, F.H., 1918. Peace River section, Alberta. Geological Survey of Canada, Summary Report 1917, part C, 1-6

McLearn, F.H., 1921. Mesozoic of Upper Peace River, B.C. Geological Survey of Canada, Summary Report 1920, part B, 1-6

McLearn, F.H., 1930. Preliminary study of the faunas of the Upper Triassic Schooler Creek Formation, western Peace River, B.C. Transactions of the Royal Society of Canada, **24**, 13-20

McLearn, F.H., 1937 a. New species from the Triassic Schooler Creek Formation. Canadian Field-Naturalist, **51**, 95-98

McLearn, F.H., 1937 b. Contributions to the Triassic of Peace River, B.C. Canadian Field-Naturalist, **51**, 127-131

McLearn, F.H., 1940 a. New Canadian Triassic ammonoids. Canadian Field-Naturalist, **54**, 47-51

McLearn, F.H., 1940 b. Triassic of Beattie Hill, Peace River Foothills, B.C. Canadian Field-Naturalist, **54,** 79-82

McLearn, F.H., 1941 a. Triassic stratigraphy of Brown Hill, Peace River Foothills, B.C.. Transactions of the Royal Society of Canada, **35**, 93-104

McLearn, F.H., 1941 b. Preliminary descriptions of some new Triassic pelecypods from the Peace River Foothills, B.C. Canadian Field-Naturalist, **55**, 31-33

McLearn, F.H., 1941 c. Triassic stratigraphy, Mahaffy Cliffs to Red Rock Spur, Peace River Foothills, B.C. Canadian Field-Naturalist, **55**, 95-100

McLearn, F.H., 1946 a. A Middle Triassic (Anisian) fauna in Halfway, Sikanni Chief and Tetsa Valleys, northeastern British Columbia. Geological Survey of Canada Paper 46-1, 2nd edition, 1948

McLearn, F.H., 1946 b. Upper Triassic faunas in Halfway, Sikanni Chief and Tetsa Valleys, northeastern British Columbia. Geological Survey of Canada Paper 46-25

McLearn, F.H., 1947 a. Upper Triassic faunas of Pardonet Hill, Peace River Foothills, British Columbia. Geological Survey of Canada Paper 47-14

McLearn, F.H., 1947 b. The Triassic *Nathorstites* fauna in northeastern British Columbia. Geological Survey of Canada Paper 47-24

McLearn, F.H., 1953. Correlation of the Triassic formations of Canada. Bulletin of the Geological Society of America, **64**, 1205-1228

McLearn, F.H., 1960. Ammonoid faunas of the Upper Triassic Pardonet Formation, Peace River Foothills, British Columbia. Geological Survey of Canada Memoir 311

McLearn, F.H., 1969. Middle Triassic (Anisian) ammonoids from northeastern British Columbia and Ellesemere Island. Geological Survey of Canada Bulletin 170

McLearn, F.H. and Kindle, E.D., 1950. Geology of northeastern British Columbia. Geological Survey of Canada Memoir 259

McMechan, M.E. and Thompson, R.I., 1989. Structural style and history of the Rocky Mountain Fold and Thrust Belt. *In*, Western Canada Sedimentary Basin – a Case History, Ricketts, B.D. (ed.), Canadian Society of Petroleum Geologists, Special Publication, **30**, 47-72

McNicoll, V.J., Harrison, J.C., Trettin, H.P. and Thorsteinsson, R., 1995. Provenance of the Devonian clastic wedge of Arctic Canada: Evidence provided by detrital zircon ages. *In*, Stratigraphic evolution of foreland basins, Dorobek, S.L. and Ross, G.M. (eds.), Society of Economic Paleontologists and Mineralogists, Special Publication, **52**, 77-93

McRoberts, C.A. and Newton, C.A., 1995. Selective extinction among end-Triassic European bivalves. Geology, **23**, 102-104

McRoberts, C.A., Furrer, H. and Jones, D.S., 1997. Palaeoenvironmental interpretation of a Triassic-Jurassic boundary section from Western Austria based on palaeoecological and geochemical data. Palaeogeography, Palaeoclimatology, Palaeoecology, **136**, 79-95

Metcalfe, I. and Isozaki, Y., 2009. Current perspectives on the Permian-Triassic boundary and end-Permian mass extinction: preface. Journal of Asian Earth Sciences, **36**, 407-412

Metcalfe, I., Nicoll, R.S., Willink, R., Ladjavadi, M. and Grice, K., 2013. Early Triassic (Induan-Olenekian) conodont biostratigraphy, global anoxia, carbon isotope excursions and environmental perturbations: New data from Western Australian Gondwana. Gondwana Research, **23**, 1136-1150

Mietto, P. and Manfrin, S., 1995. A high resolution Middle Triassic ammonoid standard scale in the Tethys Realm. A preliminary report. Bulletin de la Société Géologique de France, **166**, 539-563

Mihalynuk, M.G., Nelson, J.L. and Diakow, L.J., 1994. Cache Creek terrane entrapment: oroclinal paradox within the Canadian Cordillera. Tectonics, **13**, 575-595

Miller, E.L., Toro, J., Gehrels, G.E., Amato, J.M., Prokopiev, A., Tuchkova, M.I., Akinin, V.V., Dumitru, T.A., Moore, T.E. and Cecile, M.P., 2006. New insights into Arctic paleogeography and tectonics from U-Pb detrital zircon geochronology. Tectonics, **25**, 1-19

Mojsisovics, E. von, 1869. Über die Gliederung der oberen Triasbildungen der östlichen Alpen. Jahrbuch der Kaiserlich-Königlichen Geologische Reichsanstalt, **24**, 91-150

Mojsisovics, E. von, 1873. Das Gebirge um Hallstatt. Th. 1. Die Mollusken – Faunen der Zlambach- und Hallstätter Schichten. Abhandlungen der Kaiserlich-Königlichen Geologischen Reichsanstalt, **6**, 1-82

Mojsisovics, E. von, 1879. Die Dolomitriffe von Südtirol und Venetien. Alfred Hödler, Wien.

Mojsisovics, E. von, 1882. Die Cephalopoden der mediterranean Triasprovinz. Abhandlungen der Kaiserlich-Königlichen Geologischen Reichsanstalt, **10**, 1-322

Mojsisovics, E. von, Waagen, W.H. and Diener, C., 1895. Entwurf einer Gliederung der pelagischen Sediments des Trias-Systems. Sitzungsberichte Akademie Wissenschaft Wien, Mathematische – naturwissenschaftliche Klasse, **104**, 1279-1302

Monger, J.W.H., 1989. Overview of Cordilleran Geology. *In,* Western Canada Sedimentary Basin – A Case History, Ricketts, B.D. (ed.), Canadian Society of Petroleum Geologists, 9-45

Monger, J.W.H., and Price, R.A., 2002. The Canadian Cordillera: geology and tectonic evolution. Canadian Society of Exploration Geophysicists Recorder, February, 17-36

Monnet, C. and Bucher, H., 2005. Anisian (Middle Triassic) ammonoids from North America: quantitative biochronology and biodiversity. Stratigraphy, **2**, 281-296

Monnet, C. and Bucher, H., 2007. New Middle and Late Anisian (Middle Triassic) Ammonoid Faunas from Northwestern Nevada (USA): Taxonomy and Biochronology. Fossils and Strata, 52, 1-200

Moore, P.F., 1989. The Lower Kaskaskia Sequence – Devonian. *In,* Western Canada Sedimentary Basin – a Case History, Ricketts, B.D. (ed.), Canadian Society of Petroleum Geologists, Special Publication, **30**, 139-164

Mortensen, J.K., 1990. Geology and U-Pb geochronology of the Klondike District, west-central Yukon Territory. Canadian Journal of Earth Sciences, **27**, 903-914

Mortensen, J.K., 1992. Pre-mid-Mesozoic evolution of the Yukon-Tanana terrane, Yukon and Alaska. Tectonics, **11**, 836-853

Mortensen, J.K. and Bell, R.T., 1991. U-Pb zircon and titanite geochronology of the Mount Sedgwick pluton, northern Yukon Territory. *In,* Radiogenic age and isotope studies, Report 4. Geological Survey of Canada Paper 90-2, 19-24

Mortensen, J.K., Beranek, L., and Murphy, D.C., 2007. Permo-Triassic orogeny in the northern Cordillera: Sonoma North? Geological Society of America, Cordilleran Section

Mosher, L.C., 1968. Triassic conodonts from western North America and Europe and their correlation. Journal of Paleontology, 42, 895-946

Mosher, L.C., 1970. New conodont species as Triassic guide fossils. Journal of Paleontology, **44**, 737-742

Mosher, L.C., 1973. Triassic conodonts from British Columbia and the northern Arctic Islands. Geological Survey of Canada Bulletin, **222**, 141-193

Mosher, L.C. and Clark, D.L., 1965. Middle Triassic conodonts from the Prida Formation of northwestern Nevada. Journal of Paleontology, **39**, 551-565

Moslow, T.F., 2000. Reservoir architecture of a fine-grained turbidite system: Lower Triassic Montney Formation, Western Canada Sedimentary Basin. Deep Water Reservoirs of the World, Society of Economic Paleontologists and Mineralogists, Gulf Coast Section, 20th Annual Bob Perkins Research Conference, Houston, 42

Moslow, T.F. and Davies, G.R., 1997. Turbidite reservoir facies in the Lower Triassic Montney Formation, west-central Alberta. *In*, Triassic of the Western Canada Sedimentary Basin, Moslow, T.F. and Wittenberg, J. (eds.), Bulletin of Canadian Petroleum Geology, **45**, 507-536

Muller, J.E., 1961. Geology of Pine Pass, British Columbia. Geological Survey of Canada Map 11-1961

Müller, K.J., 1956. Triassic conodonts from Nevada. Journal of Paleontology, **30**, 818-830

Mundil, R., Ludwig, K.R., Metcalfe, I. and Renne, P.R., 2004. Age and timing of the Permian mass extinctions: U/Pb dating of closed-system zircons. Science, **305**, 1760-1763

Mundil, R., Pálfy, J., Renne, P.R. and Brack, P., 2010. The Triassic timescale: new constraints and a review of geochemical data. Geological Society of London Special Publication, **334**, 41-60

Murphy, D.C., Mortensen, J.K., Piercey, S.J., Orchard, M.J. and Gehrels, G.E., 2006. Mid-Paleozoic to early Mesozoic tectonostratigraphic evolution of Yukon-Tanana and Slide Mountain terranes and affiliated overlap assemblages, Finlayson Lake massive sulphide district, southeastern Yukon. *In*, Paleozoic Evolution and Metallogeny of Pericratonic Terranes at the Ancient Pacific Margin of North America, Canadian and Alaskan Cordillera, Colpron, M. and Nelson, J.L. (eds.), Geological Association of Canada Special Paper, **45**, 75-105

Muttoni, G., Kent, D.V., Meço, S., Balini, M., Nicora, A., Rettori, R., Gaetani, M. and Krystyn, L., 1998. Towards a better definition of the Middle Triassic magnetostratigraphy and biostratigraphy in the Tethyan realm. Earth and Planetary Science Letters, **164**, 285-302

NEB Report, 2013. Energy briefing note: The ultimate potential for unconventional petroleum from the Montney Formation of British Columbia and Alberta. National Energy Board, BC Oil and Gas Commission, Alberta Energy Regulator and BC Ministry of Natural Gas Development.

Nelson, J.L., 1993. The Sylvester allochthon: upper Paleozoic marginal basin and island arc terranes in northern British Columbia. Canadian Journal of Earth Sciences, **30**, 631-643

Nelson, J.L. and Mihalynuk, M.G., 1993. Cache Creek Ocean: closure or enclosure? Geology, **21**, 173-176

Nelson, J.L. and Colpron, M., 2007. Tectonics and metallogeny of the British Columbia, Yukon and Alaskan Cordillera, 1.8 Ga to the present. *In*, Mineral deposits of Canada: a synthesis of

major deposit types, district metallogeny, the evolution of geological provinces and exploration methods, Goodfellow, W.D. (ed.), Geological Association of Canada, Mineral Deposits Division, Special Publication, **5**, 755-791

Nelson, J.L., Harms, T.A. and Mortensen, J.K., 1998. Extensions and affiliates of the Yukon-Tanana terrane in northern British Columbia. *In,* Geological Fieldwork 1997, a summary of field activities and current research. British Columbia Ministry of Employment and Investment, Geological Survey Branch, Paper 1998-1, 7.1-7.12

Nelson, J.L., Colpron, M., Piercey, S.J., Dusel-Bacon, C., Murphy, D.C. and Roots, C.F., 2006. Paleozoic tectonic and metallogenic evolution of the pericratonic terranes in Yukon, northern British Columbia and eastern Alaska. *In,* Paleozoic Evolution and Metallogeny of Pericratonic Terranes at the Ancient Pacific Margin of North America, Canadian and Alaskan Cordillera, Colpron, M. and Nelson, J.L. (eds.), Geological Association of Canada Special Paper, **45**, 323-360

Newell, N.D., 1963. Crises in the history of life. Scientific American, **208**, 76–92

Newell, N.D., 1967. Paraconformities. *In,* Essays in Paleontology and Stratigraphy, Teichert, C. and Yochelson, E.L. (eds.), R.C. Moore Commemorative Volume, University of Kansas Press, 349– 367

Nicora, A., 1976. Conodont-fauna, stratigraphic position and relations to the Tethyan succession of the Shoshonensis Zone (Pelsonian) of Nevada. Rivista Italiana di Paleontologia e Stratigrafia, **82**, 627-648

Nicora, A., 1977. Lower Anisian platform-conodonts from the Tethys and Nevada: taxonomic and stratigraphic revision. Palaeontographica Abteilung A, **157**, 88-107

Nicora, A. and Kovács, S., 1984. Conodont fauna from the Rotelliforme, Meeki and Occidentalis Zones (Middle Triassic) of Humboldt Range, Nevada, western North America. Rivista Italiana di Paleontologia e Stratigrafia, **90**, 135-164

Nikishin, A.M., Ziegler, P., Abbott, A.D., Brunet, M. and Cloetingh, S., 2002. Permo-Triassic intraplate magmatism and rifting in Eurasia: implications for mantle plumes and mantle dynamics. Tectonophysics, **351**, 1037-1040

Nogami, Y., 1968. Trias-conodonten von Timor, Malaysien und Japan (Paleontological study of Portuguese Timor, 5). Memoirs of the Faculty of Science, Kyoto University, Series of Geology and Mineralogy, **34**, 115-136

Nokleberg, W.J., Parfenov, L.M., Monger, J.W.H., Norton, I.O., Khanchuk, A.I., Stone, D.B., Scotese, C.R., Scholl, D.W. and Fujita, K., 2000. Phanerozoic tectonic evolution of the circum-North Pacific. United States Geological Survey Professional Paper 1626

O'Connell, S.C., Dix, G.R. and Barclay, J.E., 1990. The origin, history, and regional structural development of the Peace River Arch, Western Canada. Bulletin of Canadian Petroleum Geology, **38**, 4-24

OGC Report, 2013. Hydrocarbon and by-product reserves in British Columbia, 2011. BC Oil and Gas Commission.

Ogg, J.G., 2012. Triassic. *In*, The Geologic Time Scale 2012, Gradstein, F.M., Ogg, J.G., Schmitz, M. and Ogg, G. (eds.), Elsevier, 681-730

Olsen, P.E., Shubin, N.H. and Anders, M.H., 1987. New Early Jurassic tetrapod assemblages constrain Triassic-Jurassic tetrapod extinction event. Science, **237**, 1025-1029

Olsen, P.E., Kent, D.V., Sues, H.-D., Koeberl, C., Huber, H., Montanari, A., Rainforth, E.C., Fowell, S.J., Szajna, M.J. and Hartline, B.W., 2002 a. Ascent of dinosaurs linked to an iridium anomaly at the Triassic-Jurassic boundary. Science, **296**, 1305-1307

Olsen, P.E., Koeberl, C., Huber, H., Montanari, A., Fowell, S.J., Et-Touhami, M. and Kent, D.V., 2002 b. Continental Triassic-Jurassic boundary in central Pangaea: recent progress and discussion of an Ir anomaly. *In*, Catastrophic events and mass extinctions: impacts and beyond, Koeberl, C. and MacLeod, K.G. (eds.), Geological Society of America Special Paper, **356**, 505-522

Onoue, T., Sato, H., Nakamura, T., Noguchi, T., Hidaka, Y., Shirai, N., Ebihara, M., Osawa, T., Hatsukawa, Y., Toh, Y., Koizumi, M., Harada, H., Orchard, M.J. and Nedachi, M., 2012. Deep-sea record of impact apparently unrelated to mass extinction in the Late Triassic. Proceedings of the National Academy of Sciences of the United States, **109**, 19134-19139

Orchard, M.J., 1983. *Epigondolella* populations and their phylogeny and zonation in the Norian (Upper Triassic). Fossils and Strata, **15**, 177-192

Orchard, M.J., 1991 a. Late Triassic conodont biochronology and biostratigraphy of the Kunga Group, Queen Charlotte Islands, British Columbia. Geological Survey of Canada Paper 1990-10, 173-193

Orchard, M.J., 1991 b. Upper Triassic conodont biochronology and new index species from the Canadian Cordillera. *In*, Ordovician to Triassic conodont paleontology of the Canadian Cordillera, Orchard, M.J. and McCracken, A.D. (eds.), Geological Survey of Canada Bulletin, **417**, 299-335

Orchard, M.J., 1994. Conodont biochronology around the Early-Middle Triassic boundary: new data from North America, Oman and Timor. Proceedings of the Triassic Symposium, Lausanne, Switzerland, **22**, 105-114

Orchard, M.J., 1995. Taxonomy and correlation of Lower Triassic (Spathian) segminate conodonts from Oman and revision of some species of *Neospathodus*. Journal of Paleontology, **69**, 110-122

Orchard, M.J., 2005. Multielement conodont apparatuses of Triassic Gondolelloidea. Special Papers in Palaeontology, **73**, 73-101

Orchard, M.J., 2007 a. New conodonts and zonation, Ladinian-Carnian boundary beds, British Columbia, Canada. *In*, The Global Triassic, Lucas, S.G. and Spielmann, J.A. (eds.), New Mexico Museum of Natural History and Science Bulletin, **41**, 321-330

Orchard, M.J., 2007 b. Conodont lineages from the Carnian-Norian boundary at Black Bear Ridge, northeast British Columbia. *In*, The Global Triassic, Lucas, S.G. and Spielmann, J.A. (eds.), New Mexico Museum of Natural History and Science Bulletin, **41**, 331-332

Orchard, M.J., 2007 c. A proposed Carnian-Norian boundary GSSP at Black Bear Ridge, northeast British Columbia, and a new conodont framework for the boundary interval. Albertiana, **36**, 130-141

Orchard, M.J., 2007 d. Conodont diversity and evolution through the latest Permian and Early Triassic upheavals. Palaeogeography, Palaeoclimatology, Palaeoecology, **252**, 93-117

Orchard, M.J., 2008. Lower Triassic conodonts from the Canadian Arctic, their intercalibration with ammonoid-based stages and a comparison with other North American Olenekian faunas. Polar Research, **27**, 393-412

Orchard, M.J., 2010. Triassic conodonts and their role in stage boundary definition. *In*, The Triassic Timescale, Lucas, S.G. (ed.), Geological Society of London Special Publication, **334**, 139-161

Orchard, M.J., 2013. Five new genera of conodonts from the Carnian-Norian boundary beds of Black Bear Ridge, northeast British Columbia, Canada. *In*, The Triassic System, Tanner, L.H., Spielmann, J.A. and Lucas, S.G. (eds.), New Mexico Museum of Natural History and Science Bulletin, **61**, 445-457

Orchard, M.J. and Bucher, H., 1992. Conodont-ammonoid intercalibration around the Lower-Middle Triassic boundary: Nevadan clocks help tell British Columbian time. Current Research, Part E, Geological Survey of Canada Paper, **92-1E**, 133-140

Orchard, M.J. and Krystyn, L., 1998. Conodonts of the lowermost Triassic of Spiti, and new zonations based on *Neogondolella* successions. Rivista Italiana di Paleontologia e Stratigrafia, **104**, 341-368

Orchard, M.J. and Rieber, H., 1999. Multielement *Neogondolella* (Conodonta, upper Permian-middle Triassic). Bolletino della Societa Paleontologia Italiana, **37**, 475-488

Orchard, M.J. and Tozer, E.T., 1997. Triassic conodont biochronology, its calibration with the ammonoid standard, and a biostratigraphic summary of the Western Canada Sedimentary Basin. *In*, Triassic of the Western Canada Sedimentary Basin, Moslow, T.F. and Wittenberg, J. (eds.), Bulletin of Canadian Petroleum Geology, **45**, 675-692

Orchard, M.J. and Zonneveld, J.-P., 2009. The Lower Triassic Sulphur Mountain Formation in the Wapiti Lake area: lithostratigraphy, conodont biostratigraphy, and a new biozonation for the lower Olenekian (Smithian). Canadian Journal of Earth Sciences, **46**, 757-790

Orchard, M.J., Grădinaru, E. and Nicora, A., 2007 a. A summary of the conodont succession around the Olenekian-Anisian boundary at Deşli Caira, North Dobrogea, Romania. *In,* Lucas, S.G. and Spielmann, J.A. (eds.), The Global Triassic, Bulletin of the New Mexico Museum of Natural History and Science Bulletin, **41**, 341-346

Orchard, M.J., Lehermann, D.J., Jiayong, W., Hongmei, W. and Taylor, H.J., 2007 b. Conodonts from the Olenekian-Anisian boundary beds, Guandao, Guizhou Province, China. *In,* Lucas, S.G. and Spielmann, J.A. (eds.), The Global Triassic, Bulletin of the New Mexico Museum of Natural History and Science Bulletin, **41**, 347-354

Orchard, M.J., Nassichuk, W.W. and Lin, R., 1994. Conodonts from the Lower Griesbachian *Otoceras latilobatum* bed of Selong, Tibet and the position of the Permian-Triassic boundary. Memoirs of the Canadian Society of Petroleum Geology, **17**, 823-843

Ovtcharova, M., Bucher, H., Schaltegger, U., Galfetti, T., Brayard, A., and Guex, J., 2006. New Early to Middle Triassic U-Pb ages from south China: calibration with ammonoid biochronozones and implications for the timing of Triassic biotic recovery. Earth and Planetary Science Letters, **243**, 463–475

Pálfy, J., 2003. Volcanism of the Central Atlantic Magmatic Province as a potential driving force in the End-Triassic Mass Extinction. *In,* The Central Atlantic Magmatic Province: insights from fragments of Pangea, Hames, W., McHone, J.G., Renne, P.R. and Ruppel, C. (eds.), Geophysical Monograph, 136, 255-267

Pálfy, J., Demény, A., Haas, J., Hetényi, M., Orchard, M.J. and Vető, I., 2001. Carbon isotope anomaly and other geochemical changes at the Triassic-Jurassic boundary from a marine section in Hungary. Geology, **29**, 1047-1050

Pálfy, J., Demény, A., Haas, J., Carter, E.S., Görög, A., Halász, D., Oravecz-Scheffer A., Hetényi, M., Márton, E., Orchard, M.J., Ozsvárt, P., Vető, I. and Zajzon, N., 2007. Triassic-Jurassic boundary events inferred from integrated stratigraphy of the Csővár section, Hungary. Palaeogeography, Palaeoclimatology, Palaeoecology, **244**, 11-33

Panek, R., 2000. The sedimentology and stratigraphy of the Lower Triassic Montney Formation in the subsurface of the Peace River area, northwestern Alberta. Unpublished MSc. Thesis. University of Calgary. 275 p.

Parrish, J.T., 1993. Climate of the supercontinent Pangea. Journal of Geology, **101**, 215–233

Paull, R.K., 1983. Definition and stratigraphic significance of the Lower Triassic (Smithian) conodont *Gladigondolella meeki* n. sp. in the western United States. Journal of Paleontology, **57**, 188-192

Payne, J.L., 2005. Evolutionary dynamics of gastropod size across the end-Permian extinction and through the Triassic recovery interval. Paleobiology, **31**, 269-290

Payne, J.L., Lehrmann, D.J., Wei, J., Orchard, M.J., Schrag, D.P. and Knoll, A.H., 2004. Large perturbations of the carbon cycle during recovery from the end-Permian mass extinction. Science, **305**, 506-509

Pease, V. and Vernikovsky, V., 2000. The tectonomagmatic evolution of the Taimyr Peninsula: Further constraints from new ion-microprobe data. Polarforschung, **68**, 1-3

Pease, V., Gee, D.G., Vernikovsky, V., Vernikovskaya, A. and Kireev, S., 2001. Geochronology and magmatic and metamorphic events in central Taimyr, northern Siberia. Terra Nova, **13**, 270-280

Pelletier, B.R., 1960. Triassic stratigraphy, Rocky Mountain Foothills, northeastern British Columbia. Geological Survey of Canada Paper 60-2

Pelletier, B.R., 1961. Triassic stratigraphy of the Rocky Mountains and Foothills, northeastern British Columbia. Geological Survey of Canada Paper 61-8

Pelletier, B.R., 1963. Triassic stratigraphy of the Rocky Mountains and Foothills, Peace River district, British Columbia. Geological Survey of Canada Paper 63-33

Pelletier, B.R., 1964. Triassic stratigraphy of the Rocky Mountain Foothills between Peace and Muskwa Rivers, northeastern British Columbia. Geological Survey of Canada Paper 63-33

Pelletier, B.R., 1965. Paleocurrents in the Triassic of northeastern British Columbia. *In,* Primary Sedimentary Structures and their Hydrodynamic Interpretation, Middleton, G.V. (ed.), Society of Economic Paleontologists and Mineralogists Special Publication, **12**, 233-245

Pelletier, B.R. and Stott, D.F., 1963. Geology of Trutch map-area, British Columbia. Geological Survey of Canada Paper 63-10

Pevný, J. and Salaj, J., 1997. The Anisian-Ladinian boundary at Zakázané (Slovak Karst, Western Carpathians). Zemní plyn a nafta, **42**, 97-149

Piercey, S.J., Mortensen, J.K., Murphy, D.C., Paradis, S. and Creaser, R.A., 2002. Geochemistry and tectonic significance of alkalic mafic magmatism in the Yukon-Tanana terrane, Finlayson Lake region, Yukon. Canadian Journal of Earth Sciences, **39**, 1729-1744

Pisa, G., Perri, C. and Veneri, P., 1980. Upper Anisian conodonts from Dont and M. Bivera formations, Southern Alps (Italy). Rivista Italiana di Paleontologia e Stratigrafia, **85**, 807-828

Posamentier, H.W. and Vail, P.R., 1988. Eustatic controls on clastic deposition II. Sequence and systems tract models. *In,* Sea Level Changes – An Integrated Approach, Wilgus, C.K., Hastings, B.S., Kendall, C.G.St.C., Posamentier, H.W., Ross, C.A. and Van Wagoner, J.C. (eds.), Society of Economic Paleontologists and Mineralogists Special Publication, **42**, 125-154

Poulton, T.P., 1989. Upper Absaroka to Lower Zuni: The Transition to the Foreland Basin. *In,* Western Canada Sedimentary Basin – A Case History, Ricketts, B.D. (ed.), Canadian Society of Petroleum Geologists, 233-247

Preto, N., Kustatscher, E. and Wignall, P.B., 2010. Triassic climates – state of the art and perspectives. Palaeogeography, Palaeoclimatology, Palaeoecology, **290**, 1-10

Pufahl, P.K. and Grimm, K.A., 2003. Coated phosphate grains: Proxy for physical, chemical, and ecological changes in seawater. Geology, **31**, 801-804

Purnell, M.A. and Donoghue, P.C.J., 2005. Between death and data: biases in interpretation of the fossil record of conodonts. *In*, Conodont biology and phylogeny: interpreting the fossil record, Purnell, M.A. and Donoghue, P.C.J. (eds.), Special Papers in Palaeontology, **73**, 7-26

Purnell, M.A., Donoghue, P.C.J. and Aldridge, R.J., 2000. Orientation and anatomical notation in conodonts. Journal of Paleontology, **74**, 113-122

Qi, Fazheng, 1995. Seismic stratigraphy and sedimentary facies of the Middle Triassic strata, Western Canada Sedimentary Basin, northeastern British Columbia. Unpublished PhD Thesis. University of Alberta. 219 p.

Racki, G. 1999. Silica-secreting biota and mass extinctions: survival patterns and processes. Palaeogeography, Palaeoclimatology, Palaeoecology, **154**, 107-132

Rafek, M.B., 1977. Platform Conodonts from the Middle Triassic Upper Muschelkalk of West Germany and N.E. France. Unpublished PhD Thesis. University of Bonn. 86 p.

Rahman, B., 2005. Anomalously thick sandstone bodies of the Middle Triassic Doig and Halfway formations and their exploration significance. Canadian Society of Petroleum Geologists Reservoir, **32**, 3, 14

Rahman, B. and Henderson, C.M., 2005. The nature and significance of erosion surfaces in the Middle Triassic Doig and Halfway formations, WCSB. Canadian Society of Petroleum Geologists Core Conference, Calgary, 298-299

Raup, D.M., 1979. Size of the Permo-Triassic bottleneck and its evolutionary implications. Science, **206**, 217-218

Raup, D.M., 1992. Large-body impact and extinction in the Phanerozoic. Paleobiology, **18**, 80-88

Renne, P.R., Zichao, Z., Richards, M.A., Black, M.T. and Basu, A.R., 1995. Synchrony and causal relationships between Permian-Triassic boundary crises and Siberian flood volcanism. Science, **269**, 1413-1416

Retallack, G.J., 1995. Permo-Triassic life crisis on land. Science, **267**, 77-80

Retallack, G.J., 2001. A 300-million-year record of atmospheric carbon dioxide from fossil plant cuticles. Nature, **411**, 287-290

Retallack, G.J. and Jahren, A.H., 2008. Methane release from igneous intrusion of coal during Late Permian extinction events. The Journal of Geology, **116**, 1-20

Retallack, G.J., Veevers, J.J. and Morante R., 1996. Global coal gap between Permian-Triassic extinction and Middle Triassic recovery of peat-forming plants. Geological Society of America Bulletin, **108**, 195-207

Retallack, G.J., Seyedolai, A., Krull, E.S., Holser, W.T., Ambers, C.P. and Kyte, F.T., 1998. Search for evidence of impact at the Permian-Triassic boundary in Antarctica and Australia. Geology, **26**, 979-982

Richards, B.C., 1989. Upper Kaskaskia Sequence – uppermost Devonian and Lower Carboniferous. *In,* Western Canada Sedimentary Basin – a Case History, Ricketts, B.D. (ed.), Canadian Society of Petroleum Geologists, Special Publication, **30**, 165-202

Richards, B.M., Ross, G.M. and Utting, J., 2002. U-Pb geochronology, lithostratigraphy and biostratigraphy of tuff in the Upper Fammennian to Tournaisian Exshaw Formation: evidence for a mid-Paleozoic magmatic arc on the northwestern margin of North America. *In,* Carboniferous and Permian of the world, Hills, L.V., Henderson, C.M. and Bamber, E.W. (eds.), Canadian Society of Petroleum Geologists, Memoir 19, 158-207

Richoz, S., Heindel, K., Birgel, D., Brandner, R., Mohtat, T., Horacek, M., Baud, A., Krystyn, L., Klügel, A. and Peckmann, J., 2013. Hypersaline and low-oxygen Early Triassic marine environment favor microbial mats and the formation of diagenetic carbonate crystal fans. Geological Society of Amercia Abstracts with Programs, **45**, 232

Ricketts, B.D., 1989. Introduction. *In,* Western Canada Sedimentary Basin – a Case History, Ricketts, B.D. (ed.), Canadian Society of Petroleum Geologists, Special Publication, **30**, 3-8

Riediger, C.L., Brooks, P.W., Fowler, M.G. and Snowden, L.R., 1990. Lower and Middle Triassic source rocks, thermal maturation, and oil-source rock correlations in the Peace River Embayment area, Alberta and British Columbia. Bulletin of Canadian Petroleum Geology, **38A**, 218-235

Ritter, S.M., 1989. Morphometric patterns in Middle Triassic *Neogondolella mombergensis* (Conodonta), Fossil Hill, Nevada. Journal of Paleontology, **63**, 233-245

Romano, C., Goudemand, N., Vennemann, T.W., Ware, D., Schneebeli-Herman, E., Hochuli, P.A., Brühwiler, T., Brinkmann, W. and Bucher, H., 2013. Climatic and biotic upheavals following the end-Permian mass extinction. Nature Geoscience, **6**, 57-60

Ross, G.M. and Villeneuve, M., 2003. Provenance of the Mesoproterozoic (1.45 Ga) Belt basin (western North America): another piece in the pre-Rodinia paleogeographic puzzle. Geological Society of America Bulletin, **155**, 1191-1217

Ross, G.M., Gehrels, G.E. and Patchett, P.J., 1997. Provenance of Triassic strata in the Cordilleran miogeocline, western Canada. Bulletin of Canadian Petroleum Geology, **45**, 461-473

Ross, G.M., McMechan, M.E. and Hein, F.J., 1989. Proterozoic history: the birth of the miogeocline. *In,* Western Canada Sedimentary Basin – a Case History, Ricketts, B.D. (ed.), Canadian Society of Petroleum Geologists, Special Publication, **30**, 79-104

Ruhl, M., Bonis, N.R., Reichart, G.-J., Sinninghe Damasté, J.S. and Kürschner, W.M., 2011. Atmospheric carbon injection linked to end-Triassic mass extinction. Science, **333**, 430-434

Sano, H. and Nakashima, K., 1997. Lowermost Triassic (Griesbachian) microbial bindstone-cementstone facies, southwest Japan. Facies, **36**, 1-24

Schiarizza, P., 1989. Structural and stratigraphic relationships between the Fennel Formation and Eagle Bay assemblage, western Omineca belt, south-central British Columbia: Implications for Paleozoic tectonics along the paleocontinental margin of western North America. Unpublished M.Sc. Thesis. University of Calgary. 343 p.

Schoene, B., Guex, J., Bartolini, A., Schaltegger, U. and Blackburn, T.J., 2010. Correlating the end-Triassic mass extinction and flood basalt volcanism at the 100 ka level. Geology, **38**, 387-390

Schoepfer, S., Henderson, C.M., Garrison, G.H. and Ward, P., 2012. Cessation of a productive coastal upwelling system in the Panthalassic Ocean at the Permian-Triassic Boundary. Palaeogeography, Palaeoclimatology, Palaeoecology, **313-314**, 181-188

Schoepfer, S.D., Henderson, C.M., Garrison, G.H., Foriel, J., Ward, P.D., Selby, D., Hower, J.C. and Shen, Y., 2013. Termination of a continent-margin upwelling system at the Permian-Triassic boundary, Opal Creek, Alberta, Canada. Global and Planetary Change, **105**, 21-35

Schopf, T.J.M., 1974. Permo-Triassic extinctions: relation to sea-floor spreading. Journal of Geology, **82**, 129-143

Schubert, J.K. and Bottjer, D.J., 1995. Aftermath of the Permian-Triassic mass extinction event: paleoecology of Lower Triassic carbonates in the western USA. Palaeogeography, Palaeoclimatology, Palaeoecology, **116**, 1-39

Seilacher, A., 1967. Bathymetry of trace fossils. Marine Geology, **5**, 413-428

Selwyn, A.R.C., 1877. Report on exploration in British Columbia in 1875. Geological Survey of Canada, Report of Progress 1875-76

Sepkoski, J.J., 1981. A factor analytic description of the Phanerozoic marine fossil record. Paleobiology, **7**, 36-53

Shen, S., Crowley, J.L., Wang, Y., Bowring, S.A., Erwin, D.H., Sadler, P.M., Cao, C., Rothman, D.H., Henderson, C.M., Ramezani, J., Zhang, H., Shen, Y., Wang, X., Wang, W., Mu, L., Li, W., Tang, Y., Liu, X., Liu, L., Zeng, Y., Jiang, Y. and Jin, Y., 2011. Calibrating the End-Permian Mass Extinction. Science, **334**, 1367-1372

Silberling, N.J. and Nichols, K.M., 1982. Middle Triassic molluscan fossils of biostratigraphic significance from the Humboldt Range, northwestern Nevada. U.S. Geological Survey Professional Paper 1207

Silberling, N.J. and Tozer, E.T., 1968. Biostratigraphic classification of the marine Triassic in North America. U.S. Geological Survey Special Paper 110

Silberling, N.J. and Wallace, R.E., 1969. Stratigraphy of the Star Peak Group (Triassic) and overlying Mesozoic rocks, Humboldt Range, Nevada. U.S. Geological Survey Professional Paper, **592**, 50p.

Simberloff, D.S., 1974. Permian mass extinction: effects of area on biotic equilibrium. Journal of Geology, **82**, 267-274

Simms, M.J. and Ruffel, A.H., 1989. Synchroneity of climatic change and extinctions in the Late Triassic. Geology, **17**, 265-268

Simms, M.J. and Ruffell, A.H., 1990. Climatic and biotic change in the Late Triassic. Journal of the Geological Society of London, **147**, 321–327

Sláma, J., Košler, J., Condon, D.J., Crowley, J.L., Gerdes, A., Hanchar, J.M., Horstwood, M.S.A., Morris, G.A., Nasdala, L., Norberg, N., Schaltegger, U., Schoene, B., Tubrett, M.N. and Whitehouse, M.J., 2008. Plešovice zircon – a new natural reference material for U-Pb and Hf isotopic microanalysis. Chemical Geology, **249**, 1-35

Smith, A.B., 2001. Large-scale heterogenity of the fossil record: implications for Phanerozoic biodiversity studies. Philosophical Transactions of the Royal Society of London, Series B**, 356**, 351-367

Smith, R.M.H. and Ward, P.D., 2001. Pattern of vertebrate extinctions across an event bed at the Permian-Triassic boundary in the Karoo Basin of South Africa. Geology, **29**, 1147-1150

Smith, A.G., Smith, D.G. and Funnell, B.M., 1995. Atlas of Mesozoic and Cenozoic Coastlines. Cambridge University Press.

Song, H., Wignall, P.B., Tong, J. and Yin, H., 2013. Two pulses of extinction during the Permian-Triassic crisis. Nature Geoscience, **6**, 52-56

Stanley Jr., G.D., 1988. The history of Early Mesozoic reef communities: a three-step process. Palaios, **3**, 170– 183

Stephens, M.B. and Gee, D.G., 1985. A new tectonic model for the evolution of the eugeoclinal terranes in the central Scandinavian Caledonides. *In,* The Caledonian orogen – Scandinavia and related areas, Gee, D.G. and Stuart, B.A. (eds.), John Wiley and Sons Ltd., Chichester, UK, 953-978

Stewart, J.H., 1972. Initial deposits of the Cordilleran geosyncline: evidence of Late Precambrian (<850my) continental separation. Geological Society of America Bulletin, **83**, 1345-1360

Stone, J., 1987. Review of investigative techniques used in the study of conodonts. *In,* Conodonts: Investigative Techniques and Applications, Austin, R.L. (ed.), British Micropalaeontological Society Series, Ellis Horwood Ltd., 17-34

Struik, L.C., 1994. Geology of the McLeod Lake map area (93J), British Columbia. Geological Survey of Canada, Open File 2439

Sudar, M.N., 1982. Conodonts from Bulog Limestones of the Inner Dinarides in Yugoslavia and their biostratigraphic importance. Annales Géologiques de la Péninsule Balkanique, **46**, 263-282

Sudar, M.N., 1986. Triassic microfossils and biostratigraphy of the Inner Dinarides in Yugoslavia and their biostratigraphic importance. Annales Géologiques de la Péninsule Balkanique, **50**, 150-394

Sweet, W.C., 1970. Uppermost Permian and Lower Triassic conodonts of the Salt Range and Trans-Indus Ranges, West Pakistan. *In*, Stratigraphic Boundary Problems, Permian and Triassic of West Pakistan, Kummel, B. and Teichert, C. (eds.), University of Kansas Department of Geology Special Publication, **4**, 207-275

Sweet, W.C., Mosher, L.C., Clark, D.L., Collinson, J.W. and Hasenmueller, W.A., 1971. Conodont biostratigraphy of the Triassic. Geological Society of America Memoir, **127**, 441-465

Tanner, L.H. and Lucas, S.G., 2013. Terrestrial end of Triassic extinctions: neither sudden nor severe. Geological Society of America Abstracts with Programs, **45**, 305

Tanner, L.H., Lucas, S.G. and Chapman, M.G., 2004. Assessing the record and causes of Late Triassic extinctions. Earth Science Reviews, **65**, 103-139

Tatge, U., 1956. Conodonten aus dem germanischen Muschelkalk. Paläontologische Zeitschrift, 30, 108-127

Thompson, R.I., 1989. Stratigraphy, tectonic evolution and structural analysis of the Halfway River map area (94 B), northern Rocky Mountains, British Columbia. Geological Survey of Canada Memoir 425

Tipper, H.W., Carter, E.S., Orchard, M.J. and Tozer, E.T., 1994. The Triassic-Jurassic (T-J) boundary in Queen Charlotte Islands, British Columbia defined by ammonites, conodonts and radiolarians. Geobios, **17**, 485-492

Tomašových, A. and Siblík, M., 2007. Evaluating compositional turnover of brachiopod communities during the end-Triassic mass extinction (Northern Calcareous Alps): removal of dominant groups, recovery and community reassembly. Palaegeography, Palaeoclimatology, Palaeoecology, **244**, 170-200

Tozer, E.T., 1961. The sequence of marine Triassic faunas in western Canada. Geological Survey of Canada Paper 61-6

Tozer, E.T., 1965. Latest Lower Triassic ammonoids from Ellesmere Island and northeastern British Columbia. Geological Survey of Canada Bulletin 123

Tozer, E.T., 1967. A standard for Triassic time. Geological Survey of Canada Bulletin 156

Tozer, E.T., 1971. Triassic time and ammonoids: Problems and proposals. Canadian Journal of Earth Sciences, **8**, 989-1031

Tozer, E.T., 1981. Triassic Ammonoidea: geographic and stratigraphic distribution. *In*, The Ammonoidea, House, M.R. and Senior, J.R. (eds.), Systematics Association Special Volume, **18**, 397-431

Tozer, E.T., 1982. Marine Triassic faunas of North America: their significance for assessing plate and terrane movements. Geologische Rundschau, **71**, 1077-1104

Tozer, E.T., 1984. The Trias and its ammonoids: the evolution of a timescale. Geological Survey of Canada Miscellaneous Report 35

Tozer, E.T., 1994. Canadian Triassic Ammonoid Faunas. Geological Survey of Canada Bulletin 467

Trammer, J., 1975. Stratigraphy and facies development of the Muschelkalk in the south-western Holy Cross Mts. Acta Geologica Polonica, **25**, 179-216

Trettin, H.P., Parrish, R. and Loveridge, W.D., 1987. U-Pb age determinations on Proterozoic to Devonian rocks from northern Ellesmere Island, Arctic Canada. Canadian Journal of Earth Sciences, **24**, 246-256

Trettin, H.P., Okulitch, A.V., Harrison, J.C., Brent, T.A., Fox, F.G., Packard, J.J., Smith, G.P. and Zolnai, A.I., 1991. Silurian-Early Carboniferous deformational phases and associated metamorphism and plutonism, Arctic Islands. *In*, Geology of the Innuitian Orogen and Arctic Platform of Canada and Greenland, Trettin, H.P. (ed.), Geological Survey of Canada, Geology of Canada, 293-341

Twitchett, R.J., 1999. Palaeoenvironments and faunal recovery after the end-Permian mass extinction. Palaeogeography, Palaeoclimatology, Palaeoecology, **154**, 27-37

Twitchett, R.J., 2007. The Lilliput effect in the aftermath of the end-Permian extinction event. Palaeogeography, Palaeoclimatology, Palaeoecology, **252**, 132-144

Twitchett, R.J. and Wignall, P.B., 1996. Trace fossils and the aftermath of the Permo-Triassic mass extinction: evidence from northern Italy. Palaeogeography, Palaeoclimatology, Palaeoecology, **124**, 137-151

Twitchett, R.J., Krystyn, L., Baud, A., Wheeley, J.R. and Richoz, S., 2004. Rapid marine recovery after the end-Permian mass extinction in the absence of marine anoxia. Geology, **32**, 805-808

Twitchett, R.J., Feinberg, J.M., O'Connor, D., Alvarez, W. and McCollum, L.B., 2005. Early Triassic ophiuroids: their paleoecology, taphonomy and distribution. Palaios, **20**, 213-223

Umhoeffer, P.J. and Schiarizza, P., 1996. Latest Cretaceous to early Tertiary dextral strike-slip faulting on the southeastern Yalakom fault system, southeastern Coast belt, British Columbia. Geological Society of America Bulletin, **108**, 768-785

Unterschutz, J.L.E., Creaser, R.A., Erdmer, P., Thompson, R.I. and Daughtry, K.L., 2002. North American margin origin of Quesnel terrane strata in the southern Canadian Cordillera: Inferences from geochemical and Nd isotopic characteristics of Triassic metasedimentary rocks. Geological Society of America Bulletin, **114**, 462-475

Utting, J., 1994. Palynostratigraphy of Permian and Lower Triassic rocks, Sverdrup Basin, Canadian Arctic Archipelago. Geological Survey of Canada Bulletin 478

Utting, J, Zonneveld, J.-P., MacNaughton, R.B. and Fallas, K.M., 2005. Palynostratigraphy, lithostratigraphy and thermal maturity of the Lower Triassic Toad and Grayling, and Montney formations of western Canada, and comparisons with coeval rocks of the Sverdrup Basin, Nunavut. Bulletin of Canadian Petroleum Geology, **53**, 5-24

van Achterbergh, E., Ryan, C.G., Jackson, S. and Griffin, W.L., 2001. Data reduction software for LA-ICP-MS. *In,* Laser-Ablation-ICPMS in the Earth Sciences: Principles and Applications, Sylvester, P. (ed.), Mineralogical Association of Canada Short Course Series, **29**, 239-243

van de Schootbrugge, B., Tremolada, F., Rosenthal, Y., Bailey, T.R., Feist-Burkhardt, S., Brinkhuis, H., Pross, J., Kent, D.V. and Falkowski, P.G., 2007. End-Triassic calcification crisis and blooms of organic-walled "disaster species". Palaeogeography, Palaeoclimatology, Palaeoecology, **244**, 126-141

Veevers, J.J., 1994. Pangaea: evolution of a supercontinent and its consequences for Earth's paleoclimate and sedimentary environments. *In*, Pangaea: paleoclimate, tectonics and sedimentation during accretion, zenith, and breakup of a supercontinent, Klein, G.D. (ed.), Geological Society of America Special Paper, **288**, 12-24

Veevers, J.J., Conaghan, P.J. and Shaw, S.E., 1994. Turning point in Pangaean environmental history at the Permian/Triassic (P/T) boundary. *In,* Pangaea: paleoclimate, tectonics and sedimentation during accretion, zenith, and breakup of a supercontinent, Klein, G.D. (ed.), Geological Society of America Special Paper, **288**, 187-196

Vermeesch, P., 2004. How many grains are needed for a provenance study? Earth and Planetary Science Letters, **224**, 441-451

Vernikovsky, V.A., Salanikova, E.B., Kotov, A.B., Kovach, V.P. and Yakovleva, S.Z., 1981. Precambrian granites of the Faddey terrane (northern Taimyr): New geochemical and geochronological (U-Pb, Sm-Nd) data (in Russian), Doklady Akademii Nauk, **363**, 653-657

Villeneuve, M.E., Ross, G.M., Theriault, R.J., Milles, W., Parrish, R.R. and Broome, J., 1993. Tectonic subdivision and U-Pb geochronology of the crystalline basement of the Alberta basin, western Canada. Geological Survey of Canada Bulletin 444

Villeneuve, M.E., Ryan, J.J., Gordey, S. and Piercey, S.J., 2003. Combining SHRIMP, TIMS U-Pb and Ar-Ar to resolve magmagenesis, metamorphism, and fluid flow in three coincident

magmatic arcs, Yukon-Tanana terrane, western Yukon. Eos Transactions, American Geophysical Union, **84**, Fall Meeting Supplement, V32C-1038

Visscher, H., 1992. The new STS Triassic stage nomenclature. Albertiana, **10**, 1-2

Visscher, H., Brinkhuis, H., Dilcher, D.L., Elsik, W.C., Eshet, Y., Looy, C.V., Rampino, M.R. and Traverse, A., 1996. The terminal Paleozoic fungal event: evidence of terrestrial ecosystem destabilization and collapse. Proceedings of the National Academy of Science of the United States of America, **93**, 2155-2158

Vrielynck, B., 1987. Conodontes du Trias Périméditerranéen. Systématique, stratigraphie. Documents des Laboratoires de Géologie de Lyon, **97**, 301p.

Waagen, W. and Diener, C., 1895. Untere Trias. *In,* Entwurf einer Gliederung der pelagischen Sedimente des Trias-Systems, Mojsisovics, E. von, Waagen, W. and Diener, C. (eds.) Sitzungsberichte Akademie Wissenschaft Wien, Mathematische – naturwissenschaftliche Klasse, **104**, 1271-1302

Walsh, W., Adams, C., Kerr, B. and Korol, J., 2006. Regional "shale gas" potential of the Triassic Doig and Montney formations, northeastern British Columbia. British Columbia Ministry of Energy, Mines and Petroleum Resources, Resource Development and Geoscience Branch, Petroleum Geology Open File 2006-02

Ward, P.D., Haggart, J.W., Carter, E.S., Wilbur, D., Tipper, H.W. and Evans, T., 2001. Sudden productivity collapse associated with the Triassic-Jurassic boundary mass extinction. Science, **292**, 1148-1151

Westermann, G.E., 1962. Succession and variation of *Monotis* and the associated fauna in the Norian Pine River Bridge section, British Columbia (Triassic pelecypoda). Journal of Paleontology, **36**, 745-792

Wheeler, J.O., Brookfield, A.J., Gabrielse, H., Monger, J.W.H., Tipper, H.W. and Woodsworth, G.J., 1991. Terrane map of the Canadian Cordillera. Geological Survey of Canada Map 1713A

Wignall, P.B., 2001. Large igneous provinces and mass extinctions. Earth Science Reviews, **53**, 1-33

Wignall, P.B. and Hallam, A., 1992. Anoxia as a cause of the Permian/Triassic mass extinction: facies evidence from northern Italy and the western United States. Palaeogeography, Palaeoclimatology, Palaeoecology, **93**, 21-46

Wignall, P.B. and Hallam A., 1993. Griesbachian (earliest Triassic) palaeoenvironmental changes in the Salt Range, Pakistan and southeast China and their bearing on the Permo-Triassic mass extinction. Palaeogeography, Palaeoclimatology, Palaeoecology, **102**, 215-237

Williams, M.Y., 1944. Geological reconnaissance along the Alaska Highway from Fort Nelson, British Columbia to Watson Lake, Yukon. Geological Survey of Canada Paper 44-28

Williams, M.Y. and Bocock, J.B., 1932. Stratigraphy and paleontology of Peace River vicinity of British Columbia. Transactions of the Royal Society of Canada, **26**, 197-224

Willis, A.J., 1992. Sedimentology and stratigraphic framework of the Middle Triassic Halfway Formation, Wembley oilfield, Alberta. Unpublished M.Sc. Thesis. University of Alberta. 412p.

Willis, A.J. and Moslow, T.F., 1994. Sedimentology and stratigraphy of tidal-inlet reservoirs in the Triassic Halfway Formation, Wembley Field, Alberta. Bulletin of Canadian Petroleum Geology, **42**, 245-262

Wittenburg, J., 1992. Origin and stratigraphic significance of anomalously thick sandstone trends in the Middle Triassic Doig Formation of west-central Alberta. Unpublished MSc. Thesis. University of Alberta. 600 p.

Woods, A.D., Zonneveld, J.-P. and Wakefield, R., 2013. Trace metal data from Lower and lowermost Middle Triassic rocks from Ursula Creek, British Columbia reveals persistent anoxia and variable paleoproductivity history in the aftermath of the Permian-Triassic mass extinction. Geological Society of America Abstracts with Programs, **45**, 884

Yin, H., Zhang, K., Tong, J., Yang, Z. and Wu, S., 2001. The Global Stratotype Section and Point (GSSP) of the Permian-Triassic boundary. Episodes, **24**, 102-114

Yin, H., Xie, S., Luo, G., Algeo, T.J. and Zhang, K., 2012. Two episodes of environmental change at the Permian-Triassic boundary of the GSSP section Meishan. Earth Science Reviews, **115**, 163-172

Zawidzka, K., 1975. Conodont stratigraphy and sedimentary environment of the Muschelkalk in Upper Silesia. Acta Geologica Polonica, **25**, 217-245

Zhang, K., Lai, X., Ding, M. and Liu, J., 1995. Conodont sequence and its global correlation of Permian-Triassic boundary in Meishan section, Changxing, Zhejiang Province. Earth Science, Journal of China University of Geosciences, **20**, 669-676

Zhao, L., Orchard, M.J., Tong, J., Sun, Z., Zuo, J., Zhang, S. and Yun, A., 2007. Lower Triassic conodont sequence in Chaohu, Anhui Province, China and its global correlation. Palaeogeography, Palaeoclimatology, Palaeoecology, **252**, 24-38

Zhao, L., Orchard, M.J. and Tong, J., 2004. Lower Triassic conodont biostratigraphy and speciation of *Neospathodus waageni* around the Induan-Olenekian boundary of Chaohu, Anhui Province, China. Albertiana, **29**, 41-43

Ziegler, A.M., Scotese, C.R. and Barrett, S.F., 1983. Mesozoic and Cenozoic paleogeographic maps. *In*, Tidal Friction and the Earth's Rotation, Brosche, P. and Sündermann, J. (eds.), Springer-Verlag, 240-252

Zonneveld, J.-P., 2010. The Triassic of northeastern British Columbia: sedimentary characteristics and stratigraphic architecture of conventional and unconventional reservoir

successions. Geological Association of Canada-Mineralogical Association of Canada Joint Annual Meeting (GeoCanada 2010), Williston Lake Field Trip Guidebook, 158p.

Zonneveld, J.-P., 2011. Suspending the rules: unraveling the ichnological signature of the Lower Triassic post-extinction recovery interval. Palaios, **26**, 677-681

Zonneveld, J.-P., Moslow, T.F. and Henderson, C.M., 1997. Lithofacies associations and depositional environments in a mixed siliciclastic-carbonate coastal depositional system, upper Liard Formation, Triassic, northeastern British Columbia. *In*, Triassic of the Western Canada Sedimentary Basin, Moslow, T.F. and Wittenberg, J. (eds.), Bulletin of Canadian Petroleum Geology, **45**, 474-505

Zonneveld, J.-P., Gingras, M.K. and Pemberton, S.G., 2001. Trace fossil assemblages in a Middle Triassic mixed siliciclastic-carbonate marginal marine depositional system, British Columbia. Palaeogeography, Palaeclimatology, Palaeoecology, **166**, 249-276

Zonneveld, J.-P., Ferri, F., Beatty, T.W. and Gingras, M.K., 2010 a. Unrecognized potential for thick Triassic reservoirs in frontier areas of NE British Columbia. AAPG Annual Conference, 2010

Zonneveld, J.-P., Gingras, M.K. and Beatty, T.W., 2010 b. Diverse ichnofossil assemblages following the the P-T mass extinction, Lower Triassic, Alberta and British Columbia, Canada: evidence for shallow marine refugia on the northwestern coast of Pangaea. Palaios, **25**, 368-392

Zonneveld, J.-P., MacNaughton, R.B., Utting, J., Beatty, T.W., Pemberton, S.G. and Henderson, C.M., 2010 c. Sedimentology and ichnology of the Lower Triassic Montney Formation in the Pedigree-Ring/Border-Kahntah River area, northwestern Alberta and northeastern British Columbia. *In*, Applications of Ichnology to Petroleum Exploration, Zonneveld, J.-P., Gingras, M.K. and MacEachern, J.A. (eds.), Bulletin of Canadian Petroleum Geology, **58**, 115-14

Zubin-Stathopoulos, K.D., Beauchamp, B., Davydov, V.I., Henderson, C.M., 2012. Variability of Pennsylvanian-Permian Carbonate Associations and implications for NW Pangea Paleogeography, east-central British Columbia, Canada. *In*, Gasiewicz, A. and Slowakiewicz, M. (eds.) Paleozoic Climate Cycles: Their Evolutionary and Sedimentological Impact, Geological Society, London, Special Publications, **376**, p.47-71

# APPENDIX 1

# SAMPLE TABLE

| New Conodont Samples from Surface British Columbia | | | | | | |
|---|---|---|---|---|---|---|
| **Sample No.** | **Locality** | **Height Above Base/m** | **Formation** | **Age** | **GSC No.** | **Productive** |
| 08-2009/C1 | South Halfway | 39.00 | Toad | Unknown | N/A | No |
| 08-2009/C2 | South Halfway | 88.00 | Toad | Unknown | N/A | No |
| 08-2009/C3 | South Halfway | 140.00 | Toad | Unknown | N/A | No |
| 08-2009/C4 | South Halfway | 160.00 | Toad | Unknown | N/A | No |
| 08-2009/C5 | South Halfway | 199.00 | Toad | Unknown | N/A | No |
| 08-2009/C6 | South Halfway | 216.00 | Toad | Unknown | N/A | No |
| 08-2009/C7 | South Halfway | 228.00 | Toad | Unknown | N/A | No |
| 08-2009/C8 | South Halfway | 279.00 | Toad | Unknown | N/A | No |
| 08-2009/C9 | South Halfway | 327.00 | Toad | Unknown | N/A | No |
| 08-2009/C10 | South Halfway | 397.00 | Toad | Unknown | N/A | No |
| 08-2009/C11 | South Halfway | 428.00 | Toad | Unknown | N/A | No |
| 08-2009/C12 | South Halfway | 450.00 | Toad | Unknown | N/A | No |
| 08-2009/C13 | South Halfway | 468.00 | Toad | Unknown | N/A | Yes |
| 08-2009/C14 | South Halfway | 513.00 | Toad | Unknown | N/A | Yes |
| 08-2009/C15 | South Halfway | 637.00 | Liard | Lad/Car | N/A | Yes |
| MG-10-BBR02 | Black Bear Ridge | 242.80 | Pardonet | Rhaetian | N/A | Yes |
| MG-10-BBR03 | Black Bear Ridge | 242.80 | Pardonet | Rhaetian | N/A | No |
| MG-10-BBR04 | Black Bear Ridge | 243.80 | Pardonet | Rhaetian | N/A | No |
| MG-10-BBR05 | Black Bear Ridge | 244.05 | Pardonet | Rhaetian | N/A | No |
| MG-10-GS06A | Glacier Spur | 129.00 | Liard | Ladinian | N/A | Yes |
| MG-10-GS06B | Glacier Spur | 235.00 | Liard | Ladinian | N/A | Yes |
| MG-10-GS07 | Glacier Spur | 312.30 | Liard | Ladinian | N/A | Yes |
| MG-10-GS08 | Glacier Spur | 312.70 | Liard | Ladinian | N/A | Yes |
| MG-10-GS09 | Glacier Spur | 313.00 | Liard | Ladinian | N/A | Yes |
| MG-10-GS10 | Glacier Spur | 319.30 | Liard | Ladinian | N/A | Yes |
| MG-10-BL36 | Beattie Ledge | 36.00 | Liard | Ladinian | N/A | Yes |
| MG-10-BL48.5 | Beattie Ledge | 48.50 | Liard | Ladinian | N/A | Yes |
| MG-11-MP386-C1 | Mile Post 386 | 3.50 | Toad | Ladinian | N/A | Yes |
| MG-11-MP386-C2 | Mile Post 386 | 8.00 | Toad | Ladinian | N/A | Yes |

| New Conodont Samples from Surface British Columbia | | | | | | |
|---|---|---|---|---|---|---|
| **Sample No.** | **Locality** | **Height Above Base/m** | **Formation** | **Age** | **GSC No.** | **Productive** |
| MG-11-MP386-C3 | Mile Post 386 | 12.00 | Toad | Ladinian | N/A | Yes |
| MG-11-MP386-C4 | Mile Post 386 | 14.10 | Toad | Ladinian | N/A | Yes |
| MG-11-MP386-C5 | Mile Post 386 | 17.50 | Toad | Ladinian | N/A | Yes |
| MG-11-NTP-C0 | North Tetsa Phosphate | -0.30 | Toad | Anisian | N/A | Yes |
| MG-11-NTP-C1 | North Tetsa Phosphate | 0.45 | Toad | Anisian | N/A | Yes |
| MG-11-NTP-C2 | North Tetsa Phosphate | 2.60 | Toad | Anisian | N/A | No |
| MG-11-NTP-C3 | North Tetsa Phosphate | 2.70 | Toad | Anisian | N/A | No |
| MG-11-NTP-C4 | North Tetsa Phosphate | 2.80 | Toad | Anisian | N/A | No |
| MG-11-NTP-C5 | North Tetsa Phosphate | 3.18 | Toad | Anisian | N/A | Yes |
| MG-11-NTP-C6 | North Tetsa Phosphate | 3.40 | Toad | Anisian | N/A | Yes |
| MG-11-NTP-C7 | North Tetsa Phosphate | 4.30 | Toad | Anisian | N/A | Yes |
| MG-11-NTP-C8 | North Tetsa Phosphate | 5.60 | Toad | Anisian | N/A | Yes |
| MG-11-NTP-C9 | North Tetsa Phosphate | 7.55 | Toad | Anisian | N/A | No |
| MG-11-NTP-C10 | North Tetsa Phosphate | 9.55 | Toad | Anisian | N/A | No |
| MG-11-NTP-C11 | North Tetsa Phosphate | 10.60 | Toad | Anisian | N/A | No |
| MG-11-NTP-C12 | North Tetsa Phosphate | 11.35 | Toad | Anisian | N/A | Yes |
| MG-11-NTP-C13 | North Tetsa Phosphate | >11.35 | Toad | Anisian | N/A | Yes |
| MG-11-YB-C1 | Yellow Bluffs | 1.70 | Toad | Anisian | N/A | No |
| MG-11-YB-C2 | Yellow Bluffs | 1.70 | Toad | Anisian | N/A | Yes |
| MG-11-YB-C3 | Yellow Bluffs | 3.00 | Toad | Anisian | N/A | No |
| MG-11-YB-C4 | Yellow Bluffs | 3.00 | Toad | Anisian | N/A | Yes |
| MG-11-YB-C5 | Yellow Bluffs | 3.75 | Toad | Anisian | N/A | Yes |
| MG-11-YB-C6 | Yellow Bluffs | 3.75 | Toad | Anisian | N/A | No |
| MG-11-YB-C7 | Yellow Bluffs | Talus | Toad | Anisian | N/A | Yes |
| MG-11-YB-C8 | Yellow Bluffs | 10.00 | Toad | Anisian | N/A | No |
| MG-11-YB-C9 | Yellow Bluffs | 10.00 | Toad | Anisian | N/A | Yes |
| MG-11-YB-C10 | Yellow Bluffs | 8.00 | Toad | Anisian | N/A | Yes |
| MG-11-YB-C11 | Yellow Bluffs | 13.00 | Toad | Anisian | N/A | Yes |
| MG-11-YB-C12 | Yellow Bluffs | 13.00 | Toad | Anisian | N/A | Yes |

| New Conodont Samples from Surface British Columbia | | | | | | |
|---|---|---|---|---|---|---|
| **Sample No.** | **Locality** | **Height Above Base/m** | **Formation** | **Age** | **GSC No.** | **Productive** |
| MG-11-YB-Cfloat | Yellow Bluffs | Talus | Toad | Anisian | N/A | Yes |
| MG-11-SL-C1 | Sanitary Landfill | Unknown | Toad | Unknown | N/A | No |
| MG-11-SL-C2 | Sanitary Landfill | Unknown | Toad | Unknown | N/A | No |
| MG-11-MP375W-C0 | Mile Post 375 West | Unknown | Toad | Anisian | N/A | No |
| MG-11-MP375W-C1 | Mile Post 375 West | Unknown | Toad | Anisian | N/A | No |
| MG-11-MP375W-C2 | Mile Post 375 West | Unknown | Toad | Anisian | N/A | No |
| MG-11-MP375W-C3 | Mile Post 375 West | Unknown | Toad | Anisian | N/A | Yes |
| MG-11-OS-C1 | Oyster Springs | 0.00 | Toad | Anisian | N/A | No |
| MG-11-OS-C1a | Oyster Springs | 3.00 | Toad | Anisian | N/A | No |
| MG-11-OS-C2 | Oyster Springs | 6.00 | Toad | Anisian | N/A | Yes |
| MG-11-OS-C3 | Oyster Springs | 9.00 | Toad | Anisian | N/A | No |
| MG-11-OS-C4 | Oyster Springs | 17.90 | Toad | Anisian | N/A | Yes |
| MG-11-NTPW-C1 | N Tetsa Phosphate W | Unknown | Toad | Unknown | N/A | No |
| MG-11-NTPW-C2 | N Tetsa Phosphate W | Unknown | Toad | Unknown | N/A | No |
| **Existing Conodont Samples from Surface British Columbia** | | | | | | |
| **Sample No.** | **Locality** | **Height Above Base/m** | **Formation** | **Age** | **GSC No.** | **Productive** |
| 83-TE211A | North Liard | Unknown | Toad | Anisian | 99574 | Yes |
| 83-TE211B | North Liard | Unknown | Toad | Anisian | 99575 | Yes |
| 82-B9F | Liard-Crusty | Unknown | Toad | Anisian | C-090852 | Yes |
| 00-TE-X | Liard-Brimstone | Unknown | Toad | Anisian | 42349 | Yes |
| 83-215B | East Toad River I | 2.00 | Toad | Anisian | 99588 | Yes |
| 83-215E | East Toad River I | 5.25 | Toad | Anisian | 99591 | Yes |
| 83-215F | East Toad River I | 6.00 | Toad | Anisian | 99592 | Yes |
| 83-205A | East Toad River II | 5.00 | Toad | Anisian | 99565 | Yes |
| 83-205B | East Toad River II | 10.00 | Toad | Anisian | 99564 | Yes |
| 00-TE-X | North Tetsa Hill | Unknown | Toad | Anisian | 46499 | Yes |
| 92-AH2 | Yellow Bluffs | 0.00 | Toad | Anisian | C-201902 | Yes |
| 92-AH21 | Yellow Bluffs | 21.50 | Toad | Anisian | C-201921 | Yes |
| 94-TE68294 | Mile Post 375 West | 0.00 | Toad | Anisian | 68294 | Yes |

| Existing Conodont Samples from Surface British Columbia | | | | | | |
|---|---|---|---|---|---|---|
| **Sample No.** | **Locality** | **Height Above Base/m** | **Formation** | **Age** | **GSC No.** | **Productive** |
| 92-AH26 | Mile Post 375 West | 10.00 | Toad | Anisian | C-201926 | Yes |
| 92-AH25 | Mile Post 375 West | 27.00 | Toad | Anisian | C-201925 | Yes |
| 92-AH22 | Mile Post 375 East | 4.00 | Toad | Anisian | C-201922 | Yes |
| HB-655 | Mile Post 375 East | 18.00 | Toad | Anisian | C-209952 | Yes |
| HB-656 | Mile Post 375 East | 22.00 | Toad | Anisian | C-302187 | Yes |
| 82-AH6 | Mile Post 375 East | 25.00 | Toad | Anisian | C-101077 | Yes |
| **New Conodont Samples from Subsurface British Columbia** | | | | | | |
| **Sample No.** | **Well Identifier** | **Depth Below KB/m** | **Formation** | **Age** | **GSC No.** | **Productive** |
| MG-10-JP1 | MS d-054-B/093-P9 | 2557.30 | Doig | Anisian | N/A | No |
| MG-10-JP2 | MS d-054-B/093-P9 | 2556.90 | Doig | Anisian | N/A | Yes |
| MG-10-JP3 | MS d-054-B/093-P9 | 2556.25 | Doig | Anisian | N/A | No |
| MG-10-JP4 | MS d-054-B/093-P9 | 2553.80 | Doig | Anisian | N/A | Yes |
| MG-10-JP5 | MS d-054-B/093-P9 | 2553.40 | Doig | Anisian | N/A | No |
| MG-10-JP6 | MS d-054-B/093-P9 | 2551.80 | Doig | Anisian | N/A | No |
| MG-10-JP7 | MS d-054-B/093-P9 | 2549.66 | Doig | Anisian | N/A | Yes |
| MG-10-JP8 | MS d-054-B/093-P9 | 2548.45 | Doig | Anisian | N/A | No |
| MG-11-JP1 | TA 16-17-083-25W6 | 2528.50-2529.00 | Montney | Griesbach | N/A | Yes |
| MG-11-JP2 | TA 16-17-083-25W6 | 2523.20-2524.10 | Montney | Griesbach | N/A | No |
| MG-11-JP3 | TA 16-17-083-25W6 | 2514.30-2515.30 | Montney | Griesbach | N/A | No |
| MG-11-JP4 | TA 16-17-083-25W6 | 2499.80-2501.70 | Montney | Griesbach | N/A | No |
| MG-11-JP5 | TA 16-17-083-25W6 | 2484.00-2484.80 | Montney | Griesbach | N/A | No |
| MG-11-JP6 | TA 16-17-083-25W6 | 2447.80-2448.80 | Montney | Dienerian | N/A | No |
| MG-11-JP7 | TA 16-17-083-25W6 | 2431.80-2432.40 | Montney | Dienerian | N/A | No |
| MG-11-JP8 | TA 16-17-083-25W6 | 2420.50-2421.20 | Montney | Smithian | N/A | No |
| MG-11-JP9 | TA 16-17-083-25W6 | 2402.40-2403.30 | Montney | Smithian | N/A | Yes |
| MG-11-JP10 | TA 16-17-083-25W6 | 2393.20-2394.10 | Montney | Smithian | N/A | Yes |
| MG-11-JP11 | TA 16-17-083-25W6 | 2388.70-2389.60 | Montney | Smithian | N/A | Yes |
| MG-11-JP12 | TA 16-17-083-25W6 | 2368.00-2369.00 | Montney | Spathian | N/A | No |
| MG-11-JP13 | TA 16-17-083-25W6 | 2330.80-2332.20 | Montney | Spathian | N/A | No |

| New Conodont Samples from Subsurface British Columbia | | | | | | |
|---|---|---|---|---|---|---|
| **Sample No.** | **Well Identifier** | **Depth Below KB/m** | **Formation** | **Age** | **GSC No.** | **Productive** |
| MG-11-JP14 | TA 16-17-083-25W6 | 2304.40-2305.30 | Montney | Spathian | N/A | No |
| MG-11-JP15 | TA 16-17-083-25W6 | 2276.50-2277.50 | Montney | Spathian | N/A | No |
| MG-11-JP16 | TA 16-17-083-25W6 | 2263.75-2264.70 | Montney | Spathian | N/A | No |
| MG-11-JP17 | PCK c-074-G/094-B-9 | 1951.50-1952.00 | Montney | Unknown | N/A | No |
| MG-11-JP18 | PCK c-074-G/094-B-9 | 1946.90-1947.15 | Montney | Smithian | N/A | Yes |
| MG-11-JP19 | PCK c-074-G/094-B-9 | 1945.60-1945.80 | Montney | Spathian | N/A | No |
| MG-11-JP20 | PCK c-074-G/094-B-9 | 1860.30-1860.60 | Doig | Anisian | N/A | Yes |
| MG-11-JP21 | PCK c-074-G/094-B-9 | 1858.60-1858.90 | Doig | Anisian | N/A | Yes |
| MG-11-C1 | TA 16-17-083-25W6 | 2257.43-2258.30 | Montney | Spathian | N/A | No |
| MG-11-C3 | TA 16-17-083-25W6 | 2254.44-2255.30 | Doig | Spathian | N/A | Yes |
| MG-11-C7 | TA 16-17-083-25W6 | 2241.46-2242.35 | Doig | Anisian | N/A | Yes |
| MG-11-C8 | TA 16-17-083-25W6 | 2238.74-2239.75 | Doig | Anisian | N/A | Yes |
| MG-11-C9 | TA 16-17-083-25W6 | 2236.09-2237.05 | Doig | Anisian | N/A | Yes |
| MG-11-C10 | TA 16-17-083-25W6 | 2234.10-2234.57 | Doig | Anisian | N/A | Yes |
| MG-11-C13 | TA c-085-I/094-B-01 | 2370.61-2369.96 | Doig | Anisian | N/A | Yes |
| MG-11-C14 | TA c-085-I/094-B-01 | 2368.88-2368.04 | Doig | Anisian | N/A | No |
| MG-11-C15 | TA c-085-I/094-B-01 | 2366.75-2366.06 | Doig | Anisian | N/A | No |
| MG-11-C16 | TA c-085-I/094-B-01 | 2315.22-2314.50 | Doig | Anisian | N/A | No |
| MG-11-C18 | TA c-085-I/094-B-01 | 2306.82-2306.01 | Doig | Anisian | N/A | No |
| MG-11-C21 | AD 07-13-79-15W6 | 2054.68-2054.48 | Doig | Anisian | N/A | No |
| MG-11-C22 | AD 07-13-79-15W6 | 2054.30-2054.05 | Doig | Anisian | N/A | Yes |
| MG-11-C24 | RM 08-22-82-20W6 | 1778.98-1778.70 | Doig | Unknown | N/A | No |
| MG-11-C27 | RM 08-22-82-20W6 | 1773.65-1773.21 | Doig | Unknown | N/A | No |
| MG-11-C28 | PCK d-048-A/094-B-09 | 1968.25 | Montney | Spa/Anis | N/A | No |
| MG-11-C29 | PCK d-048-A/094-B-09 | 1967.85 | Montney | Anisian | N/A | Yes |
| MG-11-C30 | PCK d-048-A/094-B-09 | 1967.30-1967.50 | Doig | Anisian | N/A | Yes |
| MG-11-C31 | PCK d-048-A/094-B-09 | 1966.00-1967.00 | Doig | Anisian | N/A | No |
| MG-11-C32 | PCK d-048-A/094-B-09 | 1964.80-1965.00 | Doig | Anisian | N/A | No |
| MG-11-C33 | PCK d-048-A/094-B-09 | 1965.00-1965.40 | Doig | Anisian | N/A | Yes |

| Existing Conodont Samples from Subsurface British Columbia | | | | | | |
|---|---|---|---|---|---|---|
| **Sample No.** | **Well Identifier** | **Depth Below KB/m** | **Formation** | **Age** | **GSC No.** | **Productive** |
| CMH-19 | TA 16-17-083-25W6 | 2527.50-2528.50 | Montney | Greisbach | N/A | Yes |
| CMH-18 | TA 16-17-083-25W6 | 2515.30-2516.30 | Montney | Griesbach | N/A | No |
| CMH-17 | TA 16-17-083-25W6 | 2495.00-2496.00 | Montney | Griesbach | N/A | No |
| **Existing Conodont Samples from Subsurface British Columbia** | | | | | | |
| **Sample No.** | **Well Identifier** | **Depth Below KB/m** | **Formation** | **Age** | **GSC No.** | **Productive** |
| CMH-16 | TA 16-17-083-25W6 | 2490.50-2491.50 | Montney | Griesbach | N/A | Yes |
| CMH-15 | TA 16-17-083-25W6 | 2470.00-2470.75 | Montney | Dienerian | N/A | Yes |
| CMH-14 | TA 16-17-083-25W6 | 2453.00-2453.75 | Montney | Smithian | N/A | No |
| CMH-13 | TA 16-17-083-25W6 | 2424.50-2425.50 | Montney | Smithian | N/A | Yes |
| CMH-12 | TA 16-17-083-25W6 | 2394.00-2395.00 | Montney | Smithian | N/A | Yes |
| CMH-11 | TA 16-17-083-25W6 | 2384.00-2385.00 | Montney | Spathian | N/A | Yes |
| CMH-10 | TA 16-17-083-25W6 | 2380.10-2381.00 | Montney | Spathian | N/A | No |
| CMH-9 | TA 16-17-083-25W6 | 2370.70-2371.50 | Montney | Spathian | N/A | Yes |
| CMH-8 | TA 16-17-083-25W6 | 2356.00-2357.00 | Montney | Spathian | N/A | No |
| CMH-7 | TA 16-17-083-25W6 | 2322.00-2323.00 | Montney | Spathian | N/A | No |
| CMH-6 | TA 16-17-083-25W6 | 2281.25-2282.00 | Montney | Spathian | N/A | No |
| CMH-5 | TA 16-17-083-25W6 | 2258.00-2259.00 | Montney | Spathian | N/A | Yes |
| CMH-3 | TA 16-17-083-25W6 | 2252.00-2253.00 | Doig | Spathian | N/A | Yes |
| CMH-4 | TA 16-17-083-25W6 | 2256.00-2257.00 | Doig | Anisian | N/A | Yes |
| CMH-2 | TA 16-17-083-25W6 | 2243.00-2244.00 | Doig | Anisian | N/A | Yes |
| CMH-1 | TA 16-17-083-25W6 | 2240.00-2241.00 | Doig | Anisian | N/A | Yes |
| TG-3884 | TG 03-06-078-22W6 | 3884.25 | Montney | Unknown | V-002493 | No |
| TG-3486 | TG 03-06-078-22W6 | 3486.00 | Montney | Griesbach | V-002492 | Yes |
| TG-3350 | TG 03-06-078-22W6 | 3350.10 | Montney | Spathian | V-002494 | Yes |
| TG-3348 | TG 03-06-078-22W6 | 3348.40 | Montney | Unknown | V-002495 | No |
| TG-3202 | TG 03-06-078-22W6 | 3202.80 | Doig | Anisian | V-002498 | No |
| TG-3192 | TG 03-06-078-22W6 | 3192.50 | Doig | Anisian | V-002497 | Yes |
| TG-3185 | TG 03-06-078-22W6 | 3185.00 | Doig | Anisian | V-002496 | Yes |
| SG-3150 | SG 16-02-078-22W6 | 3150.40 | Montney | Unknown | V-002499 | No |

| Existing Conodont Samples from Subsurface British Columbia | | | | | | |
|---|---|---|---|---|---|---|
| **Sample No.** | **Well Identifier** | **Depth Below KB/m** | **Formation** | **Age** | **GSC No.** | **Productive** |
| SG-3127 | SG 16-02-078-22W6 | 3127.54 | Montney | Unknown | V-002500 | No |
| SG-3113 | SG 16-02-078-22W6 | 3113.00 | Montney | Unknown | V-002501 | No |
| SG-30948 | SG 16-02-078-22W6 | 3094.80 | Montney | Unknown | V-002502 | No |
| SG-30944 | SG 16-02-078-22W6 | 3094.40 | Montney | Unknown | V-002503 | No |
| SG-3089 | SG 16-02-078-22W6 | 3089.00 | Montney | Unknown | V-002504 | No |
| SG-3084 | SG 16-02-078-22W6 | 3084.90 | Montney | Unknown | V-002505 | No |
| SG-3073 | SG 16-02-078-22W6 | 3073.00 | Montney | Spa/Anis | V-002506 | Yes |
| SG-3067 | SG 16-02-078-22W6 | 3067.60 | Montney | Spa/Anis | V-002507 | Yes |
| SG-3057 | SG 16-02-078-22W6 | 3057.60 | Montney | Unknown | V-002508 | No |
| SG-3052 | SG 16-02-078-22W6 | 3052.50 | Montney | Anisian | V-002509 | Yes |
| SG-3045 | SG 16-02-078-22W6 | 3045.50 | Montney | Anisian | V-002510 | Yes |
| SG-3039 | SG 16-02-078-22W6 | 3039.30 | Montney | Anisian | V-002511 | Yes |
| SG-30348 | SG 16-02-078-22W6 | 3034.80 | Doig | Anisian | V-002513 | Yes |
| SG-30346 | SG 16-02-078-22W6 | 3034.60 | Doig | Anisian | V-002512 | Yes |
| SG-3029 | SG 16-02-078-22W6 | 3029.20 | Doig | Anisian | V-002514 | No |
| SG-3020 | SG 16-02-078-22W6 | 3020.30 | Doig | Anisian | V-002515 | Yes |
| SG-2999 | SG 16-02-078-22W6 | 2999.20 | Doig | Anis/Lad | V-002516 | Yes |
| SEA-2971 | SG 16-35-078-21W6 | 2971.80 | Montney | Smithian | V-002525 | Yes |
| SEA-2970 | SG 16-35-078-21W6 | 2970.37 | Montney | Smithian | V-002526 | Yes |
| SEA-2969 | SG 16-35-078-21W6 | 2969.00 | Montney | Smithian | V-002524 | Yes |
| SEA-2781 | SG 16-35-078-21W6 | 2781.00 | Montney | Unknown | V-002517 | No |
| SEA-2773 | SG 16-35-078-21W6 | 2773.20 | Montney | Spa/Anis | V-002518 | Yes |
| SEA-2765 | SG 16-35-078-21W6 | 2765.50 | Montney | Anisian | V-002519 | No |
| SEA-2763 | SG 16-35-078-21W6 | 2763.20 | Montney | Anisian | V-002520 | No |
| SEA-2758 | SG 16-35-078-21W6 | 2758.40 | Doig | Anisian | V-002521 | Yes |
| SEA-2753 | SG 16-35-078-21W6 | 2753.75 | Doig | Unknown | V-002522 | No |
| SEA-2749 | SG 16-35-078-21W6 | 2749.00 | Doig | Unknown | V-002523 | No |
| | | | | | | |
| | | | | | | |

| New Detrital Zircon Samples from Surface British Columbia | | | | | | |
|---|---|---|---|---|---|---|
| **Sample No.** | **Locality** | **Height Above Base/m** | **Formation** | **Age** | **GSC No.** | **Productive** |
| 08-2009-Z1 | South Halfway | 376.00 | Toad | Ladinian | N/A | No |
| 08-2009-Z2 | South Halfway | 422.00 | Toad | Ladinian | N/A | No |
| 08-2009-Z3 | South Halfway | 477.00 | Toad | Ladinian | N/A | No |
| 08-2009-Z4 | South Halfway | 613.00 | Liard | Ladinian | N/A | No |
| 08-2009-Z5 | South Halfway | 634.00 | Liard | Ladinian | N/A | No |
| MG-10-UC01 | Ursula Creek | 78.90 | Toad | Smithian | N/A | No |
| MG-10-UC02 | Ursula Creek | 85.20 | Toad | Spathian | N/A | No |
| MG-10-UC03 | Ursula Creek | 124.90 | Toad | Anis/Lad | N/A | No |
| MG-10-UC04 | Ursula Creek | 129.55 | Toad | Anis/Lad | N/A | No |
| MG-10-NPP01 | Ne-Parle-Pas Point | 41.20 | Pardonet | Rhaetian | N/A | No |
| MG-10-NPP02 | Ne-Parle-Pas Point | 42.50 | Pardonet | Rhaetian | N/A | No |
| MG-10-NPP03 | Ne-Parle-Pas Point | 51.00 | Pardonet | Rhaetian | N/A | No |
| MG-10-BBR01 | Black Bear Ridge | 242.00 | Pardonet | Rhaetian | N/A | Yes |
| MG-10-BH01 | Brown Hill | 191.00 | Toad | Anisian | N/A | Yes |
| MG-10-BH02 | Brown Hill | 239.00 | Toad | Anisian | N/A | Yes |
| MG-10-GS01 | Glacier Spur | 122.60 | Liard | Ladinian | N/A | Yes |
| MG-10-GS02 | Glacier Spur | 149.00 | Liard | Ladinian | N/A | Yes |
| MG-10-GS03 | Glacier Spur | 255.00 | Liard | Ladinian | N/A | Yes |
| MG-10-GS04 | Glacier Spur | 293.80 | Liard | Ladinian | N/A | Yes |
| MG-10-GS05 | Glacier Spur | 304.00 | Liard | Ladinian | N/A | Yes |
| MG-10-FH01 | Folded Hill | 203.00 | Liard | Ladinian | N/A | No |
| MG-10-ECC01 | East Carbon Creek | 76.00 | Baldonnel | Carnian | N/A | Yes |
| MG-11-MP386-Z1 | Mile Post 386 | 10.25 | Toad | Ladinian | N/A | No |
| MG-11-MP386-Z2 | Mile Post 386 | 17.50 | Toad | Ladinian | N/A | Yes |
| MG-11-NTP-Z1 | North Tetsa Phosphate | 2.60 | Toad | Anisian | N/A | No |
| MG-11-NTP-Z2 | North Tetsa Phosphate | 2.70 | Toad | Anisian | N/A | Yes |
| MG-11-NTP-Z3 | North Tetsa Phosphate | 2.80 | Toad | Anisian | N/A | Yes |
| MG-11-NTP-Z4 | North Tetsa Phosphate | 10.60 | Toad | Anisian | N/A | No |
| MG-11-NTP-Z5 | North Tetsa Phosphate | 11.85 | Toad | Anisian | N/A | No |

| New Detrital Zircon Samples from Surface British Columbia | | | | | | |
|---|---|---|---|---|---|---|
| **Sample No.** | **Locality** | **Height Above Base/m** | **Formation** | **Age** | **GSC No.** | **Productive** |
| MG-11-YB-Z1 | Yellow Bluffs | 1.70 | Toad | Anisian | N/A | No |
| MG-11-YB-Z2 | Yellow Bluffs | 3.00 | Toad | Anisian | N/A | No |
| MG-11-YB-Z3 | Yellow Bluffs | 3.75 | Toad | Anisian | N/A | No |
| MG-11-YB-Z4 | Yellow Bluffs | 10.00 | Toad | Anisian | N/A | No |
| MG-11-YB-Z5 | Yellow Bluffs | 13.00 | Toad | Anisian | N/A | No |
| MG-11-MP375W-Z1 | Mile Post 375 West | Unknown | Toad | Anisian | N/A | Yes |
| MG-11-OS-Z1 | Oyster Springs | Unknown | Toad | Anisian | N/A | Yes |
| MG-11-OS-Z1a | Oyster Springs | 3.30 | Toad | Anisian | N/A | Yes |
| MG-11-OS-Z2 | Oyster Springs | Unknown | Toad | Anisian | N/A | No |
| JP-12-BBR01 | Black Bear Ridge | 241.80 | Pardonet | Rhaetian | N/A | Yes |
| JP-12-PC01 | Pardonet Creek | 3.60 | Pardonet | Rhaetian | N/A | Yes |
| JP-12-PC02 | Pardonet Creek | 14.35 | Pardonet | Rhaetian | N/A | Yes |
| JP-12-PC03 | Pardonet Creek | 15.45 | Pardonet | Rhaetian | N/A | No |
| JP-12-PC04 | Pardonet Creek | 15.70 | Pardonet | Rhaetian | N/A | No |
| JP-12-NPP02 | Ne-Parle-Pas Point | 37.20 | Pardonet | Rhaetian | N/A | Yes |
| JP-12-NPP03 | Ne-Parle-Pas Point | 41.20 | Pardonet | Rhaetian | N/A | Yes |
| JP-12-NPP04 | Ne-Parle-Pas Point | 41.75 | Pardonet | Rhaetian | N/A | No |
| JP-12-NPP05 | Ne-Parle-Pas Point | 42.80 | Pardonet | Rhaetian | N/A | No |
| JP-12-NPP06 | Ne-Parle-Pas Point | 43.00 | Pardonet | Rhaetian | N/A | No |
| JP-12-NPP07 | Ne-Parle-Pas Point | 43.20 | Pardonet | Rhaetian | N/A | Yes |
| JP-12-NPP08 | Ne-Parle-Pas Point | 47.25 | Pardonet | Rhaetian | N/A | Yes |
| JP-12-NPP09 | Ne-Parle-Pas Point | 48.40 | Pardonet | Rhaetian | N/A | Yes |
| JP-12-NPP10 | Ne-Parle-Pas Point | 51.20 | Pardonet | Rhaetian | N/A | No |
| **New Detrital Zircon Samples from Subsurface British Columbia** | | | | | | |
| **Sample No.** | **Well Identifier** | **Depth Below KB/m** | **Formation** | **Age** | **GSC No.** | **Productive** |
| MG-10-JPZ1 | MS d-054-B/093-P9 | 2548.45 | Doig | Anisian | N/A | No |
| MG-10-JPZ2 | MS d-054-B/093-P9 | 2549.66 | Doig | Anisian | N/A | No |
| | | | | | | |
| | | | | | | |

| New Detrital Zircon Samples from Subsurface British Columbia | | | | | | |
|---|---|---|---|---|---|---|
| **Sample No.** | **Well Identifier** | **Depth Below KB/m** | **Formation** | **Age** | **GSC No.** | **Productive** |
| MG-10-JPZ3 | MS d-054-B/093-P9 | 2551.80 | Doig | Anisian | N/A | Yes |
| MG-10-JPZ4 | MS d-054-B/093-P9 | 2553.40 | Doig | Anisian | N/A | No |
| MG-10-JPZ5 | MS d-054-B/093-P9 | 2553.80 | Doig | Anisian | N/A | No |
| MG-10-JPZ6 | MS d-054-B/093-P9 | 2556.25 | Doig | Anisian | N/A | No |
| MG-10-JPZ7 | MS d-054-B/093-P9 | 2556.90 | Doig | Anisian | N/A | No |
| MG-10-JPZ8 | MS d-054-B/093-P9 | 2557.30 | Doig | Anisian | N/A | No |
| MG-11-C1 | TA 16-17-083-25W6 | 2258.30-2257.43 | Montney | Spathian | N/A | No |
| MG-11-C2 | TA 16-17-083-25W6 | 2256.22-2255.98 | Doig | Spathian | N/A | Yes |
| MG-11-C3 | TA 16-17-083-25W6 | 2255.30-2254.44 | Doig | Spathian | N/A | No |
| MG-11-C4 | TA 16-17-083-25W6 | 2248.52-2248.05 | Doig | Anisian | N/A | No |
| MG-11-C5 | TA 16-17-083-25W6 | 2247.75-2247.21 | Doig | Anisian | N/A | No |
| MG-11-C6 | TA 16-17-083-25W6 | 2245.79-2244.62 | Doig | Anisian | N/A | No |
| MG-11-C7 | TA 16-17-083-25W6 | 2242.35-2241.46 | Doig | Anisian | N/A | No |
| MG-11-C8 | TA 16-17-083-25W6 | 2239.75-2238.74 | Doig | Anisian | N/A | No |
| MG-11-C9 | TA 16-17-083-25W6 | 2237.05-2236.09 | Doig | Anisian | N/A | No |
| MG-11-C10 | TA 16-17-083-25W6 | 2234.57-2234.10 | Doig | Anisian | N/A | No |
| MG-11-C11 | TA 16-17-083-25W6 | 2233.61-2233.08 | Doig | Anisian | N/A | No |
| MG-11-C12 | TA c-085-I/094-B-01 | 2374.17-2373.25 | Doig | Anisian | N/A | Yes |
| MG-11-C16 | TA c-085-I/094-B-01 | 2315.22-2314.50 | Doig | Anisian | N/A | Yes |
| MG-11-C17 | TA c-085-I/094-B-01 | 2310.89-2310.00 | Doig | Anisian | N/A | Yes |
| MG-11-C18 | TA c-085-I/094-B-01 | 2306.82-2306.01 | Doig | Anisian | N/A | No |
| MG-11-C19 | TA c-085-I/094-B-01 | 2295.92-2295.36 | Doig | Anisian | N/A | No |
| MG-11-C20 | AD 07-13-79-15W6 | 2056.35-2055.68 | Montney | Anisian | N/A | Yes |
| MG-11-C22 | AD 07-13-79-15W6 | 2054.30-2054.05 | Doig | Anisian | N/A | Yes |
| MG-11-C23 | RM 08-22-82-20W6 | 1779.61-1779.38 | Doig | Unknown | N/A | No |
| MG-11-C24 | RM 08-22-82-20W6 | 1778.98-1778.70 | Doig | Unknown | N/A | No |
| MG-11-C25 | RM 08-22-82-20W6 | 1775.20-1774.81 | Doig | Unknown | N/A | No |
| MG-11-C26 | RM 08-22-82-20W6 | 1774.16-1774.00 | Doig | Unknown | N/A | No |
| MG-11-C28 | PCK d-048-A/094-B-09 | 1968.25 | Montney | Spa/Anis | N/A | No |

| New Detrital Zircon Samples from Subsurface British Columbia | | | | | | |
|---|---|---|---|---|---|---|
| **Sample No.** | **Well Identifier** | **Depth Below KB/m** | **Formation** | **Age** | **GSC No.** | **Productive** |
| MG-11-C29 | PCK d-048-A/094-B-09 | 1967.85 | Montney | Spa/Anis | N/A | No |
| MG-11-C30 | PCK d-048-A/094-B-09 | 1967.30-1967.50 | Doig | Spa/Anis | N/A | No |
| MG-11-C31 | PCK d-048-A/094-B-09 | 1966.00-1967.00 | Doig | Spa/Anis | N/A | No |
| MG-11-C32 | PCK d-048-A/094-B-09 | 1964.80-1965.90 | Doig | Anisian | N/A | No |
| MG-11-C33 | PCK d-048-A/094-B-09 | 1965.00-1965.40 | Doig | Anisian | N/A | Yes |

# APPENDIX 2

# DETRITAL ZIRCON ANALYTICAL DATA

| Isotope Ratios | | | | Ages | | | | | | |
|---|---|---|---|---|---|---|---|---|---|---|
| Pb207/U235 | | Pb206/U238 | | Pb207/U235 | | Pb206/U238 | | Discordance | Preferred Age | |
| NPP-09 | | | | | | | | | | |
| 1.04835 | 0.0235 | 0.11971 | 0.00079 | 728.1 | 11.65 | 728.9 | 4.54 | -0.11 | 728.9 | 4.54 |
| 4.15058 | 0.15546 | 0.29894 | 0.00274 | 1664.3 | 30.65 | 1686 | 13.61 | -1.30 | 1676.6 | 26.67 |
| 3.04812 | 0.08449 | 0.241 | 0.00164 | 1419.8 | 21.19 | 1391.9 | 8.52 | 1.97 | 1333 | 23.54 |
| 2.29768 | 0.05762 | 0.20816 | 0.00134 | 1211.6 | 17.74 | 1219 | 7.14 | -0.61 | 1157.5 | 24.14 |
| 0.46225 | 0.00924 | 0.06162 | 0.00038 | 385.8 | 6.42 | 385.5 | 2.32 | 0.08 | 385.5 | 2.32 |
| 6.96753 | 0.21741 | 0.38207 | 0.0028 | 2107.3 | 27.71 | 2086 | 13.05 | 1.01 | 2143.6 | 18.08 |
| 1.72184 | 0.05677 | 0.17648 | 0.00155 | 1016.7 | 21.18 | 1047.7 | 8.49 | -3.05 | 1006.3 | 35.4 |
| 9.56047 | 0.20364 | 0.41442 | 0.00211 | 2393.4 | 19.58 | 2235.1 | 9.61 | 6.61 | 2578.5 | 12.21 |
| 2.55435 | 0.07552 | 0.22585 | 0.0017 | 1287.7 | 21.57 | 1312.7 | 8.92 | -1.94 | 1254.3 | 26.59 |
| 3.5413 | 0.09604 | 0.27696 | 0.00187 | 1536.5 | 21.47 | 1576 | 9.43 | -2.57 | 1507.7 | 21.75 |
| 0.72996 | 0.01373 | 0.08887 | 0.0005 | 556.5 | 8.06 | 548.8 | 2.95 | 1.38 | 548.8 | 2.95 |
| 7.02107 | 0.16603 | 0.37046 | 0.00209 | 2114.1 | 21.02 | 2031.5 | 9.81 | 3.91 | 2179 | 14.96 |
| 0.51382 | 0.01951 | 0.06818 | 0.00079 | 421 | 13.09 | 425.2 | 4.77 | -1.00 | 425.2 | 4.77 |
| 1.74466 | 0.04549 | 0.17874 | 0.00125 | 1025.2 | 16.83 | 1060.1 | 6.82 | -3.40 | 1021.4 | 28.28 |
| 0.60821 | 0.0181 | 0.07658 | 0.00067 | 482.4 | 11.43 | 475.7 | 4 | 1.39 | 475.7 | 4 |
| 0.49425 | 0.01431 | 0.06464 | 0.0006 | 407.8 | 9.72 | 403.8 | 3.61 | 0.98 | 403.8 | 3.61 |
| 1.76028 | 0.0818 | 0.16099 | 0.00195 | 1031 | 30.09 | 962.3 | 10.82 | 6.66 | 962.3 | 10.82 |
| 0.74503 | 0.0166 | 0.08487 | 0.00056 | 565.3 | 9.66 | 525.1 | 3.35 | 7.11 | 525.1 | 3.35 |
| 4.91645 | 0.16262 | 0.32521 | 0.00257 | 1805.1 | 27.91 | 1815.1 | 12.5 | -0.55 | 1749.5 | 23.06 |
| 3.47859 | 0.09337 | 0.26988 | 0.00181 | 1522.4 | 21.17 | 1540.2 | 9.19 | -1.17 | 1472.6 | 22.67 |
| 1.81501 | 0.04408 | 0.17829 | 0.00116 | 1050.9 | 15.9 | 1057.6 | 6.33 | -0.64 | 1008.3 | 26.84 |
| 13.40097 | 0.34555 | 0.5163 | 0.00311 | 2708.3 | 24.36 | 2683.5 | 13.2 | 0.92 | 2746.1 | 14.06 |
| 14.06578 | 0.44019 | 0.5406 | 0.00379 | 2754.2 | 29.67 | 2786 | 15.87 | -1.15 | 2730.3 | 15.61 |
| 2.48229 | 0.13171 | 0.21982 | 0.0029 | 1266.9 | 38.4 | 1280.9 | 15.3 | -1.11 | 1137.3 | 48.3 |
| 1.87968 | 0.05998 | 0.17973 | 0.00151 | 1073.9 | 21.15 | 1065.5 | 8.22 | 0.78 | 1011.7 | 34.01 |
| 2.60155 | 0.15637 | 0.20846 | 0.00316 | 1301.1 | 44.09 | 1220.6 | 16.87 | 6.19 | 1312.3 | 52.85 |

| Isotope Ratios | | | | Ages | | | | | | |
|---|---|---|---|---|---|---|---|---|---|---|
| Pb207/U235 | | Pb206/U238 | | Pb207/U235 | | Pb206/U238 | | Discordance | Preferred Age | |
| 0.79684 | 0.01841 | 0.08959 | 0.00062 | 595 | 10.4 | 553.1 | 3.65 | 7.04 | 553.1 | 3.65 |
| 0.48754 | 0.00783 | 0.06041 | 0.00031 | 403.2 | 5.35 | 378.1 | 1.88 | 6.23 | 378.1 | 1.88 |
| 1.81479 | 0.09923 | 0.17551 | 0.00255 | 1050.8 | 35.8 | 1042.4 | 13.96 | 0.80 | 1065.8 | 56.87 |
| 3.61362 | 0.09247 | 0.26321 | 0.00172 | 1552.5 | 20.35 | 1506.2 | 8.77 | 2.98 | 1617.7 | 21.93 |
| 4.16497 | 0.12564 | 0.30646 | 0.00231 | 1667.2 | 24.7 | 1723.3 | 11.39 | -3.36 | 1656.1 | 23.77 |
| 0.51385 | 0.01466 | 0.06596 | 0.00058 | 421 | 9.83 | 411.8 | 3.52 | 2.19 | 411.8 | 3.52 |
| 0.83843 | 0.02916 | 0.10569 | 0.00105 | 618.3 | 16.11 | 647.6 | 6.12 | -4.74 | 647.6 | 6.12 |
| 0.48883 | 0.01225 | 0.06296 | 0.00049 | 404.1 | 8.35 | 393.6 | 2.96 | 2.60 | 393.6 | 2.96 |
| **NPP-08** | | | | | | | | | | |
| 0.50518 | 0.02545 | 0.06843 | 0.00104 | 415.2 | 17.17 | 426.7 | 6.29 | -2.77 | 426.7 | 6.29 |
| 6.1384 | 0.0891 | 0.34768 | 0.00124 | 1995.7 | 12.67 | 1923.5 | 5.94 | 3.62 | 2053.3 | 10.73 |
| 6.53211 | 0.21159 | 0.3729 | 0.00283 | 2050.2 | 28.52 | 2043 | 13.28 | 0.35 | 2069.8 | 18.94 |
| 2.21611 | 0.04489 | 0.20137 | 0.00107 | 1186.1 | 14.17 | 1182.7 | 5.74 | 0.29 | 1210.1 | 20.02 |
| 4.69857 | 0.11376 | 0.31474 | 0.00183 | 1767 | 20.27 | 1764 | 9 | 0.17 | 1744.6 | 17.14 |
| 0.81061 | 0.02055 | 0.09548 | 0.00073 | 602.8 | 11.52 | 587.8 | 4.28 | 2.49 | 587.8 | 4.28 |
| 1.80895 | 0.03871 | 0.17892 | 0.00101 | 1048.7 | 13.99 | 1061.1 | 5.51 | -1.18 | 987.5 | 22.93 |
| 1.74306 | 0.07505 | 0.18018 | 0.00207 | 1024.6 | 27.78 | 1068 | 11.32 | -4.24 | 1026.2 | 45.05 |
| 0.97685 | 0.01763 | 0.11834 | 0.00061 | 692 | 9.06 | 721 | 3.52 | -4.19 | 721 | 3.52 |
| 0.52217 | 0.01204 | 0.06928 | 0.00049 | 426.6 | 8.03 | 431.8 | 2.93 | -1.22 | 417.1 | 38.65 |
| 4.81928 | 0.10298 | 0.31967 | 0.00168 | 1788.3 | 17.97 | 1788.1 | 8.18 | 0.01 | 1819.7 | 15.4 |
| 2.68956 | 0.08351 | 0.23325 | 0.00181 | 1325.6 | 22.98 | 1351.5 | 9.46 | -1.95 | 1295.3 | 27.36 |
| 0.49866 | 0.00863 | 0.06274 | 0.00034 | 410.8 | 5.85 | 392.3 | 2.07 | 4.50 | 392.3 | 2.07 |
| 0.93676 | 0.02272 | 0.10867 | 0.00076 | 671.2 | 11.91 | 665 | 4.41 | 0.92 | 665 | 4.41 |
| 4.30253 | 0.08715 | 0.30265 | 0.0015 | 1693.8 | 16.69 | 1704.4 | 7.42 | -0.63 | 1640.7 | 15.68 |
| 0.53842 | 0.02242 | 0.06885 | 0.00087 | 437.4 | 14.8 | 429.2 | 5.23 | 1.87 | 429.2 | 5.23 |
| 3.3882 | 0.08319 | 0.26433 | 0.00161 | 1501.7 | 19.25 | 1512 | 8.21 | -0.69 | 1469.6 | 20.25 |
| 6.31326 | 0.12009 | 0.37975 | 0.00174 | 2020.3 | 16.67 | 2075.1 | 8.13 | -2.71 | 2008.2 | 12.99 |

| Isotope Ratios | | | | Ages | | | | | | |
|---|---|---|---|---|---|---|---|---|---|---|
| Pb207/U235 | | Pb206/U238 | | Pb207/U235 | | Pb206/U238 | | Discordance | Preferred Age | |
| 5.77538 | 0.21047 | 0.37068 | 0.00324 | 1942.7 | 31.54 | 2032.6 | 15.24 | -4.63 | 1980.3 | 22.36 |
| 5.84511 | 0.22051 | 0.36996 | 0.00335 | 1953.1 | 32.71 | 2029.2 | 15.75 | -3.90 | 1996.2 | 22.85 |
| 7.11418 | 0.14779 | 0.38909 | 0.00194 | 2125.8 | 18.49 | 2118.6 | 9 | 0.34 | 2174.2 | 13.33 |
| 4.14544 | 0.05789 | 0.28286 | 0.00103 | 1663.3 | 11.42 | 1605.7 | 5.17 | 3.46 | 1763.1 | 12.29 |
| 2.51069 | 0.06505 | 0.21692 | 0.00146 | 1275.1 | 18.81 | 1265.6 | 7.73 | 0.75 | 1317.3 | 24 |
| 0.87089 | 0.02472 | 0.10673 | 0.00088 | 636.1 | 13.42 | 653.7 | 5.15 | -2.77 | 653.7 | 5.15 |
| 1.82313 | 0.02431 | 0.17841 | 0.00067 | 1053.8 | 8.74 | 1058.3 | 3.65 | -0.43 | 1119.2 | 15.49 |
| 3.15597 | 0.05879 | 0.24869 | 0.00119 | 1446.5 | 14.36 | 1431.7 | 6.13 | 1.02 | 1453.1 | 16.9 |
| 0.8971 | 0.04619 | 0.10128 | 0.00152 | 650.2 | 24.72 | 621.9 | 8.91 | 4.35 | 621.9 | 8.91 |
| 2.36964 | 0.08639 | 0.21367 | 0.00202 | 1233.5 | 26.03 | 1248.3 | 10.73 | -1.20 | 1251.1 | 33.73 |
| 5.86922 | 0.12217 | 0.35849 | 0.00181 | 1956.7 | 18.06 | 1975 | 8.58 | -0.94 | 1989.6 | 14.71 |
| 4.30738 | 0.14842 | 0.29044 | 0.00244 | 1694.8 | 28.39 | 1643.7 | 12.21 | 3.02 | 1763.2 | 24.48 |
| 3.95318 | 0.12339 | 0.30199 | 0.00236 | 1624.6 | 25.29 | 1701.2 | 11.69 | -4.72 | 1634.3 | 23.6 |
| 1.83191 | 0.03856 | 0.17914 | 0.00101 | 1057 | 13.83 | 1062.3 | 5.52 | -0.50 | 1040.1 | 23.23 |
| 12.07574 | 0.42996 | 0.4823 | 0.00387 | 2610.3 | 33.39 | 2537.3 | 16.85 | 2.80 | 2677.1 | 16.87 |
| 0.54897 | 0.01668 | 0.06778 | 0.00063 | 444.3 | 10.93 | 422.8 | 3.78 | 4.84 | 422.8 | 3.78 |
| 6.37504 | 0.15227 | 0.38101 | 0.00219 | 2028.8 | 20.96 | 2081 | 10.21 | -2.57 | 2019.2 | 16.19 |
| 5.87939 | 0.12847 | 0.34821 | 0.00185 | 1958.2 | 18.96 | 1926.1 | 8.83 | 1.64 | 1989.6 | 15.69 |
| 4.26043 | 0.09387 | 0.29215 | 0.00159 | 1685.8 | 18.12 | 1652.3 | 7.92 | 1.99 | 1666.6 | 17.79 |
| 1.92037 | 0.04583 | 0.18763 | 0.00119 | 1088.2 | 15.93 | 1108.5 | 6.44 | -1.87 | 1043.3 | 25.66 |
| 0.86141 | 0.01775 | 0.1037 | 0.00062 | 630.9 | 9.68 | 636 | 3.65 | -0.81 | 636 | 3.65 |
| 3.0618 | 0.06217 | 0.23184 | 0.00123 | 1423.2 | 15.54 | 1344.1 | 6.41 | 5.56 | 1503.7 | 18.86 |
| 2.23639 | 0.04671 | 0.20456 | 0.00113 | 1192.5 | 14.65 | 1199.8 | 6.03 | -0.61 | 1164.2 | 21.92 |
| 4.18965 | 0.10326 | 0.29408 | 0.00181 | 1672 | 20.2 | 1661.9 | 8.99 | 0.60 | 1688.4 | 19.62 |
| 2.77554 | 0.09816 | 0.2383 | 0.00215 | 1349 | 26.4 | 1377.9 | 11.19 | -2.14 | 1328.7 | 31.4 |
| 2.99576 | 0.18138 | 0.254 | 0.00374 | 1406.5 | 46.09 | 1459.1 | 19.21 | -3.74 | 1307.1 | 49.32 |
| 6.00409 | 0.19294 | 0.37106 | 0.00284 | 1976.4 | 27.97 | 2034.4 | 13.33 | -2.93 | 1967.4 | 20.92 |

| Isotope Ratios | | | | Ages | | | | | | |
|---|---|---|---|---|---|---|---|---|---|---|
| Pb207/U235 | | Pb206/U238 | | Pb207/U235 | | Pb206/U238 | | Discordance | Preferred Age | |
| 10.59835 | 0.32571 | 0.46187 | 0.00336 | 2488.6 | 28.51 | 2447.8 | 14.83 | 1.64 | 2636.8 | 16.67 |
| 8.16675 | 0.25711 | 0.43239 | 0.00314 | 2249.7 | 28.48 | 2316.5 | 14.14 | -2.97 | 2177.3 | 18.68 |
| 0.91563 | 0.02737 | 0.10512 | 0.00091 | 660 | 14.5 | 644.3 | 5.32 | 2.38 | 644.3 | 5.32 |
| 2.14866 | 0.06043 | 0.20128 | 0.00151 | 1164.6 | 19.49 | 1182.2 | 8.08 | -1.51 | 1202.5 | 28.44 |
| **NPP-07** | | | | | | | | | | |
| 6.77078 | 0.22108 | 0.35261 | 0.00266 | 2081.9 | 28.89 | 1947 | 12.66 | 6.48 | 2122 | 19.51 |
| 4.50206 | 0.1453 | 0.29914 | 0.00231 | 1731.4 | 26.81 | 1687 | 11.48 | 2.56 | 1736.9 | 22.93 |
| 3.54738 | 0.09475 | 0.26607 | 0.0018 | 1537.8 | 21.16 | 1520.8 | 9.19 | 1.11 | 1627.1 | 21.83 |
| 2.57695 | 0.0838 | 0.22402 | 0.00187 | 1294.1 | 23.79 | 1303.1 | 9.84 | -0.70 | 1303.5 | 29.7 |
| 9.53312 | 0.32381 | 0.46602 | 0.00379 | 2390.7 | 31.22 | 2466.1 | 16.68 | -3.15 | 2505.3 | 18.58 |
| 0.47563 | 0.02528 | 0.06505 | 0.00103 | 395.1 | 17.39 | 406.2 | 6.25 | -2.81 | 406.2 | 6.25 |
| 0.73785 | 0.02855 | 0.09218 | 0.00103 | 561.1 | 16.68 | 568.4 | 6.09 | -1.30 | 568.4 | 6.09 |
| **NPP-03** | | | | | | | | | | |
| 12.06551 | 0.34851 | 0.51259 | 0.00325 | 2609.5 | 27.08 | 2667.7 | 13.86 | -2.23 | 2612.9 | 14.01 |
| 3.65677 | 0.13314 | 0.26192 | 0.00226 | 1562 | 29.03 | 1499.7 | 11.53 | 3.99 | 1527.2 | 27.93 |
| 4.11328 | 0.08493 | 0.29522 | 0.00148 | 1656.9 | 16.87 | 1667.6 | 7.36 | -0.65 | 1625.7 | 16.43 |
| 1.75275 | 0.03339 | 0.16229 | 0.00083 | 1028.2 | 12.32 | 969.5 | 4.59 | 5.71 | 969.5 | 4.59 |
| 1.92469 | 0.07898 | 0.18974 | 0.00201 | 1089.7 | 27.42 | 1120 | 10.87 | -2.78 | 1049.7 | 42.01 |
| 0.72273 | 0.01893 | 0.09383 | 0.00072 | 552.3 | 11.16 | 578.1 | 4.27 | -4.67 | 578.1 | 4.27 |
| 1.57419 | 0.04354 | 0.16856 | 0.00126 | 960.1 | 17.17 | 1004.2 | 6.97 | -4.59 | 988.1 | 31.54 |
| 5.71264 | 0.12739 | 0.36423 | 0.00194 | 1933.3 | 19.27 | 2002.2 | 9.15 | -3.56 | 1930.7 | 15.67 |
| 4.42444 | 0.11055 | 0.31605 | 0.00193 | 1716.9 | 20.69 | 1770.4 | 9.47 | -3.12 | 1761.4 | 18.71 |
| 1.22492 | 0.06861 | 0.13387 | 0.00215 | 812 | 31.31 | 809.9 | 12.2 | 0.26 | 809.9 | 12.2 |
| 2.56548 | 0.08225 | 0.22322 | 0.00175 | 1290.9 | 23.42 | 1298.9 | 9.22 | -0.62 | 1188.7 | 29.48 |
| 0.45182 | 0.00689 | 0.06281 | 0.00031 | 378.5 | 4.82 | 392.7 | 1.85 | -3.75 | 392.7 | 1.85 |
| 0.53483 | 0.01448 | 0.07175 | 0.00059 | 435 | 9.58 | 446.7 | 3.58 | -2.69 | 446.7 | 3.58 |
| 1.82657 | 0.05296 | 0.18334 | 0.0014 | 1055 | 19.03 | 1085.2 | 7.62 | -2.86 | 1088.7 | 30.98 |

| Isotope Ratios | | | | Ages | | | | | | |
|---|---|---|---|---|---|---|---|---|---|---|
| Pb207/U235 | | Pb206/U238 | | Pb207/U235 | | Pb206/U238 | | Discordance | Preferred Age | |
| 2.35331 | 0.04967 | 0.21193 | 0.00117 | 1228.6 | 15.04 | 1239.1 | 6.22 | -0.85 | 1244.1 | 21.4 |
| 0.5543 | 0.01074 | 0.07076 | 0.00042 | 447.8 | 7.02 | 440.7 | 2.54 | 1.59 | 440.7 | 2.54 |
| 5.06029 | 0.18639 | 0.31891 | 0.00275 | 1829.5 | 31.23 | 1784.4 | 13.46 | 2.47 | 1869.3 | 24.91 |
| 1.93914 | 0.05152 | 0.17351 | 0.00121 | 1094.7 | 17.8 | 1031.4 | 6.67 | 5.78 | 1159.4 | 28.03 |
| 4.02851 | 0.16092 | 0.27703 | 0.00259 | 1640 | 32.49 | 1576.4 | 13.07 | 3.88 | 1606.8 | 29.63 |
| 5.41711 | 0.11805 | 0.31091 | 0.0017 | 1887.6 | 18.68 | 1745.2 | 8.34 | 7.54 | 2111 | 16.6 |
| 0.85349 | 0.02166 | 0.10333 | 0.00076 | 626.6 | 11.86 | 633.9 | 4.43 | -1.17 | 633.9 | 4.43 |
| 3.91738 | 0.06576 | 0.29791 | 0.0013 | 1617.3 | 13.58 | 1680.9 | 6.47 | -3.93 | 1596.9 | 16.2 |
| 3.65932 | 0.10017 | 0.27349 | 0.00186 | 1562.5 | 21.83 | 1558.5 | 9.39 | 0.26 | 1599.3 | 22.91 |
| 2.87595 | 0.07311 | 0.24071 | 0.00156 | 1375.6 | 19.15 | 1390.4 | 8.12 | -1.08 | 1414.1 | 23.6 |
| 2.71743 | 0.10827 | 0.22318 | 0.00221 | 1333.2 | 29.57 | 1298.6 | 11.67 | 2.60 | 1397.7 | 35.18 |
| 5.62945 | 0.21544 | 0.33239 | 0.00285 | 1920.6 | 33 | 1850 | 13.78 | 3.68 | 1864.4 | 25.29 |
| 0.8078 | 0.04385 | 0.0961 | 0.00152 | 601.2 | 24.63 | 591.5 | 8.93 | 1.61 | 591.5 | 8.93 |
| 1.24401 | 0.02497 | 0.13405 | 0.00076 | 820.7 | 11.3 | 810.9 | 4.33 | 1.19 | 810.9 | 4.33 |
| 4.01749 | 0.06507 | 0.29279 | 0.00127 | 1637.7 | 13.17 | 1655.4 | 6.31 | -1.08 | 1641.9 | 16.51 |
| **NPP-02** | | | | | | | | | | |
| 3.77161 | 0.14302 | 0.28425 | 0.00255 | 1586.7 | 30.43 | 1612.7 | 12.81 | -1.64 | 1443.1 | 28.28 |
| 1.77898 | 0.09399 | 0.18183 | 0.00264 | 1037.8 | 34.34 | 1077 | 14.38 | -3.78 | 1139.1 | 53.97 |
| 5.28312 | 0.11023 | 0.31358 | 0.00163 | 1866.1 | 17.81 | 1758.3 | 8.01 | 5.78 | 1993.7 | 15.17 |
| 1.01265 | 0.02833 | 0.11165 | 0.0009 | 710.2 | 14.29 | 682.3 | 5.19 | 3.93 | 682.3 | 5.19 |
| 2.86025 | 0.18682 | 0.24558 | 0.00406 | 1371.5 | 49.14 | 1415.6 | 20.99 | -3.22 | 1359.6 | 53.54 |
| 0.77 | 0.01609 | 0.09403 | 0.00058 | 579.8 | 9.23 | 579.3 | 3.39 | 0.09 | 579.3 | 3.39 |
| 0.82308 | 0.01562 | 0.09271 | 0.00052 | 609.8 | 8.7 | 571.5 | 3.06 | 6.28 | 571.5 | 3.06 |
| 0.52086 | 0.0086 | 0.06829 | 0.00034 | 425.7 | 5.74 | 425.8 | 2.08 | -0.02 | 425.8 | 2.08 |
| 4.83195 | 0.08654 | 0.30054 | 0.00133 | 1790.5 | 15.07 | 1694 | 6.6 | 5.39 | 1771.4 | 14.61 |
| 1.71447 | 0.06637 | 0.16482 | 0.00169 | 1014 | 24.83 | 983.5 | 9.37 | 3.01 | 983.5 | 9.37 |
| 2.12706 | 0.05018 | 0.19075 | 0.00119 | 1157.6 | 16.29 | 1125.4 | 6.42 | 2.78 | 1140.3 | 24.14 |

| Isotope Ratios | | | | Ages | | | | | | |
|---|---|---|---|---|---|---|---|---|---|---|
| Pb207/U235 | | Pb206/U238 | | Pb207/U235 | | Pb206/U238 | | Discordance | Preferred Age | |
| 1.80225 | 0.04362 | 0.17754 | 0.00119 | 1046.3 | 15.8 | 1053.5 | 6.51 | -0.69 | 1157.3 | 25.89 |
| 0.88598 | 0.05035 | 0.09839 | 0.00161 | 644.2 | 27.11 | 604.9 | 9.43 | 6.10 | 604.9 | 9.43 |
| 1.87797 | 0.05693 | 0.18513 | 0.00152 | 1073.3 | 20.09 | 1094.9 | 8.28 | -2.01 | 1107.7 | 31.67 |
| 6.77453 | 0.11857 | 0.39334 | 0.00174 | 2082.4 | 15.49 | 2138.3 | 8.06 | -2.68 | 2095.6 | 14.12 |
| 1.55102 | 0.03374 | 0.16224 | 0.00099 | 950.9 | 13.43 | 969.2 | 5.49 | -1.92 | 969.2 | 5.49 |
| 1.85505 | 0.06231 | 0.18618 | 0.00167 | 1065.2 | 22.16 | 1100.7 | 9.06 | -3.33 | 1010.4 | 35.45 |
| 4.38433 | 0.10252 | 0.30903 | 0.00181 | 1709.4 | 19.33 | 1735.9 | 8.93 | -1.55 | 1665.6 | 19.42 |
| 1.56391 | 0.0287 | 0.15912 | 0.00082 | 956 | 11.37 | 951.9 | 4.56 | 0.43 | 951.9 | 4.56 |
| 0.44054 | 0.01357 | 0.06205 | 0.0006 | 370.6 | 9.56 | 388.1 | 3.63 | -4.72 | 388.1 | 3.63 |
| 5.70505 | 0.16347 | 0.34476 | 0.00243 | 1932.1 | 24.76 | 1909.5 | 11.67 | 1.17 | 1958.8 | 20.43 |
| 0.86054 | 0.02174 | 0.10369 | 0.00076 | 630.4 | 11.86 | 636 | 4.46 | -0.89 | 636 | 4.46 |
| 12.51462 | 0.6396 | 0.52475 | 0.0061 | 2643.8 | 48.05 | 2719.3 | 25.79 | -2.86 | 2588.8 | 23.44 |
| 6.24455 | 0.10828 | 0.38096 | 0.00173 | 2010.7 | 15.18 | 2080.8 | 8.1 | -3.49 | 2055.4 | 15.94 |
| 2.12697 | 0.11085 | 0.20749 | 0.00295 | 1157.6 | 36 | 1215.4 | 15.73 | -4.99 | 1234.2 | 50.36 |
| 1.90856 | 0.04262 | 0.18203 | 0.00111 | 1084.1 | 14.88 | 1078 | 6.03 | 0.56 | 1060 | 25.77 |
| 0.50634 | 0.01113 | 0.06617 | 0.00045 | 416 | 7.5 | 413 | 2.7 | 0.72 | 413 | 2.7 |
| 3.65677 | 0.17714 | 0.28657 | 0.00352 | 1562 | 38.62 | 1624.4 | 17.63 | -3.99 | 1542.7 | 37.71 |
| 0.86968 | 0.02412 | 0.10409 | 0.00083 | 635.4 | 13.1 | 638.3 | 4.85 | -0.46 | 638.3 | 4.85 |
| 3.97255 | 0.13714 | 0.27595 | 0.00238 | 1628.6 | 28 | 1570.9 | 12.04 | 3.54 | 1613.1 | 27.9 |
| **PC-02** | | | | | | | | | | |
| 2.33795 | 0.05553 | 0.21051 | 0.00126 | 1223.9 | 16.89 | 1231.5 | 6.69 | -0.62 | 1120.2 | 23.89 |
| 0.55671 | 0.02378 | 0.07078 | 0.0009 | 449.4 | 15.51 | 440.8 | 5.42 | 1.91 | 440.8 | 5.42 |
| 14.02689 | 0.4622 | 0.56019 | 0.00404 | 2751.5 | 31.23 | 2867.4 | 16.7 | -4.21 | 2787.4 | 15.4 |
| 1.7212 | 0.07341 | 0.1601 | 0.00176 | 1016.5 | 27.39 | 957.3 | 9.78 | 5.82 | 957.3 | 9.78 |
| 14.76232 | 0.45528 | 0.54045 | 0.00347 | 2800 | 29.33 | 2785.3 | 14.51 | 0.52 | 2719.5 | 14.62 |
| 7.09454 | 0.27115 | 0.37635 | 0.00337 | 2123.4 | 34.01 | 2059.2 | 15.77 | 3.02 | 2220.5 | 22.51 |
| 7.28233 | 0.21863 | 0.40247 | 0.0027 | 2146.6 | 26.8 | 2180.4 | 12.41 | -1.57 | 2096.9 | 18.34 |

| Isotope Ratios | | | | Ages | | | | | | |
|---|---|---|---|---|---|---|---|---|---|---|
| Pb207/U235 | | Pb206/U238 | | Pb207/U235 | | Pb206/U238 | | Discordance | Preferred Age | |
| 7.05018 | 0.177 | 0.40778 | 0.00237 | 2117.8 | 22.33 | 2204.7 | 10.84 | -4.10 | 2104.5 | 16.41 |
| 15.77983 | 0.529 | 0.53318 | 0.00373 | 2863.6 | 32.01 | 2754.8 | 15.69 | 3.80 | 2843.4 | 15.26 |
| 19.26643 | 0.59143 | 0.5981 | 0.00383 | 3055.3 | 29.63 | 3022.2 | 15.45 | 1.08 | 3056.8 | 13.69 |
| 2.21447 | 0.05225 | 0.21123 | 0.00131 | 1185.6 | 16.51 | 1235.4 | 6.96 | -4.20 | 1225 | 24.12 |
| 3.47249 | 0.07886 | 0.27374 | 0.00152 | 1521 | 17.9 | 1559.7 | 7.7 | -2.54 | 1471.6 | 19.98 |
| 3.81243 | 0.06718 | 0.28304 | 0.00126 | 1595.4 | 14.18 | 1606.7 | 6.32 | -0.71 | 1569.9 | 16.34 |
| 2.02631 | 0.05284 | 0.19955 | 0.00135 | 1124.4 | 17.73 | 1172.9 | 7.28 | -4.31 | 1097.8 | 27.53 |
| 3.07932 | 0.08751 | 0.2593 | 0.00184 | 1427.6 | 21.78 | 1486.2 | 9.44 | -4.10 | 1441.2 | 25.01 |
| 3.30884 | 0.09024 | 0.26399 | 0.00178 | 1483.1 | 21.27 | 1510.2 | 9.07 | -1.83 | 1476.8 | 23.74 |
| 2.83282 | 0.06463 | 0.21771 | 0.0013 | 1364.3 | 17.12 | 1269.8 | 6.88 | 6.93 | 1548.2 | 21.58 |
| 2.59781 | 0.04914 | 0.2211 | 0.0011 | 1300 | 13.87 | 1287.7 | 5.78 | 0.95 | 1302.7 | 19.88 |
| 5.97088 | 0.15562 | 0.35296 | 0.00215 | 1971.6 | 22.67 | 1948.7 | 10.24 | 1.16 | 1964.5 | 18.72 |
| 13.52991 | 0.3693 | 0.47594 | 0.00289 | 2717.4 | 25.81 | 2509.6 | 12.61 | 7.65 | 2839.3 | 15.15 |
| 4.78855 | 0.09544 | 0.31004 | 0.00152 | 1782.9 | 16.74 | 1740.9 | 7.5 | 2.36 | 1745.3 | 17.71 |
| 2.41424 | 0.07296 | 0.2075 | 0.00163 | 1246.8 | 21.7 | 1215.5 | 8.72 | 2.51 | 1365.3 | 29.31 |
| 2.25439 | 0.03625 | 0.20592 | 0.00091 | 1198.2 | 11.31 | 1207.1 | 4.84 | -0.74 | 1171.3 | 19.4 |
| 1.81868 | 0.03797 | 0.17801 | 0.00101 | 1052.2 | 13.68 | 1056.1 | 5.55 | -0.37 | 1095.9 | 24.48 |
| 12.79001 | 0.33139 | 0.50834 | 0.00303 | 2664.3 | 24.4 | 2649.5 | 12.96 | 0.56 | 2754.3 | 16.09 |
| 2.26967 | 0.06252 | 0.2092 | 0.0015 | 1202.9 | 19.41 | 1224.6 | 8.01 | -1.80 | 1221.9 | 28.5 |
| 4.52888 | 0.09444 | 0.30802 | 0.0016 | 1736.3 | 17.34 | 1730.9 | 7.89 | 0.31 | 1677.4 | 19.37 |
| 3.34953 | 0.05798 | 0.2486 | 0.00115 | 1492.7 | 13.53 | 1431.2 | 5.95 | 4.12 | 1546.3 | 18.93 |
| 2.22105 | 0.11356 | 0.18673 | 0.00258 | 1187.7 | 35.8 | 1103.6 | 14.02 | 7.08 | 1508.7 | 47.68 |
| 3.87791 | 0.09196 | 0.27071 | 0.0016 | 1609.1 | 19.14 | 1544.4 | 8.12 | 4.02 | 1616.7 | 21.91 |
| 3.6509 | 0.09786 | 0.26799 | 0.00179 | 1560.7 | 21.36 | 1530.6 | 9.1 | 1.93 | 1587.2 | 24.13 |
| 2.24693 | 0.04044 | 0.1916 | 0.00098 | 1195.8 | 12.65 | 1130 | 5.31 | 5.50 | 1477.9 | 21.32 |
| **PC-01** | | | | | | | | | | |
| 3.99722 | 0.12037 | 0.30381 | 0.00226 | 1633.6 | 24.46 | 1710.2 | 11.17 | -4.69 | 1640.9 | 24.24 |

| Isotope Ratios | | | | Ages | | | | | | |
|---|---|---|---|---|---|---|---|---|---|---|
| Pb207/U235 | | Pb206/U238 | | Pb207/U235 | | Pb206/U238 | | Discordance | Preferred Age | |
| 3.39153 | 0.0809 | 0.26262 | 0.0016 | 1502.4 | 18.7 | 1503.2 | 8.18 | -0.05 | 1546.3 | 21.74 |
| 5.21302 | 0.1507 | 0.33892 | 0.00237 | 1854.7 | 24.63 | 1881.5 | 11.4 | -1.44 | 1877.3 | 21.55 |
| 3.24887 | 0.07782 | 0.26077 | 0.00159 | 1468.9 | 18.6 | 1493.8 | 8.15 | -1.70 | 1446.9 | 22.51 |
| 4.529 | 0.0786 | 0.315 | 0.00143 | 1736.3 | 14.43 | 1765.3 | 7.03 | -1.67 | 1718.2 | 17.2 |
| 1.78532 | 0.04279 | 0.1809 | 0.00118 | 1040.1 | 15.6 | 1071.9 | 6.45 | -3.06 | 1037 | 27.9 |
| 3.52645 | 0.11535 | 0.26774 | 0.00221 | 1533.2 | 25.88 | 1529.3 | 11.24 | 0.25 | 1609.1 | 27.8 |
| 5.07758 | 0.13907 | 0.31835 | 0.00209 | 1832.4 | 23.23 | 1781.6 | 10.21 | 2.77 | 1768.4 | 21.96 |
| 13.91398 | 0.65482 | 0.49798 | 0.00497 | 2743.9 | 44.58 | 2605.1 | 21.37 | 5.06 | 2716.4 | 22.65 |
| 6.33687 | 0.14727 | 0.36773 | 0.00211 | 2023.6 | 20.38 | 2018.7 | 9.93 | 0.24 | 1981.7 | 19.6 |
| 4.00073 | 0.14279 | 0.26549 | 0.00229 | 1634.3 | 28.99 | 1517.9 | 11.69 | 7.12 | 1641.1 | 29.21 |
| 4.0232 | 0.10704 | 0.29696 | 0.00199 | 1638.9 | 21.64 | 1676.2 | 9.88 | -2.28 | 1591.6 | 24.23 |
| 4.76618 | 0.13547 | 0.3081 | 0.00213 | 1779 | 23.85 | 1731.3 | 10.51 | 2.68 | 1718.9 | 24.18 |
| 14.08065 | 0.45557 | 0.52199 | 0.00386 | 2755.2 | 30.67 | 2707.6 | 16.36 | 1.73 | 2790.4 | 19.82 |
| 4.43547 | 0.09523 | 0.30781 | 0.00176 | 1719 | 17.79 | 1729.9 | 8.67 | -0.63 | 1730.2 | 21.98 |
| 0.57246 | 0.0177 | 0.07624 | 0.00072 | 459.6 | 11.43 | 473.7 | 4.32 | -3.07 | 473.7 | 4.32 |
| 5.85311 | 0.1541 | 0.37291 | 0.00248 | 1954.3 | 22.83 | 2043.1 | 11.66 | -4.54 | 1938.8 | 23.14 |
| 5.54589 | 0.29644 | 0.34265 | 0.00431 | 1907.7 | 45.98 | 1899.4 | 20.7 | 0.44 | 1974.5 | 36.09 |
| **BBR-2011** | | | | | | | | | | |
| 0.24095 | 0.00971 | 0.03509 | 0.00045 | 219.2 | 7.94 | 222.3 | 2.79 | -1.41 | 222.3 | 2.79 |
| 0.23842 | 0.00748 | 0.03549 | 0.00036 | 217.1 | 6.13 | 224.8 | 2.21 | -3.55 | 224.8 | 2.21 |
| 0.23954 | 0.01244 | 0.03557 | 0.00061 | 218 | 10.19 | 225.3 | 3.78 | -3.35 | 225.3 | 3.78 |
| 0.23157 | 0.0099 | 0.03334 | 0.00047 | 211.5 | 8.16 | 211.4 | 2.96 | 0.05 | 211.4 | 2.96 |
| 0.23038 | 0.01131 | 0.03356 | 0.00053 | 210.5 | 9.34 | 212.8 | 3.3 | -1.09 | 212.8 | 3.3 |
| 2.02057 | 0.06041 | 0.19705 | 0.0016 | 1122.5 | 20.31 | 1159.4 | 8.62 | -3.29 | 1159.4 | 8.62 |
| 0.23015 | 0.00841 | 0.03253 | 0.00037 | 210.3 | 6.94 | 206.3 | 2.32 | 1.90 | 206.3 | 2.32 |
| 2.26189 | 0.04698 | 0.2031 | 0.00115 | 1200.5 | 14.62 | 1191.9 | 6.18 | 0.72 | 1191.9 | 6.18 |
| 0.2409 | 0.01486 | 0.03383 | 0.00061 | 219.2 | 12.16 | 214.5 | 3.82 | 2.14 | 214.5 | 3.82 |

| Isotope Ratios | | | | Ages | | | | | | |
|---|---|---|---|---|---|---|---|---|---|---|
| Pb207/U235 | | Pb206/U238 | | Pb207/U235 | | Pb206/U238 | | Discordance | Preferred Age | |
| 0.2195 | 0.00868 | 0.03241 | 0.00042 | 201.5 | 7.23 | 205.6 | 2.61 | -2.03 | 205.6 | 2.61 |
| 0.23244 | 0.01076 | 0.03463 | 0.0005 | 212.2 | 8.87 | 219.5 | 3.11 | -3.44 | 219.5 | 3.11 |
| 0.23094 | 0.01393 | 0.03275 | 0.00064 | 211 | 11.49 | 207.8 | 3.97 | 1.52 | 207.8 | 3.97 |
| 0.22456 | 0.01141 | 0.03291 | 0.00051 | 205.7 | 9.46 | 208.7 | 3.2 | -1.46 | 208.7 | 3.2 |
| 0.22653 | 0.0081 | 0.03343 | 0.0004 | 207.3 | 6.71 | 212 | 2.48 | -2.27 | 212 | 2.48 |
| 0.22679 | 0.00735 | 0.03261 | 0.00034 | 207.5 | 6.09 | 206.8 | 2.14 | 0.34 | 206.8 | 2.14 |
| 0.22075 | 0.01738 | 0.03214 | 0.00076 | 202.5 | 14.46 | 203.9 | 4.76 | -0.69 | 203.9 | 4.76 |
| 0.22962 | 0.00851 | 0.03323 | 0.00038 | 209.9 | 7.02 | 210.7 | 2.38 | -0.38 | 210.7 | 2.38 |
| 0.22699 | 0.01078 | 0.03255 | 0.00048 | 207.7 | 8.92 | 206.5 | 2.99 | 0.58 | 206.5 | 2.99 |
| 0.23745 | 0.00796 | 0.03371 | 0.00037 | 216.3 | 6.53 | 213.7 | 2.28 | 1.20 | 213.7 | 2.28 |
| 0.22986 | 0.00939 | 0.03209 | 0.00043 | 210.1 | 7.76 | 203.6 | 2.7 | 3.09 | 203.6 | 2.7 |
| 2.04867 | 0.0738 | 0.19403 | 0.00185 | 1131.9 | 24.58 | 1143.2 | 9.97 | -1.00 | 1143.2 | 9.97 |
| 0.21058 | 0.00627 | 0.03151 | 0.0003 | 194 | 5.26 | 200 | 1.9 | -3.09 | 200 | 1.9 |
| 0.22437 | 0.00805 | 0.03178 | 0.00036 | 205.5 | 6.67 | 201.7 | 2.24 | 1.85 | 201.7 | 2.24 |
| 0.21962 | 0.00673 | 0.03231 | 0.00032 | 201.6 | 5.6 | 205 | 1.99 | -1.69 | 205 | 1.99 |
| 0.23725 | 0.01642 | 0.03456 | 0.00077 | 216.2 | 13.48 | 219 | 4.78 | -1.30 | 219 | 4.78 |
| 0.21687 | 0.01375 | 0.03167 | 0.00064 | 199.3 | 11.47 | 201 | 3.97 | -0.85 | 201 | 3.97 |
| 0.22244 | 0.00924 | 0.03237 | 0.00041 | 203.9 | 7.67 | 205.3 | 2.58 | -0.69 | 205.3 | 2.58 |
| 0.24249 | 0.00764 | 0.03244 | 0.00034 | 220.5 | 6.24 | 205.8 | 2.1 | 6.67 | 205.8 | 2.1 |
| 0.22979 | 0.00759 | 0.03239 | 0.00033 | 210 | 6.27 | 205.5 | 2.07 | 2.14 | 205.5 | 2.07 |
| 0.2096 | 0.00933 | 0.03045 | 0.00044 | 193.2 | 7.84 | 193.4 | 2.75 | -0.10 | 193.4 | 2.75 |
| 0.23301 | 0.01531 | 0.03229 | 0.00061 | 212.7 | 12.61 | 204.9 | 3.79 | 3.67 | 204.9 | 3.79 |
| 0.22084 | 0.00589 | 0.0322 | 0.00027 | 202.6 | 4.9 | 204.3 | 1.72 | -0.84 | 204.3 | 1.72 |
| 0.2399 | 0.00765 | 0.03332 | 0.00033 | 218.3 | 6.26 | 211.3 | 2.05 | 3.21 | 211.3 | 2.05 |
| 0.22317 | 0.00786 | 0.03285 | 0.00036 | 204.5 | 6.52 | 208.3 | 2.23 | -1.86 | 208.3 | 2.23 |
| 0.212 | 0.0075 | 0.03058 | 0.00033 | 195.2 | 6.28 | 194.2 | 2.08 | 0.51 | 194.2 | 2.08 |
| 0.22766 | 0.01045 | 0.03239 | 0.00048 | 208.3 | 8.64 | 205.5 | 3.02 | 1.34 | 205.5 | 3.02 |

| Isotope Ratios | | | | Ages | | | | | | |
|---|---|---|---|---|---|---|---|---|---|---|
| Pb207/U235 | | Pb206/U238 | | Pb207/U235 | | Pb206/U238 | | Discordance | Preferred Age | |
| 0.21839 | 0.00778 | 0.03193 | 0.00037 | 200.6 | 6.49 | 202.6 | 2.3 | -1.00 | 202.6 | 2.3 |
| 0.22213 | 0.01209 | 0.03194 | 0.00054 | 203.7 | 10.04 | 202.7 | 3.37 | 0.49 | 202.7 | 3.37 |
| 0.22942 | 0.01281 | 0.03235 | 0.00056 | 209.7 | 10.58 | 205.2 | 3.47 | 2.15 | 205.2 | 3.47 |
| 0.22453 | 0.00716 | 0.03207 | 0.00033 | 205.7 | 5.93 | 203.5 | 2.07 | 1.07 | 203.5 | 2.07 |
| 0.2068 | 0.0077 | 0.0315 | 0.00038 | 190.9 | 6.48 | 199.9 | 2.37 | -4.71 | 199.9 | 2.37 |
| 0.22035 | 0.00829 | 0.0318 | 0.00039 | 202.2 | 6.89 | 201.8 | 2.46 | 0.20 | 201.8 | 2.46 |
| 0.21199 | 0.00756 | 0.03039 | 0.00035 | 195.2 | 6.33 | 193 | 2.18 | 1.13 | 193 | 2.18 |
| 0.21797 | 0.00831 | 0.03154 | 0.00038 | 200.2 | 6.93 | 200.2 | 2.38 | 0.00 | 200.2 | 2.38 |
| 1.72469 | 0.05217 | 0.17132 | 0.00143 | 1017.8 | 19.44 | 1019.4 | 7.87 | -0.16 | 1019.4 | 7.87 |
| 0.22366 | 0.01224 | 0.03157 | 0.00054 | 205 | 10.16 | 200.4 | 3.39 | 2.24 | 200.4 | 3.39 |
| 1.91609 | 0.03375 | 0.1791 | 0.00094 | 1086.7 | 11.75 | 1062 | 5.14 | 2.27 | 1062 | 5.14 |
| 0.2214 | 0.00874 | 0.03253 | 0.00041 | 203.1 | 7.26 | 206.4 | 2.55 | -1.62 | 206.4 | 2.55 |
| 0.21553 | 0.00882 | 0.03051 | 0.00041 | 198.2 | 7.37 | 193.7 | 2.58 | 2.27 | 193.7 | 2.58 |
| 0.22138 | 0.00838 | 0.03217 | 0.0004 | 203.1 | 6.96 | 204.1 | 2.5 | -0.49 | 204.1 | 2.5 |
| 0.2244 | 0.01058 | 0.03231 | 0.00045 | 205.6 | 8.78 | 205 | 2.79 | 0.29 | 205 | 2.79 |
| 0.21747 | 0.00878 | 0.0314 | 0.00043 | 199.8 | 7.32 | 199.3 | 2.66 | 0.25 | 199.3 | 2.66 |
| 0.22267 | 0.01128 | 0.03241 | 0.00049 | 204.1 | 9.36 | 205.6 | 3.06 | -0.73 | 205.6 | 3.06 |
| **BBR-2010** | | | | | | | | | | |
| 0.22707 | 0.00992 | 0.03221 | 0.00047 | 207.8 | 8.21 | 204.3 | 2.97 | 1.68 | 204.3 | 2.97 |
| 0.25698 | 0.01177 | 0.03375 | 0.00055 | 232.2 | 9.51 | 214 | 3.41 | 7.84 | 214 | 3.41 |
| 0.22335 | 0.00976 | 0.03192 | 0.00047 | 204.7 | 8.1 | 202.5 | 2.95 | 1.07 | 202.5 | 2.95 |
| 0.21623 | 0.00747 | 0.03248 | 0.00037 | 198.8 | 6.24 | 206.1 | 2.31 | -3.67 | 206.1 | 2.31 |
| 0.19732 | 0.01616 | 0.03008 | 0.00078 | 182.9 | 13.7 | 191 | 4.86 | -4.43 | 191 | 4.86 |
| 0.226 | 0.00552 | 0.03339 | 0.00028 | 206.9 | 4.57 | 211.7 | 1.73 | -2.32 | 211.7 | 1.73 |
| 0.21322 | 0.01381 | 0.03128 | 0.00066 | 196.2 | 11.56 | 198.6 | 4.13 | -1.22 | 198.6 | 4.13 |
| 0.20726 | 0.00665 | 0.03153 | 0.00034 | 191.2 | 5.6 | 200.1 | 2.11 | -4.65 | 200.1 | 2.11 |
| 0.23038 | 0.00974 | 0.03141 | 0.00045 | 210.5 | 8.04 | 199.3 | 2.82 | 5.32 | 199.3 | 2.82 |

| Isotope Ratios | | | | Ages | | | | | | |
|---|---|---|---|---|---|---|---|---|---|---|
| Pb207/U235 | | Pb206/U238 | | Pb207/U235 | | Pb206/U238 | | Discordance | Preferred Age | |
| 0.23204 | 0.01559 | 0.03106 | 0.00067 | 211.9 | 12.85 | 197.2 | 4.18 | 6.94 | 197.2 | 4.18 |
| 0.24194 | 0.01602 | 0.03122 | 0.00067 | 220 | 13.1 | 198.2 | 4.2 | 9.91 | 198.2 | 4.2 |
| 0.21656 | 0.0071 | 0.03081 | 0.00034 | 199 | 5.93 | 195.6 | 2.14 | 1.71 | 195.6 | 2.14 |
| **ECC-01** | | | | | | | | | | |
| 10.1301 | 0.53753 | 0.4673 | 0.00576 | 2446.7 | 49.04 | 2471.7 | 25.32 | -1.02 | 2480.5 | 31.43 |
| 10.01748 | 1.78479 | 0.44468 | 0.0181 | 2436.4 | 164.49 | 2371.6 | 80.75 | 2.66 | 2463.3 | 88.66 |
| 5.31311 | 0.23238 | 0.33578 | 0.0036 | 1871 | 37.37 | 1866.3 | 17.38 | 0.25 | 1867.7 | 34.54 |
| 2.7332 | 0.20777 | 0.22799 | 0.00446 | 1337.5 | 56.51 | 1324 | 23.41 | 1.01 | 1286.9 | 73.64 |
| 4.43861 | 0.30286 | 0.31718 | 0.0053 | 1719.6 | 56.54 | 1776 | 25.95 | -3.28 | 1662 | 53.36 |
| 4.47383 | 0.49841 | 0.31892 | 0.00934 | 1726.1 | 92.45 | 1784.5 | 45.63 | -3.38 | 1986.2 | 80.72 |
| 4.35926 | 0.22415 | 0.31243 | 0.00409 | 1704.7 | 42.47 | 1752.7 | 20.07 | -2.82 | 1767.8 | 42.23 |
| 13.29975 | 1.13819 | 0.52045 | 0.00977 | 2701.2 | 80.82 | 2701.1 | 41.43 | 0.00 | 2722.6 | 40.75 |
| 1.83618 | 0.12685 | 0.18077 | 0.00325 | 1058.5 | 45.41 | 1071.2 | 17.74 | -1.20 | 968.7 | 78.48 |
| 12.22744 | 1.47688 | 0.50188 | 0.01414 | 2622 | 113.37 | 2621.9 | 60.69 | 0.00 | 2746.7 | 57.71 |
| 4.34791 | 0.42951 | 0.30731 | 0.007 | 1702.5 | 81.55 | 1727.5 | 34.53 | -1.47 | 1584.7 | 73.4 |
| 3.25775 | 0.1784 | 0.25622 | 0.00363 | 1471 | 42.55 | 1470.5 | 18.65 | 0.03 | 1443.4 | 51.68 |
| 1.08188 | 0.2699 | 0.11532 | 0.00772 | 744.6 | 131.63 | 703.6 | 44.62 | 5.51 | 703.6 | 44.62 |
| 4.86833 | 0.93749 | 0.30875 | 0.01582 | 1796.8 | 162.21 | 1734.6 | 77.93 | 3.46 | 2160.8 | 129.81 |
| 0.58201 | 0.09359 | 0.07878 | 0.00376 | 465.8 | 60.07 | 488.9 | 22.44 | -4.96 | 488.9 | 22.44 |
| 10.94243 | 0.9375 | 0.48053 | 0.00945 | 2518.2 | 79.71 | 2529.6 | 41.13 | -0.45 | 2532.1 | 46 |
| 1.82293 | 0.10257 | 0.16514 | 0.00256 | 1053.7 | 36.89 | 985.3 | 14.17 | 6.49 | 985.3 | 14.17 |
| 13.66965 | 1.47001 | 0.54492 | 0.01218 | 2727.1 | 101.75 | 2804 | 50.84 | -2.82 | 2559 | 50.61 |
| 16.88684 | 1.42574 | 0.5747 | 0.01072 | 2928.4 | 80.94 | 2927.1 | 43.87 | 0.04 | 2884 | 40.53 |
| 10.77455 | 0.65537 | 0.46684 | 0.00648 | 2503.9 | 56.52 | 2469.7 | 28.5 | 1.37 | 2435.3 | 38.09 |
| 4.45012 | 0.28223 | 0.31257 | 0.00511 | 1721.7 | 52.58 | 1753.4 | 25.11 | -1.84 | 1834.2 | 52.24 |
| 18.41095 | 3.49778 | 0.59284 | 0.02135 | 3011.5 | 182.97 | 3000.9 | 86.41 | 0.35 | 2672.7 | 72.47 |
| 1.80025 | 0.07615 | 0.18173 | 0.00214 | 1045.5 | 27.61 | 1076.4 | 11.68 | -2.96 | 950.3 | 53.91 |

| Isotope Ratios | | | | Ages | | | | | | |
|---|---|---|---|---|---|---|---|---|---|---|
| Pb207/U235 | | Pb206/U238 | | Pb207/U235 | | Pb206/U238 | | Discordance | Preferred Age | |
| 5.86509 | 0.36521 | 0.3545 | 0.00537 | 1956.1 | 54.02 | 1956 | 25.54 | 0.01 | 1914.3 | 48.2 |
| 3.25423 | 0.37365 | 0.25197 | 0.00796 | 1470.2 | 89.18 | 1448.6 | 41 | 1.47 | 1761.4 | 98.9 |
| 4.61535 | 0.46432 | 0.30784 | 0.00731 | 1752 | 83.96 | 1730.1 | 36.05 | 1.25 | 1718.5 | 75.33 |
| 4.02929 | 0.31249 | 0.30582 | 0.00614 | 1640.1 | 63.09 | 1720.1 | 30.32 | -4.88 | 1730 | 65.18 |
| 2.06885 | 0.33088 | 0.20074 | 0.00808 | 1138.6 | 109.48 | 1179.3 | 43.36 | -3.57 | 924.7 | 165.62 |
| 2.88873 | 0.21209 | 0.23836 | 0.00451 | 1379 | 55.38 | 1378.2 | 23.45 | 0.06 | 1300.6 | 72.63 |
| 6.64111 | 0.92333 | 0.3964 | 0.01263 | 2064.8 | 122.7 | 2152.4 | 58.32 | -4.24 | 1990.8 | 87.02 |
| 12.93919 | 1.66272 | 0.47338 | 0.01273 | 2675.2 | 121.12 | 2498.4 | 55.68 | 6.61 | 2523.1 | 63.48 |
| 5.53481 | 0.70346 | 0.34674 | 0.01074 | 1906 | 109.3 | 1919 | 51.43 | -0.68 | 1929.1 | 88.44 |
| 2.22633 | 0.10151 | 0.19316 | 0.00241 | 1189.4 | 31.95 | 1138.5 | 13.02 | 4.28 | 1154.2 | 55.79 |
| 15.02141 | 1.29752 | 0.54167 | 0.01038 | 2816.6 | 82.23 | 2790.4 | 43.42 | 0.93 | 2835.3 | 47.19 |
| **GS-05** | | | | | | | | | | |
| 2.1252 | 0.10819 | 0.20522 | 0.00271 | 1157 | 35.15 | 1203.3 | 14.51 | -4.00 | 1226.7 | 54.13 |
| 1.72781 | 0.08477 | 0.18026 | 0.00234 | 1018.9 | 31.56 | 1068.4 | 12.78 | -4.86 | 1096 | 57.66 |
| 4.58055 | 0.41421 | 0.32309 | 0.0073 | 1745.7 | 75.37 | 1804.8 | 35.58 | -3.39 | 1980.5 | 65.47 |
| 3.74428 | 0.18095 | 0.28991 | 0.00346 | 1580.9 | 38.73 | 1641.1 | 17.28 | -3.81 | 1620.9 | 41.01 |
| 3.18816 | 0.20625 | 0.25214 | 0.00396 | 1454.3 | 50 | 1449.5 | 20.41 | 0.33 | 1412.9 | 57.73 |
| 5.781 | 0.36542 | 0.36464 | 0.00543 | 1943.6 | 54.72 | 2004.1 | 25.64 | -3.11 | 2052.4 | 42.33 |
| 2.68661 | 0.18394 | 0.23944 | 0.00425 | 1324.8 | 50.66 | 1383.8 | 22.13 | -4.45 | 1440.2 | 64.91 |
| 5.39276 | 0.28752 | 0.33818 | 0.00415 | 1883.7 | 45.67 | 1877.9 | 20 | 0.31 | 1846.8 | 38.43 |
| 12.2304 | 1.13352 | 0.49261 | 0.0097 | 2622.2 | 86.99 | 2582 | 41.9 | 1.53 | 2609.9 | 43.03 |
| 4.43887 | 0.44329 | 0.32141 | 0.0073 | 1719.6 | 82.76 | 1796.6 | 35.62 | -4.48 | 1553 | 75.94 |
| 5.16529 | 0.13037 | 0.33514 | 0.0021 | 1846.9 | 21.47 | 1863.2 | 10.12 | -0.88 | 1828.3 | 23.15 |
| 2.92665 | 0.15068 | 0.25137 | 0.00329 | 1388.8 | 38.96 | 1445.6 | 16.95 | -4.09 | 1455.3 | 48.82 |
| 2.22805 | 0.08361 | 0.21063 | 0.00206 | 1189.9 | 26.3 | 1232.1 | 10.98 | -3.55 | 1181.9 | 40.74 |
| 5.25859 | 0.2458 | 0.33669 | 0.00358 | 1862.2 | 39.88 | 1870.7 | 17.27 | -0.46 | 1812.7 | 35.15 |
| 5.3003 | 0.24189 | 0.33038 | 0.00352 | 1868.9 | 38.98 | 1840.2 | 17.06 | 1.54 | 1864.1 | 34.46 |

| Isotope Ratios | | | | Ages | | | | | | |
|---|---|---|---|---|---|---|---|---|---|---|
| Pb207/U235 | | Pb206/U238 | | Pb207/U235 | | Pb206/U238 | | Discordance | Preferred Age | |
| 3.38216 | 0.24586 | 0.24402 | 0.00423 | 1500.3 | 56.97 | 1407.6 | 21.91 | 6.18 | 1450.4 | 63.82 |
| 3.73028 | 0.20064 | 0.28167 | 0.00369 | 1577.9 | 43.07 | 1599.8 | 18.56 | -1.39 | 1633.2 | 45.15 |
| 4.9436 | 0.32416 | 0.32011 | 0.00476 | 1809.7 | 55.38 | 1790.3 | 23.26 | 1.07 | 1738.5 | 48.24 |
| 5.84974 | 0.63134 | 0.36548 | 0.00899 | 1953.8 | 93.59 | 2008.1 | 42.46 | -2.78 | 1955 | 70.35 |
| 5.21257 | 0.3399 | 0.32775 | 0.00512 | 1854.7 | 55.55 | 1827.5 | 24.84 | 1.47 | 1968.1 | 46.81 |
| 14.10984 | 2.08605 | 0.53552 | 0.01551 | 2757.1 | 140.18 | 2764.7 | 65.12 | -0.28 | 2686.1 | 60.26 |
| 1.71861 | 0.10977 | 0.17977 | 0.00298 | 1015.5 | 41 | 1065.7 | 16.26 | -4.94 | 926 | 76.13 |
| 1.85727 | 0.0634 | 0.18394 | 0.00168 | 1066 | 22.53 | 1088.5 | 9.15 | -2.11 | 1056.1 | 42.15 |
| 1.5411 | 0.06735 | 0.16564 | 0.00192 | 946.9 | 26.91 | 988.1 | 10.63 | -4.35 | 988.1 | 10.63 |
| 1.89531 | 0.11908 | 0.17589 | 0.00295 | 1079.4 | 41.76 | 1044.5 | 16.16 | 3.23 | 1185.1 | 70.68 |
| 1.9748 | 0.09532 | 0.17301 | 0.0023 | 1106.9 | 32.53 | 1028.7 | 12.67 | 7.06 | 1381.7 | 54.06 |
| 10.46893 | 0.78874 | 0.44462 | 0.00732 | 2477.2 | 69.83 | 2371.3 | 32.68 | 4.27 | 2497.8 | 41.52 |
| 3.80919 | 0.36116 | 0.2887 | 0.00653 | 1594.7 | 76.25 | 1635 | 32.66 | -2.53 | 1551.4 | 79.46 |
| 3.9478 | 0.2879 | 0.2982 | 0.00535 | 1623.5 | 59.08 | 1682.4 | 26.56 | -3.63 | 1692.5 | 59.45 |
| 2.0964 | 0.28707 | 0.17873 | 0.006 | 1147.6 | 94.14 | 1060 | 32.82 | 7.63 | 1177.9 | 145.48 |
| 4.77823 | 0.17139 | 0.30393 | 0.00268 | 1781.1 | 30.12 | 1710.8 | 13.22 | 3.95 | 1787.4 | 33.75 |
| 1.62656 | 0.10358 | 0.16827 | 0.00287 | 980.5 | 40.04 | 1002.6 | 15.86 | -2.25 | 996 | 77.67 |
| 1.50981 | 0.10575 | 0.14498 | 0.00278 | 934.4 | 42.78 | 872.8 | 15.67 | 6.59 | 872.8 | 15.67 |
| 7.38569 | 0.42608 | 0.36148 | 0.00468 | 2159.2 | 51.59 | 1989.2 | 22.16 | 7.87 | 2113 | 40.3 |
| 2.35266 | 0.1378 | 0.22066 | 0.00325 | 1228.4 | 41.73 | 1285.4 | 17.17 | -4.64 | 1137.1 | 63.17 |
| 1.86735 | 0.06412 | 0.18897 | 0.00178 | 1069.6 | 22.7 | 1115.8 | 9.67 | -4.32 | 1093 | 44.04 |
| 7.76004 | 0.97829 | 0.42002 | 0.01111 | 2203.6 | 113.39 | 2260.6 | 50.45 | -2.59 | 2012.2 | 73.28 |
| 12.71599 | 0.9523 | 0.51716 | 0.00849 | 2658.8 | 70.5 | 2687.1 | 36.08 | -1.06 | 2697.4 | 40.5 |
| 5.47966 | 0.28456 | 0.3268 | 0.004 | 1897.4 | 44.59 | 1822.8 | 19.46 | 3.93 | 1865.8 | 42.49 |
| 2.1391 | 0.1702 | 0.19498 | 0.00399 | 1161.5 | 55.05 | 1148.3 | 21.52 | 1.14 | 1158.9 | 86.92 |
| 5.23168 | 0.40111 | 0.35143 | 0.00668 | 1857.8 | 65.36 | 1941.4 | 31.87 | -4.50 | 1985.8 | 58.48 |
| 2.01258 | 0.16116 | 0.1875 | 0.00374 | 1119.8 | 54.32 | 1107.8 | 20.28 | 1.07 | 1056.9 | 93.6 |

| Isotope Ratios | | | | Ages | | | | | | |
|---|---|---|---|---|---|---|---|---|---|---|
| Pb207/U235 | | Pb206/U238 | | Pb207/U235 | | Pb206/U238 | | Discordance | Preferred Age | |
| 4.88924 | 0.26908 | 0.31836 | 0.00432 | 1800.4 | 46.39 | 1781.7 | 21.13 | 1.04 | 1870.4 | 46.76 |
| 2.0882 | 0.1169 | 0.19765 | 0.00289 | 1144.9 | 38.44 | 1162.7 | 15.57 | -1.55 | 1102.9 | 63.91 |
| 1.76521 | 0.08018 | 0.17332 | 0.00213 | 1032.8 | 29.44 | 1030.4 | 11.71 | 0.23 | 1052.8 | 57.25 |
| 5.69497 | 0.84675 | 0.35617 | 0.01251 | 1930.6 | 128.42 | 1964 | 59.49 | -1.73 | 2031.1 | 100.3 |
| **GS-04** | | | | | | | | | | |
| 1.7791 | 0.19015 | 0.17178 | 0.00515 | 1037.9 | 69.48 | 1021.9 | 28.31 | 1.54 | 1134.6 | 125.28 |
| 0.74151 | 0.08634 | 0.09028 | 0.00337 | 563.3 | 50.34 | 557.2 | 19.95 | 1.08 | 557.2 | 19.95 |
| 1.95362 | 0.35664 | 0.18596 | 0.00913 | 1099.7 | 122.6 | 1099.5 | 49.6 | 0.02 | 1000.1 | 200.93 |
| 4.43283 | 0.36981 | 0.3003 | 0.00658 | 1718.5 | 69.12 | 1692.8 | 32.64 | 1.50 | 1947 | 64.51 |
| 1.89632 | 0.13636 | 0.1845 | 0.00371 | 1079.8 | 47.8 | 1091.5 | 20.17 | -1.08 | 1112.6 | 85.96 |
| 2.49385 | 0.30658 | 0.21836 | 0.00697 | 1270.2 | 89.1 | 1273.2 | 36.9 | -0.24 | 1200.1 | 126.81 |
| 2.82467 | 0.43361 | 0.23369 | 0.00977 | 1362.1 | 115.12 | 1353.8 | 51.03 | 0.61 | 1523.2 | 141.39 |
| 5.55984 | 0.29027 | 0.3437 | 0.0044 | 1909.9 | 44.93 | 1904.4 | 21.1 | 0.29 | 1815.9 | 41.56 |
| 1.85457 | 0.22739 | 0.17681 | 0.00597 | 1065.1 | 80.88 | 1049.5 | 32.71 | 1.46 | 1085 | 137.71 |
| 2.19654 | 0.20615 | 0.19782 | 0.00491 | 1179.9 | 65.48 | 1163.6 | 26.42 | 1.38 | 1100.6 | 102.36 |
| 4.70629 | 0.54853 | 0.32134 | 0.00948 | 1768.4 | 97.61 | 1796.3 | 46.27 | -1.58 | 1858.6 | 86.57 |
| 3.50858 | 0.14852 | 0.27011 | 0.00306 | 1529.1 | 33.45 | 1541.4 | 15.54 | -0.80 | 1566.3 | 41.69 |
| 1.62073 | 0.10704 | 0.16257 | 0.00293 | 978.3 | 41.47 | 971 | 16.25 | 0.75 | 971 | 16.25 |
| 1.91011 | 0.07017 | 0.18429 | 0.00194 | 1084.6 | 24.48 | 1090.4 | 10.55 | -0.53 | 1152.3 | 45.87 |
| 0.42951 | 0.0574 | 0.05865 | 0.00221 | 362.8 | 40.77 | 367.4 | 13.49 | -1.27 | 367.4 | 13.49 |
| 3.67825 | 0.61227 | 0.27975 | 0.0126 | 1566.7 | 132.89 | 1590.1 | 63.47 | -1.49 | 1806.1 | 135.92 |
| 13.24071 | 1.32245 | 0.52137 | 0.01222 | 2697 | 94.29 | 2705 | 51.79 | -0.30 | 2805.4 | 48.24 |
| 0.71362 | 0.10574 | 0.08981 | 0.00341 | 546.9 | 62.65 | 554.4 | 20.17 | -1.37 | 554.4 | 20.17 |
| 0.65584 | 0.06272 | 0.08246 | 0.00223 | 512.1 | 38.46 | 510.8 | 13.31 | 0.25 | 510.8 | 13.31 |
| 4.96612 | 0.21451 | 0.32726 | 0.00356 | 1813.6 | 36.51 | 1825.1 | 17.29 | -0.63 | 1807.5 | 37.84 |
| 3.07221 | 0.27049 | 0.25433 | 0.00576 | 1425.8 | 67.45 | 1460.8 | 29.62 | -2.45 | 1433.7 | 81.65 |
| 1.87418 | 0.10497 | 0.17934 | 0.00288 | 1072 | 37.08 | 1063.4 | 15.72 | 0.80 | 1249.4 | 65.43 |

| Isotope Ratios | | | | Ages | | | | | | |
|---|---|---|---|---|---|---|---|---|---|---|
| Pb207/U235 | | Pb206/U238 | | Pb207/U235 | | Pb206/U238 | | Discordance | Preferred Age | |
| 2.37828 | 0.4353 | 0.21955 | 0.0119 | 1236.1 | 130.83 | 1279.5 | 62.92 | -3.51 | 1643.8 | 177.87 |
| 10.4684 | 1.64851 | 0.46334 | 0.0273 | 2477.1 | 145.96 | 2454.3 | 120.27 | 0.92 | 2751.5 | 169.49 |
| 4.08172 | 0.73714 | 0.29155 | 0.01344 | 1650.7 | 147.29 | 1649.3 | 67.06 | 0.08 | 1708.6 | 143.3 |
| 10.69287 | 1.69818 | 0.49353 | 0.01883 | 2496.8 | 147.47 | 2585.9 | 81.28 | -3.57 | 2726.4 | 79.56 |
| 2.72564 | 0.17369 | 0.23064 | 0.00411 | 1335.5 | 47.34 | 1337.8 | 21.55 | -0.17 | 1538.3 | 64.44 |
| 16.97356 | 3.0003 | 0.58473 | 0.02154 | 2933.3 | 169.5 | 2968 | 87.6 | -1.18 | 2813.8 | 68.56 |
| 4.19903 | 0.51691 | 0.29197 | 0.00859 | 1673.8 | 100.95 | 1651.4 | 42.86 | 1.34 | 1596.6 | 96.18 |
| 3.0701 | 0.39506 | 0.24348 | 0.00714 | 1425.3 | 98.56 | 1404.7 | 37.02 | 1.45 | 1014.4 | 118.71 |
| 3.12018 | 0.17768 | 0.2535 | 0.00374 | 1437.7 | 43.79 | 1456.5 | 19.23 | -1.31 | 1412.9 | 56.92 |
| 11.94742 | 1.23839 | 0.50179 | 0.01223 | 2600.3 | 97.12 | 2621.5 | 52.48 | -0.82 | 2769.9 | 53.64 |
| 4.40172 | 0.22576 | 0.31194 | 0.00415 | 1712.7 | 42.44 | 1750.3 | 20.4 | -2.20 | 1753.7 | 47.09 |
| 3.53284 | 0.30331 | 0.27549 | 0.00617 | 1534.6 | 67.94 | 1568.6 | 31.21 | -2.22 | 1627.9 | 75.18 |
| 17.89756 | 2.85861 | 0.55216 | 0.01719 | 2984.2 | 153.6 | 2834.1 | 71.37 | 5.03 | 2801.2 | 64.08 |
| 1.00804 | 0.15278 | 0.11309 | 0.00486 | 707.9 | 77.25 | 690.7 | 28.12 | 2.43 | 690.7 | 28.12 |
| 2.41427 | 0.38382 | 0.2136 | 0.00874 | 1246.9 | 114.15 | 1248 | 46.42 | -0.09 | 1170.5 | 157.47 |
| 0.57866 | 0.0624 | 0.0753 | 0.00239 | 463.6 | 40.13 | 468 | 14.35 | -0.95 | 468 | 14.35 |
| 1.73001 | 0.09665 | 0.16842 | 0.00263 | 1019.8 | 35.95 | 1003.4 | 14.49 | 1.61 | 1051.5 | 69.69 |
| 1.82262 | 0.20618 | 0.17809 | 0.00535 | 1053.6 | 74.17 | 1056.5 | 29.28 | -0.28 | 990.8 | 132.64 |
| 1.6227 | 0.12162 | 0.16315 | 0.00344 | 979 | 47.09 | 974.2 | 19.09 | 0.49 | 1078 | 92.17 |
| 5.19703 | 0.28789 | 0.32333 | 0.00451 | 1852.1 | 47.17 | 1806 | 21.99 | 2.49 | 1908.6 | 48.33 |
| 1.6969 | 0.16463 | 0.16948 | 0.0045 | 1007.4 | 61.98 | 1009.2 | 24.79 | -0.18 | 1188.8 | 110.66 |
| 2.13244 | 0.19939 | 0.19548 | 0.0048 | 1159.4 | 64.63 | 1151 | 25.9 | 0.72 | 1177.2 | 101.13 |
| **GS-03** | | | | | | | | | | |
| 3.41552 | 0.30457 | 0.24364 | 0.00528 | 1508 | 70.04 | 1405.6 | 27.37 | 6.79 | 1570.8 | 82.32 |
| 5.18324 | 0.22434 | 0.3322 | 0.00347 | 1849.9 | 36.84 | 1849 | 16.79 | 0.05 | 1874.8 | 40.37 |
| 2.88832 | 0.13731 | 0.24133 | 0.00293 | 1378.9 | 35.86 | 1393.6 | 15.23 | -1.07 | 1432 | 51.1 |
| 4.14915 | 0.22285 | 0.29128 | 0.00383 | 1664 | 43.95 | 1647.9 | 19.13 | 0.97 | 1686 | 49.69 |

| Isotope Ratios | | | | Ages | | | | | | |
|---|---|---|---|---|---|---|---|---|---|---|
| Pb207/U235 | | Pb206/U238 | | Pb207/U235 | | Pb206/U238 | | Discordance | Preferred Age | |
| 2.25277 | 0.22813 | 0.20281 | 0.0054 | 1197.7 | 71.21 | 1190.4 | 28.94 | 0.61 | 1338.2 | 103.66 |
| 0.53257 | 0.05061 | 0.07254 | 0.00167 | 433.5 | 33.53 | 451.5 | 10.06 | -4.15 | 451.5 | 10.06 |
| 2.11269 | 0.09323 | 0.19724 | 0.00227 | 1153 | 30.41 | 1160.5 | 12.2 | -0.65 | 1139.9 | 53.8 |
| 5.51054 | 0.48548 | 0.35479 | 0.00729 | 1902.2 | 75.71 | 1957.4 | 34.67 | -2.90 | 1909.2 | 64.42 |
| 2.90096 | 0.15644 | 0.23302 | 0.00315 | 1382.2 | 40.72 | 1350.3 | 16.46 | 2.31 | 1375.3 | 56.54 |
| 3.07517 | 0.13677 | 0.24875 | 0.0028 | 1426.5 | 34.08 | 1432 | 14.46 | -0.39 | 1447 | 48.89 |
| 5.88666 | 0.39213 | 0.36195 | 0.00611 | 1959.3 | 57.82 | 1991.4 | 28.9 | -1.64 | 2178.2 | 51.73 |
| 3.46941 | 1.86227 | 0.27186 | 0.02664 | 1520.3 | 423.08 | 1550.2 | 135.03 | -1.97 | 1164.7 | 776.6 |
| 2.40285 | 0.33344 | 0.19402 | 0.00596 | 1243.5 | 99.5 | 1143.1 | 32.19 | 8.07 | 933.3 | 142.39 |
| 5.565 | 0.42794 | 0.33317 | 0.00605 | 1910.7 | 66.19 | 1853.7 | 29.25 | 2.98 | 1970.7 | 58.77 |
| 2.06249 | 0.09892 | 0.18561 | 0.00236 | 1136.4 | 32.8 | 1097.6 | 12.86 | 3.41 | 1241.8 | 58.51 |
| 18.7978 | 1.51957 | 0.57849 | 0.00962 | 3031.5 | 77.93 | 2942.6 | 39.27 | 2.93 | 2938.9 | 41.77 |
| 4.71119 | 0.41125 | 0.33135 | 0.00675 | 1769.2 | 73.12 | 1844.9 | 32.71 | -4.28 | 1668.7 | 72.22 |
| 2.62159 | 0.12581 | 0.2169 | 0.00267 | 1306.7 | 35.27 | 1265.5 | 14.14 | 3.15 | 1306.1 | 54.85 |
| 0.47093 | 0.03826 | 0.06408 | 0.00147 | 391.8 | 26.41 | 400.4 | 8.89 | -2.19 | 400.4 | 8.89 |
| 4.87787 | 0.2981 | 0.31254 | 0.00459 | 1798.4 | 51.5 | 1753.2 | 22.56 | 2.51 | 1749 | 54.37 |
| 4.84979 | 0.21108 | 0.30829 | 0.00332 | 1793.6 | 36.64 | 1732.3 | 16.34 | 3.42 | 1826.3 | 44.72 |
| 4.0499 | 0.39396 | 0.30024 | 0.00709 | 1644.3 | 79.21 | 1692.5 | 35.16 | -2.93 | 1701.4 | 81.72 |
| 4.82447 | 0.53156 | 0.3305 | 0.0088 | 1789.2 | 92.67 | 1840.8 | 42.62 | -2.88 | 1867.2 | 83.42 |
| 0.61723 | 0.04784 | 0.07729 | 0.00171 | 488.1 | 30.04 | 479.9 | 10.22 | 1.68 | 479.9 | 10.22 |
| 0.79271 | 0.05642 | 0.0871 | 0.00178 | 592.7 | 31.96 | 538.4 | 10.54 | 9.16 | 538.4 | 10.54 |
| 6.09371 | 0.24382 | 0.3552 | 0.00356 | 1989.3 | 34.9 | 1959.4 | 16.94 | 1.50 | 1978.4 | 43.17 |
| 3.75575 | 0.25764 | 0.27313 | 0.00455 | 1583.3 | 55.01 | 1556.7 | 23.03 | 1.68 | 1497 | 68.16 |
| 0.78949 | 0.08827 | 0.08679 | 0.00282 | 590.9 | 50.08 | 536.5 | 16.72 | 9.21 | 536.5 | 16.72 |
| 4.83654 | 0.35466 | 0.31053 | 0.00613 | 1791.3 | 61.7 | 1743.3 | 30.13 | 2.68 | 1903.4 | 71.44 |
| 2.16399 | 0.10565 | 0.19264 | 0.0025 | 1169.6 | 33.91 | 1135.6 | 13.53 | 2.91 | 1233.7 | 62.12 |

| Isotope Ratios | | | | Ages | | | | | | |
|---|---|---|---|---|---|---|---|---|---|---|
| Pb207/U235 | | Pb206/U238 | | Pb207/U235 | | Pb206/U238 | | Discordance | Preferred Age | |
| 0.56316 | 0.04377 | 0.06708 | 0.00156 | 453.6 | 28.43 | 418.6 | 9.41 | 7.72 | 418.6 | 9.41 |
| 12.15107 | 0.6268 | 0.49843 | 0.00622 | 2616.1 | 48.39 | 2607 | 26.75 | 0.35 | 2761.6 | 43.62 |
| 4.78326 | 0.29555 | 0.28858 | 0.00426 | 1782 | 51.89 | 1634.4 | 21.29 | 8.28 | 1753.1 | 58.67 |
| 7.77865 | 0.30943 | 0.40376 | 0.00414 | 2205.7 | 35.79 | 2186.3 | 19.03 | 0.88 | 2220.5 | 45.05 |
| 15.53133 | 0.92973 | 0.52474 | 0.0071 | 2848.4 | 57.11 | 2719.2 | 30.03 | 4.54 | 2819.3 | 45.61 |
| 2.25848 | 0.08794 | 0.20134 | 0.00215 | 1199.4 | 27.4 | 1182.5 | 11.51 | 1.41 | 1148.1 | 56.08 |
| 5.24611 | 0.33175 | 0.32906 | 0.00514 | 1860.1 | 53.93 | 1833.8 | 24.94 | 1.41 | 1933.5 | 58.63 |
| 1.75889 | 0.08488 | 0.18232 | 0.00238 | 1030.4 | 31.24 | 1079.6 | 12.96 | -4.77 | 930.7 | 68.29 |
| 4.38256 | 0.25672 | 0.3163 | 0.00469 | 1709.1 | 48.43 | 1771.7 | 22.96 | -3.66 | 1741.9 | 60 |
| **GS-02** | | | | | | | | | | |
| 5.15908 | 0.2307 | 0.33727 | 0.00352 | 1845.9 | 38.03 | 1873.5 | 16.97 | -1.5 | 1835.8 | 33.86 |
| 9.69205 | 0.91317 | 0.45618 | 0.00976 | 2406 | 86.72 | 2422.7 | 43.2 | -0.69 | 2696.1 | 46.68 |
| 4.69325 | 0.25334 | 0.32898 | 0.00419 | 1766 | 45.18 | 1833.4 | 20.3 | -3.82 | 1787.5 | 41.85 |
| 3.1875 | 0.09046 | 0.26333 | 0.00192 | 1454.1 | 21.93 | 1506.9 | 9.8 | -3.63 | 1466.8 | 28.71 |
| 4.90966 | 0.18531 | 0.32215 | 0.00287 | 1803.9 | 31.84 | 1800.2 | 13.99 | 0.21 | 1774.6 | 30.47 |
| 1.82009 | 0.05429 | 0.18597 | 0.0015 | 1052.7 | 19.55 | 1099.5 | 8.13 | -4.45 | 1034.5 | 36.01 |
| 5.12897 | 0.23608 | 0.33242 | 0.00366 | 1840.9 | 39.11 | 1850.1 | 17.72 | -0.5 | 1954.1 | 34.38 |
| 14.89601 | 2.60353 | 0.54983 | 0.01694 | 2808.6 | 166.3 | 2824.5 | 70.46 | -0.57 | 2680.9 | 131.64 |
| 0.67148 | 0.05802 | 0.08725 | 0.00203 | 521.6 | 35.25 | 539.2 | 12.04 | -3.37 | 539.2 | 12.04 |
| 1.90206 | 0.32768 | 0.18413 | 0.00788 | 1081.8 | 114.65 | 1089.5 | 42.89 | -0.71 | 1259 | 193.63 |
| 29.32518 | 1.02682 | 0.71568 | 0.00534 | 3464.5 | 34.38 | 3479.8 | 20.07 | -0.44 | 3440.2 | 20.26 |
| 5.73069 | 0.48214 | 0.35213 | 0.00613 | 1936 | 72.73 | 1944.8 | 29.25 | -0.45 | 1876.3 | 53.93 |
| 18.20313 | 1.3146 | 0.5959 | 0.00892 | 3000.5 | 69.51 | 3013.3 | 36.03 | -0.43 | 3056.6 | 31.89 |
| 1.80048 | 0.05228 | 0.18158 | 0.00144 | 1045.6 | 18.96 | 1075.6 | 7.84 | -2.87 | 1027.5 | 37.27 |
| 14.3116 | 0.70111 | 0.54793 | 0.00575 | 2770.6 | 46.49 | 2816.5 | 23.95 | -1.66 | 2819.9 | 27.51 |
| 0.7781 | 0.19542 | 0.08527 | 0.00441 | 584.4 | 111.6 | 527.5 | 26.2 | 9.74 | 527.5 | 26.2 |
| 5.41223 | 0.61834 | 0.3321 | 0.00821 | 1886.8 | 97.92 | 1848.5 | 39.75 | 2.03 | 1669.2 | 81.97 |

| Isotope Ratios | | | | Ages | | | | | | |
|---|---|---|---|---|---|---|---|---|---|---|
| Pb207/U235 | | Pb206/U238 | | Pb207/U235 | | Pb206/U238 | | Discordance | Preferred Age | |
| 4.3593 | 0.36047 | 0.29967 | 0.00583 | 1704.7 | 68.3 | 1689.7 | 28.94 | 0.88 | 1709.3 | 67.38 |
| 4.90692 | 0.46434 | 0.28969 | 0.00664 | 1803.4 | 79.82 | 1640 | 33.21 | 9.06 | 2062.9 | 66.36 |
| 14.40611 | 1.28149 | 0.56764 | 0.01094 | 2776.8 | 84.46 | 2898.1 | 44.99 | -4.37 | 2873.4 | 41.55 |
| 2.71643 | 0.60624 | 0.21558 | 0.01853 | 1333 | 165.63 | 1258.5 | 98.27 | 5.59 | 1546.3 | 314.55 |
| 1.70278 | 0.0563 | 0.16948 | 0.00155 | 1009.6 | 21.15 | 1009.2 | 8.52 | 0.04 | 1058.2 | 43.66 |
| 2.45892 | 0.07144 | 0.21488 | 0.00169 | 1260 | 20.97 | 1254.8 | 8.96 | 0.41 | 1242.7 | 36.37 |
| 4.72483 | 0.24109 | 0.32113 | 0.004 | 1771.7 | 42.76 | 1795.2 | 19.53 | -1.33 | 1847.2 | 42.69 |
| 5.00295 | 0.7175 | 0.30449 | 0.01038 | 1819.8 | 121.36 | 1713.5 | 51.3 | 5.84 | 1937.1 | 101.41 |
| 5.31255 | 0.34103 | 0.34711 | 0.00528 | 1870.9 | 54.86 | 1920.8 | 25.27 | -2.67 | 1803.7 | 51.01 |
| 1.58531 | 0.0788 | 0.16443 | 0.00222 | 964.5 | 30.95 | 981.4 | 12.31 | -1.75 | 981.4 | 12.31 |
| 0.54277 | 0.10022 | 0.06814 | 0.0032 | 440.2 | 65.96 | 425 | 19.34 | 3.45 | 425 | 19.34 |
| 17.7477 | 3.55103 | 0.54581 | 0.02076 | 2976.2 | 192.32 | 2807.7 | 86.58 | 5.66 | 2893.1 | 74.98 |
| 14.21852 | 0.75419 | 0.53287 | 0.00607 | 2764.4 | 50.32 | 2753.5 | 25.53 | 0.39 | 2703 | 33.56 |
| 0.58327 | 0.07794 | 0.07176 | 0.00253 | 466.6 | 49.98 | 446.8 | 15.21 | 4.24 | 446.8 | 15.21 |
| 11.49601 | 0.59529 | 0.513 | 0.00615 | 2564.3 | 48.37 | 2669.4 | 26.21 | -4.1 | 2580.6 | 35.73 |
| 2.19772 | 0.16789 | 0.20871 | 0.00398 | 1180.3 | 53.31 | 1221.9 | 21.24 | -3.52 | 1085.6 | 82.87 |
| 14.47538 | 1.23614 | 0.53687 | 0.00951 | 2781.4 | 81.11 | 2770.3 | 39.88 | 0.4 | 2660.7 | 44.07 |
| 4.41901 | 0.24297 | 0.31436 | 0.00431 | 1715.9 | 45.53 | 1762.1 | 21.14 | -2.69 | 1823.9 | 48.04 |
| 5.34841 | 0.22054 | 0.34895 | 0.00364 | 1876.6 | 35.27 | 1929.6 | 17.41 | -2.82 | 1968 | 39.19 |
| 1.75388 | 0.06938 | 0.16973 | 0.0018 | 1028.6 | 25.58 | 1010.6 | 9.93 | 1.75 | 977.6 | 52.89 |
| 4.95796 | 0.41354 | 0.3249 | 0.00615 | 1812.2 | 70.48 | 1813.6 | 29.93 | -0.08 | 1779.4 | 63.16 |
| 0.5915 | 0.03296 | 0.06947 | 0.00114 | 471.8 | 21.03 | 432.9 | 6.86 | 8.25 | 432.9 | 6.86 |
| **GS-01** | | | | | | | | | | |
| 3.76783 | 0.18364 | 0.29125 | 0.00364 | 1585.9 | 39.11 | 1647.8 | 18.17 | -3.90 | 1642.6 | 43.29 |
| 12.40894 | 1.29662 | 0.5058 | 0.01121 | 2635.9 | 98.19 | 2638.7 | 48.01 | -0.11 | 2516.7 | 51.08 |
| 2.07205 | 0.1864 | 0.18739 | 0.00436 | 1139.6 | 61.61 | 1107.2 | 23.66 | 2.84 | 1121.8 | 100.86 |
| 2.66809 | 0.22198 | 0.22725 | 0.00475 | 1319.7 | 61.45 | 1320.1 | 24.95 | -0.03 | 1320.7 | 81.5 |

| Isotope Ratios | | | | Ages | | | | | | |
|---|---|---|---|---|---|---|---|---|---|---|
| Pb207/U235 | | Pb206/U238 | | Pb207/U235 | | Pb206/U238 | | Discordance | Preferred Age | |
| 0.52459 | 0.04892 | 0.07102 | 0.00187 | 428.2 | 32.58 | 442.3 | 11.23 | -3.29 | 442.3 | 11.23 |
| 11.67527 | 0.35724 | 0.43451 | 0.00324 | 2578.7 | 28.62 | 2326 | 14.54 | 9.80 | 2716 | 23.64 |
| 1.68708 | 0.14451 | 0.16232 | 0.00368 | 1003.7 | 54.61 | 969.6 | 20.39 | 3.40 | 969.6 | 20.39 |
| 1.58045 | 0.11294 | 0.16337 | 0.00326 | 962.5 | 44.44 | 975.5 | 18.05 | -1.35 | 975.5 | 18.05 |
| 3.902 | 0.23885 | 0.29773 | 0.00442 | 1614.1 | 49.47 | 1680 | 21.98 | -4.08 | 1585.6 | 51.97 |
| 4.95077 | 0.40032 | 0.30243 | 0.00571 | 1811 | 68.31 | 1703.4 | 28.25 | 5.94 | 1738.8 | 61.06 |
| 3.6544 | 0.12636 | 0.27928 | 0.00252 | 1561.5 | 27.57 | 1587.8 | 12.69 | -1.68 | 1566.9 | 34.7 |
| 4.13556 | 0.17406 | 0.29157 | 0.00306 | 1661.4 | 34.41 | 1649.4 | 15.28 | 0.72 | 1645.3 | 38.56 |
| 4.37546 | 0.20368 | 0.29863 | 0.00349 | 1707.7 | 38.47 | 1684.5 | 17.31 | 1.36 | 1747 | 40.32 |
| 2.13477 | 0.05304 | 0.19795 | 0.0014 | 1160.1 | 17.18 | 1164.3 | 7.55 | -0.36 | 1135 | 33.31 |
| 0.48931 | 0.02902 | 0.06621 | 0.00114 | 404.4 | 19.79 | 413.3 | 6.91 | -2.20 | 413.3 | 6.91 |
| 12.74221 | 1.25911 | 0.52901 | 0.01137 | 2660.8 | 93.03 | 2737.3 | 47.95 | -2.88 | 2692.7 | 47.81 |
| 3.44865 | 0.2204 | 0.27424 | 0.00454 | 1515.6 | 50.31 | 1562.3 | 22.98 | -3.08 | 1618.5 | 57.66 |
| 4.36728 | 0.33905 | 0.30855 | 0.00595 | 1706.2 | 64.14 | 1733.6 | 29.3 | -1.61 | 1762.5 | 62.33 |
| 3.66933 | 0.15821 | 0.2895 | 0.00321 | 1564.7 | 34.4 | 1639 | 16.07 | -4.75 | 1554.7 | 42.09 |
| 2.06514 | 0.14451 | 0.19456 | 0.00356 | 1137.3 | 47.87 | 1146 | 19.23 | -0.76 | 1122.2 | 77.54 |
| 2.82793 | 0.09585 | 0.23906 | 0.00223 | 1363 | 25.42 | 1381.8 | 11.62 | -1.38 | 1430.6 | 38.99 |
| 5.20395 | 0.19243 | 0.32834 | 0.00304 | 1853.3 | 31.49 | 1830.3 | 14.75 | 1.24 | 1739.9 | 35.65 |
| 0.70284 | 0.04884 | 0.09114 | 0.00187 | 540.5 | 29.12 | 562.3 | 11.03 | -4.03 | 562.3 | 11.03 |
| 2.05355 | 0.1038 | 0.19341 | 0.00265 | 1133.5 | 34.52 | 1139.8 | 14.34 | -0.56 | 1164.3 | 58.97 |
| 4.18055 | 0.2801 | 0.29251 | 0.00473 | 1670.2 | 54.9 | 1654.1 | 23.61 | 0.96 | 1597.8 | 57.15 |
| 12.27632 | 0.94427 | 0.49977 | 0.00849 | 2625.8 | 72.22 | 2612.8 | 36.47 | 0.50 | 2601.6 | 42.96 |
| 0.91175 | 0.05742 | 0.10579 | 0.00192 | 658 | 30.5 | 648.3 | 11.19 | 1.47 | 648.3 | 11.19 |
| 5.22419 | 0.307 | 0.34211 | 0.0051 | 1856.6 | 50.08 | 1896.8 | 24.51 | -2.17 | 1975.7 | 48.08 |
| 0.88448 | 0.05308 | 0.10756 | 0.0019 | 643.4 | 28.6 | 658.6 | 11.06 | -2.36 | 658.6 | 11.06 |
| 2.34901 | 0.19086 | 0.2179 | 0.00441 | 1227.3 | 57.87 | 1270.7 | 23.35 | -3.54 | 1032.3 | 88.09 |
| 2.24488 | 0.24807 | 0.21137 | 0.0062 | 1195.2 | 77.63 | 1236.1 | 32.97 | -3.42 | 1266.5 | 118.13 |

| Isotope Ratios | | | | Ages | | | | | | |
|---|---|---|---|---|---|---|---|---|---|---|
| Pb207/U235 | | Pb206/U238 | | Pb207/U235 | | Pb206/U238 | | Discordance | Preferred Age | |
| 8.67146 | 0.51485 | 0.39133 | 0.00546 | 2304.1 | 54.05 | 2129 | 25.32 | 7.60 | 2368.6 | 42.35 |
| 0.6377 | 0.08135 | 0.07644 | 0.00269 | 500.9 | 50.44 | 474.8 | 16.11 | 5.21 | 474.8 | 16.11 |
| 0.99637 | 0.06595 | 0.10962 | 0.00203 | 702 | 33.54 | 670.5 | 11.81 | 4.49 | 670.5 | 11.81 |
| 4.58463 | 0.19047 | 0.32011 | 0.00349 | 1746.5 | 34.63 | 1790.2 | 17.02 | -2.50 | 1732 | 42.65 |
| 5.03348 | 0.21902 | 0.32784 | 0.00371 | 1825 | 36.86 | 1827.9 | 18.02 | -0.16 | 1857.4 | 42.82 |
| 1.8613 | 0.0925 | 0.18173 | 0.00253 | 1067.4 | 32.83 | 1076.4 | 13.83 | -0.84 | 1130.2 | 61.56 |
| 4.31274 | 0.2822 | 0.3128 | 0.00504 | 1695.8 | 53.93 | 1754.5 | 24.74 | -3.46 | 1632.2 | 58.13 |
| 1.88523 | 0.0733 | 0.17967 | 0.002 | 1075.9 | 25.8 | 1065.1 | 10.93 | 1.00 | 1113.1 | 52.76 |
| 5.21951 | 0.24307 | 0.34862 | 0.00412 | 1855.8 | 39.68 | 1928 | 19.69 | -3.89 | 1750.7 | 45.89 |
| 1.76946 | 0.05346 | 0.17616 | 0.0016 | 1034.3 | 19.6 | 1045.9 | 8.75 | -1.12 | 1061.2 | 45.86 |
| 5.90612 | 0.29939 | 0.34063 | 0.00442 | 1962.1 | 44.02 | 1889.7 | 21.27 | 3.69 | 2045.2 | 46.18 |
| MP386-Z2 | | | | | | | | | | |
| 11.28434 | 0.23991 | 0.47527 | 0.00223 | 2546.9 | 19.83 | 2506.6 | 9.77 | 1.58 | 2552.8 | 11.26 |
| 1.88581 | 0.06701 | 0.17354 | 0.00156 | 1076.1 | 23.58 | 1031.6 | 8.59 | 4.14 | 1031.5 | 36.94 |
| 4.52965 | 0.06891 | 0.31146 | 0.00118 | 1736.4 | 12.65 | 1747.9 | 5.78 | -0.66 | 1757.1 | 12.25 |
| 11.73054 | 0.2793 | 0.44779 | 0.00238 | 2583.1 | 22.28 | 2385.4 | 10.59 | 7.65 | 2725.3 | 11.95 |
| 6.37422 | 0.13732 | 0.38078 | 0.00193 | 2028.7 | 18.91 | 2079.9 | 9 | -2.52 | 2050.4 | 13.92 |
| 4.79352 | 0.09213 | 0.33502 | 0.00157 | 1783.8 | 16.15 | 1862.7 | 7.57 | -4.42 | 1799.6 | 14.29 |
| 4.9764 | 0.06533 | 0.32763 | 0.00108 | 1815.3 | 11.1 | 1826.9 | 5.23 | -0.64 | 1809.8 | 11.02 |
| 1.83168 | 0.03578 | 0.16995 | 0.00087 | 1056.9 | 12.83 | 1011.9 | 4.82 | 4.26 | 1050.7 | 21.26 |
| 2.02709 | 0.04311 | 0.19921 | 0.0011 | 1124.6 | 14.46 | 1171.1 | 5.93 | -4.13 | 1080.1 | 22.11 |
| 4.99408 | 0.11514 | 0.32729 | 0.00178 | 1818.3 | 19.5 | 1825.2 | 8.64 | -0.38 | 1793.5 | 16.31 |
| 13.52431 | 0.19754 | 0.53093 | 0.0018 | 2717 | 13.81 | 2745.4 | 7.58 | -1.05 | 2726.4 | 9.07 |
| 3.4352 | 0.09237 | 0.27481 | 0.00178 | 1512.5 | 21.15 | 1565.2 | 9.02 | -3.48 | 1446.7 | 21.75 |
| 4.98134 | 0.07004 | 0.3367 | 0.00118 | 1816.2 | 11.89 | 1870.8 | 5.69 | -3.01 | 1798.9 | 11.66 |
| 4.52295 | 0.07805 | 0.30351 | 0.00129 | 1735.2 | 14.35 | 1708.7 | 6.37 | 1.53 | 1768.3 | 13.7 |
| 12.24823 | 0.39329 | 0.52408 | 0.00372 | 2623.6 | 30.14 | 2716.4 | 15.72 | -3.54 | 2655.1 | 14.88 |

| Isotope Ratios | | | | Ages | | | | | | |
|---|---|---|---|---|---|---|---|---|---|---|
| Pb207/U235 | | Pb206/U238 | | Pb207/U235 | | Pb206/U238 | | Discordance | Preferred Age | |
| 5.62855 | 0.14506 | 0.34182 | 0.00205 | 1920.5 | 22.22 | 1895.4 | 9.86 | 1.31 | 1928.4 | 17.02 |
| 2.01746 | 0.14074 | 0.19437 | 0.00344 | 1121.4 | 47.36 | 1145 | 18.56 | -2.10 | 1057.9 | 68.79 |
| 4.74259 | 0.101 | 0.32712 | 0.00168 | 1774.8 | 17.86 | 1824.4 | 8.15 | -2.79 | 1768.6 | 15.81 |
| 3.36418 | 0.06806 | 0.26046 | 0.00132 | 1496.1 | 15.84 | 1492.2 | 6.73 | 0.26 | 1509.1 | 17.36 |
| 1.87256 | 0.03374 | 0.18888 | 0.00091 | 1071.4 | 11.93 | 1115.3 | 4.94 | -4.10 | 1052.3 | 19.95 |
| 4.71001 | 0.11612 | 0.31615 | 0.00187 | 1769 | 20.65 | 1770.9 | 9.16 | -0.11 | 1797.2 | 17.84 |
| 11.79548 | 0.23663 | 0.48424 | 0.00219 | 2588.3 | 18.78 | 2545.7 | 9.53 | 1.65 | 2603.7 | 11.57 |
| 5.28499 | 0.15985 | 0.33136 | 0.00231 | 1866.4 | 25.82 | 1845 | 11.19 | 1.15 | 1816.4 | 20.34 |
| 4.51521 | 0.13634 | 0.30015 | 0.00219 | 1733.8 | 25.1 | 1692.1 | 10.86 | 2.41 | 1812.7 | 21.55 |
| 4.55336 | 0.06783 | 0.3047 | 0.00115 | 1740.8 | 12.4 | 1714.6 | 5.66 | 1.51 | 1734.9 | 13.28 |
| 2.13252 | 0.05975 | 0.19026 | 0.00139 | 1159.4 | 19.37 | 1122.8 | 7.55 | 3.16 | 1222.5 | 27.89 |
| 4.55306 | 0.06931 | 0.31976 | 0.00123 | 1740.7 | 12.67 | 1788.6 | 5.99 | -2.75 | 1691.6 | 13.6 |
| 6.11548 | 0.10984 | 0.36706 | 0.00159 | 1992.5 | 15.67 | 2015.5 | 7.52 | -1.15 | 1990.5 | 13.65 |
| 3.05949 | 0.13006 | 0.22938 | 0.00232 | 1422.6 | 32.53 | 1331.2 | 12.19 | 6.42 | 1366.2 | 35.09 |
| 1.90955 | 0.03916 | 0.18383 | 0.00101 | 1084.4 | 13.67 | 1087.9 | 5.5 | -0.32 | 1108.2 | 22.4 |
| 3.93456 | 0.08542 | 0.29371 | 0.00158 | 1620.8 | 17.58 | 1660.1 | 7.9 | -2.42 | 1624.7 | 18.03 |
| 2.11276 | 0.03487 | 0.19848 | 0.00088 | 1153 | 11.38 | 1167.2 | 4.75 | -1.23 | 1155.4 | 18.37 |
| 2.0344 | 0.0323 | 0.19676 | 0.00085 | 1127.1 | 10.81 | 1157.9 | 4.57 | -2.73 | 1120.8 | 18.15 |
| 5.17155 | 0.11786 | 0.31981 | 0.00172 | 1847.9 | 19.39 | 1788.8 | 8.41 | 3.20 | 1798.7 | 17.17 |
| 2.92942 | 0.07462 | 0.24494 | 0.00157 | 1389.5 | 19.28 | 1412.3 | 8.13 | -1.64 | 1363.4 | 23.07 |
| 6.37786 | 0.16416 | 0.37538 | 0.00225 | 2029.2 | 22.59 | 2054.7 | 10.54 | -1.26 | 1983.3 | 17.43 |
| 4.7343 | 0.11631 | 0.32448 | 0.00192 | 1773.3 | 20.59 | 1811.6 | 9.34 | -2.16 | 1741.6 | 18.67 |
| 0.73694 | 0.0152 | 0.0906 | 0.00055 | 560.6 | 8.88 | 559.1 | 3.24 | 0.27 | 559.1 | 3.24 |
| 4.71644 | 0.06411 | 0.29532 | 0.00106 | 1770.2 | 11.39 | 1668.1 | 5.28 | 5.77 | 1853.9 | 13.47 |
| 15.0695 | 0.26052 | 0.536 | 0.00219 | 2819.6 | 16.46 | 2766.7 | 9.21 | 1.88 | 2866.4 | 11.76 |
| 6.57637 | 0.2261 | 0.37261 | 0.00289 | 2056.2 | 30.3 | 2041.6 | 13.55 | 0.71 | 1980.4 | 21.49 |
| 1.44455 | 0.03199 | 0.14718 | 0.0009 | 907.6 | 13.29 | 885.1 | 5.04 | 2.48 | 885.1 | 5.04 |

| Isotope Ratios | | | | Ages | | | | | | |
|---|---|---|---|---|---|---|---|---|---|---|
| Pb207/U235 | | Pb206/U238 | | Pb207/U235 | | Pb206/U238 | | Discordance | Preferred Age | |
| 4.24463 | 0.1014 | 0.29716 | 0.00173 | 1682.7 | 19.63 | 1677.2 | 8.6 | 0.33 | 1653.9 | 19.44 |
| 5.12284 | 0.09437 | 0.30989 | 0.00141 | 1839.9 | 15.65 | 1740.2 | 6.93 | 5.42 | 1827.5 | 15.76 |
| 6.10541 | 0.17259 | 0.34883 | 0.00229 | 1991 | 24.66 | 1929 | 10.92 | 3.11 | 1961.7 | 19.31 |
| 3.16174 | 0.04827 | 0.24712 | 0.00101 | 1447.9 | 11.78 | 1423.6 | 5.21 | 1.68 | 1465.1 | 16.37 |
| OS-Z1a | | | | | | | | | | |
| 5.2052 | 0.13194 | 0.32933 | 0.00243 | 1853.5 | 21.59 | 1835.1 | 11.78 | 0.99 | 1858.6 | 24.55 |
| 10.17841 | 0.38387 | 0.46662 | 0.00455 | 2451.1 | 34.87 | 2468.7 | 19.99 | -0.72 | 2487.8 | 26.06 |
| 3.92576 | 0.06686 | 0.29551 | 0.00166 | 1619 | 13.78 | 1669 | 8.24 | -3.09 | 1605 | 20.34 |
| 16.45205 | 0.40467 | 0.56538 | 0.00365 | 2903.4 | 23.54 | 2888.8 | 15.03 | 0.50 | 2863.4 | 17.15 |
| 4.69054 | 0.46978 | 0.29112 | 0.00711 | 1765.6 | 83.83 | 1647.1 | 35.48 | 6.71 | 1619.7 | 90.68 |
| 2.0734 | 0.05935 | 0.17656 | 0.00159 | 1140.1 | 19.61 | 1048.1 | 8.72 | 8.07 | 1223.6 | 37.4 |
| 1.76362 | 0.04937 | 0.17673 | 0.00158 | 1032.2 | 18.14 | 1049.1 | 8.64 | -1.64 | 1050 | 38.85 |
| 2.38404 | 0.05049 | 0.21847 | 0.00148 | 1237.8 | 15.15 | 1273.8 | 7.83 | -2.91 | 1190.5 | 27.97 |
| 6.06029 | 0.19 | 0.36156 | 0.0031 | 1984.6 | 27.32 | 1989.5 | 14.68 | -0.25 | 1939.4 | 27.52 |
| 2.88097 | 0.08995 | 0.22126 | 0.00205 | 1376.9 | 23.53 | 1288.5 | 10.85 | 6.42 | 1393.2 | 36.06 |
| 2.89197 | 0.06201 | 0.23728 | 0.00162 | 1379.8 | 16.18 | 1372.6 | 8.43 | 0.52 | 1407.6 | 26.37 |
| 2.06577 | 0.08374 | 0.1899 | 0.00231 | 1137.5 | 27.73 | 1120.9 | 12.52 | 1.46 | 1171.4 | 52.4 |
| 5.38533 | 0.21329 | 0.34924 | 0.00369 | 1882.5 | 33.92 | 1930.9 | 17.65 | -2.57 | 1787 | 35.68 |
| 2.1108 | 0.09319 | 0.19712 | 0.0026 | 1152.3 | 30.42 | 1159.8 | 14.02 | -0.65 | 1163.6 | 56.68 |
| 2.06019 | 0.07072 | 0.20254 | 0.00213 | 1135.7 | 23.46 | 1188.9 | 11.43 | -4.68 | 1186.8 | 44.69 |
| 3.36066 | 0.05441 | 0.26322 | 0.00144 | 1495.3 | 12.67 | 1506.3 | 7.37 | -0.74 | 1487.3 | 21.02 |
| 3.26926 | 0.16265 | 0.25097 | 0.00354 | 1473.8 | 38.68 | 1443.5 | 18.23 | 2.06 | 1532.2 | 51.95 |
| 2.54623 | 0.11303 | 0.22147 | 0.00291 | 1285.4 | 32.36 | 1289.6 | 15.35 | -0.33 | 1318.4 | 52.7 |
| 0.99954 | 0.11995 | 0.11969 | 0.00425 | 703.6 | 60.91 | 728.8 | 24.44 | -3.58 | 728.8 | 24.44 |
| 1.54908 | 0.04528 | 0.14977 | 0.00142 | 950.1 | 18.04 | 899.7 | 7.99 | 5.30 | 899.7 | 7.99 |
| 16.29457 | 0.59579 | 0.57447 | 0.00512 | 2894.2 | 34.98 | 2926.1 | 20.95 | -1.10 | 2926.1 | 22.48 |
| 0.45803 | 0.0189 | 0.06172 | 0.00085 | 382.9 | 13.16 | 386 | 5.15 | -0.81 | 386 | 5.15 |

| Isotope Ratios | | | | Ages | | | | | | |
|---|---|---|---|---|---|---|---|---|---|---|
| Pb207/U235 | | Pb206/U238 | | Pb207/U235 | | Pb206/U238 | | Discordance | Preferred Age | |
| 3.93849 | 0.08289 | 0.27445 | 0.0018 | 1621.6 | 17.04 | 1563.3 | 9.09 | 3.60 | 1563.3 | 24.25 |
| 5.65898 | 0.18369 | 0.35216 | 0.00315 | 1925.1 | 28.01 | 1944.9 | 15.04 | -1.03 | 1944.9 | 29.72 |
| 3.09065 | 0.06384 | 0.24205 | 0.00163 | 1430.4 | 15.85 | 1397.3 | 8.46 | 2.31 | 1397.3 | 25.65 |
| 3.1919 | 0.16096 | 0.25129 | 0.00355 | 1455.2 | 38.99 | 1445.1 | 18.3 | 0.69 | 1445.1 | 53.61 |
| 12.23644 | 0.57008 | 0.52052 | 0.00593 | 2622.7 | 43.73 | 2701.4 | 25.14 | -3.00 | 2701.4 | 30.02 |
| 4.6007 | 0.19202 | 0.30835 | 0.0036 | 1749.4 | 34.81 | 1732.6 | 17.76 | 0.96 | 1732.6 | 39.45 |
| 1.71095 | 0.07701 | 0.17232 | 0.00239 | 1012.6 | 28.85 | 1024.9 | 13.12 | -1.21 | 1024.9 | 61.59 |
| 5.30899 | 0.14919 | 0.33402 | 0.0027 | 1870.3 | 24.01 | 1857.8 | 13.02 | 0.67 | 1857.8 | 27.76 |
| 3.32121 | 0.13335 | 0.25683 | 0.00306 | 1486 | 31.33 | 1473.6 | 15.67 | 0.83 | 1473.6 | 42.74 |
| 4.39163 | 0.10944 | 0.30281 | 0.00225 | 1710.8 | 20.61 | 1705.2 | 11.13 | 0.33 | 1705.2 | 27.12 |
| 0.77603 | 0.08206 | 0.08907 | 0.00295 | 583.2 | 46.91 | 550 | 17.47 | 5.69 | 550 | 17.47 |
| 1.8979 | 0.07297 | 0.18892 | 0.00222 | 1080.4 | 25.57 | 1115.5 | 12.03 | -3.25 | 1115.5 | 51.98 |
| 0.51348 | 0.02085 | 0.06154 | 0.00087 | 420.8 | 13.99 | 385 | 5.3 | 8.51 | 385 | 5.3 |
| 13.99522 | 0.68527 | 0.56368 | 0.00665 | 2749.4 | 46.4 | 2881.8 | 27.43 | -4.82 | 2881.8 | 30.04 |
| 3.16377 | 0.22196 | 0.23537 | 0.00479 | 1448.4 | 54.13 | 1362.6 | 24.99 | 5.92 | 1362.6 | 72.53 |
| 2.09531 | 0.09488 | 0.19966 | 0.00273 | 1147.3 | 31.12 | 1173.5 | 14.68 | -2.28 | 1173.5 | 58.06 |
| 2.41435 | 0.07792 | 0.21927 | 0.00218 | 1246.9 | 23.17 | 1278 | 11.51 | -2.49 | 1278 | 40.77 |
| 3.14176 | 0.18346 | 0.23993 | 0.00398 | 1443 | 44.98 | 1386.3 | 20.7 | 3.93 | 1386.3 | 62.38 |
| 11.46331 | 0.63419 | 0.45667 | 0.00624 | 2561.6 | 51.67 | 2424.9 | 27.63 | 5.34 | 2424.9 | 35.99 |
| 4.27337 | 0.12954 | 0.28376 | 0.00253 | 1688.2 | 24.94 | 1610.3 | 12.7 | 4.61 | 1610.3 | 32.41 |
| 5.61815 | 0.11705 | 0.34288 | 0.00226 | 1918.9 | 17.96 | 1900.5 | 10.84 | 0.96 | 1900.5 | 24.52 |
| 3.99099 | 0.0769 | 0.28388 | 0.00182 | 1632.4 | 15.64 | 1610.9 | 9.13 | 1.32 | 1610.9 | 25.81 |
| 1.75717 | 0.05655 | 0.1695 | 0.00174 | 1029.8 | 20.83 | 1009.4 | 9.59 | 1.98 | 1009.4 | 45.5 |
| 2.18346 | 0.07407 | 0.19376 | 0.00203 | 1175.8 | 23.63 | 1141.7 | 10.94 | 2.90 | 1141.7 | 44.79 |
| 2.08837 | 0.07436 | 0.18366 | 0.00203 | 1145 | 24.45 | 1087 | 11.05 | 5.07 | 1087 | 47.1 |
| 4.34189 | 0.36334 | 0.31751 | 0.00753 | 1701.4 | 69.06 | 1777.5 | 36.84 | -4.47 | 1777.5 | 79.29 |
| 4.57684 | 0.17051 | 0.31019 | 0.00331 | 1745.1 | 31.04 | 1741.6 | 16.27 | 0.20 | 1741.6 | 38.14 |

| Isotope Ratios | | | | Ages | | | | | | |
|---|---|---|---|---|---|---|---|---|---|---|
| Pb207/U235 | | Pb206/U238 | | Pb207/U235 | | Pb206/U238 | | Discordance | Preferred Age | |
| 3.5206 | 0.13907 | 0.27472 | 0.00315 | 1531.9 | 31.24 | 1564.7 | 15.91 | -2.14 | 1564.7 | 43.79 |
| 3.64731 | 0.12447 | 0.2865 | 0.00289 | 1559.9 | 27.19 | 1624 | 14.47 | -4.11 | 1624 | 38.79 |
| 2.22662 | 0.06988 | 0.19236 | 0.00187 | 1189.5 | 21.99 | 1134.1 | 10.12 | 4.66 | 1134.1 | 42.5 |
| **OS-Z1** | | | | | | | | | | |
| 6.51844 | 0.24787 | 0.38067 | 0.00355 | 2048.4 | 33.48 | 2079.4 | 16.58 | -1.51 | 1970.6 | 28.2 |
| 4.37524 | 0.13225 | 0.28939 | 0.00233 | 1707.7 | 24.98 | 1638.5 | 11.64 | 4.05 | 1630 | 28.29 |
| 2.07203 | 0.0552 | 0.20267 | 0.00161 | 1139.6 | 18.24 | 1189.7 | 8.62 | -4.40 | 1080 | 33.08 |
| 2.13294 | 0.07729 | 0.20401 | 0.00203 | 1159.5 | 25.05 | 1196.8 | 10.85 | -3.22 | 1102 | 39.89 |
| 11.72774 | 0.37384 | 0.48153 | 0.00381 | 2582.9 | 29.82 | 2533.9 | 16.6 | 1.90 | 2561.5 | 22.43 |
| 5.91351 | 0.11625 | 0.34784 | 0.00215 | 1963.2 | 17.07 | 1924.3 | 10.29 | 1.98 | 1957.5 | 22.34 |
| 3.93116 | 0.11076 | 0.29329 | 0.00233 | 1620.1 | 22.81 | 1658 | 11.59 | -2.34 | 1654.5 | 27.91 |
| 3.31453 | 0.08202 | 0.25197 | 0.00184 | 1484.5 | 19.3 | 1448.6 | 9.45 | 2.42 | 1491.7 | 27.62 |
| 5.3787 | 0.16222 | 0.33481 | 0.00272 | 1881.5 | 25.82 | 1861.7 | 13.11 | 1.05 | 1932.6 | 26.44 |
| 11.04328 | 0.42854 | 0.4808 | 0.00449 | 2526.8 | 36.13 | 2530.7 | 19.55 | -0.15 | 2588.6 | 24.46 |
| 7.0938 | 0.20558 | 0.38386 | 0.0029 | 2123.3 | 25.79 | 2094.3 | 13.5 | 1.37 | 2035.9 | 24.6 |
| 2.15321 | 0.03852 | 0.19392 | 0.00121 | 1166.1 | 12.4 | 1142.6 | 6.52 | 2.02 | 1194.9 | 26.83 |
| 2.40669 | 0.10276 | 0.20788 | 0.00238 | 1244.6 | 30.63 | 1217.5 | 12.7 | 2.18 | 1299.6 | 43.13 |
| 14.88707 | 0.25262 | 0.56365 | 0.00319 | 2808 | 16.15 | 2881.7 | 13.16 | -2.62 | 2759 | 19.48 |
| 3.91524 | 0.08939 | 0.2842 | 0.00196 | 1616.8 | 18.47 | 1612.5 | 9.86 | 0.27 | 1658 | 25.79 |
| 4.68749 | 0.0544 | 0.31582 | 0.00162 | 1765 | 9.71 | 1769.3 | 7.96 | -0.24 | 1731.4 | 21.72 |
| 4.07133 | 0.11 | 0.28605 | 0.00218 | 1648.6 | 22.02 | 1621.8 | 10.9 | 1.63 | 1645.9 | 27.62 |
| 0.92548 | 0.01339 | 0.10823 | 0.00063 | 665.3 | 7.06 | 662.5 | 3.67 | 0.42 | 662.5 | 3.67 |
| 4.85724 | 0.11334 | 0.33312 | 0.0023 | 1794.9 | 19.65 | 1853.5 | 11.1 | -3.26 | 1753.8 | 25.19 |
| 4.87875 | 0.13691 | 0.30907 | 0.00238 | 1798.6 | 23.65 | 1736.1 | 11.73 | 3.47 | 1795.4 | 26.99 |
| 5.27208 | 0.14021 | 0.35387 | 0.00269 | 1864.4 | 22.7 | 1953.1 | 12.79 | -4.76 | 1939.4 | 25.87 |
| 3.4506 | 0.06478 | 0.25745 | 0.00161 | 1516 | 14.78 | 1476.8 | 8.24 | 2.59 | 1527.4 | 25.44 |
| 1.53382 | 0.03471 | 0.15343 | 0.00112 | 944 | 13.91 | 920.1 | 6.23 | 2.53 | 920.1 | 6.23 |

| Isotope Ratios | | | | Ages | | | | | | |
|---|---|---|---|---|---|---|---|---|---|---|
| Pb207/U235 | | Pb206/U238 | | Pb207/U235 | | Pb206/U238 | | Discordance | Preferred Age | |
| 2.25797 | 0.06231 | 0.20613 | 0.00168 | 1199.3 | 19.42 | 1208.2 | 8.98 | -0.74 | 1218.2 | 33.33 |
| 5.88384 | 0.12594 | 0.36976 | 0.00242 | 1958.9 | 18.58 | 2028.3 | 11.37 | -3.54 | 1882.4 | 24.61 |
| 1.88769 | 0.03504 | 0.18669 | 0.00119 | 1076.8 | 12.32 | 1103.4 | 6.45 | -2.47 | 953.9 | 29.68 |
| 5.78091 | 0.11729 | 0.34581 | 0.00221 | 1943.6 | 17.56 | 1914.6 | 10.57 | 1.49 | 1938.5 | 24.34 |
| 5.42536 | 0.15763 | 0.34009 | 0.00268 | 1888.9 | 24.91 | 1887.1 | 12.88 | 0.10 | 1861.7 | 27.6 |
| 6.49308 | 0.17564 | 0.38565 | 0.00289 | 2045 | 23.8 | 2102.6 | 13.47 | -2.82 | 2019.5 | 26.02 |
| 5.0727 | 0.08789 | 0.32864 | 0.00198 | 1831.6 | 14.7 | 1831.8 | 9.62 | -0.01 | 1858.7 | 24.47 |
| 5.50331 | 0.24888 | 0.36267 | 0.00394 | 1901.1 | 38.86 | 1994.8 | 18.65 | -4.93 | 1751.9 | 34.85 |
| 3.05317 | 0.06086 | 0.25312 | 0.00166 | 1421 | 15.25 | 1454.6 | 8.53 | -2.36 | 1384.4 | 27.93 |
| 0.60399 | 0.01963 | 0.07515 | 0.00079 | 479.8 | 12.42 | 467.1 | 4.77 | 2.65 | 467.1 | 4.77 |
| **MP375W-Z1** | | | | | | | | | | |
| 2.36436 | 0.244 | 0.20671 | 0.00599 | 1231.9 | 73.64 | 1211.3 | 31.99 | 1.67 | 1220.6 | 125.45 |
| 2.0196 | 0.09353 | 0.19689 | 0.00273 | 1122.1 | 31.45 | 1158.6 | 14.71 | -3.25 | 1050 | 60.4 |
| 4.08807 | 0.11481 | 0.27893 | 0.0023 | 1651.9 | 22.91 | 1586 | 11.62 | 3.99 | 1635.2 | 29.73 |
| 1.77569 | 0.05174 | 0.17079 | 0.0016 | 1036.6 | 18.93 | 1016.4 | 8.83 | 1.95 | 1042.4 | 41.07 |
| 2.44723 | 0.1755 | 0.20386 | 0.00415 | 1256.6 | 51.69 | 1196 | 22.22 | 4.82 | 1211 | 84.11 |
| 2.93198 | 0.14381 | 0.24015 | 0.00345 | 1390.2 | 37.14 | 1387.5 | 17.96 | 0.19 | 1387.5 | 55.24 |
| 3.97361 | 0.22999 | 0.29364 | 0.0047 | 1628.8 | 46.95 | 1659.7 | 23.43 | -1.90 | 1585.7 | 57.56 |
| 3.8711 | 0.10729 | 0.27335 | 0.00231 | 1607.7 | 22.36 | 1557.8 | 11.72 | 3.10 | 1638.1 | 31.64 |
| 4.82778 | 0.20948 | 0.30779 | 0.00381 | 1789.8 | 36.5 | 1729.8 | 18.76 | 3.35 | 1865 | 42.32 |
| 13.10092 | 1.01359 | 0.5471 | 0.01054 | 2686.9 | 72.99 | 2813.1 | 43.91 | -4.70 | 2738.2 | 47.48 |
| 0.66609 | 0.02347 | 0.07957 | 0.00098 | 518.3 | 14.31 | 493.6 | 5.83 | 4.77 | 493.6 | 5.83 |
| 2.08792 | 0.4347 | 0.19442 | 0.01216 | 1144.8 | 142.94 | 1145.3 | 65.62 | -0.04 | 1292.8 | 257.1 |
| 5.12967 | 0.17778 | 0.33579 | 0.00344 | 1841 | 29.45 | 1866.4 | 16.62 | -1.38 | 1810.8 | 39.27 |
| 5.00324 | 0.18558 | 0.33318 | 0.00362 | 1819.9 | 31.39 | 1853.8 | 17.51 | -1.86 | 1783.4 | 41.56 |
| **D-54-B/93-P-9 2551.8** | | | | | | | | | | |
| 4.62554 | 0.15094 | 0.31184 | 0.00301 | 1753.9 | 27.24 | 1749.8 | 14.8 | 0.23 | 1705.9 | 38.3 |

| Isotope Ratios | | | | Ages | | | | | | |
|---|---|---|---|---|---|---|---|---|---|---|
| Pb207/U235 | | Pb206/U238 | | Pb207/U235 | | Pb206/U238 | | Discordance | Preferred Age | |
| 4.51846 | 0.29096 | 0.28452 | 0.00524 | 1734.4 | 53.54 | 1614.1 | 26.28 | 6.94 | 1931.2 | 61.16 |
| 3.90132 | 0.09917 | 0.27913 | 0.00229 | 1614 | 20.54 | 1587 | 11.56 | 1.67 | 1630.4 | 35.44 |
| 4.27748 | 0.19842 | 0.31612 | 0.00419 | 1689 | 38.18 | 1770.7 | 20.52 | -4.84 | 1651.6 | 50.04 |
| 4.29357 | 0.40326 | 0.30189 | 0.00774 | 1692.1 | 77.35 | 1700.7 | 38.32 | -0.51 | 1697.3 | 89.38 |
| 5.2217 | 0.22511 | 0.33828 | 0.00416 | 1856.2 | 36.74 | 1878.4 | 20.05 | -1.20 | 1828.6 | 46.33 |
| 11.04004 | 0.75466 | 0.50081 | 0.00855 | 2526.5 | 63.64 | 2617.3 | 36.74 | -3.59 | 2429.6 | 50.38 |
| 0.55011 | 0.03561 | 0.07113 | 0.00152 | 445.1 | 23.33 | 443 | 9.16 | 0.47 | 443 | 9.16 |
| 2.99914 | 0.10094 | 0.24833 | 0.00265 | 1407.4 | 25.63 | 1429.8 | 13.68 | -1.59 | 1409.8 | 47.27 |
| 4.11027 | 0.21981 | 0.3077 | 0.00468 | 1656.3 | 43.68 | 1729.4 | 23.09 | -4.41 | 1499.4 | 62.14 |
| 3.31551 | 0.14089 | 0.26601 | 0.00353 | 1484.7 | 33.15 | 1520.5 | 17.97 | -2.41 | 1501.2 | 57.89 |
| 14.60547 | 0.88555 | 0.572 | 0.00936 | 2789.9 | 57.62 | 2916 | 38.39 | -4.52 | 2823.6 | 53.33 |
| 1.76047 | 0.072 | 0.17895 | 0.00241 | 1031 | 26.49 | 1061.2 | 13.18 | -2.93 | 972.8 | 67.65 |
| 3.77234 | 0.14646 | 0.29141 | 0.00375 | 1586.9 | 31.16 | 1648.5 | 18.71 | -3.88 | 1573.6 | 59.77 |
| **NTP-Z3** | | | | | | | | | | |
| 4.15801 | 0.12768 | 0.28389 | 0.00211 | 1665.8 | 25.13 | 1610.9 | 10.57 | 3.30 | 1714.1 | 22.69 |
| 2.91022 | 0.12442 | 0.23741 | 0.00248 | 1384.6 | 32.31 | 1373.2 | 12.95 | 0.82 | 1352.3 | 36.36 |
| 1.91827 | 0.03478 | 0.18459 | 0.0009 | 1087.5 | 12.1 | 1092 | 4.89 | -0.41 | 1087.2 | 20 |
| 1.431 | 0.01827 | 0.14173 | 0.00052 | 902 | 7.63 | 854.4 | 2.93 | 5.28 | 854.4 | 2.93 |
| 4.02021 | 0.13587 | 0.3046 | 0.00253 | 1638.3 | 27.48 | 1714.1 | 12.51 | -4.63 | 1668.3 | 25.24 |
| 25.719 | 0.60338 | 0.63554 | 0.00327 | 3335.9 | 22.93 | 3171.5 | 12.87 | 4.93 | 3488.1 | 10.22 |
| 4.36255 | 0.09477 | 0.2857 | 0.00148 | 1705.3 | 17.94 | 1620 | 7.42 | 5.00 | 1665.6 | 16.97 |
| 1.99986 | 0.028 | 0.18588 | 0.00071 | 1115.5 | 9.48 | 1099 | 3.84 | 1.48 | 1082.7 | 16.25 |
| 15.04492 | 0.38271 | 0.55364 | 0.00315 | 2818.1 | 24.22 | 2840.3 | 13.06 | -0.79 | 2873.1 | 12.39 |
| 2.78888 | 0.06603 | 0.22158 | 0.00134 | 1352.6 | 17.7 | 1290.2 | 7.07 | 4.61 | 1398.1 | 21.71 |
| 4.08596 | 0.12869 | 0.28346 | 0.00217 | 1651.5 | 25.69 | 1608.7 | 10.88 | 2.59 | 1688.9 | 23.72 |
| 6.28626 | 0.18857 | 0.3635 | 0.0025 | 2016.5 | 26.28 | 1998.7 | 11.84 | 0.88 | 1998.6 | 19.01 |
| 3.56891 | 0.16899 | 0.27463 | 0.00319 | 1542.6 | 37.56 | 1564.2 | 16.16 | -1.40 | 1534.8 | 36.92 |

| Isotope Ratios | | | | Ages | | | | | | |
|---|---|---|---|---|---|---|---|---|---|---|
| Pb207/U235 | | Pb206/U238 | | Pb207/U235 | | Pb206/U238 | | Discordance | Preferred Age | |
| 5.87304 | 0.0799 | 0.34188 | 0.0012 | 1957.3 | 11.8 | 1895.7 | 5.77 | 3.15 | 2037.5 | 11.99 |
| 3.73806 | 0.09849 | 0.27708 | 0.0018 | 1579.6 | 21.11 | 1576.6 | 9.1 | 0.19 | 1605.3 | 21.32 |
| 4.96269 | 0.13377 | 0.31767 | 0.00205 | 1813 | 22.78 | 1778.3 | 10.01 | 1.91 | 1825.8 | 19.51 |
| 0.46225 | 0.01381 | 0.06386 | 0.00059 | 385.8 | 9.59 | 399 | 3.57 | -3.42 | 399 | 3.57 |
| 2.92281 | 0.0574 | 0.23749 | 0.0012 | 1387.8 | 14.86 | 1373.6 | 6.25 | 1.02 | 1374.5 | 18.92 |
| 4.46035 | 0.12625 | 0.28534 | 0.00196 | 1723.6 | 23.48 | 1618.2 | 9.83 | 6.12 | 1800.1 | 21.22 |
| 3.06487 | 0.12608 | 0.24133 | 0.00245 | 1424 | 31.49 | 1393.6 | 12.71 | 2.13 | 1423.2 | 34.51 |
| 3.90659 | 0.11974 | 0.26656 | 0.00201 | 1615 | 24.78 | 1523.3 | 10.25 | 5.68 | 1705.4 | 23.95 |
| 13.61454 | 0.49929 | 0.53709 | 0.00433 | 2723.3 | 34.69 | 2771.2 | 18.17 | -1.76 | 2731.5 | 17.29 |
| 3.50752 | 0.13006 | 0.2727 | 0.00252 | 1528.9 | 29.3 | 1554.5 | 12.78 | -1.67 | 1570.3 | 29.92 |
| 2.18285 | 0.04092 | 0.19085 | 0.00097 | 1175.6 | 13.05 | 1126 | 5.24 | 4.22 | 1235.9 | 20.51 |
| 1.56412 | 0.05086 | 0.16127 | 0.0014 | 956.1 | 20.14 | 963.9 | 7.76 | -0.82 | 963.9 | 7.76 |
| 1.16213 | 0.02208 | 0.12587 | 0.00069 | 783 | 10.37 | 764.3 | 3.96 | 2.39 | 764.3 | 3.96 |
| 3.32944 | 0.05592 | 0.2591 | 0.00116 | 1488 | 13.11 | 1485.2 | 5.94 | 0.19 | 1504.9 | 17.44 |
| 4.04306 | 0.12713 | 0.28698 | 0.00222 | 1642.9 | 25.6 | 1626.4 | 11.14 | 1.00 | 1682.2 | 24.88 |
| 4.04392 | 0.08095 | 0.29624 | 0.00152 | 1643.1 | 16.3 | 1672.6 | 7.58 | -1.80 | 1649.7 | 18.46 |
| 5.15616 | 0.13187 | 0.33637 | 0.00212 | 1845.4 | 21.75 | 1869.2 | 10.22 | -1.29 | 1859.8 | 20.14 |
| 2.27535 | 0.10539 | 0.2048 | 0.00243 | 1204.7 | 32.67 | 1201 | 13 | 0.31 | 1199.2 | 44.76 |
| 2.03632 | 0.13463 | 0.17651 | 0.00277 | 1127.7 | 45.02 | 1047.9 | 15.17 | 7.08 | 963.7 | 65.16 |
| 1.68234 | 0.03418 | 0.17042 | 0.00095 | 1001.9 | 12.94 | 1014.4 | 5.24 | -1.25 | 933.3 | 25.17 |
| **NTP-Z2** | | | | | | | | | | |
| 2.44707 | 0.0518 | 0.22493 | 0.00142 | 1256.6 | 15.26 | 1307.9 | 7.47 | -4.08 | 1256.6 | 15.26 |
| 3.08935 | 0.07545 | 0.25424 | 0.0018 | 1430.1 | 18.73 | 1460.3 | 9.24 | -2.11 | 1430.1 | 18.73 |
| 0.57855 | 0.01706 | 0.07677 | 0.0007 | 463.5 | 10.97 | 476.8 | 4.16 | -2.87 | 476.8 | 4.16 |
| 13.63678 | 0.36755 | 0.54829 | 0.00395 | 2724.8 | 25.5 | 2818 | 16.45 | -3.42 | 2724.8 | 25.5 |
| 3.37276 | 0.09454 | 0.27571 | 0.00215 | 1498.1 | 21.95 | 1569.7 | 10.86 | -4.78 | 1498.1 | 21.95 |
| 0.87846 | 0.02432 | 0.10642 | 0.00088 | 640.2 | 13.15 | 651.9 | 5.15 | -1.83 | 651.9 | 5.15 |

| Isotope Ratios | | | | Ages | | | | | | |
|---|---|---|---|---|---|---|---|---|---|---|
| Pb207/U235 | | Pb206/U238 | | Pb207/U235 | | Pb206/U238 | | Discordance | Preferred Age | |
| 4.77603 | 0.11837 | 0.3148 | 0.00221 | 1780.7 | 20.81 | 1764.3 | 10.85 | 0.92 | 1780.7 | 20.81 |
| 12.96989 | 0.47394 | 0.46105 | 0.00422 | 2677.5 | 34.45 | 2444.2 | 18.61 | 8.71 | 2677.5 | 34.45 |
| 3.51743 | 0.11601 | 0.27413 | 0.00244 | 1531.1 | 26.08 | 1561.7 | 12.34 | -2.00 | 1531.1 | 26.08 |
| 1.8454 | 0.05409 | 0.18251 | 0.00153 | 1061.8 | 19.3 | 1080.7 | 8.34 | -1.78 | 1061.8 | 19.3 |
| 4.57159 | 0.1457 | 0.31914 | 0.00272 | 1744.1 | 26.55 | 1785.5 | 13.28 | -2.37 | 1744.1 | 26.55 |
| 15.07129 | 0.60088 | 0.55232 | 0.00536 | 2819.8 | 37.96 | 2834.8 | 22.26 | -0.53 | 2819.8 | 37.96 |
| 6.00276 | 0.21997 | 0.37622 | 0.00362 | 1976.2 | 31.9 | 2058.6 | 16.94 | -4.17 | 1976.2 | 31.9 |
| 2.42319 | 0.05962 | 0.20974 | 0.00153 | 1249.5 | 17.68 | 1227.4 | 8.15 | 1.77 | 1249.5 | 17.68 |
| 2.41321 | 0.07738 | 0.21671 | 0.00196 | 1246.5 | 23.02 | 1264.5 | 10.37 | -1.44 | 1246.5 | 23.02 |
| 4.80047 | 0.1337 | 0.31917 | 0.0025 | 1785 | 23.41 | 1785.7 | 12.24 | -0.04 | 1785 | 23.41 |
| 6.33961 | 0.3674 | 0.38943 | 0.00555 | 2023.9 | 50.83 | 2120.2 | 25.74 | -4.76 | 2023.9 | 50.83 |
| 1.96366 | 0.06923 | 0.18582 | 0.00185 | 1103.1 | 23.72 | 1098.7 | 10.07 | 0.40 | 1103.1 | 23.72 |
| 5.00029 | 0.15546 | 0.32334 | 0.0028 | 1819.4 | 26.31 | 1806 | 13.64 | 0.74 | 1819.4 | 26.31 |
| 1.86554 | 0.05808 | 0.17967 | 0.00162 | 1069 | 20.58 | 1065.2 | 8.86 | 0.36 | 1069 | 20.58 |
| 0.91159 | 0.04696 | 0.10912 | 0.00168 | 657.9 | 24.94 | 667.6 | 9.78 | -1.47 | 667.6 | 9.78 |
| 4.89456 | 0.13089 | 0.31794 | 0.00252 | 1801.3 | 22.55 | 1779.7 | 12.32 | 1.20 | 1801.3 | 22.55 |
| 4.348 | 0.12109 | 0.29311 | 0.0024 | 1702.5 | 22.99 | 1657 | 11.96 | 2.67 | 1702.5 | 22.99 |
| 4.47945 | 0.12722 | 0.29851 | 0.00247 | 1727.2 | 23.58 | 1683.9 | 12.28 | 2.51 | 1727.2 | 23.58 |
| 4.19507 | 0.12298 | 0.29928 | 0.00255 | 1673.1 | 24.04 | 1687.7 | 12.66 | -0.87 | 1673.1 | 24.04 |
| 2.5218 | 0.08278 | 0.21931 | 0.00206 | 1278.3 | 23.87 | 1278.2 | 10.9 | 0.01 | 1278.3 | 23.87 |
| 5.05284 | 0.16727 | 0.33435 | 0.00311 | 1828.2 | 28.06 | 1859.4 | 15.02 | -1.71 | 1828.2 | 28.06 |
| 5.69215 | 0.39981 | 0.31825 | 0.00533 | 1930.2 | 60.66 | 1781.2 | 26.09 | 7.72 | 1930.2 | 60.66 |
| 0.42901 | 0.01377 | 0.05888 | 0.00059 | 362.5 | 9.78 | 368.8 | 3.57 | -1.74 | 368.8 | 3.57 |
| **07-13-79-15W6 02** | | | | | | | | | | |
| 2.06526 | 0.04905 | 0.19067 | 0.00119 | 1137.4 | 16.25 | 1125 | 6.42 | 1.09 | 1174.7 | 23.57 |
| 4.19196 | 0.15334 | 0.29667 | 0.00263 | 1672.4 | 29.99 | 1674.8 | 13.07 | -0.14 | 1677.8 | 25.87 |
| 4.67217 | 0.13137 | 0.32033 | 0.00217 | 1762.3 | 23.52 | 1791.3 | 10.59 | -1.65 | 1759.8 | 19.34 |

| Isotope Ratios | | | | Ages | | | | | | |
|---|---|---|---|---|---|---|---|---|---|---|
| Pb207/U235 | | Pb206/U238 | | Pb207/U235 | | Pb206/U238 | | Discordance | Preferred Age | |
| 3.09705 | 0.06888 | 0.24813 | 0.00138 | 1432 | 17.07 | 1428.8 | 7.13 | 0.22 | 1405 | 18.93 |
| 0.74972 | 0.02473 | 0.08489 | 0.00086 | 568.1 | 14.35 | 525.2 | 5.1 | 7.55 | 525.2 | 5.1 |
| 3.8525 | 0.09798 | 0.28196 | 0.00176 | 1603.8 | 20.5 | 1601.2 | 8.87 | 0.16 | 1609 | 19.37 |
| 2.90948 | 0.07248 | 0.23615 | 0.00152 | 1384.4 | 18.83 | 1366.6 | 7.91 | 1.29 | 1467 | 21.57 |
| 1.77769 | 0.10719 | 0.18043 | 0.00289 | 1037.3 | 39.18 | 1069.3 | 15.76 | -3.08 | 1021.5 | 62.35 |
| 1.64822 | 0.03871 | 0.17069 | 0.00108 | 988.9 | 14.84 | 1015.9 | 5.97 | -2.73 | 979.6 | 26.25 |
| 3.33193 | 0.09845 | 0.25546 | 0.00189 | 1488.6 | 23.08 | 1466.6 | 9.7 | 1.48 | 1505.7 | 23.92 |
| 11.5174 | 0.63196 | 0.51704 | 0.00639 | 2566 | 51.26 | 2686.6 | 27.16 | -4.70 | 2569.7 | 23.73 |
| 13.23295 | 0.34134 | 0.52677 | 0.00303 | 2696.4 | 24.35 | 2727.8 | 12.81 | -1.16 | 2703.2 | 12.28 |
| 13.93231 | 0.22702 | 0.53098 | 0.00201 | 2745.1 | 15.44 | 2745.6 | 8.45 | -0.02 | 2717.3 | 9.85 |
| 5.20518 | 0.10143 | 0.33072 | 0.00156 | 1853.5 | 16.6 | 1841.9 | 7.54 | 0.63 | 1794.8 | 14.56 |
| 3.05385 | 0.04758 | 0.24504 | 0.001 | 1421.2 | 11.92 | 1412.9 | 5.17 | 0.58 | 1423.9 | 15 |
| 0.54437 | 0.0263 | 0.06932 | 0.00102 | 441.3 | 17.29 | 432.1 | 6.16 | 2.08 | 432.1 | 6.16 |
| 4.30753 | 0.12357 | 0.27963 | 0.00194 | 1694.8 | 23.64 | 1589.5 | 9.76 | 6.21 | 1722.2 | 21.1 |
| 3.98473 | 0.0862 | 0.28886 | 0.00156 | 1631.1 | 17.56 | 1635.8 | 7.8 | -0.29 | 1632.6 | 17.52 |
| 0.47692 | 0.01212 | 0.06321 | 0.0005 | 396 | 8.33 | 395.1 | 3.02 | 0.23 | 395.1 | 3.02 |
| 4.44554 | 0.05871 | 0.30546 | 0.00106 | 1720.9 | 10.95 | 1718.3 | 5.26 | 0.15 | 1727.9 | 12.62 |
| 6.02938 | 0.13785 | 0.35805 | 0.00196 | 1980.1 | 19.91 | 1972.9 | 9.3 | 0.36 | 1965.3 | 15.86 |
| 2.90909 | 0.09508 | 0.25241 | 0.00211 | 1384.3 | 24.7 | 1450.9 | 10.87 | -4.81 | 1410.9 | 28.07 |
| 0.45378 | 0.01509 | 0.05526 | 0.00059 | 379.9 | 10.54 | 346.8 | 3.58 | 8.71 | 346.8 | 3.58 |
| **07-13-79-15W6 Z1** | | | | | | | | | | |
| 4.71664 | 0.05977 | 0.28299 | 0.00095 | 1770.2 | 10.62 | 1606.4 | 4.77 | 9.25 | 1952.6 | 11.49 |
| 2.44883 | 0.05207 | 0.22118 | 0.00124 | 1257.1 | 15.33 | 1288.1 | 6.54 | -2.47 | 1278.6 | 20.89 |
| 0.31974 | 0.01018 | 0.04129 | 0.00044 | 281.7 | 7.83 | 260.8 | 2.7 | 7.42 | 260.8 | 2.7 |
| 10.29134 | 0.27088 | 0.4259 | 0.0026 | 2461.3 | 24.36 | 2287.2 | 11.74 | 7.07 | 2620.7 | 14.06 |
| 2.45899 | 0.03896 | 0.19422 | 0.00084 | 1260.1 | 11.44 | 1144.2 | 4.53 | 9.20 | 1440.3 | 16.16 |
| 1.84933 | 0.01823 | 0.17862 | 0.00051 | 1063.2 | 6.5 | 1059.4 | 2.79 | 0.36 | 1026.2 | 13.24 |

| Isotope Ratios | | | | Ages | | | | | | |
|---|---|---|---|---|---|---|---|---|---|---|
| Pb207/U235 | | Pb206/U238 | | Pb207/U235 | | Pb206/U238 | | Discordance | Preferred Age | |
| 0.74162 | 0.01856 | 0.09454 | 0.0007 | 563.4 | 10.82 | 582.3 | 4.12 | -3.35 | 582.3 | 4.12 |
| 1.91269 | 0.02704 | 0.18566 | 0.00073 | 1085.5 | 9.43 | 1097.8 | 3.95 | -1.13 | 1071.8 | 16.7 |
| 13.56721 | 0.28795 | 0.53905 | 0.00264 | 2720 | 20.07 | 2779.5 | 11.07 | -2.19 | 2727.3 | 11.86 |
| 4.08979 | 0.09951 | 0.2961 | 0.00178 | 1652.3 | 19.85 | 1672 | 8.88 | -1.19 | 1637.6 | 19.32 |
| 0.52407 | 0.00941 | 0.06797 | 0.00038 | 427.9 | 6.27 | 423.9 | 2.28 | 0.93 | 423.9 | 2.28 |
| 6.35723 | 0.09186 | 0.36767 | 0.00135 | 2026.4 | 12.68 | 2018.4 | 6.36 | 0.39 | 1990.8 | 12.61 |
| 6.54758 | 0.16967 | 0.38827 | 0.00239 | 2052.3 | 22.83 | 2114.8 | 11.09 | -3.05 | 2000.2 | 17.5 |
| 2.11101 | 0.0441 | 0.1932 | 0.00107 | 1152.4 | 14.39 | 1138.7 | 5.8 | 1.19 | 1134.3 | 22.69 |
| 2.43088 | 0.10258 | 0.20148 | 0.00213 | 1251.8 | 30.36 | 1183.3 | 11.43 | 5.47 | 1211.8 | 39.19 |
| 2.10721 | 0.06831 | 0.19893 | 0.00168 | 1151.2 | 22.32 | 1169.6 | 9.03 | -1.60 | 1123.5 | 32.79 |
| 2.73447 | 0.07022 | 0.22615 | 0.00151 | 1337.9 | 19.09 | 1314.3 | 7.94 | 1.76 | 1376.6 | 24.15 |
| 5.63426 | 0.21676 | 0.34115 | 0.00307 | 1921.4 | 33.18 | 1892.2 | 14.75 | 1.52 | 1876.3 | 25.37 |
| 2.52726 | 0.04544 | 0.21157 | 0.00105 | 1279.9 | 13.08 | 1237.2 | 5.57 | 3.34 | 1419 | 19.18 |
| 4.80315 | 0.11059 | 0.31215 | 0.00181 | 1785.5 | 19.35 | 1751.3 | 8.89 | 1.92 | 1849.5 | 18.7 |
| 5.51674 | 0.0922 | 0.34533 | 0.0015 | 1903.2 | 14.37 | 1912.2 | 7.21 | -0.47 | 1891.1 | 15.79 |
| 2.34146 | 0.06565 | 0.21158 | 0.00155 | 1225 | 19.95 | 1237.2 | 8.27 | -1.00 | 1218 | 28.26 |
| 0.51995 | 0.01025 | 0.06794 | 0.00041 | 425.1 | 6.85 | 423.7 | 2.5 | 0.33 | 423.7 | 2.5 |
| 1.62817 | 0.04326 | 0.16622 | 0.00121 | 981.2 | 16.71 | 991.3 | 6.67 | -1.03 | 991.3 | 6.67 |
| 6.52318 | 0.32966 | 0.36088 | 0.00436 | 2049 | 44.49 | 1986.3 | 20.63 | 3.06 | 2185.4 | 30.15 |
| **C-085-I/094-B-1 Z2** | | | | | | | | | | |
| 4.68831 | 0.11863 | 0.33299 | 0.00235 | 1765.2 | 21.18 | 1852.8 | 11.36 | -4.96 | 1697.6 | 24.3 |
| 3.93578 | 0.1858 | 0.30027 | 0.00366 | 1621.1 | 38.22 | 1692.6 | 18.16 | -4.41 | 1480.7 | 43.96 |
| 3.93037 | 0.1221 | 0.29124 | 0.00253 | 1620 | 25.15 | 1647.7 | 12.61 | -1.71 | 1648.4 | 30.35 |
| 1.90221 | 0.16362 | 0.17866 | 0.00454 | 1081.9 | 57.25 | 1059.7 | 24.81 | 2.05 | 1172.2 | 103.82 |
| 3.68843 | 0.08686 | 0.28445 | 0.00196 | 1568.9 | 18.81 | 1613.8 | 9.83 | -2.86 | 1561.4 | 25.46 |
| 2.72325 | 0.07703 | 0.23641 | 0.00196 | 1334.8 | 21.01 | 1368 | 10.23 | -2.49 | 1383.7 | 32.31 |
| 3.2133 | 0.06626 | 0.25823 | 0.00164 | 1460.4 | 15.97 | 1480.8 | 8.39 | -1.40 | 1501.2 | 24.7 |

| Isotope Ratios | | | | Ages | | | | | | |
|---|---|---|---|---|---|---|---|---|---|---|
| Pb207/U235 | | Pb206/U238 | | Pb207/U235 | | Pb206/U238 | | Discordance | Preferred Age | |
| 5.60083 | 0.31491 | 0.32382 | 0.00454 | 1916.2 | 48.44 | 1808.4 | 22.1 | 5.63 | 1903 | 45.06 |
| 12.97614 | 0.42844 | 0.52225 | 0.00427 | 2677.9 | 31.13 | 2708.7 | 18.07 | -1.15 | 2702.6 | 23.44 |
| 4.31877 | 0.10956 | 0.29626 | 0.00216 | 1696.9 | 20.92 | 1672.7 | 10.72 | 1.43 | 1718.2 | 27.42 |
| 2.97983 | 0.11536 | 0.25528 | 0.00276 | 1402.5 | 29.43 | 1465.7 | 14.17 | -4.51 | 1392.9 | 42.23 |
| 2.17245 | 0.06293 | 0.19596 | 0.0017 | 1172.3 | 20.14 | 1153.6 | 9.16 | 1.60 | 1208.9 | 37.4 |
| C-085-I/094-B-1 4 | | | | | | | | | | |
| 1.81309 | 0.05288 | 0.17972 | 0.00138 | 1050.2 | 19.09 | 1065.4 | 7.54 | -1.45 | 935.7 | 30.77 |
| 4.3333 | 0.09767 | 0.31328 | 0.00173 | 1699.7 | 18.6 | 1756.8 | 8.48 | -3.36 | 1616.2 | 16.93 |
| 2.80696 | 0.05943 | 0.24192 | 0.00132 | 1357.4 | 15.85 | 1396.7 | 6.85 | -2.90 | 1305.6 | 19.26 |
| 3.31996 | 0.06522 | 0.26931 | 0.00134 | 1485.8 | 15.33 | 1537.3 | 6.79 | -3.47 | 1397.4 | 17.12 |
| 4.3914 | 0.10382 | 0.31327 | 0.00181 | 1710.7 | 19.55 | 1756.8 | 8.9 | -2.69 | 1636.7 | 17.78 |
| 6.70107 | 0.11255 | 0.38935 | 0.00159 | 2072.8 | 14.84 | 2119.8 | 7.39 | -2.27 | 2003.7 | 12.33 |
| 4.31673 | 0.06624 | 0.30752 | 0.0012 | 1696.6 | 12.65 | 1728.5 | 5.93 | -1.88 | 1633.1 | 13.44 |
| 1.78412 | 0.02526 | 0.1804 | 0.0007 | 1039.7 | 9.21 | 1069.1 | 3.85 | -2.83 | 929.4 | 17.02 |
| 5.32017 | 0.17122 | 0.32968 | 0.00249 | 1872.1 | 27.51 | 1836.8 | 12.09 | 1.89 | 1820.1 | 21.32 |
| 1.53437 | 0.03987 | 0.16014 | 0.00115 | 944.3 | 15.97 | 957.6 | 6.39 | -1.41 | 957.6 | 6.39 |
| 1.789 | 0.03554 | 0.17704 | 0.00095 | 1041.5 | 12.94 | 1050.8 | 5.23 | -0.89 | 1000.8 | 22.57 |
| 0.54024 | 0.0123 | 0.07179 | 0.0005 | 438.6 | 8.11 | 446.9 | 3 | -1.89 | 446.9 | 3 |
| 5.88752 | 0.20987 | 0.35423 | 0.00295 | 1959.4 | 30.94 | 1954.8 | 14.02 | 0.23 | 1905.5 | 22.79 |
| 5.29506 | 0.13726 | 0.33726 | 0.00209 | 1868.1 | 22.14 | 1873.5 | 10.07 | -0.29 | 1787.1 | 18.95 |
| 2.07137 | 0.04234 | 0.1878 | 0.00103 | 1139.4 | 14 | 1109.5 | 5.61 | 2.62 | 1154.6 | 22.13 |
| 3.08455 | 0.05134 | 0.25376 | 0.00111 | 1428.9 | 12.76 | 1457.9 | 5.73 | -2.03 | 1369 | 17.08 |
| 3.17947 | 0.04829 | 0.24751 | 0.00103 | 1452.2 | 11.73 | 1425.6 | 5.3 | 1.83 | 1562.4 | 15.88 |
| 3.54709 | 0.062 | 0.26849 | 0.00122 | 1537.8 | 13.85 | 1533.1 | 6.2 | 0.31 | 1521.2 | 17 |
| 3.43891 | 0.04628 | 0.27686 | 0.00102 | 1513.3 | 10.59 | 1575.5 | 5.16 | -4.11 | 1449.9 | 15.46 |
| 4.4622 | 0.12537 | 0.29918 | 0.00205 | 1724 | 23.31 | 1687.3 | 10.16 | 2.13 | 1691.9 | 22.16 |

| Isotope Ratios | | | | Ages | | | | | | |
|---|---|---|---|---|---|---|---|---|---|---|
| Pb207/U235 | | Pb206/U238 | | Pb207/U235 | | Pb206/U238 | | Discordance | Preferred Age | |
| C-085-I/094-B-1 Z1 | | | | | | | | | | |
| 4.98863 | 0.20739 | 0.33185 | 0.00531 | 1817.4 | 35.16 | 1847.3 | 25.71 | -1.65 | 1954 | 37.82 |
| 4.97371 | 0.11497 | 0.32638 | 0.00434 | 1814.9 | 19.54 | 1820.8 | 21.07 | -0.33 | 1829.7 | 26.8 |
| 1.81204 | 0.059 | 0.16902 | 0.00256 | 1049.8 | 21.3 | 1006.7 | 14.1 | 4.11 | 1135.8 | 44.01 |
| 1.444 | 0.02531 | 0.14413 | 0.00187 | 907.4 | 10.52 | 868 | 10.54 | 4.34 | 868 | 10.54 |
| 0.4936 | 0.01717 | 0.06729 | 0.0011 | 407.4 | 11.67 | 419.8 | 6.65 | -3.04 | 419.8 | 6.65 |
| 1.83423 | 0.05692 | 0.17909 | 0.00265 | 1057.8 | 20.39 | 1062 | 14.48 | -0.40 | 1009.3 | 43.36 |
| 2.45391 | 0.10319 | 0.21336 | 0.00353 | 1258.6 | 30.33 | 1246.7 | 18.73 | 0.95 | 1224.5 | 49.96 |
| 1.8189 | 0.06167 | 0.18588 | 0.00286 | 1052.3 | 22.21 | 1099 | 15.56 | -4.44 | 1045.1 | 46.73 |
| 4.78713 | 0.08813 | 0.31776 | 0.00413 | 1782.6 | 15.46 | 1778.8 | 20.18 | 0.21 | 1796.4 | 25.18 |
| 0.45818 | 0.01553 | 0.06151 | 0.001 | 383 | 10.81 | 384.8 | 6.1 | -0.47 | 384.8 | 6.1 |
| 4.65775 | 0.23809 | 0.31878 | 0.00561 | 1759.7 | 42.73 | 1783.8 | 27.42 | -1.37 | 1715.4 | 46.48 |
| 1.78587 | 0.08345 | 0.18161 | 0.00325 | 1040.3 | 30.41 | 1075.8 | 17.71 | -3.41 | 939.4 | 62.31 |
| 5.36655 | 0.15931 | 0.33226 | 0.00476 | 1879.5 | 25.41 | 1849.3 | 23.04 | 1.61 | 1907.5 | 31.02 |
| 3.47901 | 0.1271 | 0.2584 | 0.00401 | 1522.5 | 28.81 | 1481.6 | 20.56 | 2.69 | 1520 | 40.34 |
| 1.65094 | 0.03442 | 0.15179 | 0.00208 | 989.9 | 13.18 | 911 | 11.65 | 7.97 | 911 | 11.65 |
| 3.48824 | 0.10908 | 0.25803 | 0.00382 | 1524.6 | 24.68 | 1479.7 | 19.58 | 2.95 | 1530.3 | 36.51 |
| 9.46444 | 0.31954 | 0.46971 | 0.00696 | 2384.1 | 31.01 | 2482.3 | 30.52 | -4.12 | 2443.1 | 29.41 |
| 4.24236 | 0.11475 | 0.30804 | 0.00438 | 1682.3 | 22.23 | 1731 | 21.6 | -2.89 | 1651.6 | 32.37 |
| D-048-A/094-B-9 01 | | | | | | | | | | |
| 4.0444 | 0.13908 | 0.28825 | 0.0063 | 1643.2 | 27.99 | 1632.8 | 31.54 | 0.63 | 1647 | 37.33 |
| 4.11893 | 0.1302 | 0.29438 | 0.00636 | 1658.1 | 25.83 | 1663.4 | 31.68 | -0.32 | 1668.8 | 34.83 |
| 4.47902 | 0.23728 | 0.30122 | 0.00712 | 1727.1 | 43.97 | 1697.4 | 35.29 | 1.72 | 1611 | 49.96 |
| 2.60662 | 0.09412 | 0.23602 | 0.00524 | 1302.5 | 26.5 | 1366 | 27.31 | -4.88 | 1270.4 | 45.28 |
| 6.31369 | 0.17567 | 0.34689 | 0.00732 | 2020.4 | 24.39 | 1919.7 | 35.05 | 4.98 | 2023.4 | 28.85 |
| 13.84941 | 0.42103 | 0.54519 | 0.0115 | 2739.5 | 28.79 | 2805.1 | 47.96 | -2.39 | 2721.7 | 25.32 |
| 0.57927 | 0.01944 | 0.07722 | 0.00173 | 464 | 12.5 | 479.5 | 10.35 | -3.34 | 479.5 | 10.35 |

| Isotope Ratios | | | | Ages | | | | | | |
|---|---|---|---|---|---|---|---|---|---|---|
| Pb207/U235 | | Pb206/U238 | | Pb207/U235 | | Pb206/U238 | | Discordance | Preferred Age | |
| 0.52615 | 0.01786 | 0.06947 | 0.00157 | 429.3 | 11.89 | 433 | 9.46 | -0.86 | 433 | 9.46 |
| 14.43287 | 0.61737 | 0.54227 | 0.01191 | 2778.6 | 40.62 | 2793 | 49.8 | -0.52 | 2825.4 | 29.18 |
| 3.15232 | 0.12088 | 0.25874 | 0.00577 | 1445.6 | 29.56 | 1483.4 | 29.54 | -2.61 | 1440.3 | 43.76 |
| 1.94269 | 0.05617 | 0.18555 | 0.00399 | 1095.9 | 19.38 | 1097.2 | 21.67 | -0.12 | 1117.6 | 41.29 |
| 0.54851 | 0.02448 | 0.07234 | 0.00172 | 444 | 16.05 | 450.2 | 10.34 | -1.40 | 450.2 | 10.34 |
| 2.07721 | 0.05273 | 0.20018 | 0.00422 | 1141.3 | 17.4 | 1176.3 | 22.64 | -3.07 | 1087.5 | 37.57 |
| 4.55998 | 0.1044 | 0.31793 | 0.00659 | 1742 | 19.07 | 1779.6 | 32.21 | -2.16 | 1678.4 | 29.54 |
| 3.92138 | 0.12266 | 0.28018 | 0.00599 | 1618.1 | 25.31 | 1592.3 | 30.16 | 1.59 | 1631.3 | 35.91 |
| 4.26718 | 0.15826 | 0.27534 | 0.00607 | 1687.1 | 30.51 | 1567.9 | 30.68 | 7.07 | 1842.9 | 38.33 |
| 12.09229 | 0.80275 | 0.48886 | 0.01184 | 2611.6 | 62.26 | 2565.7 | 51.27 | 1.76 | 2565.1 | 41.46 |
| 3.37828 | 0.09924 | 0.25741 | 0.00549 | 1499.4 | 23.01 | 1476.6 | 28.17 | 1.52 | 1659.2 | 35.64 |
| 5.91865 | 0.15425 | 0.34444 | 0.00718 | 1964 | 22.64 | 1908 | 34.42 | 2.85 | 1942.6 | 30.01 |
| 0.87468 | 0.0391 | 0.10611 | 0.00253 | 638.1 | 21.18 | 650.1 | 14.72 | -1.88 | 650.1 | 14.72 |
| 1.72448 | 0.08213 | 0.17441 | 0.00416 | 1017.7 | 30.61 | 1036.4 | 22.83 | -1.84 | 1078.6 | 66.45 |
| 1.84506 | 0.05687 | 0.17441 | 0.00375 | 1061.7 | 20.3 | 1036.4 | 20.58 | 2.38 | 1037.5 | 45.5 |
| 5.68773 | 0.18985 | 0.34997 | 0.00748 | 1929.5 | 28.82 | 1934.5 | 35.72 | -0.26 | 1960.1 | 35.01 |
| 1.94964 | 0.0576 | 0.17555 | 0.00375 | 1098.3 | 19.83 | 1042.6 | 20.54 | 5.07 | 1103.2 | 43.52 |
| 5.70039 | 0.13736 | 0.3521 | 0.00727 | 1931.4 | 20.81 | 1944.6 | 34.65 | -0.68 | 1909.2 | 31.3 |
| 10.39938 | 0.34982 | 0.48377 | 0.01024 | 2471 | 31.16 | 2543.7 | 44.51 | -2.94 | 2488.1 | 31.42 |
| 3.83343 | 0.11303 | 0.28236 | 0.00597 | 1599.8 | 23.74 | 1603.2 | 30.01 | -0.21 | 1656.7 | 36.94 |
| 4.20999 | 0.28025 | 0.29384 | 0.00744 | 1676 | 54.62 | 1660.7 | 37.05 | 0.91 | 1592.4 | 62.45 |
| 5.75094 | 0.2258 | 0.35049 | 0.00764 | 1939.1 | 33.96 | 1936.9 | 36.49 | 0.11 | 1897.4 | 39.64 |
| 0.51987 | 0.02879 | 0.06619 | 0.00171 | 425.1 | 19.23 | 413.2 | 10.37 | 2.80 | 413.2 | 10.37 |
| 1.75983 | 0.16354 | 0.18212 | 0.00576 | 1030.8 | 60.17 | 1078.6 | 31.4 | -4.64 | 1034.1 | 124.93 |
| 0.57109 | 0.02661 | 0.07428 | 0.00178 | 458.7 | 17.2 | 461.9 | 10.69 | -0.70 | 461.9 | 10.69 |
| **BH-02** | | | | | | | | | | |
| 10.88624 | 0.48035 | 0.45442 | 0.00462 | 2513.5 | 41.03 | 2414.9 | 20.47 | 3.92 | 2635 | 26.88 |

| Isotope Ratios | | | | Ages | | | | | | |
|---|---|---|---|---|---|---|---|---|---|---|
| Pb207/U235 | | Pb206/U238 | | Pb207/U235 | | Pb206/U238 | | Discordance | Preferred Age | |
| 3.76188 | 0.13233 | 0.26225 | 0.00245 | 1584.7 | 28.22 | 1501.3 | 12.53 | 5.26 | 1736.9 | 33 |
| 2.24531 | 0.04365 | 0.20165 | 0.00117 | 1195.3 | 13.66 | 1184.2 | 6.29 | 0.93 | 1230.4 | 25.57 |
| 1.85131 | 0.07332 | 0.18257 | 0.00202 | 1063.9 | 26.11 | 1081 | 11.01 | -1.61 | 1063.5 | 48.49 |
| 13.01253 | 0.41319 | 0.53078 | 0.00397 | 2680.6 | 29.94 | 2744.7 | 16.73 | -2.39 | 2724.4 | 21.29 |
| 5.3879 | 0.30167 | 0.32862 | 0.00449 | 1882.9 | 47.95 | 1831.7 | 21.79 | 2.72 | 1972.8 | 42.46 |
| 2.88601 | 0.07883 | 0.23067 | 0.00172 | 1378.3 | 20.6 | 1338 | 9 | 2.92 | 1375.5 | 30.37 |
| 4.26232 | 0.50492 | 0.30963 | 0.0092 | 1686.1 | 97.43 | 1738.9 | 45.29 | -3.13 | 1769.5 | 101.28 |
| 1.87524 | 0.12906 | 0.17588 | 0.00324 | 1072.4 | 45.58 | 1044.4 | 17.75 | 2.61 | 1151.9 | 80.34 |
| 17.10112 | 0.57384 | 0.6045 | 0.00467 | 2940.5 | 32.19 | 3048 | 18.78 | -3.66 | 2991.3 | 20.85 |
| 0.60624 | 0.06522 | 0.0697 | 0.0024 | 481.2 | 41.23 | 434.4 | 14.47 | 9.73 | 434.4 | 14.47 |
| 3.82868 | 0.25206 | 0.28737 | 0.00478 | 1598.8 | 53 | 1628.4 | 23.95 | -1.85 | 1737.8 | 55.79 |
| 3.3978 | 0.33444 | 0.27304 | 0.007 | 1503.9 | 77.22 | 1556.2 | 35.46 | -3.48 | 1666.9 | 86.16 |
| 0.59695 | 0.02995 | 0.07691 | 0.00118 | 475.3 | 19.04 | 477.7 | 7.07 | -0.50 | 477.7 | 7.07 |
| 3.23393 | 0.19475 | 0.26536 | 0.00406 | 1465.3 | 46.71 | 1517.2 | 20.71 | -3.54 | 1499.9 | 57.55 |
| 2.14659 | 0.11007 | 0.20026 | 0.00265 | 1164 | 35.52 | 1176.7 | 14.21 | -1.09 | 1020.2 | 58.38 |
| 4.09803 | 0.1918 | 0.29974 | 0.00342 | 1653.9 | 38.2 | 1690 | 16.94 | -2.18 | 1569.5 | 41.41 |
| 4.05809 | 0.1284 | 0.28938 | 0.0024 | 1645.9 | 25.77 | 1638.4 | 11.98 | 0.46 | 1675.7 | 31.12 |
| 4.61054 | 0.1652 | 0.3167 | 0.0029 | 1751.2 | 29.9 | 1773.6 | 14.18 | -1.28 | 1804.2 | 32.28 |
| 1.8309 | 0.08949 | 0.17681 | 0.0024 | 1056.6 | 32.1 | 1049.5 | 13.13 | 0.67 | 1130.3 | 58.91 |
| 13.78396 | 0.84205 | 0.54553 | 0.0074 | 2735 | 57.83 | 2806.6 | 30.85 | -2.62 | 2807.3 | 33.07 |
| 3.85716 | 0.10099 | 0.26301 | 0.00194 | 1604.8 | 21.11 | 1505.2 | 9.89 | 6.21 | 1808 | 28.34 |
| 0.74307 | 0.06245 | 0.09395 | 0.00227 | 564.2 | 36.38 | 578.9 | 13.39 | -2.61 | 578.9 | 13.39 |
| 2.16581 | 0.08233 | 0.19653 | 0.00202 | 1170.1 | 26.41 | 1156.6 | 10.9 | 1.15 | 1118.3 | 45.23 |
| 3.21441 | 0.16199 | 0.26137 | 0.00345 | 1460.6 | 39.03 | 1496.8 | 17.61 | -2.48 | 1547.2 | 49.05 |
| 4.86929 | 0.25439 | 0.33668 | 0.00427 | 1797 | 44.01 | 1870.7 | 20.61 | -4.10 | 1737.9 | 43.49 |
| 1.45371 | 0.22553 | 0.15451 | 0.00737 | 911.4 | 93.33 | 926.2 | 41.14 | -1.62 | 926.2 | 41.14 |
| 3.03269 | 0.10358 | 0.25127 | 0.00231 | 1415.9 | 26.08 | 1445 | 11.91 | -2.06 | 1423.7 | 37.51 |

| Isotope Ratios | | | | Ages | | | | | | |
|---|---|---|---|---|---|---|---|---|---|---|
| Pb207/U235 | | Pb206/U238 | | Pb207/U235 | | Pb206/U238 | | Discordance | Preferred Age | |
| 17.98623 | 1.13185 | 0.58135 | 0.0076 | 2989 | 60.53 | 2954.3 | 30.98 | 1.16 | 2979.1 | 31.77 |
| 0.57374 | 0.04388 | 0.07548 | 0.0017 | 460.4 | 28.31 | 469.1 | 10.16 | -1.89 | 469.1 | 10.16 |
| 2.95006 | 0.07865 | 0.24084 | 0.00183 | 1394.9 | 20.22 | 1391.1 | 9.49 | 0.27 | 1422 | 32.65 |
| 2.27537 | 0.07638 | 0.21596 | 0.00205 | 1204.7 | 23.68 | 1260.5 | 10.86 | -4.63 | 1244.4 | 40.83 |
| 11.97861 | 0.51274 | 0.49413 | 0.00504 | 2602.7 | 40.11 | 2588.5 | 21.73 | 0.55 | 2726 | 29.69 |
| 3.36272 | 0.24488 | 0.26866 | 0.00481 | 1495.8 | 56.99 | 1534 | 24.44 | -2.55 | 1531.6 | 65.84 |
| 3.12289 | 0.23701 | 0.25478 | 0.0049 | 1438.3 | 58.37 | 1463.1 | 25.19 | -1.72 | 1376.1 | 73.44 |
| 3.36821 | 0.22095 | 0.26101 | 0.0043 | 1497 | 51.36 | 1495 | 21.98 | 0.13 | 1567.3 | 60.77 |
| 3.82574 | 0.11319 | 0.27987 | 0.0023 | 1598.2 | 23.82 | 1590.7 | 11.56 | 0.47 | 1644.1 | 33.9 |
| 9.27337 | 0.60426 | 0.44477 | 0.00684 | 2365.4 | 59.72 | 2372 | 30.52 | -0.28 | 2543.1 | 41.64 |
| 2.25252 | 0.07881 | 0.2117 | 0.00206 | 1197.6 | 24.6 | 1237.9 | 10.98 | -3.37 | 1158.6 | 44.16 |
| 13.77191 | 0.91001 | 0.51385 | 0.00751 | 2734.2 | 62.55 | 2673 | 31.98 | 2.24 | 2766.3 | 38.27 |
| 1.7327 | 0.14201 | 0.1724 | 0.00381 | 1020.8 | 52.77 | 1025.3 | 20.93 | -0.44 | 1007.4 | 98.18 |
| 6.2514 | 0.20364 | 0.37577 | 0.00329 | 2011.7 | 28.52 | 2056.5 | 15.41 | -2.23 | 2066.6 | 33.77 |
| 3.94632 | 0.20078 | 0.28132 | 0.00365 | 1623.2 | 41.22 | 1598 | 18.35 | 1.55 | 1667.1 | 48.63 |
| 0.85116 | 0.02581 | 0.10231 | 0.00097 | 625.3 | 14.16 | 627.9 | 5.67 | -0.42 | 627.9 | 5.67 |
| **BH-01** | | | | | | | | | | |
| 4.6566 | 0.18385 | 0.32744 | 0.00319 | 1759.5 | 33 | 1826 | 15.5 | -3.78 | 1776 | 32.75 |
| 1.84514 | 0.09412 | 0.17648 | 0.00251 | 1061.7 | 33.59 | 1047.7 | 13.73 | 1.32 | 1179.2 | 59.02 |
| 7.7134 | 0.73593 | 0.38749 | 0.00823 | 2198.2 | 85.76 | 2111.2 | 38.23 | 3.96 | 2346.3 | 55.1 |
| 5.22672 | 0.28856 | 0.35247 | 0.0048 | 1857 | 47.06 | 1946.4 | 22.86 | -4.81 | 1966.7 | 41.51 |
| 1.6937 | 0.10306 | 0.17794 | 0.00293 | 1006.2 | 38.85 | 1055.7 | 16.03 | -4.92 | 970.6 | 74.11 |
| 1.69347 | 0.04356 | 0.16614 | 0.00125 | 1006.1 | 16.42 | 990.8 | 6.89 | 1.52 | 990.8 | 6.89 |
| 3.27712 | 0.28288 | 0.27036 | 0.00609 | 1475.6 | 67.16 | 1542.6 | 30.89 | -4.54 | 1574.9 | 79.38 |
| 5.03721 | 0.19621 | 0.33362 | 0.00315 | 1825.6 | 33 | 1855.9 | 15.25 | -1.66 | 1793 | 31.92 |
| 0.51304 | 0.0407 | 0.06932 | 0.00178 | 420.5 | 27.32 | 432.1 | 10.72 | -2.76 | 432.1 | 10.72 |
| 3.9623 | 0.22391 | 0.27433 | 0.00378 | 1626.5 | 45.82 | 1562.8 | 19.13 | 3.92 | 1656.4 | 47.76 |

| Isotope Ratios | | | | Ages | | | | | | |
|---|---|---|---|---|---|---|---|---|---|---|
| Pb207/U235 | | Pb206/U238 | | Pb207/U235 | | Pb206/U238 | | Discordance | Preferred Age | |
| 12.75305 | 0.79233 | 0.51548 | 0.00682 | 2661.6 | 58.5 | 2680 | 29.03 | -0.69 | 2705.5 | 31.8 |
| 2.10767 | 0.27 | 0.19464 | 0.00654 | 1151.3 | 88.22 | 1146.5 | 35.28 | 0.42 | 1150.2 | 136.53 |
| 14.46948 | 0.85999 | 0.55764 | 0.00694 | 2781 | 56.45 | 2856.9 | 28.72 | -2.73 | 2721.9 | 30.22 |
| 2.10627 | 0.07825 | 0.19649 | 0.00201 | 1150.9 | 25.58 | 1156.4 | 10.83 | -0.48 | 1210.7 | 42.77 |
| 3.92487 | 0.26518 | 0.28938 | 0.0049 | 1618.8 | 54.67 | 1638.5 | 24.52 | -1.22 | 1695 | 56.6 |
| 5.7466 | 0.21005 | 0.34205 | 0.00302 | 1938.4 | 31.61 | 1896.5 | 14.5 | 2.16 | 1876.4 | 30.51 |
| 2.03986 | 0.10451 | 0.19422 | 0.0027 | 1128.9 | 34.91 | 1144.2 | 14.58 | -1.36 | 1170.4 | 58.75 |
| 4.61729 | 0.20469 | 0.31887 | 0.00347 | 1752.4 | 37 | 1784.2 | 16.96 | -1.81 | 1707.6 | 38.12 |
| 4.54114 | 0.13772 | 0.31492 | 0.00248 | 1738.5 | 25.24 | 1764.9 | 12.16 | -1.52 | 1710.7 | 29.75 |
| 3.73058 | 0.25413 | 0.28587 | 0.00503 | 1578 | 54.55 | 1620.9 | 25.22 | -2.72 | 1731.7 | 58.68 |
| 15.10401 | 1.42625 | 0.56056 | 0.01026 | 2821.8 | 89.93 | 2869 | 42.37 | -1.67 | 2803.9 | 41.19 |
| 16.18605 | 1.61899 | 0.52585 | 0.01036 | 2887.8 | 95.65 | 2724 | 43.76 | 5.67 | 2748.5 | 45.01 |
| 4.88562 | 0.21364 | 0.32039 | 0.00341 | 1799.8 | 36.86 | 1791.6 | 16.64 | 0.46 | 1772.9 | 37.35 |
| 17.3778 | 1.93487 | 0.55194 | 0.01215 | 2955.9 | 106.9 | 2833.2 | 50.47 | 4.15 | 2863.1 | 48.03 |
| 17.92822 | 0.55948 | 0.5713 | 0.00424 | 2985.9 | 30.01 | 2913.2 | 17.38 | 2.43 | 3025.4 | 22.95 |
| 14.09185 | 1.03736 | 0.53214 | 0.00866 | 2755.9 | 69.79 | 2750.5 | 36.44 | 0.20 | 2858.3 | 37.89 |
| 3.78159 | 0.16721 | 0.27495 | 0.00313 | 1588.8 | 35.51 | 1565.9 | 15.82 | 1.44 | 1642.1 | 41.61 |
| 3.00229 | 0.13012 | 0.25328 | 0.00292 | 1408.2 | 33.01 | 1455.4 | 15 | -3.35 | 1449 | 44.7 |
| 4.70744 | 0.17962 | 0.31153 | 0.00302 | 1768.6 | 31.96 | 1748.2 | 14.86 | 1.15 | 1794.2 | 35.3 |
| 0.56854 | 0.03387 | 0.06912 | 0.00127 | 457.1 | 21.92 | 430.8 | 7.66 | 5.75 | 430.8 | 7.66 |
| 5.35314 | 0.16886 | 0.34264 | 0.00284 | 1877.4 | 26.99 | 1899.4 | 13.63 | -1.17 | 1880.4 | 31.46 |
| 4.16174 | 0.15669 | 0.28665 | 0.0028 | 1666.5 | 30.82 | 1624.8 | 14.01 | 2.50 | 1676.4 | 37.29 |
| 4.26429 | 0.18149 | 0.31335 | 0.00347 | 1686.5 | 35.01 | 1757.2 | 17.04 | -4.19 | 1778.8 | 39.87 |
| 2.82831 | 0.30895 | 0.24196 | 0.00636 | 1363.1 | 81.94 | 1396.9 | 33.02 | -2.48 | 1264.1 | 106.64 |
| 0.81775 | 0.02325 | 0.09941 | 0.00087 | 606.8 | 12.98 | 610.9 | 5.11 | -0.68 | 610.9 | 5.11 |
| 9.47287 | 0.4182 | 0.44399 | 0.00466 | 2384.9 | 40.55 | 2368.5 | 20.81 | 0.69 | 2403.8 | 33.13 |
| 4.37826 | 0.21195 | 0.29465 | 0.00341 | 1708.2 | 40.02 | 1664.7 | 17 | 2.55 | 1642 | 43.49 |

| Isotope Ratios | | | | Ages | | | | | | |
|---|---|---|---|---|---|---|---|---|---|---|
| Pb207/U235 | | Pb206/U238 | | Pb207/U235 | | Pb206/U238 | | Discordance | Preferred Age | |
| 4.49886 | 0.30613 | 0.32204 | 0.00538 | 1730.8 | 56.53 | 1799.7 | 26.26 | -3.98 | 1746.5 | 56.39 |
| 4.69143 | 0.19537 | 0.31571 | 0.00334 | 1765.7 | 34.86 | 1768.7 | 16.36 | -0.17 | 1739.6 | 39.44 |
| 5.32844 | 0.24243 | 0.31904 | 0.00361 | 1873.4 | 38.9 | 1785 | 17.65 | 4.72 | 1863.3 | 40.59 |
| 32.98501 | 1.71919 | 0.74357 | 0.00832 | 3580.2 | 51.37 | 3583.8 | 30.76 | -0.10 | 3598.7 | 28.49 |
| 12.53264 | 0.66541 | 0.50458 | 0.00609 | 2645.2 | 49.93 | 2633.4 | 26.11 | 0.45 | 2640.6 | 35.1 |
| 14.48235 | 1.66614 | 0.54821 | 0.01364 | 2781.8 | 109.27 | 2817.7 | 56.79 | -1.29 | 2808.6 | 55.48 |
| **16-17-083-25W6 Z1** | | | | | | | | | | |
| 1.51022 | 0.04692 | 0.14674 | 0.00145 | 934.5 | 18.98 | 882.6 | 8.14 | 5.55 | 882.6 | 8.14 |
| 1.54514 | 0.03295 | 0.162 | 0.0012 | 948.6 | 13.15 | 967.9 | 6.68 | -2.03 | 967.9 | 6.68 |
| 3.83015 | 0.10988 | 0.27569 | 0.00236 | 1599.1 | 23.1 | 1569.6 | 11.95 | 1.84 | 1629.2 | 11.95 |
| 3.99197 | 0.14066 | 0.29699 | 0.00291 | 1632.6 | 28.61 | 1676.3 | 14.48 | -2.68 | 1562 | 14.48 |
| 4.89392 | 0.27697 | 0.31857 | 0.00456 | 1801.2 | 47.72 | 1782.7 | 22.32 | 1.03 | 1762.5 | 22.32 |
| 2.41105 | 0.10109 | 0.20263 | 0.00247 | 1245.9 | 30.09 | 1189.4 | 13.23 | 4.53 | 1293 | 13.23 |
| 5.07942 | 0.15581 | 0.2993 | 0.00266 | 1832.7 | 26.02 | 1687.8 | 13.2 | 7.91 | 1947.6 | 13.2 |
| 1.46926 | 0.0377 | 0.15005 | 0.00128 | 917.8 | 15.5 | 901.2 | 7.17 | 1.81 | 901.2 | 7.17 |
| 4.14346 | 0.10502 | 0.30363 | 0.00238 | 1662.9 | 20.73 | 1709.3 | 11.74 | -2.79 | 1605.2 | 11.74 |
| 4.49365 | 0.12138 | 0.31986 | 0.0026 | 1729.8 | 22.44 | 1789.1 | 12.7 | -3.43 | 1682.1 | 12.7 |
| 5.92277 | 0.18047 | 0.37051 | 0.0032 | 1964.6 | 26.47 | 2031.8 | 15.04 | -3.42 | 1924.3 | 15.04 |
| 5.81239 | 0.16173 | 0.34753 | 0.00284 | 1948.3 | 24.11 | 1922.8 | 13.6 | 1.31 | 1935.4 | 13.6 |
| 1.46935 | 0.05144 | 0.15946 | 0.00175 | 917.9 | 21.15 | 953.8 | 9.73 | -3.91 | 953.8 | 9.73 |
| 2.63066 | 0.13856 | 0.2294 | 0.00324 | 1309.2 | 38.75 | 1331.4 | 16.99 | -1.70 | 1175.9 | 16.99 |
| 1.98068 | 0.09234 | 0.19282 | 0.00256 | 1109 | 31.46 | 1136.6 | 13.85 | -2.49 | 1039.8 | 13.85 |
| 3.93802 | 0.12943 | 0.29682 | 0.00283 | 1621.5 | 26.61 | 1675.5 | 14.07 | -3.33 | 1564.2 | 14.07 |
| 4.58056 | 0.1938 | 0.3226 | 0.0037 | 1745.7 | 35.26 | 1802.4 | 18.01 | -3.25 | 1684.8 | 18.01 |
| 2.12801 | 0.11545 | 0.19235 | 0.00301 | 1157.9 | 37.48 | 1134.1 | 16.25 | 2.06 | 1184.8 | 16.25 |
| 4.17587 | 0.24309 | 0.29031 | 0.00431 | 1669.3 | 47.69 | 1643.1 | 21.52 | 1.57 | 1535.6 | 21.52 |
| 5.58087 | 0.18189 | 0.36522 | 0.00341 | 1913.2 | 28.06 | 2006.9 | 16.1 | -4.90 | 1831.9 | 16.1 |

| Isotope Ratios | | | | Ages | | | | | | |
|---|---|---|---|---|---|---|---|---|---|---|
| Pb207/U235 | | Pb206/U238 | | Pb207/U235 | | Pb206/U238 | | Discordance | Preferred Age | |
| 0.39284 | 0.01165 | 0.05551 | 0.0006 | 336.4 | 8.49 | 348.3 | 3.64 | -3.54 | 348.3 | 3.64 |
| 5.59341 | 0.23992 | 0.36055 | 0.00413 | 1915.1 | 36.95 | 1984.8 | 19.57 | -3.64 | 1874.6 | 19.57 |
| 2.04475 | 0.14272 | 0.19749 | 0.00384 | 1130.5 | 47.59 | 1161.8 | 20.65 | -2.77 | 1103.2 | 20.65 |
| 2.29175 | 0.12514 | 0.21517 | 0.00335 | 1209.7 | 38.6 | 1256.3 | 17.76 | -3.85 | 1221.1 | 17.76 |
| 0.55445 | 0.03315 | 0.07326 | 0.0014 | 447.9 | 21.66 | 455.8 | 8.39 | -1.76 | 455.8 | 8.39 |
| 0.67985 | 0.03229 | 0.07741 | 0.00121 | 526.7 | 19.52 | 480.7 | 7.24 | 8.73 | 480.7 | 7.24 |
| 2.71196 | 0.08776 | 0.21664 | 0.00225 | 1331.7 | 24.01 | 1264.1 | 11.94 | 5.08 | 1537.2 | 11.94 |
| 3.55453 | 0.11619 | 0.24467 | 0.00249 | 1539.4 | 25.9 | 1410.9 | 12.92 | 8.35 | 1691.7 | 12.92 |
| 1.6382 | 0.07488 | 0.15224 | 0.00212 | 985 | 28.82 | 913.5 | 11.84 | 7.26 | 913.5 | 11.84 |
| 2.19015 | 0.05545 | 0.20929 | 0.00184 | 1177.9 | 17.65 | 1225.1 | 9.82 | -4.01 | 1114.4 | 9.82 |
| 4.70409 | 0.17527 | 0.29252 | 0.00328 | 1768 | 31.2 | 1654.1 | 16.37 | 6.44 | 1998.9 | 16.37 |
| 4.96894 | 0.1279 | 0.31735 | 0.00278 | 1814.1 | 21.76 | 1776.8 | 13.63 | 2.06 | 1859.1 | 13.63 |
| 1.74982 | 0.06705 | 0.17144 | 0.00206 | 1027.1 | 24.76 | 1020 | 11.33 | 0.69 | 1009.3 | 11.33 |